Colossal Aromatic Molecules

A thesis submitted in partial fulfillment of the requirements for the degree of

Doctor of Philosophy in Chemistry

at the

University of Canterbury

by

Jayne Louise Ferguson

University of Canterbury
Christchurch
New Zealand

2013

Acknowledgements

Over four years ago, I never imagined that a drink at The Foundry after the NZIC quiz night and the decision to apply for a summer scholarship with Dr. Chris Fitchett the next day would lead me complete a PhD thesis under Chris' supervision. Thank you Chris, for guiding me through this time, for your constant encouragement, patience, support and of course all of those Staff Club beers! I have thoroughly enjoyed being your first student, and figuring out this PhD journey together. I would like to thank Prof. Peter Steel, for introducing to me to the infamous Winstenstein reaction, and also Assoc. Prof. Paul Kruger for his encouragement. The support from all members of staff is greatly appreciated, especially those involved with X-ray crystallography, Chris, Matt, Jan and Peter, thank you for always taking the time to share your extensive knowledge.

I would also like to thank the past and present members of Team Fitchett, Robbie, Paul, Will, Chris, Emma, Anthony, Sam and Aimee, for making the lab and office and enjoyable place to spend my time, as well as the past and present members of the Steel group that I have had the privilege of sharing an office with these last few years. Particularly, I would like to thank Dr. Jeni Burgess for showing me the ropes in the lab at the start of my time here, and Dr. Matt Polson for sharing your considerable chemistry knowledge and cooking me many dinners. I have also been fortunate enough to be welcomed into the 853 office for Wednesday curry train and Friday baking. Without Dr. Chris Hawes my time here would have been lot more challenging, thank you for the afternoon tea breaks and sharing many a beer with me throughout the course of our studies, especially as the going got tough.

Thank you to all of the technical staff, especially Wayne Mackay, for all the work you do around the department and your smiling faces. Thank you also to Dr. Marie Squire for running many Mass Spec samples and assisting with NMR, thank you also for sharing in all the excitement when the chemistry was working, and encouraging me to keep going when it wasn't. A thank you must also go to the College of Science for a PhD Scholarship and the NZIC and Evans fund for assisting with travel to conferences. I would also like to thank Graham Townsend, and the staff over at Bridging Programmes, for providing part-time employment teaching Headstart over the summers.

Thank you to all of my friends outside the Chemistry department, especially Ange, Stef, Kathryn, Aleisha and Kelly, you may not have understood entirely what I was doing but you always took the time to listen. I would also like to thank my parents, Janice and Willie, for your support as I followed this path, and also thank you to my siblings, Amy, Tracey and Tim. And finally, to my husband Alan, thank you for putting up with me writing this thesis during the start of our married life together. Thank you for believing in me when I didn't believe in myself and thank you for all of your support and love.

Table of contents

Abstract

This thesis describes the preparation of a series of compounds containing π-excessive, five-membered, heterocyclic rings with peripheral aryl substituents, designed to investigate their oxidative cyclodehydrogenation and/or photocyclisation to form curved, fused aromatic systems with a heterocyclic atom at the core of the compound. The ability of these compounds to undergo oxidative cyclodehydrogenation was investigated using a range of conditions, including the use of Lewis acidic transition metals, organic reagents and light as catalysts to carry out the desired carbon-carbon bond forming reactions. Two backbone linked 2,2'-biimidazole ligands were prepared to investigate their coordination chemistry with a range of different metal ions and counter ions.

Two families of model compounds, including ten previously unreported compounds, were prepared and subjected to various conditions for oxidative cyclodehydrogenation and photocyclisation resulting in the isolation of compounds with one carbon-carbon bond formed between the peripheral aryl rings in the same position on the heterocyclic ring, nineteen previously unreported compounds were isolated. Additionally, in one case oxidative cyclodehydrogenation resulted in the formation of two carbon-carbon bonds, producing a highly strained aromatic compound containing a heterocyclic ring. Photocyclisation of one family of compounds resulted in the formation of a different heterocyclic core dependent upon the substituent on the nitrogen atom. Five pentaarylpyrrole compounds, three of which were previously unreported, were also prepared after the exploration of various synthetic routes towards the pentaarylpyrrole motif. Photocyclisation also resulted in the formation of one carbon-carbon bond. The compounds resulting from oxidative cyclodehydrogenation and photocyclisation were characterised by NMR spectroscopy, UV/vis spectroscopy and fluorometry, where possible X-ray crystallography was also used.

The coordination chemistry of backbone linked 2,2'-biimidazole ligands to various metal ions could be controlled by the length of the backbone linker. The ethyl linked 2,2'-biimidazole ligand formed bridging and monodentate coordination compounds with various metal ions, the metallosupramolecular assemblies produced with silver ions could be controlled by the anion present. Discrete coordination complexes were usually formed, but in two cases metallopolymers were produced. The propyl linked 2,2'-biimidazole ligand formed exclusively discrete, chelating complexes with copper (II) metal ions. Eighteen coordination complexes were prepared during the course of this study characterized by X-ray crystallography, and NMR spectroscopy where appropriate.

Abbreviations

NMR: Nuclear Magnetic Resonance

COSY: Correlation Spectroscopy

HSQC: Heteronuclear Single Quantum Coherence

HMBC: Heteronuclear Multiple Bond Correlation

IR: Infrared

MP: Melting Point

UV/Vis: Ultraviolet/Visible

ESMS: Electrospray Mass Spectrometry

TGA: Thermogravimetric Analysis

PAH: Polycyclic aromatic hydrocarbon

HBC: Hexa-*peri*-hexabenzocoronene

MLCT: Metal to ligand charge transfer

Atom Colour Scheme:

Black: Carbon

Light Blue: Nitrogen

Grey: Hydrogen

Red: Oxygen

Green: Chlorine, Fluorine

Dark Blue: Copper, Cobalt

Light purple: Cadmium

Magenta: Silver

Yellow: Sulfur

Chapter One:

Introduction

1.1 General introduction to organic electronic devices

The discovery of the organic light emitting diode,[1] organic field effect transistor[2] and organic photovoltaic cell[3] in the mid 1980's has garnered increasing attention towards to the possibility of commercial organic electronic devices. Initially, the 2000 Chemistry Nobel Prize awarded to Heeger,[4] MacDiarmid[5] and Shirakawa[6] for "the discovery and development of conductive polymers"[7] in the late 1970's drove the push towards new 'soft' materials for electronics.[8] There are many advantages for implementation of 'soft' materials into electronic devices; the flexibility of the polymers and small molecules, the reduction in size of the devices by the use of these new organic materials, the ability to change the properties of the new materials as desired through organic synthesis and a decrease in manufacturing costs.[9]

The most important physical process for application of organic polymers and small molecules in organic electronic devices is the ability of the compound to carry charge over a long range.[10] Electronic charge is usually carried through the π-orbitals of the organic compound, in conducting polymers charge is transported along the π-system of the conjugated chain of the polymers, while in self assembled small molecules charge can hop from one molecule to another through interacting π-orbitals from different molecules. There are many factors that influence the ability of a compound to carry charge; the supramolecular ordering of small molecules in the bulk has a profound influence on the charge carrying ability of the molecule due to the alignment or misalignment of the π-orbitals from different molecules.[11] Many different methods exist for measuring the charge carrying ability of organic materials.[11a,12] Although the short range charge transport can be measured, more important for device performance is the long range charge carrier transport, commonly measured by time of flight (TOF) experiments or directly by implementation in a device. The underlying mechanism of charge transport in organic materials is not well understood,[13] but has been the subject of extensive investigation, both theoretically and experimentally, in an attempt to provide a set of guidelines for the development of new organic materials.[10,13,14]

The implementation of organic materials into commercial devices is still to overcome many challenges.[9b,15] The presence of impurities in organic materials can significantly disrupt the charge carrying ability, and the synthesis of most π-conjugated molecules is not trivial. Processing of the organic materials into thin films for devices can alter the supramolecular ordering of the material,[11a] and solubility of the organic compounds for application in traditional processing techniques is also an issue.[16] Despite these limitations research into new materials for application in organic electronic devices continues as organic electronic devices continue to find a place beside traditional silicon based devices.

1.1.1 Carbon based materials in organic electronic devices

The late 1980's and early 1990's heralded the discovery of fullerenes[17] and carbon nanotubes.[18] These all carbon allotropes have been the subject of considerable attention as new materials for organic electronics[19] due to their unique physical properties and chemical behavior owing to the presence of fused π conjugated benzene rings.[9b] Currently, carbon nanotubes can be produced on relatively large scales through various techniques,[20] but there also exists routes to carbon nanotubes[21] and fullerenes[22] through controlled organic synthesis using precursor aromatic molecules. Carbon nanotubes in particular have been incorporated into a variety of devices for their desirable properties and their ease of integration into existing manufacturing methods.[23] Currently the strength and electron carrying ability of individual carbon nanotubes far exceed that of bulk carbon nanotube materials, and extensive research effort is being directed towards reliably producing single carbon nanotubes of a defined size.[24]

The push towards using all carbon allotropes in organic electronic devices was increased by the isolation of single sheets of graphene in 2004 by Geim and Novoselov,[25] and they were awarded the Nobel Prize in Physics in 2010[26,27] for "groundbreaking experiments regarding the two-dimensional material graphene".[28] Previously only few layer thick sheets of graphite had been isolated and studied[29] and the isolation of a single layer of graphene was thought to be impossible as two dimensional crystals were believed to be thermodynamically unstable.[30] The two dimensional single layer graphene sheets were isolated by micromechanical exfoliation; this technique involves peeling a single layer of graphene from highly oriented pyrolytic graphite (HOPG) using Scotch tape. The isolation of graphene using this method allowed for chemists and physicists alike to experimentally confirm the remarkable properties of this material that were predicted by theory. Graphene has exceeded expectations displaying many important properties, such as, transparency, mechanical strength, quantum effects and thermal conductivity.[31] As such, many reviews have been published on graphene and its emerging applications in a variety of fields.[32] Despite the many favorable properties that single layers of graphene display, and the predicted application of these single layer sheets in a variety of different fields, the large scale synthesis of high quality single layers of graphene sheets remains an obstacle.[33]

1.1.2 Routes towards the synthesis of graphene sheets

There are many different routes for the synthesis of graphene sheets. Preparation of graphene oxide by the oxidation and exfoliation of graphite sheets, followed by reduction of the graphene oxide is a common technique for the large scale preparation of graphene.[34] The individual sheets isolated from this exfoliation process are not pure and show significant variation in their properties. Chemical vapor deposition (CVD),[35] thermal decomposition of SiC,[36] and preparation of graphite intercalation

compounds[37] are also common techniques employed in the synthesis of graphene.[30,38] Each method has advantages and disadvantages, with large scale preparations resulting in less than perfect sp^2 delocalisation in the graphene sheets due to defects, while preparation techniques where pure graphene can be achieved are usually difficult or impossible to scale up to industrial demands.[39] Recently the unzipping of carbon nanotubes with $KMnO_4$ and H_2SO_4 to form graphene sheets has also been reported.[40]

Another possibility for the synthesis of pristine graphene sheets is organic synthesis.[30,32d,41] This bottom up approach using controlled, rational, organic synthesis allows for total control over the size and shape of the graphene sheet formed. All-benzenoid polycyclic aromatic hydrocarbons (PAH's) can be considered as subunits of graphene, and are sometimes referred to as 'nano-gaphene',[39a] owing to their small size in comparison to the graphene sheets produced by other methods. Polycyclic aromatic hydrocarbons typically range in size from 1 – 3 nm, and they are one of the most investigated class of compounds since their discovery as a component of coal tar nearly a century ago.[42]

1.2 Polycyclic aromatic hydrocarbons

1.2.1 Types of polycyclic aromatic hydrocarbons

The polycyclic aromatic hydrocarbons are a large class of molecules, of which the all-benzenoid PAH's are only a small group.[43] Graphene can be considered an infinite member of this all-benzenoid class, while triphenylene, **1.1**, is the smallest. The all-benzenoid PAH's differentiate themselves from other PAH's due to the ability of the π-electrons to be assigned into to only Clar aromatic sextets. Triphenylene, **1.1**, can then be represented as three individual benzene rings joined by carbon-carbon single bonds, as shown in figure 1.1. The four fused isomers of **1.1** are also shown in figure 1.1, and in each case **1.2** – **1.5** cannot be drawn using only Clar sextets. Compounds **1.2**, **1.3** and **1.4** possess two Clar sextets, while **1.5** has only one Clar sextet.

The distribution of the π-electrons of triphenylene into only Clar sextets results in higher stability and lower reactivity compared to other fused isomers where only some of the π electrons can be assigned to a Clar sextet. This stability and low reactivity is the case for all all-benzoid hydrocarbons when compared to their non-benzenoid isomers and as a result the all-benzenoid PAH's have played an important role in the development of the theory of PAH's and aromaticity.[44]

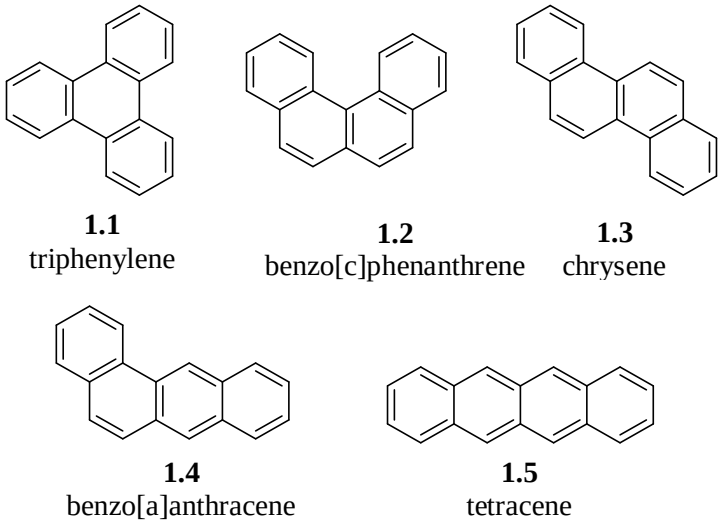

1.1 triphenylene

1.2 benzo[c]phenanthrene

1.3 chrysene

1.4 benzo[a]anthracene

1.5 tetracene

Figure 1.1. Triphenylene, **1.1**, the smallest member of the all benzenoid class and its four isomers.

The all-benzenoid PAH's, as well as other planar disc-like molecules, have become the subject of intensive interest as materials for organic electronics due to their ability to form highly ordered columnar liquid crystalline phases when substituted with peripheral alkyl groups,[45] shown in figure 1.2. Charge transport can along the column, while the alkyl groups help to prevent intercolumnar hopping of the charge carriers, increasing their lifetime and allowing the alkyl chains to act as insulators between the columns.[45b,46] Hexaalkylthio substituted triphenylene was one of the first discotic compounds to be studied using TOF measurements.[47] The charge carrier mobility of the liquid crystal was dependent on both the supramolecular order[48] and the thermotropic state of the molecules.

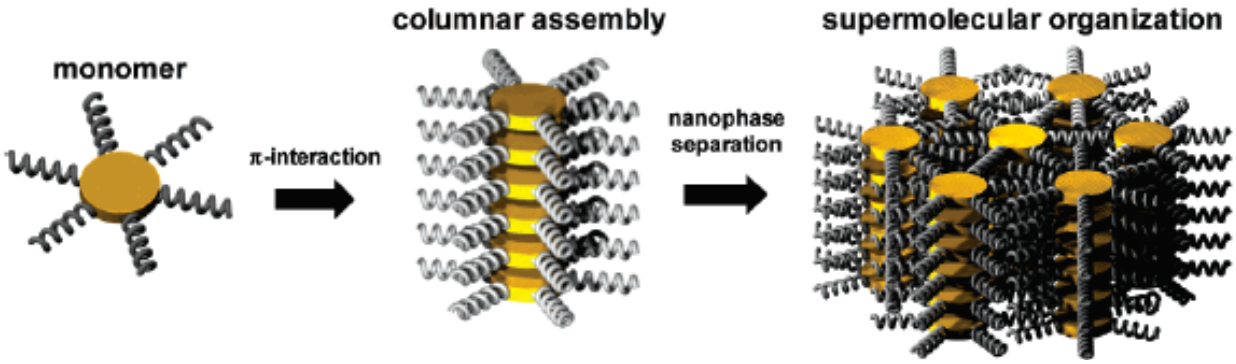

Figure 1.2 Schematic illustration of the columnar ordering and overall supramolecular organisation of discotic liquid crystalline materials.[49]

The charge carrier mobility is dependent not only on the molecular order and thermotropic state but also the size and π overlap of the discotic aromatic core.[50] Many discotic aromatic cores have been

investigated for their ability to form discotic liquid crystalline compounds and some of the most successful are shown in figure 1.3. Porphyrin, **1.6**,[51] phthalocyanine, **1.7**,[51d,52] perylene diimide, **1.8**,[53] and hexa-*peri*-hexabenzocoronene (HBC), **1.9**,[49,54] all display charge carrier mobilities greater than that of triphenylene, **1.1**.

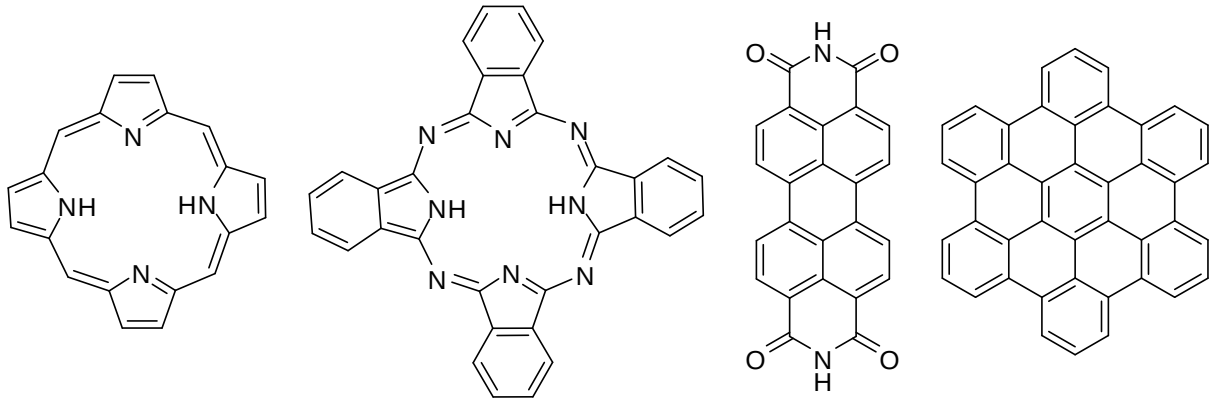

1.6 **1.7** **1.8** **1.9**

Figure 1.3. Aromatic cores for the formation of discotic liquid crystalline compounds.

All-benzenoid PAH's with larger core sizes than triphenylene have been the subject of intensive investigation, not only as potential materials for organic electronics, but for fundamental study on the mechanism of charge transport between molecules in columnar liquid crystal phases. HBC, **1.9**, is a D_{6h} symmetric all-benzenoid PAH, sometimes referred to as 'super-benzene' due to its shape and extensive π-delocalised system, and it has been at the forefront of investigations into the formation of discotic liquid crystalline compounds as charge carrier transporting materials for organic electronic devices.[49,54a,b]

1.2.2 Routes towards the synthesis of all benzenoid polycyclic aromatic hydrocarbons

HBC was first synthesised in 1958 by Clar *et al.*,[55] and subsequently both Halleaux *et al*.[56] and Schmidt *et al*.[57] also reported syntheses of HBC. Clar's synthetic strategy, shown in scheme 1.1, employed the dimerisation of 2:3–7:8-dibenzo-*peri*-naphthene, **1.10**, to form tetrabenzoperopyrene, **1.11**. Tetrabenzoperopyrene was then heated to 400˚ and HBC was formed in low yield after recrystallisation from boiling pyrene. Unfortunately all of these methods use very harsh conditions and produced the desired HBC molecule in low yields. The difficult preparation of HBC hindered further investigation into its properties and application until the development of a milder, general route to HBC and derivatives by Müllen and co-workers in 1995.[58]

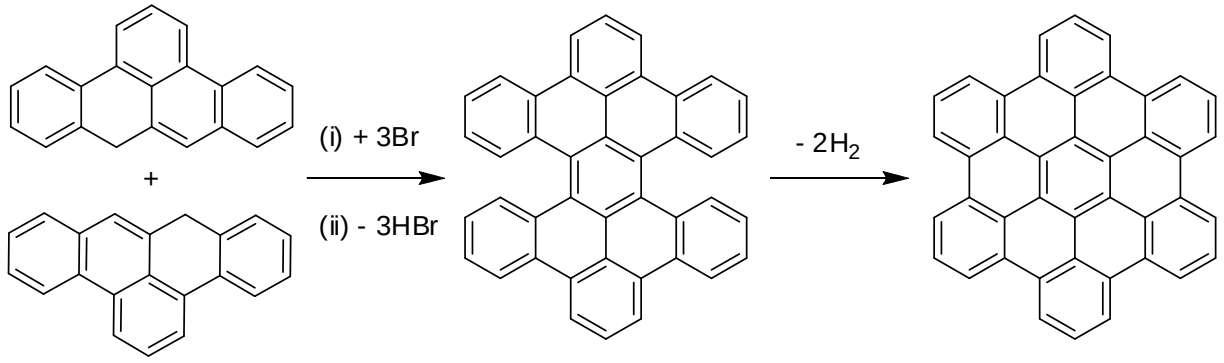

1.10 **1.11** **1.9**

Scheme 1.1. The first reported synthesis of HBC, **1.9**, by Clar *et al.* in 1958.[55]

The route to HBC taken by Müllen and co-workers utilises oxidative cyclodehydrogenation between suitable branched oligophenylene precursors,[59] as shown in scheme 1.2a. Initially, cobalt catalysed cyclotrimerisation of diphenylacetylene derivatives, **1.12**, was used to synthesise the required hexaphenylbenzene derivatives, **1.13**, for oxidative cyclodehydrogenation into HBC.[58,60] Another method to hexaphenylbenzene derivatives, shown in scheme 1.2b, is now commonly employed, the Diels-Alder reaction between tetraphenylcyclopentadienone derivatives, **1.14**, and diphenylacteylene derivatives.[61] This route has the advantage of allowing different symmetry in the substitution pattern around the HBC core.

Organic synthesis gives intimate control of the size and shape of the HBC derivative. The size and shape of the HBC core has a significant effect on the optoelectronic properties of the resulting compound.[45f,62] The greater the size of the aromatic core the greater the π-delocalisation of electrons and subsequently a bathochromic shift is seen in the UV/vis spectra. A colour change is also observed as the size of the aromatic core increases, HBC is a yellow powder, while the largest graphite fragment (with 222 carbon atoms) isolated using rational organic synthesis is black.[63] A range of compounds closely related to the HBC core, but possessing different symmetries in their aromatic core, and not fully benzenoid, were synthesised and studied through UV/vis and photoluminescence spectroscopy.[62c] A reduction in the symmetry of the aromatic core leads to more symmetry forbidden transitions that are now allowed, and subsequently broadening of the absorption peaks in the UV/vis spectrum is observed. The molecular absorption coefficients of all compounds were within the same range and differences in the peripheral alkyl substitution of the aromatic core does not affect the electronic spectra.

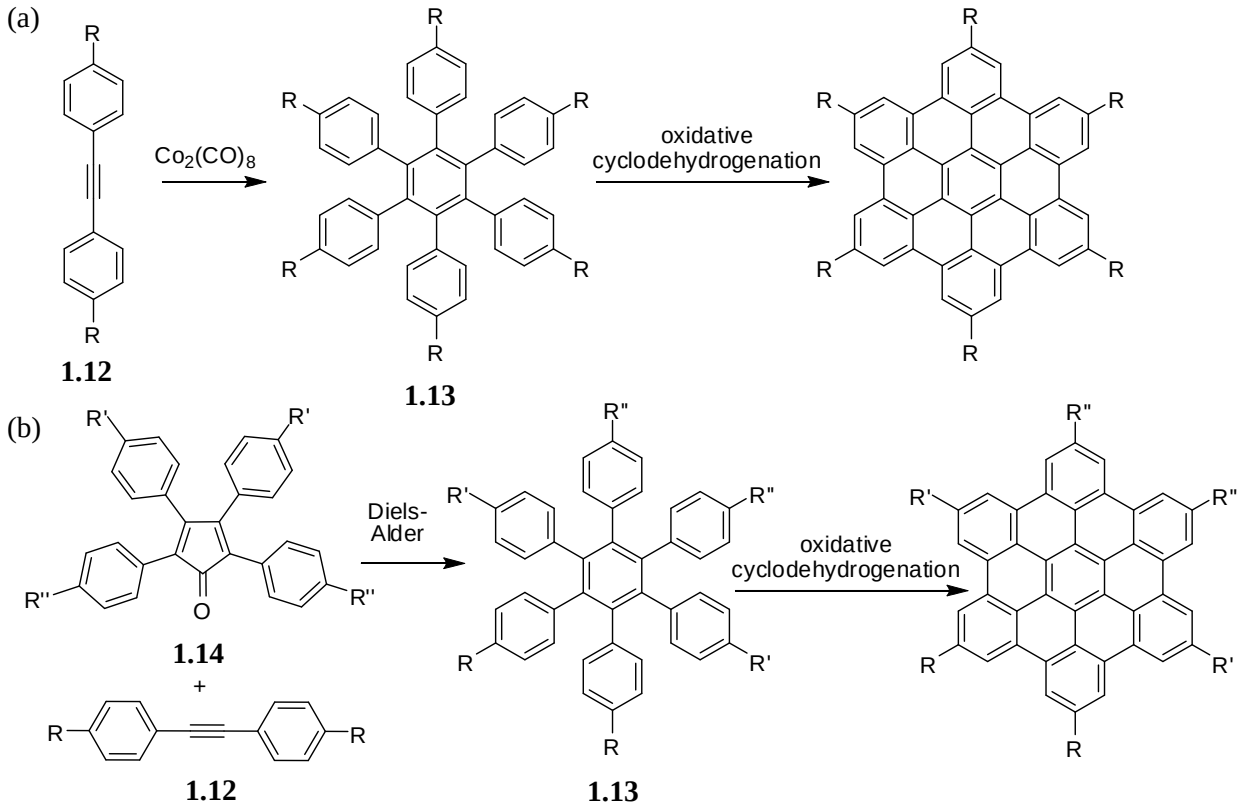

Scheme 1.2. General routes to substituted HBC's, (a) cobalt catalysed trimerisation of diphenylacetylenes followed by oxidative cyclodehydrogenation to give 6 fold symmetric HBC's,[58,59,60] (b) Diels-Alder reaction between diphenylacteylenes and tetraphenylcyclopentadienones to give HBC's of lower symmetry.[61]

Fully benzenoid aromatic cores with lower symmetries than that of HBC have also been synthesised and studied, through simple modification of the diphenylacetylene precursor for the Diels-Alder reaction with tetraphenylcyclopentadienones.[61b] These oligiophenylene derivatives are then cyclodehydrogenated to form the HBC derivative. Again, the optical properties are different to HBC, with similar trends seen in the UV/vis spectra as those discussed above.

HBC and larger derivatives are generally insoluble in common organic solvents; this complicates the isolation and purification of these compounds, and hinders their characterisation by general methods. MALDI – TOF mass spectroscopy is commonly used to characterize large HBC derivatives insoluble in common organic solvents.[64] The addition of peripheral solubilising groups around the aromatic core can overcome this solubility problem in many cases. The length and branching of the solubilising alkyl groups can be used to control the properties of the resultant discotic liquid crystals.[49]

1.2.3 Supramolecular organisation of all benzenoid polycyclic aromatic hydrocarbons

Rational organic synthesis also allows for direct control of the functional groups at the periphery and their substitution pattern around the aromatic core. This allows for the supramolecular assembly and electronic properties of the molecules to be controlled.[65] Simple six fold alkylphenyl substitution on to the HBC core induces a helical columnar packing arrangement,[66] while the degree of branching in peripheral alkyl chains can control the aggregation of the molecules.[67] The pitch of the helical arrangement can be controlled by exploiting hydrophilic/hydrophobic interactions, due to the varying substitution pattern of the hydrophilic and hydrophobic groups around the aromatic core.[65b,68] Hydrogen bonding functionality has been introduced with amido or urea functionality close to the aromatic core to promote closer, more ordered interactions between molecules within a self assembled column.[69] Hydrogen bonding within columns, by addition of a carboxylic acid group at the end of a long alkyl spacer, can change the overall packing arrangement of the columnar assembly.[70] Furthermore, water soluble HBC assemblies with peripheral negatively charged side chains were recently synthesised, the columnar assembly can then recruit biological molecules through electrostatic interactions with the negatively charged side chains.[71]

HBC molecules that do not self assemble into columnar packing arrangements and instead assemble into discrete tubular nanostructures up to 10 μm long, were synthesised in 2004.[72] The gemini shaped HBC molecule was peripherally substituted with dodecyl and triethylene glycol chains. The pitch of the tubular nanostructure could be controlled by the solvent present during the self assembly process.[72-73] By appending allylic functionalities to the termini of the triethylene glycol chains the HBC molecules spontaneously form tubular structures when acyclic diene metathesis is performed with Grubbs catalyst in DCM. Without the addition of Grubbs catalyst the tubular structures do not form in DCM.[74] The solubility of the tubular structures can also be controlled by photochemistry. Coumarin units appended on the end of the triethylene glycol chains form dimers when irradiated at $\lambda > 300$ nm, rendering the tubular structure insoluble, this reaction can also be reversed by irradiation at lower wavelengths.[75] A range of HBC molecules with this general gemini structure have now been synthesised to provide greater understanding of the structural requirement for the self assembly process.[75]

The peripheral functional groups appended to the HBC core can also be charge transport materials in their own right, creating a columnar supramolecular assembly where a coaxial double cable is formed for efficient hole transport.[76] Dipole interactions can also be exploited to increase the aggregation between molecules in a column,[77] and also to determine the overall nature of the packing arrangement.[78]

Peripheral halide functionalisation of HBC allows for the implementation of transitional metal coupling reactions. Insoluble six fold symmetric compound **1.15**, shown in figure 1.4, is used as key building block to functional HBC derivatives through Pd-catalysed coupling reactions. When reacted with solubilising acetylenes in a Sonogashira coupling reaction[79] a series of soluble HBC derivatives were obtained. A series of mono-(**1.16a)**, di-(**1.16b – d)**, and tri-bromo (**1.16e)** substituted HBC molecules, shown in figure 1.4, have also been prepared for further functionalisation through transition metal coupling.[61c,80]

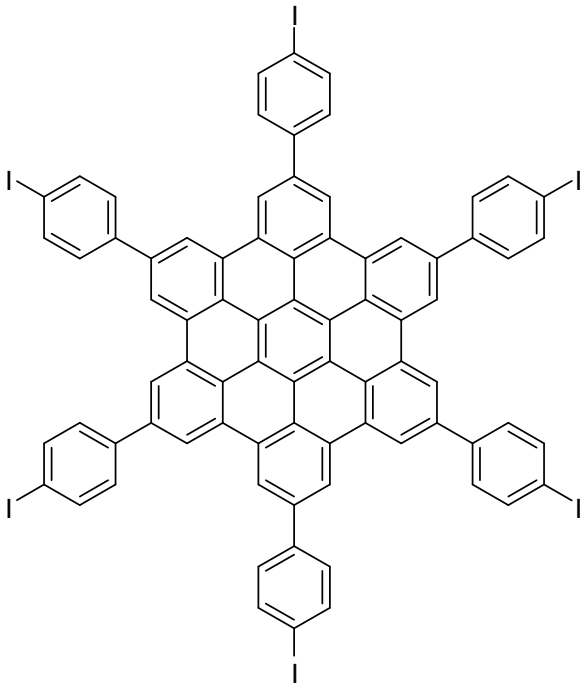

1.15

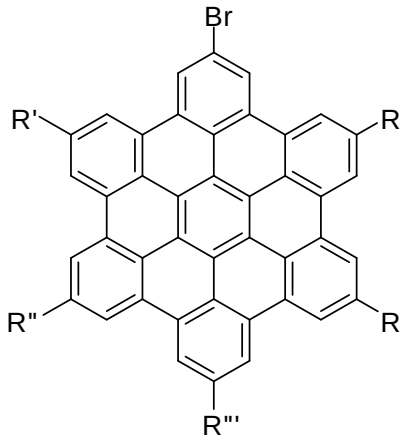

1.16a R, R', R'', R''' = $C_{12}H_{25}$
1.16b R' = Br, R, R'', R''' = $C_{12}H_{25}$
1.16c R'' = Br, R, R', R''' = $C_{12}H_{25}$
1.16d R''' = Br, R, R', R'' = $C_{12}H_{25}$
1.16e R', R'' = Br, R, R''' = $C_{12}H_{25}$

Figure 1.4. HBC precursor molecules **1.15** and **1.16** that undergo transition metal coupling reactions to form functional HBC derivatives.[61c,79,80]

A closely related compound to HBC is hexa-*cata*-hexabenzocoronene, **1.17**, shown in figure 1.5, which was prepared in 2005 by Nuckolls and co-workers.[81] The synthesis was based around the high yielding final step, in which bis olefins, **1.18**, undergo stilbene type photocyclisation to form **1.17** in 83% yield. Unlike HBC, **1.17** is not planar. Steric congestion from the peripheral carbon atoms twists the outer phenyl rings out of plane by ~ 20˚. The non-planar cores of **1.17** do not prevent the aggregation of **1.17** when the periphery is substituted by four alkoxy chains, and **1.17** forms columnar liquid crystalline phases and displays high charge carrier mobility. When eight alkoxy chains are substituted around the periphery of **1.17**, the crystalline fibers formed can be transferred into field effect transistors with an elastomer stamp.[82]

The curved nature of **1.17** allows for different molecular interactions than the flat HBC molecules described above. Interactions with fullerene molecules are possible due to the nature of the curvature in **1.17**. This fullerene interaction allows for the synthesis of efficient photovoltaic cells, where **1.17** acts as the donor molecule and fullerene as the acceptor.[83] An improved methodology towards the synthesis of the bis olefins, **1.18**, was reported in 2009,[84] enabling a range of substitution patterns and oxidative cyclodehydrogenation can also be employed on the bis olefin precursors, **1.18**, as some functional groups are not tolerant to the photocyclisation conditions.[84]

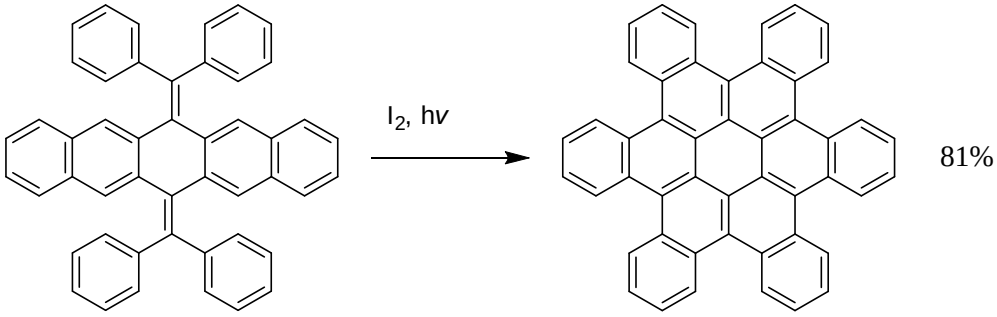

1.18 **1.17**

Figure 1.5. Synthesis of hexa-*cata*-hexabenzocoronene, **1.17**, in high yield by photocyclisation of precursor **1.18**.[81]

1.2.4 Applications of polycyclic aromatic hydrocarbons in devices

For applications in devices precise control over the supramolecular order during processing is essential. If the supramolecular order cannot be controlled the charge carrying ability of the material, and the performance of the device, suffers. Discotic liquid crystals posses many desirable properties for implementation in devices as they spontaneously self assemble into columns allowing charge to be carried through the column, they are soluble in common organic solvents, and they are dynamic materials allowing for self healing of defects present in the columnar liquid crystal.[45c,49] Columnar liquid crystals can align in one of two directions on the electrode surface in the device. For applications in field effect transistors an edge-on organisation is desired, whilst a face on arrangement is desired for photovoltaic cells and light emitting diodes. Control of the supramolecular order and alignment is determined during the processing of these materials into thin films on the surface electrode of the device. For HBC liquid crystals a variety of techniques have been used to control both the alignment and increase the supramolecular order of the resultant thin film.[45c] Zone casting has been used to align molecules of HBC with sixfold dodecyl alkyl substitution edge on to the surface electrode, and the resulting field effect transistor displayed high mobility of charge carriers.[85] Magnetic alignment of a sixfold phenyldodecyl alkyl substituted HBC increased the charge carrier mobility even further.[86] Lagmuir – Blodgett techniques

have been used to form thin films of amphiphilic HBC derivatives. Two distinct phases resulted from this processing technique, with distinct differences in their electronic properties.[87]

For photovoltaic devices both a donor and an acceptor molecule are required. HBC (donor) and perylene tetracarboxy diimide (PDI) (acceptor) have been blended together by simple solution processing for application in devices. Simple spin coating of a HBC/PDI mix from solution was first employed in 2001, and the resulting field effect transistor displayed a high external quantum efficiency of 34% at 490 nm, corresponding to an overall power conversion efficiency of 2%.[88] The high efficiency is attributed to the charge transfer between the donor and acceptor molecules through the conjugated π systems. The length and branching of the alkyl chains of the donor HBC molecules influences the amount of light that can be absorbed by these molecules, decreasing the device efficiency.[89] Solution processing of blends of donor and acceptor molecules lacks any control over the overall ordering of the material, allowing no way to decrease the amount of defects that lead to low device performance.

The donor and acceptor molecules can also be covalently linked together to provide defined pathways for the charge transport of electrons and holes. Initially, one PDI molecule was covalently attached to an HBC core through an acetylene linker.[90] The donor/acceptor dyad formed self assembled into coaxial columns, allowing for possible separate pathways for electron and hole transport. Initial measurements indicated that the material exhibited ambipolar transport.[90-91] Further covalently linked HBC/PDI molecules have also appeared in the literature,[92] most recently a six fold covalent attachment of PDI molecules around an HBC molecule has been reported, as part of a series of HBC/PDI dyads. These dyad molecules were synthesised in order to determine the interactions between the HBC and PDI molecules and how this affects their overall supramolecular organisation.[93] The sixfold substituted HBC/PDI compounds assembled in a coaxial column fashion for dual hole and electron transport, but did not display photoinduced electron transfer between the HBC and PDI, essential for the operation of a solar cell. The lack of electron transfer was ascribed to the distance of greater than 1 mm between the donor and acceptor parts of the molecule. The other HBC/PDI molecules in the series did not assemble into coaxial columns and instead formed a column where the HBC and PDI molecules are alternating. This direct overlap of donor and acceptor molecules allowed for photoinduced electron transfer to occur.[93]

The use of HBC and other discotic aromatic cores that form columnar liquid crystals for applications in organic electronic devices still needs to overcome some hurdles. The charge carrier mobility of the processed thin films does not yet match those of the parent aromatic core, possibly due to the inability to prevent defects in the long range order during processing. Synthetic and purification hurdles prevent large

amounts of these materials from being synthesised and fabrication of the devices needs to be suitable for industry procedures.

1.3 Oxidative cyclodehydrogenation and the Scholl reaction

Oxidative cyclodehydrogenation of branched oligiophenylene compounds is the final and key reaction step for the synthesis of many polycyclic aromatic compounds.[54b] The Scholl reaction has been defined as the intramolecular cyclodehydrogenation of aromatic nuclei resulting in the formation of a condensed ring system, under the influence of aluminium chloride. A broader definition of the Scholl reaction in recent times is "the elimination of two aryl bonded hydrogens accompanied by the formation of an aryl-aryl bond under the influence of Friedel – Crafts catalysts".[94] It is named as such for the pioneering work of Scholl, who first reported in 1910 that 1,1'-binaphthyl, **1.19**, could be condensed to form perylene, **1.20**, in an aluminium chloride melt,[95] shown in scheme 1.3. The harsh conditions employed and the sometimes complex product mixtures prevented the widespread application of the Scholl reaction in organic synthesis, until milder conditions were developed by Kovacic in the 1960's for the polymerisation of benzene,[96] an intermolecular Scholl-type reaction. These milder conditions use aluminium chloride, with copper chloride was employed as the oxidant, rather than air. The final polyphenylbenzene products depended upon the catalyst:oxidant ratio, the amount of water present and the length of the reaction. The presence of a trace amount of water, or the presence of hydrogen chloride is necessary for the reaction to proceed.[97]

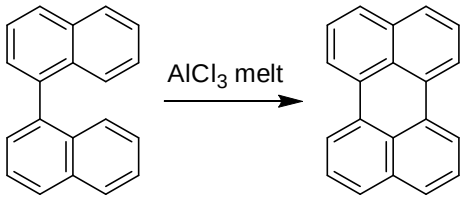

1.19 **1.20**

Scheme 1.3. Oxidative cyclodehydrogenation of 1,1'-binaphthyl, **1.19**, to form perylene, **1.20**, an early example of the Scholl reaction.[95]

The development of milder conditions for the Scholl reaction allowed the study of this reaction to extend to more complicated systems, where more than one carbon-carbon bond is formed. The room temperature reaction of diphenyltriphenylene, **1.21**, with $AlCl_3$, $CuCl_2$ in CS_2 for 2 days, formed the fully cyclodehydrogenated product tribenzo[*b*, *n*, *pqr*]perylene, **1.22**, in 77% yield,[98] shown in scheme 1.4. Two carbon-carbon bonds have been formed during the course of this reaction from unsubstituted and unactivated aryl rings. Not long after the report of the formation of **1.22** from **1.21**, the same group, lead

by Müllen, reported the formation six new carbon-carbon bonds to form HBC from hexaphenylbenzene.[58] Since this time an increasing number of carbon-carbon bonds have been formed through oxidative cyclodehydrogenation of suitable oligophenylene derivatives using $AlCl_3$ with either $CuCl_2$ or $Cu(OTf)_2$ as an oxidant.[99] The use of a milder Lewis acid, iron (III) chloride, rendered the presence of additional oxidants unnecessary,[60d,61a] and iron (III) chloride is well known to catalyse oxidative carbon-carbon bond forming reactions.[100]

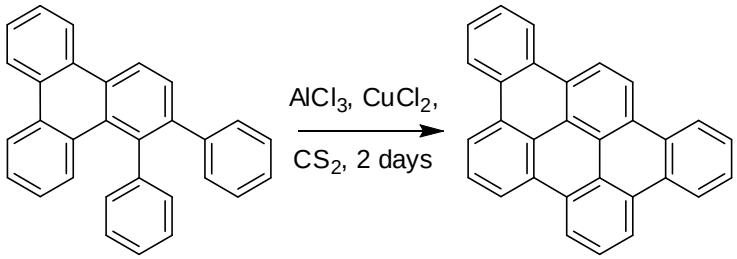

77%

1.21 **1.22**

Scheme 1.4. The formation of two carbon-carbon bonds using oxidative cyclodehydrogenation under mild conditions.[98]

1.3.1 Reagents for oxidative cyclodehydrogenation

Since these initial reports Müllen and coworkers have pioneered the development of $AlCl_3$/oxidant and $FeCl_3$ as reagents for the planarisation of suitable oligophenylene derivatives to all planar all benzenoid PAH's.[49] A variety of other reagents and conditions have also been employed to carry out various other oxidative cyclodehydrogenation reactions. The use of heavy metal Lewis acidic catalysts has been popular, with $MoCl_5$, $Tl(CF_3CO_2)_3$ and CoF_3 employed as reagents for oxidative cyclodehydrogenation. $MoCl_5$ can polymerise benzene under Kovacic type conditions,[101] and it has also been used alongside other Lewis acid catalysts such as $TiCl_4$, $SnCl_4$ and $SiCl_4$ for intramolecular aryl coupling reactions.[102] Oxidative coupling using $Tl(CF_3CO_2)$ has also been reported, although the presence of CF_3CO_2H is usually required.[103] Oxidative dimerisation of a novel fluoranthene based PAH has been achieved using $MoCl_5$[104]. Various vanadium oxides and chlorides have also been employed.[101,103c,105] The reaction of $Pb(OAc)_4$ with $BF_3.OEt_2$ has been investigation for the intermolecular coupling of benzene molecules.[106] Potassium melts have recently been used for the synthesis of perylene from 1,1'-binapthyl, the same reaction reported by Scholl in 1910. Pressure and heat are also required, but the reaction proceeds in greater than 95% yield.[107]

Heavy metal Lewis acidic catalysts are not required to carry out oxidative cyclodehydrogenation reactions, and a variety of organic acidic catalysts and oxidants have been used. Hypervalent iodine, $(CF_3COO)_2I^{III}C_6H_5$, with $BF_3.Et_2O$ in dichloromethane cyclises various biaryl compounds linked by a heteratom resulting in the formation of various heterocycles.[108] DDQ/CH_3SO_3H has recently been employed by Zhai *et al*. for the six fold oxidative cyclodehydrogenation of hexaphenylbenzene, forming HBC.[109] This reagent system has proven useful for the successful oxidative cyclodehydrogenation of electron poor hexaphenylbenzene precursors, the use of $FeCl_3$ was not successful in this case.[110] The DDQ/CH_3SO_3H reagent system has also been employed for the final oxidative cyclodehydrogenation of precursors for the formation of PAH's with low numbers of Clar sextets.[111]

Photocyclisation conditions can also be employed to carry out oxidative cyclodehydrogenation. The photocyclisation of stillbene-type precursors to form more complex aromatic systems has been well studied.[84,112,113] Usually I_2 and propylene oxide are used as oxidants,[114] although early reports of these photocyclisation reactions used air as the oxidant.[115] The formation of hexa-*cata*-hexabenzocoronene, **1.17**, employed photocyclisation conditions for the final oxidative cyclodehydrogenation step,[81] see figure 1.5. Photocyclisation and $FeCl_3$ have been used in a two step procedure for the complete cyclodehydrogenation of a tetrabenzocoronene.[116]

1.3.2 Unexpected products from cyclodehydrogenation reactions

Despite the attractiveness of the Scholl reaction in organic chemistry, allowing the formation of multiple carbon-carbon bonds in a single step from unactivated aryl rings, up to 54 new carbon-carbon bonds has been reported,[63] it does suffer from some inherent drawbacks. The conditions employed for oxidative cyclodehydrogenation often result in formation of chlorinated side products,[42,117] and some functional groups are intolerant to the reaction conditions employed.[60c] If rotational isomers exist the regioselectivity of the Scholl reaction is unpredictable, and in a few cases partially cyclodehydrogenated and rearranged compounds have been observed.

Recently, Müllen and coworkers synthesised a tetra dodecyl substituted quinquephenyl, **1.23**,[118] that possesses rotational conformers to determine the regioselectivity of the Scholl reaction. Surprisingly, only one of the two possible products was formed from oxidative cyclodehydrogenation, a tribenzoperylene. The tribenzoperylene formed arises from the cyclodehydrogenation of the slightly more sterically hindered isomer. Another group subsequently synthesised a more sterically encumbered compound, tetra *tert*butyl substituted quinquephenyl, **1.24**,[119] and subjected this compound to oxidative cyclodehydrogenation, shown in scheme 1.5. It was expected that the *tert*butyl groups would provide

enough steric hinderance to prefer the formation the tetrabenzanthracene, **1.25**, arising from **1.24** in the trans orientation. Instead dibenzopicene, **1.26**, was preferentially formed in 80% yield, arising from **1.24** in the more sterically hindered cis orientation, and only 8% of **1.25** was isolated. Other attempts to use blocking groups to direct the regioselectivity of this reaction have also been reported.[120]

As well as rotational isomerisation, unexpected products can arise from the 1,2 phenyl shift of oligiophenylene precursors during cyclodehydroegnation.[117a,121] The rearrangement of these precursors to form unexpected cyclodehydrogenated products is difficult to control and prevents the rational organic synthesis of some desired molecular architectures, as well as the formation of complex reaction mixtures that are difficult to purify and separate when the rearrangement products are not degenerate.[121b]

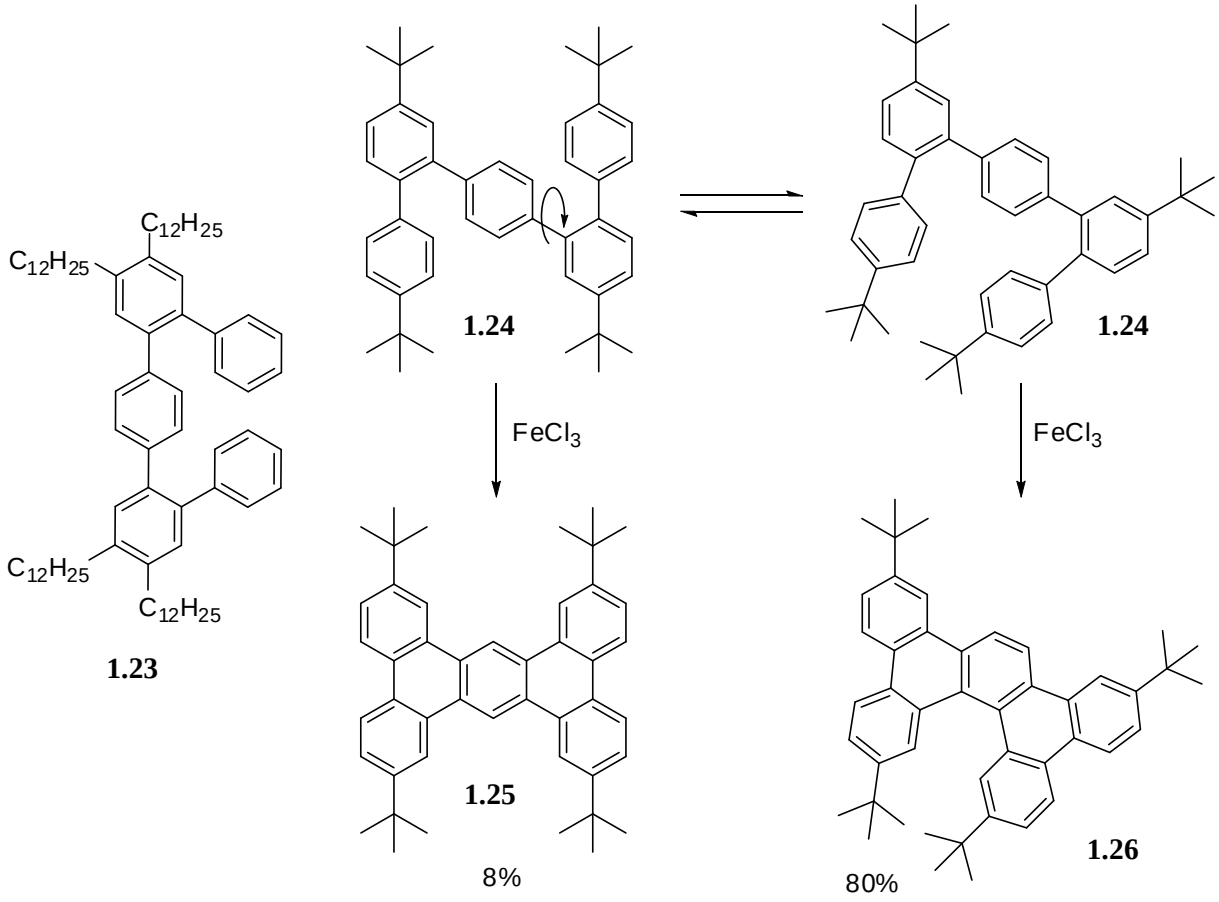

Scheme 1.5. Surprising regioselectivity of the Scholl reaction, the more sterically hindered oligiophenylene precursor is preferred for the oxidative cyclodehydrogenation.[118,119]

The addition of peripheral heteroatom substitutents on HBC and derivatives is desirable, as this allows another method to tune the electronic nature of the aromatic core. Six fold alkoxy substituted hexaphenylbenzene, **1.27**, was employed as a precursor to six fold alkoxy substituted HBC, **1.28**. Initial

attempts to cyclodehydrogenate **1.27** were met with the apparent formation of an extended quinonoid system, **1.29**.[60c] This was not entirely unsurprising as alkoxy groups are well known to undergo both ether cleavage and oxidations to quinonoid aromatic structures.[60c,122] A much later paper by Wadumethrige and Rathore,[60e] disproved the assignment of the product of the cyclodehydrogenation of **1.27**, and the formation of an bis spirocyclic dienone structure, **1.30** was assigned as the correct product, determined by X-ray crystallography (shown in scheme 1.6). This was not the first observation of the formation of a spirocyclic product from the oxidative cyclodehydrogenation of alkoxy substituted hexaphenylbenzene precursors.[121a,123]

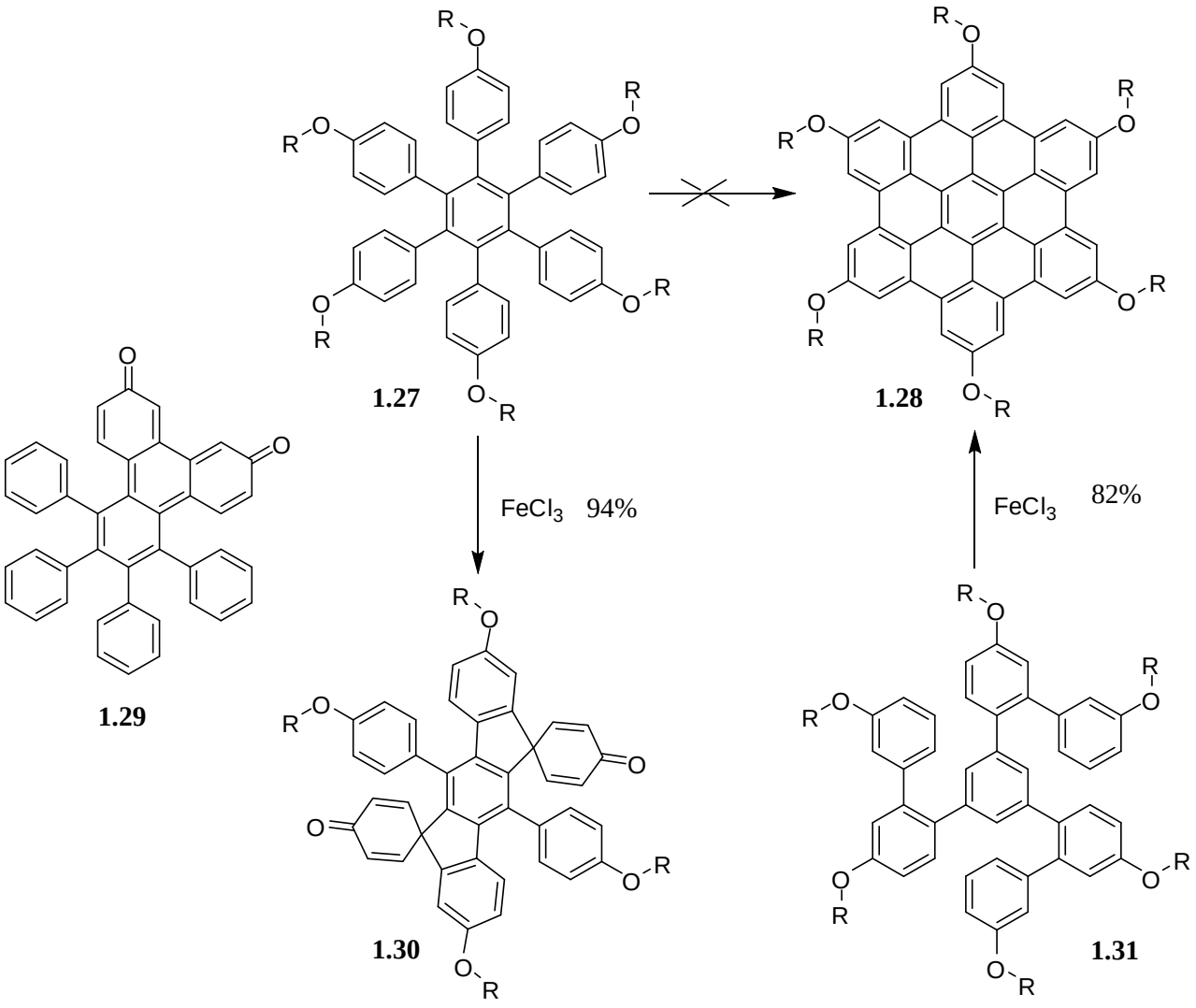

Scheme 1.6. Formation of an bis spirocyclic dienone structure, **1.30**, from oxidative cyclodehydrogenation of a six fold alkoxy substituted hexaphenylbenzene, **1.27**, and subsequent formation of sixfold alkoxy substituted HBC, **1.28**, using a 1,3,5-trisbiphenylbenzene, **1.31**.[60c,e]

The formation of a hexa alkoxy substituted HBC was first reported in 2005, by Zhang *et al.*[124] The synthesis was achieved by employing a hexaphenylbenzene precursor where electron withdrawing fluorine groups were substituted ortho to the alkoxy groups, and the subsequent cyclodehydrogenation proceeded in low yields. In 2008 the synthesis of **1.28** was finally achieved,[60e] using an alternative precursor to hexaphenylbenzenes. A 1,3,5-trisbiphenylbenzene precursor, **1.31**, was subjected to oxidative cyclodehydrogenation and **1.28** was formed in nearly quantitative yield.

The synthesis of alkoxy substituted HBC derivatives by the cyclodehydrogenation of hexaphenylbenzene precursors is often met with difficulty and spirocyclic products are often formed preferentially. The synthesis of a para disubstituted alkoxy hexaphenylbenzene and subsequent cyclodehydrogenation[121a] forms a bis spirocyclic dienone much like **1.30**, as well as the desired HBC derivative. Mechanistic considerations lead to the conclusion that the ortho, para directing nature of the methoxy groups promote the formation of the spirocyclic product, the mechanism of the Scholl reaction is discussed further in section 1.3.3.[121a,123b]

The isolation of some partially cyclised products from the Scholl reaction gives some insight into the possible mechanism of this reaction, and suggests that the formation of each carbon-carbon bond proceeds in a stepwise rather than concerted manner.[125] The first partially cyclised intermediate, **1.32**, was isolated from the Scholl reaction of hexaphenylbenzene in 2000,[60a] and is shown in figure 1.6. It was identified by ^{1}H-NMR spectroscopy and assigned as the product arising from the formation of four new carbon-carbon bonds, with one phenyl ring untouched by cyclodehydrogenation. The presence of other partially cyclodehydrogenated compounds were also identified but not able to be isolated, and the

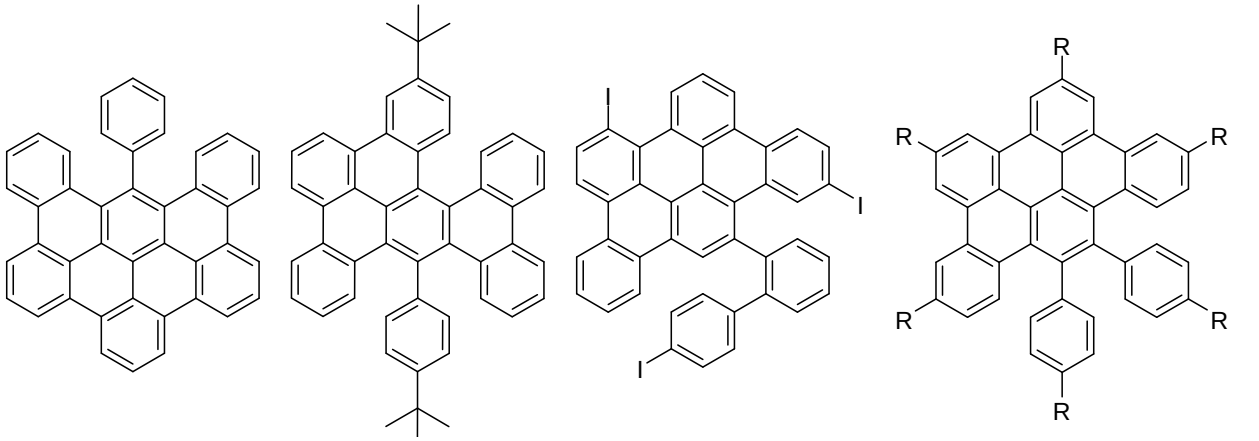

1.32 **1.33** **1.34** **1.35** R = Ph-O-$(CH_2CH_2O)_3CH_3$

Figure 1.6. Partially cyclodehydrogenated compounds formed during the oxidative cyclodehydrogenation of oligophenylene precursors.[60a,126,128]

The use of 1,3,5-trisbiphenylbenzene precursors and the related 1,4-diphenyl-2,5-biphenylbenzene precursors has also lead to the isolation of partially cyclodehydrogenated products, **1.33** and **1.34**,[126] shown in figure 1.6. Unlike the case where **1.32** could be further reacted on to form HBC, partially cyclodehydrogenated compound **1.34** could not be further cyclodehydrogenated to form the related three fold iodo substituted HBC derivative.[126a] Compound **1.34** is highly insoluble in common organic solvents, including the solvent (DCM) the cyclodehydrogenation is performed in, and the authors ascribe the inability of **1.34** to undergo any further cyclodehydrogenation to this insolubility and the steric hinderance of the free biphenyl unit.[126a] In contrast, compound **1.33**, will undergo further oxidative cyclodehydrogenation to form the remaining three carbon-carbon bonds and the corresponding para di*tert*butyl substituted HBC derivative, but only when **1.33** was isolated and resubjected to oxidative cyclodehydrogenation conditions. The presence of the two *tert*butyl groups were hypothesized to stabilise the radical cations[127] formed during oxidative cyclodehydrogenation, requiring two independent cyclodehydrogenation reactions.[126a] Crystal structures of **1.33** and a soluble derivative of **1.34** were also obtained to support the assigned structures.

Another semi-fused intermediate, **1.35**, from the Scholl reaction of hexaphenylbenzene precursors was isolated in 2009 by Lu and Moore.[128] Compound **1.35** was produced in the same reaction mixture that also contained the corresponding HBC derivative, and subjecting isolated **1.35** to further cyclodehydrogenation forms the expected HBC derivative. The time that the cyclodehydrogenation reaction was allowed to proceed impacted the yield of **1.35** that was produced. Only 20 minutes difference in reaction time (from 70 min to 90 min) allowed the transformation of **1.35**, as the main reaction product at 70 min, to the full cyclodehydrogenated HBC precursor at 90 min. This indicates that the formation of **1.35** is a kinetically favoured reaction intermediate, rather than a thermodynamically favoured reaction product.[128]

The cyclodehydrogenation reaction reaches limitations when applied to large oligophenylene systems. Full cyclodehydrogenation of large oligiophenylene systems where over 120 hydrogen atoms need to be removed to form over 60 new carbon-carbon bonds, requires a conversion of 99% for each carbon-carbon bond, leading to only a total yield of 28% for the final product.[129] Partial cyclodehydrogenation to form 3-dimensional propeller systems rather than planarised 2-dimensional graphite systems is usually observed in these cases.[129]

In some cases, the choice of Lewis acid catalyst for the Scholl reaction will control the cyclodehydrogenation product formed. In 2002, Draper *et al*. reported the formation of a nitrogen

containing HBC derivative, **1.37**,[130] and later the coordination chemistry of **1.37** was investigated.[131] Compound **1.37** was formed in 49% yield by the oxidative cyclodehydrogenation of the appropriate hexaphenylbenzene, **1.36**, using $AlCl_3$ and $CuCl_2$, shown in scheme 1.7. In 2005 the same group isolated a related half cyclised compound, **1.38**,[132] in 32% yield by the oxidative cyclodehydrogenation of the same hexaphenylbenzene precursor, **1.36**. In this case $FeCl_3$ was used for the oxidative cyclodehydrogenation reaction, and a 35% yield of **1.37** was isolated from the same reaction mixture. No evidence for the formation of **1.38** was seen when $AlCl_3/CuCl_2$ was used to form **1.37** from **1.36**.

Surprisingly, further cyclodehydrogenation of **1.38** was not successful using either $AlCl_3/CuCl_2$ or $FeCl_3$. The authors conclude that **1.38** is a thermodynamically stable product in its own right, and they speculate that the mechanism of the formation of **1.38** may be different to that of **1.37**.[132] Further examples of partially cyclodehydrogenated products have been reported with the incorporation of only one pyrimidyl ring into the hexaphenylbenzene precursor.[133] Full cyclodehydrogenation only occurs when the 2-position of the pyrimidine ring is substituted, in this case by a *tert*butyl group. When the 2-position of the pyrimidine ring is unsubstituted cyclodehydrogenation only affords two carbon-carbon bonds, ortho to the two pyrimidine nitrogen atoms. The resultant partially cyclodehydrogenated product could not be cyclodehydrogenated further, just like compound **1.38**. The reason for this difference in reactivity towards cyclodehydrogenation by substitution in the 2-position could be a result of many factors, the authors suggest that hindering coordination by a metal ion to the pyrimidyl nitrogen atoms by the *tert*butyl group increases the reactivity of the precursor towards full cyclodehydrogenation.

This difference in reactivity between $AlCl_3/CuCl_2$ and $FeCl_3$ as reagents for oxidative cyclodehydrogenation has also been exploited for an all carbon system, where only one bond was required to be formed by cyclodehydrogenation. The precursor 3-(1-naphthyl)perylene, **1.39**, was subjected to oxidative cyclodehydrogenation and depending on the system used the desired terrylene, **1.40**, was formed or its isomer possessing a five membered ring, **1.41**,[134] shown in scheme 1.8.

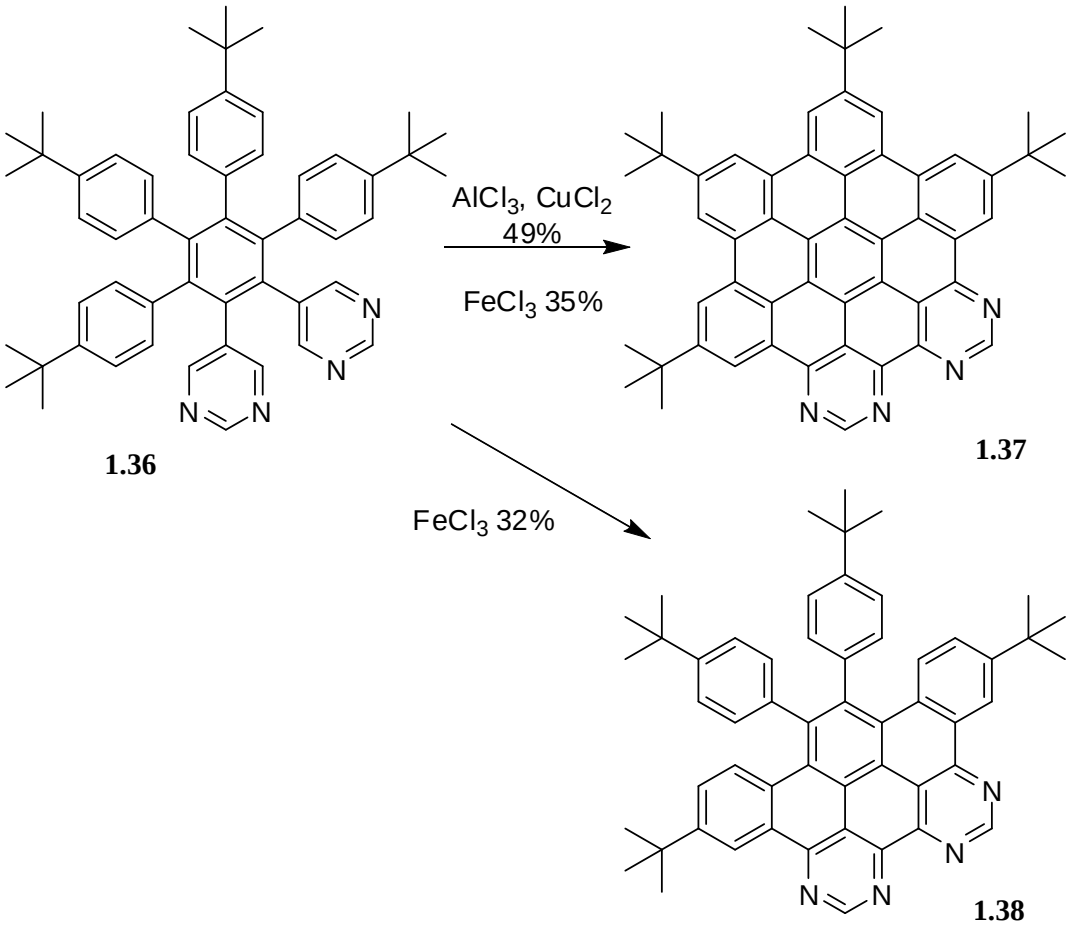

Scheme 1.7. Differences in products obtained using different oxidative cyclodehydrogenation reagents from the same precursor, **1.36**.[130,132]

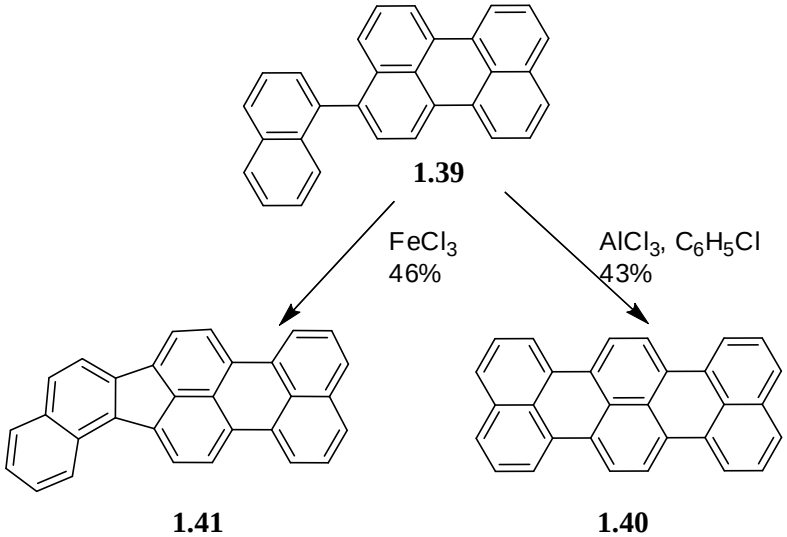

Scheme 1.8. Two different cyclodehydrogenated products, **1.40** and **1.41**, obtained using different reagents with the same precursor, **1.39**.[134]

1.3.3 Mechanism of the Scholl reaction

The isolation of partially cyclodehydrogenated products, unexpectedly rearranged products and the formation of different products when different reagents are used to carry out the Scholl reaction requires the reaction mechanism of the Scholl reaction to be studied. In recent years a series of papers has emerged in the literature from the groups of King,[125,135] Müllen[121a,127] and Rathore[136] concerning the reaction mechanism of the Scholl reaction for the cyclodehydrogenation of hexaphenylbenzene to HBC. There are currently two proposed possibilities for the carbon-carbon bond formation, radical cation and arenium cation pathways.[94]

Shown in figure 1.7 is the arenium ion mechanism (proton transfer), favoured by the group of King, and the radical cation mechanism (electron transfer), favoured by the groups of Müllen and Rathore. Both mechanisms lead to the formation of the same product, and distinguishing between acid and electron – transfer based catalysis is extremely difficult.[137]

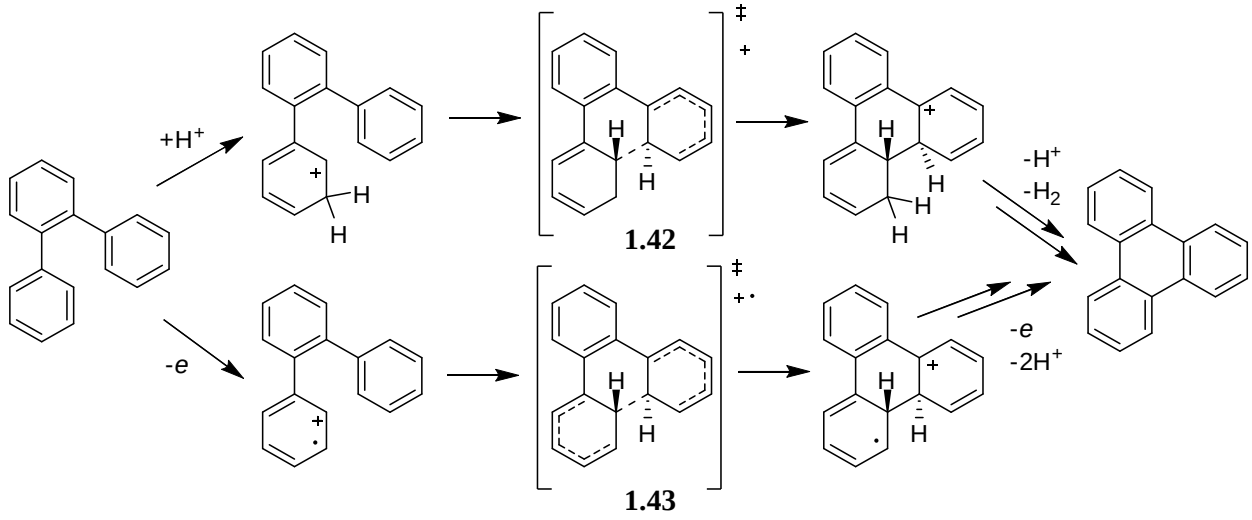

Figure 1.7. Arenium cation (top) and radial cation (bottom) mechanisms for the Scholl reaction.

King and co-workers favour the arenium ion (proton transfer) mechanism for the Scholl reaction because calculation of the carbon-carbon bond forming transition states, **1.42** and **1.43**, indicate that the transition state arising from the arenium ion pathway, **1.42**, is lower in energy.[125,135a] The requirement of water or HCl in order for the Scholl reaction to proceed[97] implicates the presence of Brønstead acids for the protonation, but Lewis acids could also be responsible. The formation of multiple carbon-carbon bonds is also predicted by King to increase the speed of the reaction as the energy of the transition state decreases in each contiguous carbon-carbon bond forming reaction. The radical cation mechanism is discounted by King as calculations demonstrate that it requires a strong oxidant for radical generation, stronger than

those employed in the Scholl reaction, and that the Scholl reaction can occur in acidic media that do not promote radical cation formation.[135a]

The groups of Müllen[127] and Rathore[136] separately conducted theoretical and experimental studies on the mechanism of the Scholl reaction, and both groups support the radical cation mechanism for the Scholl reaction. The preference for the radical cation mechanism in both groups is result of experimental observations that polynuclear hydrocarbons form radical cations when exposed to aluminium halides,[138] that dehydrogenation can occur with electrochemical oxidation,[139] and that the oxidants employed in the Scholl reaction are strong enough to effect the initial one electron oxidation. The group lead by Rathore, also determined experimentally that cyclodehydrogenation does not occur when an oligiophenylene precursor is exposed to a strong Brønstead acid or Lewis acid, but when exposed to DDQ/H^+, a well known oxidant system which oxidizes aromatic electron donors to radical cations, cyclodehydrogenation does occur.[136]

The arenium ion mechanism is discounted by these groups owing to the necessary protonation of a carbon atom meta to an electron donating phenyl group, which is strongly disfavoured. The role of the oxidant in the arenium ion mechanism is relegated to the as yet unknown oxidation steps to convert the dihydroaromatic intermediate to triphenylene. Rathore and co-workers argue that weak oxidants like I_2 and O_2 are known to perform this oxidation, yet with the arenium cation mechanism strong oxidants such as $FeCl_3$ and $CuCl_2$ are required. All groups acknowledge that the presence, however small, of the possibility of the other competing mechanism, due to the known interconversion of the carbocations and cation radicals under the conditions of the Scholl reaction.

Oxidative cyclodehydrogenation reactions are not the only way in which to form carbon-carbon bonds between aryl rings. Many transition metal catalysed routes towards the formation of carbon-carbon bonds and in particular, carbon-carbon bonds between aryl rings,[140] exist. Unfortunately, these transition metal catalysed reactions usually require some kind of functionalisation on one or both of the carbon atoms to be joined. In the synthesis of PAH's like HBC this functionalisation can be difficult to achieve. The functional groups required are not always tolerant to the reaction conditions required for the synthesis of the precursor molecules and the extra functional groups can provide too much steric hinderance to form the precursor molecules. Fluorine atoms have recently been employed to activate polycyclic aromatic precursors towards forming carbon-carbon bonds across cove regions forming curved polycyclic aromatic compounds by the formation of five-membered rings, by solid state catalysis with γ-Al_2O_3.[141] Recently,

ring closing metathesis has been employed for the synthesis of some smaller PAH's.[142] Ring closing metathesis allows for complete control over the regioselectivity of the reaction.

1.4 Curved aromatic compounds

PAH's comprised of entirely of fused benzene rings will strive to adopt a planar conformation. All of the examples of PAH's discussed above form planar graphitic sheets after oxidative cyclodehydrogenation. Only the example of hexa-*cata*-hexabenzocoronene, **1.17** discussed above is distorted from planarity, due to the steric congestion caused by some of the peripheral carbon atoms. Enforcing non planarity onto PAH's has become a topic of increasing interest of the last few decades,[143] and is usually achieved by steric congestion on the outside of the aromatic core, or by embedding non six membered rings in the aromatic core, **1.17** is an example of the former.

1.4.1 Strategies for enforcing curvature

Simple steric congestion in the form of halide substitution at every available carbon atom was used to synthesise a non-planar triphenylene, **1.44**, in 1994.[144] Compound **1.44** could not be prepared by direct chlorination of triphenylene, and a low yielding (2%) cyclotrimerisation strategy proved successful. Enough sample was obtained for recrystallisation and subsequent analysis by X-ray crystallography, which revealed an overall end to end twist of one naphthalene unit of 56.6˚. Pascal has synthesised many acene units that exhibit significant twisting due to phenyl substitution around the acene core.[145] The largest end to end twist reported to date is 144˚, observed in a pentacene unit, **1.45**, first synthesised in 2004,[146] and shown in figure 1.8. The anthracene daughter to this pentancene unit, **1.46**,[147] has a 65.7˚ twist from end to end.

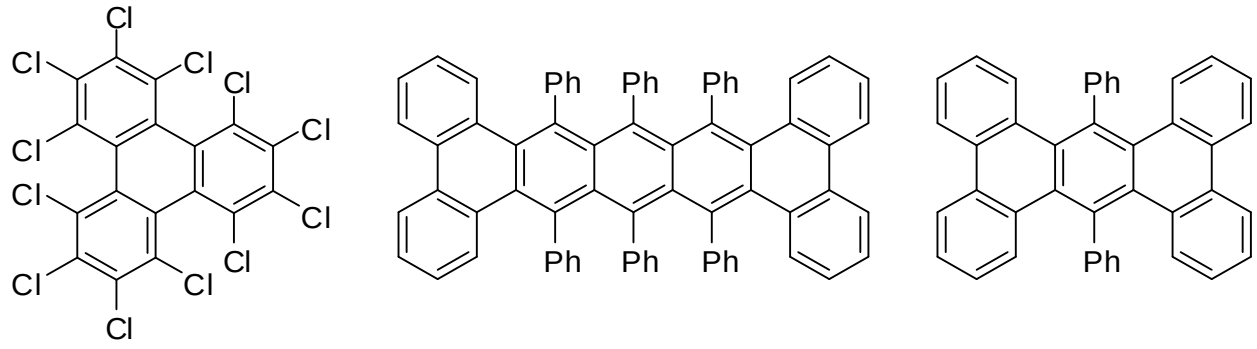

1.44 **1.45** **1.46**

Figure 1.8. Twisted polycyclic aromatic compounds synthesised by Pascal and coworkers.[144,146,147]

Very recently Nuckolls and co-workers described the synthesis and performance in solar cells and thin film transistors of three large disorted PAH's, octabenzocircumbiphenyls, **1.47**,[148] closely related to hexa-*cata*-hexabenzocoronene, **1.17**, and shown in figure 1.9. The synthesis of **1.47** was achieved in a similar manner to that of **1.17**, where in this case photocyclisation of a tris olefin precursor was the key final step. The tetra and octa dodecyloxy substituted compounds are soluble in common organic solvents. The contorted nature of **1.47** again allowed close molecular contact with a fullerene derivative and power conversion efficiencies of up to 2.9% were observed in a photovoltaic device.

The planar core of HBC can also be disorted from planarity if enough peripheral substitution is present around the aromatic core of the molecule. Compound **1.48** was synthesised in 2005[149] by the oxidative cyclodehydrogenation of the corresponding hexaphenylbenzene precursor. An X-ray crystal structure revealed that although the central benzene core was almost planar (all six carbon atoms were coplanar to within 0.014Å) the outer benzene rings were flipped up and down in an alternating manner to reduce the steric congestion imparted by the methoxy groups, and **1.48** was in a centrosymmetric conformation. X-ray crystal structures were also obtained with hexafluorobenzene and fullerene.

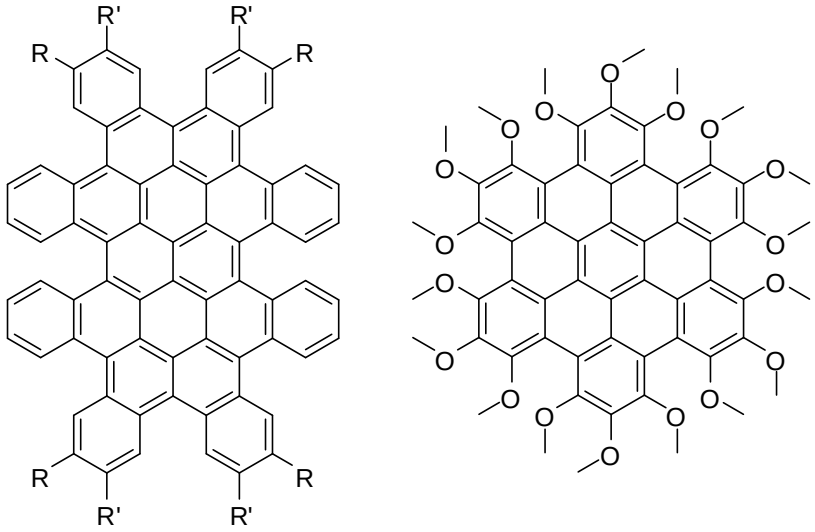

1.47 R, R' = H
R = $OC_{12}H_{25}$, R' = H
R, R' = $OC_{12}H_{25}$

1.48

Figure 1.9. Contorted PAH's closely related to hexabenzocoronenes.[148,149]

1.4.2 Rational organic synthesis of curved aromatic compounds

The synthesis of curved PAH's by embedding a non six membered ring into the core of the molecule has captured the imagination of many organic chemists due to the possibility of the rational chemical

synthesis of fullerenes and other curved molecules. The first rational organic synthesis of a curved geodesic shaped PAH was of corannulene, **1.49**, in 1965 by Bath and Lawton,[150] outlined in scheme 1.9. Although the synthetic route was low yielding (> 1% overall yield from acenaphthalene, **1.50**), the interest generated from the synthesis of this molecule set the tone for the rational organic synthesis of curved PAH molecules.

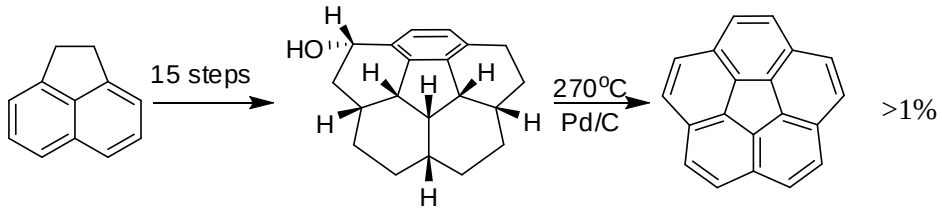

Scheme 1.9. Barth and Lawtons route to corannulene.[150]

In 1991, Scott and co workers published a short synthesis to corannulene using flash vacuum pyrolysis (FVP).[151] A bis acetylene fluoranthene, **1.51**, undergoes cyclisation to corannulene, **1.49**, in ~10% yield. The low yield could not be increased as polymerisation of the bis acetylene occurs before sublimation and cyclisation. Tetrabromo bis acetylene fluoranthene, **1.52**, also undergoes cyclisation under FVP conditions to produce **1.49** in a higher yield (~40%).[151] The synthesis was improved even further in 1997 by the same group, using a three step synthesis from acenaphthalenequinone, **1.53**, via the key chlorovinyl compound, **1.54**, in an overall 26% yield.[152] Figure 1.10 outlines the synthetic strategies used by Scott in the 1990's for the synthesis of corannulene.

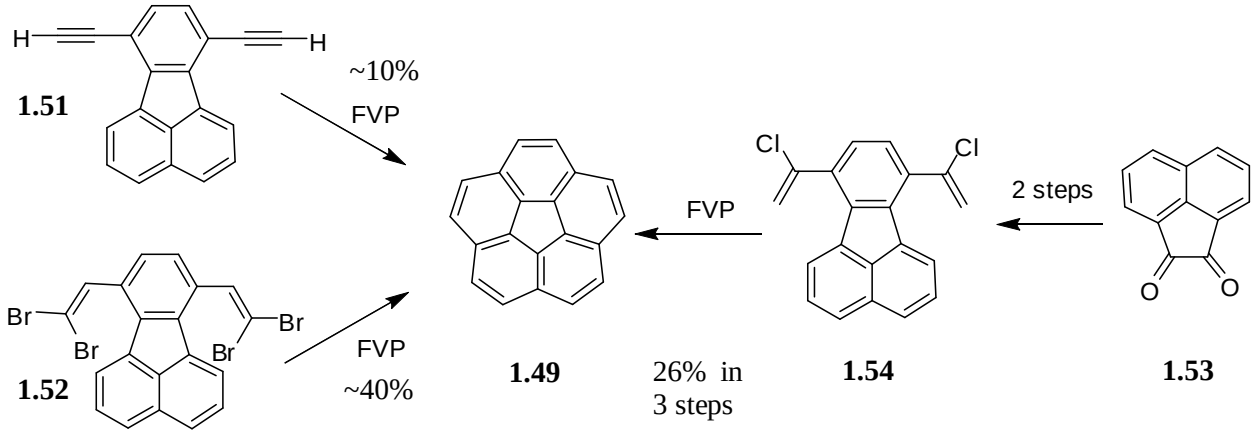

Figure 1.10. Various synthetic routes to corannulene using FVP by Scott and co workers.[151,152]

The first route to corannulene not requiring the use of FVP was published by Siegel in 1996.[153] The tetrabromoalkylated floranthene derivative, **1.55**, was cyclised and aromatized by $TiCl_3/LiAlH_4$ and DDQ

to form a dimethylated corannulene derivative, **1.56**, as shown in scheme 1.10. The purely solution phase synthesis allows for the introduction of substituents on the corannulene core that are not compatible with the harsh conditions required for FVP.

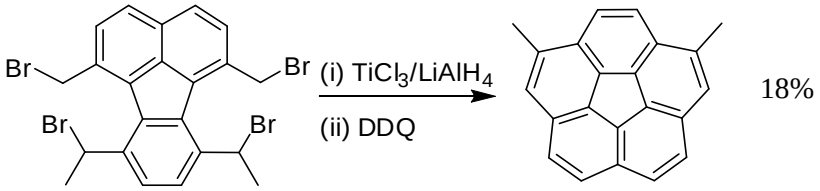

1.55 **1.56**

Scheme 1.10. First solution phase synthesis of a corannulene derivative.[153]

According to Euler's rule, 12 isolated pentagons embedded in a planar hexagonal sheet will yield a closed surface, and the chemical equivalent of this is fullerene. Fullerene, formally known as buckminsterfullerene, was first isolated in 1985[17] by the vaporisation of graphite, and isolatable quantities were first synthesised through this method in 1990.[154] The Nobel Prize was awarded to Curl,[155] Kroto[156] and Smalley[157] for "their discovery of fullerenes".[158] It would be another 11 years before the first rational organic chemical synthesis of fullerenes was reported by Scott and co workers,[22a,159] using an aldol trimerisation and FVP as the two key final steps, outlined below in scheme 1.11.

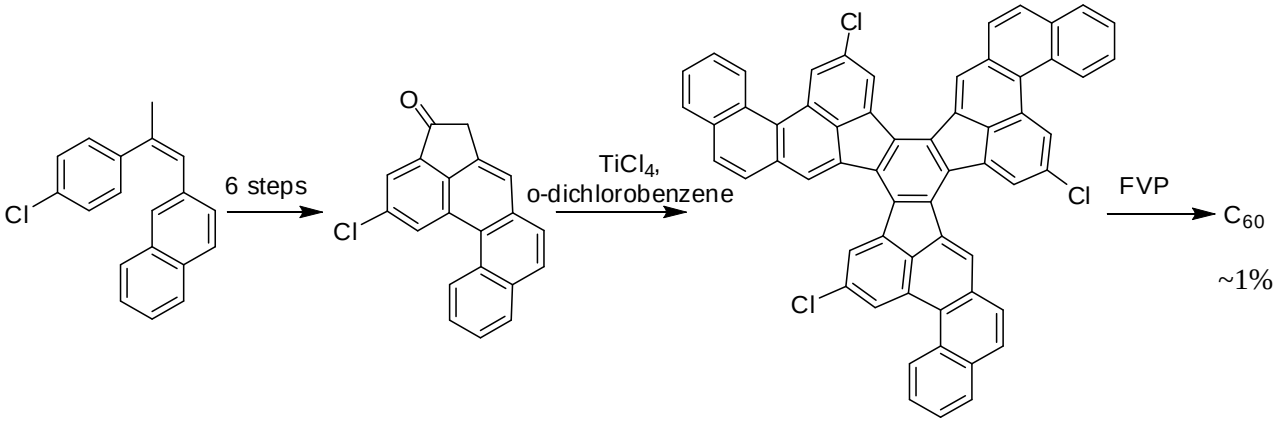

Scheme 1.11. First rational organic synthesis of fullerene, C_{60}.[159]

The development of FVP techniques[143c] and solution phase synthesises of corannulene allows for further development of the curved PAH's. The groups of Scott,[143c,143d,160] Siegel,[143b] Sygula[161] and Rabideau[143a] have all pioneered extensions and derivatisations to the corannulene core. Corannulene derivatives[162] such as those shown in figure 1.11 stack into one dimensional columnar array. One of these derivatives, **1.57**,[162c] has greater pyrimidalisation of the central carbon atoms than that seen in fullerene. The systematic study of all indenocorannules found that the greater the strain in the curved PAH the more

ordered the one dimensional columns are.[162c] Liquid crystalline corannulene derivatives have also been prepared.[163] Very recently, the synthesis of coraunulene derivatives was extended to the synthesis of an endcap unit of a single walled carbon nanotube,[21h] and it is envisaged that these end cap units can be used to template the formation of single walled carbon nanotubes of controlled size and shape.

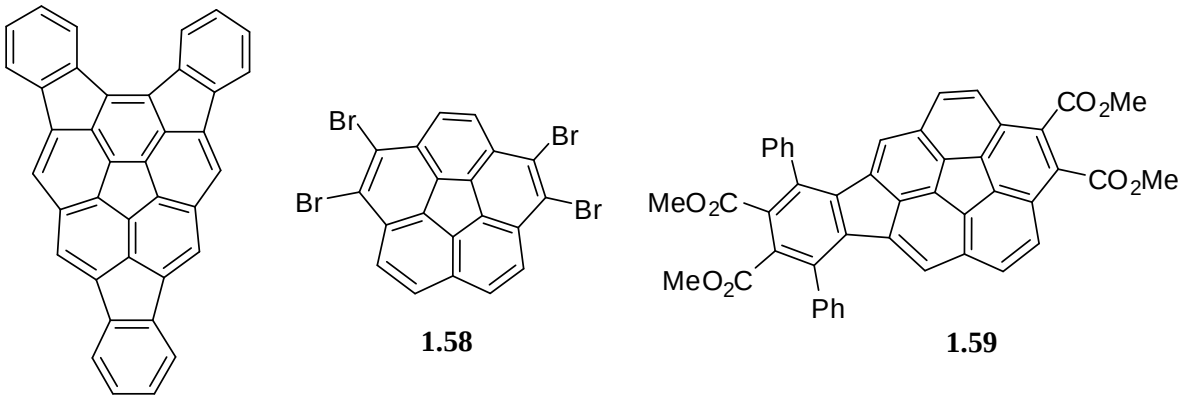

1.57 **1.58** **1.59**

Figure 1.11. Corannulene derivatives that pack into one dimensional columnar arrays.[162]

Four and seven membered rings have also recently been incorporated into the core of PAH's. Tetrabenzoquadrannulene, **1.60**, shown in figure 1.12, has recently been synthesised, its crystal structure and a crystal structure of **1.60** with fullerene has also been described.[164] Although the synthesis is low yielding, enough **1.60** was isolated to determine that it is stable under a variety of conditions, including exposure to light, brief treatment with acid (TsOH) or base (^{t}BuOK), and air. The key step in the synthesis of **1.60** was cyclotrimerisation by a tetraalkyne precursor with the four membered core already introduced into the molecule. The co-crystal of **1.60** with fullerene reveals the close interaction of the two components, due to the complementary curved π systems of **1.60** and fullerene.

A seven membered ring has recently been incorporated into an HBC core by the addition of an additional carbon atom on the periphery of the aromatic core, **1.61**.[165] The additional carbon atom, making up the seven membered ring, imparts a rare saddle shaped geometry onto the molecule. The only other π-systems to display this saddle shape are [7]circulene,[166] **1.62**, and [7.7]circulene.[167] Curved compound **1.61** is synthesised through oxidative cyclodehydrogenation of hexaphenylbenzene type precursor, the heptagon ring is pre built into this precursor, so only five carbon-carbon bonds need to be formed in the final step. Compound **1.61** has similar emission and absorption to alkylated HBC's but its visible light absorption is much more intense, attributed to the lower symmetry of **1.61**.

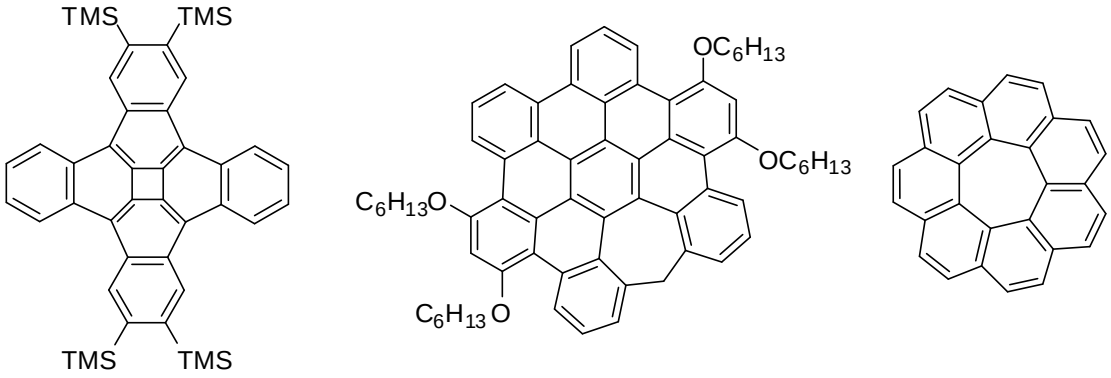

1.60 **1.61** **1.62**

Figure 1.12. Two recent examples of curved PAH's with four and seven membered rings embedded in the aromatic core.[164a,165,166]

1.5 Heteroatom containing polycyclic aromatic compounds

1.5.1 Nitrogen containing polycyclic aromatic compounds

Incorporation of heteroatoms into the core of PAH's provides an opportunity for modification of the electronic properties of the PAH core. The first example of a HBC derivative with heteroatoms embedded in the periphery of the aromatic HBC core was **1.37**, shown in scheme 1.7. The incorporation of electronegative nitrogen atoms into the periphery of the HBC core depletes the π electron density allowing **1.37** to be electron accepting and increases the charge carrier ability. The dipole created by the addition of nitrogen atoms allows **1.37** to be soluble in common organic solvents, and its optical properties can be measured. The UV/vis displays the expected bands of the HBC core with the presence of two additional bands, while the strong fluorescence of **1.37** is quenched by the addition of acid, showing the effect the π electron distribution has on the optical properties.

Careful design of the precursor hexaphenylbenzene derivative allows for placement of nitrogen atoms around the HBC periphery of **1.37** to facilitate the coordination of metal ions. The coordination of Ru(II) and Pd(II) to **1.37** and **1.38** has been investigated.[131,132,168] Metal coordination alters the photophysical properties[169] so that the complex formed between Ru(II) and **1.37** is both a near IR emitter[170] and a black MLCT absorber,[171] as is the case for the complex between Ru(II) and **1.38**.

The incorporation of terpyridine (terpy) units into π conjugated systems is an area of developing interest,[172] and the incorporation of terpy units to the HBC core is a recent achievement.[173] Initially, an acetylene linker or direct peripheral substitution, **1.63**, was used to bridge the terpy unit to the HBC core, although no complexes with Ru(terpy) were reported.[173a] More recently terpy has been incorporated

directly into the HBC core,[173b] forming **1.64**, as shown in figure 1.13. The cyclodehydrogenation of **1.64** suffers from low yields due to the activation of the carbon atoms ortho and para to the nitrogen atom of the central pyridine ring, rather than the desired meta activation. Only small quantities of **1.64** were able to be prepared, not enough to study its photophysical properties upon complexation with ruthenium. Partially cyclised compound **1.65** is the major product from the cyclodehydrogenation to form **1.64**, and complexes of **1.65** and its precursor with Ru(terpy) have been prepared. They show similar properties to that of $Ru(terpy)_2$ due to the minimal interactions from the non planar arrangement of the terpy and PAH/phenylene core.

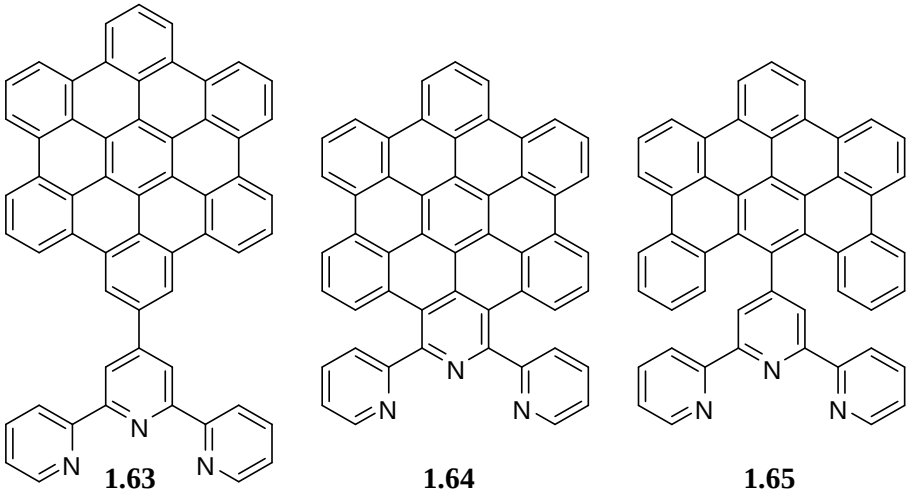

1.63 **1.64** **1.65**

Figure 1.13. Recently prepared HBC derivatives incorporating terpyridine units.[173]

Nitrogen containing heteroaromatic rings have also been employed to bridge two HBC units. The reaction of an α diketone HBC derivative with benzenetetramine produced a tetraazaanthracene bridge between the two HBC cores.[174] The preparation of a large copper phthalocyanine derivative was also possible from the α diketone HBC derivative.[174]

1.5.2 Other heteroatom containing polycyclic aromatic compounds

The incorporation of π excessive heteroaromatic rings into the core of HBC derivatives is not well explored. The oxidative cyclodehydrogenation of hexapyrrolylbenzene produces a planar PAH with six interior nitrogen atoms, and is the only reported example of a pyrrole containing HBC-like derivative, having 13 fused aromatic rings and a planar structure. Thiophene rings have recently received attention for incorporation into HBC derivatives. Three benzothiophene rings have been attached to the periphery of an HBC core, **1.66**,[175] while more recently one thiophene ring has been incorporated directly into the periphery of HBC forming **1.67**, shown in figure 1.14 and a dimer.[176] The optical and electrochemical properties of **1.67** are similar to those of the alkylated HBC derivatives.

Curved hexa-*cata*-hexabenzocoronenes have also been synthesised with four thiophene rings incorporated directly into the periphery, **1.68**.[177] The curved structure allows for formation of one dimensional columnar arrays and when combined with an acceptor fullerene molecule the fullerene is guided into spaces between the columns, forming a ball and socket motif.[177,178] The resulting solar cells show promise for organic electronic applications, with power conversion efficiencies of up to 2.7%.[178]

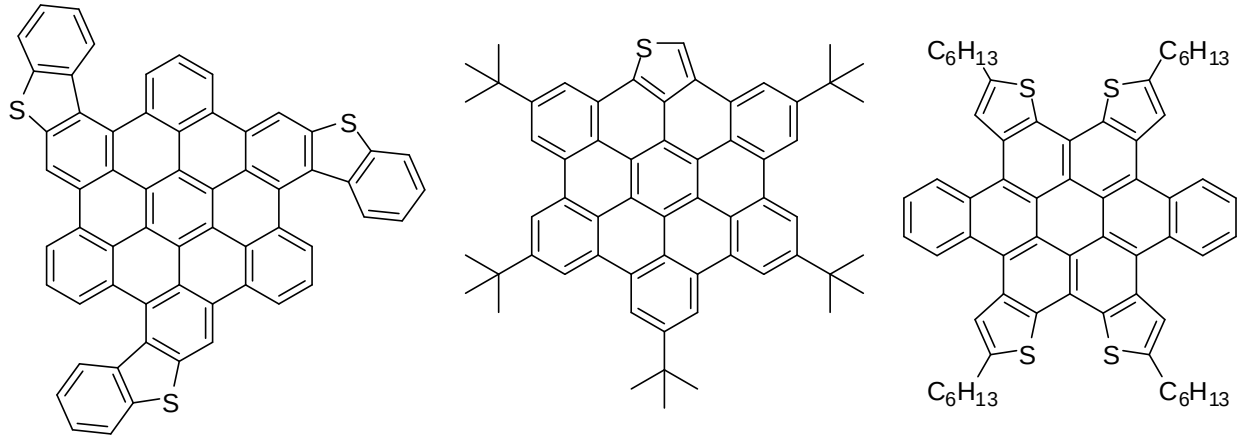

1.66 **1.67** **1.68**

Figure 1.14. Thiophene containing HBC derivatives that have recently been prepared.[175,176.177]

A PAH containing a central thiophene core, **1.69**, shown in figure 1.15, has also been prepared by the oxidative cyclodehydrogenation of the tetraphenylthiophene precursor.[179] Compound **1.69** forms a dianion and the sulphur atom can be extruded from **1.69** with a series of C-S bond cleavages. Phosphole containing π conjugated compounds are gaining attention as functional materials owing to the reactivity of the phosphorus to tune the properties of compounds for different applications.[180] A planar PAH with a central phosphole core was recently prepared, **1.70**, shown in figure 1.15.[181] The PAH has a similar structure to that of **1.69**, but was prepared through photocyclisation of a tetraarylphosphole, the phosphole was too reactive for the Scholl reaction to be employed. The tetraaryl phosphole precursor had a carbon-carbon bond between the two phenyl rings in the 3- and 4-position of the phosphole already formed. The reactive σ^3,λ^3-P allows for direct tuning of the photophysical properties. A coordination complex with Au coordinating to two molecules of **1.70** was also prepared and the crystal structure of the complex shows packing of the complex into one dimensional columns through π – π interactions.

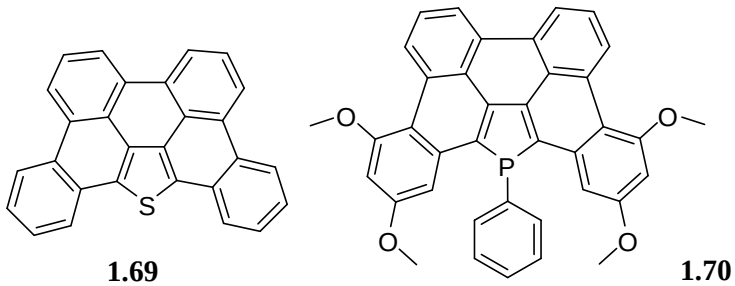

1.69 **1.70**

Figure 1.15. Planar phosphorus containing PAH.[179,181]

1.6 Scope of thesis

This thesis aims to explore the incorporation of π excessive pyrrole rings into the core of PAH's, using appropriate indole and pyrrole precursors with peripheral aryl substitution and their subsequent oxidative cyclodehydrogenation and/or photocyclisation. The routes taken towards the appropriately substituted indole and pyrrole precursors are such that the substitution around the heterocyclic core can be controlled and easily varied to probe the effect of different functionalisation on the aryl rings where the carbon-carbon bond forming reactions take place. Known literature methods were applied for the carbon-carbon bond forming reactions, with the change from indole to tetraarylpyrrole to pentaarylpyrrole cores allowing control over the number of expected carbon-carbon bond forming reactions.

Chapter Two investigates the use of 2,3-diarylindole compounds in Scholl reactions to form a dibenzo[*a*,*c*]carbazole core by the formation of a carbon-carbon bond between the aryl rings in the 2- and 3-positions of the indole core. Eight different 2,3-diarylindoles were used, with the substitution on the nitrogen atom and the substitution at the 4-position of the aryl rings systematically varied. Photocyclisation to form the desired bond between the aryl rings 2- and 3-positions was also carried out.

Chapter Three uses tetraarylpyrrole compounds with the opportunity for the formation of three new carbon-carbon bonds between the peripheral aryl rings. Six different tetraarylpyrroles were used to investigate carbon-carbon bond forming reactions, and again the substitution on the nitrogen atom and the 4-position of the peripheral aryl rings were systematically varied. Both the Scholl reaction and photocyclisation reaction conditions were used, with the difference in the substitution on the nitrogen atom allowing the formation of different heterocyclic cores from these carbon-carbon bond forming reactions.

Chapter Four investigates different routes towards the synthesis of pentaarylpyrrole compounds. The ability to systematically vary the peripheral aryl groups by the changing the substitution at the 4-position

of the aryl rings was a key requirement for the synthesis of these pentaarylpyrroles. Once a route had been established to pentaarylpyrroles three new compounds, and two known compounds, were synthesised, and the Scholl reaction and photocyclisation reaction investigated with pentaphenylpyrrole.

Chapter Five uses a heterocyclic five membered ring system, imidazole, as the base for exploring the metallosupramolecular chemistry of two backbone linked biimidazole ligands with a range of metal salts. A variety of different coordination modes were observed with these ligands. The coordination to silver salts produced a range of coordination modes forming discrete or polymeric species depending on the coordinating strength of the anion used, while the coordination to copper (I) salts produced discrete dinuclear species. The coordination to copper (II) salts also produced discrete species with the two different ligands producing two different coordination modes, monodenate or chelating, due to the difference in the restrictiveness of the tethering backbone

Characterisation of the previously unknown precursor compounds and products obtained from the formation of carbon-carbon bonds studied in Chapters Two – Four were carried out using ^{1}H-NMR spectroscopy, UV/visible spectroscopy, fluorometry and X-ray crystallography where possible. Characterisation of the complexes formed in Chapter Five relied mainly on X-ray crystallography and where appropriate ^{1}H-NMR spectroscopy.

1.7 References

(1) Burroughes, J. H.; Jones, C. A.; Friend, R. H. *Nature* **1988**, *335*, 137

(2) Tsumura, A.; Koezuka, H.; Ando, T. *Appl. Phys. Lett.* **1986**, *49*, 1210.

(3) Tang, C. W. *Appl. Phys. Lett.* **1986**, *48*, 183.

(4) Heeger, A. J. *Angew. Chem. Int. Ed.* **2001**, *40*, 2591.

(5) MacDiarmid, A. G. *Angew. Chem. Int. Ed.* **2001**, *40*, 2581.

(6) Shirakawa, H. *Angew. Chem. Int. Ed.* **2001**, *40*, 2574.

(7) http://www.nobelprize.org/nobel_prizes/chemistry/laureates/2000/.

(8) Tsutsui, T.; Fujita, K. *Adv. Mater.* **2002**, *14*, 949.

(9) (a) Kelley, T. W.; Baude, P. F.; Gerlach, C.; Ender, D. E.; Muyres, D.; Haase, M. A.; Vogel, D. E.; Theiss, S. D. *Chem. Mater.* **2004**, *16*, 4413, (b) Zhong, C.; Duan, C.; Huang, F.; Wu, H.; Cao, Y. *Chem. Mater.* **2011**, *23*, 326.

(10) Coropceanu, V.; Cornil, J.; da Silva Filho, D. A.; Olivier, Y.; Silbey, R.; Brédas, J.-L. *Chem. Rev.* **2007**, *107*, 926.

(11) (a) Shirota, Y.; Kageyama, H. *Chem. Rev.* **2007**, *107*, 953, (b) Kaiser, A. B.; Skakalova, V. *Chem. Soc. Rev.* **2011**, *40*, 3786.

(12) Saeki, A.; Koizumi, Y.; Aida, T.; Seki, S. *Acc. Chem. Res.* **2012**, *45*, 1193.

(13) Troisi, A. *Chem. Soc. Rev.* **2011**, *40*, 2347.

(14) (a) Brédas, J.-L.; Beljonne, D.; Coropceanu, V.; Cornil, J. *Chem. Rev.* **2004**, *104*, 4971, (b) Warman, J. M.; de Haas, M. P.; Dicker, G.; Grozema, F. C.; Piris, J.; Debije, M. G. *Chem. Mater.* **2004**, *16*, 4600, (c) Brédas, J.-L.; Norton, J. E.; Cornil, J.; Coropceanu, V. *Acc. Chem. Res.* **2009**, *42*, 1691.

(15) (a) Moulin, E.; Cid, J.-J.; Giuseppone, N. *Adv. Mater.* **2013**, *25*, 477, (b) Wang, C.; Dong, H.; Hu, W.; Liu, Y.; Zhu, D. *Chem. Rev.* **2012**, *112*, 2208.

(16) (a) Teichler, A.; Perelaer, J.; Schubert, U. S. *J. Mater. Chem. C* **2013**, *1*, 1910, (b) Wen, Y.; Liu, Y.; Guo, Y.; Yu, G.; Hu, W. *Chem. Rev.* **2011**, *111*, 3358.

(17) Kroto, H. W.; Heath, J. R.; O'Brien, S. C.; Curl, R. F.; Smalley, R. E. *Nature* **1985**, *318*, 162

(18) (a) Iijima, S. *Nature* **1991**, *354*, 56, (b) Monthioux, M.; Kuznetsov, V. L. *Carbon* **2006**, *44*, 1621, (c) Boehm, H. P. *Carbon* **1997**, *35*, 581.

(19) (a) Baughman, R. H.; Zakhidov, A. A.; de Heer, W. A. *Science* **2002**, *297*, 787, (b) Gruner, G. *J. Mater. Chem.* **2006**, *16*, 3533, (c) Hoheisel, T. N.; Schrettl, S.; Szilluweit, R.; Frauenrath, H. *Angew. Chem. Int. Ed.* **2010**, *49*, 6496.

(20) (a) Zhang, Q.; Huang, J.-Q.; Qian, W.-Z.; Zhang, Y.-Y.; Wei, F. *Small* **2013**, *9*, 1237, (b) Onoa, G. B.; Thomas, B. O. R.; Michael, E. W.; Henry, I. S. *Nanotechnology* **2005**, *16*, 2799, (c)

Mukhopadhyay, K.; Koshio, A.; Sugai, T.; Tanaka, N.; Shinohara, H.; Konya, Z.; Nagy, J. B. *Chem. Phys. Lett.* **1999**, *303*, 117.

(21) (a) Hirst, E. S.; Jasti, R. *J. Org. Chem.* **2012**, *77*, 10473, (b) Jasti, R.; Bertozzi, C. R. *Chem. Phys. Lett.* **2010**, *494*, 1, (c) Jasti, R.; Bhattacharjee, J.; Neaton, J. B.; Bertozzi, C. R. *J. Am. Chem. Soc.* **2008**, *130*, 17646, (d) Omachi, H.; Matsuura, S.; Segawa, Y.; Itami, K. *Angew. Chem. Int. Ed.* **2010**, *49*, 10202, (e) Yamago, S.; Watanabe, Y.; Iwamoto, T. *Angew. Chem. Int. Ed.* **2010**, *49*, 757, (f) Itami, K. *Pure Appl. Chem.* **2012**, *84*, 907, (g) Nishiuchi, T.; Feng, X.; Enkelmann, V.; Wagner, M.; Müllen, K. *Chem. Eur. J.* **2012**, *18*, 16621, (h) Scott, L. T.; Jackson, E. A.; Zhang, Q.; Steinberg, B. D.; Bancu, M.; Li, B. *J. Am. Chem. Soc.* **2012**, *134*, 107.

(22) (a) Scott, L. T.; Boorum, M. M.; McMahon, B. J.; Hagen, S.; Mack, J.; Blank, J.; Wegner, H.; de Meijere, A. *Science* **2002**, *295*, 1500, (b) Otero, G.; Biddau, G.; Sanchez - Sanchez, C.; Caillard, R.; Lopez, M. F.; Rogero, C.; Palomares, F. J.; Cabello, N.; Basanta, M. A.; Ortega, J.; Mendez, J.; Echavarren, A. M.; Perez, R.; Gomez - Lor, B.; Martin - Gago, J. A. *Nature* **2008**, *454*, 865

(23) De Volder, M. F. L.; Tawfick, S. H.; Baughman, R. H.; Hart, A. J. *Science* **2013**, *339*, 535.

(24) Watson, T. J. *Nat. Nanotechnol.* **2007**, *2*, 605.

(25) Novoselov, K. S.; Geim, A. K.; Morozov, S. V.; Jiang, D.; Zhang, Y.; Dubonos, S. V.; Grigorieva, I. V.; Firsov, A. A. *Science* **2004**, *306*, 666.

(26) (a) Geim, A. K. *Angew. Chem. Int. Ed.* **2011**, *50*, 6966, (b) Novoselov, K. S. *Angew. Chem. Int. Ed.* **2011**, *50*, 6986.

(27) Dresselhaus, M. S.; Araujo, P. T. *ACS Nano* **2010**, *4*, 6297.

(28) http://www.nobelprize.org/nobel_prizes/physics/laureates/2010/.

(29) Xuekun, L.; Minfeng, Y.; Hui, H.; Rodney, S. R. *Nanotechnology* **1999**, *10*, 269.

(30) Allen, M. J.; Tung, V. C.; Kaner, R. B. *Chem. Rev.* **2010**, *110*, 132.

(31) (a) Geim, A. K. *Science* **2009**, *324*, 1530, (b) Castro Neto, A. H.; Guinea, F.; Peres, N. M. R.; Novoselov, K. S.; Geim, A. K. *Rev. Mod. Phys.* **2009**, *81*, 109.

(32) (a) Novoselov, K. S.; Fal'ko, V. I.; Colombo, L.; Gellert, P. R.; Schwab, M. G.; Kim, K. *Nature* **2012**, *490*, 192, (b) Huang, X.; Yin, Z.; Wu, S.; Qi, X.; He, Q.; Zhang, Q.; Yan, Q.; Boey, F.; Zhang, H. *Small* **2011**, *7*, 1876, (c) Wan, X.; Huang, Y.; Chen, Y. *Acc. Chem. Res.* **2012**, *45*, 598, (d) Weiss, N. O.; Zhou, H.; Liao, L.; Liu, Y.; Jiang, S.; Huang, Y.; Duan, X. *Adv. Mater.* **2012**, *24*, 5782, (e) Pang, S.; Hernandez, Y.; Feng, X.; Müllen, K. *Adv. Mater.* **2011**, *23*, 2779, (f) Geim, A. K., Novoselov, K. S. *Nat. Mater.* **2007**, *6*, 183, (g) Chua, C. K.; Pumera, M. *Chem. Soc. Rev.* **2013**, *42*, 3222, (h) Zhan, D.; Yan, J.; Lai, L.; Ni, Z.; Liu, L.; Shen, Z. *Adv. Mater.* **2012**, *24*, 4055, (i) Pumera, M. *Chem. Soc. Rev.* **2010**, *39*, 4146, (j) Rodriguez-Perez, L.; Herranz, M. a. A.; Martin, N. *Chem. Commun.* **2013**, *49*, 3721, (k) Huang, X.; Zeng, Z.; Fan, Z.; Liu, J.; Zhang, H.

Adv. Mater. **2012**, *24*, 5979, (l) Zhu, Y.; James, D. K.; Tour, J. M. *Adv. Mater.* **2012**, *24*, 4924, (m) Sahoo, N. G.; Pan, Y.; Li, L.; Chan, S. H. *Adv. Mater.* **2012**, *24*, 4203.

(33) (a) Ruoff, R. *Nat. Nanotechnol.* **2008**, *3*, 10, (b) Forrest, S. R. *Nature* **2004**, *428*, 911

(34) (a) Hummers, W. S.; Offeman, R. E. *J. Am. Chem. Soc.* **1958**, *80*, 1339, (b) Boehm, H. P.; Clauss, A.; Fischer, G. O.; Hofmann, U. *Z. Naturf.* **1962**, *17*, 150, (c) Tung, V. C.; Allen, M. J.; Yang, Y.; Kaner, R. B. *Nat. Nanotechnol.* **2009**, *4*(d) Compton, O. C.; Nguyen, S. T. *Small* **2010**, *6*, 711.

(35) (a) Sukang, B.; Hyeongkeun, K.; Youngbin, L.; Xiangfan, X.; Park, J.-S.; Zheng, Y.; Balakrishnan, J.; Lei, T.; Kim, H. R.; Song, Y. I.; Kim, Y.-J.; Kim, K. S.; Özyilmaz, B.; Ahn, J.-H.; Hong, B. H.; Iijima, S. *Nat. Nanotechnol.* **2010**, *5*, 574, (b) Kim, K. S.; Zhao, Y.; Jang, H.; Lee, S. Y.; Kim, J. M.; Kim, K. S.; Ahn, J.-H.; Kim, P.; Choi, J.-Y.; Hong, B. H. *Nature* **2009**, *457*, 706, (c) Sutter, P. W.; Flege, J.-I.; Sutter, E. A. *Nat. Mater.* **2008**, *7*, 406

(36) Berger, C.; Song, Z.; Li, X.; Wu, X.; Brown, N.; Naud, C.; Mayou, D.; Li, T.; Hass, J.; Marchenkov, A. N.; Conrad, E. H.; First, P. N.; de Heer, W. A. *Science* **2006**, *312*, 1191.

(37) (a) Li, X.; Wang, X.; Zhang, L.; Lee, S.; Dai, H. *Science* **2008**, *319*, 1229, (b) Li, X.; Zhang, G.; Bai, X.; Sun, X.; Wang, X.; Wang, E.; Dai, H. *Nat. Nanotechnol.* **2008**, *3*, 538.

(38) Inagaki, M.; Kim, Y. A.; Endo, M. *J. Mater. Chem.* **2011**, *21*, 3280.

(39) (a) Chen, L.; Hernandez, Y.; Feng, X.; Müllen, K. *Angew. Chem. Int. Ed.* **2012**, *51*, 7640, (b) Dreyer, D. R.; Ruoff, R. S.; Bielawski, C. W. *Angew. Chem. Int. Ed.* **2010**, *49*, 9336.

(40) Kosynkin, D. V.; Higginbotham, A. L.; Sinitskii, A.; Lomeda, J. R.; Dimiev, A.; Price, B. K.; Tour, J. M. *Nature* **2009**, *458*, 872.

(41) Yan, X.; Li, L.-S. *J. Mater. Chem.* **2011**, *21*, 3295.

(42) Müller, M.; Kübel, C.; Müllen, K. *Chem. Eur. J.* **1998**, *4*, 2099.

(43) (a) Harvey, R. G. *Polycyclic Aromatic Hydrocarbons*; Wiley: New York, 1997, (b) Clar, E. *Polycyclic Hydrocarbons*; Academic Press: London, 1964.

(44) (a) Watson, M. D.; Fechtenkötter, A.; Müllen, K. *Chem. Rev.* **2001**, *101*, 1267, (b) Clar, E. *The Aromatic Sextet*; John Wiley and Sons: London, 1972, (c) Randić, M. *Chem. Rev.* **2003**, *103*, 3449.

(45) (a) Sergeyev, S.; Pisula, W.; Geerts, Y. H. *Chem. Soc. Rev.* **2007**, *36*, 1902, (b) Pisula, W.; Zorn, M.; Chang, J. Y.; Müllen, K.; Zentel, R. *Macromol. Rapid. Commun.* **2009**, *30*, 1179, (c) Kaafarani, B. R. *Chem. Mater.* **2011**, *23*, 378, (d) Kumar, S. *Chem. Soc. Rev.* **2006**, *35*, 83, (e) Laschat, S.; Baro, A.; Steinke, N.; Giesselmann, F.; Hägele, C.; Scalia, G.; Judele, R.; Kapatsina, E.; Sauer, S.; Schreivogel, A.; Tosoni, M. *Angew. Chem. Int. Ed.* **2007**, *46*, 4832, (f) Grimsdale, A. C.; Müllen, K. *Angew. Chem. Int. Ed.* **2005**, *44*, 5592.

(46) Warman, J. M.; Piris, J.; Pisula, W.; Kastler, M.; Wasserfallen, D.; Müllen, K. *J. Am. Chem. Soc.* **2005**, *127*, 14257.

(47) Adam, D.; Schuhmacher, P.; Simmerer, J.; Haussling, L.; Siemensmeyer, K.; Etzbach, K. H.; Ringsdorf, H.; Haarer, D. *Nature* **1994**, *371*, 141.

(48) Hoeben, F. J. M.; Jonkheijm, P.; Meijer, E. W.; Schenning, A. P. H. J. *Chem. Rev.* **2005**, *105*, 1491.

(49) Wu, J.; Pisula, W.; Müllen, K. *Chem. Rev.* **2007**, *107*, 718.

(50) van de Craats, A. M.; Warman, J. M. *Adv. Mater.* **2001**, *13*, 130.

(51) (a) Sakurai, T.; Tashiro, K.; Honsho, Y.; Saeki, A.; Seki, S.; Osuka, A.; Muranaka, A.; Uchiyama, M.; Kim, J.; Ha, S.; Kato, K.; Takata, M.; Aida, T. *J. Am. Chem. Soc.* **2011**, *133*, 6537, (b) Castella, M.; Lopez-Calahorra, F.; Velasco, D.; Finkelmann, H. *Chem. Commun.* **2002**, 2348, (c) Schouten, P. G.; Warman, J. M.; de Haas, M. P.; Fox, M. A.; Pan, H.-L. *Nature* **1991**, *353*, 736, (d) Imahori, H.; Umeyama, T.; Kurotobi, K.; Takano, Y. *Chem. Commun.* **2012**, *48*, 4032, (e) Drain, C. M.; Batteas, J. D.; Flynn, G. W.; Milic, T.; Chi, N.; Yablon, D. G.; Sommers, H. *P. Nat. Acad. Sci. USA* **2002**, *99*, 6498, (f) Qi, M.-H.; Liu, G.-F. *J. Mater. Chem.* **2003**, *13*, 2479, (g) Kroeze, J. E.; Koehorst, R. B. M.; Savenije, T. J. *Adv. Funct. Mater.* **2004**, *14*, 992.

(52) (a) Kimura, M.; Narikawa, H.; Ohta, K.; Hanabusa, K.; Shirai, H.; Kobayashi, N. *Chem. Mater.* **2002**, *14*, 2711, (b) Sergeyev, S.; Debever, O.; Pouzet, E.; Geerts, Y. H. *J. Mater. Chem.* **2007**, *17*, 3002.

(53) (a) Struijk, C. W.; Sieval, A. B.; Dakhorst, J. E. J.; van Dijk, M.; Kimkes, P.; Koehorst, R. B. M.; Donker, H.; Schaafsma, T. J.; Picken, S. J.; van de Craats, A. M.; Warman, J. M.; Zuilhof, H.; Sudhölter, E. J. R. *J. Am. Chem. Soc.* **2000**, *122*, 11057, (b) An, Z.; Yu, J.; Jones, S. C.; Barlow, S.; Yoo, S.; Domercq, B.; Prins, P.; Siebbeles, L. D. A.; Kippelen, B.; Marder, S. R. *Adv. Mater.* **2005**, *17*, 2580, (c) Nolde, F.; Pisula, W.; Müller, S.; Kohl, C.; Müllen, K. *Chem. Mater.* **2006**, *18*, 3715.

(54) (a) Pisula, W.; Feng, X.; Müllen, K. *Chem. Mater.* **2011**, *23*, 554, (b) Simpson, C. D.; Wu, J.; Watson, M. D.; Mullen, K. *J. Mater. Chem.* **2004**, *14*, 494, (c) Holmes, A. B.; Jones, D. J.; Purushothaman, B.; Seyler, H.; Wong, W. W. H. *Pure Appl. Chem.* **2012**, *84*, 1047.

(55) (a) Clar, E.; Ironside, C. T. *Proc. Chem. Soc.* **1958**, 150, (b) Clar, E.; Ironside, C. T.; Zander, M. *J. Chem. Soc.* **1959**, 142.

(56) Halleux, A.; Martin, R. H.; King, G. S. D. *Helv. Chim. Acta* **1958**, *129*, 1177.

(57) Hendel, W.; Khan, Z. H.; Schmidt, W. *Tetrahedron* **1986**, *42*, 1127.

(58) Stabel, A.; Herwig, P.; Müllen, K.; Rabe, J. P. *Angew. Chem. Int. Ed.* **1995**, *34*, 1609.

(59) Berresheim, A. J.; Müller, M.; Müllen, K. *Chem. Rev.* **1999**, *99*, 1747.

(60) (a) Kubel, C.; Eckhardt, K.; Enkelmann, V.; Wegner, G.; Mullen, K. *J. Mater. Chem.* **2000**, *10*, 879, (b) Herwig, P.; Kayser, C. W.; Müllen, K.; Spiess, H. W. *Adv. Mater.* **1996**, *8*, 510, (c) Weiss, K.; Beernink, G.; Dotz, F.; Birkner, A.; Mullen, K.; Woll, C. H. *Angew. Chem. Int. Ed.* **1999**, *38*, 3748, (d) Fechtenkötter, A.; Saalwächter, K.; Harbison, M. A.; Müllen, K.; Spiess, H. W. *Angew. Chem. Int. Ed.* **1999**, *38*, 3039(e) Wadumethrige, S. H.; Rathore, R. *Org. Lett.* **2008**, *10*, 5139.

(61) (a) Iyer, V. S.; Wehmeier, M.; Brand, J. D.; Keegstra, M. A.; Müllen, K. *Angew. Chem. Int. Ed.* **1997**, *36*, 1604, (b) Wu, J.; Tomović, Ž.; Enkelmann, V.; Müllen, K. *J. Org. Chem.* **2004**, *69*, 5179, (c) Ito, S.; Wehmeier, M.; Brand, J. D.; Kübel, C.; Epsch, R.; Rabe, J. P.; Müllen, K. *Chem. Eur. J.* **2000**, *6*, 4327.

(62) (a) Rieger, R.; Müllen, K. *J. Phys. Org. Chem.* **2010**, *23*, 315, (b) Debije, M. G.; Piris, J.; de Haas, M. P.; Warman, J. M.; Tomović, Ž.; Simpson, C. D.; Watson, M. D.; Müllen, K. *J. Am. Chem. Soc.* **2004**, *126*, 4641, (c) Kastler, M.; Schmidt, J.; Pisula, W.; Sebastiani, D.; Müllen, K. *J. Am. Chem. Soc.* **2006**, *128*, 9526, (d) Wang, Z.; Tomović, Ž.; Kastler, M.; Pretsch, R.; Negri, F.; Enkelmann, V.; Müllen, K. *J. Am. Chem. Soc.* **2004**, *126*, 7794.

(63) Simpson, C. D.; Brand, J. D.; Berresheim, A. J.; Przybilla, L.; Räder, H. J.; Müllen, K. *Chem. Eur. J.* **2002**, *8*, 1424.

(64) (a) Przybilla, L.; Brand, J.-D.; Yoshimura, K.; Räder, H. J.; Müllen, K. *Anal. Chem.* **2000**, *72*, 4591, (b) Cristadoro, A.; Räder, H. J.; Müllen, K. *Rapic Commun. Mass Sp.* **2007**, *21*, 2621, (c) Cristadoro, A.; Räder, H. J.; Müllen, K. *Rapic Commun. Mass Sp.* **2008**, *22*, 2463.

(65) (a) Wheeler, S. E. *CrystEngComm* **2012**, *14*, 6140, (b) Feng, X.; Marcon, V.; Pisula, W.; Hansen, M. R.; Kirkpatrick, J.; Grozema, J.; Andrienko, D.; Kremer, K.; Müllen, K. *Nat. Mater.* **2009**, *8*, 421, (c) Wheeler, S. E. *J. Am. Chem. Soc.* **2011**, *133*, 10262, (d) Pisula, W.; Feng, X.; Müllen, K. *Adv. Mater.* **2010**, *22*, 3634.

(66) Pisula, W.; Tomović, Ž.; Watson, M. D.; Müllen, K.; Kussmann, J.; Ochsenfeld, C.; Metzroth, T.; Gauss, J. *J. Phys. Chem. B.* **2007**, *111*, 7481.

(67) Kastler, M.; Pisula, W.; Wasserfallen, D.; Pakula, T.; Müllen, K. *J. Am. Chem. Soc.* **2005**, *127*, 4286.

(68) Feng, X.; Pisula, W.; Kudernac, T.; Wu, D.; Zhi, L.; De Feyter, S.; Müllen, K. *J. Am. Chem. Soc.* **2009**, *131*, 4439.

(69) Dou, X.; Pisula, W.; Wu, J.; Bodwell, G. J.; Müllen, K. *Chem. Eur. J.* **2008**, *14*, 240.

(70) Wasserfallen, D.; Fischbach, I.; Chebotareva, N.; Kastler, M.; Pisula, W.; Jäckel, F.; Watson, M. D.; Schnell, I.; Rabe, J. P.; Spiess, H. W.; Müllen, K. *Adv. Funct. Mater.* **2005**, *15*, 1585.

(71) Yin, M.; Shen, J.; Pisula, W.; Liang, M.; Zhi, L.; Müllen, K. *J. Am. Chem. Soc.* **2009**, *131*, 14618.

(72) Hill, J. P.; Jin, W.; Kosaka, A.; Fukushima, T.; Ichihara, H.; Shimomura, T.; Ito, K.; Hashizume, T.; Ishii, N.; Aida, T. *Science* **2004**, *304*, 1481.

(73) Jin, W.; Fukushima, T.; Niki, M.; Kosaka, A.; Ishii, N.; Aida, T. *P. Nat. Acad. Sci. USA* **2005**, *102*, 10801.

(74) Jin, W.; Fukushima, T.; Kosaka, A.; Niki, M.; Ishii, N.; Aida, T. *J. Am. Chem. Soc.* **2005**, *127*, 8284.

(75) Motoyanagi, J.; Fukushima, T.; Ishii, N.; Aida, T. *J. Am. Chem. Soc.* **2006**, *128*, 4220.

(76) Wu, J.; Baumgarten, M.; Debije, M. G.; Warman, J. M.; Müllen, K. *Angew. Chem. Int. Ed.* **2004**, *43*, 5331.

(77) (a) Foster, E. J.; Jones, R. B.; Lavigueur, C.; Williams, V. E. *J. Am. Chem. Soc.* **2006**, *128*, 8569, (b) Chen, L.; Dou, X.; Pisula, W.; Yang, X.; Wu, D.; Floudas, G.; Feng, X.; Mullen, K. *Chem. Commun.* **2012**, *48*, 702.

(78) Feng, X.; Pisula, W.; Zhi, L.; Takase, M.; Müllen, K. *Angew. Chem. Int. Ed.* **2008**, *47*, 1703.

(79) Wu, J.; Watson, M. D.; Zhang, L.; Wang, Z.; Müllen, K. *J. Am. Chem. Soc.* **2004**, *126*, 177.

(80) Fechtenkötter, A.; Tchebotareva, N.; Watson, M.; Müllen, K. *Tetrahedron* **2001**, *57*, 3769.

(81) Xiao, S.; Myers, M.; Miao, Q.; Sanaur, S.; Pang, K.; Steigerwald, M. L.; Nuckolls, C. *Angew. Chem. Int. Ed.* **2005**, *44*, 7390.

(82) Xiao, S.; Tang, J.; Beetz, T.; Guo, X.; Tremblay, N.; Siegrist, T.; Zhu, Y.; Steigerwald, M.; Nuckolls, C. *J. Am. Chem. Soc.* **2006**, *128*, 10700.

(83) Tremblay, N. J.; Gorodetsky, A. A.; Cox, M. P.; Schiros, T.; Kim, B.; Steiner, R.; Bullard, Z.; Sattler, A.; So, W.-Y.; Itoh, Y.; Toney, M. F.; Ogasawara, H.; Ramirez, A. P.; Kymissis, I.; Steigerwald, M. L.; Nuckolls, C. *ChemPhysChem* **2010**, *11*, 799.

(84) Plunkett, K. N.; Godula, K.; Nuckolls, C.; Tremblay, N.; Whalley, A. C.; Xiao, S. *Org. Lett.* **2009**, *11*, 2225.

(85) Pisula, W.; Menon, A.; Stepputat, M.; Lieberwirth, I.; Kolb, U.; Tracz, A.; Sirringhaus, H.; Pakula, T.; Müllen, K. *Adv. Mater.* **2005**, *17*, 684.

(86) Shklyarevskiy, I. O.; Jonkheijm, P.; Stutzmann, N.; Wasserberg, D.; Wondergem, H. J.; Christianen, P. C. M.; Schenning, A. P. H. J.; de Leeuw, D. M.; Tomović, Ž.; Wu, J.; Müllen, K.; Maan, J. C. *J. Am. Chem. Soc.* **2005**, *127*, 16233.

(87) Reitzel, N.; Hassenkam, T.; Balashev, K.; Jensen, T. R.; Howes, P. B.; Kjaer, K.; Fechtenkötter, A.; Tchebotareva, N.; Ito, S.; Müllen, K.; Bjørnholm, T. *Chem. Eur. J.* **2001**, *7*, 4894.

(88) Schmidt-Mende, L.; Fechtenkötter, A.; Müllen, K.; Moons, E.; Friend, R. H.; MacKenzie, J. D. *Science* **2001**, *293*, 1119.

(89) Li, J. L.; Kastler, M.; Pisula, W.; Robertson, J. W. F.; Wasserfallen, D.; Grimsdale, A. C.; Wu, J. S.; Müllen, K. *Adv. Funct. Mater.* **2007**, *17*, 2528.

(90) Mativetsky, J. M.; Kastler, M.; Savage, R. C.; Gentilini, D.; Palma, M.; Pisula, W.; Müllen, K.; Samorì, P. *Adv. Funct. Mater.* **2009**, *19*, 2486.

(91) Zaumseil, J.; Sirringhaus, H. *Chem. Rev.* **2007**, *107*, 1296.

(92) (a) Wu, J.; Qu, J.; Tchebotareva, N.; Müllen, K. *Tetrahedron Lett.* **2005**, *46*, 1565, (b) Samorì, P.; Fechtenkötter, A.; Reuther, E.; Watson, M. D.; Severin, N.; Müllen, K.; Rabe, J. P. *Adv. Mater.* **2006**, *18*, 1317.

(93) Dössel, L. F.; Kamm, V.; Howard, I. A.; Laquai, F.; Pisula, W.; Feng, X.; Li, C.; Takase, M.; Kudernac, T.; De Feyter, S.; Müllen, K. *J. Am. Chem. Soc.* **2012**, *134*, 5876.

(94) Balaban, A. T.; Nenitzescu, C. D. *Friedel-Crafts and Related Reactions*; Interscience: New York, 1964.

(95) Scholl, R.; Seer, C.; Weitzenbock, R. *Chem. Ber.* **1910**, *43*, 2202

(96) (a) Kovacic, P.; Kyriakis, A. *J. Am. Chem. Soc.* **1963**, *85*, 454, (b) Kovacic, P.; Oziomek, J. *J. Org. Chem.* **1964**, *29*, 100.

(97) Baddeley, G. *J. Chem. Soc.* **1950**, 994.

(98) Müller, M.; Mauermann-Düll, H.; Wagner, M.; Enkelmann, V.; Müllen, K. *Angew. Chem. Int. Ed.* **1995**, *34*, 1583.

(99) (a) Müller, M.; Petersen, J.; Strohmaier, R.; Günther, C.; Karl, N.; Müllen, K. *Angew. Chem. Int. Ed.* **1996**, *35*, 886, (b) Morgenroth, F.; Reuther, E.; Müllen, K. *Angew. Chem. Int. Ed.* **1997**, *36*, 631, (c) Müller, M.; Iyer, V. S.; Kübel, C.; Enkelmann, V.; Müllen, K. *Angew. Chem. Int. Ed.* **1997**, *36*, 1607.

(100) Sarhan, A. A. O.; Bolm, C. *Chem. Soc. Rev.* **2009**, *38*, 2730.

(101) Kovacic, P.; Lange, R. M. *J. Org. Chem.* **1965**, *30*, 4251.

(102) Kramer, B.; Fröhlich, R.; Waldvogel, Siegfried R. *Eur. J. Org. Chem.* **2003**, *2003*, 3549.

(103) (a) McKillop, A.; Turrell, A. G.; Young, D. W.; Taylor, E. C. *J. Am. Chem. Soc.* **1980**, *102*, 6504, (b) Magnus, P.; Schultz, J.; Gallagher, T. *J. Am. Chem. Soc.* **1985**, *107*, 4984(c) Schwartz, M. A.; Pham Phuong Thi, K. *J. Org. Chem.* **1988**, *53*, 2318.

(104) Debad, J. D.; Morris, J. C.; Lynch, V.; Magnus, P.; Bard, A. J. *J. Am. Chem. Soc.* **1996**, *118*, 2374.

(105) Kupchan, S. M.; Dhingra, O. P.; Kim, C.-K. *J. Org. Chem.* **1978**, *43*, 4076.

(106) Aylward, J. B. *J. Chem. Soc. B.* **1967**, 1268.

(107) Rickhaus, M.; Belanger, A. P.; Wegner, H. A.; Scott, L. T. *J. Org. Chem.* **2010**, *75*, 7358.

(108) (a) Takada, T.; Arisawa, M.; Gyoten, M.; Hamada, R.; Tohma, H.; Kita, Y. *J. Org. Chem.* **1998**, *63*, 7698, (b) Churruca, F.; SanMartin, R.; Carril, M.; Urtiaga, M. K.; Solans, X.; Tellitu, I.; Domínguez, E. *J. Org. Chem.* **2005**, *70*, 3178.

(109) Zhai, L.; Shukla, R.; Rathore, R. *Org. Lett.* **2009**, *11*, 3474.

(110) Jones, D. J.; Purushothaman, B.; Ji, S.; Holmes, A. B.; Wong, W. W. H. *Chem. Commun.* **2012**, *48*, 8066.

(111) (a) Chen, T.-A.; Liu, R.-S. *Org. Lett.* **2011**, *13*, 4644, (b) Chen, T.-A.; Liu, R.-S. *Chem. Eur. J.* **2011**, *17*, 8023.

(112) (a) Blackburn, E. V.; Timmons, C. J. *Quart. Rev. Chem. Soc* **1969**, *23*, 482, (b) Laarhoven, W. H.; Cuppen, T. J. H. M.; Nivard, R. J. F. *Recueil* **1968**, *87*, 687.

(113) Mallory, F. B.; Mallory, C. W. *Photocyclization of Stilbenes and Related Molecules*; Wiley: New York, 1984.

(114) Liu, L.; Yang, B.; Katz, T. J.; Poindexter, M. K. *J. Org. Chem.* **1991**, *56*, 3769.

(115) Wood, C. S.; Mallory, F. B. *J. Org. Chem.* **1964**, *29*, 3373.

(116) Zhang, X.; Jiang, X.; Zhang, K.; Mao, L.; Luo, J.; Chi, C.; Chan, H. S. O.; Wu, J. *J. Org. Chem.* **2010**, *75*, 8069.

(117) (a) Dötz, F.; Brand, J. D.; Ito, S.; Gherghel, L.; Müllen, K. *J. Am. Chem. Soc.* **2000**, *122*, 7707, (b) Cao, X.-Y.; Zi, H.; Zhang, W.; Lu, H.; Pei, J. *J. Org. Chem.* **2005**, *70*, 3645.

(118) Dössel, L.; Gherghel, L.; Feng, X.; Müllen, K. *Angew. Chem. Int. Ed.* **2011**, *50*, 2540.

(119) Pradhan, A.; Dechambenoit, P.; Bock, H.; Durola, F. *Angew. Chem. Int. Ed*. **2011**, *50*, 12582.

(120) Danz, M.; Tonner, R.; Hilt, G. *Chem. Commun.* **2012**, *48*, 377.

(121) (a) Dou, X.; Yang, X.; Bodwell, G. J.; Wagner, M.; Enkelmann, V.; Müllen, K. *Org. Lett.* **2007**, *9*, 2485, (b) Ormsby, J. L.; Black, T. D.; Hilton, C. L.; Bharat; King, B. T. *Tetrahedron* **2008**, *64*, 11370.

(122) Closs, F.; Haeussling, L.; Henderson, P.; Ringsdorf, H.; Schuhmacher, P. *J. Chem. Soc., Perkin Trans. 1* **1995**, 829.

(123) (a) Feng, X.; Pisula, W.; Takase, M.; Dou, X.; Enkelmann, V.; Wagner, M.; Ding, N.; Müllen, K. *Chem. Mater*. **2008**, *20*, 2872, (b) Gregg, D. J.; Ollagnier, C. M. A.; Fitchett, C. M.; Draper, S. M. *Chem. Eur. J.* **2006**, *12*, 3043.

(124) Zhang, Q.; Prins, P.; Jones, S. C.; Barlow, S.; Kondo, T.; An, Z.; Siebbeles, L. D. A.; Marder, S. R. *Org. Lett.* **2005**, *7*, 5019.

(125) Rempala, P.; Kroulík, J.; King, B. T. *J. Am. Chem. Soc.* **2004**, *126*, 15002.

(126) (a) Feng, X.; Wu, J.; Enkelmann, V.; Müllen, K. *Org. Lett.* **2006**, *8*, 1145, (b) Wu, J.; Gherghel, L.; Watson, M. D.; Li, J.; Wang, Z.; Simpson, C. D.; Kolb, U.; Müllen, K. *Macromolecules* **2003**, *36*, 7082.

(127) Di Stefano, M.; Negri, F.; Carbone, P.; Müllen, K. *Chem . Phys.* **2005**, *314*, 85.

(128) Lu, Y.; Moore, J. S. *Tetrahedron Lett.* **2009**, *50*, 4071.

(129) Simpson, C. D.; Mattersteig, G.; Martin, K.; Gherghel, L.; Bauer, R. E.; Räder, H. J.; Müllen, K. *J. Am. Chem. Soc.* **2004**, *126*, 3139.

(130) Draper, S. M.; Gregg, D. J.; Madathil, R. *J. Am. Chem. Soc.* **2002**, *124*, 3486.

(131) Draper, S. M.; Gregg, D. J.; Schofield, E. R.; Browne, W. R.; Duati, M.; Vos, J. G.; Passaniti, P. *J. Am. Chem. Soc.* **2004**, *126*, 8694.

(132) Gregg, D. J.; Bothe, E.; Höfer, P.; Passaniti, P.; Draper, S. M. *Inorg. Chem.* **2005**, *44*, 5654.

(133) Nagarajan, S.; Barthes, C.; Gourdon, A. *Tetrahedron* **2009**, *65*, 3767.

(134) Avlasevich, Y.; Kohl, C.; Mullen, K. *J. Mater. Chem.* **2006**, *16*, 1053.

(135) (a) Rempala, P.; Kroulík, J.; King, B. T. *J. Org. Chem.* **2006**, *71*, 5067, (b) King, B. T.; Kroulík, J.; Robertson, C. R.; Rempala, P.; Hilton, C. L.; Korinek, J. D.; Gortari, L. M. *J. Org. Chem.* **2007**, *72*, 2279.

(136) Zhai, L.; Shukla, R.; Wadumethrige, S. H.; Rathore, R. *J. Org. Chem.* **2010**, *75*, 4748.

(137) Rathore, R.; Kochi, J. K. *Acta Chem. Scand.* **1998**, *52*, 114.

(138) Rooney, J. J.; Pink, R. C. *Proc. Chem. Soc.* **1961**, 142.

(139) (a) Ronlan, A.; Hammerich, O.; Parker, V. D. *J. Am. Chem. Soc.* **1973**, *95*, 7132, (b) Ronlan, A.; Parker, V. D. *J. Org. Chem.* **1974**, *39*, 1014 (c) Rathore, R.; Kochi, J. K. *J. Org. Chem.* **1995**, *60*, 7479

(140) Kuhl, N.; Hopkinson, M. N.; Wencel-Delord, J.; Glorius, F. *Angew. Chem. Int. Ed.* **2012**, *51*, 10236.

(141) (a) Amsharov, K. Y.; Kabdulov, M. A.; Jansen, M. *Angew. Chem. Int. Ed.* **2012**, *51*, 4594, (b) Siegel, J. S. *Nature* **2012**, *486*, 327.

(142) Bonifacio, M. C.; Robertson, C. R.; Jung, J.-Y.; King, B. T. *J. Org. Chem.* **2005**, *70*, 8522.

(143) (a) Rabideau, P. W.; Sygula, A. *Acc. Chem. Res.* **1996**, *29*, 235, (b) Wu, Y.-T.; Siegel, J. S. *Chem. Rev.* **2006**, *106*, 4843, (c) Tsefrikas, V. M.; Scott, L. T. *Chem. Rev.* **2006**, *106*, 4868, (d) Scott, L. T.; Bronstein, H. E.; Preda, D. V.; Ansems, R. B. M.; Bratcher, M. S.; Hagen, S. *Pure Appl. Chem.* **1999**, *71*, 209, (e) Kawase, T.; Kurata, H. *Chem. Rev.* **2006**, *106*, 5250(f) Lu, X.; Chen, Z. *Chem. Rev.* **2005**, *105*, 3643, (g) Myśliwiec, D.; Stępień, M. *Angew. Chem. Int. Ed.* **2013**, *52*, 1713.

(144) (a) Shibata, K.; Kulkarni, A. A.; Ho, D. M.; Pascal, R. A. *J. Am. Chem. Soc.* **1994**, *116*, 5983, (b) Shibata, K.; Kulkarni, A. A.; Ho, D. M.; Pascal, R. A. *J. Org. Chem.* **1995**, *60*, 428.

(145) Pascal, R. A. *Chem. Rev.* **2006**, *106*, 4809.

(146) (a) Lu, J.; Ho, D. M.; Vogelaar, N. J.; Kraml, C. M.; Pascal, R. A. *J. Am. Chem. Soc.* **2004**, *126*, 11168, (b) Lu, J.; Ho, D. M.; Vogelaar, N. J.; Kraml, C. M.; Bernhard, S.; Byrne, N.; Kim, L. R.; Pascal, R. A. *J. Am. Chem. Soc.* **2006**, *128*, 17043.

(147) Pascal, R. A.; McMillan, W. D.; Van Engen, D.; Eason, R. G. *J. Am. Chem. Soc.* **1987**, *109*, 4660.

(148) Xiao, S.; Kang, S. J.; Wu, Y.; Ahn, S.; Kim, J. B.; Loo, Y.-L.; Siegrist, T.; Steigerwald, M. L.; Li, H.; Nuckolls, C. *Chem. Sci.* **2013**, *4*, 2018.

(149) Wang, Z.; Dötz, F.; Enkelmann, V.; Müllen, K. *Angew. Chem. Int. Ed.* **2005**, *44*, 1247.

(150) Barth, W. E.; Lawton, R. G. *J. Am. Chem. Soc.* **1966**, *88*, 380.

(151) Scott, L. T.; Hashemi, M. M.; Meyer, D. T.; Warren, H. B. *J. Am. Chem. Soc.* **1991**, *113*, 7082.

(152) Scott, L. T.; Cheng, P.-C.; Hashemi, M. M.; Bratcher, M. S.; Meyer, D. T.; Warren, H. B. *J. Am. Chem. Soc.* **1997**, *119*, 10963.

(153) Seiders, T. J.; Baldridge, K. K.; Siegel, J. S. *J. Am. Chem. Soc.* **1996**, *118*, 2754.

(154) Kratschmer, W.; Lamb, L. D.; Fostiropoulos, K.; Huffman, D. R. *Nature* **1990**, *347*, 354.

(155) Curl, R. F. *Angew. Chem. Int. Ed.* **1997**, *36*, 1566.

(156) Kroto, H. *Angew. Chem. Int. Ed.* **1997**, *36*, 1578.

(157) Smalley, R. E. *Angew. Chem. Int. Ed.* **1997**, *36*, 1594.

(158) http://www.nobelprize.org/nobel_prizes/chemistry/laureates/1996/.

(159) Boorum, M. M.; Vasil'ev, Y. V.; Drewello, T.; Scott, L. T. *Science* **2001**, *294*, 828.

(160) Scott, L. T. *Angew. Chem. Int. Ed.* **2004**, *43*, 4994.

(161) Sygula, A. *Eur. J. Org. Chem.* **2011**, *2011*, 1611.

(162) (a) Wu, Y.-T.; Hayama, T.; Baldridge, K. K.; Linden, A.; Siegel, J. S. *J. Am. Chem. Soc.* **2006**, *128*, 6870, (b) Wu, Y.-T.; Bandera, D.; Maag, R.; Linden, A.; Baldridge, K. K.; Siegel, J. S. *J. Am. Chem. Soc.* **2008**, *130*, 10729, (c) Filatov, A. S.; Scott, L. T.; Petrukhina, M. A. *Cryst. Growth. Des.* **2010**, *10*, 4607, (d) Steinberg, B. D.; Jackson, E. A.; Filatov, A. S.; Wakamiya, A.; Petrukhina, M. A.; Scott, L. T. *J. Am. Chem. Soc.* **2009**, *131*, 10537, (e) Marcinow, Z.; Sygula, A.; Ellern, A.; Rabideau, P. W. *Org. Lett.* **2001**, *3*, 3527.

(163) Miyajima, D.; Tashiro, K.; Araoka, F.; Takezoe, H.; Kim, J.; Kato, K.; Takata, M.; Aida, T. *J. Am. Chem. Soc.* **2009**, *131*, 44.

(164) (a) Bharat; Bhola, R.; Bally, T.; Valente, A.; Cyrański, M. K.; Dobrzycki, Ł.; Spain, S. M.; Rempała, P.; Chin, M. R.; King, B. T. *Angew. Chem. Int. Ed.* **2010**, *49*, 399, (b) Kumar, B.; King,

B. T. *J. Org. Chem.* **2012**, *77*, 10617, (c) King, B. T.; Olmstead, M. M.; Baldridge, K. K.; Kumar, B.; Balch, A. L.; Gharamaleki, J. A. *Chem. Commun.* **2012**, *48*, 9882.

(165) Luo, J.; Xu, X.; Mao, R.; Miao, Q. *J. Am. Chem. Soc.* **2012**, *134*, 13796.

(166) (a) Yamamoto, K.; Harada, T.; Nakazaki, M.; Naka, T.; Kai, Y.; Harada, S.; Kasai, N. *J. Am. Chem. Soc.* **1983**, *105*, 7171, (b) Yamamoto, K.; Harada, T.; Okamoto, Y.; Chikamatsu, H.; Nakazaki, M.; Kai, Y.; Nakao, T.; Tanaka, M.; Harada, S.; Kasai, N. *J. Am. Chem. Soc.* **1988**, *110*, 3578.

(167) (a) Yamamoto, K.; Saitho, Y.; Iwaki, D.; Ooka, T. *Angew. Chem. Int. Ed.* **1991**, *30*, 1173, (b) Yamamoto, K. *Pure Appl. Chem.* **1993**, *65*, 157

(168) Gregg, D. J.; Fitchett, C. M.; Draper, S. M. *Chem. Commun.* **2006**, 3090.

(169) Anderson, P. A.; Richard Keene, F.; Meyer, T. J.; Moss, J. A.; Strouse, G. F.; Treadway, J. A. *J. Chem. Soc., Dalton Trans.* **2002**, 3820.

(170) Treadway, J. A.; Strouse, G. F.; Ruminski, R. R.; Meyer, T. J. *Inorg. Chem.* **2001**, *40*, 4508.

(171) Anderson, P. A.; Strouse, G. F.; Treadway, J. A.; Keene, F. R.; Meyer, T. J. *Inorg. Chem.* **1994**, *33*, 3863.

(172) Wild, A.; Winter, A.; Schluetter, F.; Schubert, U. S. *Chem. Soc. Rev.* **2011**, *40*, 1459.

(173) (a) Murphy, F. A.; Draper, S. M. *J. Org. Chem.* **2010**, *75*, 1862, (b) Graczyk, A.; Murphy, F. A.; Nolan, D.; Fernandez-Moreira, V.; Lundin, N. J.; Fitchett, C. M.; Draper, S. M. *Dalton Trans.* **2012**, *41*, 7746.

(174) Fogel, Y.; Kastler, M.; Wang, Z.; Andrienko, D.; Bodwell, G. J.; Müllen, K. *J. Am. Chem. Soc.* **2007**, *129*, 11743.

(175) Feng, X.; Wu, J.; Ai, M.; Pisula, W.; Zhi, L.; Rabe, J. P.; Müllen, K. *Angew. Chem. Int. Ed.* **2007**, *46*, 3033.

(176) Martin, C. J.; Gil, B.; Perera, S. D.; Draper, S. M. *Chem. Commun.* **2011**, *47*, 3616.

(177) Gorodetsky, A. A.; Chiu, C.-Y.; Schiros, T.; Palma, M.; Cox, M.; Jia, Z.; Sattler, W.; Kymissis, I.; Steigerwald, M.; Nuckolls, C. *Angew. Chem. Int. Ed.* **2010**, *49*, 7909.

(178) Kang, S. J.; Kim, J. B.; Chiu, C.-Y.; Ahn, S.; Schiros, T.; Lee, S. S.; Yager, K. G.; Toney, M. F.; Loo, Y.-L.; Nuckolls, C. *Angew. Chem. Int. Ed.* **2012**, *51*, 8594.

(179) Benshafrut, R.; Rabinovitz, M.; Hoffman, R. E.; Ben-Mergui, N.; Müllen, K.; Iyer, V. S. *Eur. J. Org. Chem.* **1999**, *1999*, 37.

(180) Ren, Y.; Baumgartner, T. *Dalton Trans.* **2012**, *41*, 7792.

(181) Bouit, P.-A.; Escande, A.; Szűcs, R.; Szieberth, D.; Lescop, C.; Nyulászi, L.; Hissler, M.; Réau, R. *J. Am. Chem. Soc.* **2012**, *134*, 6524.

Chapter Two:

2,3-Diarylindole compounds

2.1 Introduction

The indole ring system is a biologically privileged moiety, and is one of the most ubiquitous heterocyclic ring structures found in nature.[1,2] The amino acid tryptophan, one of the twenty proteinogenic amino acids, contains an indole ring, as shown in figure 2.1a. Due to its fluorescence properties, tryptophan acts as a fluorescent probe in the study of protein conformations, as the fluorescence signal of the tryptophan molecule changes depending on the environment around the protein.[3] Indole moieties are commonly found in natural products and biological molecules. Serotonin, shown in figure 2.1b, a monoamine neurotransmitter derived from tryptophan, has been implicated in the regulation of mood, sleep and also memory.[4]

Many drug molecules available today contain an indole moiety, and are used to treat a wide range of conditions.[5] Triptans are an important class of drugs containing an indole ring[6] and are used in the treatment of headaches and migranes. Sumatriptan, shown in figure 2.1c, is a first generation triptan drug and was the first member of the triptan family to be introduced on the drug market. Indomethacin, shown in figure 2.1c, is a non-steroidal anti-inflammatory drug containing an indole ring.[7] There are many other classes of drugs that also contain indole moieties.

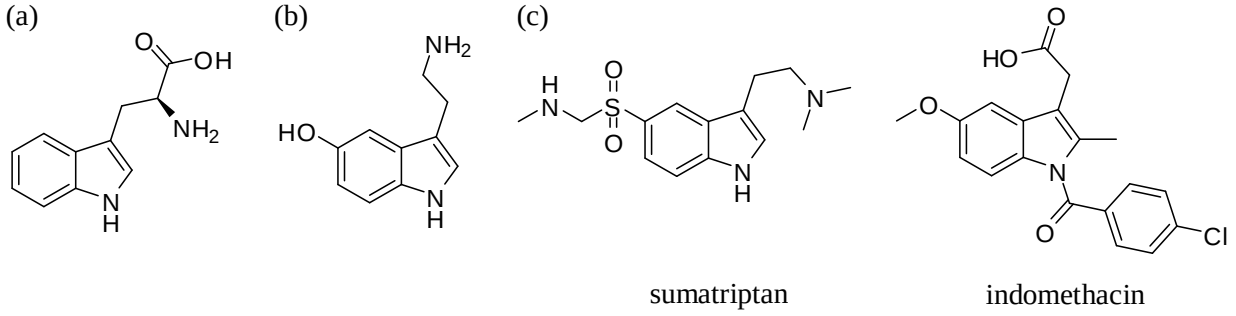

Figure 2.1 Biologically relevant molecules containing an indole ring system, (a) tryptophan, (b) serotonin, and (c) two pharmaceuticals.

Due to the biological importance of the indole functional group many methods exist for the synthesis of the indole ring and variously substituted derivatives.[2,5,8,9] The Fischer indole synthesis[10] is one of the oldest and most commonly used methods for the preparation of the indole ring. It utilises an appropriately substituted phenyl hydrazine and enolisable ketone to produce the desired indole ring under acidic conditions,[2,5,8a] as shown in scheme 2.1. The availability of the desired hydrazine precursor can impose limitations on the use of this reaction in some instances.

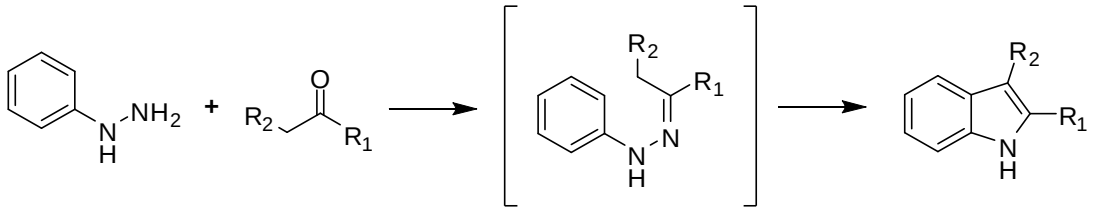

Scheme 2.1. General scheme for the Fischer indole synthesis.

More recently, the transitional metal mediated synthesis of indole rings has been widely employed[2,8b,9] due the tolerance of these catalysts to a wide range of functional groups, and the range of precursors that can be employed. The formation of the indole ring is often achieved by palladium catalysis using ortho-substituted anilines and substituted alkynes, preparation of the indole is often achieved in a one-pot reaction. The Larock indole synthesis, shown in scheme 2.2, utilises an appropriately substituted acetylene and ortho substituted iodoaniline to form an indole ring via heteroannulation, with substitution in the 2- and 3-positions resulting from substitution on the acetylene.[5] This synthesis was successfully employed in the total synthesis of psychotrimine in 2008,[11] where gram quantities of the 2-iodoaniline precursor was isolated before formation of the indole ring with the protected acetylene.

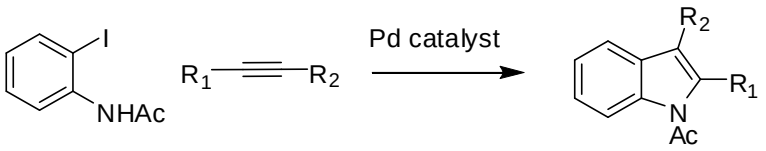

Scheme 2.2. General scheme for the Larock indole synthesis.

A series of 2,3-diarylindoles were targeted in this project as simple model systems for a series of pentarylpyrrole compounds to undergo oxidative cyclodehydrogenation using a variety of conditions. The 2,3-diarylindole model system simplifies the number of possible carbon-carbon bonds that can be formed by oxidative cyclodehydrogenation reactions. Five possible carbon-carbon bonds can be formed by oxidative cyclodehydrogenation of pentaarylpyrrole compounds, yet only one carbon-carbon bond should be formed by the oxidative cyclodehydrogenation of 2,3-diarylindole compounds. Two carbon-carbon bonds can be formed by the oxidative cyclodehydrogenation of 1,2,3-triarylindole compounds. The reduction in the number of possible carbon-carbon bonds able to be formed through oxidative cyclodehydrogenation reactions should allow for ease of determination of the resulting products from the reaction. Oxidative cyclodehydrogenation of a series of 2,3-diarylindole compounds will produce a family of dibenzo[*a*,*c*]carbazole compounds, some of these desired dibenzo[*a*,*c*]carbazole compounds have already been synthesised,[12,13] allowing for simple identification of the desired products.

2.2 Synthesis of N-substituted-2,3-diarylindoles

2.2.1 Synthesis of NH-2,3-diarylindoles, ***2.1*** *–* ***2.4***

Although there are many methods available for the synthesis of indole scaffolds, a synthesis was required for the formation of N*H*-2,3-diarylindoles where variation in the substitution of the aryl groups in the 4-position could be easily achieved. To this end, four N*H*-2,3-diarylindoles, **2.1**, **2.2**, **2.3** and **2.4**, were synthesised following the method of Szmuszkovicz *et al*.[14] The condensation of aniline and the appropriate benzoin derivative under acidic conditions gave the corresponding indoles in moderate yields (~ 50%), as shown in scheme 2.3. Benzoin, **2.1a**, and anisoin, **2.2a**, were commercially available, whilst 4,4'-dimethylbenzoin, **2.3a**, and 4,4'-di*tert*butylbenzoin, **2.4a**, were synthesised via a benzoin condensation with one equivalent of potassium cyanide and two equivalents of the appropriately substituted benzaldehyde precursor, in good yields (~ 85%).

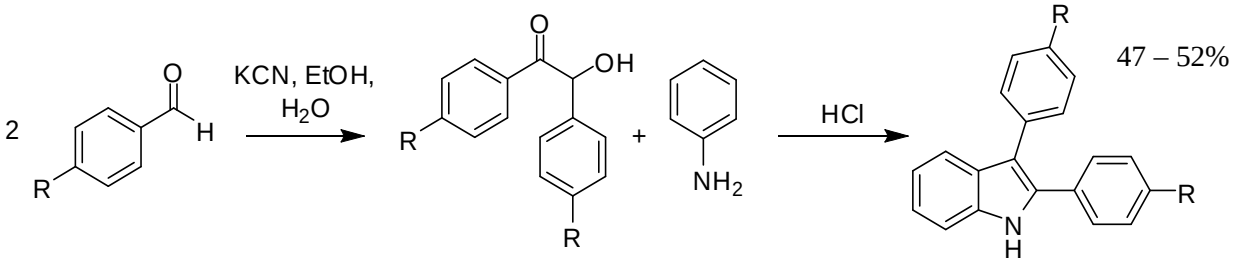

2.1a – 2.4a

2.1 R = H
2.2 R = OMe
2.3 R = Me
2.4 R = ^{t}Bu

Scheme 2.3. Synthesis of N*H*-2,3-diarylindoles.

N*H*-2,3-diphenylindole, **2.1**, and N*H*-2,3-bis(4-methoxyphenyl)indole, **2.2**, have both been previously synthesised. Due to intense interest from both the chemical and biological communities in synthetic methodologies towards the indole core, both **2.1**[15] and **2.2**[16] have been the target of various synthetic routes. Both compounds have also been investigated for their biological properties, with **2.2** prepared by Szmuszkovicz *et al*. as an anti-inflammatory agent.[14]

N*H*-2,3-bis(4-methylphenyl)indole, **2.3**, was prepared during the course of this study by Chen *et al*., using a Pd catalysed intermolecular coupling between aniline and 1,2-bis(4-methylphenyl)acetylene.[17] Before this study Zhang *et al*. prepared **2.3** using solid phase synthesis, whereby **2.3** was synthesised via a one-pot Suzuki cross coupling of a 2,3-dibromoindole derivative with 4-methylphenyl boronic acid.[18]

The determination of a structure by X-ray crystallography allows the three-dimensional nature of the molecule to be examined. The structural information obtained from X-ray crystallography was analysed

during the course of this study as it allows the distance between the ortho carbon atoms of the phenyl rings that are to undergo oxidative cyclodehydrogenation to be determined.

A single crystal of **2.3** suitable for X-ray diffraction was grown by the recrystallisation of **2.3** from ethyl acetate and hexane. The crystal structure solved in the monoclinic space group $P2_1/c$, with three crystallographically independent molecules of **2.3** present in the asymmetric unit, one molecule of **2.3** is shown in figure 2.2a. The three crystallographically independent molecules of **2.3** differ only in the twist of the phenyl rings in the 2- and 3-position of the indole core. The phenyl ring in the 3-position of the indole is twisted out of plane more than 15˚ relative to the phenyl ring in the 2-position (twist angles are 26.7(1)˚, 32.3(1)˚ and 32.7(1)˚ for the phenyl ring in the 2-position, 47.6(1)˚, 47.7(1)˚ and 49.1(1)˚ for the phenyl ring in the 3-position). The distance between the ortho carbon atoms of the phenyl rings are 3.223(2) Å, 3.224(2) Å, 3.257(2) Å, and this is comparable to the distance between the ortho carbon atoms of hexaphenyl benzene (smallest distance = 3.343 Å),[19] which has been successfully cyclodehydrogenated to form HBC using a variety of techniques.[20] Molecules of **2.3** pack together in a herringbone arrangement, shown in figure 2.2b. Each molecule of **2.3** displays face-to-face and edge-to-face π − π interactions with adjacent molecules through both the indole core and both phenyl rings. The nitrogen hydrogen atoms are involved in N−H···π hydrogen bonding interactions with the six-membered ring of the indole core in an adjacent unit (N···centroid distances = 3.406(1) Å, 3.469(2) Å and 3.700(2) Å). These interactions help to stabilise the herringbone arrangement of molecules.

N*H*-2,3-bis(4-*tert*butylphenyl)indole, **2.4**, prepared in two steps from 4-*tert*butylbenzaldehyde (43%), has not been previously reported in the literature and was fully characterised during the course of this study. The ^{1}H-NMR spectrum is as expected from the other substituted N*H*-2,3-diarylindoles prepared, with a broad NH peak observed at 8.19 ppm, and two peaks for the *tert*butyl groups (integrating for nine protons each) observed at 1.38 ppm and 1.33 ppm. The remaining 12 aromatic protons are observed between 7.68 ppm and 7.11 ppm.

(a) (b)

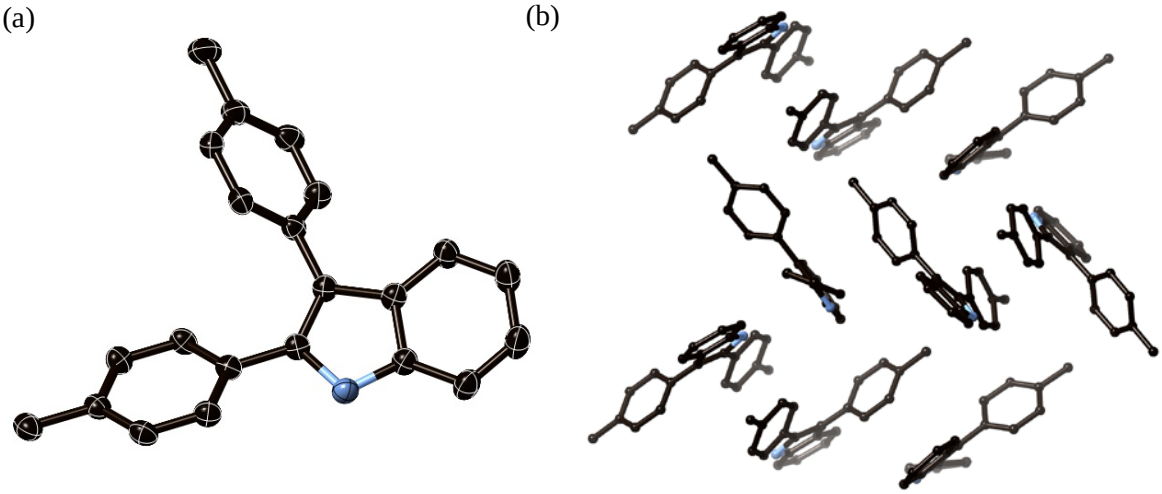

Figure 2.2. (a) One molecule of **2.3**, (b) herringbone packing of molecules of **2.3**, hydrogen atoms have been removed for clarity.

2.2.2 Synthesis of N-ethyl and N-benzyl-2,3-diarylindoles, ***2.5*** *–* ***2.12***

To prevent reaction with the lewis acids required for the Scholl-type cyclodehydrogenation in the following section, the ability of the lewis basic nitrogen functionality of each N*H*-2,3-diarylindole, **2.1** – **2.4**, to coordinate to the lewis acid needs to be removed. Substitution on the nitrogen atoms by ethyl and benzyl groups removes the N*H* functionality and gives protected indoles **2.5** – **2.12**, in reasonable yields (65% to 84%). Following a modified literature procedure,[14,21] sodium hydride was used to deprotonate the N*H*-2,3-diarylindoles before the addition of ethyl bromide or benzyl bromide, as shown in scheme 2.4.

Indoles **2.5**, **2.6** and **2.9** have all been previously prepared by other groups. N-ethyl-2,3-diphenylindole, **2.5**, was first synthesised in 1910 by the reaction of benzoin with N-ethylaniline in the presence of zinc chloride.[22] Very little has appeared in the literature since this time, although **2.5** has been used for quantitative ^{13}C-NMR studies detailing the shifts in the phenyl carbon in the 2- and 3-position of the indole ring.[23] N-benzyl-2,3-diphenylindole, **2.9**, has been synthesised by a variety of methods,[24] but not by the method used here, and no further studies were reported.

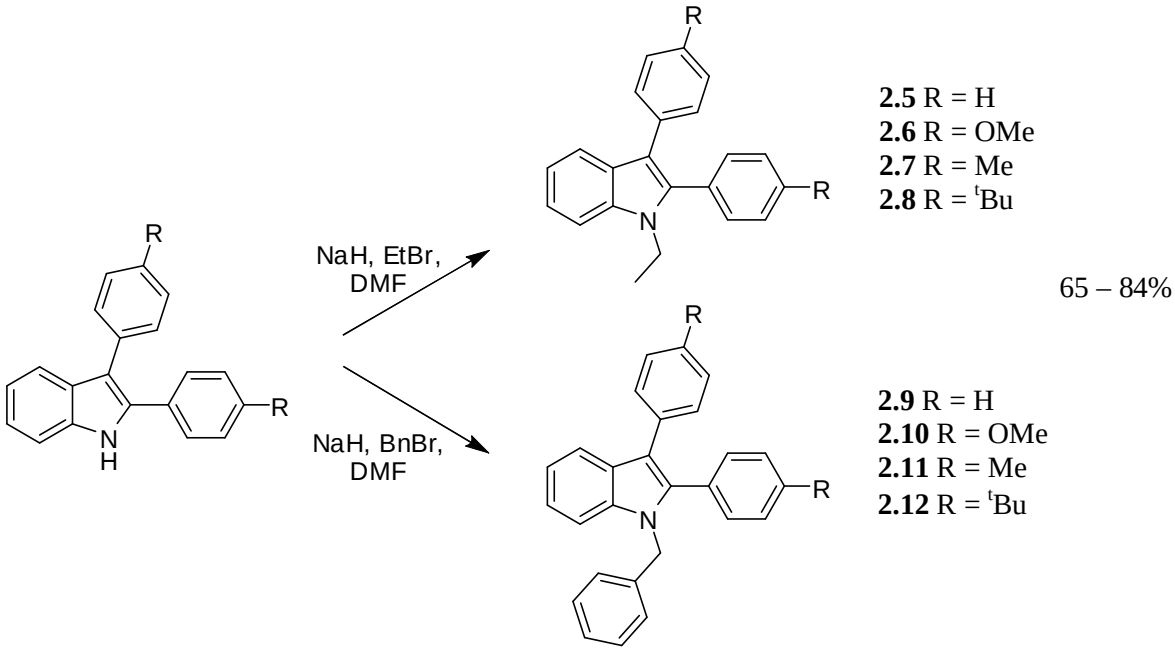

Scheme 2.4. Ethylation and benzylation of N*H*-2,3-diarylindoles.

Crystals of **2.5** were grown by the slow diffusion of methanol into a dichloromethane solution of **2.5**. The crystal structure was solved in the monoclinic space group $P2_1/c$, with one molecule of **2.5** present in the asymmetric unit, shown in figure 2.3a. Much like the crystal structure of **2.3** described above, the phenyl rings in the 2- and 3-positions are twisted out of plane from the central indole core (55.5(1)˚ and 52.8(1)˚ respectively). The large difference in twist angles from the indole core between the 2- and 3-positions seen in the crystal structure of **2.3** are not present in this structure, the phenyl ring in the 2-position is twisted out of plane by just over 3˚ more than the phenyl ring in the 3-position, this is presumably due to differences in crystal packing of the two molecules. The distance between the two ortho carbon atoms, C15 and C17, of the phenyl rings is 3.571(1) Å, a slightly larger distance (~ 0.3 Å) than that observed for **2.3** above. Again the molecules adopt a herringbone packing arrangement, shown in figure 2.3b, due to the N-ethyl substitution there are no N−H···π interactions to further stabilise this packing.

N-ethyl-2,3-bis(4-methoxyphenyl)indole, **2.6**, has been investigated for its potential as an anti-inflammatory agent,[14] and also has been used as fluorescent probe for the estrogen receptor.[25] Surprisingly there has been no report of the synthesis of N-benzyl-2,3-bis(4-methoxyphenyl)indole, **2.10**, despite its ease of synthesis in a reasonable yield (35%) through only two steps from commercially available starting materials.

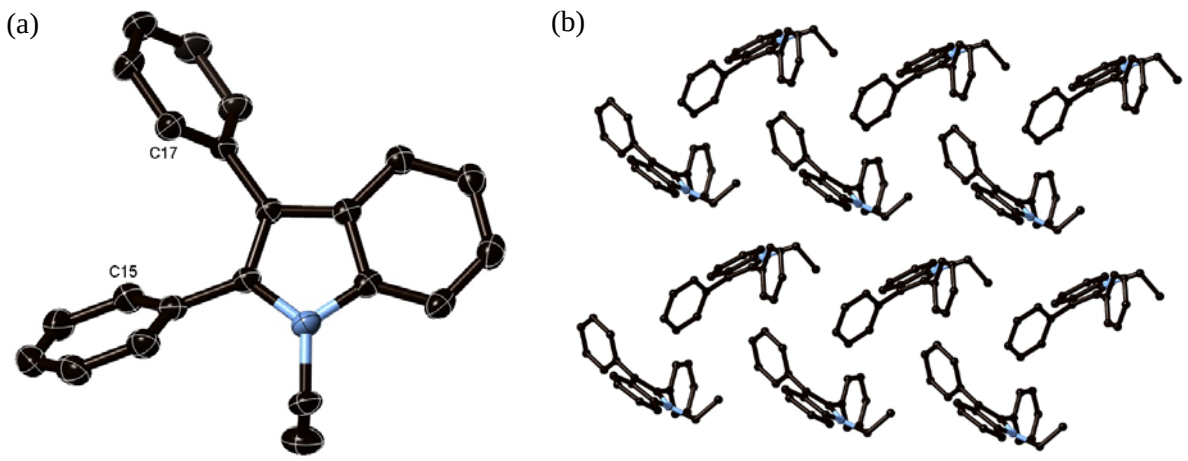

Figure 2.3. (a) Asymmetric unit of **2.5**, (b) herringbone packing of molecules of **2.5**, hydrogen atoms have been removed for clarity.

N-ethyl-2,3-bis(4-methylphenyl)indole, **2.7**, and N-benzyl-2,3-bis(4-methylphenyl)indole, **2.11**, have not been previously reported in the literature. In this study both **2.7** and **2.11** were synthesised in three steps in reasonable overall yield (44% and 41%) from 4-methylbenzaldehyde, and fully characterised. A crystal of **2.11** was obtained by recrystallisation of the bulk material using ethyl acetate and hexane. The crystal structure was solved in the monoclinic space group $P2_1/n$, with one molecule of **2.11** and half a solvent hexane molecule present in the unit cell, as shown in figure 2.4a. As expected the 4-methylphenyl rings at the 2- and 3-position are twisted out of plane relative to the indole core by 48.1(1)˚ and 42.9(1)˚, respectively. The hexane solvent molecule is slightly disordered and does not have any strong interactions with the molecules of **2.11**. The distance between the ortho carbons atoms, C15 and C18, is 3.298(1) Å. The bulky benzyl group prevents the molecules from adopting a herringbone packing arrangement, and adjacent units of **2.11** form only weak face-to-face and edge-to-face π – π interactions through the six membered ring of the indole core and the methylphenyl rings in the 2- and 3-positions of the indole core. The benzyl phenyl ring displays edge-to-face interactions with the five membered ring of the indole core and the 2-methylphenyl ring of adjacent units. The edge-to-face π – π interactions of the benzyl ring of **2.11** are shown in figure 2.4b.

N-ethyl-2,3-bis(4-*tert*butylphenyl)indole, **2.8**, and N-benzyl-2,3-bis(4-*tert*butylphenyl)indole, **2.12**, have not been previously reported in the literature and were fully characterised during the course of this study. Both **2.8** and **2.12** were prepared in three steps in a reasonable overall yield (29% and 28%, respectively) from 4-*tert*butylbenzaldehyde.

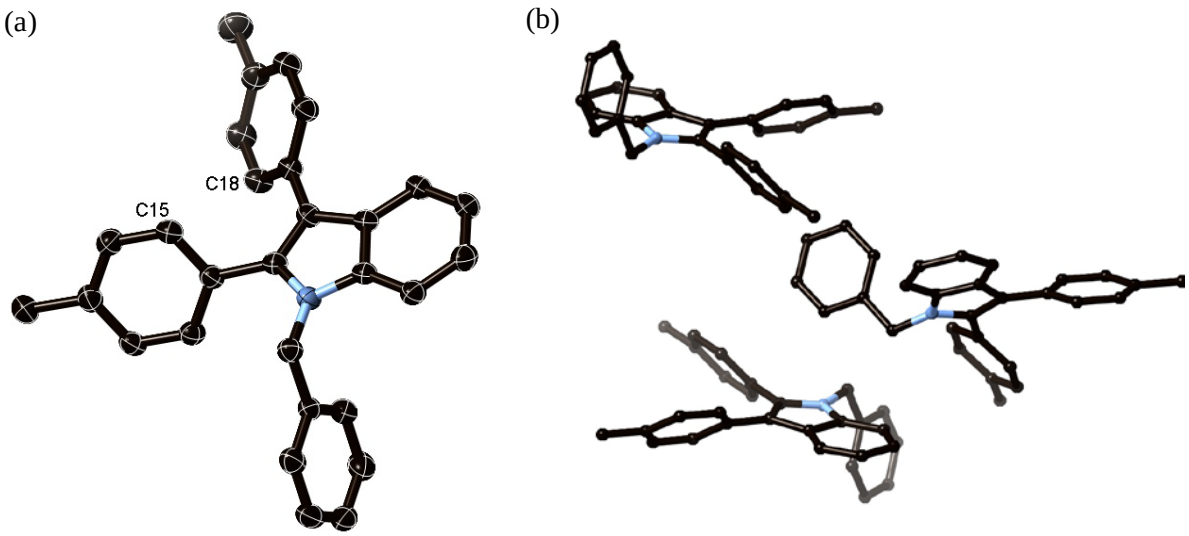

Figure 2.4. (a) Asymmetric unit of **2.11**, (b) π – π interactions between adjacent molecules of **2.11**, solvent molecules and hydrogen atoms have been removed for clarity.

Crystals suitable for X-ray crystallography were grown for both **2.8** and **2.12** by recrystallisation of bulk material from ethyl actetate and hexane. The crystal structures of both **2.8** and **2.12** solved in the monoclinic space group $P2_1/c$, with one molecule present in the asymmetric unit, shown in figure 2.5a and figure 2.5b, respectively. The phenyl rings in the 2- and 3-positions of **2.8** twist out of plane relative to the indole core by 50.3(1)˚ and 48.1(1)˚. The *tert*butyl group of the aryl group in the 3-position of the indole core of compound **2.8** is disordered over two positions because of rotation of this *tert*butyl group, one position has 67% occupancy, and the other 33% occupancy. The twist in the phenyl groups of **2.12** relative to the indole core are similar to **2.8**, 66.2(1)˚ and 39.2(1)˚, respectively, and there is no disorder in the *tert*butyl groups. The distance between the ortho carbon atoms, C15 and C21, are 3.414(1) Å for **2.8**, and 3.616(1) Å for **2.12**. These distances are slightly larger than those observed in the previous crystal structures collected for the 2,3-diarylindoles, **2.3**, **2.5**, and **2.11**, this may be a result of the presence of the bulky *tert*butyl group decorating the periphery of both phenyl rings, crystal packing effects may also be playing a role in the increased distance.

The molecules of **2.8** display edge-to-face π – π interactions between the indole core and phenyl ring in the 2-position (C···centroid distance = 3.527(1) Å), while the ethyl group and *tert*butyl groups have C–H···π interactions with the indole core (C···centroid = 3.415(1) Å and 3.635(1) Å, respectively). The packing of **2.8** is shown in figure 2.6.

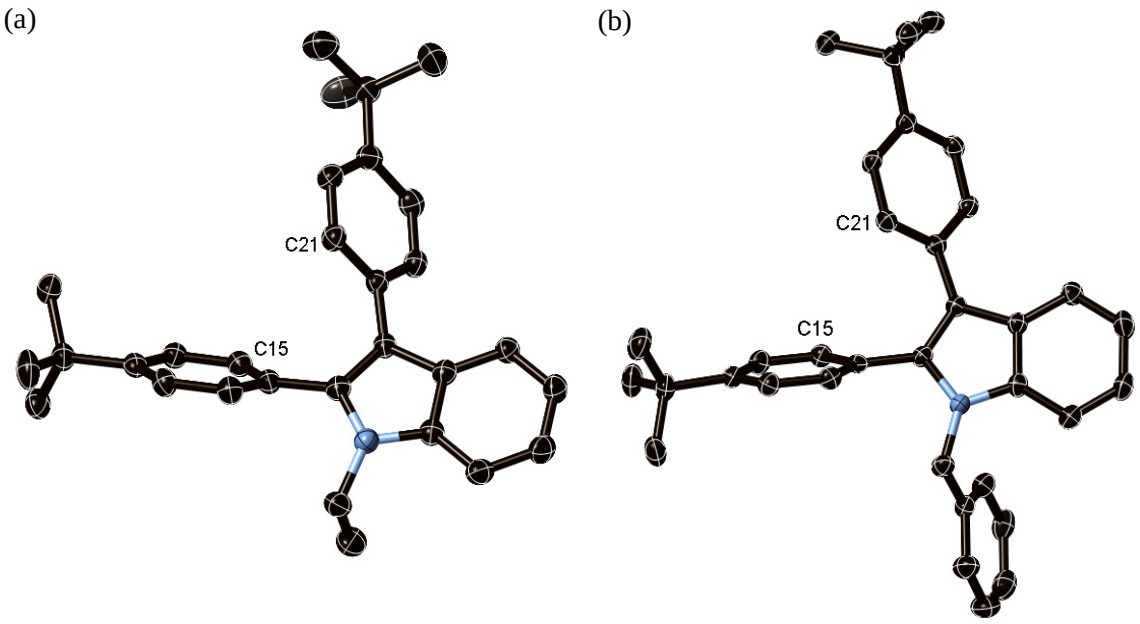

Figure 2.5. (a) asymmetric unit of **2.8**, (b) asymmetric unit of **2.12**, *tert*butyl group disorder not shown and hydrogen atoms have been removed for clarity.

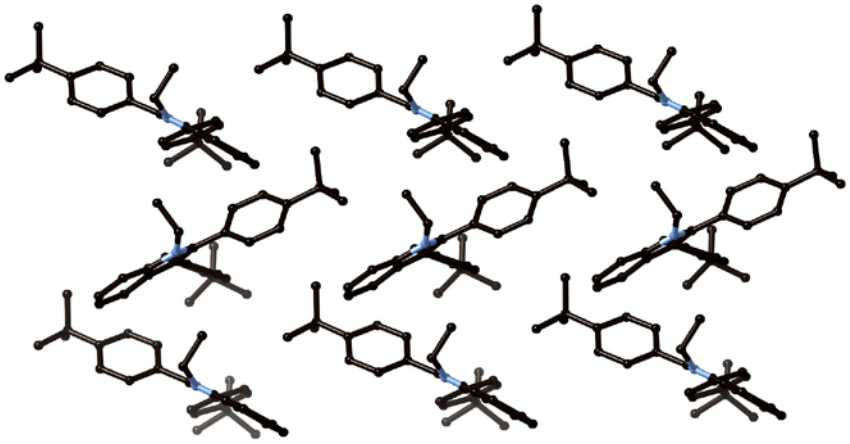

Figure 2.6 Packing of **2.8**, hydrogen atoms have been removed for clarity.

The benzyl substitution has a considerable effect on the packing of **2.12**, in comparison to **2.8**. The bulk of the benzyl group causes molecules of **2.12** to pack in layers, with edge-to-face π – π interactions between the indole core and the 2-phenyl group (C – plane distance = 3.562(1) Å) and weak C – H···π interactions between the *tert*butyl group and the benzyl group (C – plane distance = 4.042(1) Å) are still present in the packing arrangement, shown in figure 2.7.

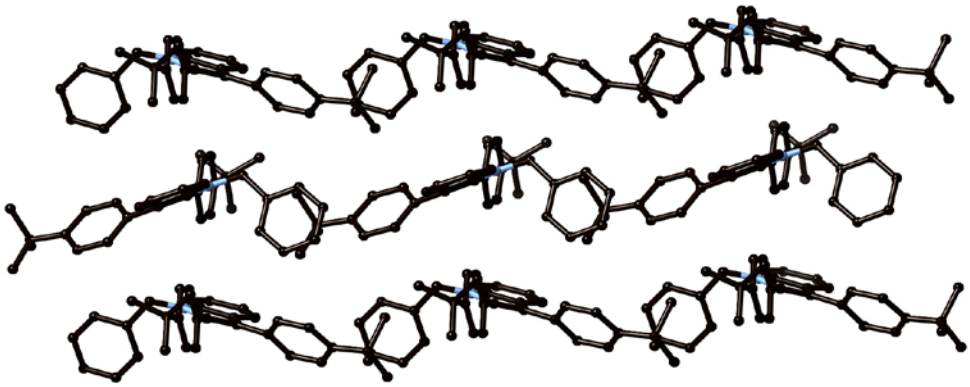

Figure 2.7 Packing of **2.12**, hydrogen atoms have been removed for clarity.

2.2.3 Synthesis of N-phenyl-2,3-diphenylindole, ***2.13***

There are several methods for the synthesis of N-phenyl-substituted indoles, including that of N-phenyl-2,3-diphenylindole. The first report of the synthesis of **2.13** came in 1910,[22] by the condensation of diphenyl amine and benzoin in the presence of $ZnCl_2$. The same paper also reported that **2.13** could also be prepared by the reaction of benzoin with the diphenyl amine hydrochloride salt. More recently transition metals have been employed to form N-substituted indoles, including **2.13**, in one pot.[26,27] Titanium tetrachloride and *tert*butyl amine were used to catalyse a hydroamination based Fischer indole synthesis between aryl hydrazines and alkynes,[26] whilst palladium acetate has been used to catalyse direct and decarboxylative arylations of N-substituted-2-carboxyindoles.[27]

Attempts were made to synthesise **2.13** using diphenyl amine and benzoin in the presence of zinc chloride, but unfortunately only starting materials were recovered, even after refluxing for extended periods. An alternative method to formation of N-substituted-2,3-diphenyl indoles like **2.13** is an Ullmann-type reaction, where a copper catalyst catalyses the reaction between an N*H* indole with the appropriate halosubstituted phenyl group. The Buchwald-Hartwig amination[28,29] is also commonly employed to form carbon-nitrogen bonds between various heterocycles and appropriately halogenated aromatic groups. Many transition metals and conditions have been reported for the direct arylation of the nitrogen atom of the indole ring,[30,31] as well as various other nucleophilic heterocycles.[31,32] Transition metals are not always necessary to catalyse the direct arylation of the nitrogen atom of the indole ring, the use of a only a strong base can also be sufficient, although the subsequent S_NAr reaction often proceeds in low yields.[33] Formation of the appropriate N-substituted indole and then direct arylation at the 2- and 3-positions of the indole core by phenyl boronic acids, catalysed by copper trifluoroactetate, has also been reported.[34]

Transition metal catalyzed Ullmann − type coupling between a halosubstituted benzene and an NH indole derivative was the preferred method as a range of N*H*-2,3-diaryl substituted indoles had already been prepared (**2.1 – 2.4**). With bromobenzene and iodobenzene employed as the haloarene, various reaction conditions were trialled with N*H*-2,3-diphenylindole **2.1**. Both copper oxide and copper iodide were trialled as catalysts for the reaction, with potassium carbonate employed as the base, but in all cases mainly starting material was returned, along with a small amount of unidentified products, none of which corresponded to **2.13**, as judged by mass spectrometry and ^{1}H-NMR spectroscopy.

The transition metal free route of Cano *et al*.[33] was then attempted, using indole as a model for the more sterically hindered N*H*-2,3-diarylindoles. The reaction between iodobenzene and indole in the presence of potassium hydroxide gave N-phenylindole in reasonable yield (43%) after column chromatography. With this encouraging result, **2.1** and iodobenzene were reacted together in the presence of potassium hydroxide, and after column chromatography **2.13** was isolated in low yield (25%). Mass spectrometry confirmed the presence of **2.13** (observed as [**2.13** + Na]$^{+}$), but the ^{1}H-NMR spectrum, shown in figure 2.8, did not match the various, differing spectra reported in the literature.[26,27,35] Although the expected number of protons were present with the expected chemical shift (~ 7.0 – 8.0 ppm) in the ^{1}H-NMR spectrum of **2. 13**, the presence of 2 separate downfield shifted doublets (7.81 ppm and 7.70 ppm) was not reported in the literature, instead one doublet, integrating to one proton, is most commonly reported at ~ 7.95 ppm. The multiplet from 7.40 – 7.05 ppm is normally reported from 7.60 – 7.15 ppm.

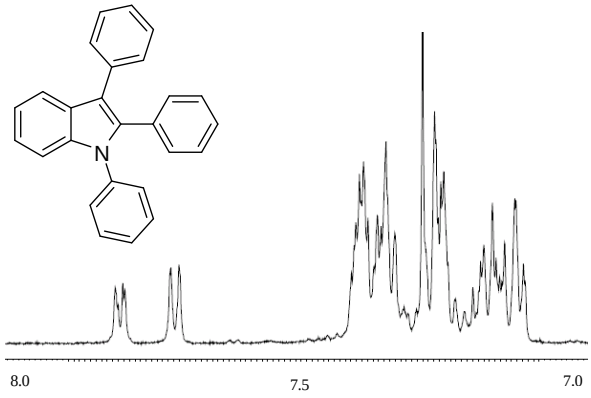

Figure 2.8. ^{1}H-NMR spectrum of the aromatic region of **2.13**.

To confirm the structure of the obtained product crystals suitable for X-ray crystallography were grown from the slow evaporation of a dichloromethane solution. As hoped, the crystal structure confirmed that **2.13** had indeed been synthesised. The structure of **2.13** was solved in the monoclinic space group $P2_1/n$, with one **2.13** molecule present in the asymmetric unit, as shown in figure 2.9a. As might be expected, due to the symmetric nature of the indole ring, the nitrogen atom is disordered over two positions, with

both the 1- and 3-positions occupied by a nitrogen atom 50% of the time, and a carbon atom the other 50% of the time. Like the crystal structures of all N*H* and N-substituted indoles obtained, the three phenyl rings are twisted out of the plane of the indole core by 50.5(1)˚, 48.6(1)˚ and 68.5(1)˚, respectively. The phenyl rings in the 3-position display edge-to-face π – π interactions with an indole core of an adjacent molecule of **2.13** (C to plane distance = 3.542(4) Å and 3.665(5) Å). All three phenyl rings also display edge-to-face π – π interactions with other phenyl rings of adjacent molecules of **2.13**, as shown in figure 2.9b. The ^{1}H-NMR spectrum of the crystals isolated match the ^{1}H-NMR spectrum of the bulk material shown in figure 2.8.

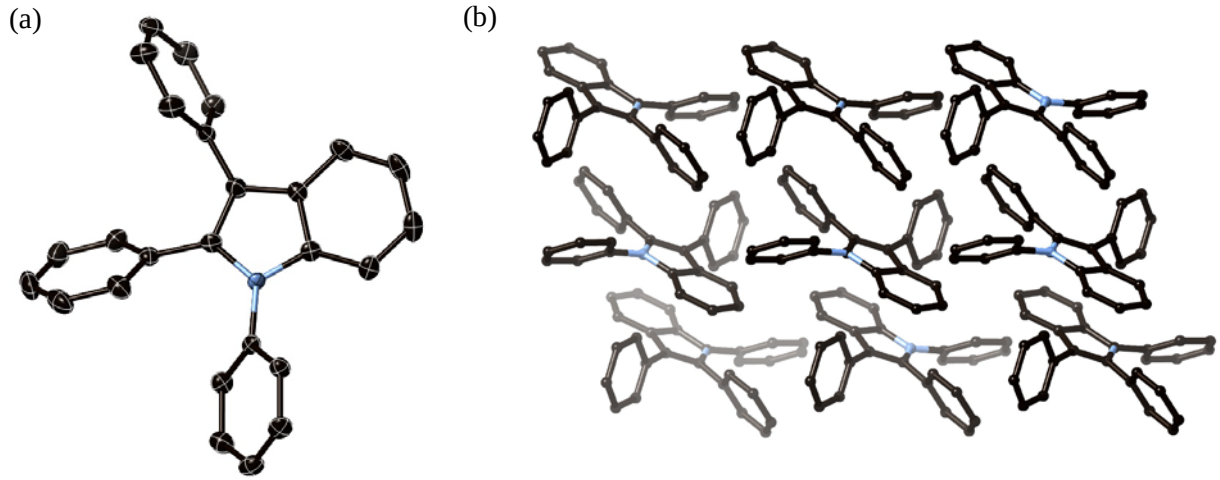

Figure 2.9. (a) Asymmetric unit of **2.13**, (b) packing of **2.13**, showing edge-to-face π – π interactions between adjacent phenyl rings, only one nitrogen atom position is shown and hydrogen atoms have been omitted for clarity.

Compound **2.2** was also used as a starting material, employing the reaction conditions described above in an attempt to produce N-phenyl-2,3-bis(4-methoxyphenyl)indole, **2.14**. After quenching of the reaction **2.14** was detected with mass spectrometry, but could not be isolated cleanly with column chromatography.

2.3 Attempted synthetic routes for the at oxidative cyclodehydrogenation of N-substituted-2,3-diarylindoles using Lewis acidic transition metals

With the protected 2,3-diarylindoles, **2.5** – **2.12**, in hand oxidative cyclodehydrogenation could be investigated. The 2,3-diarylindoles are expected to form only one bond by oxidative cyclodehydrogenation, ie formation of a carbon-carbon bond between the ortho carbons on the phenyl rings in the 2- and 3-position of the indole core, to give the corresponding dibenzo[*a*,*c*]carbazole, as shown in scheme 2.5.

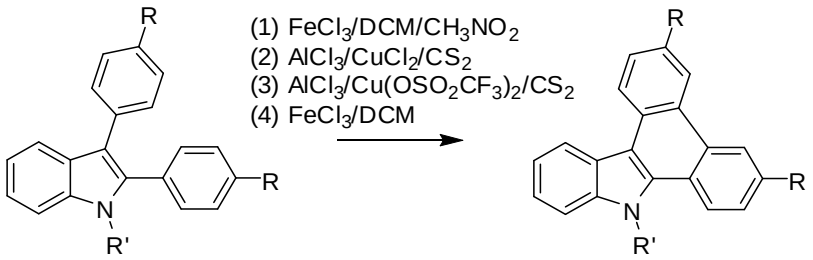

2.15 R = H, R' = Et
2.16 R = OMe, R' = Et
2.17 R = Me, R' = Et
2.18 R = ^{t}Bu, R' = Et

2.19 R = H, R' = Bn
2.20 R = OMe, R' = Bn
2.21 R = Me, R' = Bn
2.22 R = ^{t}Bu, R' = Bn

Scheme 2.5. General scheme and common reagents employed for the formation of dibenzo[*a*,*c*]carbazoles from 2,3-diarylindoles by oxidative cyclodehydrogenation.

The formation of dibenzo[*a*,*c*]carbazole scaffolds from 2,3-diarylindoles is not unprecedented. Photocyclisation of various N*H*-2,3-diphenylindoles with a single methyl substitution at the 5-, 6- or 7-position to produce the corresponding dibenzo[*a*,*c*]carbazole has been previously reported.[12] The conversion of 2,3-diarylindoles to dibenzo[*a*,*c*]carbazoles was reported as early as 1969 by Szmuszkovicz,[13] with the photocyclisation of N*H*-2,3-bis(4-methoxyphenyl)indole, **2.2**, to 3,6-dimethoxy-dibenzo[*a*,*c*]carbazole, **2.24**, outlined in scheme 2.6.

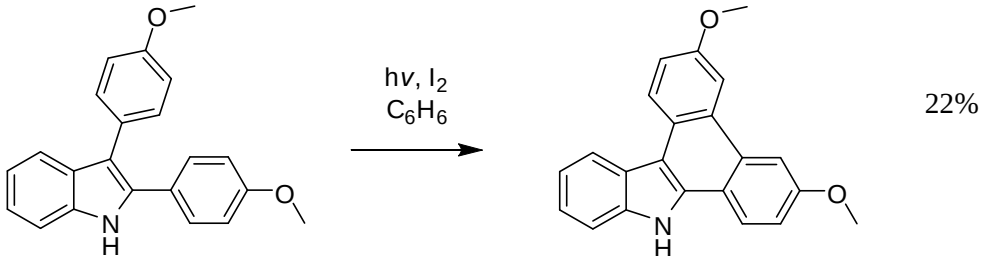

2.2 **2.24**

Scheme 2.6. First reported synthesis of a dibenzo[*a*,*c*]carbazole scaffold from a 2,3-diarylindole.[13]

Although the photocyclisation of the indole core to the corresponding dibenzo[*a*,*c*]carbazole looked to be a facile route for the formation of the desired carbon-carbon bond, the 2,3-diarylindole scaffold was synthesised in this study primarily as a simple model to develop a set of conditions that could be used for the oxidative cyclodehydrogenation of more complex aryl substituted pyrrole architectures using chemical means. Furthermore, there is no literature precedent for the formation of dibenzo[*a*,*c*]carbazoles from 2,3-diarylindoles using oxidative cyclodehydrogenation.

Various reagents have been used for the intramolecular Scholl reaction, with transition metal catalysed reactions using $FeCl_3$, $AlCl_3/CuCl_2$ and $AlCl_3/Cu(OTf)_2$ the most commonly employed. While various

other transition metals, organic reagents and oxidants have been used in the intramolecular oxidative cyclodehydrogenation of all carbon containing precursors,[20] only $FeCl_3$ and $CuCl_2/AlCl_3$ have been used for the successful oxidative cyclodehydrogenation of nitrogen containing precursors.[36, 37] Using these two reagents appeared the natural place to start developing reaction conditions for indole precursors **2.5** – **2.12**. Electron donating substituents, such as methoxy groups and disubstituted amines, have been used to activate precursor molecules towards intramolecular cyclodehydrogenation,[38] and as a result attention was initially focused on the intramolecular oxidative cyclodehydrogenation of compounds **2.6** and **2.10** with $FeCl_3$.

2.3.1 Attempted synthetic routes for oxidative cyclodehydrogenation using $FeCl_3$

The most common literature conditions employed for oxidative cyclodehydrogenation of oligophenylenes involves addition of a nitromethane solution of anhydrous $FeCl_3$ in a large excess (typically eight to 15 times excess of $FeCl_3$ for each carbon-carbon bond to be formed) to an anhydrous dichloromethane solution of the appropriate precursor, with a constant stream of argon bubbling through the solution for the duration of the reaction, typically thirty minutes – four hours.

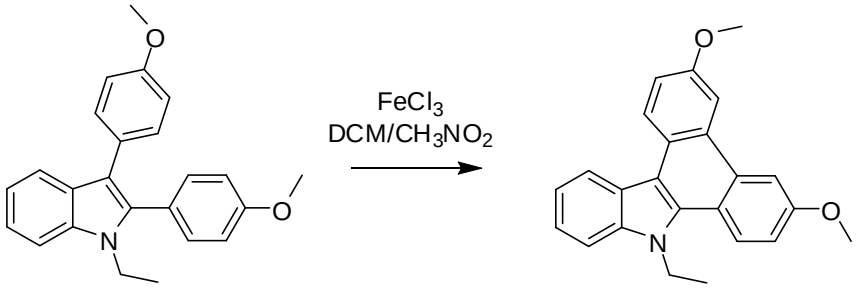

2.6 **2.16**

Scheme 2.7. Attempted conversion of **2.6** into **2.16** using standard literature conditions.

This approach was used as a first attempt for the conversion of **2.6** to 9-ethyl-3,6-dimethoxy-dibenzo[*a*,*c*] carbazole, **2.16**, as shown in scheme 2.7, with an eight times excess of $FeCl_3$ used. The reaction was monitored by TLC, and quenched after 24 hours. ^{1}H-NMR spectroscopy indicates the formation of a mixture of cyclodehydrogenated products, as evidenced by the downfield movement of some protons. Oxidative intramolecular cyclodehydrogenation between two phenyl groups possessing a para substituted methoxy group have been shown to form spirocyclic enone compounds as well as the expected cyclodehydrogenated product. This could be the reason for multiple products being observed in the ^{1}H-NMR spectrum of the crude reaction mixture. Unfortunately, none of the various products could be isolated by purification with column chromatography and the crude reaction mixture was not stable when stored in air and exposed to light, taking on a deep brown colour after 12 hours. The ^{1}H-NMR spectrum

of the brown, oily material showed significant broadening of peaks, perhaps due to stacking of the products and the mixture of products present in the crude product.

The $FeCl_3$ does not need to be added to the reaction as a solution and can instead be introduced to the reaction as a solid.[39] This approach was trialled, in this case a 15 times excess of $FeCl_3$ was used and after 24 hours the reaction was quenched. After purification with column chromatography the ^{1}H-NMR spectrum indicates the isolation of only one cyclodehydrogenated product, albeit in poor yield (12%). The cyclodehydrogenated product was assigned as the expected **2.16**, and the ^{1}H-NMR spectrum of the product is shown in figure 2.10, along with the ^{1}H-NMR spectrum of the precursor indole **2.6** for comparison. As expected the formation of a carbon-carbon bond between the two phenyl rings in the 2- and 3-position has deshielded the adjacent protons moving them significantly downfield, and the appearance of two deshielded singlets also indicates the formation of **2.16**. The protons belonging to the ethyl group and methoxy groups have also moved downfield relative to parent compound **2.6** (ethyl group: 4.75 ppm from 4.13 ppm and 1.66 ppm from 1.28 ppm, methoxy groups: 4.04 ppm and 4.03 ppm from 3.85 ppm and 3.80 ppm). Unfortunately, the light yellow solid isolated decomposes to a dark brown oil when stored in air and exposed to light after 12 hours. Again broadening of the peaks in the ^{1}H-NMR spectrum is observed for this dark brown oil, extra proton peaks are also observed suggesting that the product is possibly decomposing into a less symmetrical product. Attempts to crystallize **2.16** were also unsuccessful, as **2.16** decomposes in solution over the course of 12 hours from a lightly coloured solution to a dark brown solution. Mass spectrometry is consistent with the formation of **2.16**, observed as a radical cation.

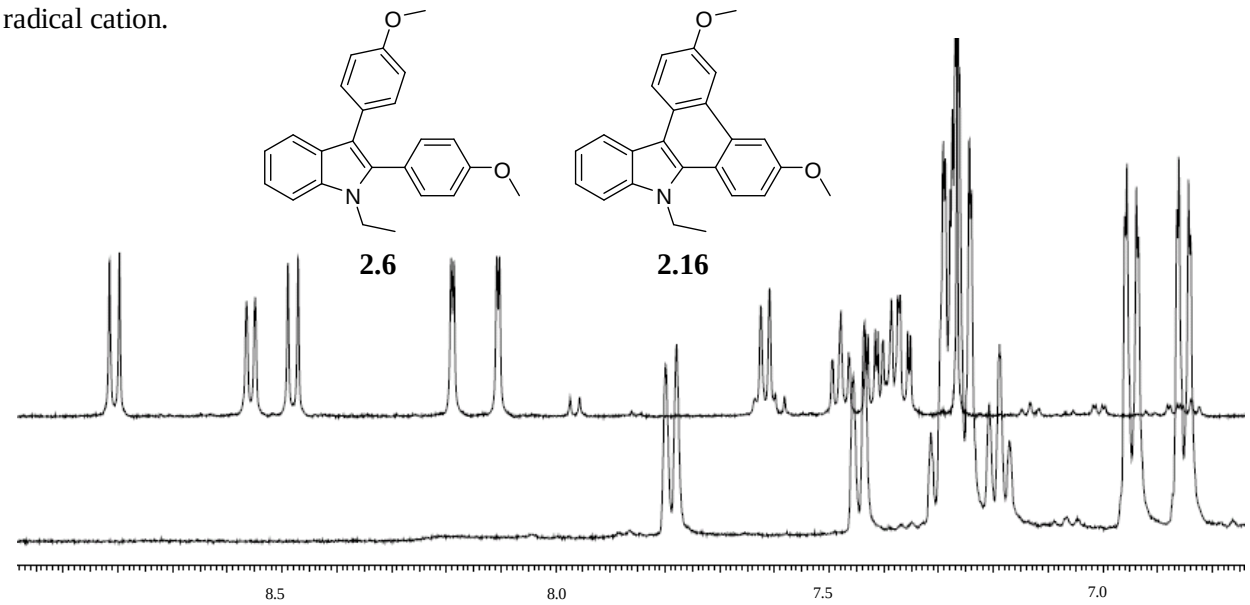

Figure 2.10. ^{1}H-NMR spectrum of the aromatic region of **2.16** and **2.6**, showing the downfield shift of protons in the spectrum of **2.16**. Top spectrum is **2.16**, bottom spectrum is **2.6**.

Despite the instability of **2.16**, $FeCl_3$ has been sucessfully used for the first time to cyclodehydrogenate an N-substituted-2,3-diarylindole to form a dibenzo[*a*,*c*]carbazole. With this result in hand, **2.10** was subjected to the same conditions as above. Pleasingly after purification with column chromatography 9-benzyl-3,6-dimethoxy-dibenzo[*a*,*c*]carbazole, **2.20**, was isolated albeit in low yield (23%). This is the first report of **2.20**, and accordingly the molecule was fully characterised. The aromatic region of the ^{1}H-NMR spectrum of **2.20** is, as expected, similar to **2.16**. The singlet arising from the methylene benzyl group has been shifted considerably downfield from the starting indole **2.10** (~ 0.7 ppm). Like **2.16**, compound **2.20** was also observed to decompose when stored in the presence of air and light, as well as in solution. Decomposition of **2.20** did not happen as rapidly, and as result crystals suitable for X-ray crystallography were able to be grown from the slow diffusion of diisopropyl ether into a benzene solution of **2.20**. Compound **2.20** crystallises in the triclinc space group *P*-1, with one molecule of **2.20** present in the asymmetric unit, as shown in figure 2.11a. The formation of a carbon-carbon bond between the ortho carbons of the phenyl rings in the 2- and 3-positions of the indole (C15···C19 = 1.468(2) Å) has formed the carbazole core and as a result the phenyl groups are forced into planarity. This is in contrast to the considerable twist of the phenyl rings in the 2- and 3-positions out of the plane of the indole core, observed in all parent indole molecules where crystal structures where able to be collected.

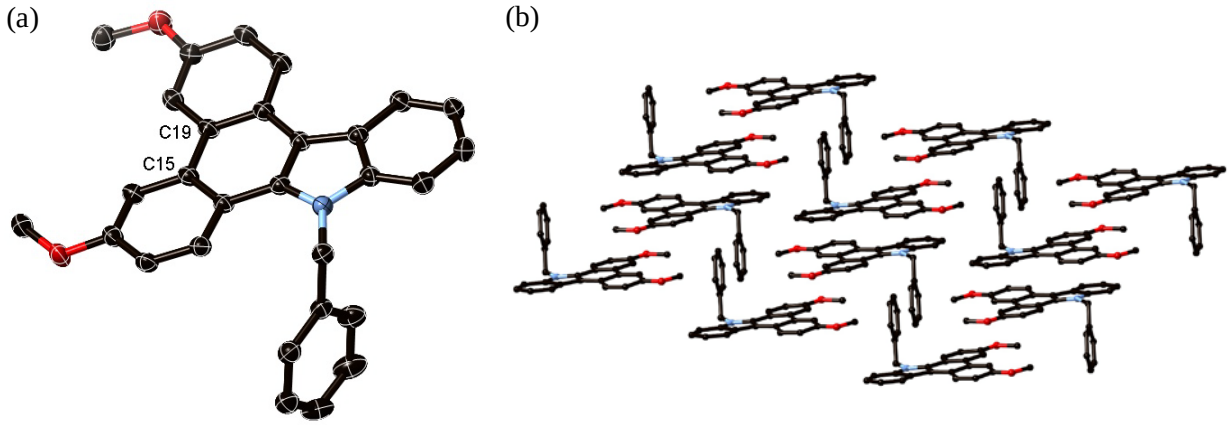

Figure 2.11. (a) Asymmetric unit of **2.20**, (b) packing between adjacent units of **2.20**, hydrogen atoms have been removed for clarity.

As expected from the increased π conjugation molecules of **2.20** pack together with extensive face-to-face π – π interactions, as shown in figure 2.11b. The dibenzo[*a*,*c*]carbazole core displays face-to-face π – π interactions with an adjacent dibenzo[*a*,*c*]carbazole core (centroid···centroid distances range from 3.341(1) Å to 3.498(1) Å) and edge-to-face π – π interactions with a benzyl group of a different molecule (C···centroid distance = 3.732(2) Å). The benzyl groups also interact with the peripheral methoxy groups in an egde on fashion (C···centroid distances range from 3.569(1) Å to 4.041(2) Å).

The set of conditions described above was then used to investigate the oxidative cyclodehydrogenation of the remaining benzyl protected 2,3-diarylindoles **2.9**, **2.11** and **2.12**, as **2.10** appeared to be more stable than **2.6** once isolated. Unfortunately, in each case low yields of cyclodehydrogenated products (as judged by the integrals of downfield shifts of protons relative to the precursor indole in the ^{1}H-NMR spectra of the crude reaction mixture) and the formation of multiple products prevented the isolation of any of the corresponding dibenzo[*a,c*]carbazoles. The use of $FeCl_3$ in the Scholl reaction of oligophenylenes to form all carbon planar structures is often reported to suffer from undesirable chlorination on the periphery of the molecules.[40] This may be the cause of the multiple products found in the ^{1}H-NMR spectrum of these reactions. Adding $FeCl_3$ as a solid may also lower the yield of the reactions, as $FeCl_3$ has a low solubility in dichloromethane, although as mentioned above, dissolving the $FeCl_3$ in nitromethane prior to addition into the reaction mixture did not lead to any products that were able to be isolated.

The reaction of compound **2.11** with $FeCl_3$ dissolved in nitromethane was attempted, two cyclodehydrogenated products were observed with ^{1}H-NMR spectroscopy, but they could not be seperated by column chromatography. Mass spectroscopy did not show any formation of the expected dibenzo[*a,c*]carbazole and the peaks present in the mass spectrum could not be assigned to any cyclodehydrogenated products, despite the observation of downfield shifted protons and the appearance of downfield shifted singlets consistent with the formation of dibenzo[*a,c*]carbazoles. This could be due to decompostion of the material in solution before the mass spectrum could be measured, and the seperation was not further persued.

Despite being unable to isolate any more dibenzo[*a,c*]carbazoles from the corresponding benzyl protected 2,3-diarylindole precursors, attempts were made at the formation of dibenzo[*a,c*]carbazoles from the prepared ethyl protected 2,3-diarylindole precursors **2.5**, **2.7** and **2.8**. Again $FeCl_3$ was used, both as a solid, and dissolved in nitromethane before addition to the reaction mixture. Unfortunately, in the case of **2.5** and **2.7** no cyclodehydrogenated products could be isolated from either of the reaction conditions. Compound **2.8** was reacted with 15 times equivalence of solid $FeCl_3$. After quenching the reaction and purification with column chromatography the ^{1}H-NMR spectrum of the isolated solid appears to be 9-ethyl-3,6-di*tert*butyl-dibenzo[*a,c*]carbazole, **2.18**, and peaks corresponding to $[M^{\cdot}]^{+}$ and $[MH]^{+}$ are observed in the mass spectrum. Decolouration of **2.18** to a brown oil occurs over 24 hours, as observed with **2.16** again suggesting that the ethyl substituted dibenzo[*a,c*]carbazoles formed through oxidative cyclodehydrogenation with $FeCl_3$ are not stable when isolated.

To further investigate the use of $FeCl_3$ for the cyclodehydrogenation of 2,3-diarylindole molecules **2.2** and **2.4** were subjected to the successful cyclodehydrogenation conditions (i.e. 15x equivalents of $FeCl_3$ added as a solid to the reaction mixture) described above. The ^{1}H-NMR spectrum and mass spectroscopy for both of the crude reaction mixtures did not indicate any cyclodehydrogenation, although mass spectroscopy does show a peak close to the expected mass for the dimerisation of starting materials. Unfortunately, this peak could not be assigned to a reasonable dimer product and purification did not lead to any clean product. Very recently a product corresponding to dimerisation and cyclodehydrogenation of a N*H* pyrrole compound has been isolated in good yield (71%) using similar conditions for the Scholl reaction.[41] Four equivalents of $FeCl_3$ were used to form three carbon-carbon bonds (two cyclodehydrogenation reactions and one dimerisation).

2.3.2 Attempted synthetic routes for oxidative cyclodehydrogenation using $AlCl_3$/oxidant

Clearly, low yields, the formation of multiple products, problematic separation, isolation of cyclodehydrogenated products and decomposition of the isolated products indicates that the cyclodehydrogenation of N-substituted-2,3-diarylindoles using $FeCl_3$ is not ideal. Use of $AlCl_3$ with either $CuCl_2$ or $Cu(OTf)_2$ as the terminal oxidant is also a route known to produce polycyclic aromatic molecules from oligophenylene precursors,[20] and also heterocyclic precursors.[37] Both $AlCl_3$/$CuCl_2$ and $AlCl_3$/$Cu(OTf)_2$ were used in attempts to form **2.16** from precursor **2.6**. In both cases the reactions were run in degassed CS_2, monitored with TLC and quenched after 4 days, as the TLC did not show any changes after this time. In each case no products could be isolated from the reaction mixture and ^{1}H-NMR spectroscopy indicated little to no formation of cyclodehydrogenated product in each case.

Attempts at oxidative intramolecular cyclodehydrogenation with transition metal lewis acids and oxidants using 2,3-diarylindoles as model systems for arylsubstituted pyrrole molecules has illustrated the difficulty in the control of the Scholl reaction often alluded to in the literature.[38] Despite the successful formation of three dibenzo[*a*,*c*]carbazoles from 2,3-diarylindoles the reaction is not high yielding and purification of products is difficult. Subsequent chapters will detail attempts at oxidative cyclodehydrogenation through various chemical means of other heterocyclic model systems.

2.4 Photocyclisation of 2,3-diarylindole derivatives

Despite reports on the formation of dibenzo[*a*,*c*]carbazoles from N*H*-2,3-diarylindoles in the late 1960's and early 1970's using photochemical techniques, no further reports on the photocyclisation of 2,3-diarylindoles have appeared. There are only two cases where N-substituted-2,3-diarylindoles have been used to form the corresponding 9-substituted-dibenzo[*a*,*c*]carbazoles, both cases were reported by Mudry

and Frasca in the same 1974 paper,[12] 9-phenyl-dibenzo[*a*,*c*]carbazole, **2.28**, and 9-methyl-dibenzo[*a*,*c*]carbazole, **2.29**, were obtained in 77% and 65% yield respectively from the photocyclisation of the corresponding N-substituted-2,3-diphenylindoles **2.13** and **2.27**.

Interestingly, two minor products are also observed when **2.27** and **2.13** were subjected to photocyclisation conditions, as shown in scheme 2.8. For both cases Mudry and Frasca hypothesise that that the photooxidation to form **2.32** and **2.33**, and the photooxidation and bond cleavage to form **2.30** and **2.31** is a result of the substitution on the nitrogen atom of the 2,3-diarylindole. The photocyclisation to form **2.28** and **2.29** occurs in the singlet state, whilst Mudry and Frasca speculate that N-substitution facilitates intersystem crossing to the triplet state, allowing photooxidation with ground state oxygen (rather than photooxidation arising from the reaction of singlet oxygen with ground state indole molecules) to occur. These photooxidation products are not observed when the nitrogen atom of the indole is unsubstituted. It is also interesting to note that in the case of **2.13** only one carbon-carbon bond is formed between the ortho carbon atoms of the phenyl rings in the 2- and 3-position. It appears that there is no interaction with the ortho carbon of the phenyl group substituted on the nitrogen atom. No explanation is given in the text, although the lack of carbon-carbon bond formation could be a result of electronic effects, spin states resulting from the nitrogen substitution or that the there is not enough stillbene character between the nitrogen atom and C2 to facilitate another photocyclisation.

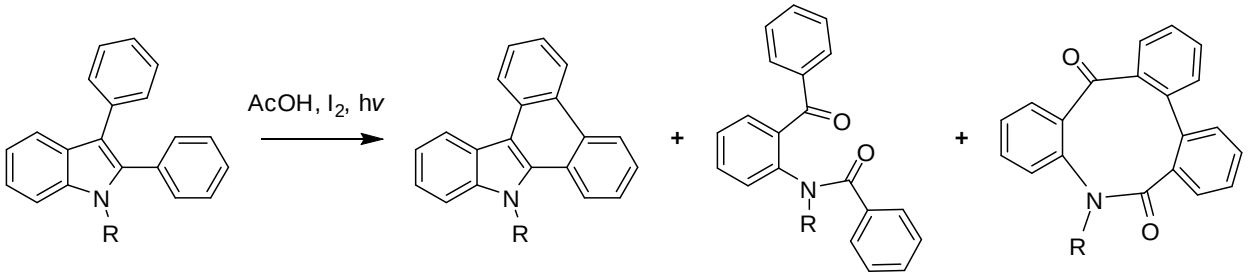

2.13 R = Ph	**2.28** R = Ph (77%)	**2.30** R = Ph (14%)	**2.32** R = Ph (10%)
2.27 R = Me	**2.29** R = Me (65%)	**2.31** R = Me (25%)	**2.33** R = Me (1%)

Scheme 2.8. Photocyclisation products of **2.13** and **2.27** as reported by Mudry and Frasca.[12]

As well as photocyclisation of 2,3-diarylindoles, dibenzo[*a*,*c*]carbazoles have previously been synthesised through a variety of methods. Larock has pioneered the synthesis of fused polycyclic aromatics by palladium catalysed annulations of arynes and 2-halobiaryls.[42] When the biaryl used is a 3-(2-iodophenyl)indole, the resulting product is a dibenzo[*a*,*c*]carbazole, obtained in high yields. Palladium catalysis is also used for the intramolecular cyclisation of 2-(2-bromoaryl)-3-arylindole compounds into the corresponding dibenzo[*a*,*c*]carbazoles.[43] Photomediated cyclisation of diarylamide anions has also been used to synthesise dibenzo[*a*,*c*]carbazoles.[44]

With 2,3-diarylindoles **2.3** – **2.12** already in hand, photocyclisation of these precursors was carried out. The photocyclisation of **2.1** and **2.2** is already known.[12,13] All photocyclisation reactions were carried out in a Rayonet photoreactor irradiating with 300nm light over 12 hours. All reactions were performed in a quartz tube with toluene as the solvent, 1.1 equivalents of I_2 and 5mL of propylene oxide were used in each case.[45] A constant stream of argon was bubbled through the reaction solution for the duration of the reaction to remove oxygen.

*2.4.1 Photocyclisation of NH-2,3-diarylindoles **2.3** and **2.4***

Initially, N*H*-2,3-diarylindoles **2.3** and **2.4** were subjected to the photocyclisation conditions described above. Pleasingly, after washing the reaction mixture with a solution of sodium thiosulfate to remove the excess I_2, and purification with column chromatography, the previously unreported 3,6-dimethyl-dibenzo[*a*,*c*]carbazole, **2.25**, and 3,6-di*tert*butyl-dibenzo[*a*,*c*]carbazole, **2.26**, were isolated in reasonable yields of 58% and 40%, respectively. Both compounds were fully characterised, and each ^{1}H-NMR spectrum displayed significant downfield shifting of protons.

Crystals of **2.26** suitable for X-ray crystallography were obtained by recrystallisation from ethyl actetate and hexanes. Compound **2.26** crystallises in the monoclinic space group $P2_1/c$, with one molecule of **2.26** present in the asymmetric unit, as shown in figure 2.12a. Like the crystal structure of **2.20**, the formation of a dibenzo[*a*,*c*]carbazole core by forming a carbon-carbon bond between the ortho carbon atoms of the phenyl rings in the 2- and 3-positions (C15···C21 = 1.465(2) Å) has planarised these phenyl groups with respect to the original indole core. The molecules of **2.26** pack together in layers, displaying extensive face-to-face (centroid to centroid distances = range from 3.335(2) Å to 3.505(2) Å) π – π interactions with one adjacent dibenzo[*a*,*c*]carbazole core, much like those observed in the packing of **2.20**, and shown in figure 2.12b. The N*H* group of the carbazole core is prevented from participating in any hydrogen bonding interactions due to the bulkiness of the two peripheral *tert*butyl groups, preventing close contacts with another moiety. The bulky *tert*butyl groups participate in C–H···π interactions with two adjacent molecules (C···centroid distances = 3.483(1) Å and 3.689(1) Å).

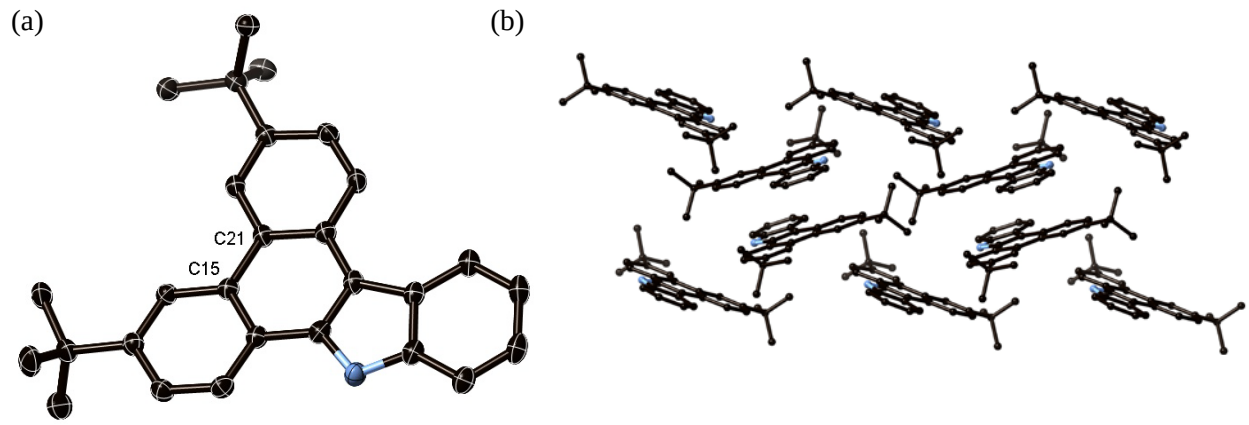

Figure 2.12. (a) Asymmetric unit of **2.26**, (b) crystal packing of **2.26**, hydrogen atoms have been removed for clarity.

*2.4.2 Photocyclisation of N-ethyl-2,3-diarylindoles **2.5** – **2.8***

With the successful photocyclisation of N*H*-2,3-diarylindoles **2.3** and **2.4** the N-ethyl-2,3-diarylindoles **2.5** – **2.8** were then subjected to the standard photocyclisation conditions described above. With argon used to degass the reaction mixture before and during irradiation it was hoped that no photooxidation products would be isolated as products, and indeed this was the case. All 9-ethyl-dibenzo[*a*,*c*]carbazoles, **2.15** – **2.18**, were isolated in moderate to good yields after column chromatography (64%, 60%, 87% and 89% respectively). All four compounds **2.15** – **2.18** have not previously appeared in the literature and were fully characterised during the course of this study.

The ^{1}H-NMR spectra of the aromatic region for all four compounds are shown in figure 2.13a − d, the ^{1}H-NMR spectrum of **2.16** formed by photocyclisation matched the ^{1}H-NMR spectrum of **2.16** formed by oxidative cyclodehydrogenation with solid $FeCl_3$. The three compounds **2.16** − **2.18** have methoxy, methyl and *tert*butyl substitution at the 3- and 6-position of the dibenzo[*a*,*c*]carbazole core, respectively. This substitution gives rise to a recognizable pattern of the proton environments in the ^{1}H-NMR spectrum from 8 ppm downfield. In each case two downfield shifted singlets and three down field shifted doublets are observed. The two ethyl resonances observed at ~ 4.1 ppm and ~ 1.3 ppm in the starting indole compounds also shift downfield to ~ 4.9 ppm and ~ 1.7 ppm respectively. All proton peaks in all four spectra are able to be assigned through 2-dimensional COSY and TOCSY experiments. A high resolution mass spectrum was measured for all four compounds, with $[MH]^+$ and $[M^{\cdot}]^+$ peaks observed in all cases apart from **2.16**, where only $[MH]^+$ is observed. All data is consistent with the formation of **2.15** – **2.18**.

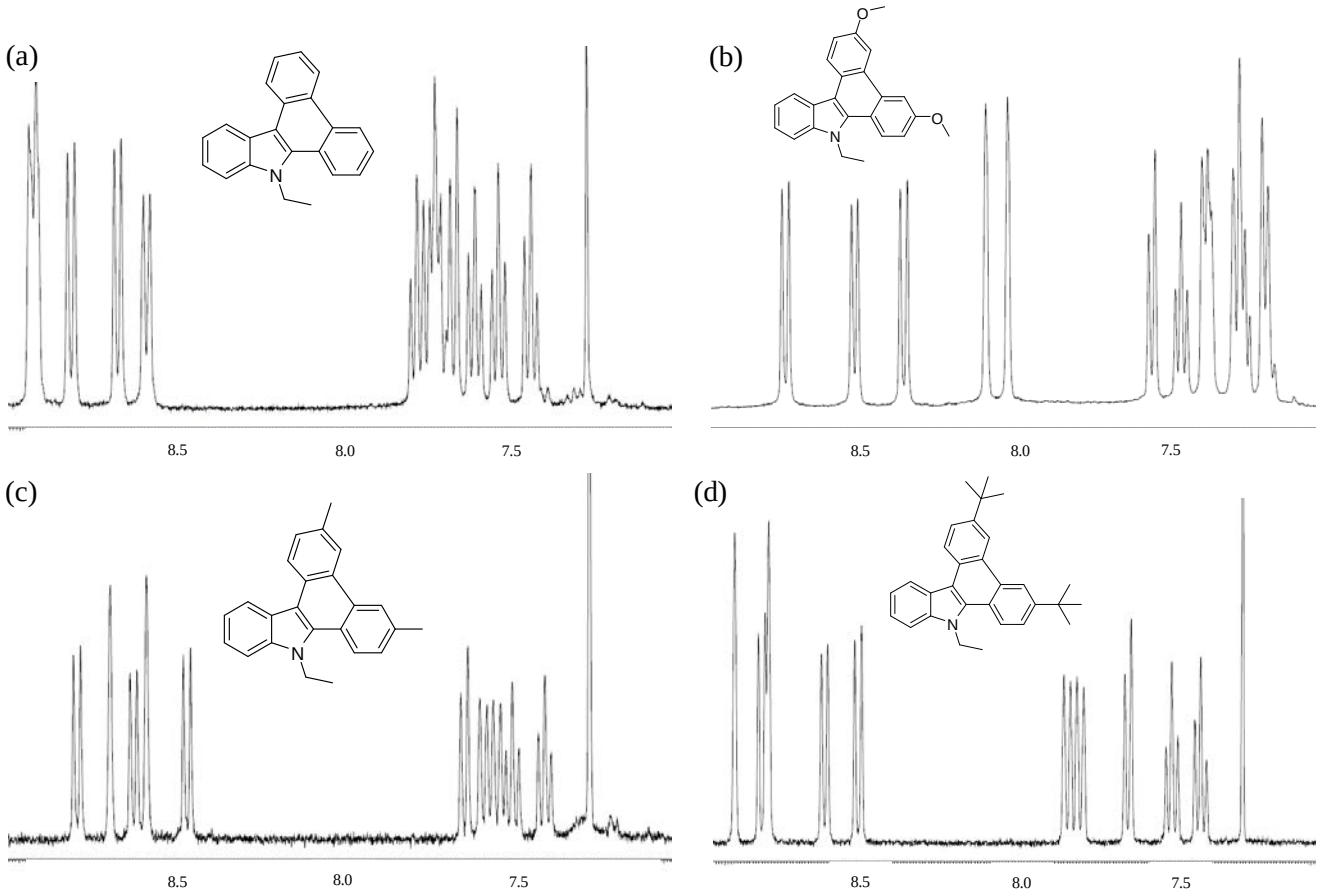

Figure 2.13. ^{1}H-NMR spectra of the aromatic region of 9-ethyl-dibenzo[*a*,*c*]carbazoles, (a) **2.15**, (b), **2.16**, (c) **2.17**, (d) **2.18**.

Crystals of **2.15** suitable for X-ray crystallography were obtained by recrystallisation with ethyl actetate and hexanes. Compound **2.15** crystallises in the monoclinic space group $P2_1/c$, with one molecule of **2.15** present in the asymmetric unit, as shown in figure 2.14a. The carbon-carbon bond formed (C15···C17 = 1.465(2) Å) is comparable to the corresponding carbon-carbon bond lengths in the crystal structures of **2.20** and **2.26**. Comparison to the crystal structure obtained for the precursor 2,3-diarylindole **2.5** reveals that the carbon-carbon distance between C15 and C17 for **2.5** is 3.571(1) Å due to the twisting of the phenyl rings out of the plane of the indole core. The photocyclisation to form a carbon-carbon bond between these two atoms has brought C15 and C17 over 2.1 Å closer together, and twist angles between the phenyl groups and the indole core have reduced from 124.5(1)˚ and 127.2(1)˚ in compound **2.5** to 2.4(1)˚ and 5.0(1)˚ respectively in compound **2.15**.

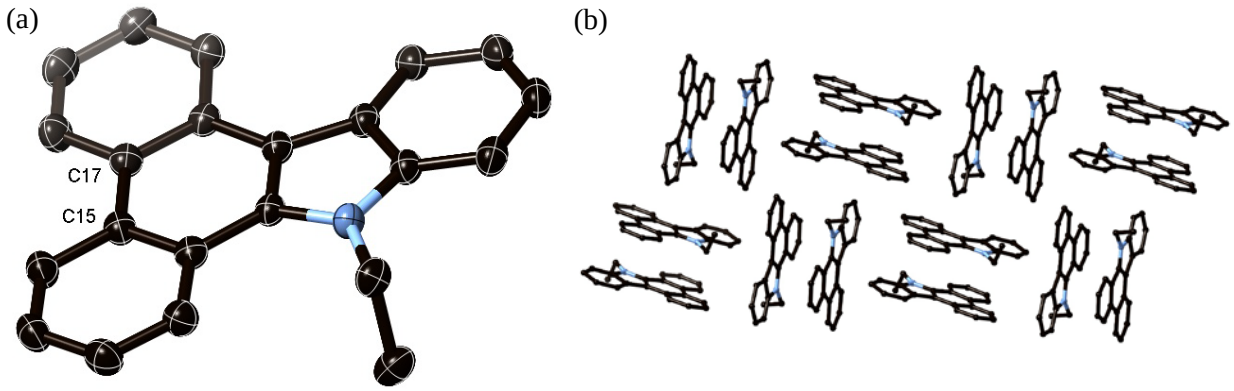

Figure 2.14. (a) Asymmetric unit of **2.15**, (b) edge-to-face and face-to-face π – π crystal packing interactions between molecules of **2.15**, hydrogen atoms have been removed for clarity.

Again each molecule of **2.15** displays face-to-face π – π interactions with one other molecule of **2.15** (centroid to centroid distances range from 3.412(1) Å and 3.518(1) Å). Each molecule of **2.14** also displays edge-to-face π – π interactions with two other adjacent molecules of **2.15** (carbon to centroid distances range from 3.670(1) Å to 3.877(1) Å). These packing interactions are shown in figure 2.14b. The ethyl group does not have any strong interactions with adjacent molecules.

Crystals suitable for X-ray diffraction were also obtained by the recrystallisation of **2.17** from ethyl acetate and hexanes. Compound **2.17** crystallises in the orthorhombic space group *Pbca*, with one molecule of **2.17** present in the asymmetric unit, shown in figure 2.15a. As expected the newly formed carbon-carbon bond (C15···C18 = 1.465(2) Å) is comparable to bond lengths of the newly formed bond in the crystal structures obtained for compounds **2.15**, **2.20** and **2.26**. The crystal packing is dominated by edge-to-face π – π interactions (C to centroid distances range from 3.752(2) Å to 3.795(2) Å) and C–H···π interactions involving the peripheral methyl groups of compound **2.17** (C to centroid interactions range from 3.467(2) Å to 3.681(2) Å), shown in figure 2.15b. Slipped face-to-face π – π interactions are also present between adjacent dibenzo[*a*,*c*]carbazole cores (centroid to centroid distances range from 3.487(2) Å to 3.535(2) Å).

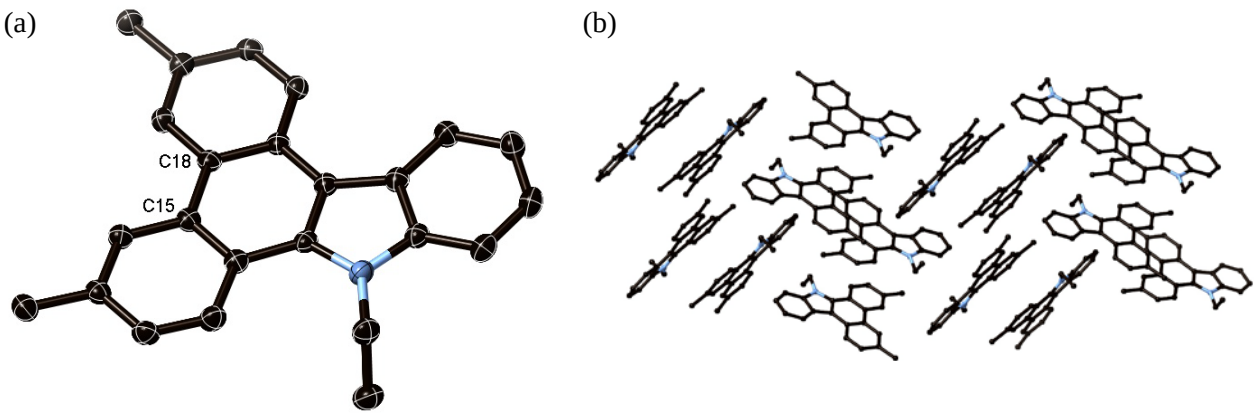

Figure 2.15. (a) Asymmetric unit of **2.17**, (b) crystal packing of **2.17**, hydrogen atoms have been removed for clarity.

*2.4.3 Photocyclisation of N-benzyl-2,3-diarylindoles **2.9** – **2.12***

With the successful isolation of compounds **2.15** – **2.18** from the corresponding 2,3-diarylindoles **2.5** – **2.8** in good yields without formation of any undesirable photooxidation products, the photocyclisation of N-benzyl-2,3-diarylindoles **2.9**, **2.11** and **2.12** was carried out under the standard photocyclisation conditions. Each of the three 2,3-diarylindole precursors, **2.9**, **2.11** and **2.12**, produced the corresponding 9-benzyl-dibenzo[*a*,*c*]carbazoles, **2.19**, **2.21** and **2.22** in 84%, 56% and 78% respectively. Although **2.20** was already been prepared from **2.10** by oxidative cyclodehydrogenation in low yields (23%) using $FeCl_3$, **2.20** was also prepared by photocyclisation of **2.10** in a considerably higher yield of 62%. Again all four compounds **2.19** – **2.22** have not been previously reported in the literature and accordingly they were fully characterised during the course of this study.

Shown in figure 2.16a – d is the aromatic region of the ^{1}H-NMR spectra for all four compounds. In each case the singlet arising from the methylene benzyl protons is shifted downfield (observed at ~ 6.0 ppm) from the precursor 2,3-diarylindole (observed at ~ 5.3 ppm). As in the case of the 9-ethyl-3,6-disubstitued-dibenzo[*a*,*c*]carbazoles, **2.16** – **2.18**, the three 9-benzyl-3,6-disubstituted-dibenzo[*a*,*c*]carbazoles, **2.20** – **2.22**, all display two newly formed singlets and three additional doublets significantly shifted downfield. The ^{1}H-NMR spectra of **2.19** – **2.22** were considerably harder to assign than the 9-ethyl-dibenzo[*a*,*c*]carbazoles due to the presence of additional proton resonances from the benzyl group overlapping with the remaining carbazole peaks. A high resolution mass spectrum was measured for all four compounds, with $[MH]^+$ and $[M\cdot]^+$ peaks observed in all cases apart from **2.19**, where only $[MH]^+$ is observed. All data is consistent with the formation of **2.19** – **2.22**.

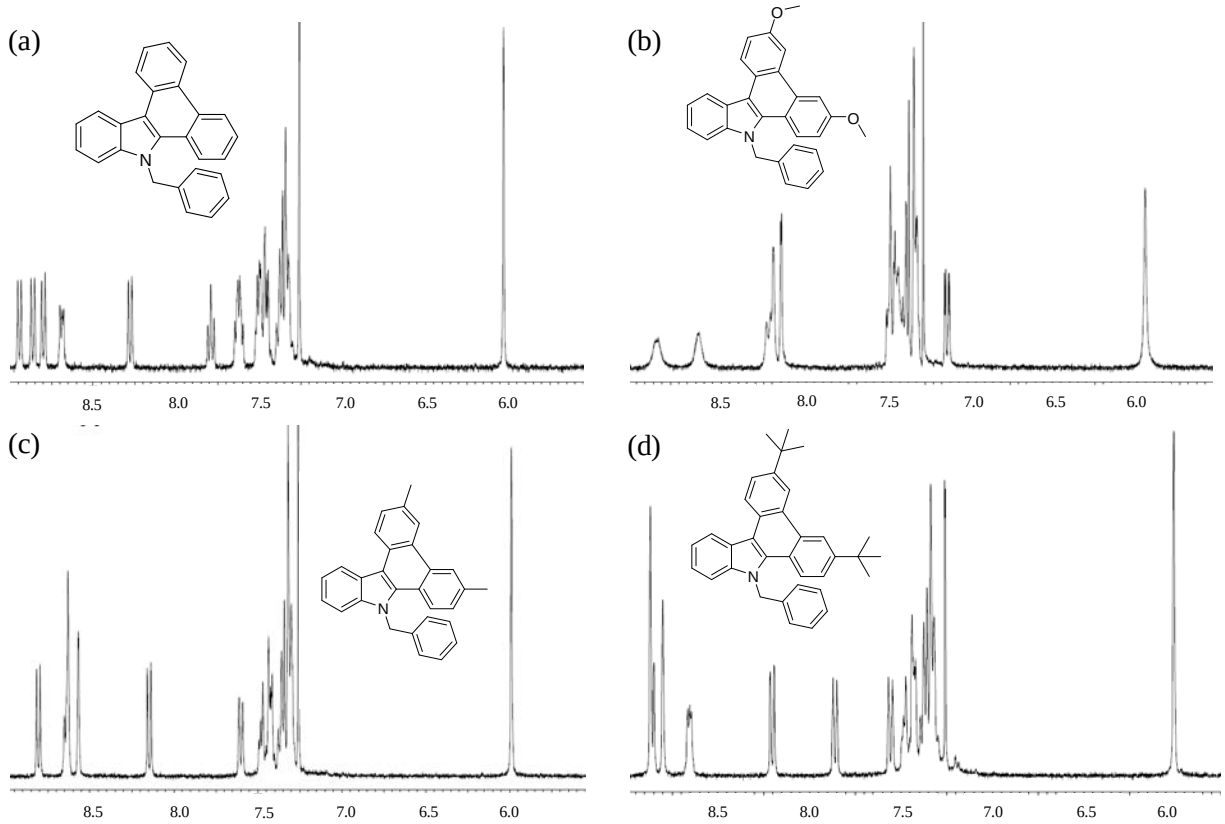

Figure 2.16. ^{1}H-NMR spectra of the aromatic region of 9-benzyl-dibenzo[*a*,*c*]carbazoles, (a) **2.19**, (b), **2.20**, (c) **2.21**, (d) **2.22**.

Crystals of **2.21** were isolated by recrystallisation using ethyl acetate and hexanes. The crystal structure was solved in the triclinic space group *P*-1, with one molecule of **2.21** present in the asymmetric unit, shown in figure 2.17a. The carbon-carbon bond formed during the course of the reaction (C15···C18 = 1.461(3) Å) is a similar distance to the other four crystal structures of dibenzo[*a*,*c*]carbazoles obtained, **2.15**, **2.17**, **2.20** and **2.26**. In comparison to the crystal structure of **2.11**, the distance between C15 and C18 has decreased by ~ 1.8 Å (C15 ··· C18 = 3.298(1) Å for **2.11**), this is comparable to the ~ 2.1 Å difference in the distance between C15 and C17 seen in the crystal structures of **2.5** and **2.15**. The molecules of **2.21** pack together with slipped face-to-face (centroid to centroid distances = 3.536(1) Å and 3.551(1) Å) and C–H···π (C to centroid distances = 3.642(2) Å and 3.892(3) Å) interactions dominating. These interactions form layers of **2.21**, with the benzyl group displaying edge-to-face π – π interactions (C to centroid distance = 3.778(2) Å) with a molecule of **2.21** in a neighbouring stack, as shown in figure 2.17b. This packing arrangement is different from both the corresponding 9-ethyl-dibenzo[*a*,*c*] carbazole, **2.17**, and the precursor 2,3-diarylindole, **2.11**, possibly due to a combination of the bulkiness of the benzyl group and the more extended π system resulting from the formation of the carbon-carbon bond between C15 and C18.

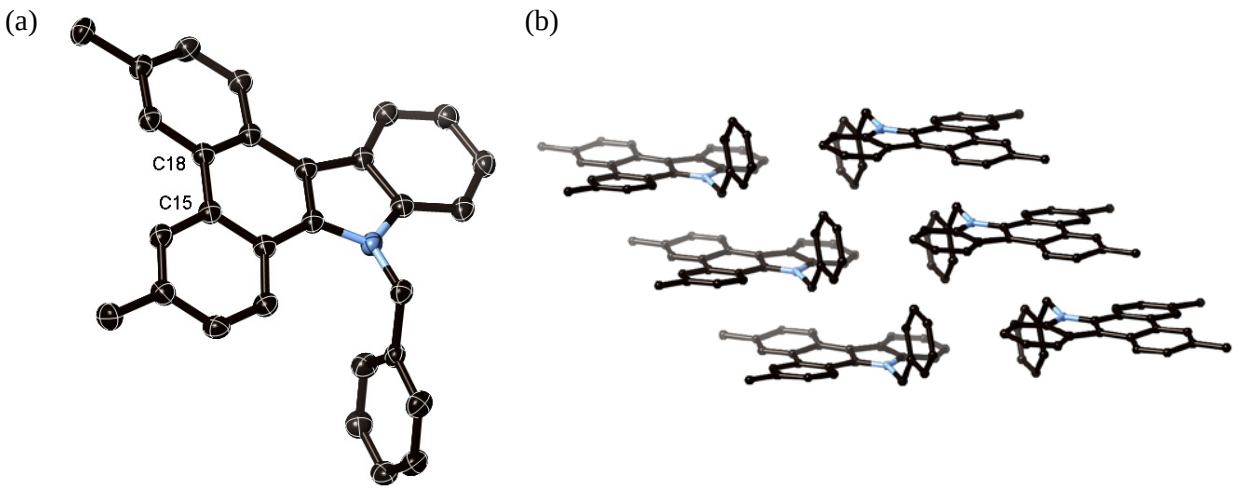

Figure 2.17. (a) Asymmetric unit of **2.21**, (b) packing of **2.21** showing the face-to-face and C–H ···π interactions between the molecules, hydrogen atoms have been removed for clarity.

2.4.5 Analysis of intramolecular distances from X-ray crystallography

Shown below in table 2.1 and 2.2 are the distances between the ortho carbon atoms in the crystal structures of the 2,3-diarylindoles both before and after cyclodehydrogenation. As expected the distances decrease considerably (~ 1.8 Å) with the formation of a carbon-carbon bond between these atoms in the dibenzo[*a*,*c*]carbazoles. The distance between the ortho carbon atoms in the 2,3-diarylindoles **2.3**, **2.5**, **2.8**, **2.11**, **2.12** and **2.13** varies from 3.223(2) Å to 3.616(1) Å, most likely due to the different crystal packing seen in the various crystal structures. The carbon-carbon bond distance in the dibenzo[*a*,*c*]carbazoles is typical of a single bond between two sp^2 hybridised carbon atoms. The bond distances range from 1.461(3) Å – 1.468(2) Å.

Compound	R group	N-substitution	Distance
2.3	Methyl	Hydrogen	3.223(2), 3.224(2), 3.257(2)
2.5	Hydrogen	Ethyl	3.571(1)
2.8	*Tert*butyl	Ethyl	3.414(1)
2.11	Methyl	Benzyl	3.298(1)
2.12	*Tert*butyl	Benzyl	3.616(1)
2.13	Hydrogen	Phenyl	3.381(5), 3.680(6)

Table 2.1. Distances between ortho carbon atoms in X-ray structures of 2,3-diarylindoles.

Compound	R group	N-substitution	Distance
2.15	Hydrogen	Ethyl	1.465(2)
2.17	Methyl	Ethyl	1.465(2)
2.20	Methoxy	Benzyl	1.468(2)
2.21	Methyl	Benzyl	1.461(3)
2.26	*Tert*butyl	Hydrogen	1.465(2)

Table 2.2. Bond distances between ortho carbon atoms in X-ray structures of dibenzo[*a*,*c*]carbazoles.

2.4.6 Analysis of change in NMR shifts resulting from cyclodehydrogenation

Shown below in table 2.3 is the change in chemical shift as a direct result of a carbon-carbon bond being formed between the peripheral aryl rings of the 2,3-diarylindole compounds, **2.5** – **2.12**, to form the corresponding dibenzo[*a*,*c*]carbazoles, **2.15** – **2.22**. In each case the increase in π conjugation to form the dibenzo[*a*,*c*]carbazoles has resulted in a downfield shift of the functional groups directly attached to the nitrogen atom by ~ 0.73 ppm. These groups were used to measure the difference in chemical shift as they are not crowded by other peaks in the ^{1}H-NMR spectrum of both the 2,3-diarylindole and the dibenzo[*a*,*c*]carbazoles. The compounds with methoxy substitution in the 4-position of the peripheral aryl rings are not as affected by the increase in π conjugation due to the strong electron donating nature of this group.

Compound	functional group measured	difference in chemical shift compared to ( )	Compound	functional group measured	difference in chemical shift compared to ( )
2.15	ethyl CH_2	0.76 ppm (**2.5**)	**2.19**	benzyl CH_2	0.73 ppm (**2.9**)
2.16	ethyl CH_2	0.60 ppm (**2.6**)	**2.20**	benzyl CH_2	0.68 ppm (**2.10**)
2.17	ethyl CH_2	0.75 ppm (**2.7**)	**2.21**	benzyl CH_2	0.71 ppm (**2.11**)
2.18	ethyl CH_2	0.76 ppm (**2.8**)	**2.22**	benzyl CH_2	0.72 ppm (**2.12**)

Table 2.3. Change in chemical shift as a result of carbon-carbon bond forming reactions.

2.5 Optical properties

The formation of a carbon-carbon bond between the ortho carbon atoms of the phenyl rings in the 2,3-diarylindoles, **2.3** – **2.12**, extends the π conjugation of the system to form dibenzo[*a*,*c*]carbazoles, **2.15** – **2.22**, **2.25** and **2.26**. Emission and excitation spectra were measured for each 2,3-diarylindole and corresponding dibenzo[*a*,*c*]carbazole. The difference in absorption and emission spectra of incompletely and completely fused aromatic compounds has previously been observed in the literature for both carbon derivatives[40,46] and heterocyclic derivatives.[36a,37,47] With each carbon-carbon bond formed between the

external aryl rings, the planarity and rigidity of the fused compounds is increased, allowing the fine structure and vibronic coupling of the absorption and emission bands to be observed.[48] The increased π conjugation of the completely cyclised, fused compounds is responsible for a bathochromic shift and increase in ε observed in the UV/visible spectra in comparison to the incompletely cyclised derivatives.[36a,46b] The 2,3-diarylindole precursor compounds can be considered to be incompletely cyclised when compared to their corresponding dibenzo[*a*,*c*]carbazole compounds, and as a result the change in emission and excitation spectra would be expected to follow the trends outlined above for incompletely and completely cyclised HBC derivatives.

Figure 2.18a shows the absorption spectra for all N-substituted-2,3-diarylindoles, **2.5** – **2.12**, figure 2.18b shows the absorption spectra for the corresponding 9-substituted-dibenzo[*a*,*c*]carbazoles, **2.15** – **2.22**, and figure 2.18c shows the absorption spectra for the N*H*-2,3-diarylindoles, **2.3** and **2.4** and the corresponding dibenzo[*a*,*c*]carbazoles, **2.25** and **2.26**. The general shape of the absorption spectra remains consistent for the 2,3-diarylindoles, **2.3** – **2.12** and the dibenzo[*a*,*c*]carbazoles, **2.15** – **2.22**, **2.25** and **2.26**. The shape of the absorbance and emission spectra are not affected by peripheral substitution around the 2,3-diarylindole or dibenzo[*a*,*c*]carbazole core, or by the type of substitution on the nitrogen atom. As expected due to the increase in π conjugation the λ_{max} of the dibenzo[*a*,*c*]derivatives is redshifted by ~ 6200 cm^{-1}. The λ_{max} of the 2,3-diarylindoles is observed at ~ 235 nm and λ_{max} of the dibenzo[*a*,*c*]carbazoles is observed at ~ 275 nm. The increase in π conjugation also leads to a significantly larger ε_{max} of the dibenzo[*a*,*c*]carbazole derivatives than their corresponding 2,3-diarylindole derivatives, in most cases ε_{max} is almost doubled.

The rigidity and planarity of the dibenzo[*a*,*c*]carbazoles allows for the fine structure in the UV/visible bands to be observed, particularly for the bands present at ~ 300 nm and ~ 360 nm. In contrast the fine structure in the absorption bands of the 2,3-diarylindoles is lost due to the flexibility of these compounds. The λ_{max} of the strongly electron donating, methoxy substituted 2,3-diarylindoles, **2.6** and **2.10**, are redshifted by 1059 cm^{-1} and 2067 cm^{-1} respectively, compared to **2.5** and **2.9**, and the λ_{max} of the two lowest energy absorption bands of the dibenzo[*a*,*c*]carbazoles, **2.16** and **2.20**, are redshifted by 1412 cm^{-1} and 1539 cm^{-1} (**2.16**) and 1536 cm^{-1} and 1556 cm^{-1} (**2.20**) compared to their unsubstituted derivatives, **2.5**, **2.9**, **2.15** and **2.19**. This bathochromic shift is most likely due to an increase in the HOMO of the ground state of the methoxy substituted compounds. In the case of the dibenzo[*a*,*c*]carbazoles the strongest absorption band at ~ 277 nm does not show any bathochromic shift, possibly due the methoxy groups donating into orbitals not affected by this transition. The weaker electron donating compounds, having either methyl or *tert*butyl substitution, have smaller bathochromic shifts.

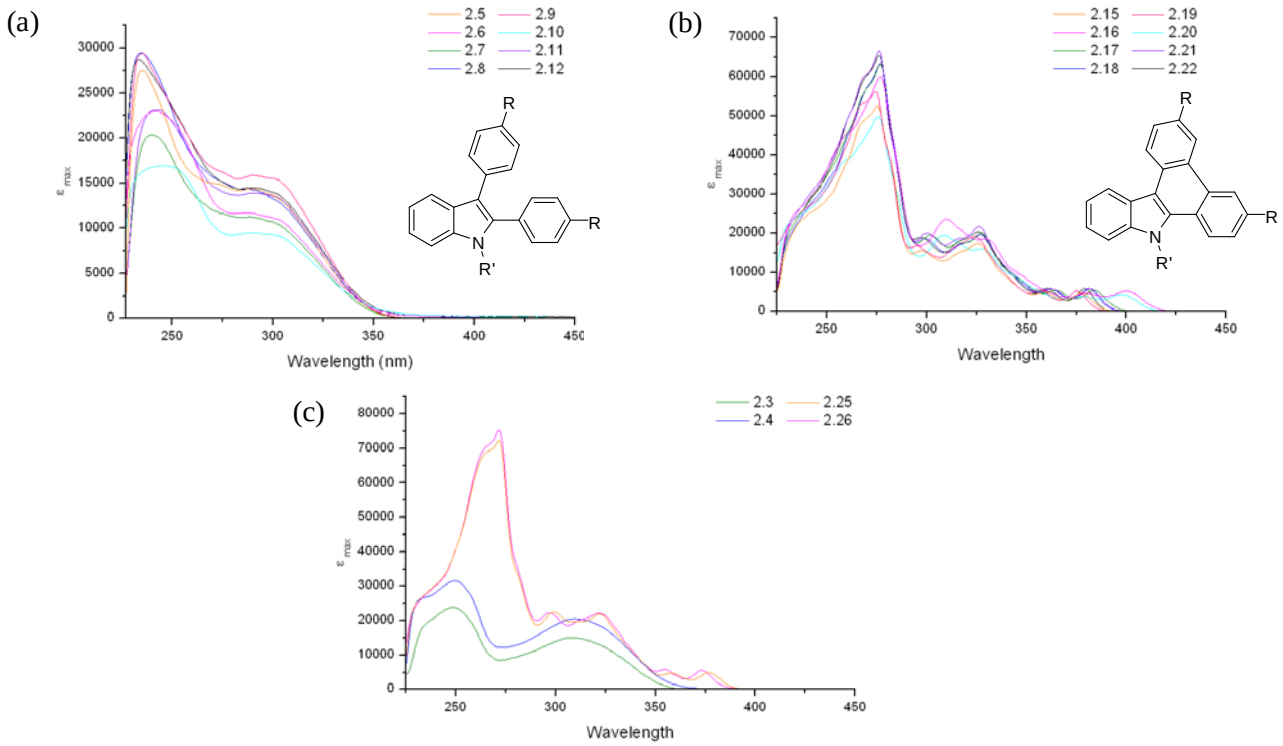

Figure 2.18. UV/visible spectra of (a) **2.5** – **2.12**, (b) **2.15** – **2.22**, (c) **2.3**, **2.4**, **2.25** and **2.26**, all spectra were measured in dichloromethane at room temperature, concentrations ~ 10^{-6} mol.L^{-1}, R = H, OMe, Me, ^{t}Bu, R' = Et, Bn.

Figure 2.19 shows the normalised absorption and emission spectra for the precursor 2,3-diarylindole compounds, figure 2.19a shows the N-ethyl-2,3-diarylindoles, **2.5** – **2.8**, figure 2.19b shows the N-benzyl-2,3-diarylindoles, **2.9** – **2.12**, and figure 2.19c shows the N*H*-2,3-diarylindoles, **2.3** and **2.2.** Like the absorption spectrum, the fine structure in the emission bands of the 2,3-diarylindole compounds cannot be seen because of the flexibility of these compounds. This means that all 2,3-diarylindole compounds have a broad emission spectrum with λ_{max} ~ 417 nm. Again, the methoxy substituted 2,3-diarylindoles **2.6** and **2.10** have a slight redshift in the emission spectra compared to their unsubstituted derivatives, the redshift in the emission spectra is much smaller compared to the redshift in the absorption spectra, 112 cm^{-1} for **2.6** and 173 cm^{-1} for **2.10**.

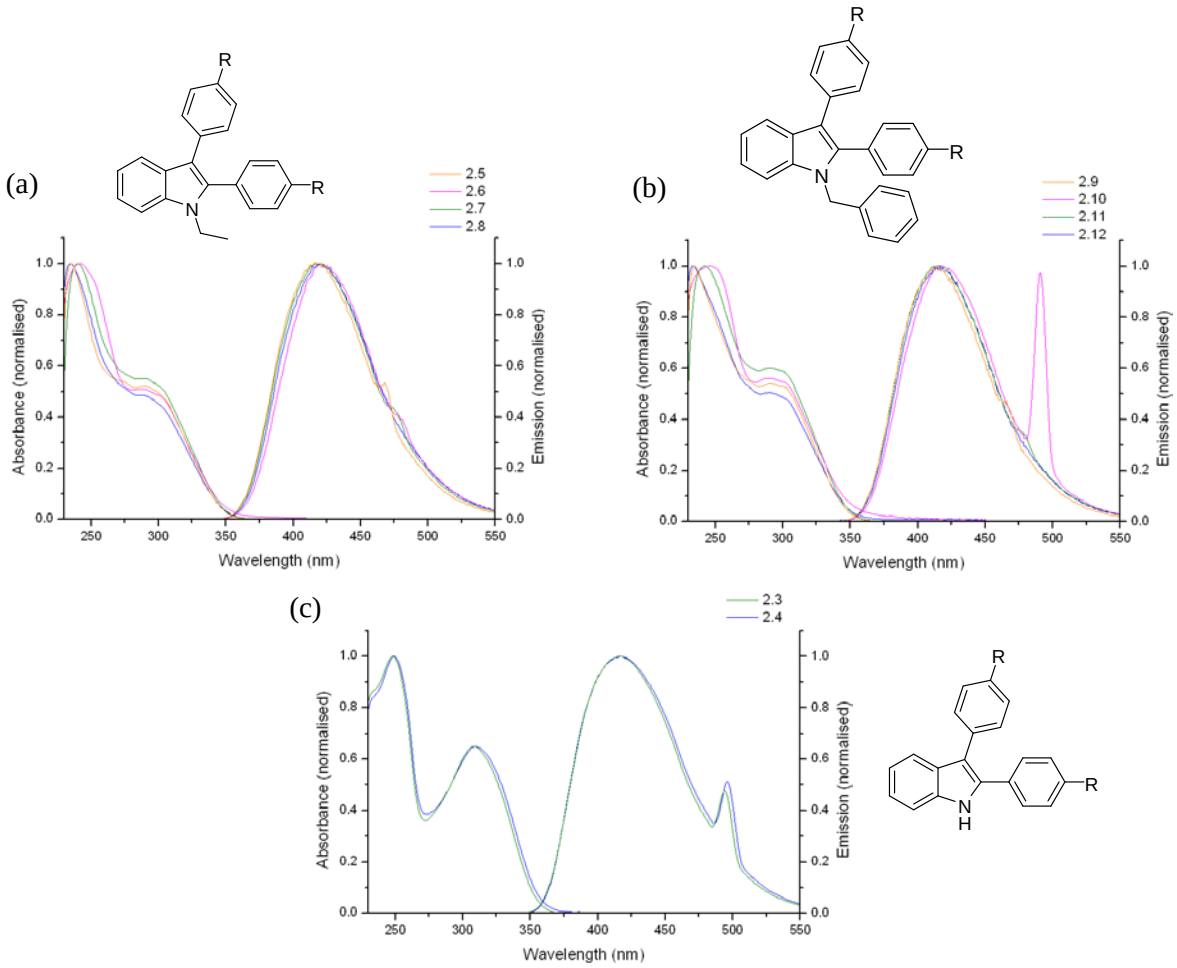

Figure 2.19. UV/visible and photoluminescence spectra of (a) **2.5** – **2.8**, (b) **2.9** – **2.12**, (c) **2.3** and **2.4**, all measured in dichloromethane at room temperature, concentrations ~ 10^{-6} mol.L^{-1}, R = H, OMe, Me, ^{t}Bu.

Figure 2.20 shows the normalised absorption and emission spectra for the photocyclised dibenzo[*a*,*c*]carbazole compounds, figure 2.20a shows the 9-ethyl-dibenzo[*a*,*c*]carbazoles, **2.15** – **2.18**, figure 2.20b shows the 9-benzyl-dibenzo[*a*,*c*]carbazoles, **2.19** – **2.22**, and figure 2.20c shows the dibenzo[*a*,*c*]carbazoles, **2.25** and **2.26**. Because of the rigidity and planarity imposed on the dibenzo[*a*,*c*]carbazoles by the formation of the carbon-carbon bond some fine structure and vibronic coupling can be observed in the emission spectra of these compounds. The dibenzo[*a*,*c*]compounds emit at a slightly higher energy (blueshifted) than their precursor 2,3-diarylindole compounds, ~ 1660 cm^{-1}. The emission of the methoxy substituted compounds, **2.16** and **2.20**, is redshifted compared to the emission of the unsubstituted compounds, **2.15** and **2.19**. The bathochromic shifts are larger than those observed in the emission spectra of the corresponding 2,3-diarylindoles, **2.6** and **2.10**, compound **2.16** is bathochromically shifted 1897 cm^{-1} and **2.20** is bathochromically shifted 1876 cm^{-1}, whereas the bathochromic shifts in the emission of **2.6** and **2.10** were only ~ 150 cm^{-1}.

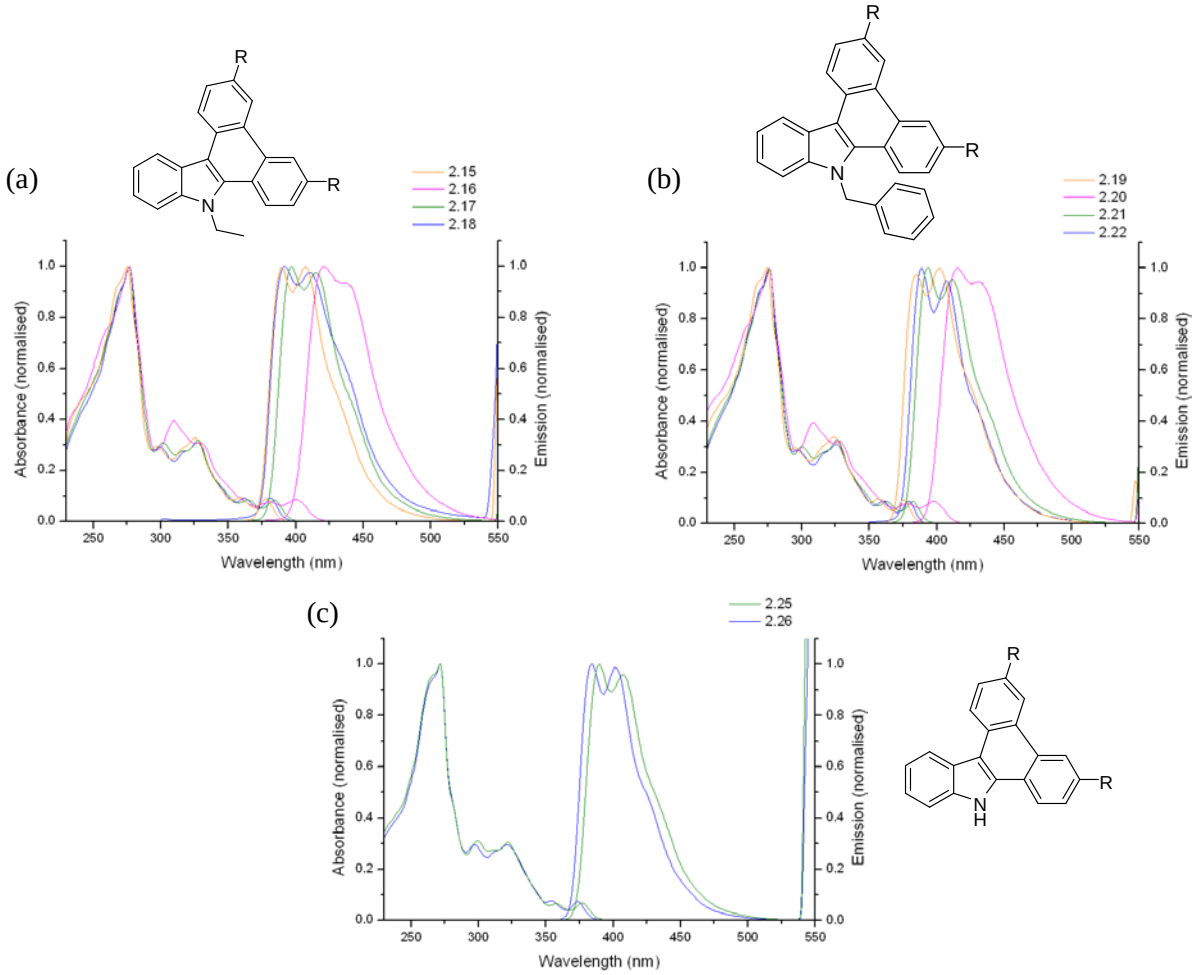

Figure 2.20. UV/visible and photoluminescence spectra of (a) **2.15** – **2.18**, (b) **2.19** – **2.22**, (c) **2.25** and **2.26**, all measured in dichloromethane at room temperature, concentrations ~ 10^{-6} mol.L^{-1}.

Table 2.4 summarises the main features of the absorption and emission spectra of the 2,3-diarylindole compounds **2.3** – **2.12**, shown in figures 2.18a, 2.18c and 2.19. Table 2.5 summarises the main features of the absorption and emission spectra of the dibenzo[*a*,*c*]carbazoles shown in figures 2.18b, 2.18c and 2.20. Extinction coefficients are given for the absorption bands.

	absorption		fluorescence		Absorption		fluorescence
	λ_{max} (nm)	ε (L.mol^{-1}cm^{-1})	λ_{max} (nm)		λ_{max} (nm)	ε (L.mol^{-1}cm^{-1})	λ_{max} (nm)
2.5	235, 289	27519, 14503	421	**2.9**	235, 290	28781, 16042	414
2.6	241, 287	20856, 10467	423	**2.10**	247, 290	18433, 10363	417
2.7	240, 289	18386, 10658	420	**2.11**	242, 291	20729, 13050	415
2.8	235, 288	30065, 14707	421	**2.12**	233, 290	27928, 14247	416
2.3	248, 308	22605, 16726	416	**2.4**	249, 310	31542, 20477	417

Table 2.4 Summary of the absorption and fluorescence maxima of **2.3** – **2.12**.

	absorption		fluorescence		absorption		fluorescence
	λ_{max} (nm)	ε (L.mol^{-1}cm^{-1})	λ_{max} (nm)		λ_{max} (nm)	ε (L.mol^{-1}cm^{-1})	λ_{max} (nm)
2.15	275, 297, 326, 359, 378	52363, 15472, 17219, 4877, 4659	389, 407	**2.19**	274, 295, 324, 357, 375	56103, 16745, 19190, 5568, 5247	385, 402
2.16	277, 310, 329, 380, 400	59286, 23439, 18347, 4693, 5080	420, 435	**2.20**	276, 309, 327, 378, 398	49464, 19528, 16030, 3900, 4416	415, 431
2.17	277, 302, 327, 365, 384	61425, 19026, 19612, 5226, 5212	397, 414	**2.21**	276, 300, 326, 363, 382	65698, 19672, 21264, 5463, 5570	394, 411
2.18	277, 299, 327, 362, 381	63644, 18444, 19505, 5523, 5688	392, 410	**2.22**	276, 297, 325, 360, 379	66433, 19674, 20986, 6390, 6227	389, 407
2.25	272, 299, 325, 357, 377	72416, 22763, 21116, 4836, 4956	390, 407	**2.26**	272, 297, 321, 355, 373	74773, 22095, 22128, 5805, 5599	384, 401

Table 2.5 Summary of the absorption and fluorescence maxima of **2.15** – **2.22**, **2.25** and **2.26**.

Shown in figure 2.21a are the normalised absorption and emission spectra of the unsubstituted precursor 2,3-diarylindole compounds, **2.5** and **2.9**, and the corresponding dibenzo[*a*,*c*]carbazoles, **2.15** and **2.19**. Figure 2.21b shows the normalised absorption and emission methoxy substituted precursor 2,3-diarylindole compounds **2.6** and **2.10**, along with their corresponding dibenzo[*a*,*c*]carbazoles, **2.16** and **2.20**. Figure 2.21a and 2.21b show the effect on the optical properties by enforced planarization and rigidity resulting from the formation of one carbon-carbon bond. The difference in λ_{max} resulting from increased π conjugation is clearly shown, and a comparison between figures 2.21a and 2.21b illustrates the pronounced bathochromic shift in the emission spectra of the methoxy substituted compounds.

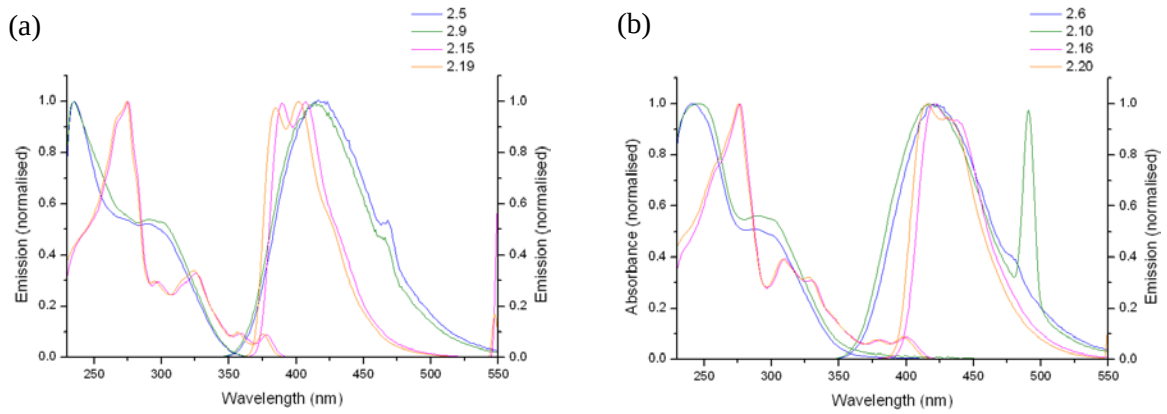

Figure 2.21 UV/visible and photoluminescence spectra of (a) **2.5**, **2.9**, **2.15** and **2.19**, and (b) **2.6**, **2.10**, **2.16**, **2.20**, all measured in dichloromethane at room temperature, concentrations ~ 10^{-6} mol.L^{-1}.

2.6 Attempted synthesis of metal coordinating 2,3-diarylindoles

The incorporation of a terpyridine (terpy) group directly to the 2,3,-diarylindole scaffold allowing the formation of a metal complex was also explored. Incorporating a metal coordinating group to the N*H*-2,3-diarylindoles, **2.1** – **2.4**, already prepared also allows for incorporation of a terpy group to the corresponding dibenzo[*a*,*c*]carbazoles, through photocyclisation. This will give a platform to compare the different optical properties between the metal complexes formed from these two compounds. The metal complexes formed will hopefully incorporate the desirable optical properties from the metal and the appended 2,3-diarylindole enables the π conjugation of the complex to be controlled by photocyclisation. This should allow control of the bathochromic shift and extinction coefficient, as discussed for the differences in optical properties of the 2,3-diarylindoles and corresponding dibenzo[*a*,*c*]carbazoles above. To the best of our knowledge terpy has never been directly attached to an indole ring before, and the route taken to the desired terpy appended indole compounds, **2.27**, is shown in figure 2.22.

The synthetic strategy for appending the terpy group onto the indole core is shown in scheme 2.9. The key 4-chloro terpy molecule, **2.28**, has previously been prepared by Constable and Ward[49] and was targeted for substitution directly onto the indole. There is some literature precedence for the substitution of **2.28** onto N*H* heterocyclic rings. Accorsi *et al.*[50] recently prepared a terpy appended carbazole ligand by deprotonation of the carbazole with KO^{t}Bu, followed by electrophilic substitution of **2.28**. Synthesis of **2.28** following the method of Ward and Constable proceeded in good yields, from ethyl pyridine-2-carboxylate and acetone.

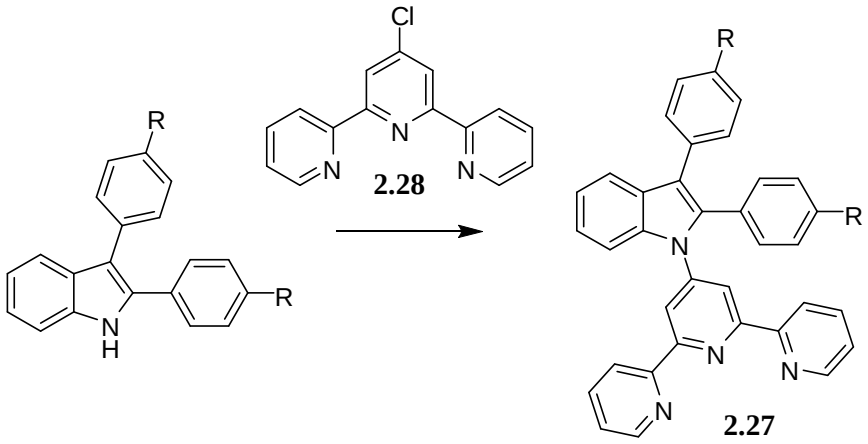

Figure 2.22. The key step in the preparation of the desired terpy appended 2,3-diarylindoles, **2.27**.

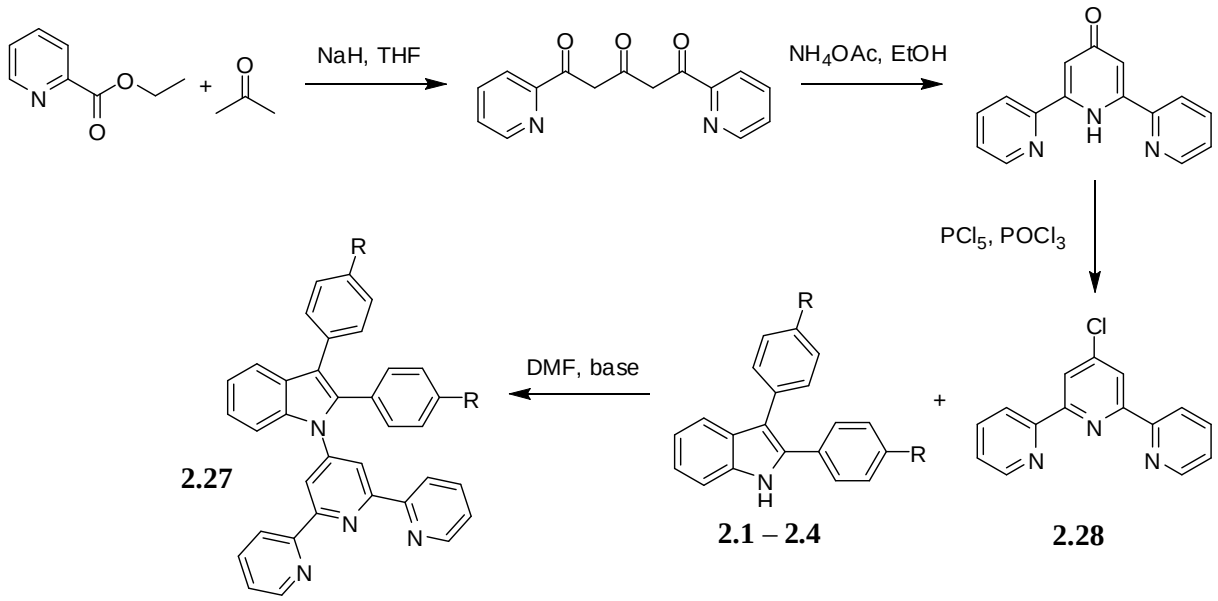

Scheme 2.9. Synthetic route for the formation of key intermediate **4.28** and desired compounds **4.27**.[49]

Initially, the substitution of **2.28** onto the nitrogen atom of **2.2** was attempted using the conditions for substitution onto the nitrogen atom of N*H*-2,3-diarylindoles outlined in section 2.2.2. Unfortunately the only products isolated from this reaction are starting materials, even when the reaction is heated. The conditions for substitution outlined by Accorsi *et al*. also resulted in the isolation of only starting materials from the reaction. It would appear that the steric hindrance encountered by peripheral aryl substitution in the 2- and 3-position of the indole core is not able to be overcome using these conditions for substitution.

Another synthetic strategy, also incorporating compound **2.28**, was used in another attempt to form the desired terpy appended 2,3-diarylindoles. Compound **2.28** can be used to form a terpy ruthenium complex, **2.29**, and the coordination of **2.28** to a metal ion activates the 4-position of the central pyridine ring towards nucleophilic attack. Various examples of nucelophilic attack at the 4-position of the central pyridine ring of complex **2.29** have been reported in the literature,[51] and it was hoped this activation would allow for the formation of the desired terpy appended 2,3-diarylindole ruthenium complexes, **2.30**, as outlined in scheme 2.10.

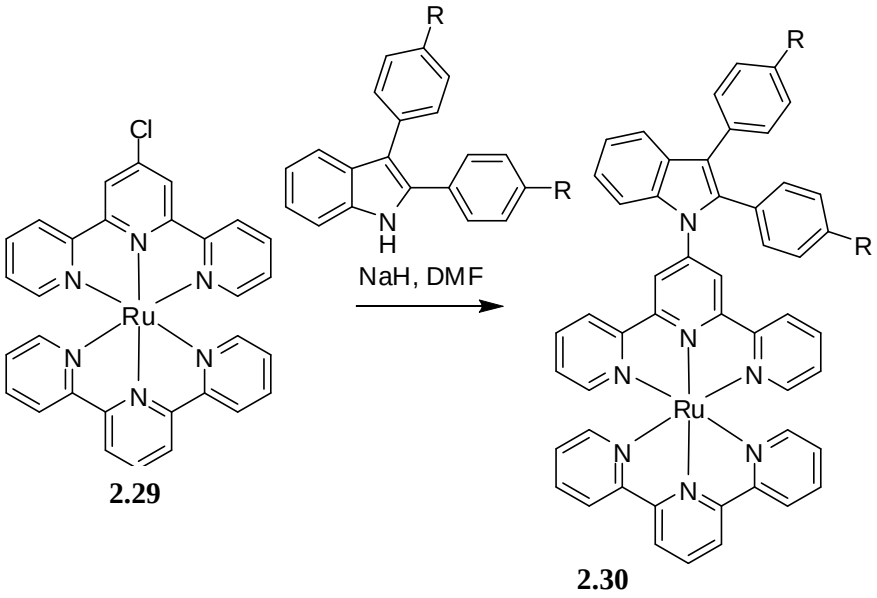

Scheme 2.10. Synthesis of desired terpy appended 2,3-diarylindole ruthenium complexes, **2.30**, by employing a terpy ruthenium complex, **2.29**.[51]

The synthesis of complex **2.29** from readily available Ru(terpy)Cl_3 has previously been reported[52] and the synthesis of **2.29** proceeded in good yields, as did a crude reaction where the formation of the desired complex using indole as the nucelophile was attempted, but unfortunately the use of **2.2** in scheme 2.10 did not produce any of the desired complex **2.30**. The difficulty in carrying out the desired substitution reaction meant that efforts toward metal coordinating versions of 2,3-diarylindoles were not pursued further.

2.7 Summary

The synthesis and characterisation of five new N-susbtituted-2,3-diarylindole compounds with ethyl and benzyl substitution on the nitrogen atom of the indole ring system has been carried out along with the synthesis of three known N-substituted-2,3-diarylindole compounds to form a family of compounds to act

as model system for investigation into oxidative cyclodehydrogenation of heterocyclic ring systems. Attempts at oxidative cyclodehydrogenation with various reagents were carried out with the family of model compounds, resulting in the isolation of only one stable dibenzo[*a*,*c*]carbazole, 9-benzyl-3,6-dimethoxy-dibenzo[*a*,*c*]carbazole, **2.20**, in low yields. Photocyclisation was also investiagted as an alternative method to forming the desired carbon-carbon bond between the peripheral aryl rings. Each N-substituted-2,3-diarylindole underwent photocyclisation to form the corresponding dibenzo[*a*,*c*]carbazole, in good yields. Two precursor N*H*-2,3-diarylindoles not previously photocyclised also underwent photocyclisation forming the corresponding dibenzo[*a*,*c*]carbazole.

The change in optical properties as the result of the formation of a carbon-carbon bond was investigated using UV/vis spectroscopy and fluorometry. The rigidity imposed by the carbon-carbon bond formation allows for the fine structure and some vibronic coupling to be seen the spectra of the dibenzo[*a*,*c*]carbazoles, while the more flexible 2,3-diarylindoles have broad absorbance and emission spectra.

Two different synthetic strategies were also investigated in an attempt to form N-substituted-2,3-diarylindole compounds that could coordinate to metal atoms. Metal coordination to the 2,3-diarylindole scaffold would offer the ability to change the optical properties of the ligand through photocyclisation but both strategies failed to substitute the required terpyridine unit onto the nitrogen atom of the indole ring.

2.8 References

(1) (a) Horton, D. A.; Bourne, G. T.; Smythe, M. L. *Chem. Rev.* **2003**, *103*, 893, (b) Sundberg, R. J. *Indoles*; Academic Press: London, 1996.

(2) Humphrey, G. R.; Kuethe, J. T. *Chem. Rev.* **2006**, *106*, 2875.

(3) (a) Vivian, J. T.; Callis, P. R. *Biophys. J.* **2001**, *80*, 2093, (b) Kim, J. E.; Arjara, G.; Richards, J. H.; Gray, H. B.; Winkler, J. R. *J. Phys. Chem. B.* **2006**, *110*, 17656, (c) Royer, C. A. *Chem. Rev.* **2006**, *106*, 1769(d) Lackowicz, J. *Principles of Fluorescence Spectroscopy*; 2nd ed.; Plenum: New York, 1999.

(4) (a) Berger, M.; Gray, J. A.; Roth, B. L. *Annu. Rev. Med.* **2009**, *60*, 355, (b) Williams, E.; Stewart-Knox, B.; Helander, A.; McConville, C.; Bradbury, I.; Rowland, I. *Biol. Psych.* **2006**, *71*, 171.

(5) Inman, M.; Moody, C. J. *Chem. Sci.* **2013**, *4*, 29.

(6) Kochanowska-Karamyan, A. J.; Hamann, M. T. *Chem. Rev.* **2010**, *110*, 4489.

(7) Hart, F. D.; Boardman, P. L. *Br. Med. J.* **1963**, *5363*, 965

(8) (a) Gribble, G. W. *J. Chem. Soc., Perkin Trans. 1* **2000**, 1045, (b) Cacchi, S.; Fabrizi, G. *Chem. Rev.* **2011**, *111*, PR215, (c) Taber, D. F.; Tirunahari, P. K. *Tetrahedron* **2011**, *67*, 7195.

(9) (a) Hegedus, L. S. *Angew. Chem. Int. Ed.* **1988**, *27*, 1113(b) Cacchi, S.; Fabrizi, G. *Chem. Rev.* **2005**, *105*, 2873.

(10) Robinson, B. *Chem. Rev.* **1963**, *63*, 373.

(11) Newhouse, T.; Baran, P. S. *J. Am. Chem. Soc.* **2008**, *130*, 10886.

(12) Mudry, C. A.; Frasca, A. R. *Tetrahedron* **1974**, *30*, 2983.

(13) Szmuszkovicz, J. *Org. Prep. & Procedures* **1969**, *1*, 105.

(14) Szmuszkovicz, J.; Glenn, E. M.; Heinzelman, R. V.; Hester, J. B.; Youngdale, G. A. *J. Med. Chem.* **1966**, *9*, 527.

(15) (a) Nakamura, Y.; Ukita, T. *Org. Lett.* **2002**, *4*, 2317, (b) Smith, A. L.; Stevenson, G. I.; Swain, C. J.; Castro, J. *Tetrahedron Lett.* **1998**, *39*, 8317, (c) Fuerstner, A.; Hupperts, A.; Ptock, A.; Janssen, E. *J. Org. Chem.* **1994**, *59*, 5215, (d) Shen, M.; Leslie, B. E.; Driver, T. G. *Angew. Chem. Int. Ed.* **2008**, *47*, 5056, (e) Lu, B. Z.; Zhao, W.; Wei, H.-X.; Dufour, M.; Farina, V.; Senanayake, C. H. *Org. Lett.* **2006**, *8*, 3271, (f) Shen, M.; Li, G.; Lu, B. Z.; Hossain, A.; Roschangar, F.; Farina, V.; Senanayake, C. H. *Org. Lett.* **2004**, *6*, 4129.

(16) (a) Cacchi, S.; Fabrizi, G.; Goggiamani, A. *Adv. Synth. Catal.* **2006**, *348*, 1301, (b) Liu, Y.; Gribble, G. W. *Tetrahedron Lett.* **2000**, *41*, 8717.

(17) Chen, X.; Li, X.; Wang, N.; Jin, J.; Lu, P.; Wang, Y. *Eur. J. Org. Chem.* **2012**, *2012*, 4380.

(18) Zhang, H.-C.; Ye, H.; White, K. B.; Maryanoff, B. E. *Tetrahedron Lett.* **2001**, *42*, 4751.

(19) Bart, J. C. J. *Acta. Cryst. B* **1968**, *24*, 1277

(20) (a) Simpson, C. D.; Wu, J.; Watson, M. D.; Mullen, K. *J. Mater. Chem.* **2004**, *14*, 494, (b) Wu, J.; Pisula, W.; Müllen, K. *Chem. Rev.* **2007**, *107*, 718, (c) Müller, M.; Kübel, C.; Müllen, K. *Chem. Eur. J.* **1998**, *4*, 2099.

(21) Kuo, W.-J.; Chen, Y.-H.; Jeng, R.-J.; Chan, L.-H.; Lin, W.-P.; Yang, Z.-M. *Tetrahedron* **2007**, *63*, 7086.

(22) Richards, M. B. *J. Chem. Soc., Trans.* **1910**, *97*, 977.

(23) Biswas, K. M.; Dhara, R. N.; Mallik, H.; Halder, S.; Sinha-Chaudhuri, A.; Saha, A.; Ganguly, D.; De, P.; Brahmachari, A. S. *Monatsh Chem* **1996**, *127*, 111.

(24) (a) Baccolini, G.; Dalpozzo, R.; Todesco, P. E. *J. Chem. Soc., Perkin Trans. 1* **1988**, 971, (b) Wagner, P. J.; Cao, Q. *Tetrahedron Lett.* **1991**, *32*, 3915.

(25) Koulocheri, Sophia D.; Haroutounian, Serkos A. *Eur. J. Org. Chem.* **2001**, *2001*, 1723.

(26) Ackermann, L.; Born, R. *Tetrahedron Lett.* **2004**, *45*, 9541.

(27) Miyasaka, M.; Fukushima, A.; Satoh, T.; Hirano, K.; Miura, M. *Chem. Eur. J.* **2009**, *15*, 3674.

(28) Hartwig, J. F. *Angew. Chem. Int. Ed.* **1998**, *37*, 2046.

(29) (a) Wolfe, J. P.; Wagaw, S.; Marcoux, J.-F.; Buchwald, S. L. *Acc. Chem. Res.* **1998**, *31*, 805, (b) Hartwig, J. F. *Acc. Chem. Res.* **1998**, *31*, 852.

(30) (a) Bellina, F.; Calandri, C.; Cauteruccio, S.; Rossi, R. *Eur. J. Org. Chem.* **2007**, *2007*, 2147, (b) Antilla, J. C.; Klapars, A.; Buchwald, S. L. *J. Am. Chem. Soc.* **2002**, *124*, 11684, (c) Haneda, S.; Adachi, Y.; Hayashi, M. *Tetrahedron* **2009**, *65*, 10459, (d) Rao, R. K.; Naidu, A. B.; Jaseer, E. A.; Sekar, G. *Tetrahedron* **2009**, *65*, 4619, (e) Jocula, L.; Djakovitch, L. *Adv. Synth. Catal.* **2009**, *351*, 673.

(31) Swapna, K.; Murthy, S. N.; Nageswar, Y. V. D. *Eur. J. Org. Chem.* **2010**, *2010*, 6678.

(32) (a) Cristau, H.-J.; Cellier, P. P.; Spindler, J.-F.; Taillefer, M. *Chem. Eur. J.* **2004**, *10*, 5607, (b) Zhang, H.; Cai, Q.; Ma, D. *J. Org. Chem.* **2005**, *70*, 5164, (c) Klapars, A.; Antilla, J. C.; Huang, X.; Buchwald, S. L. *J. Am. Chem. Soc.* **2001**, *123*, 7727, (d) Xu, Z.-L.; Li, H.-X.; Ren, Z.-G.; Du, W.-Y.; Xu, W.-C.; Lang, J.-P. *Tetrahedron* **2011**, *67*, 5282.

(33) Cano, R.; Ramón, D. J.; Yus, M. *J. Org. Chem.* **2011**, *76*, 654.

(34) Ban, I.; Sudo, T.; Taniguchi, T.; Itami, K. *Org. Lett.* **2008**, *10*, 3607.

(35) Cao, C.; Shi, Y.; Odom, A. L. *Org. Lett.* **2002**, *4*, 2853.

(36) (a) Gregg, D. J.; Bothe, E.; Höfer, P.; Passaniti, P.; Draper, S. M. *Inorg. Chem.* **2005**, *44*, 5654, (b) Takase, M.; Enkelmann, V.; Sebastiani, D.; Baumgarten, M.; Müllen, K. *Angew. Chem. Int. Ed.* **2007**, *46*, 5524.

(37) Draper, S. M.; Gregg, D. J.; Madathil, R. *J. Am. Chem. Soc.* **2002**, *124*, 3486.

(38) King, B. T.; Kroulík, J.; Robertson, C. R.; Rempala, P.; Hilton, C. L.; Korinek, J. D.; Gortari, L. M. *J. Org. Chem.* **2007**, *72*, 2279.

(39) Herwig, P. T.; Enkelmann, V.; Schmelz, O.; Müllen, K. *Chem. Eur. J.* **2000**, *6*, 1834.

(40) Luo, J.; Xu, X.; Mao, R.; Miao, Q. *J. Am. Chem. Soc.* **2012**, *134*, 13796.

(41) Gońka, E.; Myśliwiec, D.; Lis, T.; Chmielewski, P. J.; Stępień, M. *J. Org. Chem.* **2013**, *78*, 1260.

(42) (a) Liu, Z.; Zhang, X.; Larock, R. C. *J. Am. Chem. Soc.* **2005**, *127*, 15716, (b) Liu, Z.; Larock, R. C. *J. Org. Chem.* **2007**, *72*, 223, (c) Dubrovskiy, A. V.; Markina, N. A.; Larock, R. C. *Org. & Biomol. Chem.* **2013**, *11*, 191.

(43) Cacchi, S.; Fabrizi, G.; Goggiamani, A.; Iazzetti, A. *Org. & Biomol. Chem.* **2012**, *10*, 9142.

(44) Budén, M. a. E.; Vaillard, V. A.; Martin, S. E.; Rossi, R. A. *J. Org. Chem.* **2009**, *74*, 4490.

(45) Liu, L.; Yang, B.; Katz, T. J.; Poindexter, M. K. *J. Org. Chem.* **1991**, *56*, 3769.

(46) (a) Rieger, R.; Müllen, K. *J. Phys. Org. Chem.* **2010**, *23*, 315, (b) Lu, Y.; Moore, J. S. *Tetrahedron Lett.* **2009**, *50*, 4071.

(47) (a) Tovar, J. D.; Rose, A.; Swager, T. M. *J. Am. Chem. Soc.* **2002**, *124*, 7762, (b) Behof, W. J.; Wang, D.; Niu, W.; Gorman, C. B. *Org. Lett.* **2010**, *12*, 2146.

(48) (a) Nijegorodov, N. I.; Downey, W. S. *J. Phys. Chem.* **1994**, *98*, 5639, (b) Nijegorodov, N.; Zvolinsky, V.; Luhanga, P. V. C. *J. Photochem. & Photobiol. A.* **2008**, *196*, 219, (c) Wu, J.; Watson, M. D.; Tchebotareva, N.; Wang, Z.; Müllen, K. *J. Org. Chem.* **2004**, *69*, 8194.

(49) Constable, E. C.; Ward, M. D. *J. Chem. Soc., Dalton Trans.* **1990**, 1405.

(50) Accorsi, G.; Armaroli, N.; Cardinali, F.; Wang, D.; Zheng, Y. *J. Alloy Compd.* **2009**, *485*, 119.

(51) (a) Constable, E. C.; Thompson, A. M. W. C.; Harveson, P.; Macko, L.; Zehnder, M. *Chem. Eur. J.* **1995**, *1*, 360, (b) Constable, E. C.; Housecroft, C. E.; Neuburger, M.; Poleschak, I.; Zehnder, M. *Polyhedron* **2003**, *22*, 93.

(52) Constable, E. C.; Harverson, P.; Housecroft, C. E.; Nordlander, E.; Olsson, J. *Polyhedron* **2006**, *25*, 437.

Chapter Three:

2,3,4,5-Tetraarylpyrrole compounds

3.1 Introduction

Pyrrole, a π-excessive five-membered heterocyclic ring, plays an important role in biology and chemistry. For example, porphyrins are π-conjugated macrocyclic ring systems made up of four pyrrole rings bridged by a methylene spacer, as shown in figure 3.1. Some porphyrins are naturally occurring; heme is a biologically relevant porphyrin that coordinates to iron and is incorporated into many enzymes, including the cytochrome P450's,[1] the group of enzymes responsible for oxidation of organic substrates. Due to their conjugated aromatic systems porphyrins are also of interest as new materials for applications in organic electronics.[2] Porphyrins can form coordination complexes with a range of different metals, and have been used as the basis of many supramolecular structures.[3]

The pyrrole ring is also found in a wide range of natural products and is a key structural component in many drug molecules. Atorvastatin,[4] a cholesterol lowering drug sold under the trade name of Lipitor, shown in figure 3.1, is one of the top selling drugs worldwide and consists of a pyrrole core substituted with various aryl, amide and alkyl groups. Pyrrole is also the key component in some antibacterial compounds and marine natural products. The marinopyrroles,[5] marinopyrrole A is shown in figure 3.1, are metabolites isolated from a *Streptomyces* species, with a unique N,C2 link between the bis pyrrole moieties not seen previously in the isolation of natural products. They show good inhibitory activity against the metacillin resistant *Staphylococcus-aureus*.

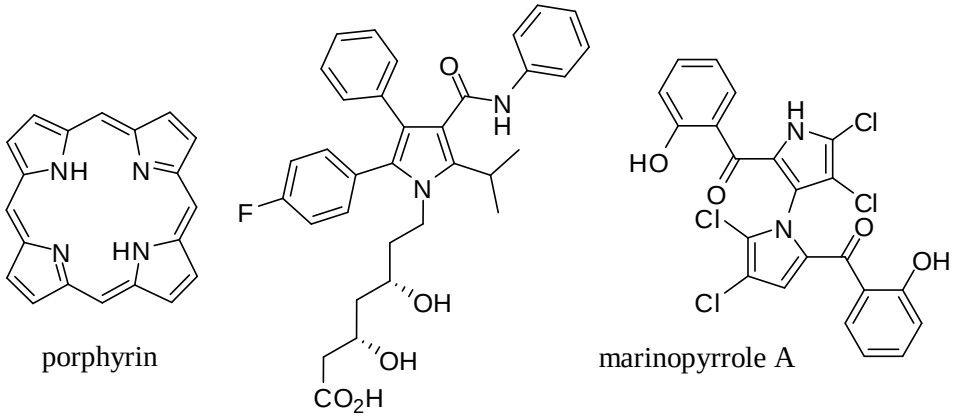

Figure 3.1. Examples of the pyrrole core in biology, drug molecules and marine natural products.

Recently attention has turned to pyrroles and their derivatives for their application in materials chemistry. Porphyrins and their derivatives can self assemble into one dimensional columns in liquid crystalline compounds with the correct substitution on the periphery of the porphyrin core.[6] Another class of compounds, the BODIPY dyes have also recently become the subject of attention for their possible

application as chemosensors and biological probes due to their intense fluorescence and strong UV absorption.[7]

Pyrroles are also used as key structural platforms in organic chemistry and as such there exist many methods for their formation.[8] Classically the pyrrole ring was synthesised using the Paal – Knorr reaction, the condensation of 1,4-butadiones and a primary or secondary amine to form the pyrrole core. Paal and Knorr first reported this reaction independently in 1884,[9] and this method is still used widely for the synthesis of pyrrole compounds. The diketone and amine compounds allow for the incorporation of a wide range of functional groups onto the pyrrole core, simple 2,5-dimethyl substituted pyrroles can be formed by the reaction of hexane-2,5-diones with a variety of alkyl and aryl substituted amines.[10,11] The synthesis of a variety of tetraaryl substituted pyrrole compounds for applications in organic LED's was achieved using the Paal – Knorr condensation of a 1,2,3,4-tetraaryl-1,4-butadione compound, and subsequent substitution of the nitrogen atom of the pyrrole ring gave the desired compounds.[12]

There are a wide variety of methods available for the formation of multisubstituted pyrrole cores due to the requirement for their synthesis in both chemistry and biology. The use of multicomponent reactions for pyrrole synthesis allows for the incorporation of a broad range of substituents onto the pyrrole core, and the method used for synthesis depends on the type of functional group required.[8a] A brief discussion of multicomponent reactions for the synthesis of pentaarylsubstituted pyrrole cores will follow in Chapter 4. The π-excessive pyrrole core means that it is more activated than benzene towards electrophilic aromatic substitution reactions, usually these occur at the 2- or 5-position on the pyrrole ring.[10,13]

The formation of a family of N-substituted-2,3,4,5-tetraarylpyrrole compounds was targeted as a more complex model system for studying the oxidative cyclodehydrogenation reaction. The presence of four peripheral aryl groups positioned around the pyrrole core allows for up to three carbon-carbon bond forming reactions to occur from oxidative cyclodehydrogenation. Increasing the number of carbon-carbon bonds able to be formed through oxidative cyclodehydrogenation increases the possibility of a complex mixture of compounds, if one product is not thermodynamically favoured over the other possible reaction products. Formation of only one carbon-carbon bond can now occur in two different places around the pyrrole core, as can the formation of only two carbon-carbon bonds. The oxidative cyclodehydrogenation of aryl rings attached to a pyrrole core has not been previously reported in the literature, although carbon-carbon bond forming reactions between the ortho carbon atoms attached to other π-excessive heterocycles, i.e. thiophene, have been studied.[14]

3.2 Synthesis of N-substituted-2,3,4,5-tetraarylpyrroles

3.2.1 Synthesis of NH-2,3,4,5-tetraarylpyrroles, ***3.1 – 3.4***

In order to prepare a family of 2,3,4,5-tetraarylpyrrole compounds as model compounds for exploring different oxidative cyclodehydrogenation reaction conditions, a synthesis was required that allowed the substitution at the 4-position of the aryl ring to be easily varied. In 2008, MacLean *et al*. published a synthesis of N*H*-2,3,4,5-tetraphenylpyrrole, **3.1**, by the condensation of 2 equivalents of benzoin with ammonium acetate,[15] as shown in Scheme 3.1. Despite the numerous other methods available to prepare N*H*-2,3,4,5-tetraphenylpyrrole, this method appealed because the starting benzoin compound lends itself easily to variation in the substitution at the 4-position of the aryl rings. Additionally, four different benzoin derivatives had already been prepared in the course of this study for the preparation of a family of 2,3-diarylindole compounds, also used as models for oxidative cyclodehydrogenation in Chapter 2. The synthesis of **3.1**, **3.3** and **3.4** proceeded as expected in moderate yields (56%, **3.1**, 52%, **3.3**, 53%, **3.4**). The low yields were not problematic as all benzoin compounds were readily available through commercial sources (benzoin and anisoin) or condensation of the appropriate aldehyde (4,4'-dimethylbenzoin and 4,4'-di*tert*butylbenzoin).

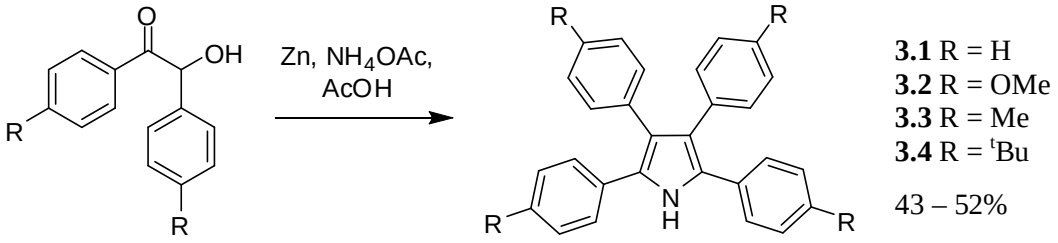

Scheme 3.1. Synthesis of N*H*-2,3,4,5-tetraarylpyrroles, **3.1** – **3.4**.

Compound **3.1** is commonly prepared using classical Paal – Knorr conditions by the condensation of 1,2,3,4-tetraphenyl-1,4-butadione with an ammonium salt.[12a] This method is high yielding (76%)[12a] but systematic variation of the 4-position of the aryl groups requires the synthesis of the appropriate 1,2,3,4-tetraaryl-1,4-butadione in each case, which is much more synthetically challenging than the one step preparation of benzoin derivatives from the appropriate benzaldehyde. Desylamine and desoxybenzoin have also been employed to form **3.1**.[16] A variation on the Paal – Knorr synthesis of **3.1** was recently reported using 1,2,3,4-tetraphenylbut-2-ene and ammonium formate under microwave irradiation, and is catalysed by Pd/C.[17] Compound **3.1** has been investigated for its use as an antioxidant in comparison to a phenolic antioxidant di-*tert*butylhydroxyanisole along with a range of other pyrrole derivatives.[15] The dielectric constant of **3.1** has also been measured, along with a variety of other pyrrole derivatives, in different solvents to determine the conformation and rotation of the substituents in solution.[18]

Surprisingly, despite their preparation in only two steps from the readily available appropriately substituted benzaldehyde, N*H*-2,3,4,5-tetra(4-methylphenyl)pyrrole, **3.3** and N*H*-2,3,4,5-tetra(4-*tert*butylphenyl)pyrrole, **3.4**, have not been previously prepared in the literature. Each compound was characterised and all data was consistent with the formation of **3.3** and **3.4**. The ^{1}H NMR spectrum of each compound is as expected when compared to the known compound **3.1**.

MacLean *et al*. also report the synthesis of N*H*-2,3,4,5-tetra(4-methoxyphenyl)pyrrole, **3.2**, but in a much lower yield (23%) compared to the formation of **3.1**.[15] Unfortunately, despite repeated attempts the synthesis of **3.2** was unsuccessful in this case. The carbonyl carbon atom of anisoin is less nucleophilic than benzoin due to the electron donating methoxy groups of anisoin, making electrophilic attack at this carbonyl carbon atom by the ammonium acetate much more difficult. Apart from this report there are only few other references in the literature to the preparation of **3.2**,[19] and most reports are concerned with the electrochemical oxidation of **3.2**.[20]

3.2.2 Attempts at the synthesis of NH-2,3,4,5-tetra(p-methoxyphenyl)pyrrole

In order to obtain the family of N*H* -2,3,4,5-tetraarylpyrrole compounds it was desirable to complete the synthesis of **3.2**, adding to the family a more electron donating substituent to the peripheral phenyl groups on the pyrrole ring. After the failed condensation of anisoin and ammonium acetate mentioned in the previous section, another route was required for the formation of **3.2**. 1,2,3,4-tetra(4-methoxyphenyl)-buta-1,4-dione, **3.11**, was synthesised in two steps from anisoin following the method of Carter *et al*.[21] and Kuo *et al*.[12a] shown in scheme 3.2. Anisoin was reduced with granulated tin and hydrochloric acid to give deoxyanisoin which was then oxidatively dimerised with iodine and sodium methoxide to give the desired compound **3.11** in 68% yield. With compound **3.11** in hand condensation with ammonium acetate was attempted, but frustratingly no **3.2** was able to be isolated from the reaction. It would appear that presence of four peripheral, electron donating methoxyphenyl groups greatly hinders the condensation to form a pyrrole ring. Although it was frustrating to not add another member to the N*H*-2,3,4,5-tetraarylpyrrole family, the three compounds **3.1**, **3.3** and **3.4** still allowed for sufficient exploration of oxidative cyclodehydrogenation conditions on aryl-substituted pyrrole compounds.

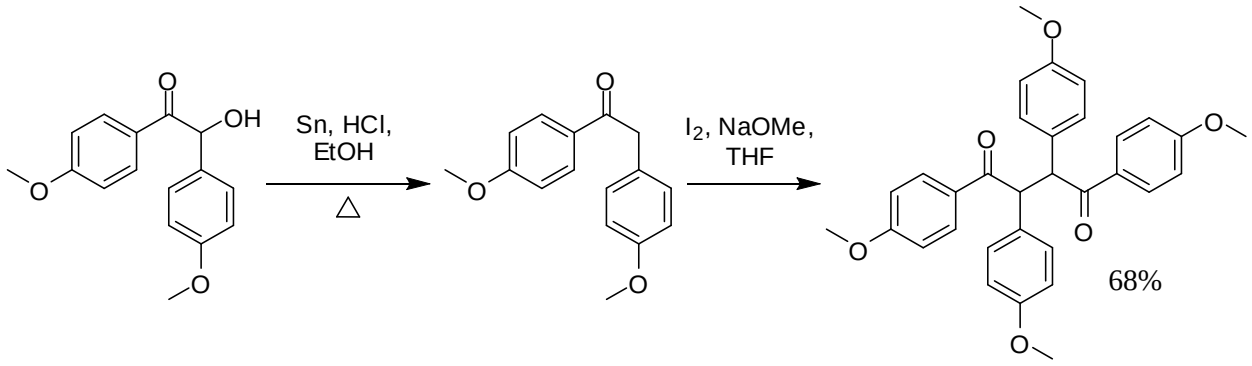

3.11

Scheme 3.2. Preparation of **3.11** in two steps from anisoin.

3.2.3 Synthesis of N-ethyl and N-benzyl-tetraarylpyrroles, ***3.5 – 3.10***

The N*H*-2,3,4,5-tetraarylpyrroles, **3.1**, **3.3**, **3.4**, required protection by substitution on the nitrogen atom of the pyrrole ring to prevent coordination of this Lewis basic nitrogen atom with the Lewis acids employed in subsequent oxidative cyclodehydrogenation reactions. In a similar manner to the N*H*-2,3-diarylindole compounds prepared in Chapter 2, the nitrogen atom was substituted by both ethyl and benzyl protecting groups. Each N*H*-2,3,4,5-tetraarylpyrrole was deprotonated with sodium hydride and then either ethyl bromide or benzyl bromide was added to afford compounds **3.5** – **3.10** after an aqueous work up, shown in scheme 3.3.

N-ethyl-2,3,4,5-tetraphenylpyrrole, **3.5**, has been previously prepared from **3.1**, using the conditions described above. Compound **3.5** and a range of other tetraaryl substituted pyrrole molecules were synthesised to evaluate their device performance in organic light emitting diodes.[12a] The bulky phenyl groups around the pyrrole core helped to restrict the packing of these molecules, preventing aggregation in thin films. There are no other reports of the synthesis of **3.5** or its properties in the literature. There is only brief mention of N-benzyl-2,3,4,5-tetraphenylpyrrole, **3.8**, in the literature. In contrast to compounds **3.5** and **3.8**, the preparation of N-methyl-2,3,4,5-tetraphenylpyrrole is relatively well known in the literature. There are a variety of methods published to produce N-methyl-2,3,4,5-tetraphenylpyrrole.[22] Most recently a copper catalysed reaction between phenylboronic acid and N-methylpyrrole was reported to form N-methyl-2,3,4,5-tetraphenylpyrrole in 51% yield.[22a]

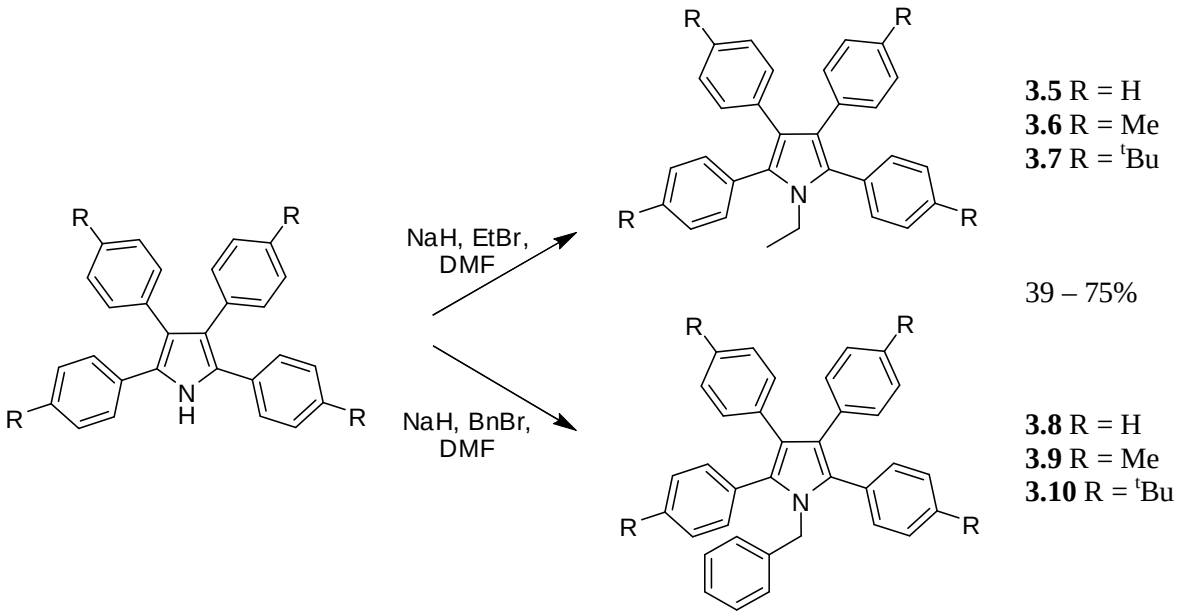

Scheme 3.3. Ethylation and benzylation of N*H*-2,3,4,5-tetraarylpyrroles.

Surprisingly, N-ethyl-2,3,4,5-tetra(4-methylphenyl)pyrrole, **3.6**, N-ethyl-2,3,4,5-tetra(4-*tert*butylphenyl) pyrrole, **3.7**, N-benzyl-2,3,4,5-tetra(4-methylphenyl)pyrrole, **3.9**, and N-benzyl-2,3,4,5-tetra(4-*tert*butyl phenyl)pyrrole, **3.10**, are all unknown compounds. The synthesis of **3.6** and **3.9** from N*H*-pyrrole **3.3** and the synthesis of **3.7** and **3.10** from N*H*-pyrrole **3.4** all proceed in moderate yields (69% and 75% from pyrrole **3.3**) and low yields (39% and 43% from pyrrole **3.4**). Each compound was fully characterised during the course of this study. The ^{1}H-NMR spectrum of each compound was as expected with the CH_2 quartet and CH_3 triplet corresponding to the ethyl protection observed at ~ 3.9 ppm and ~ 0.9 ppm, while the characteristic methylene proton singlet from the benzyl protection of **3.9** and **3.10** observed at ~ 5.0 ppm. Due to the symmetric nature of **3.6** – **3.10**, the methyl and *tert*butyl substitution of the peripheral aryl rings was observed as two singlets in each case, with the methyl protons present at ~ 2.3 ppm for compounds **3.6** and **3.9**, while the *tert*butyl protons were present at ~ 1.2 ppm for compounds **3.7** and **3.10**.

3.3 Attempted synthetic routes for the oxidative cyclodehydrogenation of N-substituted-2,3,4,5-tetraarylpyrroles using Lewis acidic transition metals

The prepared N-substituted-2,3,4,5-tetraarylpyrrole compounds, **3.5** – **3.10** synthesised above provide another platform to study the oxidative cyclodehydrogenation reaction. As opposed to Chapter 2, there are five different possibilities for the oxidative cyclodehydrogenation reaction of N-substituted-2,3,4,5-tetraarylpyrrole, all of the expected products are shown in figure 3.2. Ideally the oxidative

cyclodehydrogenation of N-substituted-2,3,4,5-tetraarylpyrrole compounds will form three new carbon-carbon bonds, only two carbon-carbon bond forming reactions away from the targeted fully cyclodehydrogenated pentaarylpyrrole compounds. However, there is a strong possibility of only one or two carbon-carbon bonds forming in the oxidative cyclodehydrogenation reaction, as partially cyclised products have been previously observed for oxidative cyclodehydrogenation reaction of both all carbon[23] and heterocyclic precursors.[24]

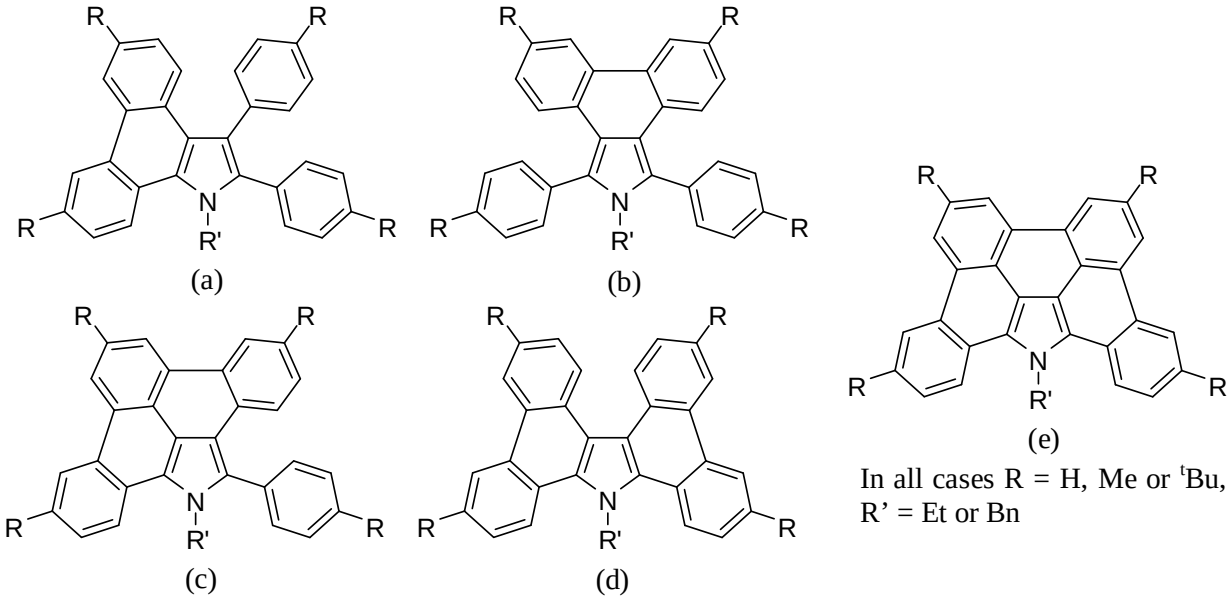

Figure 3.2. Possible combinations of carbon-carbon bonds that could be formed by the oxidative cyclodehydrogenation of N-substituted-2,3,4,5-tetraarylpyrrole compounds, **3.5** – **3.10**.

In 2007 Takase *et al*. reported the only example of a cyclodehydrogenation reaction where a pyrrole unit was incorporated.[25] In this example pyrrole is used as a peripheral aryl group and undergoes cyclodehydrogenation, rather than acting as the core structural unit to which aryl groups are attached to undergo cyclodehydrogenation (compounds **3.5** – **3.10**). Six pyrrole molecules were substituted onto a benzene core to form hexapyrrolylbenzene, **3.12**, and cyclodehydrogenated using $FeCl_3$ to form hexapyrrolohexaazacoronene, **3.13**, as shown in scheme 3.4. To help with solubility and isolation 3,4-dibromopyrrole and 3,4-di(4-trifluoromethylphenyl)pyrrole were also used a starting materials and their synthesis to hexapyrrolylbenzene derivatives and subsequent cyclodehydrogenation also proceeded successfully. A crystal structure was obtained of the cyclodehydrogenated hexa(3,4-di(4-trifluoromethylphenyl))pyrrolylbenzene compound, demonstrating the planarity of the azacoronene core. The carbon-carbon bond distance formed by cyclodehydrogenation between the pyrrole rings is 1.48(1) Å, longer than the expected distance for a carbon-carbon bond in a conjugated aromatic system, and closer to that of a single bond between two separate aromatic systems, as seen for the carbon-carbon bond

formed between two aryl rings of 2,3-diarylindoles in Chapter 2, typically ~ 1.47 Å. This planarity of **3.13** results from the use of a six membered ring as the core molecule, when pyrrole is used as the central core the five membered ring should impart non-planarity onto the resulting molecule when two or more bonds are formed adjacent to each other by oxidative cyclodehydrogenation. Hydrazine rather than methanol is used to quench the reaction, and the reason for this is unclear as problems with the quenching and purification of the reaction mixture are not mentioned.

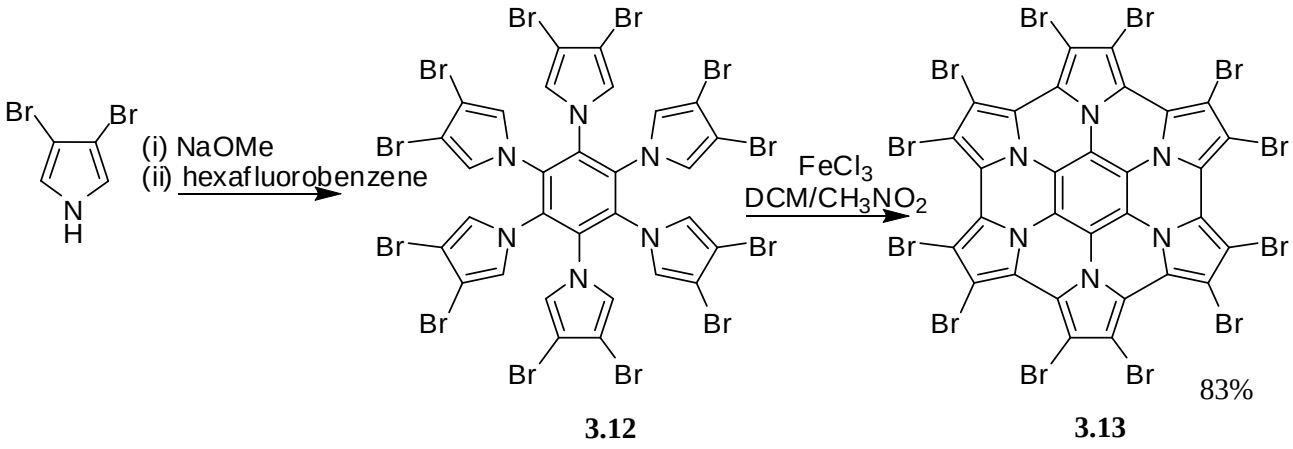

3.12 **3.13**

Scheme 3.4. Synthesis of hexapyrrolylbenzene and subsequent cyclodehydrogenation forming a hexaazacoronene core.[25]

*3.3.1 Attempted synthetic routes for oxidative cyclodehydrogenation using $FeCl_3$ with N-ethyl-2,3,4,5-tetraarylpyrroles **3.5**, **3.6** and **3.7***

To investigate the cyclodehydrogenation of 2,3,4,5-tetraarylpyrrole compounds, the N-ethyl-2,3,4,5-tetraarylpyrroles, **3.5**, **3.6** and **3.7**, were employed initially, with $FeCl_3$ used as both the lewis acid and oxidant. As up to three carbon-carbon bonds can be formed from the oxidative cyclodehydrogenation of 2,3,4,5-tetraarylpyrrole compounds 45 equivalents of $FeCl_3$ were used, 15 equivalents of $FeCl_3$ for each carbon-carbon bond to be formed.

Firstly, **3.5** was subjected to oxidative cyclodehydrogenation, with 45 equivalents of $FeCl_3$ dissolved in the minimum amount of nitromethane and added dropwise to a solution of **3.5** dissolved in anhydrous dichloromethane, with a constant stream of argon bubbling through the reaction mixture. After one hour the reaction was quenched with methanol. As well as protecting the nitrogen atom from reacting with the lewis acids employed in cyclodehydrogenation reactions the characteristic peaks in the ^{1}H-NMR spectrum arising from both the ethyl and benzyl group allow for the observation of different cyclodehydrogenation products, especially when the aromatic region of the spectrum is crowded. As seen in the previous

chapter, cyclodehydrogenation deshields the protons moving their peaks downfield in the ^{1}H-NMR spectrum.

In this case the crude ^{1}H-NMR spectrum indicated the presence of at least three different cyclodehydrogenated products, as judged by the presence of three different CH_2 quartets arising from the ethyl groups, present from 5.2 – 5.0 ppm. The peaks in the aromatic region of the spectrum were also shifted downfield from the spectrum of **3.5**, indicating that a cyclodehydrogenation reaction has taken place. Unfortunately, despite repeated attempts at purification using column chromatography and various solvent systems no single product could be isolated from the reaction mixture. Mass spectrometry did not give any clear evidence for the products that may have formed from this reaction. Identical reaction conditions were also employed, but the reaction mixture was left to stir under an atmosphere of argon overnight, in an attempt to form only the most stable cyclodehydrogenation product. This approach was also unsuccessful as the same three CH_2 quartets arising from the ethyl groups of the different products were present in the ^{1}H-NMR spectrum of the crude reaction mixture.

Despite being unable to isolate any products from the cyclodehydrogenation of **3.5** with 45 equivalents of $FeCl_3$ compounds **3.6** and **3.7** were also subjected to the same cyclodehydrogenation conditions. Unfortunately, after quenching of the reaction mixture in a similar method to the above reaction the same result was obtained and no products were able to be isolated using column chromatography.

As demonstrated in the previous chapter, $FeCl_3$ does not need to be added to the reaction mixture dropwise as solution in nitromethane, and can instead be added to the reaction directly as a solid.[26] This approach provided the only successful cyclodehydrogenation reaction using Lewis acidic transition metal catalysts in the previous chapter and so it was also trialled for compounds **3.5**, **3.6** and **3.7**. Initially 45 equivalents of $FeCl_3$ were added directly to a solution of **3.5** in anhydrous dichloromethane with a constant stream of argon bubbling through the reaction mixture. After stirring the reaction overnight and quenching with methanol, purification of the reaction mixture was attempted. Upon attempting to dissolve the product in the minimum amount of dichloromethane to purify the crude reaction mixture by column chromatography, a solid formed which was filtered, washed with a small amount of dichloromethane and isolated in a low 8% yield. Pleasingly, the solid was soluble enough in deuterated chloroform to collect a ^{1}H-NMR spectrum. The ^{1}H-NMR spectrum revealed the presence of only one cyclodehydrogenated product, **3.14**, and its ^{1}H-NMR spectrum is shown in figure 3.3.

The aromatic protons of **3.14** integrate for 12 protons, two less protons than if the desired three carbon-carbon bonds had formed, and interestingly the aromatic region also lacks the expected triplet peaks from the unsubstituted peripheral phenyl rings. The spectrum also contains two unexpected singlet peaks present at 8.69 ppm and 8.58 ppm. This indicates both that carbon-carbon bonds have formed between the ortho carbon atoms on the peripheral phenyl groups from cyclodehydrogenation, and that substitution has occurred at the para position on all four of the peripheral aryl groups. The resulting singlets must then arise from the meta proton between these two positions. To explain the presence of 12 aromatic proton signals only two carbon-carbon bonds must have formed, along with para substitution at all four of the aryl groups, rather than the formation of three carbon-carbon bonds, which would give rise to 14 aromatic proton signals. There are two possibilities for the position of the two new carbon-carbon bonds in **3.14**; either the carbon-carbon bonds have formed so that both ortho carbon atoms of one phenyl ring in position 3 or 4 on the pyrrole core are involved in cyclodehydrogenation (see figure 3.2c) creating an unsymmetrical product, or only one ortho carbon atom from each phenyl ring is involved in cyclodehydrogenation (see figure 3.2d) giving rise to a symmetrical product. The presence of only six peaks in the aromatic region of the ^{1}H-NMR spectrum (four doublet peaks and two singlet peaks) indicate that a symmetrical product with the carbon-carbon bonds arranged like that of figure 3.2d must have formed. The ethyl peaks of **3.14** have also shifted downfield due to the formation of a more aromatic product, the CH_2 quartet is now at 5.12 ppm and the CH_3 triplet is at 1.70 ppm compared to 3.90 ppm and 0.97 ppm for **3.5**, respectively.

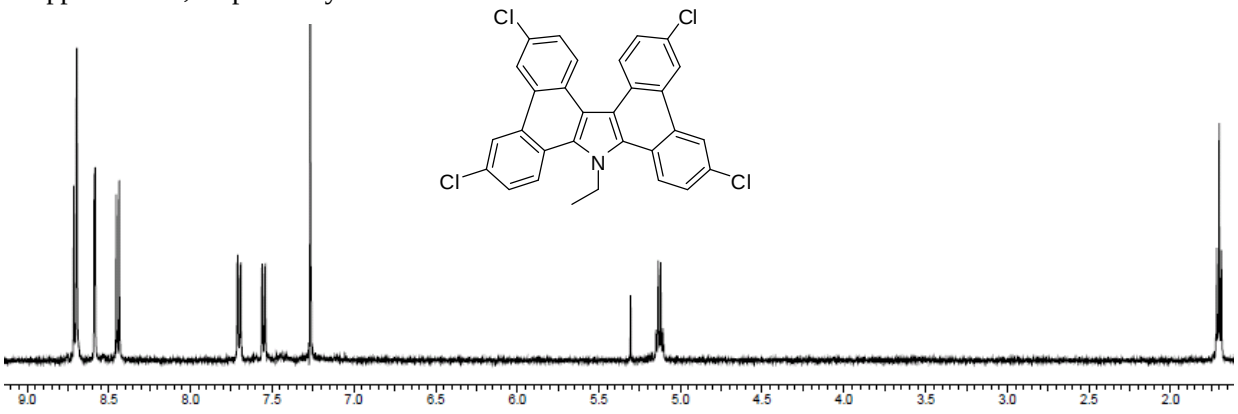

Figure 3.3. ^{1}H-NMR spectrum of **3.14** obtained from the reaction of **3.5** with 45 equivalents of solid $FeCl_3$.

The substitution at all four para positions of the peripheral phenyl groups of **3.14** is most likely by chlorine atoms, as chlorinated side products are often encountered when performing oxidative cyclodehydrogenation using $FeCl_3$.[27] If the para substitution on the peripheral phenyl groups is in fact chlorine then the product formed from the reaction between **3.5** and 45 equivalents of solid $FeCl_3$ would

be 3,6,12,15-tetrachloro-9-ethyl-tetrabenzo[*a*,*c*,*g*,*i*]carbazole, **3.14**, as shown in scheme 3.5. Unfortunately a mass spectrum could not be obtained of **3.14**. The rest of the crude reaction mixture was purified, but no other products or more **3.14** were able to be isolated. It is clear from the low yield of **3.14** that this is not the only product formed from the reaction of **3.5** and 45 equivalents of $FeCl_3$, but it is the only product that was able to be isolated.

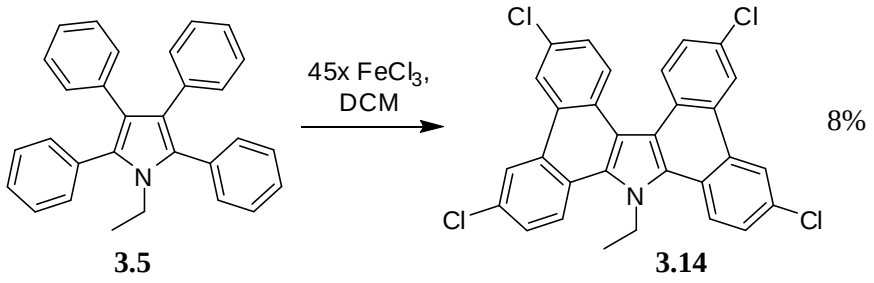

3.5 **3.14**

Scheme 3.5. Formation of cyclodehydrogenation product **3.14** from **3.5**.

Compound **3.14** is sparingly soluble in dichloromethane and pleasingly the slow evaporation of a dilute dichloromethane solution formed crystals suitable for X-ray crystallography. The X-ray crystal structure was solved in the triclinic space group *P*-1 with one molecule of **3.14** present in the asymmetric unit, as shown in figure 3.3, confirming the chlorination at all four para positions of the peripheral phenyl groups. Unlike the previous chapter, where the formation of a carbon-carbon bond between the ortho carbon atoms of the phenyl rings in the 2- and 3-positions on the indole ring served to planarise the resulting dibenzo[*a*,*c*]carbazole, the formation of two carbon-carbon bonds, one between the ortho carbon atoms of the phenyl rings in the 2- and 3-position, and one between the ortho carbon atoms in the 4- and 5-position does not result in a planar structure. In fact the phenyl rings in the 3- and 4-positions are twisted at an angle of 38.1(1)˚ to each other, and at 20.3(1)˚ and 18.2(1)˚ to the central pyrrole core. The twisting present in the structure does not result in elongation of the carbon-carbon bonds formed (C11···C14 = 1.472(3) Å and C25···C28 = 1.496(3) Å). The carbon-chlorine bonds range from 1.736(3) Å to 1.746(3) Å, as expected for a carbon-chlorine single bond. The twisting of **3.14** is presumably to minimise the steric clash between the ortho hydrogen atoms of the phenyl rings in the 3- and 4-position, as shown in figure 3.4.

The four chlorine atoms present in compound **3.14** and the considerable twisting of the molecule both play a significant role in the crystal packing. The chlorine atoms in the para position of the phenyl groups in the 3- and 4-position on the pyrrole core of **3.14** interact with chlorine atoms in the same position of another molecule of **3.14**. These halogen-halogen interactions between the chlorine atoms (Cl···Cl = 3.405(1) Å) forms a dimer, with the two molecules of **3.14** related about an inversion centre, as shown in

figure 3.5. Halogen-halogen interactions are well documented in supramolecular assemblies and can control the overall crystal packing of the molecule.[28] The remaining two chlorine atoms (in the para position of the phenyl groups in the 2- and 5-position of the pyrrole core) hydrogen bond with peripheral hydrogen atoms in neighbouring units (C···Cl ranges from 3.610(2) Å to 3.881(3) Å).

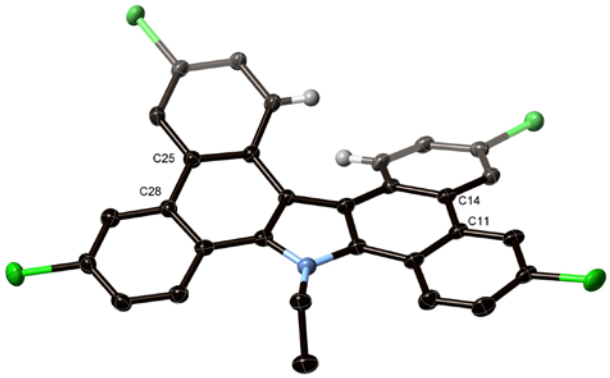

Figure 3.4. Asymmetric unit of **3.14**, all hydrogen atoms apart from the two contributing to the twist of the molecule have been removed for clarity.

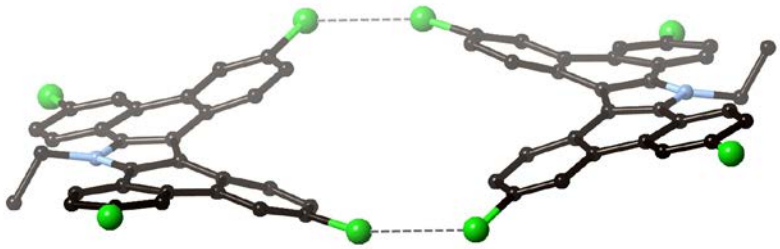

Figure 3.5. Halogen – halogen interactions between the chlorine atoms of the phenyl rings in position 3 and 4 on the pyrrole core, hydrogen atoms have been removed for clarity.

The overall packing of **3.14** in the solid state also displays weak face-to-face π – π stacking interactions (centroid to centroid distances range from 3.665(3) Å and 3.894(2) Å) between the peripheral phenyl groups and also between the pyrrole core and the peripheral phenyl rings causing the dimers to pack in layers, as shown in figure 3.6.

With the first successful oxidative cyclodehydrogenation of a 2,3,4,5-tetraarylpyrrole molecule, identical reaction conditions were employed for tetraarylpyrroles **3.6** and **3.7**. Unfortunately, in both cases the ^{1}H-NMR spectrum of the crude reaction mixture indicated three cyclodehydrogenation products present as well as a large amount of starting tetraarylpyrrole. Although purification was attempted no products could be isolated cleanly from the reaction mixture. The presence of a large amount of starting compound in the reactions of **3.6** and **3.7** was not observed in the crude ^{1}H-NMR spectrum of the reaction of **3.5** to produce

3.14. The presence of a large amount of starting compound could indicate that chlorination in the para position of the peripheral aryl groups is necessary to activate the 2,3,4,5-tetraarylpyrrole molecules towards cyclodehydrogenation. Compounds **3.6** and **3.7** block the para position from chlorination as they are already substituted with methyl and *tert*butyl groups, respectively.

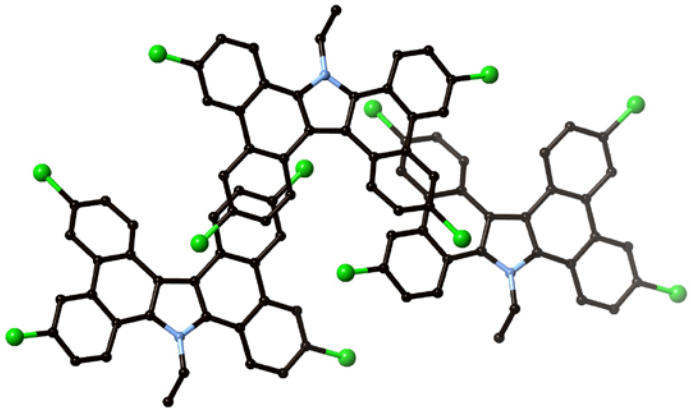

Figure 3.6. Face-to-face π – π interactions of adjacent molecules of **3.14**, hydrogen atoms have been removed for clarity.

Further attempts were made to isolate and purify cyclodehydrogenation products from the reaction of 2,3,4,5-tetraarylpyrroles with $FeCl_3$ that did not have chlorination of the para position of the peripheral aryl groups. Fewer equivalents of $FeCl_3$ per carbon-carbon bond to be formed were employed in the cyclodehydrogenation of **3.5** in an attempt to isolate cyclodehydrogenation products that were not chlorinated. Keeping in mind that the only product isolated, **3.14**, contained only two carbon-carbon bonds when 45 equivalents of $FeCl_3$ was employed (22.5 equivalents formation of two carbon-carbon bonds and for tetra chlorination), both 24 and 15 equivalents of $FeCl_3$ were trialled with tetraarylpyrrole **3.5**. Frustratingly, in each case a mixture of products were observed in the crude ^{1}H-NMR spectrum and no products were able to be isolated by column chromatography.

Tetraarylpyrroles **3.6** and **3.7** were also subjected to further cyclodehydrogenation with fewer equivalents of $FeCl_3$. Both 30 and 15 equivalents of $FeCl_3$ were trialled and added to the reaction mixture as both a solid and dissolved in nitromethane. In some cases a small amount of cyclodehydrogenated product was observed by ^{1}H-NMR spectroscopy, but mostly only starting material was recovered. In some cases the products observed early on in the reaction by thin layer chromatography did not appear to be stable when the reaction was continued overnight. In these cases the reactions were repeated and quenched after product formation, unfortunately no cyclodehydrogenation products were able to be isolated successfully.

*3.3.2 Oxidative cyclodehydrogenation using $FeCl_3$ with N-benzyl-2,3,4,5-tetraarylpyrroles, **3.8**, **3.9** and **3.10***

With the successful isolation and purification of one cyclodehydrogenated compound, **3.14**, from the reaction of N-ethyl-2,3,4,5-tetraarylpyrrole compounds, **3.5**, **3.6** and **3.7**, the cyclodehydrogenation of the N-benzyl-2,3,4,5-tetraarylpyrrole compounds **3.8**, **3.9** and **3.10** was attempted. Despite only small amounts of cyclodehydrogenation products observed in the ^{1}H-NMR spectra of **3.6** and **3.7**, the corresponding N-benzyl-2,3,4,5-tetraarylpyrrole compounds **3.9** and **3.10** were trialled, as the benzyl group may play a role in the stabilisation of the final product, as observed for the cyclodehydrogenation using $FeCl_3$ of the 2,3-diarylindoles in the previous chapter.

The same cyclodehydrogenation conditions that were employed for the isolation of **3.14** from **3.5**, were initially employed for the cyclodehydrogenation of **3.8**. Unfortunately, after quenching the reaction, a mixture of cyclodehydrogenation products, as determined by the number of benzylic protons in the ^{1}H-NMR spectrum, were isolated. Isolation and purification of these products was attempted using column chromatography, but the various products could not be separated.

Different ratios of $FeCl_3$ were then employed for the cyclodehydrogenation of **3.8**, **3.9** and **3.10**, as monitoring the above reaction and the reactions of the N-ethyl-2,3,4,5-tetraarylpyrroles, **3.5**, **3.6** and **3.7**, with thin layer chromatography seemed to suggest a decomposition of products when the reactions were left to stir overnight despite the reactions being incomplete after eight hours. An excess of $FeCl_3$ may be responsible for the observed decomposition when the reactions were left to stir overnight. Both 30 and 15 equivalent of $FeCl_3$ per molecule to be cyclodehydrogenated was employed, and initially the $FeCl_3$ was added to the reaction as a solid as the only cyclodehydrogenated products isolated by using chemical means in this study have been obtained in this way.

Frustratingly, the addition of 30 equivalents of solid $FeCl_3$ to **3.8**, **3.9** and **3.10** produced various cyclodehydrogenation products that could not be isolated. The addition of 15 equivalents of $FeCl_3$ to **3.8**, **3.9** and **3.10**, also produces various cyclodehydrogenation products, but in all three cases one cyclodehydrogenation product was able to be isolated by column chromatography. Further purification of the isolated products was achieved by recrystallisation, and the cyclodehydrogenated compounds were obtained in low yields (25% − 38%). Analysis of the ^{1}H-NMR spectra, shown in figure 3.7, indicates that one carbon-carbon bond has been formed by oxidative cyclodehydrogenation. In each case the new carbon-carbon bond has formed in the same position as seen by the similarity of the ^{1}H-NMR spectrum in the downfield region from 7.5 ppm to 9 ppm to the ^{1}H-NMR spectra of the dibenzo[*a*,*c*]carbazoles

presented in Chapter 2. The formation of only one carbon-carbon bond is confirmed by mass spectrometry.

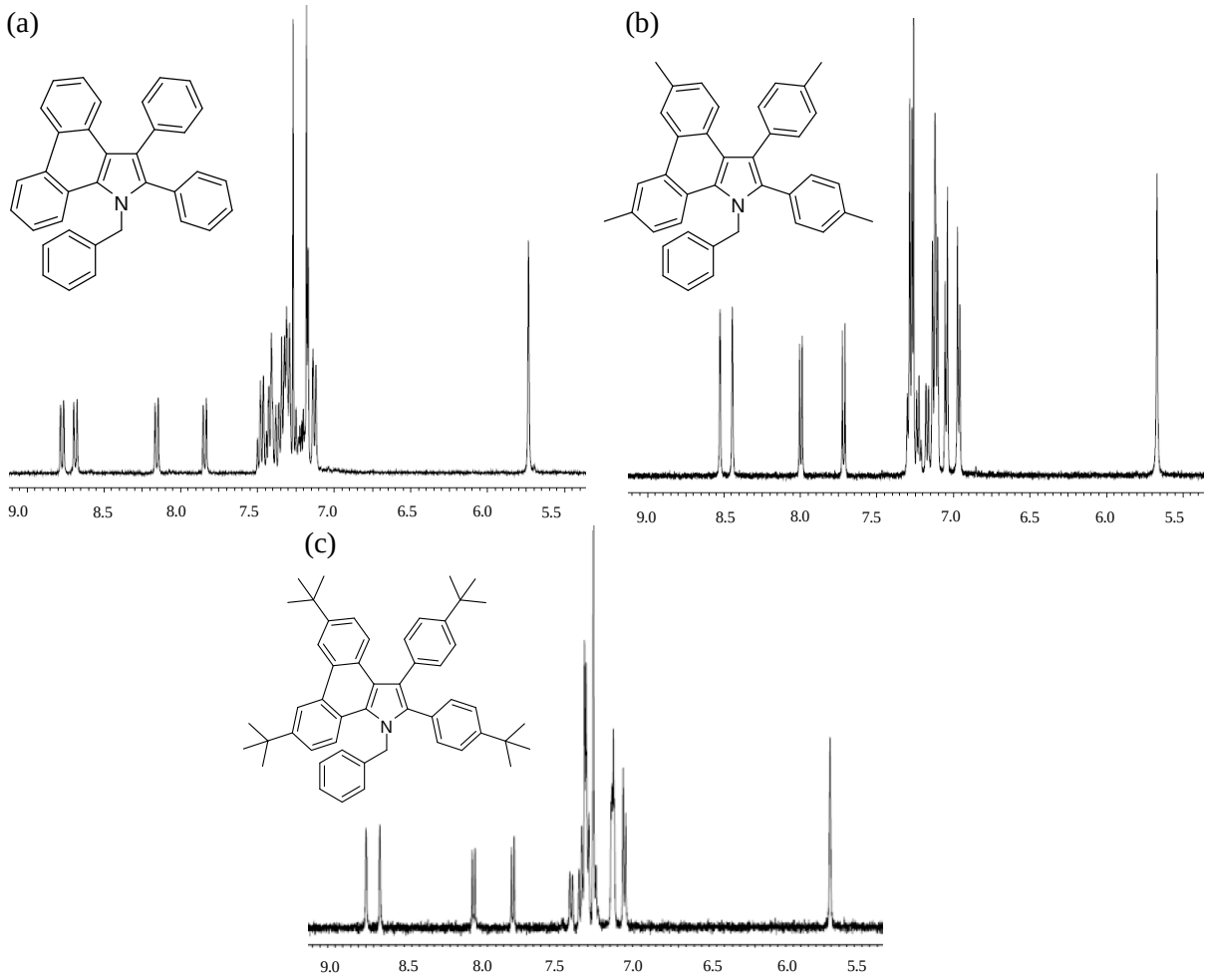

Figure 3.7. ^{1}H-NMR spectrum of the aromatic region of the N-benzyl-2,3-diphenyldibenzo[*e*,*g*]indole compounds, (a) **3.15**, (b) **3.16**, (c) **3.17**.

As shown in figure 3.2 the carbon-carbon bond can form in one of two positions; either between the peripheral aryl groups in the 2- and 3-positions of the pyrrole core (figure 3.2a), creating an unsymmetrical product, or between the peripheral aryl groups in the 3- and 4-positions of the pyrrole core (figure 3.2b), creating a symmetrical product. The ^{1}H-NMR spectra of **3.16** and **3.17** indicate the formation of an unsymmetrical product (figure 3.2a) by the presence of two singlet peaks observed significantly upfield, rather than the presence of one upfield shifted singlet, which would be expected for a symmetrical product. The lack of singlet peaks from cyclodehydrogenation in the ^{1}H-NMR spectrum of **3.15** indicates that no para substitution has occurred during the course of the cyclodehydrogenation. The methylene benzyl singlet is moved considerably downfield in each case from ~ 5.1 ppm in the precursor

compounds **3.8**, **3.9** and **3.10** to ~ 5.7 ppm in the cyclodehydrogenated products **3.15**, **3.16** and **3.17**. The aromatic region from ~ 7ppm to ~ 7.5 ppm is crowded due to the two free peripheral aryl groups and the proton resonances from the aromatic benzyl protons.

The ^{1}H-NMR spectra and mass spectrometry indicate that the reaction of all three N-benzyl-2,3,4,5-tetraarylpyrrole compounds, **3.8**, **3.9** and **3.10**, has formed the corresponding N-benzyl-2,3-diaryldibenzo[*e*,*g*]indole compounds, **3.15**, **3.16** and **3.17**, shown in figure 3.8. This is the first reported preparation of N-benzyl-2,3-diaryldibenzo[*e*,*g*]indole compounds, and along with the preparation of **3.14** above, demonstrates that compounds with a pyrrole core can undergo cyclodehydrogenation reactions of their peripheral aryl groups to form carbon-carbon bonds. All three compounds were fully characterised during the course of this study.

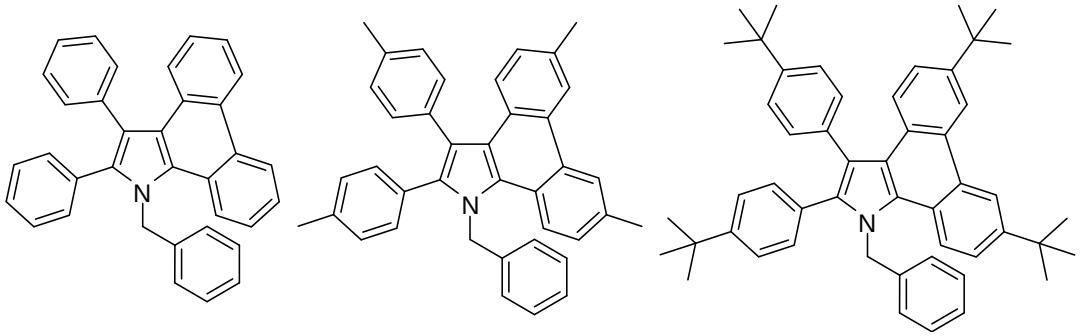

3.15 **3.16** **3.17**

Figure 3.8. Cyclodehydrogenated compounds isolated from the reactions of **3.8**, **3.9** and **3.10** (a) N-benzyl-2,3-diphenyl-dibenzo[*e*,*g*]indole, **3.15**, (b) N-benzyl-2,3-di(4-methylphenyl)-6,9-dimethyl-dibenzo[*e*,*g*]indole, **3.16**, (c) N-benzyl-2,3-di(4-*tert*butylphenyl)-6,9-di*tert*butyl-dibenzo[*e*,*g*]indole, **3.17**.

Despite the use of identical conditions for the oxidative cyclodehydrogenation of N-ethyl-2,3,4,5-tetraarylpyrrole compounds, **3.5**, **3.6** and **3.7**, previously, no evidence was found in the ^{1}H-NMR spectra for the formation of the corresponding N-ethyl-2,3-diaryl-dibenzo[*e*,*g*]indole compounds. The substitution at the nitrogen atom of the pyrrole core must play more of a role in the Scholl reaction than simply just protecting the nitrogen atom from reaction with the lewis acid. The subtle change in protecting group from ethyl to benzyl affects the type of products obtained from the reaction mixture, further demonstrating the well known difficulty in controlling the products obtained from the Scholl reaction.[29,30] Crystals suitable for X-ray crystallography were grown of all three cyclodehydrogenation products, **3.15**, **3.16** and **3.17**, by the slow diffusion of methanol into a benzene solution of the compound and figure 3.9a – c are shows the asymmetric units of all three compounds.

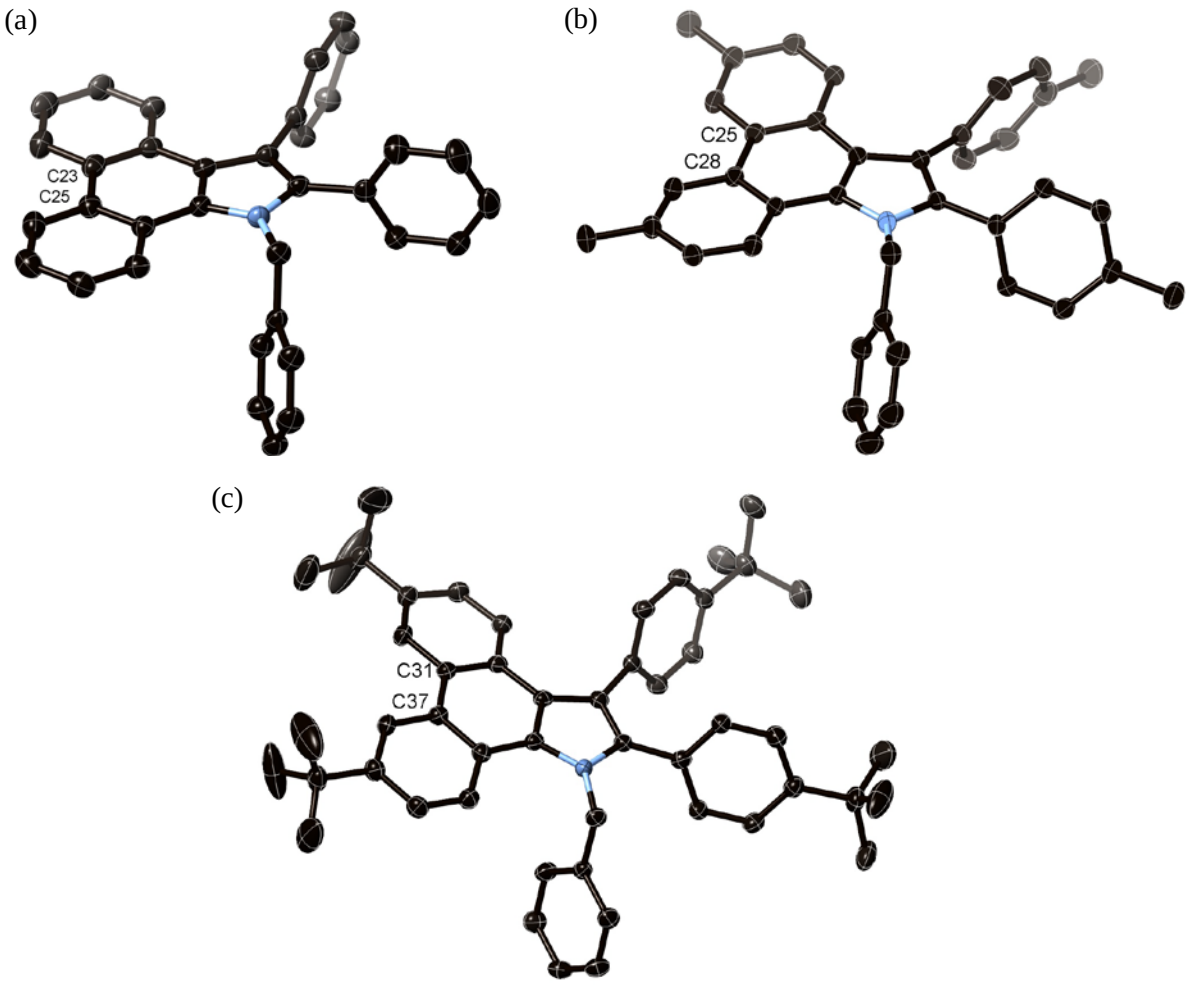

Figure 3.9. Asymmetric units of (a) **3.15**, (b) **3.16**, (c) **3.17**, hydrogen atoms and solvent benzene molecules have been removed for clarity.

Compound **3.15** crystallised in the monoclinic space group $P2_1/c$, and the new carbon-carbon bond formed between C23 and C25 has a bond length of 1.467(2) Å. The formation of only one carbon-carbon bond allows the newly formed dibenzo[*e*,*g*]indole core to be planar, as opposed to the twisting of the tetrabenzo[*a*,*c*,*g*,*i*]carbazole core seen in the crystal structure of compound **3.14**. The peripheral phenyl rings in the 2- and 3-position of the pyrrole ring that were not involved in the cyclodehydrogenation reaction twist at angles of 87.8(1)˚ and 77.1(1)˚, respectively to the dibenzo[*e*,*g*]indole core. Molecules of **3.15** display extensive edge-to-face π – π stacking interactions between the dibenzo[*e*,*g*]indole core and the two peripheral phenyl rings (C···centroid distances range from 3.686(2) Å to 3.829(2) Å) in units of **3.15** both above and below the compound, stacking the molecules of **3.15** into columns. The benzyl group displays face-to-face π – π stacking interactions with a peripheral phenyl ring (centroid to centroid distances = 3.330(2) Å) of a neighbouring molecule of **3.15** in the same column. The benzyl ring also

displays edge-to-face π – π stacking interactions with a peripheral phenyl ring (C···centroid distance = 3.664(2) Å) of an adjacent molecule of **3.15** in different columns, allowing interactions between the columns of **3.15**. The π – π stacking interactions and columns formed between molecules of **3.15** are shown in figure 3.10.

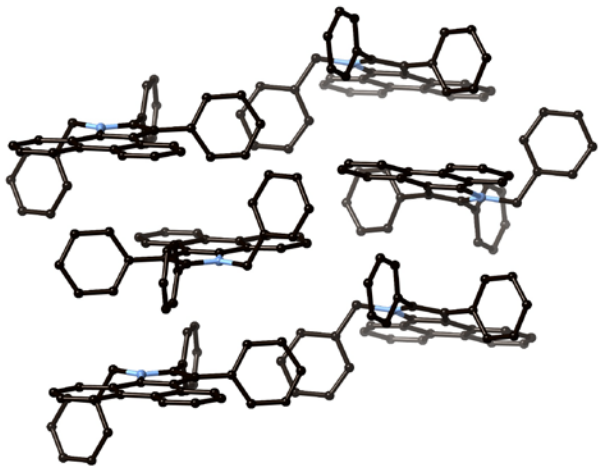

Figure 3.10. Edge-to-face and face-to-face π – π stacking interactions between adjacent molecules of **3.15** to form a column of molecules linked by interactions between the benzyl groups, hydrogen atoms have been removed for clarity.

Compound **3.16** also crystallises in the monoclinic space group $P2_1/c$, with one solvent molecule of benzene present in the asymmetric unit along with one molecule of **3.16**. The new carbon-carbon bond formed between C25 and C28 has a distance of 1.466(2) Å, very similar to that of **3.15**. Again the dibenzo[*e*,*g*]indole core is planar with the peripheral 4-methylphenyl groups at the 2- and 3-position of the pyrrole ring twisted at 54.1(1)˚ and 77.6(1)˚ to the dibenzo[*e*,*g*]indole core respectively. In this case face-to-face π – π stacking interactions between dibenzo[*e*,*g*]indole cores of molecules of **3.16** both above and below stack the molecules of **3.16** together in columns (centroid to centroid distances range from 3.769(2) Å to 3.912(2) Å), and each solvent benzene molecule also participates in face-to-face π – π stacking interactions with the peripheral 4-methylphenyl group in the 2-position of the pyrrole core (centroid to centroid distance = 3.765(3) Å). The methyl groups of the phenyl rings participate in edge-to-face π – π stacking interactions with the benzene solvent molecules (C···centroid distance = 3.762(3) Å) and the benzyl group of a molecule of **3.16** in an adjacent column (C···centroid = 3.567(3) Å). The benzyl groups also display edge-to-face π – π stacking interactions with the peripheral 4-methylphenyl group in the 2-position of the pyrrole core of a molecule in the same column (C···centroid distances range from 3.628(2) Å to 3.902(2) Å). The face-to-face and edge-to-face π – π stacking interactions between molecules of **3.16**, as well as the columns of molecules of **3.16** formed are shown in figure 3.11.

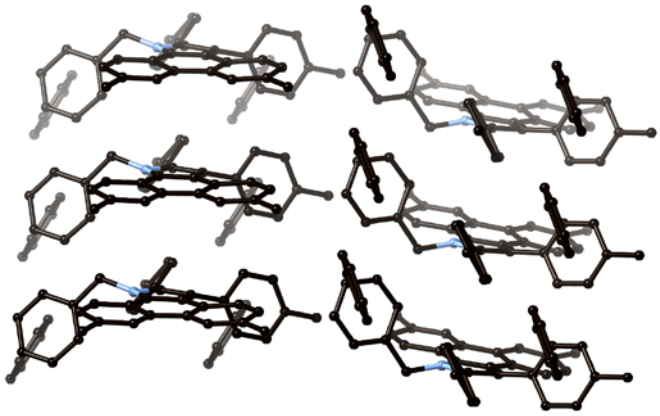

Figure 3.11. Edge-to-face and face-to-face π – π stacking interactions between adjacent molecules of **3.16**, hydrogen atoms have been removed for clarity.

Finally, compound **3.17** crystallised in the orthorhombic space group *Pbcn*, with one disordered solvent molecule of benzene present in the asymmetric unit along with one molecule of **3.17**. Two of the *tert*butyl groups have increased thermal motion due to the freedom of movement around the central carbon atom. The new carbon-carbon bond formed between C31 and C37 has a distance of 1.470(4) Å and again results in the formation of a planar dibenzo[*e*,*g*]indole core. The two peripheral 4-*tert*butylphenyl groups in the 2- and 3-position of the pyrrole ring twist out of the plane of the dibenzo[*e*,*g*]indole core by 64.8(1)˚ and 66.1(1)˚, respectively. Compound **3.17** displays edge-to-face π – π stacking interactions between the dibenzo[*e*,*g*]indole core and the 4-*tert*butylphenyl groups in the 2- and 3-position of the pyrrole ring with molecules of **3.17** both above and below (C···centroid distances range from 3.621(3) Å to 3.924(3) Å) to again form columns of **3.17**. The molecules in the columns are offset from each other due to the bulky *tert*butyl groups. These columns are further supported by weak edge-to-face π – π stacking interactions between the benzyl group of **3.17** and the *tert*butylphenyl group in the 2-position of the pyrrole ring of a neighbouring molecule of **3.17** in the same column (C···centroid distances = 3.964(3) Å and 3.949(3) Å). The bulky *tert*butyl groups prevent π – π interactions between the columns. The disordered benzene solvent molecules do not have any strong interactions with **3.17**. Figure 3.12 shows the π – π stacking interactions between molecules of **3.17** to form distinct columns.

Because of the extended aromaticity of the dibenzo[*e*,*g*]indole core and the remaining phenyl rings, all three molecules are able to form columns resulting from the extensive edge-to-face and face-to-face π – π stacking present. The peripheral methyl and *tert*butyl substitution does not affect the ability of molecules of **3.16** and **3.17** to form columns, but the interactions between the columns is minimised the bulkier the group substituted on the periphery.

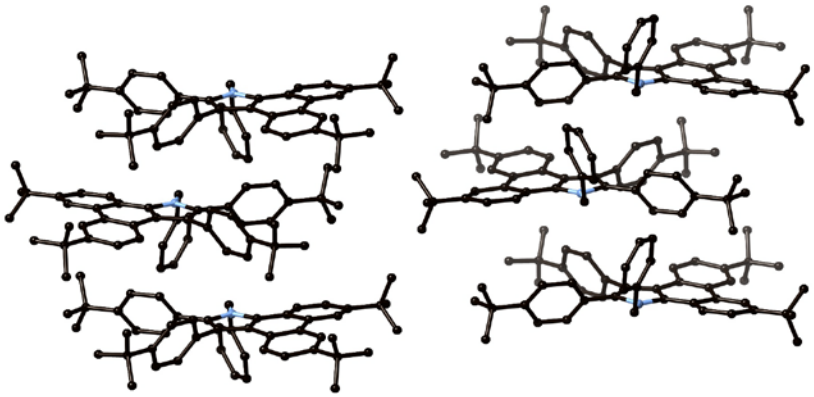

Figure 3.12. Edge-to-face π – π stacking interactions between molecules of **3.17** to form distinct columns, hydrogen atoms and benzene solvent molecules have been removed for clarity.

All three compounds **3.8**, **3.9** and **3.10** were also subjected to oxidative cyclodehydrogenation using 15 equivalents of $FeCl_3$ dissolved in the minimum amount of nitromethane. Pleasingly, after quenching the reactions with methanol and purification with column chromatography, all three compounds **3.15**, **3.16** and **3.17** were obtained in similar yields to above.

Despite the documented attempts above using 45 equivalents of $FeCl_3$, no cyclodehydrogenation products were able to be isolated, but the use of 15 equivalents of $FeCl_3$ allowed for the isolation of cyclodehydrogenation products where one carbon-carbon bond had been formed. This opens the possibility of forming each carbon-carbon bond from oxidative cyclodehydrogenation in a stepwise fashion over three subsequent reactions, using 15 equivalents of $FeCl_3$ each time. Unfortunately, the low yields obtained for the formation of **3.15**, **3.16** and **3.17** prevented enough of these compounds being synthesised for this route to forming a curved polycyclic heteroaromatic compound to be pursued.

*3.3.3 Attempted synthetic routes for oxidative cyclodehydrogenation and simultaneous Friedel-Crafts alkylation using $FeCl_3$ with 2,3,4,5-tetraarylpyrrole **3.5***

The Friedel-Crafts alkylation and oxidative cyclodehydrogenation of hexaphenylbenzene **3.18** to form a soluble hexabenzohexacoronene derivative, **3.19**, using $FeCl_3$ as both the required strong lewis acid catalyst and as the oxidant was reported by Rathore *et al.* in 2003.[31] Solubility is often an issue in the isolation and characterisation of polycyclic aromatic compounds, but the preparation of the appropriately substituted compounds before cyclodehydrogenation can also be synthetically challenging. This one pot reaction, shown in scheme 3.6, does not require the synthesis of the appropriately substituted precursor

compounds, instead cyclodehydrogenation and alkylation occur in one pot, with almost 100% conversion from **3.18** to **3.19**.

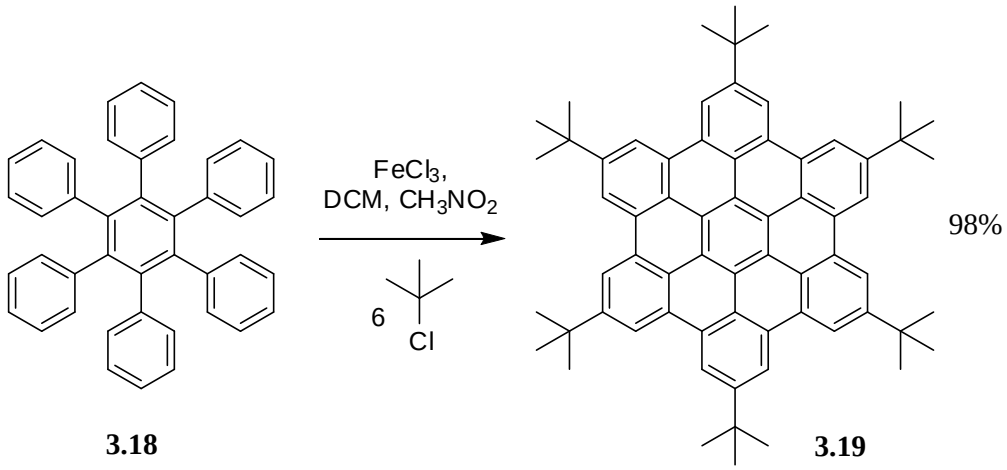

Scheme 3.6. Synthesis of a soluble hexabenzohexacorene derivative, **3.19**, from hexaphenylbenzene, **3.18**, by Friedel-Crafts alkylation and cyclodehydrogenation in a one pot reaction.[31]

N-ethyl-2,3,4,5-tetraphenylpyrrole, **3.5**, was chosen to investigate the scope of this reaction on the tetraarylpyrrole model compounds, as cyclodehydrogenation and para-substitution has already been observed when **3.5** was reacted with $FeCl_3$ to form **3.14**. Initially, the reaction of **3.5** and *tert*butylchloride with 12 equivalents of $FeCl_3$ was carried out exactly as described in the literature; a few drops of $FeCl_3$ dissolved in nitromethane was added to **3.5** dissolved in dry dichloromethane with a constant stream of argon bubbling through the solution. After three hours the remainder of the $FeCl_3$ solution was added and two hours later the reaction was quenched with methanol. The addition of a small amount of $FeCl_3$ initially is required to catalyse Friedel-Crafts alkylation, and the cyclodehydrogenation reaction proceeds after the addition of the remaining $FeCl_3$ solution.[31] After quenching of the reaction mixture ^{1}H-NMR spectroscopy indicated the presence of cyclodehydrogenated compounds by the observation of downfield shifted peaks, but unfortunately no characteristic singlet peaks were observed for the meta protons if both para alkylation and cyclodehydrogenation had occurred, as in the case of **3.14**.

To determine if para alkylation was able to occur in this manner the reaction was repeated and only a few drops of $FeCl_3$ dissolved in nitromethane solution was added. Thin layer chromatography indicates the formation of four or five products, plus the presence of **3.5** after 30 minutes of reaction time. After this point no change occurs in the thin layer chromatography in the remaining reaction time, suggesting that the reaction has consumed the catalytic $FeCl_3$ in the first 30 minutes and no new reactions are occurring. Frustratingly, the ^{1}H-NMR spectrum of the reaction mixture shows only starting material present,

indicating that only a very small amount of alkylated or cyclodehydrogenated product has formed. It appears that the small amount of $FeCl_3$ is not being used as catalytic lewis acid for the Friedel-Crafts alkylation, so the reaction was re-run with all of the $FeCl_3$ solution added initially in one go and the reaction was then monitored by thin layer chromatography. The reaction mixture almost immediately forms four or five products, but over the course of the reaction the amount of new product does not increase and **3.5** is not consumed. Addition of another 12 equivalents of $FeCl_3$ dissolved in nitromethane was added but this did not increase the yield of any new products and again mainly **3.5** was isolated from the reaction mixture.

The Friedel-Crafts alkylation and cyclodehydrogenation of **3.5** does not occur as readily, if at all, as that of hexaphenylbenzene, **3.18**, as evidenced by the reactions above. Oxidative cyclodehydrogenation with N-ethyl-2,3,4,5-tetraphenylpyrroles using $FeCl_3$ dissolved in nitromethane has already been observed in this study to form many products, none of which can be isolated. The addition of *tert*butyl chloride may be complicating this already problematic reaction, producing even more products. No Friedel – Crafts alkylations of any phenyl substituted pyrroles have been reported where the alkylation occurs on the phenyl ring. It may be that *tert*butyl chloride is reacting in an unexpected manner with the pyrrole ring that further complicates the cyclodehydrogenation reaction.

3.3.4 Attempted synthetic routes for oxidative cyclodehydrogenation using $AlCl_3$ with N-substituted-2,3,4,5-tetraarylpyrroles, ***3.5*** *–* ***3.10***

As outlined in Chapter 2 other lewis acidic transition metal catalysts besides $FeCl_3$ have also been used to perform oxidative cyclodehydrogenation reactions. Various N-ethyl-2,3,4,5-tetraarylpyrroles, **3.5** – **3.7**, and N-benzyl-2,3,4,5-tetraarylpyrroles, **3.8** – **3.10**, were subjected to oxidative cyclodehydrogenation with $AlCl_3$ using $CuCl_2$ or $Cu(OTf)_2$ as the oxidant. The reactions were monitored with thin layer chromatography and allowed to run for 72 hours or more, but frustratingly in each case multiple products were detected, that could not be separated or isolated. ^{1}H-NMR spectroscopy and mass spectrometry did not help in identifying any products, although the proton integrals obtained from ^{1}H-NMR spectroscopy of the reaction mixture showed that any cyclodehydrogenation products that were formed were present in a very low yield. Varying these reaction conditions from the literature was not pursued due to the low yields of products.

3.4 Photocyclisation of N-substituted-2,3,4,5-tetraarylpyrroles

After the successful photocyclisation of 2,3-diarylindoles to form dibenzo[*a*,*c*]carbazoles in the previous chapter, the N-substituted-2,3,4,5-tetraarylpyrroles, **3.5** – **3.10**, were subjected to photocyclisation under

similar conditions. Unlike the 2,3-diarylindoles, successful photocyclisation reactions of 2,3,4,5-tetraarylpyrroles have not previously been reported. A 1968 report by Laarhoven *et al*. investigated the photocyclisation of a range of compounds with five and six membered heterocyclic rings as the core of the compound with peripheral aryl groups.[32] They report that the photocyclisation reactions of N*H*-2,3,4,5-tetraphenylpyrrole, **3.20**, and 2,3,4,5-tetraphenylfuran, **3.21**, is confusing, with these two compounds undergoing rapid photolysis. Although they obtained some UV/vis evidence for the photocyclisation of these compounds no products were isolated from the reaction. Interestingly, they also report that 2,3,4,5-tetraphenylthiophene, **3.22**, does not undergo any photocyclisation reaction, but 2,3-diphenylthiophene, **3.23**, and 2,3-diphenylfuran, **3.24**, do undergo the expected stillbene-type photocyclisation reaction to the corresponding phenanthro-[9,10-*b*]-thiophene, **3.25**, and phenanthro-[9,10-*b*]-furan, **3.26**.[32,33] Figure 3.13 shows the discrepancy in the photocyclisation behavior of these similar compounds.

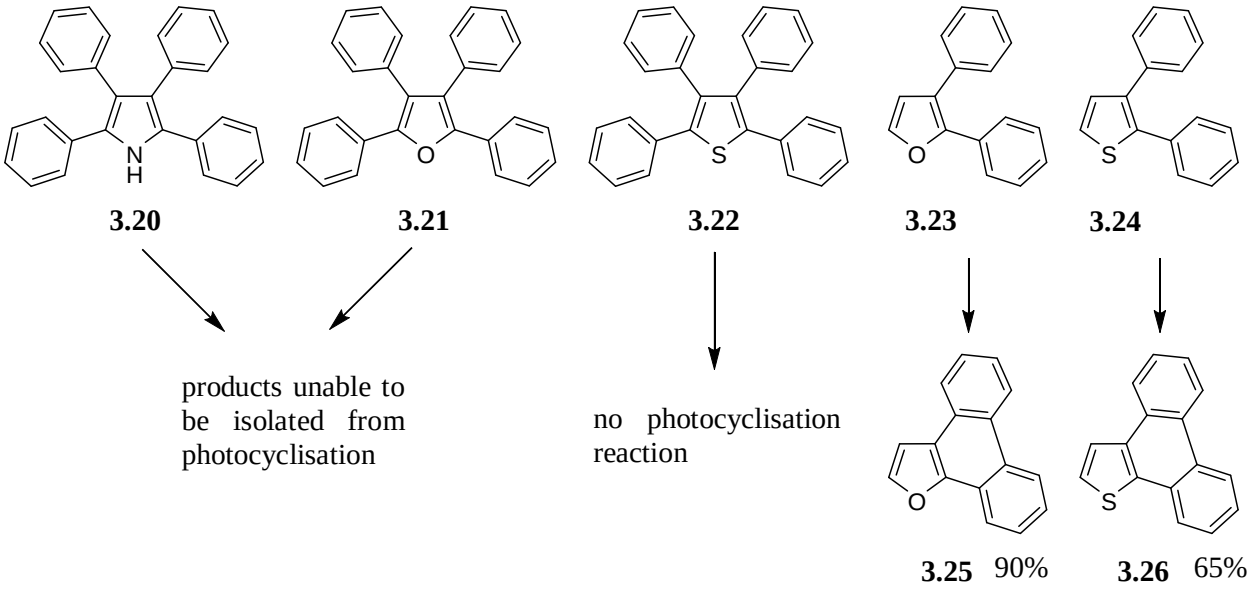

Figure 3.13. Differences in reactivity of compounds containing a five – membered heterocycle at the core of the compound.

The photocyclisation of N*H*-2,3-diphenylpyrrole also proceeds as expected, to form the corresponding dibenzo[*e*,*g*]indole,[34] and 4,5-diphenylimidazole also undergoes photocyclisation to produce phenanthro-[9,10-*d*]-imidazole.[35] Since these first reports appeared in the literature in the 1960's and 1970's the apparent differences in reactivity to photocyclisation of aryl-substituted five-membered heterocycles has not been investigated.

*3.4.1 Photocyclisation of N-ethyl-2,3,4,5-tetraarylpyrroles **3.5** – **3.7***

Initially the N-ethyl-2,3,4,5-tetraarylpyrroles **3.5** – **3.7** were subjected to the same photocyclisation conditions as those described in the previous chapter.[36] As there are three carbon-carbon bonds that can be formed by photocyclisation of N-substituted-2,3,4,5-tetraarylpyrroles 3.3 equivalents of I_2 were employed for each reaction, 1.1 equivalents of I_2 for each carbon-carbon bond to be formed.

All three N-ethyl-2,3,4,5-tetraphenylpyrroles formed one carbon-carbon bond when subjected to photocyclisation conditions, even with the presence of 3.3 equivalents of I_2, as shown in figure 3.14. The photocyclisation proceeds in good yields (69% − 73%) forming the carbon-carbon bond in the same position as that observed when **3.15**, **3.16** and **3.17** were formed from the oxidative cyclodehydrogenation of **3.8**, **3.9** and **3.10** using $FeCl_3$. The photocyclisation of N-ethyl-2,3,4,5-tetraphenylpyrroles, **3.5**, **3.6** and **3.7**, forms the corresponding N-ethyl-2,3-diaryl-dibenzo[*e,g*]indole cores, **3.27**, **3.28** and **3.29**, complementing the series of N-benzyl-2,3- diaryl-dibenzo[*e,g*]indoles, **3.15**, **3.16** and **3.17**, previously prepared.

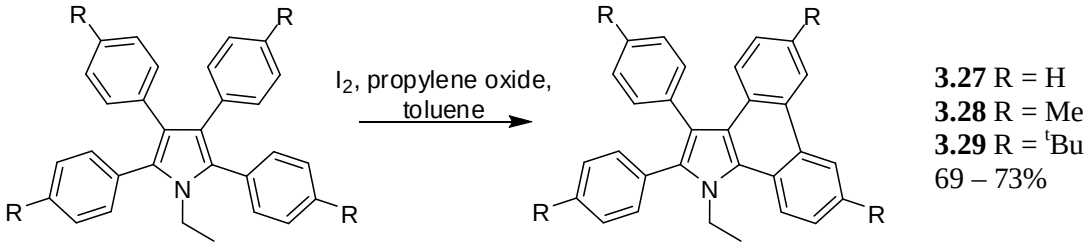

Figure 3.14. Formation of N-ethyl-2,3-diaryl-dibenzo[*e,g*]indoles from their corresponding N-ethyl-2,3,4,5-tetraarylpyrrole precursors, **3.5**, **3.6** and **3.7** (a) N-ethyl-2,3-diphenyl-dibenzo[*e,g*]indole, **3.27**, (b) N-ethyl-2,3-di(4-methylphenyl)-6,9-dimethyl-dibenzo[*e,g*]indole, **3.28**, (c) N-ethyl-2,3-di(4-*tert*butylphenyl)-6,9-di*tert*butyl-dibenzo[*e,g*]indole, **3.29**.

Each compound displays the characteristic downfield shift of protons in the ^{1}H-NMR spectrum, shown in figure 3.15, as a result of the additional aromaticity of the resulting compound by the formation of a carbon-carbon bond. The downfield shifted peaks are similar to that seen for compounds **3.15** – **3.17**, due to the formation of the same 2,3-diaryl-dibenzo[*e,g*]indole core. The para substituted compounds **3.28** and **3.29** have two singlet peaks and two doublet peaks that are observed from 9.0 ppm to 7.7 ppm, while **3.27** has only upfield shifted doublet peaks in this region due to the lack of para substitution. As expected the CH_2 quartet and CH_3 triplet arising from the N-ethyl substitution of all three compounds is moved downfield due to the formation of a carbon-carbon bond. The CH_2 quartet is now observed at ~ 4.5 ppm for all three compounds **3.27**, **3.28** and **3.29**, compared to the precursor compounds where the CH_2 quartet

is observed at ~3.8 ppm, and the triplet is now observed at ~ 1.4 ppm, compared to the precursor compounds where the CH_3 triplet is observed at ~ 0.9 ppm.

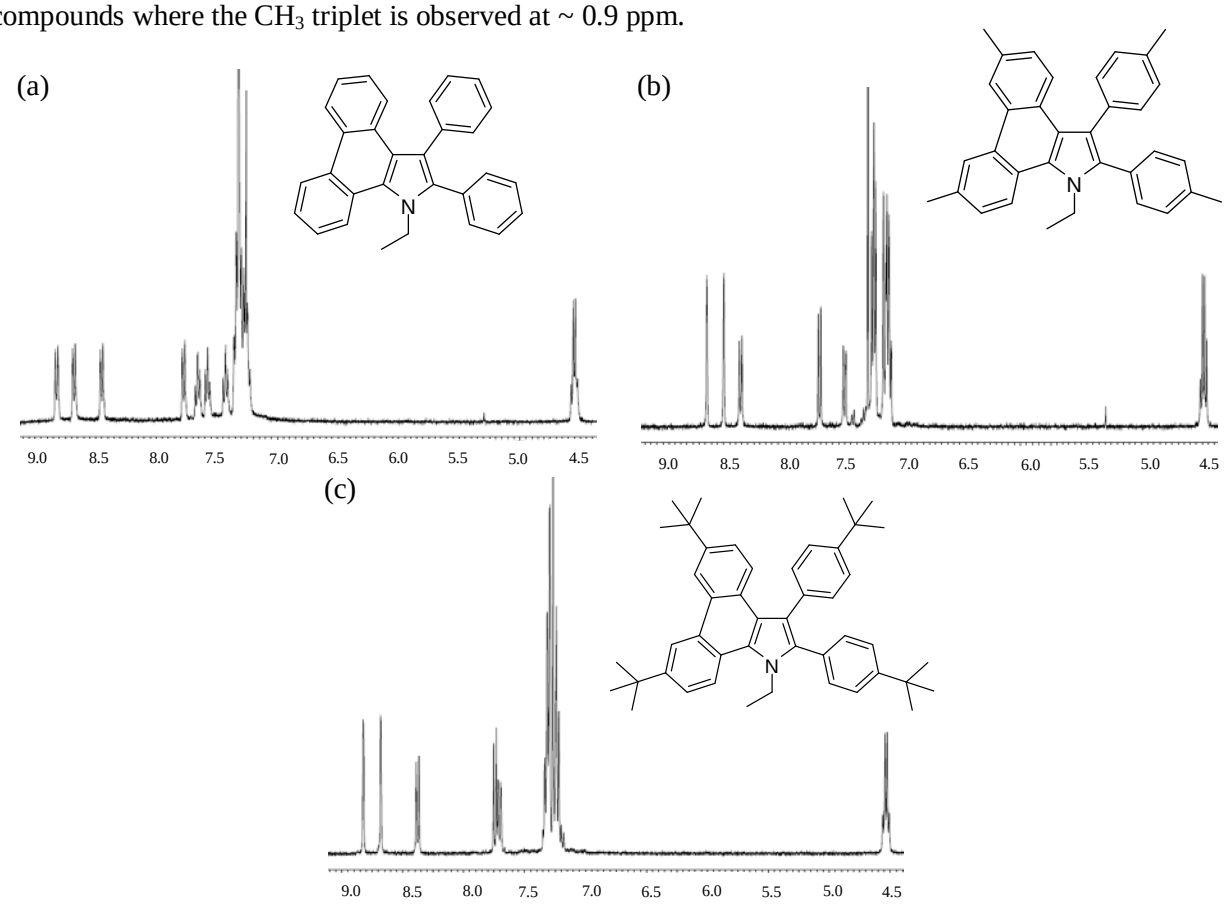

Figure 3.15. ^{1}H-NMR spectrum of N-ethyl-2,3-diaryl-dibenzo[*e*,*g*]indole compounds, (a) **3.27**, (b) **3.28**, (c) **3.29**.

The formation of the N-ethyl-2,3-diaryl-dibenzo[*e*,*g*]indole structure was confirmed by X-ray crystallography. Crystals of **3.28** were grown from the diffusion of methanol into a benzene solution of **3.28**. The crystal structure was solved in the triclinic space group *P*-1, with one molecule of **3.28** present in the asymmetric unit along with one disordered solvent benzene molecule, shown in figure 3.16. The new carbon-carbon bond formed between C25 and C28 again forms the planar dibenzo[*e*,*g*]indole unit (C25···C28 = 1.467(3) Å), and the two remaining peripheral 4-methylphenyl groups in the 2- and 3-position of the central pyrrole ring are twisted at angles of 109.4(1)˚ and 104.3(1)˚, respectively to the indole core. The molecules of **3.28** do not pack together in columns with extensive π – π stacking interaction like the crystal packing observed for compounds **3.15**, **3.16** and **3.17**, and instead molecules of **3.28** form a capsule around the disordered benzene molecule, shown in figure 3.17.

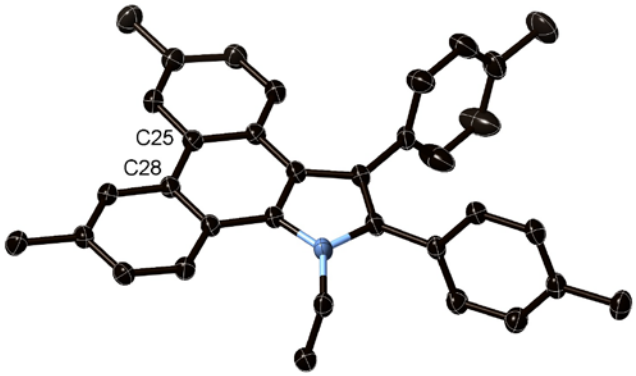

Figure 3.16. Asymmetric unit of **3.28**, solvent benzene molecule and hydrogen atoms have been removed for clarity.

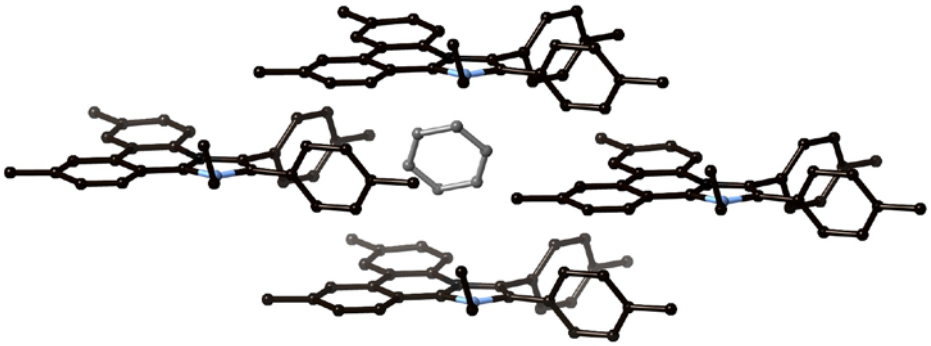

Figure 3.17. Molecules of **3.28** forming a cage around the disordered solvent benzene molecule (shown in grey), and hydrogen atoms have been removed for clarity.

3.4.2 Further cyclodehydrogenation of photocyclised N-ethyl-2,3,4,5-tetraarylpyrroles

The photocyclisation of N-ethyl-2,3,4,5-tetraarylpyrroles **3.5**, **3.6** and **3.7** forming the corresponding N-ethyl-2,3-diaryl-dibenzo[*e*,*g*]indoles **3.27**, **3.28** and **3.29** proceeds in much higher yields than the oxidative cyclodehydrogenation of N-benzyl-2,3,4,5-tetraarylpyrroles **3.8**, **3.9** and **3.10** forming the corresponding N-benzyl-2,3-diaryl-dibenzo[*e*,*g*]indoles **3.15**, **3.16** and **3.17**. This high yielding photocyclisation approach allows for the synthesis of a reasonable quantity of **3.27**, **3.28** and **3.29** to explore the stepwise formation of more carbon-carbon bonds through cyclodehydrogenation or photocyclisation, as shown in scheme 3.7. There are three different core structures that can be obtained by the formation of additional carbon-carbon bonds. The formation of an additional carbon-carbon bond could form a 9-ethyl-tetrabenzo[*a*,*c*,*g*,*i*]carbazole core, **3.31**, like that found in compound **3.14**, or the carbon-carbon bond could form between the aryl rings in the 3- and 4-position of the pyrrole core, **3.30**. If two carbon-carbon bonds are formed the fully cyclodehydrogenated core **3.32** will be obtained.

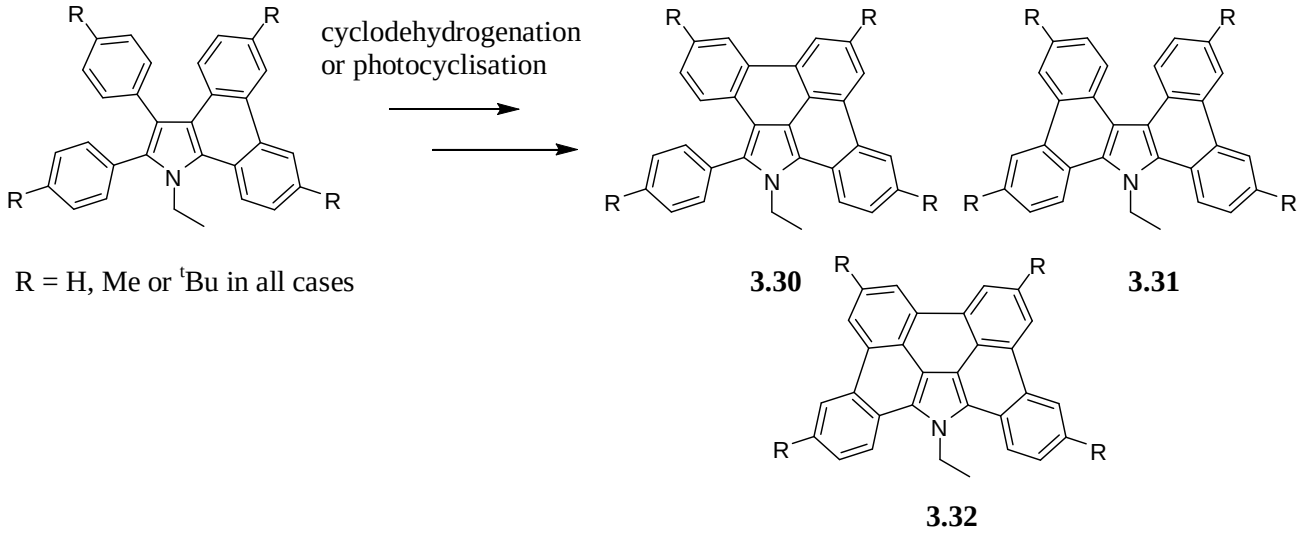

Scheme 3.7. Possible formation of new carbon-carbon bonds by stepwise photocyclisation or oxidative cyclodehydrogenation catalysed by lewis acidic transition metals.

Firstly, compound **3.27** was subjected to the standard photocyclisation reaction conditions with 2.2 equivalents of I_2 used, 1.1 equivalents for each carbon-carbon bond to be formed. After standard quenching of the reaction mixture, the ^{1}H-NMR spectrum and mass spectrometry indicated the presence of only starting compound **3.27**. In a 2010 paper Zhang *et al*. used both photocyclisation and cyclodehydrogenation to form curved polycyclic aromatic hydrocarbon 1.2,3.4,7.8,9.10-tetrabenzocoronene, **3.33**, from an olefin precursor molecule, **3.34**.[37] Photocyclisation formed two of the required four carbon-carbon bonds and after isolation of the partially cyclised compound, **3.35**, the remaining two carbon-carbon bonds were formed by oxidative cyclodehydrogenation using $FeCl_3$, as shown in scheme 3.8. Extension of the photocyclisation reaction time to convert **3.34** directly to **3.33** was not successful, and was attributed to the diminished double bond character of the olefin units once the photocyclisation occurred, preventing further stillbene type photocyclisation after the formation of the two carbon-carbon bonds. This loss of double bond character may also be why more carbon-carbon bonds do not form by photocyclisation after the initial conversion of the N-ethyl-2,3,4,5-tetraarylpyrrole compounds, **3.5**, **3.6** and **3.7**, to the N-ethyl-2,3-diaryl-dibenzo[*e,g*]indole compounds, **3.27**, **3.28** and **3.29** by the formation of only one carbon-carbon bond. The formation of a mixture of two photocyclisation products with one and two carbon-carbon bonds formed from a tetraaryl substituted phosphole has also been recently reported[38] and extension of the photocyclisation reaction time did not alter the yields of the two products.

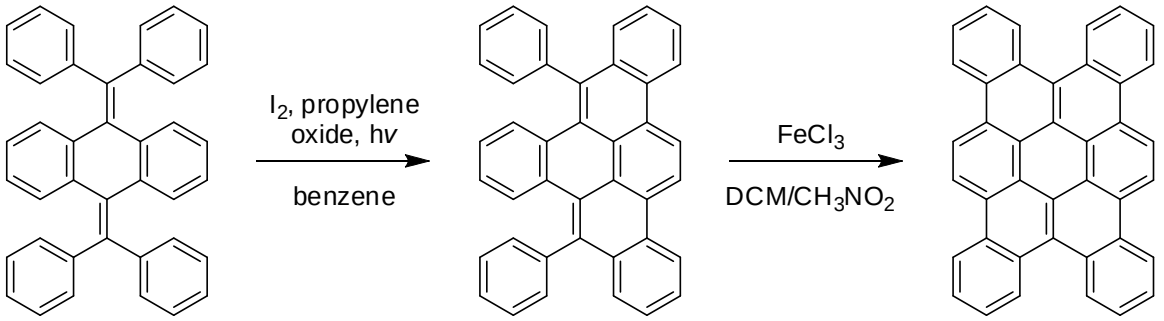

Scheme 3.8. Synthesis of tetrabenzocoronene, **3.33**, using both photocyclisation and oxidative cyclodehydrogenation.[37]

The report by Zhang *et al*. suggests that photocyclisation and oxidative cyclodehydrogenation can work in tandem to produce curved aromatic molecules through different methods of carbon-carbon bond formation. Compound **3.27** was subjected to oxidative cyclodehydrogenation conditions using 15 equivalents of $FeCl_3$ dissolved in a small amount of nitromethane. The reaction was quenched after five hours and the crude ^{1}H-NMR of the reaction mixture indicated a very small amount of cyclodehydrogenated product has been formed, but mainly starting material was present in the reaction mixture. Unfortunately no successful cyclodehydrogenation reactions were performed using $FeCl_3$ on the precursor N-ethyl-2,3,4,5-tetraarylpyrrole compounds, although successful cyclodehydrogenation reactions were able to be performed on the precursor N-benzyl-2,3,4,5-tetraarylpyrrole compounds. This could indicate that further carbon-carbon bond forming reactions by oxidative cyclodehydrogenation with $FeCl_3$ on the N-ethyl-2,3,4,5-tetraarylpyrroles may not be successful.

*3.4.3 Photocyclisation of N-benzyl-2,3,4,5-tetraarylpyrroles, **3.8**, **3.9** and **3.10***

The low yielding oxidative cyclodehydrogenation using $FeCl_3$ prevented enough N-benzyl-2,3-diaryl-dibenzo[*e,g*]indole compounds, **3.15**, **3.16**, and **3.17**, from being synthesised to investigate the stepwise carbon-carbon bond formation by photocyclisation and/or oxidative cyclodehydrogenation. Owing to the high yielding formation of N-ethyl-2,3-diaryl-dibenzo[*e,g*]indole compounds, **3.27**, **3.28** and **3.29**, by photocyclisation, it was hoped that formation of N-benzyl-2,3-diaryl-dibenzo[*e,g*]indole compounds, **3.15**, **3.16** and **3.17**, by photocyclisation of N-benzyl-2,3,4,5-tetraarylpyrroles, **3.8**, **3.9** and **3.10** in an analogous manner would also occur in high yields. This would allow for investigation into the stepwise formation of carbon-carbon bonds using oxidative cyclodehydrogenation as the N-benzyl-2,3,4,5-tetraarylpyrroles have already formed stable products, **3.15**, **3.16** and **3.17** through cyclodehydrogenation.

All three N-benzyl-2,3,4,5-tetraarylpyrrole compounds, **3.8**, **3.9** and **3.10** were subjected to the standard photocyclisation reaction conditions, using 3.3 equivalents of I_2 per molecule, 1.1 equivalents of I_2 per carbon-carbon bond to be formed. After removal of excess I_2, thin layer chromatography and ^{1}H-NMR spectroscopy showed the formation of multiple products in the reaction mixture, not the clean high yielding formation of only one product as observed for the N-ethyl-2,3,4,5-tetraarylpyrrole compounds.

In all three cases, only one product from the photocyclisation reaction was able to be isolated by column chromatography. Compounds **3.36**, **3.37** and **3.38** were isolated from the photocyclisation of **3.8**, **3.9** and **3.10** respectively, in low yields (4% − 5%). The ^{1}H-NMR spectra of compounds **3.36**, **3.37** and **3.38** are very similar and are shown in figure 3.18a – c. The spectra display some unusual features that have not previously been observed for photocyclisation or oxidative cyclodehydrogenation products in the course of this study.

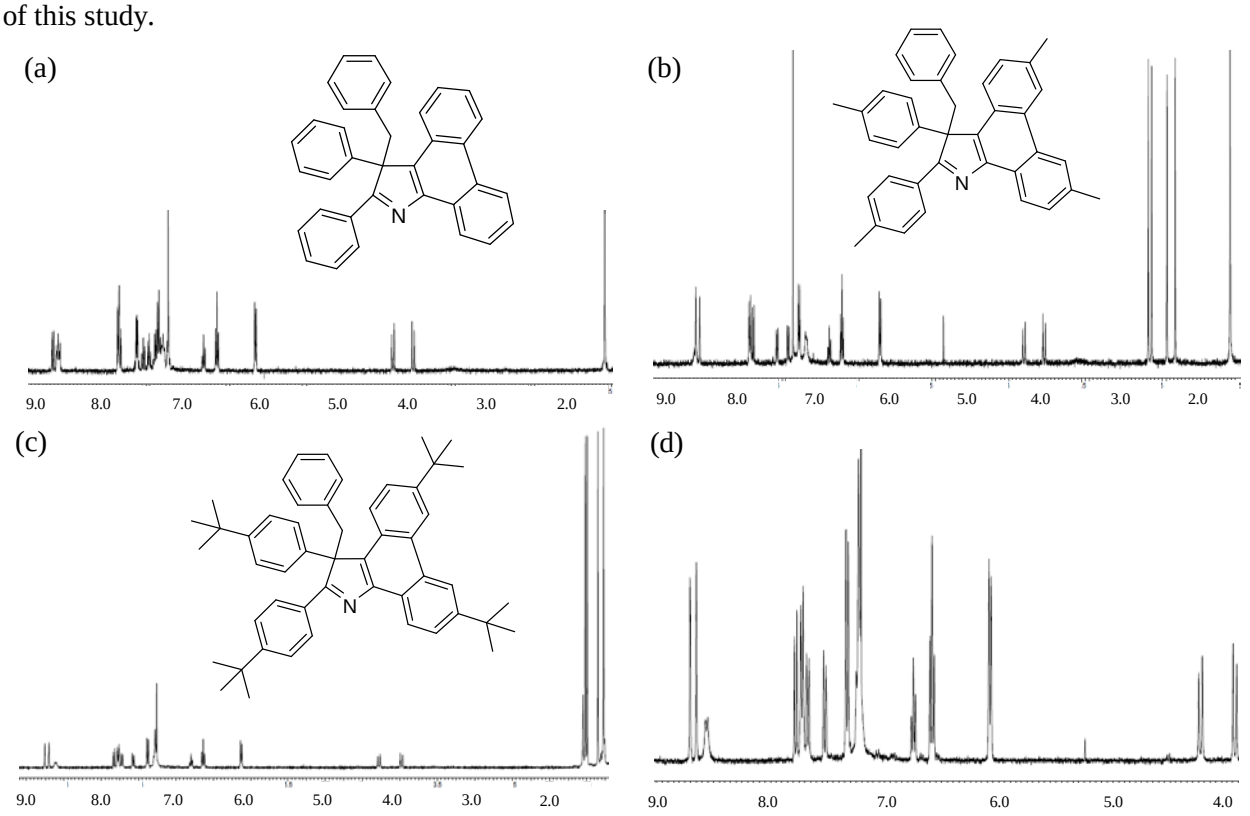

Figure 3.18. ^{1}H-NMR spectrum of (a) **3.36**, (b) **3.37**, (c) **3.38**, (d) enlarged ^{1}H-NMR spectrum of the aromatic region of **3.38**.

The singlet methylene benzyl peak present in the starting N-benzyl-2,3,4,5-tetraarylpyrrole compounds, observed at ~ 5.0 ppm, is shifted significantly upfield in the ^{1}H-NMR spectra of all three photocyclisation products, **3.36**, **3.37** and **3.38**, and in addition the two benzyl methylene protons are now observed in two

magnetically inequivalent environments as doublets at ~ 4.3 ppm and ~ 4.0 ppm. These protons are coupled together with a coupling constant of ~ 12.5Hz, indicative of sp^3 methylene protons, and are also as observed to be coupled together in the 2-D COSY experiment in all three cases. The presence of two proton environments, rather than a single proton environment indicates that the benzyl ring is somehow locked into a conformation, either through a carbon-carbon bond being formed from the benzyl to a peripheral aryl ring attached to the pyrrole core, or by restriction of the movement of the benzyl group on the NMR timescale. In the case of **3.37** and **3.38**, the methyl and *tert*butyl groups respectively are in four magnetically different environments. Mass spectrometry indicates the formation of one only carbon-carbon bond, but the proton environments are considerably different than those observed for **3.15**, **3.16** and **3.17**. In these cases the methylene benzyl remains a single environment and is shifted downfield to ~ 5.7 ppm.

The carbon-carbon bond could also form to produce a compound like that shown in figure 3.2b. The formation of a carbon-carbon bond between the aryl rings in the 3- and 4-position of the pyrrole ring would produce a symmetrical compound, and there are too many aromatic proton resonances for this to be the case. 2-D COSY and TOCSY experiments indicate the benzyl ring has not formed a carbon-carbon bond to a peripheral aryl group attached to the pyrrole core, because the expected doublet, triplet, triplet splitting pattern of an unsubstituted phenyl ring in the same spin coupled system is observed in both the COSY and TOCSY. These three peaks corresponding to the benzyl ring protons are also moved upfield, but not as far as the methylene benzyl protons. There are no other protons observed in the same spin coupled system in all three cases.

The aromatic region of the ^{1}H-NMR spectra is more complicated due to the presence of protons from the four peripheral aryl groups as well as the benzyl ring. As seen previously for the formation of one carbon-carbon bond between the aryl rings in the 2- and 3-positions of the pyrrole ring there are two downfield shifted singlet peaks at in the region from 8.5 ppm to 8.8 ppm for the compounds with para substitution on the peripheral aryl rings, **3.37** and **3.38**. This suggests that the new carbon-carbon formed, as indicated by mass spectrometry, has formed between the peripheral aryl rings in the 2- and 3-positions of the pyrrole ring. These peaks are not coupled to any other protons, as determined by 2-D COSY and TOCSY experiments. The other peaks in the aromatic region are harder to analyse due to the crowding in this region.

In the aromatic region of the ^{1}H-NMR spectra of **3.36**, **3.37** and **3.38** there is at least one peak under the chloroform signal. The ^{1}H-NMR spectrum of **3.38** was also collected in CD_2Cl_2, shown in figure 3.19, and

a broadened peak integrating to four protons is observed, the other aromatic peaks shift a small amount but otherwise the spectrum is the same. The aromatic protons integrate for 19 protons, two less than the starting compound **3.10**, again indicating the formation of only one carbon-carbon bond. From the ^{1}H-NMR spectrum, 2-D correlations from COSY, TOCSY, HSQC and HMBC experiments and mass spectrometry the overall structure of these photocyclisation products could not be determined.

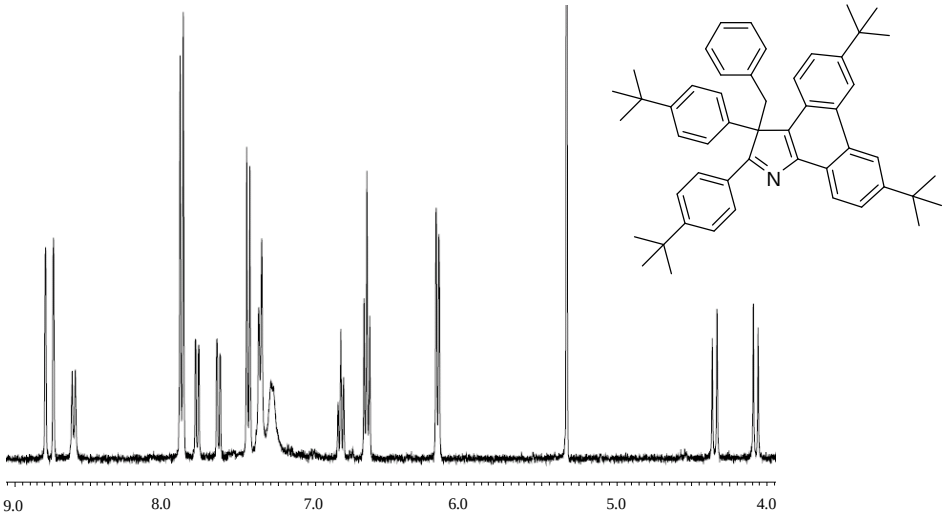

Figure 3.19. ^{1}H-NMR spectrum of **3.38** collected in CD_2Cl_2.

Fortunately, crystals suitable for X-ray crystallography were grown from the slow diffusion of methanol into a benzene solution of **3.37**. Compound **3.37** crystallises in the triclinic space group *P*-1 with one molecule present in the asymmetric unit, the crystal structure of **3.37** is shown in figure 3.20. As expected from the ^{1}H-NMR spectrum of **3.37**, a carbon-carbon bond has formed between the peripheral 4-methylphenyl rings in the 4- and 5-position of the pyrrole ring (C32···C35 = 1.462(2) Å) to form a dibenzo[*e,g*]indole core. The benzyl ring has shifted from the nitrogen atom of the pyrrole ring to the carbon atom in the 3-position of the pyrrole ring, resulting in the localisation of double bonds between N1 and C2, and C4 and C5 (N1···C2 = 1.295(2) Å, C4···C5 = 1.361(2) Å), and single bonds between N1 and C5, C2 and C3, and C3 and C4 (N1···C5 = 1.415(2) Å, C2···C3 = 1.539(2) Å and C3···C4 = 1.521(2) Å). The movement of the benzyl group to C3 results in the sp^3 hybridisation of this atom. The 4-methylphenyl rings in the 2- and 3-positions are twisted out of the plane of the dibenzo[*e,g*]indole core by 20.8(1)˚ and 94.1(1)˚, respectively.

Molecules of **3.37** pack together with extensive face-to-face π – π stacking interactions between benzyl groups in neighbouring molecules and the dibenzo[*e,g*]indole groups in neighbouring molecules (centroid to plane distances = 3.354(2) Å, 3.423(1) Å and 3.484(1) Å), forming a grid like packing motif, shown in

figure 3.21. Weak edge-to-face π – π stacking interactions between the 4-methylphenyl rings stabilise the formation of this grid like packing (C··· centroid = 3.975(2) Å).

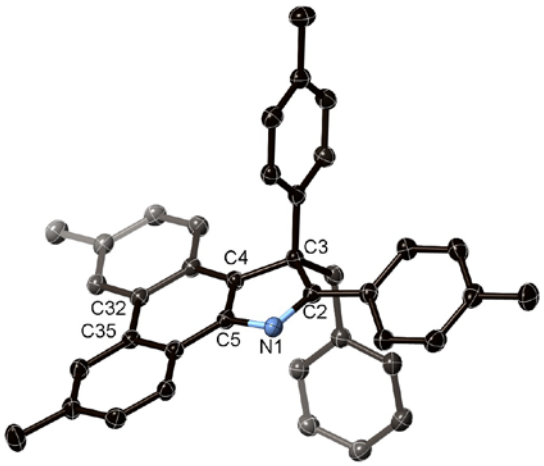

Figure 3.20. Asymmetric unit of **3.37**, hydrogen atoms have been removed for clarity.

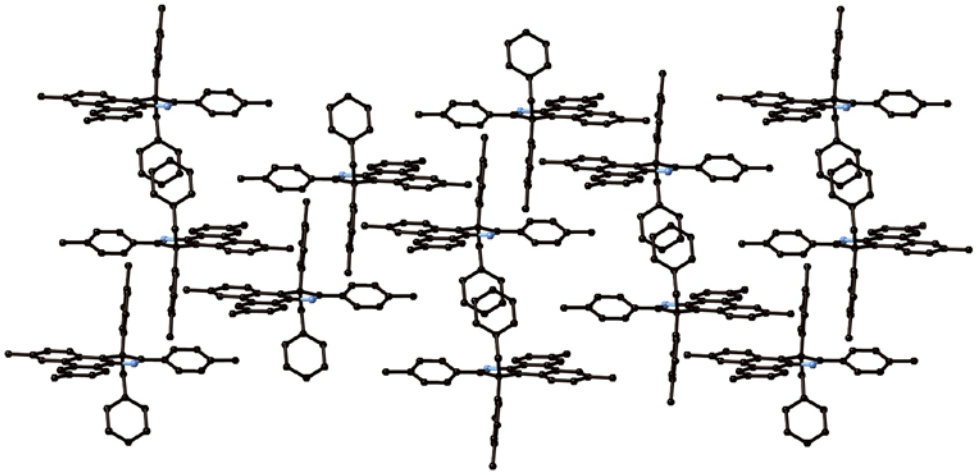

Figure 3.21. π – π stacking interactions between molecules of **3.37**, hydrogen atoms have been removed for clarity.

The methylene benzyl hydrogens are pro-chiral in the crystal structure of **3.37** obtained, explaining the splitting of this peak in the ^{1}H-NMR spectrum, and the benzyl group sits below the dibenzo[*e*,*g*]indole core, shielding these protons and explaining the upfield shift of both the methylene and benzyl ring protons in the ^{1}H-NMR spectrum. The ^{1}H-NMR spectrum of all three compounds **3.36**, **3.37** and **3.38** have similar features, including the upfield shift and splitting of the methylene benzyl peaks, and the downfield shifts of some proton peaks resulting from the formation of one carbon-carbon bond. The crystal structure of **3.37** gives confirmation of the structure of the product obtained from the photocyclisation reaction of **3.9** to form **3.37**. The structures of **3.36** and **3.38** must be the same, differing

only by the substitution in the para position of the peripheral aryl rings. The structures of all three 3-benzyl-2,3-diaryl-dibenzo[*e,g*]indoles, **3.36**, **3.37** and **3.38** formed by the photocyclisation of N-benzyl-2,3,4,5-tetraarylpyrroles is shown in figure 3.22.

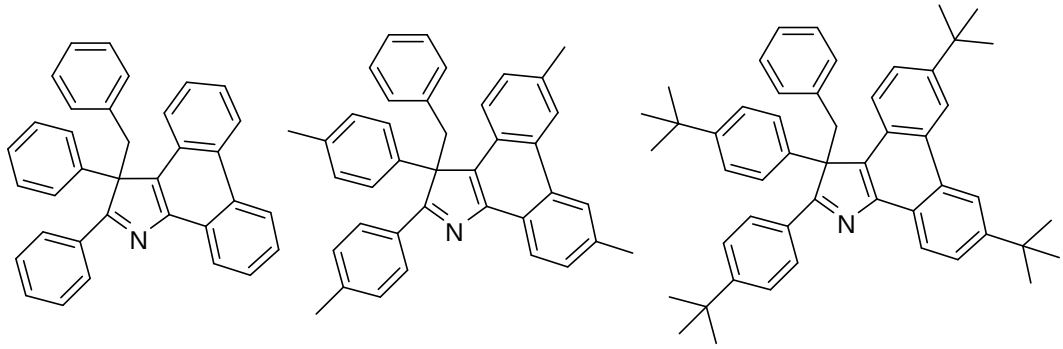

3.36 **3.37** **3.38**

Figure 3.22. Photocyclisation products isolated from the reactions of **3.8**, **3.9** and **3.10** (a) 3-benzyl-2,3-diphenyl-dibenzo[*e,g*]indole, **3.36**, (b) 3-benzyl-2,3-di(4-methylphenyl)-6,9-dimethyl-dibenzo[*e,g*]indole, **3.37**, (c) 3-benzyl-2,3-di(4-*tert*butylphenyl)-6,9-di*tert*butyl-dibenzo[*e,g*]indole, **3.38**.

Photoisomerisation of N-benzylpyrrole to 2-benzylpyrrole and 3-benzylpyrrole has previously been observed by Patterson *et al*. in 13% and 3% yield respectively.[39] The photoisomerisation of N-(1-phenylethyl)-2,5-dimethylpyrrole also produces the 2- and 3-substituted photoisomerisation products in 12% and 5% yield. In both cases, when the 2-substituted photoisomerisation product is irradiated no 3-substituted product is observed in the reaction mixture.[39,40] The lack of photoisomerisation from the 2-substituted pyrroles to the 3-substituted pyrroles suggests that the 3-substituted pyrroles arise from a photochemically allowed direct 1,3-shift.[39] Similar photoisomerisation behavior is also observed for N-acetylpyrroles.[41]

Simultaneous photocyclisation and 1,3 photochemical shift have not been previously observed for five membered heterocyclic ring systems. The 3-benzyl-2,3-diaryl-dibenzo[*e,g*]indoles isolated from the reaction mixtures by column chromatography were not the only products formed from the photocyclisation of the N-ethyl-2,3,4,5-tetraarylpyrroles, thin layer chromatography indicated the formation of 5 or 6 products, but extensive efforts to isolate these compounds by column chromatography were not successful. Mass spectrometry indicates the presence of a compound where the benzyl group has been lost and photocyclisation has also occurred, whether this is an effect from mass spectrometry or one of the products formed in the reaction is not clear as none of this product could be isolated.

Extension of the reaction time did not increase the yield of **3.36**, **3.37** and **3.38**. The low yielding photocyclisation and 1,3-photochemical shift of the precursor N-benzyl-2,3,4,5-tetraarylpyrroles is in stark contrast to the high yielding photocyclisation of the precursor N-ethyl-2,3,4,5-tetraarylpyrroles. Thin layer chromatography and ^{1}H –NMR spectroscopy also give clear evidence that more than one compound is being formed in the reaction, but only one compound was able to be isolated.

Only one carbon-carbon bond is formed in the product isolated from the photocyclisation reaction of the N-benzyl-2,3,4,5-tetraphenylpyrroles. In attempts to reduce to number of products formed, 2.2 equivalents and 1.1 equivalents of I_2 per precursor molecule were trialled. In both cases this did not reduced the number of products formed in the reaction, as judged by thin layer chromatography.

3.4.4 Analysis of change in NMR shifts resulting from cyclodehydrogenation and photocyclisation

Shown below in table 3.1 is the change in chemical shift as a direct result of a carbon-carbon bond being formed between the peripheral aryl rings of the 2,3,4,5-tetraarylpyrrole compounds, **3.5** – **3.10**, to form the corresponding 2,3-diaryl-dibenzo[*e*,*g*]indoles, **3.15** – **3.17** and **3.27** – **3.29**. As discussed in Chapter 2, the increase in π conjugation results in a downfield shift of the functional groups directly attached to the nitrogen atom by ~ 0.65 ppm. On the other hand, the benzylic protons of the 3-benzyl-2,3-diaryl-dibenzo[*e*,*g*]indoles, **3.36** – **3.38**, are shifted significantly upfield, as a direct result of the benzyl ring no longer being attached a heterocyclic atom involved in a conjugated π system, and instead attached to a sp^3 hybridised carbon atom.

Compound	functional group measured	difference in chemical shift	Compound	functional group measured	difference in chemical shift
3.15	benzyl CH_2	0.65 ppm	**3.27**	ethyl CH_2	0.65 ppm
3.16	benzyl CH_2	0.65 ppm	**3.28**	ethyl CH_2	0.65 ppm
3.17	benzyl CH_2	0.71 ppm	**3.29**	ethyl CH_2	0.67 ppm
3.36	benzyl CH_2	-0.76 ppm and -1.03 ppm	**3.37**	benzyl CH_2	-0.75 ppm and -1.02 ppm
3.38	benzyl CH_2	-0.65 ppm and -0.92 ppm			

Table 3.1. Change in chemical shift as a result of carbon-carbon bond forming reactions and/or 1,3-migration.

3.5 Attempts at oxidative cyclodehydrogenation of N-substituted-2,3,4,5-tetraarylpyrroles using organic reagents

The Scholl reaction requires a strong acid and an oxidant, and in many cases the same species can fulfill both roles. The type of strong acid and oxidant are not limited to Lewis acidic transition metals and oxidants and a variety of organic reagents have been successfully used to implement the Scholl reaction. Organic reagents such as DDQ/H^+ and $(CF_3COO)_2I^{III}C_6H_5$ (PIFA)/$BF_3.OEt_2$ have recently been employed in the Scholl reaction of small oligophenylene precursors. These organic reagents provide some advantages over the traditional transition metal reagents, a large excess of organic reagent is generally not required, and in the case where DDQ is employed as the organic oxidant DDQ-H_2 can be recovered at the end of the reaction and recycled back into DDQ.

3.5.1 Oxidative cyclodehydrogenation using DDQ/H^+

DDQ was first employed as an oxidant for the Scholl reaction with CH_3SO_3H as the strong acid by Zhai *et al*. in 2009.[42] Along with the formation of a range of substituted triphenylenes from the corresponding o-terphenyls, a hexaphenylbenzene derivative, **3.39**, in the presence of DDQ/H^+ underwent the Scholl reaction to form six new carbon-carbon bonds, giving the corresponding HBC derivative, **3.40**, shown in scheme 3.9.

Using DDQ/CH_3SO_3H as an oxidant/catalyst system for the cyclodehydrogenation of the already synthesised N-substituted pyrroles **3.5** – **3.10** was appealing as a different reagent for the Scholl reaction may be more reactive towards the highly substituted pyrrole system. DDQ in the presence of a strong acid is known to produce the corresponding radical cation of the aromatic precursor,[43] and it follows that using these conditions to carry out the Scholl reaction the proposed radical cation mechanism should apply.

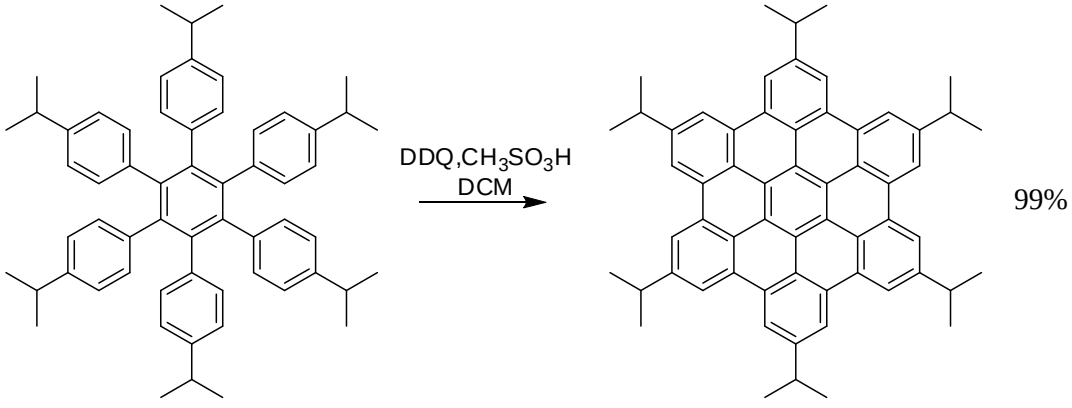

3.39 **3.40**

Scheme 3.9. Oxidative cyclodrehydrogenation of a hexaphenylbenzene precursor using DDQ/CH_3SO_3H as the catalyst/oxidant system.[42]

Both **3.6** and **3.9** were subjected to oxidative cyclodehydrogenation using the conditions as described by Zhai *et al*.[42] At 0 ˚C the dichloromethane solution of N-substituted-2,3,4,5-tetra(4-methylphenyl)pyrrole precursor was treated with acid, then DDQ added and the reaction was monitored with TLC. In each case the reaction was quenched after 24 hours with a solution of saturated sodium bicarbonate. Purification by column chromatography afforded **3.28** and **3.16** in low yield from the corresponding precursor. The ^{1}H-NMR spectrum and mass spectrum matched the previously obtained data for **3.28** and **3.16**.

The formation of only one bond from the oxidative cyclodehydrogenation reaction with DDQ/CH_3SO_3H indicates that N-substituted-2,3,4,5-tetraaryl precursors are not more reactive towards cyclodehydrogenation with this particular reagent system. Although the formation of only one bond is frustrating, it perhaps indicates that this particular system is not able to form more carbon-carbon bonds to introduce a significant amount of strain into the molecule without harsher reaction conditions.

3.5.2 Attempts at oxidative cyclodehydrogenation using $(CF_3COO)_2I^{III}C_6H_5$ (PIFA)/$BF_3.OEt_2$

Another organic system that has been used for the formation of carbon-carbon bonds between aryl rings is $(CF_3COO)_2I^{III}C_6H_5$ (PIFA)/$BF_3.OEt_2$.[44] PIFA also forms radial cations with aromatic compounds so the radical cation mechanism for the Scholl reaction should also be the preferred mechanism in this case.

Compound **3.5** was subjected to oxidative cyclodehydrogenation following the standard literature conditions.[44a] Compound **3.5** was dissolved in dichloromethane and cooled to -40 ˚C, after addition of a dichloromethane solution of PIFA and $BF_3.OEt_2$ the reaction mixture was stirred for four hours. After quenching with sodium carbonate and subsequent purification no evidence was found in the ^{1}H-NMR spectrum or mass spectrum for any cyclodehydrogenation reactions occuring.

3.6 Attempted synthesis of backbone fused N*H*-2,3,4,5-tetraarylpyrrole

None of the N-substituted-2,3,4,5-tetraarylpyrrole compounds synthesised and subjected to oxidative cyclodehydrogenation have formed a carbon-carbon bond between the aryl rings in the 3- and 4-position of the pyrrole ring. As mentioned in section 3.4.2 a tetraarylphosphole compound has been recently synthesised,[38] with a carbon-carbon bond formed between the 3- and 4-position already installed. The resulting compound was able to undergo photocyclisation, whereby two carbon-carbon bonds were formed between the aryl rings in the 2- and 3-position and the 4- and 5-position of the phosphole. The resulting compound has all three possible carbon-carbon bonds formed between the ortho carbon atoms in adjoining aryl rings.

To circumvent the need to form the carbon-carbon bond between the aryl rings in the 3- and 4-position through cyclodehydrogenation reactions, a precursor pyrrole compound, **3.41**, was envisaged where the carbon-carbon bond between the phenyl rings in the 3- and 4-position was already preinstalled. The retrosynthetic analysis to **3.41**, shown in figure 3.23, requires the formation of a diketone, **3.43**, for Paal – Knorr condensation with an ammonium salt. The N*H*-tetraphenyl pyrrole, **3.42**, formed from the condensation will then be able to undergo substitution at the nitrogen atom with ethyl or benzyl bromide to form the desired compounds, using the conditions described above in section 3.2.3. The synthesis of compound **3.43** has already been described by Dennis *et al*.[45] employing a Knoevenagel condensation of 1,3-diphenylacetone and phenanthrenequinone, to form **3.44**, followed by photooxidative ring opening forming the required diketone **3.43**. The synthesis of **3.43** was competed following the method of Dennis *et al*. from 1,3-diphenylacetone and phenanthrenequinone.

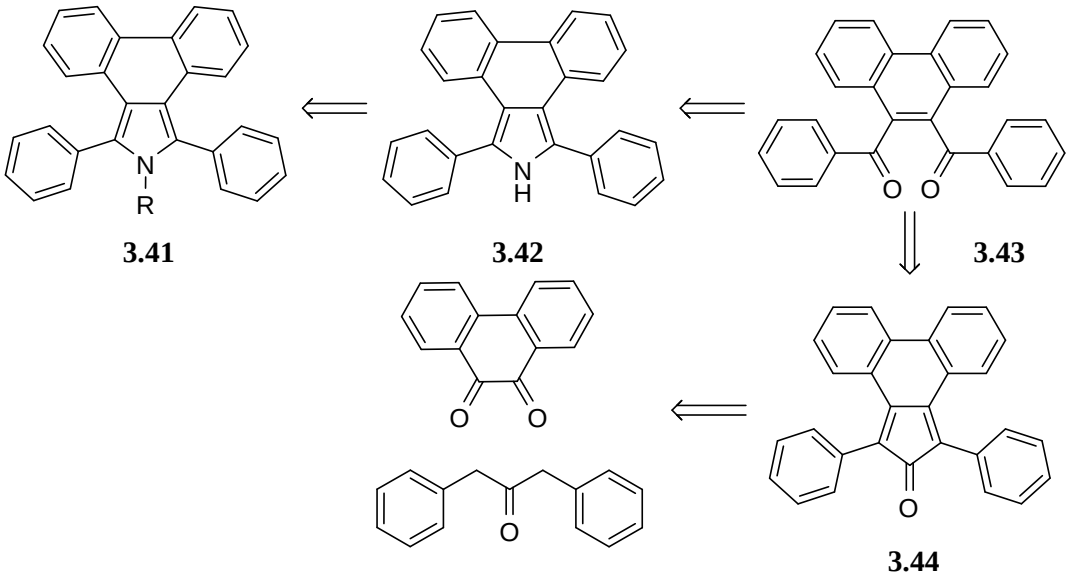

3.41 **3.42** **3.43** **3.44**

Figure 3.23. Retrosynthetic analysis for the formation of compound **3.41**.

The Paal – Knorr condensation of **3.43** to form **3.42** proved to be much more difficult. Initial attempts at the condensation of the diketone with ammonium acetate were not successful, and it appeared from mass spectroscopy that only one condensation reaction was occurring no matter the length of time the reaction was run for, or the excess of ammonium acetate added. Presumably, the imine formed from only one condensation is unable to react any further with the other carbonyl, due to the localised double bond present. To drive the reaction forward to the formation of the desired N*H*-pyrrole, **3.42**, a reductive amination was employed, by addition of an excess of zinc dust to the reaction mixture. Pleasingly the addition of zinc has an immediate effect on the reaction, with an additional spot appearing on the TLC.

After another 24 hours TLC indicates that the undesired mono condensation product is still present and another excess of zinc dust was added. After 24 hours the TLC shows no change and the reaction was quenched and purified using column chromatography. The resulting compound was isolated in low yields (20%), but identification of this compound proved difficult. The ^{1}H-NMR spectrum of the isolated compound was different to that of the single condensation product, with the aromatic protons shifted downfield, presumably due the formation of the desired aromatic pyrrole core deshielding the protons. Mass spectrometry did not indicate that any of the desired **3.42** was present, and the low yields prevented further analysis.

Crystals of the isolated compound were grown by the slow evaporation of a dichloromethane solution. The compound crystallises in the orthorhombic space group *Pbca* with one molecule of **3.42** present in the asymmetric unit, as shown in figure 3.24. The ^{1}H-NMR spectrum of these crystals matched the ^{1}H-NMR spectrum of the isolated material, and pleasingly the X-ray structure confirms that compound **3.42** has been formed. The preinstalled carbon-carbon bond between the ortho carbon atoms of the phenyl rings in the 3- and 4-positions has served to almost planarise these phenyl rings. The phenyl rings in the 3- and 4- positions deviate only slightly away from the plane of the pyrrole ring (6.6(1)˚ and 11.4(1)˚), while the phenyl rings in the 2- and 5- position of the pyrrole ring are twisted at much larger angles (56.1(1)˚ and 42.9(1)˚), as expected. The distance between the carbon atoms that are expected to form a carbon-carbon bond using oxidative cyclodehydrogenation or photocyclisation are 3.308(1) Å and 3.313(1) Å apart, comparable to those seen in the X-ray crystal structures of the precursor 2,3-diarylindoles in Chapter 2, ~ 3.2 Å.

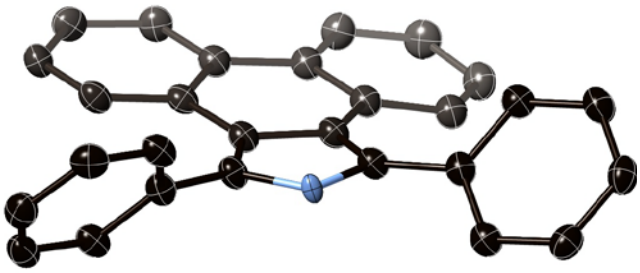

Figure 3.24. Asymmetric unit of **3.42**, hydrogen atoms have been removed for clarity.

The crystal packing of **3.42** is dominated by the formation of complementary N*H*–π (N···C = 3.653(1) Å) interactions, as shown in figure 3.25, and edge-to-face π – π interactions (C–plane distance = 3.519(1) Å) between the pyrrole N*H* nitrogen and the phenyl rings in the 2- and 5-position in adjacent molecules. The pyrrole ring and the fused backbone of a neighbouring compound also participate in face-to-face π – π interactions (centroid···centroid distance = 3.757(1) Å), and the fused backbone also participates in edge-

to-face π – π interactions with an unfused aryl ring in a different neighbouring compound (C···centroid distance = 3.602(1) Å).

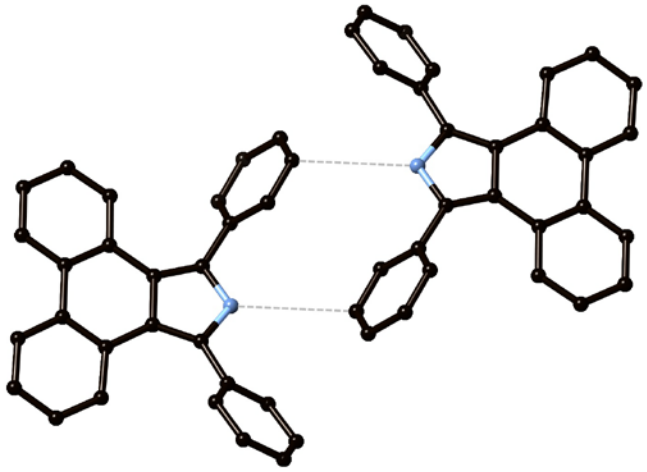

Figure 3.25. Complementary N*H* ··· π and edge-to-face π – π interactions between molecules of **3.42**.

With a small amount of **3.42** in hand, substitution of the nitrogen atom with an ethyl group, using ethyl bromide as the electrophilic reactant, was attempted. Unfortunately, after following the conditions outlined in 3.2.3, no desired N-ethyl substituted **3.41** was able to be isolated from the reaction mixture. ^{1}H-NMR spectroscopy and mass spectroscopy did not provide any evidence for the formation of N-ethyl substituted **3.41**. With the low yielding synthesis of **3.42** making it difficult to synthesise larger quantities of the precursor the synthesis of **3.41** was abandoned.

3.7 Optical properties

Emission and excitation spectra were measured for each 2,3,4,5-tetraarylpyrrole compound prepared **3.1**, **3.3** – **3.10**, and the corresponding N-substituted-2,3-diaryl-dibenzo[*e*,*g*]indole compound, prepared by oxidative cyclodehydrogenation or photocyclisation, **3.15** – **3.17** and **3.27** – **3.29**. For the same reasons as described in Chapter 2, a difference in the absorption and emission spectra between the precursor compounds and partially fused products is expected. Although the partially fused compounds **3.15** – **3.17** and **3.27** – **3.29** will not be as rigid as the products discussed in Chapter 2, they should still be more rigid than their precursor compounds **3.5** – **3.10**, allowing for some fine structure and vibronic coupling to be observed. The increase in π-conjugation by partial fusion of the precursors should also allow for a bathochromic shift to be observed in the partially fused compounds **3.15** – **3.17** and **3.27** – **3.29**.

Figure 3.26a shows the absorption spectra of the N*H*-2,3,4,5-tetraarylpyrroles, **3.1**, **3.3** and **3.4**, figure 3.26b shows the absorption spectra of the N-substituted-2,3,4,5-tetrarylpyrroles, **3.5** – **3.10**, figure 3.26c

shows the absorption spectra of the corresponding N-substituted-2,3-diaryl-dibenzo[*e*,*g*]indoles, **3.15** – **3.17** and **3.27** – **3.29** and figure 3.26d shows the absorption spectra of the 3-benzyl-2,3-diaryl-dibenzo[*e*,*g*]indoles, **3.36** – **3.38**. The shape of the absorption spectra remain consistent for each type of compound and the spectra are not affected by peripheral substitution of the aryl rings or substitution on the nitrogen atom. The substitution on the peripheral aryl rings are only weakly electron donating (methyl and *tert*butyl).

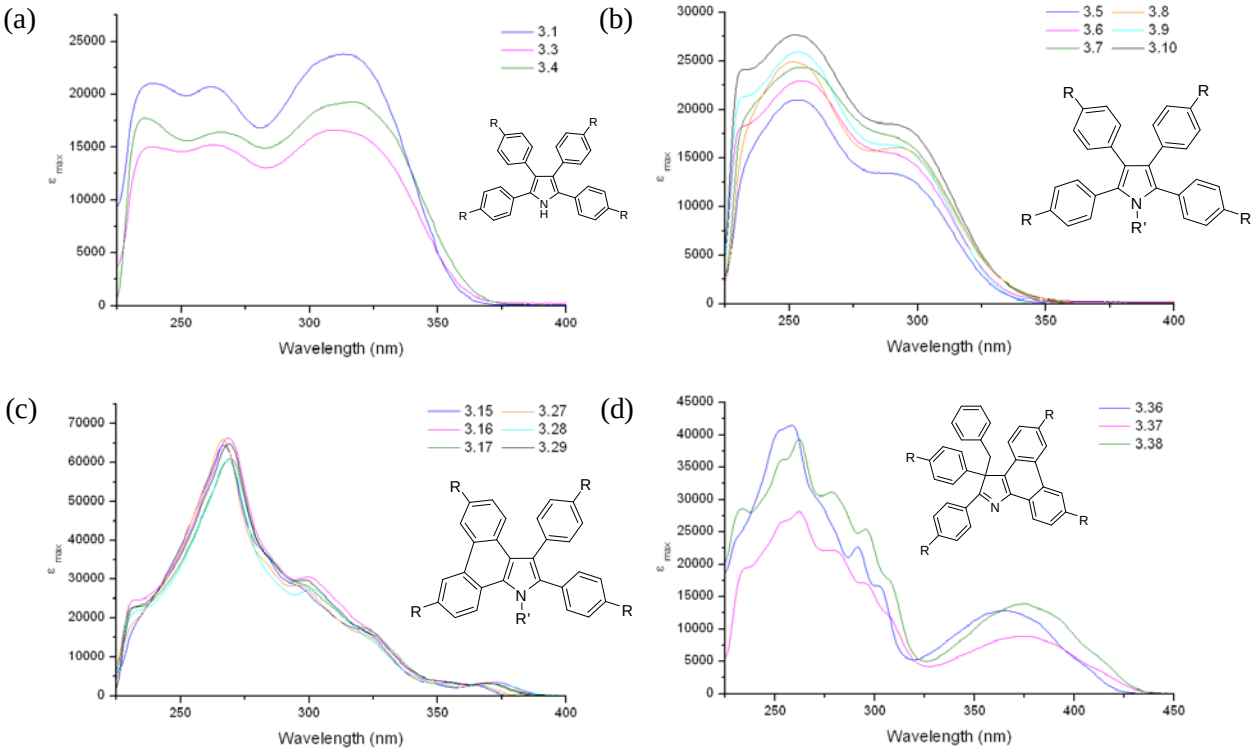

Figure 3.26 UV/visible spectra of (a) **3.1**, **3.3**, **3.4**, (b) **3.5** – **3.10**, (c) **3.15** – **3.17**, **3.27** – **3.29**, (d) **3.36** – **3.38**, all spectra were measured in dichloromethane at room temperature, concentrations ~ 10^{-6} mol.L^{-1}, R = H, Me, ^{t}Bu, R' = Et, Bn.

As discussed in Chapter 2, the formation of a carbon-carbon bond increasing the π-conjugation results in a red shift of the λ_{max} in the absorption spectra. This is observed for the N-substituted-2,3-diaryl-dibenzo[*e*,*g*]indoles compared to their N-substituted-2,3,4,5-tetraarylpyrrole precursors, with a redshift in λ_{max} of ~ 2000 cm^{-1}. The λ_{max} of the N-substituted-2,3,4,5-tetraarylpyrroles is ~255 nm and the λ_{max} of the N-substituted-2,3-diaryl-dibenzo[*e*,*g*]indoles is ~ 270 nm. The 3-benzyl-2,3-diaryl-dibenzo[*e*,*g*]indoles, λ_{max} ~ 260 nm, are not as redshifted as the N-substituted-2,3-diaryl-dibenzo[*e*,*g*]indoles (only ~ 1200 cm^{-1}) compared to their precursor N-benzyl-2,3,4,5-tetraarylpyrroles as the pyrrole ring has lost its aromaticity, but two aryl rings have been joined by a carbon-carbon bond. The increase in π-conjugation

of the N-substituted-2,3-diaryl-dibenzo[*e*,*g*]indoles also results in a significantly larger ε compared to the N-substituted-2,3,4,5-tetraarylpyrroles.

The broad absorption of the precursor compounds **3.1**, **3.3** – **3.10** is a result of the flexibility of these compounds. Fine structure and some vibronic coupling can be seen in the absorption spectra of the cyclodehydrogenated and photocyclised compounds, **3.15** – **3.17**, **3.27** – **3.29** and **3.36** – **3.38**, as a result of some rigidity being introduced to the system through the formation of a carbon-carbon bond. These N-substituted-2,3-diaryl-dibenzo[*e*,*g*]indole compounds are more flexible than the cyclodehydrogenated and photocyclised compounds in presented Chapter 2 due to the presence of uncyclised peripheral aryl rings, and the fine structure and vibronic coupling is not as pronounced. The 3-benzyl-2,3-diaryl-dibenzo[*e*,*g*]indoles have the most fine structure and vibronic coupling in this series of compounds, with a complicated absorption profile.

Figure 3.27 shows the normalised absorption and emission spectra for the precursor 2,3,4,5-tetraarylpyrroles, figure 3.27a shows the N*H*-2,3,4,5-tetraarylpyrroles, **3.1**, **3.3** and **3.4**, figure 3.27b shows the N-ethyl-2,3,4,5-tetraarylpyrroles, **3.5** – **3.7**, and figure 3.27c shows the N-benzyl-2,3,4,5-tetraarylpyrroles, **3.8** – **3.10**. There is no fine structure in the emission of these precursor compounds due to the flexibility of the compounds. All precursor compounds have a broad emission spectrum with λ_{max} ~ 392 nm. There is a slight redshift in the emission spectra for the N-benzyl-2,3,4,5-tetraarylpyrroles, **3.8** – **3.10**, due to the peripheral aryl methyl and *tert*butyl substitution (257 cm^{-1} and 447 cm^{-1}, respectively).

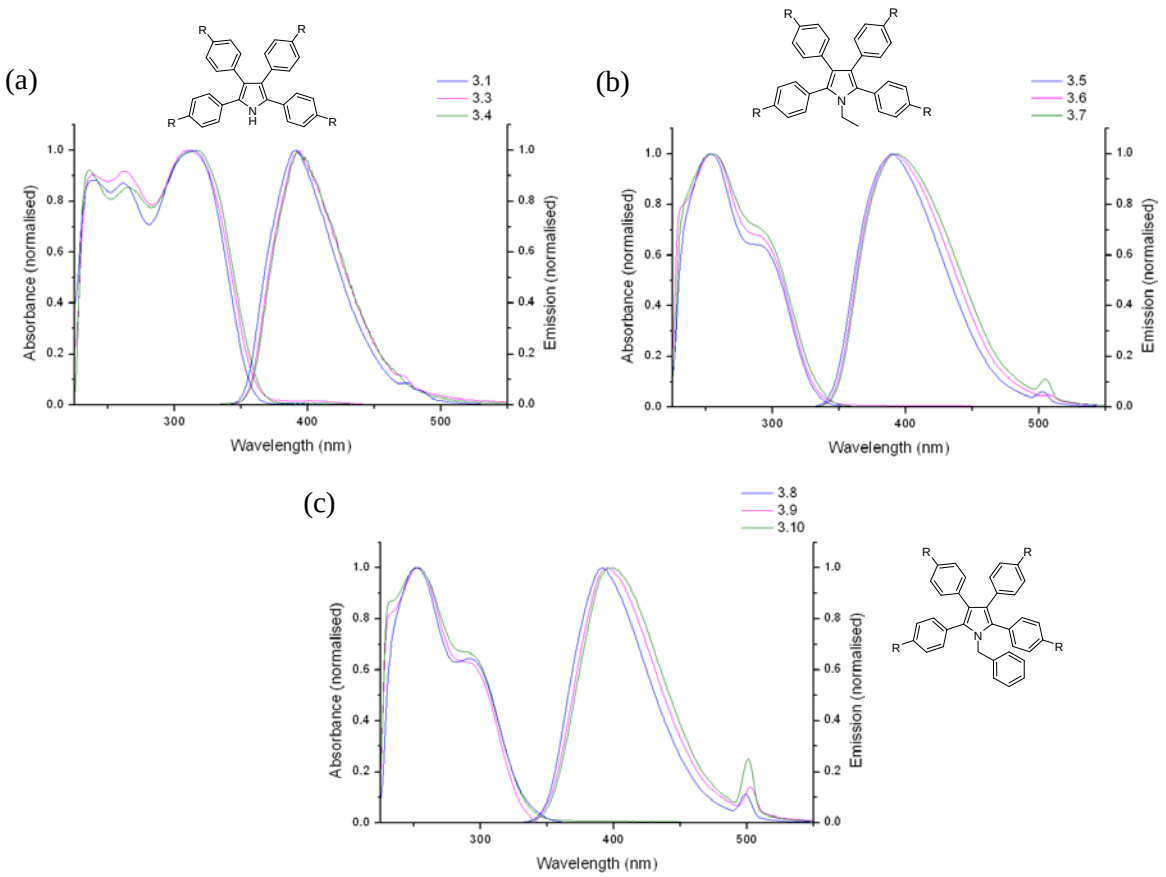

Figure 3.27 UV/visible and photoluminescence spectra of (a) **3.1**, **3.3**, **3.4**, (b) **3.5** – **3.7**, (c) **3.8** – **3.10**, all measured in dichloromethane at room temperature, concentrations ~ 10^{-6} mol.L^{-1}, R = H, Me, ^{t}Bu.

Figure 3.28 shows the normalised absorption and emission spectra for the cyclodehydrogenated and photocyclised partially fused compounds, figure 3.28a shows the N-ethyl-2,3-diaryl-dibenzo[*e*,*g*]indoles, **3.27** – **3.29**, figure 3.28b shows the N-benzyl-2,3-diaryl-dibenzo[*e*,*g*]indoles, **3.15** – **3.17**, figure 3.28c shows the 3-benzyl-2,3-diaryl-dibenzo[*e*,*g*]indoles, **3.36** – **3.38**. Again the increase in rigidity from the formation of a carbon-carbon bond allows for some fine structure and vibronic coupling to be seen in both the absorption and emission spectra of the N-substituted-2,3-diaryl-dibenzo[*e*,*g*]indoles. Vibronic coupling is seen in the emission spectra of the N-substituted-2,3-diaryl-dibenzo[*e*,*g*]indoles with peripheral aryl substitution, **3.28**, **3.29**, **3.16** and **3.17**. The weak electron donating ability of the peripheral methyl and *tert*butyl groups red shifts the emission spectra (~ 600 cm^{-1} and 350 cm^{-1}, respectively) of the N-substituted-2,3-diaryl-dibenzo[*e*,*g*]indoles. The λ_{max} of the emission spectra of the N-substituted-2,3-diphenyl-dibenzo[*e*,*g*]indoles, **3.27** and **3.15**, is almost the same as the precursor compounds λ_{max} = 394 nm. The emission spectra of the 3-benzyl-2,3-diaryl-dibenzo[*e*,*g*]indoles show some vibronic coupling, but the fine structure is much more pronounced in the UV/visible spectra. The emission of the 3-benzyl-2,3-diaryl-dibenzo[*e*,*g*]indoles is significantly red shifted (~ 3500 cm^{-1}) compared to that of the precursor

N-benzyl-2,3,4,5-tetraarylpyrrole compounds, λ_{max} of **3.36**, **3.37** and **3.38** are 453 nm, 463 nm, and 461 nm respectively.

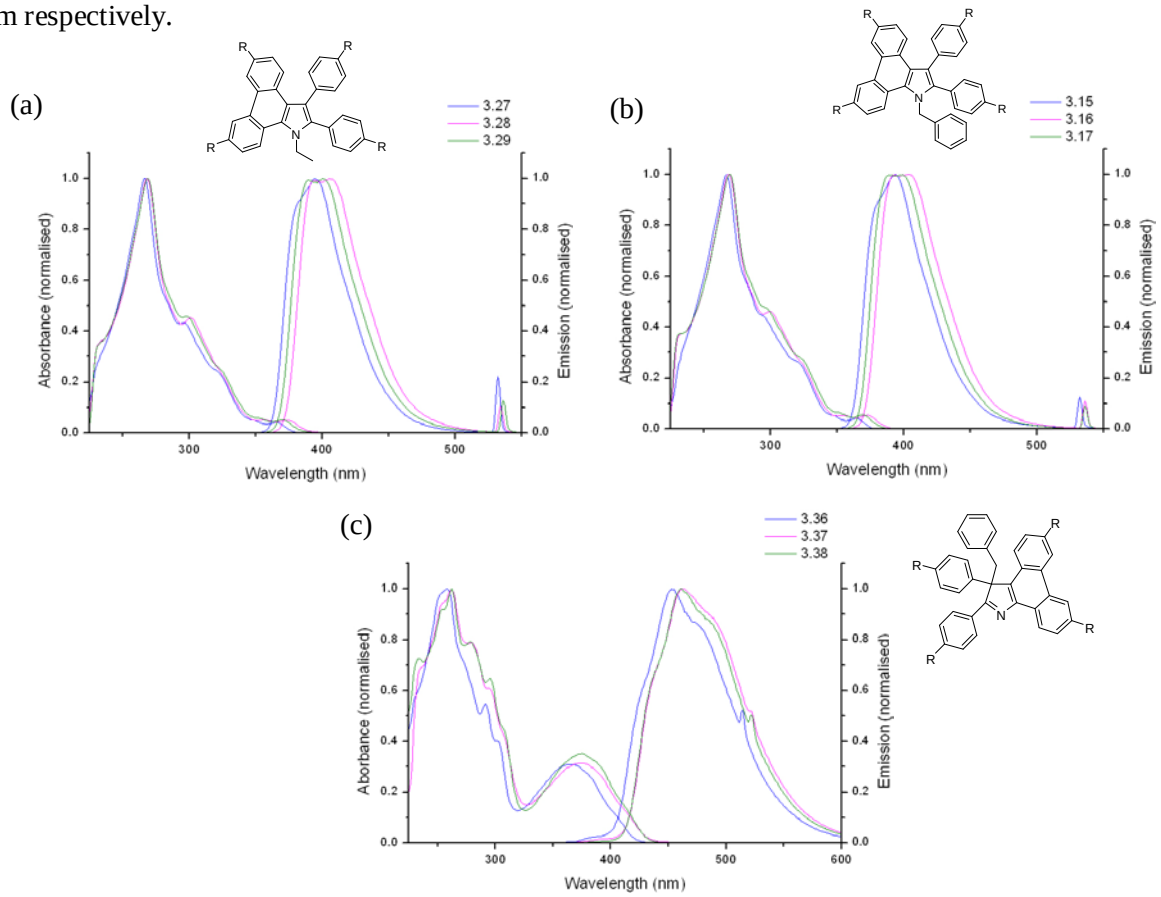

Figure 3.28 UV/visible and photoluminescence spectra of (a) **3.27** – **3.29**, (b) **3.15** – **3.17**, (c) **3.36** – **3.38**, all measured in dichloromethane at room temperature, concentrations ~ 10^{-6} mol.L^{-1}, R = H, Me, ^{t}Bu.

Table 3.2 summarises the main features of the absorption and emission spectra of the 2,3,4,5-tetraarylpyrroles, **3.1**, **3.3** – **3.10**, shown in figures 3.26a, 3.26b and 3.27. Table 3.3 summarises the main features of the absortion and emission spectra of the partially fused compounds, **3.15** – **3.17**, **3.27** – **3.29** and **3.36** – **3.38**, shown in figures 3.26c, 3.26d and 3.28.

	absorption		fluorescence		absorption		fluorescence
	λ_{max} (nm)	ε (L.mol^{-1}cm^{-1})	λ_{max} (nm)		λ_{max} (nm)	ε (L.mol^{-1}cm^{-1})	λ_{max} (nm)
3.1	239, 262, 313	20939, 20731, 23806	392	**3.3**	238, 262, 309	14879, 15138, 16400	394
3.4	236, 265, 316	18524, 17423, 20350	392				
3.5	253,285	20831, 13475	390	**3.6**	256, 289	22312, 14988	392
3.7	255, 287	24323, 17437	393				
3.8	251, 291	27416, 16018	392	**3.9**	253, 284	25573, 16291	396
3.10	253, 289	26405, 17660	399				

Table 3.2 Summary of the absorption and fluorescence maxima of **3.1**, **3.3** – **3.10**.

	absorption		fluorescence		absorption		fluorescence
	λ_{max} (nm)	ε (L.mol^{-1}cm^{-1})	λ_{max} (nm)		λ_{max} (nm)	ε (L.mol^{-1}cm^{-1})	λ_{max} (nm)
3.27	267, 296, 319, 365	65681, 28569, 16423, 2655	394	**3.28**	268, 301, 323, 374	61052, 27660, 14852, 3140	394, 405
3.29	269, 298, 324, 371	64653, 30069, 16262, 3291	390, 400				
3.15	267, 294, 318, 365	62766, 28055, 17661, 3071	394	**3.16**	269, 299, 322, 373	64982, 30645, 17828, 3551	393, 403
3.17	269, 296, 323, 369	62144, 29750, 17470, 3472	389, 399				
3.36	258, 291, 301, 364	40432, 23671, 17474, 13590	453	**3.37**	262, 281, 294, 306, 375	30986, 24451, 19158, 13655, 9741	463
3.38	262, 279, 295, 307, 375	43251, 34494, 28320, 19733, 15564	461				

Table 3.3. Summary of the absorption and fluorescence maxima of **3.27** – **3.29**, **3.15** – **3.17** and **3.36** – **3.38** .

Shown in figure 3.29a are the normalised absorption and emission spectra of N*H*-2,3,4,5-tetra(4-methylphenyl)pyrrole, **3.3**, and the N-substituted-2,3,4,5-tetra(4-methylphenyl)pyrroles, **3.6** and **3.9**. Figure 3.29b shows the N-substituted-2,3,4,5-tetra(4-methylphenyl)pyrroles, **3.6** and **3.9**, along with the

corresponding partially fused N-substituted-2,3-di(4-methylphenyl)-6,9-dimethyl-dibenzo[*e*,*g*]indoles, **3.28** and **3.16**, and figure 3.29c shows the precursor N-benzyl-2,3,4,5-tetra(4-methylphenyl)pyrrole, **3.19**, along with the two different partially fused compounds obtained through cyclodehydrogenation and photocyclisation respectively, **3.16** and **3.37**. These figures illustrate the differences in both the absorption and emission spectra when the aromatic system is changed, either by cyclodehydrogenation or photocyclisation, and the absorption and emission spectra are also changed when the nitrogen atom on the pyrrole ring is substituted from a hydrogen atom to an ethyl or benzyl group.

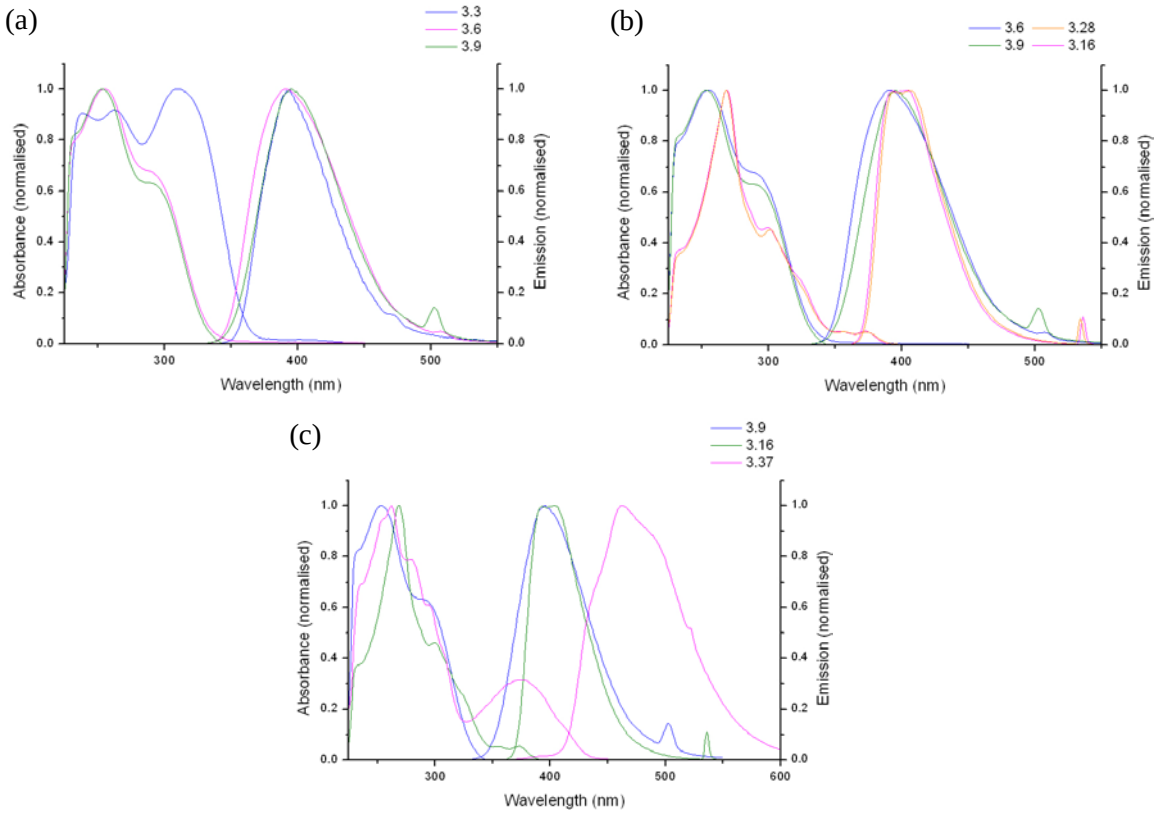

Figure 3.29 UV/visible and photoluminescence spectra of (a) **3.3**, **3.6** and **3.9** (b) **3.6**, **3.9**, **3.26** and **3.19** (c) **3.9**, **3.16** and **3.37**, all measured in dichloromethane at room temperature, concentrations ~ 10^{-6} mol.L^{-1}.

3.8 Summary

The synthesis and characterisation of four new N-substituted-2,3,4,5-tetraarylpyrrole compounds has been carried out along with the synthesis of their corresponding, previously unknown, precursor N*H*-2,3,4,5-tetraarylpyrrole compounds. Along with two already known N-substituted-2,3,4,5-tetraarylpyrrole compounds a family of model compounds with more than one position for the formation of carbon-carbon bonds through oxidative cyclodehydrogenation and photocyclisation were investigated. When subjected

to oxidative cyclodehydrogenation with $FeCl_3$, the N-benzyl-2,3,4,5-tetraarylpyrrole compounds formed only one carbon-carbon bond resulting in the corresponding N-benzyl-2,3-diaryl-dibenzo[*e*,*g*]indole compounds in low yields. The carbon-carbon bond forms between the peripheral aryl rings in the 2- and 3-position of the pyrrole ring in each case. Cyclodehydrogenation of the N-ethyl-2,3,4,5-tetraarylpyrrole compounds was also attempted. In all cases multiple products were formed as judged by ^{1}H-NMR spectroscopy and in only one case could a product be isolated, in low yield. The isolated compound, 3,6,12,15-tetrachloro-9-ethyl-tetrabenzo[*a*,*c*,*g*,*i*]carbazole, has formed two carbon-carbon bonds and undergone chlorination of all four phenyl rings. The carbon-carbon bonds formed impart significant twisting onto the tetrabenzo[*a*,*c*,*g*,*i*]carbazole core.

Photocyclisation of the N-substituted-2,3,4,5-tetraphenylpyrrole compounds was also carried out, with the photocyclisation of N-ethyl-2,3,4,5-tetraphenylpyrroles forming the corresponding N-ethyl-2,3-diaryl-dibenzo[*e*,*g*]indole compounds in good yields, completing the family of N-substituted-2,3-diaryl-dibenzo[*e*,*g*]indoles that were prepared by oxidative cyclodehydrogenation. The N-benzyl-2,3,4,5-tetraarylpyrroles, also underwent photocyclisation, forming multiple products, with one, 3-benzyl-2,3-diaryl-dibenzo[*e*,*g*]indoles, isolated in low yields. The isolated compounds have formed one carbon-carbon bond but the benzyl group has also undergone a 1,3-photochemical shift, destroying the aromaticity of the pyrrole core. The N-ethyl-2,3-diaryl-dibenzo[*e*,*g*]indoles prepared through photocyclisation were subjected to further photocyclisation and oxidative cyclodehydrogenation without success. The optical properties of the N-substituted-2,3-diaryl-dibenzo[*e*,*g*]indoles, 3-benzyl-2,3-diaryl-dibenzo[*e*,*g*]indoles and their precursors were measured with the formation of a carbon-carbon bond allowing for the fine structure and vibronic coupling to be observed in these compounds. The 3-benzyl-2,3-diphenyl-dibenzo[*e*,*g*]indole compounds have complicated UV/vis spectra.

Attempts were also made at the synthesis of a tetraphenylpyrrole compound with the carbon-carbon bond between the phenyl rings in the 3- and 4-position preinstalled. Low yields prevented the synthesis of this desired compound.

3.9 References

(1) (a) Shaik, S.; Kumar, D.; de Visser, S. P.; Altun, A.; Thiel, W. *Chem. Rev.* **2005**, *105*, 2279, (b) Denisov, I. G.; Makris, T. M.; Sligar, S. G.; Schlichting, I. *Chem. Rev.* **2005**, *105*, 2253, (c) Meunier, B.; de Visser, S. P.; Shaik, S. *Chem. Rev.* **2004**, *104*, 3947.

(2) (a) Imahori, H.; Umeyama, T.; Kurotobi, K.; Takano, Y. *Chem. Commun.* **2012**, *48*, 4032, (b) Drain, C. M.; Batteas, J. D.; Flynn, G. W.; Milic, T.; Chi, N.; Yablon, D. G.; Sommers, H. *P. Natl. Acad. Sci. USA* **2002**, *99*, 6498, (c) D'Urso, A.; Fragala, M. E.; Purrello, R. *Chem. Commun.* **2012**, *48*, 8165.

(3) (a) Goldberg, I. *CrystEngComm* **2002**, *4*, 109, (b) Karmakar, A.; Goldberg, I. *CrystEngComm* **2010**, *12*, 4095.

(4) Roth, B. D. In *Progress in Medicinal Chemistry*; F.D. King, A. W. O. A. B. R., Scott, L. D., Eds.; Elsevier, 2002; Vol. Volume 40.

(5) Hughes, C. C.; Prieto-Davo, A.; Jensen, P. R.; Fenical, W. *Org. Lett.* **2008**, *10*, 629.

(6) (a) Schouten, P. G.; Warman, J. M.; de Haas, M. P.; Fox, M. A.; Pan, H.-L. *Nature* **1991**, *353*, 736, (b) Castella, M.; Lopez-Calahorra, F.; Velasco, D.; Finkelmann, H. *Chem. Commun.* **2002**, 2348, (c) Sakurai, T.; Tashiro, K.; Honsho, Y.; Saeki, A.; Seki, S.; Osuka, A.; Muranaka, A.; Uchiyama, M.; Kim, J.; Ha, S.; Kato, K.; Takata, M.; Aida, T. *J. Am. Chem. Soc.* **2011**, *133*, 6537.

(7) Loudet, A.; Burgess, K. *Chem. Rev.* **2007**, *107*, 4891.

(8) (a) Estevez, V.; Villacampa, M.; Menendez, J. C. *Chem. Soc. Rev.* **2010**, *39*, 4402, (b) Ferreira, V. F.; de Souza, M. C. B. V.; Cunha, A. C.; Pereira, L. O. R.; Ferreira, M. L. G. *Org. Prep. Proced. Int.* **2001**, *33*, 411.

(9) (a) Paal, C. *Ber. Dtsch. Chem. Ges.* **1884**, *17*, 2756, (b) Knorr, L. *Ber. Dtsch. Chem. Ges.* **1884**, *17*, 2863.

(10) Jones, R. A.; Bean, G. P. *The Chemistry of Pyrroles*; Academic Press: London, 1977.

(11) (a) Katritzky, A. R.; Yousaf, T. I.; Chen, B. C.; Guang-Zhi, Z. *Tetrahedron* **1986**, *42*, 623, (b) Banik, B. K.; Samajdar, S.; Banik, I. *J. Org. Chem.* **2003**, *69*, 213.

(12) (a) Kuo, W.-J.; Chen, Y.-H.; Jeng, R.-J.; Chan, L.-H.; Lin, W.-P.; Yang, Z.-M. *Tetrahedron* **2007**, *63*, 7086, (b) Li, C.-S.; Tsai, Y.-H.; Lee, W.-C.; Kuo, W.-J. *J. Org. Chem.* **2010**, *75*, 4004.

(13) Eicher, T.; Hauptmann, S. *The Chemistry of Heterocyles*; Wiley: Weinheim, 2003.

(14) Benshafrut, R.; Rabinovitz, M.; Hoffman, R. E.; Ben-Mergui, N.; Müllen, K.; Iyer, V. S. *Eur. J. Org. Chem.* **1999**, *1999*, 37.

(15) MacLean, P. D.; Chapman, E. E.; Dobrowolski, S. L.; Thompson, A.; Barclay, L. R. C. *J. Org. Chem.* **2008**, *73*, 6623.

(16) Davidson, D. *J. Org. Chem.* **1938**, *03*, 361.

(17) Rao, H. S. P.; Jothilingam, S.; Scheeren, H. W. *Tetrahedron* **2004**, *60*, 1625.

(18) Cumper, C. W. N.; Wood, J. W. M. *J. Chem. Soc. B.* **1971**, 1811.

(19) King, F. E.; Paterson, G. D. *J. Chem. Soc.* **1936**, 400

(20) (a) Bewick, A.; Serve, D.; Joslin, T. A. *J. Electroanal. Chem. Interfacial Electrochem.* **1983**, *154*, 81, (b) Grossi, P. J.; Marchetti, L.; Ramasseul, R.; Rassat, A.; Serve, D. *J. Electroanal. Chem. Interfacial Electrochem.* **1978**, *87*, 353, (c) Libert, M.; Caullet, C.; Huguet, J. *Bull. Soc. Chim. Fr.* **1972**, 3639.

(21) Carter, P. H.; Cymerman, C. J.; Lack, R. E.; Moyle, M. *Org. Syn.* **1960**, *40*, 16.

(22) (a) Ban, I.; Sudo, T.; Taniguchi, T.; Itami, K. *Org. Lett.* **2008**, *10*, 3607, (b) Merlic, C. A.; Baur, A.; Aldrich, C. C. *J. Am. Chem. Soc.* **2000**, *122*, 7398, (c) Vo-Quang, L.; Vo-Quang, Y. *J. Heterocyclic Chem.* **1982**, *19*, 145.

(23) (a) Kubel, C.; Eckhardt, K.; Enkelmann, V.; Wegner, G.; Mullen, K. *J. Mater. Chem.* **2000**, *10*, 879, (b) Lu, Y.; Moore, J. S. *Tetrahedron Lett.* **2009**, *50*, 4071(c) Feng, X.; Wu, J.; Enkelmann, V.; Müllen, K. *Org. Lett.* **2006**, *8*, 1145.

(24) (a) Gregg, D. J.; Bothe, E.; Höfer, P.; Passaniti, P.; Draper, S. M. *Inorg. Chem.* **2005**, *44*, 5654, (b) Graczyk, A.; Murphy, F. A.; Nolan, D.; Fernandez-Moreira, V.; Lundin, N. J.; Fitchett, C. M.; Draper, S. M. *Dalton Trans.* **2012**, *41*, 7746.

(25) Takase, M.; Enkelmann, V.; Sebastiani, D.; Baumgarten, M.; Müllen, K. *Angew. Chem. Int. Ed.* **2007**, *46*, 5524.

(26) Herwig, P. T.; Enkelmann, V.; Schmelz, O.; Müllen, K. *Chem. Eur. J.* **2000**, *6*, 1834.

(27) Luo, J.; Xu, X.; Mao, R.; Miao, Q. *J. Am. Chem. Soc.* **2012**, *134*, 13796.

(28) (a) Sarma, J. A. R. P.; Desiraju, G. R. *Acc. Chem. Res.* **1986**, *19*, 222 228, (b) Pedireddi, V. R.; Reddy, D. S.; Goud, B. S.; C., C. D.; Rae, D. R.; Desiraju, G. R. *J. Chem. Soc., Perkin Trans. 2* **1994**, 2353, (c) Desiraju, G. R.; Parthasarathy, R. *J. Am. Chem. Soc.* **1989**, *111*, 8725

(29) (a) Weiss, K.; Beernink, G.; Dötz, F.; Birkner, A.; Müllen, K.; Wöll, C. H. *Angew. Chem. Int. Ed.* **1999**, *38*, 3748, (b) Gregg, D. J.; Ollagnier, C. M. A.; Fitchett, C. M.; Draper, S. M. *Chem. Eur. J.* **2006**, *12*, 3043.

(30) Dou, X.; Yang, X.; Bodwell, G. J.; Wagner, M.; Enkelmann, V.; Müllen, K. *Org. Lett.* **2007**, *9*, 2485.

(31) Rathore, R.; Burns, C. L. *J. Org. Chem.* **2003**, *68*, 4071.

(32) Laarhoven, W. H.; Cuppen, T. J. H. M.; Nivard, R. J. F. *Recl. Trav. Chim. Pay. B.* **1968**, *87*, 687

(33) Blackburn, E. V.; Timmons, C. J. *Q. Rev. Chem. Soc.* **1969**, *23*, 482.

(34) Padwa, A.; Ku, H.; Mazzu, A. *J. Org. Chem.* **1978**, *43*, 381.

(35) Cooper, J. L.; Wasserman, H. H. *J. Chem. Soc. D: Chem. Commun.* **1969**, 200.

(36) Liu, L.; Yang, B.; Katz, T. J.; Poindexter, M. K. *J. Org. Chem.* **1991**, *56*, 3769.

(37) Zhang, X.; Jiang, X.; Zhang, K.; Mao, L.; Luo, J.; Chi, C.; Chan, H. S. O.; Wu, J. *J. Org. Chem.* **2010**, *75*, 8069.

(38) Bouit, P.-A.; Escande, A.; Szűcs, R.; Szieberth, D.; Lescop, C.; Nyulászi, L.; Hissler, M.; Réau, R. *J. Am. Chem. Soc.* **2012**, *134*, 6524.

(39) Patterson, J. M.; Burka, L. T. *Tetrahedron Lett.* **1969**, *10*, 2215.

(40) D'Auria, M. *Heterocycles* **1996**, *43*, 1305

(41) Patterson, J. M.; Bruser, D. M. *Tetrahedron Lett.* **1973**, *14*, 2959.

(42) Zhai, L.; Shukla, R.; Rathore, R. *Org. Lett.* **2009**, *11*, 3474.

(43) (a) Rathore, R.; Zhu, C.; Lindeman, S. V.; Kochi, J. K. *J. Chem. Soc., Perkin Trans. 2* **2000**, 1837, (b) Eberson, L.; P. Hartshorn, M.; Persson, O. *J. Chem. Soc., Perkin Trans. 2* **1997**, 195, (c) Handoo, K. L.; Gadru, K. *Curr. Sci.* **1986**, *55*, 920

(44) (a) Churruca, F.; SanMartin, R.; Carril, M.; Urtiaga, M. K.; Solans, X.; Tellitu, I.; Domínguez, E. *J. Org. Chem.* **2005**, *70*, 3178, (b) Takada, T.; Arisawa, M.; Gyoten, M.; Hamada, R.; Tohma, H.; Kita, Y. *J. Org. Chem.* **1998**, *63*, 7698.

(45) Dennis, G. D.; Edwards-Davis, D.; Field, L. D.; Masters, A. F.; Maschmeyer, T.; Ward, A. J.; Buys, I. E.; Turner, P. *Aust. J. Chem.* **2006**, *59*, 135.

Chapter Four:

Pentaarylpyrrole compounds

4.1 Introduction

The π-excessive, five-membered heterocyclic ring, pyrrole can be considered as an electronic replacement for benzene as it has six π electrons. By replacing the benzene core of the hexaphenylbenzene precursor to HBC with a pyrrole ring the resulting pentaphenylpyrrole precursor, **4.1**, should undergo oxidative cyclodehydrogenation forming five new carbon-carbon bonds between the peripheral phenyl rings. The formation of five new carbon-carbon bonds should result in the formation of a compound, **4.2**, with corannulene-like curvature induced by the central five-membered ring and the incorporation of a heteroatom into the core of a PAH, as shown in figure 4.1. Incorporation of a heteroatom into the core of a HBC derivative, coupled with the expected curvature from the five membered ring, should confer new and interesting chemical and physical properties onto this molecule.

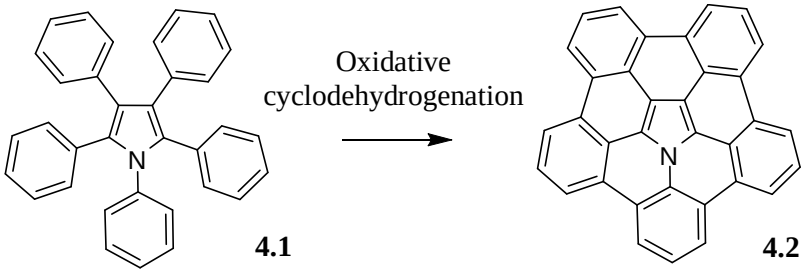

Figure 4.1 Envisaged oxidative cyclodehydrogenation of **4.1** to form **4.2**.

The synthesis of precursor **4.1**, a sterically hindered pentaaryl substituted pyrrole, poses a significant synthetic challenge. Up until 2010 there existed only few routes to synthesise pentaphenylpyrrole. These routes do not easily allow controlled variability in the peripheral aryl groups of the molecule, and most reactions reported to form pentaphenylpyrrole were low yielding.[1] More recently transition metal catalysed reactions have played an important role in the synthesis of sterically encumbered heterocyclic derivatives. The steric hindrance required for the placement of five phenyl rings around the pyrrole core leads to the failure of reactions that are known to form less sterically hindered pyrroles. In 2004 Rao *et al.*[2] attempted the formation of pentaphenylpyrrole by a microwave reaction of 1,2,3,4-tetraphenylbutenedione and anilinium formate catalysed by Pd/C. This strategy was used successfully to prepare various tri- and tetra-phenylpyrrole derivatives using the appropriate precursor, but the formation of pentaphenylpyrrole failed. The authors do observe reduction of the double bond of the 1,2,3,4-tetraphenylbutenedione, and formation of the expected imine, but the required cyclisation did not occur. Steric factors preventing the cyclisation reaction are cited by the authors for the lack of formation of the desired pentaphenylpyrrole.

In 2010, Feng *et al*. reported a Suzuki coupling route to pentaarylpyrrole, discussed in section 4.4 below. Following this Chen *et al*.[3] reported in late 2012 another metal catalysed route for the synthesis of a range of pentaarylpyrrole compounds. The route to these compounds followed a $PdCl_2$ and $CuCl_2$ catalysed reaction between diarylacetylenes and aniline derivatives, with variability in the peripheral aryl groups able to be introduced through both reaction components. Electron donating substituents in the para position decreased the yield of the formation of the pentaarylpyrroles.[3] In this study the incorporation of electron donating substituents is desirable, as the electron donating nature can activate the precursor molecules towards cyclodehydrogenation.

Computational studies on the expected cyclodehydrogenated product from the reaction, **4.2**, along with a range of other curved heteroatom containing conjugated molecules, was carried out in 2010.[4] These calculations indicate that **4.2** should indeed display curvature induced by the five membered pyrrole ring. Importantly, these calculations also indicated that **4.2** should be stable when synthesised, indicated by a range of parameters all indicating higher stability than C_{222}, the largest graphite sheet synthesised using oxidative cyclodehydrogenation. The stability of the heteroatom containing conjugated molecules studied is attributed to the all benzenoid nature of the compounds, with the π electrons able to be assigned completely into Clar sextets in each case, including that of **4.2**.

4.2 Attempted synthesis of pentaaryl pyrroles using a Paal – Knorr approach

*4.2.1 Synthesis of required 1,2,3,4-tetraaryl-1,4-butadiones, **4.3** – **4.5***

There are a wide range of methods for the synthesis of multiply substituted pyrroles. Ideally, a route towards pentaaryl substituted pyrrole derivatives was required that allowed for the synthesis of a family of compounds where the 4-position of the peripheral aryl groups could be easily modified. The simplest route to the pentaaryl substituted pyrroles, keeping in mind these conditions, appeared to be the synthesis of 1,2,3,4,5-tetraaryl-1,4-butadiones and subsequent Pall – Knorr condensation with aniline derivatives to form the desired pyrrole. The steric congestion around the pyrrole core will be quite large and could potentially inhibit the cyclisation. Pall – Knorr condensation reactions with aniline and substituted butadiones are well known.[5,6]

Another appeal of using the Pall – Knorr condensation reaction to form pentaaryl substituted compounds is the relative ease of synthesis of the appropriate precursors. Aniline, **4.9**, and 4-anisidine, **4.10**, are commercially available, with 4-*tert*butylaniline, **4.11**, synthesised in two steps in high yields from *tert*butyl benzene.[7] The required 1,2,3,4,-tetraaryl-1,4-butadiones can be synthesised from the oxidative dimerisation of two deoxybenzoin molecules.[8] With the appropriate benzoin molecules in hand from the

synthesis of 2,3-diarylindoles and 2,3,4,5-tetraarylpyrroles in Chapters 2 and 3 respectively, the benzoin molecules could be reduced to the required deoxybenzoins,[9] allowing for the synthesis of the 1,2,3,4-tetraaryl-1,4-butadiones, **4.3**, **4.4** and **4.5** in two steps, as shown in Scheme 4.1.

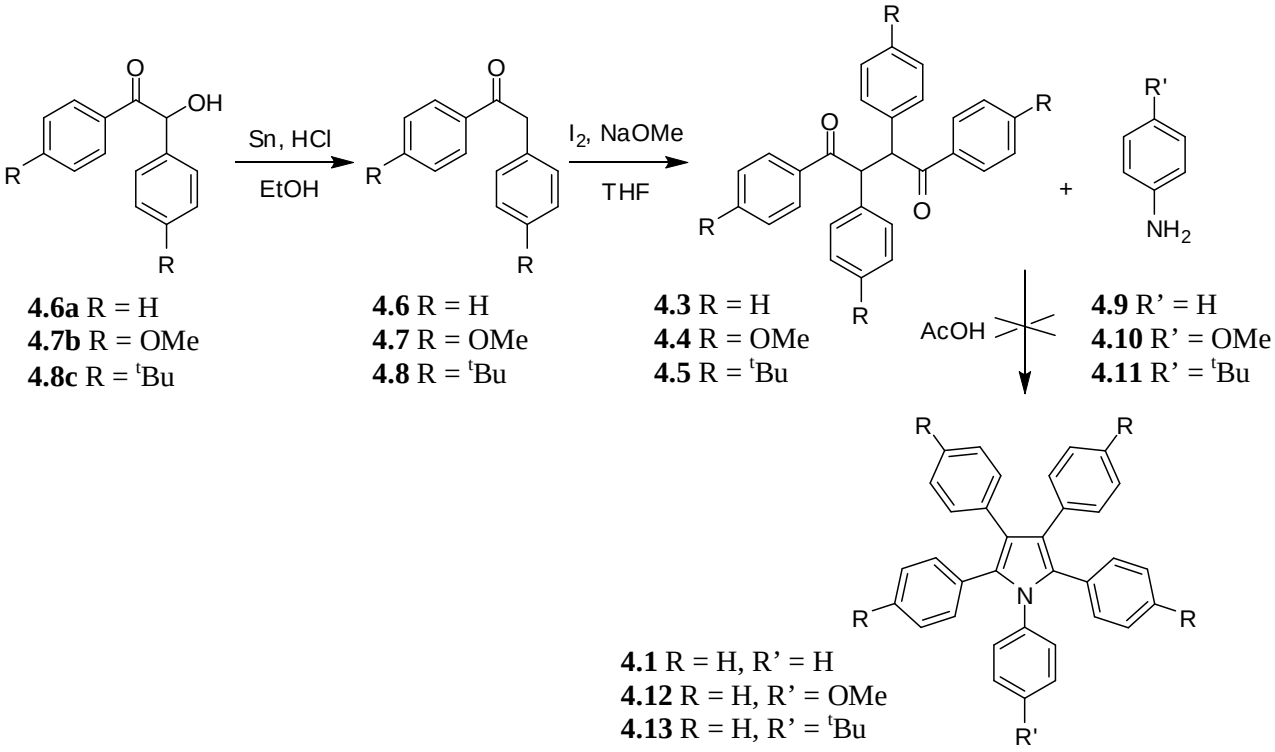

4.6a R = H
4.7b R = OMe
4.8c R = ^{t}Bu

4.6 R = H
4.7 R = OMe
4.8 R = ^{t}Bu

4.3 R = H
4.4 R = OMe
4.5 R = ^{t}Bu

4.9 R' = H
4.10 R' = OMe
4.11 R' = ^{t}Bu

4.1 R = H, R' = H
4.12 R = H, R' = OMe
4.13 R = H, R' = ^{t}Bu

Scheme 4.1. Attempted synthesis of pentaarylpyrroles using the Pall – Knorr condensation between 1,2,3,4-tetraaryl-1,4-butadiones and aniline derivatives.[8,9]

Following the method of Carter *et al*.[9] benzoin, **4.6a**, anisoin, **4.7b**, and 4,4'-di*tert*butylbenzoin, **4.8a**, were reduced with tin chloride to form the corresponding deoxybenzoin compounds, **4.6**,[10] **4.7**,[9] and **4.8**,[11] all of which have been previously synthesised. The deoxybenzoins were then subjected to the oxidative dimerisation conditions described by Kuo *et al*.[8] The synthesis of **4.4** has already been described in Chapter 3, and the oxidative dimerisation of **4.3** and **4.5** proceed in reasonable yields (~ 65%). Compounds **4.3**[8] and **4.4**[12] have been previously reported while **4.5** is unknown.

*4.2.2 Attempts at Paal – Knorr condensation with 1,2,3,4-tetraaryl-1,4-butadiones, **4.3** – **4.5** and aniline*

With compounds **4.3** – **4.5** in hand the Pall – Knorr condensation with aniline, and aniline derivatives, could be carried out. Initially, the Pall – Knorr condensation was attempted with **4.3** and aniline, **4.9**, in refluxing acetic acid. After two hours a white solid precipitated from the reaction mixture, which was filtered and isolated. Unfortunately the ^{1}H-NMR spectrum matched the literature ^{1}H-NMR spectrum for 2,3,4,5-tetraphenylfuran, **4.14**, shown in figure 4.2, rather than the desired 1,2,3,4,5-pentaphenylpyrrole,

4.1. The steric hindrance of incorporating aniline to form the desired pyrrole compound has not been overcome and instead intramolecular condensation of **4.3** has occurred.

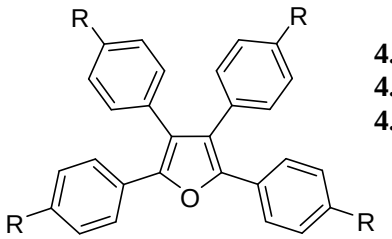

4.14 R = H
4.15 R = OMe
4.16 R = ^{t}Bu

Figure 4.2. 2,3,4,5-tetraarylfurans formed by the intramolecular cyclisation of **4.3** – **4.5** respectively.

Compound **4.14** has been previously synthesised by many groups, using a variety of methods, including from the dione **4.3**.[13] A X-ray crystal structure of **4.14** has not been reported, and the slow evaporation of a dichloromethane solution of **4.14** gave crystals suitable for X-ray crystallography. The X-ray crystal structure was solved in the monoclinic space group *C*2/*c*, with one molecule of **4.14** present in the asymmetric unit, as shown in figure 4.3. As expected the phenyl rings adopt a propeller confirmation around the periphery of the furan ring, with the phenyl rings twisted at 19.9(1)˚, 34.0(1)˚, 42.8(1)˚ and 62.5(1)˚ out of the plane of the furan core. The crystal packing of **4.14** is dominated by edge-to-face π – π interactions.

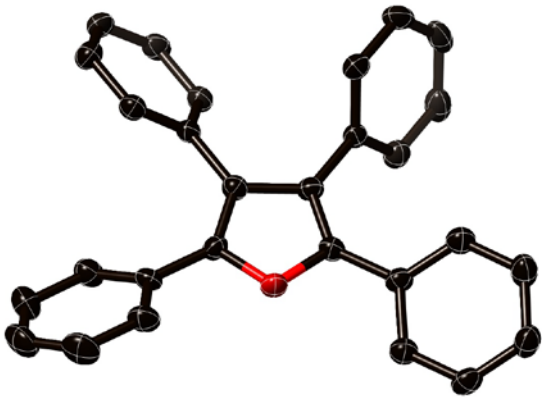

Figure 4.3. Asymmetric unit of **4.14**, hydrogen atoms have been removed for clarity.

The Paal – Knorr reaction was also carried out between the two remaining butadiones, **4.4** and **4.5**, with aniline, **4.9**. In each case, the same conditions as described above were used. The corresponding furans, **4.15** and **4.16**, were isolated in ~ 80% yield, and both have previously been reported in the literature.[14] A crystal of **4.15** was grown from the slow evaporation of a dichloromethane solution. The X-ray crystal structure was solved in the triclinic space group *P*-1, and two molecules of **4.15** were present in the

asymmetric unit. One peripheral methoxy group, of the methoxyphenyl in the 2-position of the furan ring, in one molecule, is disordered over two positions. One position is occupied 60% of the time, the other 40%. The only other difference in the two molecules present in the asymmetric unit is the twisting of the 4-methoxyphenyl rings around the furan ring, in one molecule the phenyl rings are twisted at angles 2.7(1)˚, 20.5(1)˚, 68.9(1)˚ and 97.1(1)˚of out of the plane of the furan core, while the molecule with methoxy disorder the phenyl rings are twisted out of the plane of the furan core by 4.0(1)˚, 4.1(1)˚, 63.4(1)˚ and 75.4(1)˚. In each molecule the 4-methoxyphenyl rings in the 2- and 5-position are almost coplanar with the furan core. One molecule of **4.15** is shown in figure 4.4. The crystal structure packing is dominated by hydrogen bonding between the methoxy oxygen atom and the hydrogen atoms of the 4-methoxyphenyl rings, along with edge-to-face π – π interactions between the 4-methoxyphenyl rings and the furan ring.

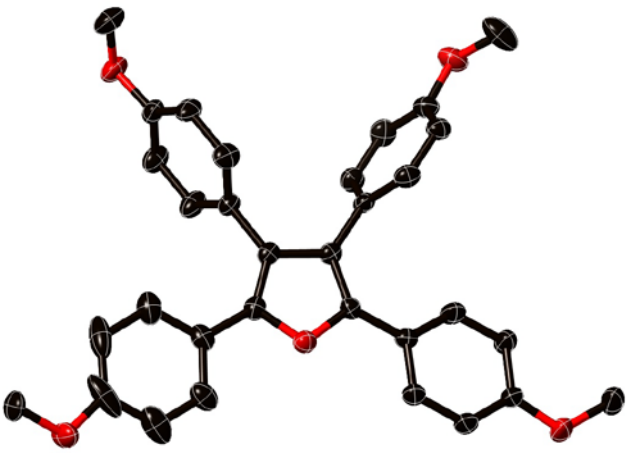

Figure 4.4 One molecule present in the asymmetric unit of **4.15**, hydrogen atoms have been removed for clarity, and methoxy disorder is not shown.

To try and drive the 1,2,3,4-tetraaryl-1,4-butadiones, **4.3** – **4.5**, towards an intermolecular Pall – Knorr condensation to form the desired pentaarylpyrroles, **4.1**, **4.12** and **4.13**, rather than a intramolecular condensation forming the 2,3,4,5-tetraarylfurans, **4.13** – **4.15**, a range of different conditions for the condensation were trialled using dione **4.3** and aniline, **4.9**. The amount of aniline, the acid used (HCl or AcOH), the time (2 – 48 hours) and the pressure the reaction was carried out under were all varied, but in all cases these modifications to the reaction conditions were unsuccessful, and only furan **4.14** was isolated.

4.2.3 Attempts at oxidative cyclodehydrogenation of 2,3,4,5-tetraarylfurans, ***4.14 – 4.16***

With furans **4.14** – **4.16** in hand, the oxidative cyclodehydrogenation of these precursors was attempted. There is no literature precedent for the oxidative cyclodehydrogenation of furans. Although the attempted photocyclisation of **4.14** has been carried out,[15] no products were able to be isolated from the reaction mixture. The oxidative cyclodehydrogenation of the corresponding 2,3,4,5-tetraphenylthiophene has been reported using $AlCl_3$ and $CuCl_2$ in CS_2.[16] Using these conditions the oxidative cyclodehydrogenation of **4.14** and **4.15** were attempted. In each case the reactions were quenched when the TLC stopped changing (three days and five days, respectively) and attempts were made at purification. In both cases multiple products were seen on the TLC plate and ^{1}H-NMR spectroscopy confirms this. Unfortunately, purification with column chromatography was not successful in isolating any products in either case. The oxidative cyclodehydrogenation of **4.14** and **4.15** was also attempted using $FeCl_3$. In each case only starting material was recovered.

4.3 Synthesis of pentaarylpyrroles by münchnone formation and subsequent 1,3-dipolar addition of diphenylacetylene

4.3.1 Synthesis of münchnone precursors, ***4.18*** *and* ***4.21***

Another route towards the formation of pentaarylpyrroles was required due to the formation of exclusively 2,3,4,5-tetraphenylfurans when the Paal – Knorr condensation was attempted. When devising a new route to the pentaaryl pyrroles, it was important to introduce the phenyl substituted nitrogen atom into the synthetic scaffold early on in the synthesis, so that the desired pyrrole ring can form. One method of incorporating the phenyl substituted nitrogen into the synthetic scaffold before the bulk of the steric hindrance is introduced is to form a münchnone, **4.17** by the cyclodehydration of N-phenyl-N-benzoyl-phenylglycine, **4.18**, as shown in scheme 4.2.

Münchnones are mesoionic compounds,[17] a class of compounds whose structure can only be accurately represented using polar resonances. The münchnones are named as such for the place of their discovery, Münich. The formation of münchnones and their subsequent 1,3-dipolar addition using acetylene derivatives to form pyrrole ring has been extensively studied,[18] and the regioselectivity of the 1,3-dipolar addition when unsymmetrical acetylenes are used has been of particular interest.[19]

A model system, where the substitution on the nitrogen atom is a methyl group, rather than a phenyl group was also prepared to ensure the 1,3-dipolar addition of the diphenyl acetylene to the münchnone derivatives occurs as expected to form the desired N-methyl-2,3,4,5-tetraphenylpyrrole, **4.19**. The steric

hindrance of the 1,3 dipolar addition, bringing four phenyl groups together, should not be affected by the substitution on the nitrogen atom.

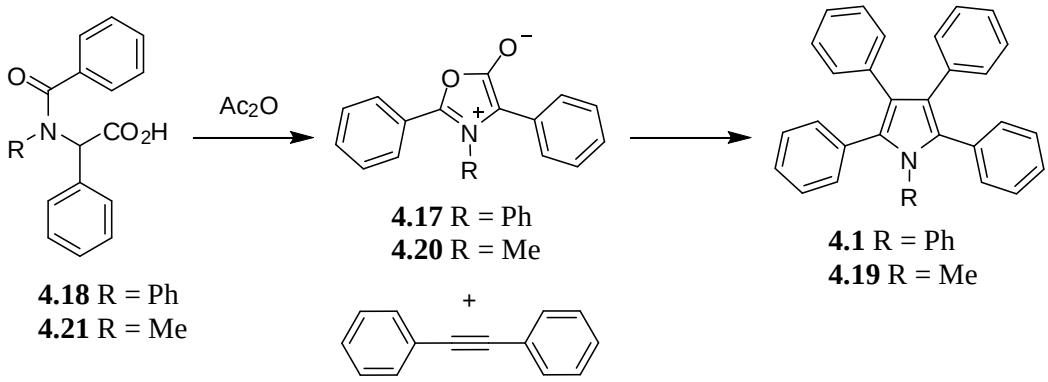

Scheme 4.2. Desired synthesis of pentaphenylpyrrole by the dehydration of N-phenyl-N-benzoyl-phenylglycine, and 1,3-dipolar addition using diphenyl acetylene.

Precursor compounds **4.18** and **4.21** were synthesised in the same manner, following modified literature procedures,[20] as outlined in scheme 4.3 below. Phenyl acetic acid was protected as an ethyl ester, and then brominated. The appropriate amine was substituted and then benzoyl chloride was used to form the amide

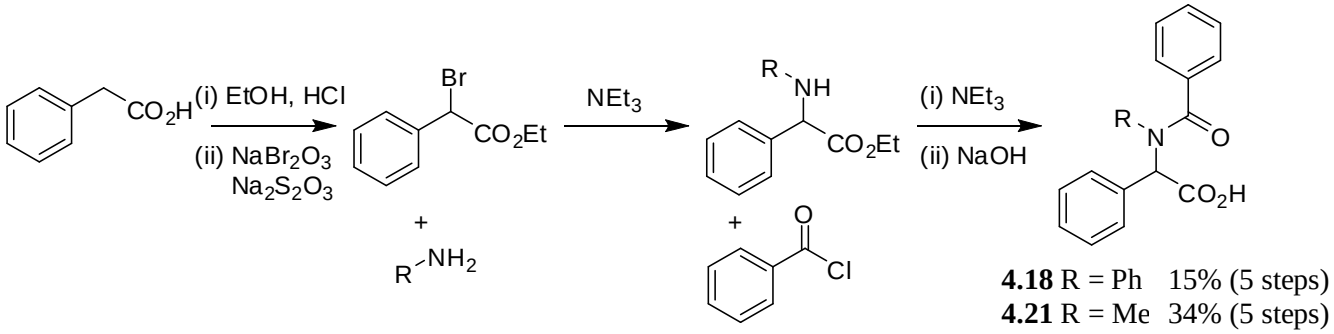

Scheme 4.3. General procedure for the synthesis of **4.17** and **4.18** following literature procedures from phenyl acetic acid.[20]

*4.3.2 1,3-dipolar additions of diphenyl acetylenes with münchone precursors, **4.18** and **4.21**, and münchnones, **4.17** and **4.20***

With **4.18** and **4.21** in hand the preparation of the targeted münchnones could be carried out. Although normally prepared *in situ* and reacted with acetylenes immediately, münchnones can be isolated and subjected to the 1,3-dipolar addition in a separate step, although this often results in lower yields.[21] Both **4.18** and **4.21** were dehydrated with acetic anhydride to form the corresponding münchnones **4.17** and

4.20, but the compounds were difficult to purify and decomposed over the course of a few days. Compound **4.21** was treated with acetic anhydride to form münchnone **4.20** *in situ*, followed by the addition of diphenyl acetylene for **4.21** to undergo 1,3 dipolar addition. Pleasingly, N-methyl-2,3,4,5-tetraphenyl pyrrole, **4.19**, was formed, as judged by comparison of its ^{1}H-NMR spectrum to a known literature ^{1}H-NMR spectrum.[22]

With the encouraging formation of **4.19**, compound **4.18** was subjected to the same conditions for the *in situ* formation of **4.17** and subsequent addition of diphenylacetylene. After purification of the reaction mixture the ^{1}H-NMR spectrum matched the spectrum of pentaphenylpyrrole **4.1** published by Feng *et al*.,[23] and mass spectrometry also indicated the formation of **4.1**. Although the reaction mixture was difficult to purify, and the reaction was low yielding (15%), using *in situ* münchnone formation has been successful for the formation of pentaphenylpyrrole. A crystal of **4.1** suitable for X-ray crystallography was also obtained, a polymorph of that isolated by Feng *et al*.[23] The crystal structure solves in the monoclinic space group $P2_1/n$, with one molecule of **4.1** present in the asymmetric unit, shown in figure 4.5a. The main difference in the crystal structure of **4.1** compared to that obtained by Feng *et al*, is the degree of twisting out of the phenyl rings out of the plane of the central pyrrole ring.[23] In the crystal isolated by Feng *et al*. the twist angles are 40.1˚, 48.0˚, 53.2˚, 56.1˚ and 60.1˚, while in the crystal isolated here the twist angles are 39.1(1)˚, 49.2(1)˚, 53.3(1)˚, 55.8(1)˚ and 56.8(1)˚.

The slight difference in the twisting of the phenyl rings affects the overall packing motif of the structures. The molecules of **4.1** crystallised by Feng *et al*., pack into molecular columns, with the axis of the column perpendicular to the plane of the pyrrole ring, and each molecule is aligned in the same way, with a distance between the pyrrole rings of 5.14 Å.[23] While the molecules of **4.1** crystallised here also stack into columns, each column consists of molecules of **4.1** facing alternate ways, with edge-to-face $\pi - \pi$ interactions (C – centroid distance = 3.553(1) Å and 3.797(1) Å) between the pyrrole rings and the peripheral phenyl rings in the column, as shown in figure 4.5b.

Despite the success of using a münchnone for the synthesis of **4.1**, this synthetic scheme does have several drawbacks. Firstly, the final step of the reaction proceeds in low yields, and secondly the synthesis of N-substituted-N-benzoyl-phenylglycines, **4.18** and **4.21**, is five synthetic steps from the starting phenyl acetic acid. Around the time the synthesis of **4.1** was completed we became aware of the synthesis of pentaphenylpyrrole and other aryl substituted pyrrole derivatives by Feng *et al*,[23] using a Suzuki coupling approach of 1,2,5-triphenylpyrrole derivatives. The synthetic strategy towards three new and two known pentaarylpyrrole derivatives is outlined below.

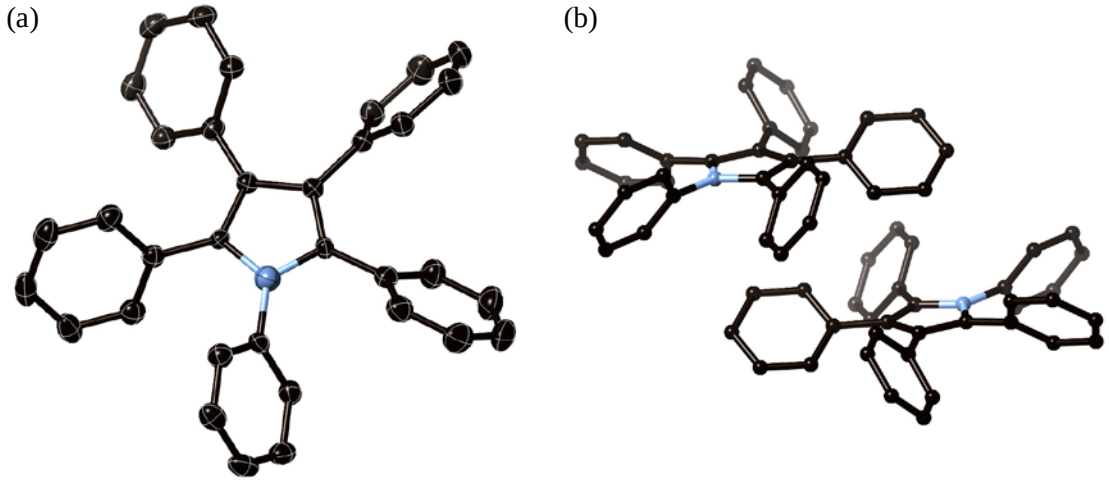

Figure 4.5. (a) Asymmetric unit of **4.1**, (b) edge-to-face π – π interactions between alternating molecules of **4.1** in a column, hydrogen atoms have been removed for clarity.

4.4 Synthesis of pentaarylpyrroles using a Suzuki coupling

As outlined in scheme 4.4, Feng *et al*., synthesised pentaphenylpyrrole, **4.1**, in four steps.[23] Phenyl acetylene was oxidatively coupled to form bisphenyl butadiyne, which was then reacted with aniline to form 1,2,5-triphenylpyrrole, **4.22**, catalysed by copper chloride. The 1,2,5-triphenylpyrrole was then brominated forming 1,2,5-triphenyl-3,4-dibromopyrrole, **4.23**. Compound **4.23** was then subjected to a Suzuki coupling reaction with phenyl boronic acid, **4.24**, to form desired pentaphenylpyrrole, **4.1**.

The synthesis of 3,4-diarylpyrrole derivatives from the Suzuki coupling of arylboronic acids and 3,4-dibromopyrroles has been previously observed in the literature.[24] Additionally, the synthesis of pentaphenylpyrrole from the Suzuki coupling of 1,2,5-triphenyl-3,4-dibromopyrrole and phenyl boronic acid[23] is not the only report of the synthesis of sterically crowded pyrrole derivatives through Suzuki coupling with aryl boronic acids.[25] 2,3,4,5-Tetrabromopyrroles have been used for a four-fold Suzuki coupling with a variety of aryl boronic acids, and the regioselectivity of the reaction can be controlled, with the 2- and 5-position of the pyrrole ring more reactive than the 3- and 4- positions.[25a]

The synthesis of the required 1,2,5-triphenylpyrrole, **4.22**, was achieved in this case by the Paal – Knorr condensation of 1,4-diphenylbutane, **4.25**, and aniline, **4.9**, rather than the copper chloride catalysed reaction of bisphenyl butadiyne and aniline. 1,4-diphenyl-1,4-butanedione, **4.25**, was synthesised by the reduction of trans-1,4-diphenyl-1,4-butenedione,[26] which was prepared by the reaction of benzene and fumaryl chloride under Friedel – Crafts conditions.[27] With compound **4.22** in hand, bromination proceeded in good yields to form **4.23**. Phenyl boronic acid, **4.24**, was prepared according to the literature

procedure.[28] Although the purification of **4.24** by washing with hexanes was disrupted due to the February 2011 earthquake, recrystallisation with water over four months later provided **4.24** for the Suzuki coupling reaction with **4.23**. Pleasingly, the Suzuki coupling proceeded to form pentaphenylpyrrole, although the reaction proceeded in lower yields than those reported (45% compared to 82%).

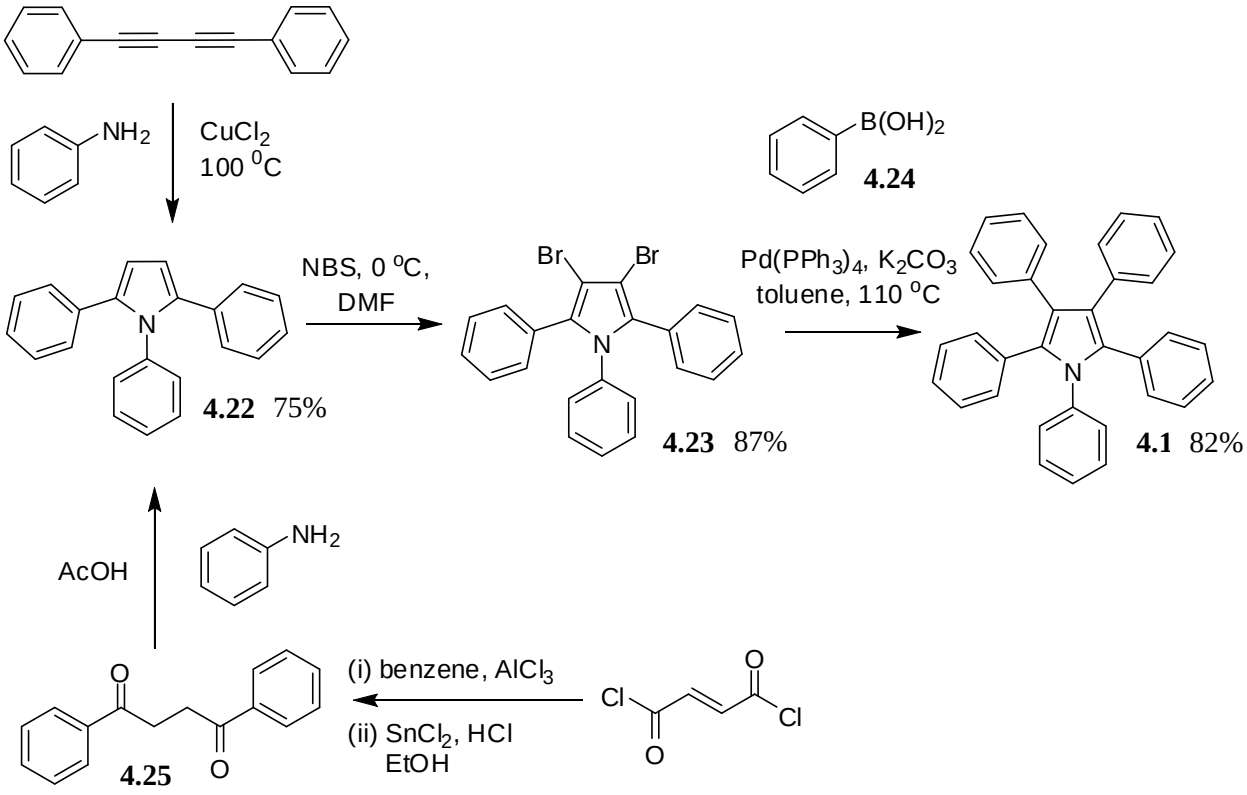

Scheme 4.4. Synthesis of pentaphenyl pyrrole using a Suzuki coupling approach.[23]

With a route to pentaphenylpyrroles in hand, the peripheral aryl substituents can be systematically varied by substitution of the 4-position in the aniline and the phenylboronic acid. Firstly, the synthesis of **4.12** and **4.13** were targeted by variation of the aniline used in the Paal – Knorr condensation to form the 1,2,5-tetraarylpyrrole derivative. 4-*tert*butylaniline, **4.11** was prepared following literature procedure,[7] both **4.10** and **4.11** underwent the Paal – Knorr condensation in moderate yields (60%) with **4.25**, to form 1-(4-methoxyphenyl)-2,5-diphenylpyrrole, **4.26**, and 1-(4-*tert*butylphenyl)-2,5-diphenylpyrrole, **4.27**, respectively, as shown in scheme 4.5.

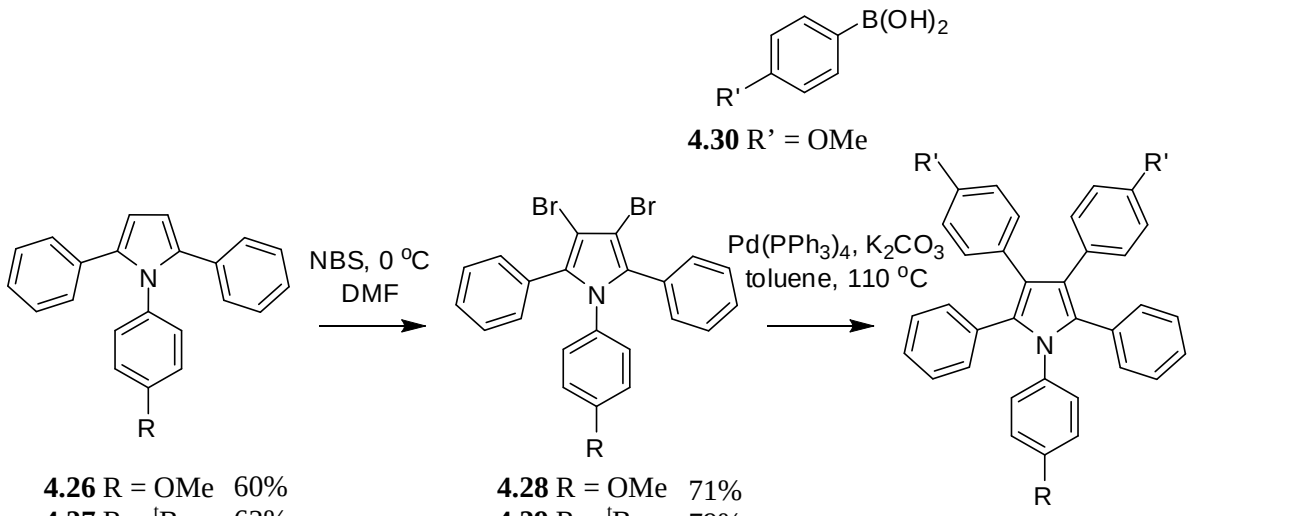

4.30 R' = OMe

4.26 R = OMe 60%
4.27 R = ^{t}Bu 62%

4.28 R = OMe 71%
4.29 R = ^{t}Bu 79%

4.12 R = OMe, R' = H 33%
4.13 R = ^{t}Bu, R' = H 26%
4.31 R = H, R' = OMe 26%
4.32 R = OMe, R' = OMe 25%

Scheme 4.5. Synthesis of pentaarylpyrroles, following the method of Feng *et al*.[23]

With compounds **4.26** and **4.27** in hand the synthesis of pentaarylpyrroles **4.12** and **4.13** could be completed following the method of Feng *et al*. and shown in scheme 4.5. Bromination of **4.26** and **4.27** formed 1-(4-methoxyphenyl)-2,5-diphenyl-3,4-dibromopyrrole, **4.28** (71%) and 1-(4-*tert*butylphenyl)-2,5-diphenyl-3,4-dibromopyrrole, **4.29** (79%), respectively. The Suzuki coupling reaction to form the desired pentaarylpyrroles **4.12** and **4.13** proceeded in low yields (33% and 26%). Compounds **4.27** – **4.29** and **4.13** have not been previously prepared in the literature, and compound **4.12** was only recently reported.[3]

Another aryl boronic acid, 4-methoxyphenyl boronic acid, **4.30**, was also prepared following a literature procedure,[29] and used in the Suzuki coupling reaction with **4.23** and **4.28** to form 1,2,5-triphenyl-3,4-di(4-methoxyphenyl)pyrrole, **4.31** and 1,3,4-tri(4-methoxyphenyl)-2,5-diphenylpyrrole, **4.32**, in moderate yields (26% and 25%). Again these compounds have not been previously prepared in the literature.

A crystal of **4.32** suitable for X-ray crystallography was obtained by the slow diffusion of methanol into a benzene solution of **4.32**. The structure solved in the triclinic space group *P*-1, with one molecule of **4.32** present in the asymmetric unit, as shown in figure 4.6a. As observed in the crystal structure of pentaphenylpyrrole, **4.1**, the peripheral phenyl and 4-methoxyphenyl groups are twisted out of the plane of the central pyrrole core in this case at angles of 40.8(1)˚, 41.9(1)˚, 57.0(1)˚, 60.8(1)˚ and 68.3(1)˚

(compared with the twist angles of **4.1**: 39.1(1)˚, 49.2(1)˚, 53.3(1)˚, 55.8(1)˚ and 56.8(1)˚). The peripheral 4-methoxyphenyl group in the 3-position of the pyrrole ring forms a hydrogen bond from the oxygen of the methoxy group to a hydrogen atom of the phenyl ring on the 4-methoxyphenyl group in the 1-position of the pyrrole ring of a neighbouring molecule (C···O = 3.344(2) Å). The 4-methoxyphenyl group in the 3-position of this neighbouring molecule forms a reciprocal hydrogen bond back, forming a dimer of **4.32** molecules, held together by two complementary hydrogen bonds, as shown in figure 4.6b.

(a) (b)

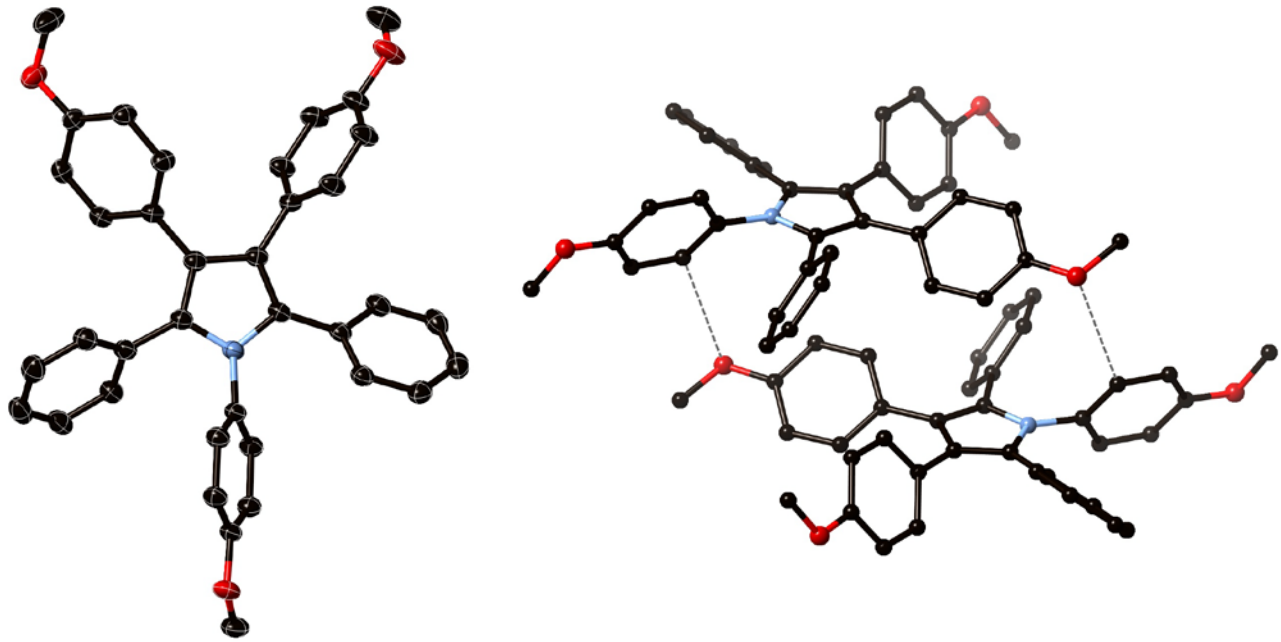

Figure 4.6. (a) Asymmetric unit of **4.32**, (b) complementary hydrogen bonding between two molecules of **4.32**, hydrogen atoms have been removed for clarity.

The oxygen atom of the 4-methoxyphenyl group in the 3-position of the pyrrole ring also forms a hydrogen bond to a CH_3 hydrogen atom, also from the 4-methoxyphenyl group in the 1-position if the pyrrole ring, in a different neighbouring group (C···O = 3.478(2) Å). This hydrogen bond is formed between neighbouring molecules to form a layer of molecules of **4.32**, while the hydrogen bonding discussed above, and shown in figure 4.6b, occurs between these layers of molecules, shown in figure 4.7. There is also extensive edge-to-face $\pi - \pi$ interaction between the peripheral phenyl rings of neighbouring **4.32** compounds.

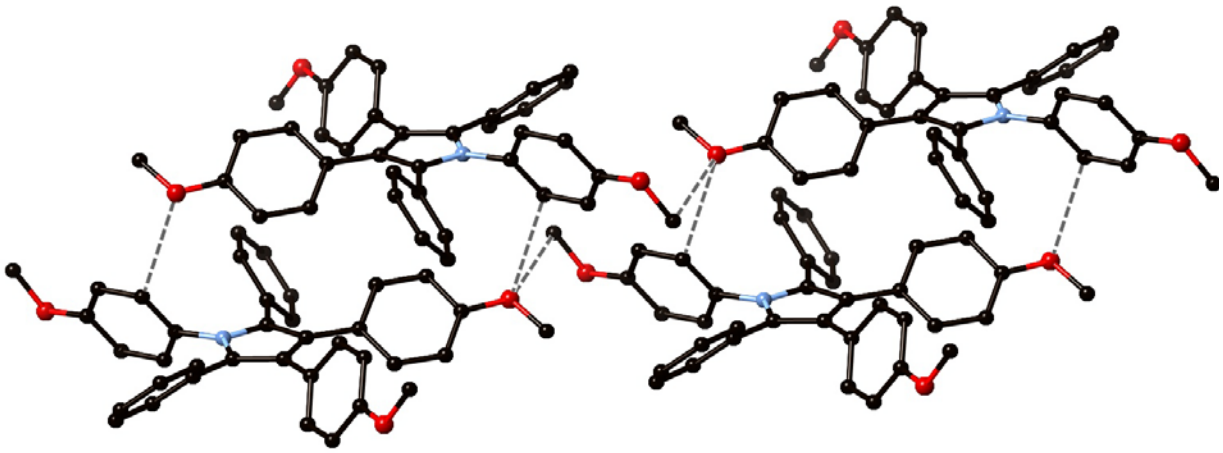

Figure 4.7. Hydrogen bonding within and between layers of **4.30**.

4.5 Cyclodehydrogenation and photocyclisation attempts with pentaarylpyrroles

Despite the limited success of forming carbon-carbon bonds using the Scholl reaction with either $FeCl_3$ or $AlCl_3$/oxidant outlined in Chapter 2 and Chapter 3, both of these approaches were trialled for **4.1**. Firstly, eight equivalents of $FeCl_3$ per carbon-carbon bond to be formed was added as a solid to a dichloromethane solution of **4.1**, with argon bubbling through the reaction mixture. The reaction was monitored with thin layer chromatography and quenched after 24 hours. ^{1}H-NMR spectroscopy of the crude reaction mixture is in agreement with thin layer chromatography, showing that a mixture of products formed. Encouragingly, the ^{1}H-NMR spectrum shows the downfield shifting of some aromatic peaks, consistent with that observed for previous carbon-carbon bond forming reactions described in previous chapters. Frustratingly, attempts at purification with column chromatography could not isolate a single product from the reaction and a mass spectrum obtained of the mixture displayed peaks for material that could not be assigned to the mass to a reasonable cyclodehydrogenation product. Again the isolated product mixture suffered from decomposition over the course of 24 hours.

The $AlCl_3/CuCl_2$ catalyst system was also trialled for the oxidative cyclodehydrogenation of **4.1**. The reaction was quenched after six days, after which point thin layer chromatography did not show any change. Again a mixture of products formed, as judged by thin layer chromatography and a ^{1}H-NMR spectrum of the crude reaction mixture. The integrals of the downfield shifted peaks indicate that the formation of carbon-carbon bonds has proceeded in low yields, consistent with that found for the use of this catalyst system in the previous chapters. Although purification with column chromatography was attempted the different products could not be separated.

Photocyclisation of **4.1** was also attempted, using the conditions outlined in Chapter 2.[30] After irradiation of 5.1 equivalents of I_2, 5 mL of propylene oxide and **4.1** overnight, with argon bubbling though the solution, the reaction mixture was quenched, I_2 was removed by washing with $Na_2S_2O_3$ and then purified. The ^{1}H-NMR spectrum indicates the formation of only one product, and mass spectrometry confirms this. The mass corresponds to that of the formation of only one carbon-carbon bond. There are three separate positions in which the carbon-carbon bond can form, as shown in figure 4.8. Judging by previous products obtained by photocyclisation the carbon-carbon bond is most likely to form in the position shown in figure 4.8b, between the peripheral phenyl rings in the 2- and 3-position of the phenyl ring. In no cases in Chapter 3 did a carbon-carbon bond form between the peripheral phenyl rings in the 3- and 4-position, carbon-carbon bonds formed though photocyclisation, and though oxidative cyclodehydrogenation, only formed between peripheral phenyl rings in the 2- and 3-position. In the case of 1,2,3-triphenylindole presented in Chapter 2, the literature photocyclisation of this compound only forms one carbon-carbon bond, between the peripheral phenyl rings in the 2- and 3-position and no carbon-carbon bond formation is seen between the phenyl rings in the 1- and 2-position.[31]

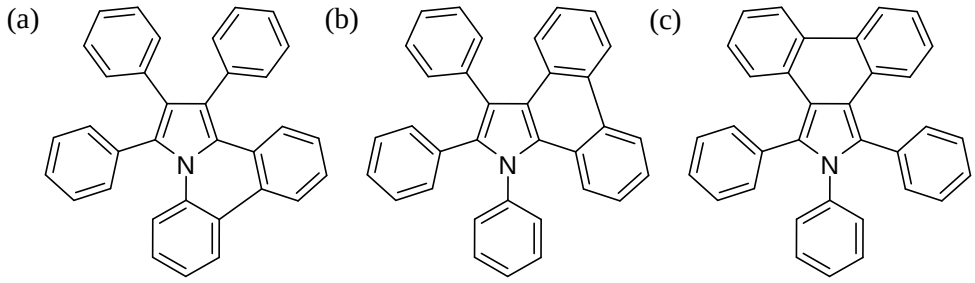

Figure 4.8. The three possible positions for formation of a carbon-carbon bond of **4.1**.

The ^{1}H-NMR spectrum of the product obtained from photocyclisation, is shown in figure 4.9. There are three downfield shifted protons, with two protons, both doublets, significantly downfield shifted (8.72 ppm and 8.68 ppm). The two protons shifted furthest downfield are most likely the protons ortho to the carbon-carbon bond formed, as the most downfield shifted protons in the ^{1}H-NMR spectrum of the cyclodehydrogenated and photocyclised products formed in Chapter 3 were the protons ortho to the carbon-carbon bond formed. Numerous attempts were made at growing a crystal of the product of the reaction to be able to determine the absolute position of formation of the carbon-carbon bond, but no suitable crystals for X-ray diffraction were grown. The complicated nature of the ^{1}H-NMR spectrum does not allow for the absolute position of the carbon-carbon bond formed to be determined, but the product can be tentatively assigned that that shown in figure 4.8b.

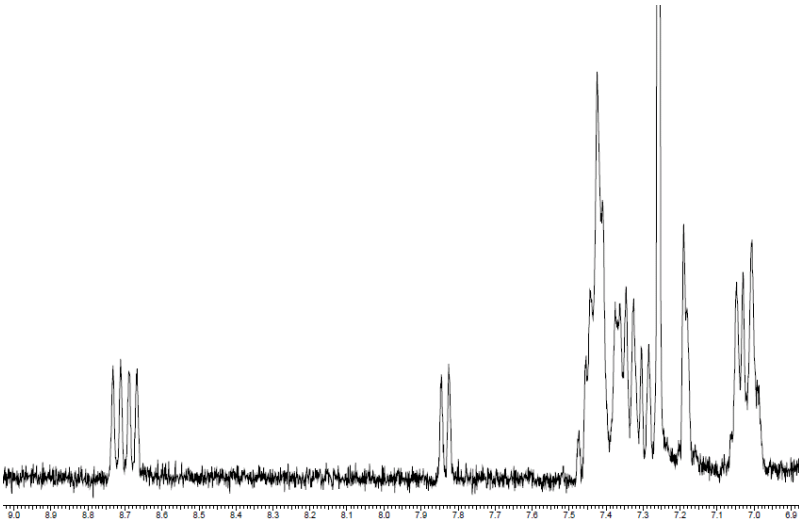

Figure 4.9. ^{1}H-NMR spectrum of the aromatic region of the product isolated from the photocyclisation reaction of **4.1**.

4.6 Optical properties

The absorption spectra of each of the five pentaarylpyrroles prepared were measured and are shown in figure 4.10. As expected the absorption spectra are similar to that of the N-substituted-2,3,4,5-tetraarylpyrroles measured in Chapter 3, as the only difference is the substitution on the nitrogen atom. There are two main absorption bands at ~ 257 nm and ~ 296 nm compared to ~ 253 nm and ~ 288 nm for the N-substituted-2,3,4,5-tetraarylpyrroles present in Chapter 3. As expected, due to the flexible nature of the compounds, the absorption spectra are broad with no fine structure observed. The two pentaarylpyrrole compounds with two and three electron donating 4-methoxyphenyl groups around the periphery of the pyrrole core, **4.31** and **4.32**, respectively, have a larger ε_{max} than the pyrroles with only one 4-methoxyphenyl group, **4.12** or no 4-methoxyphenyl groups, **4.1** and **4.13**. Table 4.1 summarises the main features of the absorption spectra shown in figure 4.10.

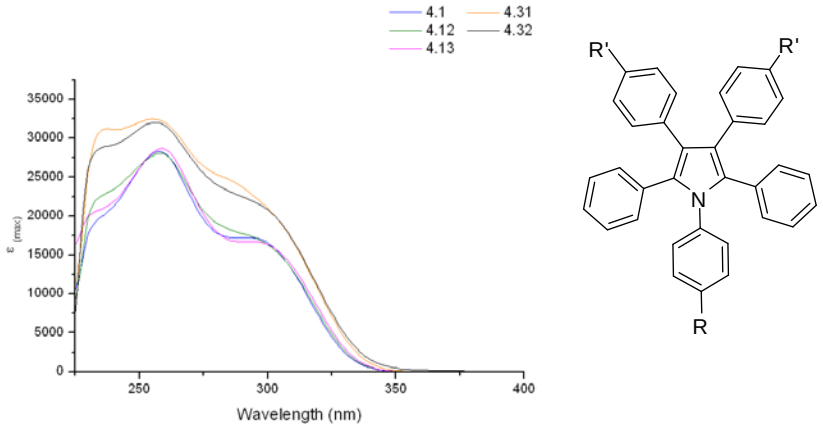

Figure 4.10. Absorption spectra of the five prepared pentaarylpyrrole compounds, **4.1**, **4.12** and **4.13**, **4.31** and **4.32**, R = H, OMe, ^{t}Bu, R' = H, OMe.

	absorption			absorption	
	λ_{max} (nm)	ε (L.mol^{-1}cm^{-1})		λ_{max} (nm)	ε (L.mol^{-1}cm^{-1})
4.1	258, 293	27935, 17168	**4.31**	255, 297	32112, 21821
4.12	258, 296	28545, 17402	**4.32**	256, 296	32053, 21900
4.13	259, 294	28678, 16777			

Table 4.1. Summary of the absorption maxima for compounds **4.1**, **4.12** and **4.13**, **4.31** and **4.32**.

4.7 Attempted synthesis of metal coordinating N-substituted-2,3,4,5-tetraarylpyrroles

The formation of a metal coordinating pentaarylpyrrole derivative was also targeted. In order to follow the same synthetic route of Feng *et al.*[23] the synthesis of a 1-(4'-(4-aminophenyl)2.2':6,2''-terpyridine)-2,5-diphenylpyrrole, **4.33**, was required as the first step towards the synthesis of a pentaphenylpyrrole compound that is able to coordinate to a metal, outlined in scheme 4.6. The synthesis of the key amine 4'-(4-aminophenyl)-2,2':6,2''terpyridine, **4.34**, has been reported in the literature.[32] The amine functionality of compound **4.34** has been exploited to form metal coordinating perylene bisimide ligands,[33] and the amine functionality has also been condensed with maleic anhydride,[32] forming a ligand which was coordinated to ruthenium and attached to a native heme protein.[34]

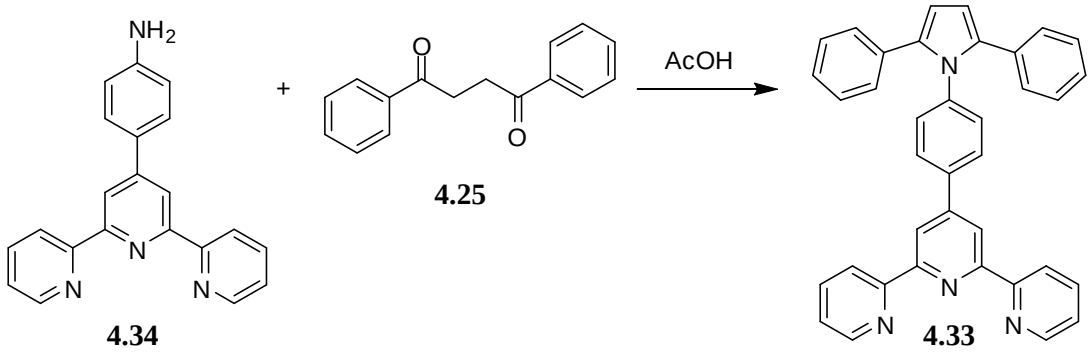

Scheme 4.6. Synthesis of the required tri substituted pyrrole, **4.31**, for the synthesis of pentaarylpyrroles with the ability to coordinate to metals.[23,32]

Following literature procedure,[32] the synthesis of **4.34** was completed using Krönke's salt, 2-acetylpyridine and 4-nitrobenzaldehyde. Encouraged by the successful formation of 1,2,5-triphenylpyrroles, **4.22**, **4.26** and **4.27**, from aniline derivatives and **4.25**, the synthesis of **4.33** from **4.34** and **4.25** was attempted using the same conditions. Unfortunately, mass spectroscopy indicates the formation of 4'-(4-acetylphenyl)-2,2':6,2''terpyridine, and this synthetic scheme was not developed any further.

4.8 Summary

The synthesis of pentaarylpyrrole compounds has been explored through three different synthetic strategies. Three 1,2,3,4-tetraaryl-1,4-butadiones were prepared and their condensation with aniline was investigated. The resulting intramolecular condensation of the 1,2,3,4-tetraaryl-1,4-butadiones formed 2,3,4,5-tetraarylfurans. These compounds were investigated for their ability to undergo oxidative cyclodehydrogenation, with no success.

N-methyl-2,3,4,5-tetraphenylpyrrole and pentaphenylpyrrole were successfully formed by the *in situ* formation of the appropriate münchnones from their N-substituted-N-benzoyl-phenylglycine compounds and subsequent 1,3-dipolar addition of diphenylacetylene. This route formed the desired pentaphenylpyrrole in low yields.

Another route to pentaphenylpyrrole derivatives with the opportunity to vary the aryl groups as desired was undertaken to form three new pentaarylpyrrole compounds and two known pentaarylpyrrole compounds. This key step of this synthetic route utilises the Suzuki coupling of arylboronic acids with 1,2,5-triaryl-3,4-dibromopyrrole compounds. The N-aryl groups and the aryl groups in the 3- and 4-position of the pyrrole core were systematically varied, and the optical properties measured. The use of 4-

methoxyphenyl groups increases the ε_{max} of these compounds compared to the pentaphenylpyrrole derivative prepared.

Attempts were also made towards the synthesis of a pentaarylpyrrole compound capable of coordinating to a metal. The synthesis of 4'-(4-aminophenyl)-2,2':6,2''terpyridine was achieved following literature procedures, but attempts to form the desired 1,2,5-triarylpyrrole from this terpyridine derivative and 1,4-diphenyl-1,4-butadione were not successful.

4.9 References

(1) (a) Ranganathan, S.; Kar, S. K. *Tetrahedron Lett.* **1971**, *12*, 1855, (b) Roth, H. J.; George, H.; Assadi, F.; Rimek, H. J. *Angew. Chem. Int. Ed.* **1968**, *7*, 946, (c) Braye, E. H.; Hübel, W.; Caplier, I. *J. Am. Chem. Soc.* **1961**, *83*, 4406, (d) Wakatsuki, Y.; Kuramitsu, T.; Yamazaki, H. *Tetrahedron Lett.* **1974**, *15*, 4549, (e) Rigaudy, J.; Baranne-Lafont, J. *Tetrahedron Lett.* **1965**, *6*, 1375.

(2) Rao, H. S. P.; Jothilingam, S.; Scheeren, H. W. *Tetrahedron* **2004**, *60*, 1625.

(3) Chen, X.; Li, X.; Wang, N.; Jin, J.; Lu, P.; Wang, Y. *Eur. J. Org. Chem.* **2012**, *2012*, 4380.

(4) Gao, X.; Zhang, S. B.; Zhao, Y.; Nagase, S. *Angew. Chem. Int. Ed.* **2010**, *49*, 6764.

(5) (a) Eicher, T.; Hauptmann, S. *The Chemistry of Heterocyles*; Wiley: Weinheim, 2003, (b) Jones, R. A.; Bean, G. P. *The Chemistry of Pyrroles*; Academic Press: London, 1977.

(6) (a) Wang, B.; Gu, Y.; Luo, C.; Yang, T.; Yang, L.; Suo, J. *Tetrahedron Lett.* **2004**, *45*, 3417, (b) Srinivas, R.; Thirupathi, B.; Kumar, J. K. P.; Prasad, A. N.; Reddy, B. M. *Curr. Org. Chem.* **2012**, *16*, 2482.

(7) Craig, D. *J. Am. Chem. Soc.* **1935**, *57*, 195.

(8) Kuo, W.-J.; Chen, Y.-H.; Jeng, R.-J.; Chan, L.-H.; Lin, W.-P.; Yang, Z.-M. *Tetrahedron* **2007**, *63*, 7086.

(9) Carter, P. H.; Cymerman, C. J.; Lack, R. E.; Moyle, M. *Org. Synth.* **1960**, *40*, 16.

(10) Ballard, D. A.; Dehn, W. M. *J. Am. Chem. Soc.* **1932**, *54*, 3969.

(11) Han, G. Y.; Han, P. F.; Perkins, J.; McBay, H. C. *J. Org. Chem.* **1981**, *46*, 4695.

(12) (a) Cymerman-Craig, J.; Moyle, M.; Rowe-Smith, P.; Wailes, P. C. *Aust. J. Chem.* **1956**, *9*, 391, (b) Mortensen, D. S.; Rodriguez, A. L.; Carlson, K. E.; Sun, J.; Katzenellenbogen, B. S.; Katzenellenbogen, J. A. *Journal of Medicinal Chemistry* **2001**, *44*, 3838.

(13) Gurdere, M. B.; Budak, Y.; Ceylan, M. *Asian J. Chem.* **2008**, *20*, 1425.

(14) Hussain, M.; Khera, R. A.; Hung, N. T.; Langer, P. *Org. Biomol. Chem.* **2011**, *9*, 370.

(15) Laarhoven, W. H.; Cuppen, T. J. H. M.; Nivard, R. J. F. *Recl. Trav. Chim. Pay. B* **1968**, *87*, 687

(16) Benshafrut, R.; Rabinovitz, M.; Hoffman, R. E.; Ben-Mergui, N.; Müllen, K.; Iyer, V. S. *Eur. J. Org. Chem.* **1999**, *1999*, 37.

(17) Baker, W.; Ollis, W. D. *Quart. Rev., Chem. Soc.* **1957**, *11*, 15.

(18) (a) Padwa, A.; Lim, R.; MacDonald, J. G.; Gingrich, H. L.; Kellar, S. M. *J. Org. Chem.* **1985**, *50*, 3816, (b) Anderson, W. K.; Corey, P. F. *J. Org. Chem.* **1977**, *42*, 559.

(19) (a) Avalos, M.; Babiano, R.; Cabanillas, A.; Cintas, P.; Jiménez, J. L.; Palacios, J. C.; Aguilar, M. A.; Corchado, J. C.; Espinosa-García, J. *J. Org. Chem.* **1996**, *61*, 7291, (b) Huisgen, R. *Angew. Chem. Int. Ed.* **1963**, *2*, 565, (c) Huisgen, R. *Angew. Chem. Int. Ed.* **1963**, *2*, 633, (d) Padwa, A.;

Burgess, E. M.; Gingrich, H. L.; Roush, D. M. *J. Org. Chem.* **1982**, *47*, 786, (e) Gotthardt, H.; Huisgen, R.; Bayer, H. O. *J. Am. Chem. Soc.* **1970**, *92*, 4340.

(20) (a) Kikuchi, D.; Sakaguchi, S.; Ishii, Y. *J. Org. Chem.* **1998**, *63*, 6023, (b) Bélanger, G.; April, M.; Dauphin, É.; Roy, S. *J. Org. Chem.* **2007**, *72*, 1104.

(21) Huisgen, R.; Gotthardt, H.; Bayer, H. O.; Schaefer, F. C. *Chem. Ber.* **1970**, *103*, 2611.

(22) Ban, I.; Sudo, T.; Taniguchi, T.; Itami, K. *Org. Lett.* **2008**, *10*, 3607.

(23) Feng, X.; Tong, B.; Shen, J.; Shi, J.; Han, T.; Chen, L.; Zhi, J.; Lu, P.; Ma, Y.; Dong, Y. *J. Phys. Chem. B* **2010**, *114*, 16731.

(24) (a) Fukuda, T.; Sudo, E.-i.; Shimokawa, K.; Iwao, M. *Tetrahedron* **2008**, *64*, 328, (b) Tsurumaki, E.; Inokuma, Y.; Easwaramoorthi, S.; Lim, J. M.; Kim, D.; Osuka, A. *Chem. Eur. J.* **2008**, *15*, 237, (c) Bando, Y.; Sakamoto, S.; Yamada, I.; Haketa, Y.; Maeda, H. *Chem. Commun.* **2012**, *48*, 2301.

(25) (a) Dang, T. T.; Ahmad, R.; Dang, T. T.; Reinke, H.; Langer, P. *Tetrahedron Lett.* **2008**, *49*, 1698, (b) Lakshmi, V.; Ravikanth, M. *J. Org. Chem.* **2011**, *76*, 8466, (c) Ishizuka, T.; Sankar, M.; Yamada, Y.; Fukuzumi, S.; Kojima, T. *Chem. Commun.* **2012**, *48*, 6481.

(26) Bailey, P. S.; Lutz, R. E. *J. Am. Chem. Soc.* **1948**, *70*, 2412.

(27) (a) Lutz, R. E. *Org. Synth.* **1940**, *20*, 29, (b) Conant, J. B.; Lutz, R. E. *J. Am. Chem. Soc.* **1923**, *45*, 1303

(28) Liu, S.-J.; Zhao, Q.; Fan, Q.-L.; Huang, W. *Eur. J. Inorg. Chem.* **2008**, *2008*, 2177

(29) Percec, V.; Bera, T. K.; De, B. B.; Sanai, Y.; Smith, J.; Holerca, M. N.; Barboiu, B.; Grubbs, R. B.; Fréchet, J. M. J. *J. Org. Chem.* **2001**, *66*, 2104.

(30) Liu, L.; Yang, B.; Katz, T. J.; Poindexter, M. K. *J. Org. Chem.* **1991**, *56*, 3769.

(31) Mudry, C. A.; Frasca, A. R. *Tetrahedron* **1974**, *30*, 2983.

(32) Koohmareh, G. A.; Sharifi, M. *J. Appl. Polym. Sci.* **2010**, *116*, 179.

(33) Dobrawa, R.; Lysetska, M.; Ballester, P.; Grüne, M.; Würthner, F. *Macromolecules* **2005**, *38*, 1315.

(34) Peterson, J. R.; Smith, T. A.; Thordarson, P. *Chem. Commun.* **2007**, 1899.

Chapter Five:

Coordination chemistry of backbone linked 2,2’-biimidazole compounds

5.1 Introduction

Supramolecular chemistry has been described by Lehn as the 'designed chemistry of the intermolecular bond'.[1] This description clearly demonstrates the shift in thoughts of chemists from designing molecules through covalent, intramolecular bonds, to designing assemblies of molecules held together by weak, non-covalent intermolecular forces such as hydrogen bonding, $\pi - \pi$ stacking, ionic interactions and van der Waals forces. [2,3] Although individually these intramolecular forces are quite weak, when a large number are employed the additive nature of these forces allows for the formation of very robust structures.[4] The weak intramolecular forces involved in supramolecular chemistry allow for the disruption and formation of interactions to ensure that the final species formed is the most thermodynamically stable. This process of disruption and reformation of weak interactions to arrive at the most stable product is known as self assembly.[5,6]

Hydrogen bonding interactions are commonly encountered in supramolecular assemblies, as well as in a large number of biological systems, such as the assembly of complementary pairs of bases to form the helical structure of DNA. Hydrogen bonds occur between a hydrogen atom bonded to an electronegative atom (donor) and a neighbouring electronegative atom (acceptor),[2] for example nitrogen and oxygen atoms can act as both donor and acceptor atoms in hydrogen bonding, whilst halides such as chlorine and bromine are hydrogen bond acceptors. Strong hydrogen bonds can direct the formation of supramolecular assemblies,[7] and can be almost as strong as covalent bonds, whilst weak hydrogen bonds serve to stabilise the supramolecular structure formed.[5] The donor atom does not need to be particularly electronegative, C – H bonds often participate in weak hydrogen bonding interactions,[8] and the acceptor atom(s) do not need to possess a lone pair of electrons, alkenes and π systems can also act as acceptor groups.[9] A range of hydrogen bonding parameters used to determine the strength of the hydrogen bond is shown in table 5.1.[5] Hydrogen bonds are directional in nature, the more distorted the bond is from linearity the weaker the hydrogen bond tends to be in a simple D–H$^{\cdots}$A system. The directional nature of hydrogen bonds allows them to be an essential tool for installing complementarity into molecules for supramolecular assembly, and in turn directing the formation of desired supramolecular assemblies.[8b] Acceptor atoms with the ability to interact with two or more hydrogen atoms can be used to construct extended hydrogen bonding networks within the supramolecular assembly.

A–H···B	Strong	Medium	Weak
Bond energy (kJ. mol^{-1})	120 − 60	60 − 16	<12
H···B bond length (Å)	1.2 – 1.5	1.5 – 2.2	2.2 – 3.2
A···B bond length (Å)	2.2 – 2.5	2.5 – 3.2	3.2 – 4.0
Bond angles (˚)	175 − 180	130 − 180	90 − 150
Examples	Proton sponge	Acids, alcohols	C – H hydrogen bonds

Table 5.1. Common hydrogen bonding parameters.[5]

Other weak interactions between molecules stabilise the formation of supramolecular assemblies,[10] although none of these interactions are as directional as the hydrogen bond. Interactions between aromatic moieties in organic chemistry and in biological systems have long been observed and these interactions are also found in supramolecular aggregations,[11] although they are rarely the only type of interaction present.[12] Edge-to-face and face-to-face π – π stacking interactions are the most common type of interaction found in supramolecular assemblies,[13,14] and are shown in figure 5.1. Hunter and Sanders proposed in 1990[14] a model for favourable interactions between aromatic units by considering the contributions from the π electrons and the σ framework separately. This model gives rise to a set of rules for favourable π – π interactions for both neutral and polarised aromatic systems, whereby offset face-to-face and edge-to-face interactions are greatly favoured over direct face-to-face interactions. Recently Martinez and Iverson proposed that there is no special interaction between two aromatic units.[15] That is, the packing seen in aromatic systems can be attributed to other forces present in the association of all molecules.[15,16] Typically the interplanar separation between face-to-face π stacked molecules ranges from 3.3 Å to 3.8 Å,[11] and the aromatic rings tend to be offset rather than parallel. Often a combination of edge-to-face and face-to-face π – π interactions are present in supramolecular assemblies.[11] Other types of aromatic interactions such as anion – π[17] interactions can also stabilise supramolecular assemblies.

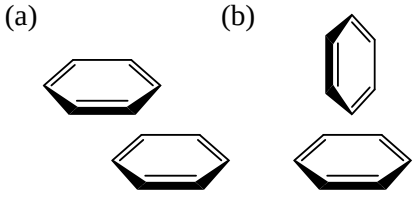

Figure 5.1. (a) Face-to-face and (b) edge-to-face π – π interactions.

As well as using weak interactions to hold molecules together metallosupramolecular chemistry[18] utilises the interactions between metal ions and organic ligands to form supramolecular species. The interactions

between the metal and ligand are usually much stronger than the weak interactions present in supramolecular assemblies, although the strength of the interaction between the metal and ligand is dependent upon the nature of both.[19] The metal ligand bond needs to be weak enough to allow for reversibility during the self assembly process, but robust enough to form a stable supramolecular assembly. Metallosupramolecular chemistry has been used in the construction of various architectures including helicates,[20] cantenanes,[21] rotaxanes,[22] knots[23] and cages.[24] Using metal atoms in constructing metallosupramolecular assemblies allows for the incorporation of properties from the metal atoms into the overall structure of the assembly, to form functional supramolecular architectures.[25]

Information is encoded into both the metal and ligand to direct the assembly of the components through molecular recognition. The encoding of both metal and ligand allows for the formation of simple to complex architectures in one pot through self assembly of the individual metal and ligand components.[26] To obtain the desired product both metal and ligand must contain the correct encoding information. One of the key components able to be encoded in the metal atom is its preferred geometry. Shown in figure 5.2a are some common metal geometries encountered in metallosupramolecular assemblies, it is important for the metal atoms to have a reasonably predictable coordination geometry in order to form the desired assembly. The metal ion can also be used as a template for the formation of supramolecular assemblies.[27] Distortion around the metal centre is not uncommon in metallosupramolecular assemblies. To quantify the degree of distortion away from the idealized geometry τ_4[28] and τ_5[29] values can be easily calculated for four and five coordinate geometries respectively, shown in figure 5.2b are the equations to calculate τ_4 and τ_5 values. For a metal centre with four coordinate geometry $\tau_4 = 1.00$ corresponds to a metal centre with perfect tetrahedral geometry and $\tau_4 = 0$ corresponds to perfect square planar geometry, intermediate values correspond to a distortion away from these two idealised geometries. Similarly, $\tau_5 = 0$ corresponds to a metal centre with square pyramidal geometry, whilst $\tau_5 = 1.00$ corresponds to a trigonal bipyramidal geometry.

Ligands used in metallosupramolecular chemistry must be able to bond to metal atoms in a reasonably reliable fashion.[30] Ligands can be designed to bridge two or more metal atoms to form supramolecular assemblies containing multiple metal atoms.[31] The ligand also needs to contain the appropriate donor atom so that the metal − ligand bonds are labile enough to allow for corrections during the self assembly process, but robust enough to form a stable assembly. Commonly nitrogen containing heterocycles are used as ligands in metallosupramolecular assemblies.[32]

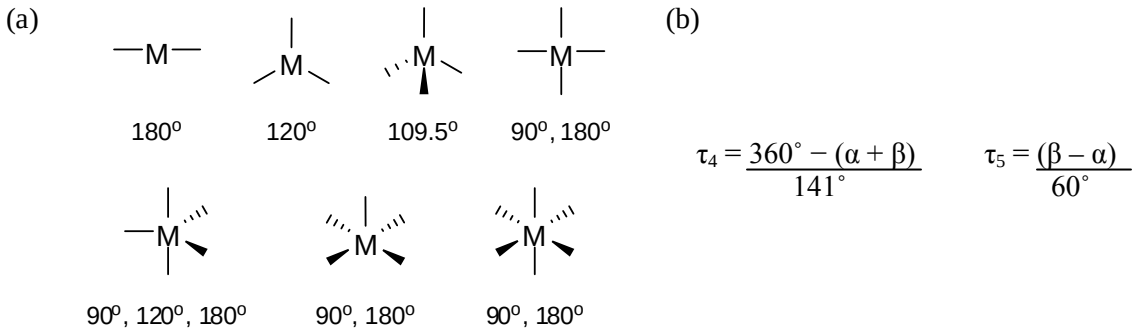

Figure 5.2. (a) Some common metal atom geometries encountered in metallosupramolecular chemistry and their associated angles, (b) equations for the calculation of τ_4[28] and τ_5[29] values.

By far the most commonly used biheterocycle in coordination chemistry is the chelating, bidentate, ligand 2,2'-bipyridine (figure 5.3a).[33] A five membered analogue of 2,2'-bipyridine, 2,2'-biimidazole (figure 5.3b), has also been used to form various supramolecular assemblies with a variety of metal atoms.[34] As well as chelating metal centres,[34c] as is the case for 2,2'-bipyridine, 2,2'-biimidazole can also coordinate to two metal centres, in either a convergent,[34d,35] shown in figure 5.3c, or a divergent[34e,35] fashion, shown in figure 5.3d. The additional N*H* group present in the 2,2'-biimidazole scaffold also allows for hydrogen bonding interactions to occur to direct the formation of supramolecular assemblies.[36]

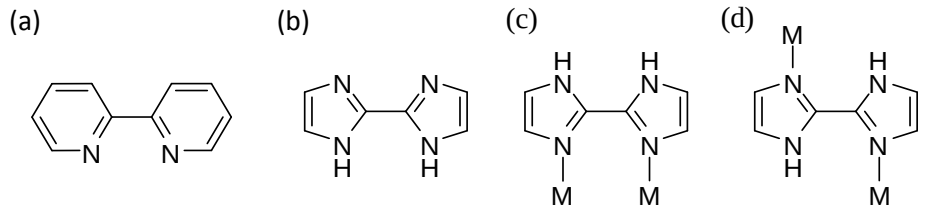

Figure 5.3. (a) 2,2'-bipyridine, (b) 2,2'-biimidazole, (c) convergent coordination and (d) divergent coordination of 2,2'-biimidazole.

The supramolecular assembly formed from 2,2'-biimidazole can depend on the anion used.[35] In combination with Ag_2O and H_2SO_4, or $AgNO_3$ and oxalic acid, a one dimensional chain is formed where two 2,2'-biimidazole ligands convergently bridge two silver atoms to form dinuclear Ag_2(2,2'-biimidazole)$_2$ units. These units are linked through the respective anions and the one dimensional chains are linked by hydrogen bonding interactions between the respective anions and the uncoordinated nitrogen atoms of the 2,2'-biimidazole ligand. When 2,2'-biimidazole is combined with $AgNO_3$,[34d]

$Ag(CH_3COO)$ and ClO_4^-, or $AgNO_3$ and nicotinic acid, a one dimensional polymeric helicate is formed rather than dinuclear unit, and the 2,2'-biimidazole divergently bridges two silver atoms to grow the polymer.

Hydrogen bonding interactions through the imidazole ligand can be blocked by substitution of one nitrogen atom on each ring, ie 1,1'-dimethyl-2,2'-biimidazole, and in combination with $AgNO_3$ a one dimensional polymeric helicate is formed,[37] similar to the polymeric helicates described above. In combination with $CuSO_4$ four molecules of 1,1'-dimethyl-2,2'-biimidazole bridge two copper atoms, with a molecule of water bound in the axial position of each copper centre, to give a water capped quadruple helicate.[38] Zinc and cadmium complexes of 1,1'-dimethyl-2,2'-biimidazole have diverse coordination modes dependent on the anion used.[39]

The formation of metallosupramolecular assemblies can also be controlled by the anions present, as seen in the coordination of 2,2'-biimidazole to various silver salts above. Oxyanions, such as carboxylate,[40] nitrate,[41] sulfate[42] and phosphate,[43] and halides[44] can form moderate to strong hydrogen bonds with hydrogen donor groups in the supramolecular assembly, and they can also occupy coordination sites around the metal centre to impose a set mode of coordination onto the ligand. It can be difficult to predict how many anions will coordinate to the metal centre and in which positions, often resulting in an unpredictable supramolecular assembly.[19] Anions can also template the formation of supramolecular assemblies,[45,46] Cui *et. al.* showed that the pitch of a helix can be altered by the anion present.[47] Changing the anion present from nitrate to hexafluorophosphate and then to perchlorate changed the pitch of the one dimensional helix from 2_1 to 3_1 and then 4_1, shown in figure 5.4. Supramolecular assemblies controlled by anion $-\pi$ interactions,[48] weak hydrogen bonds between anions and hydrogen bond donors and poorly coordinating anions are less common.[45]

With the correct combination of metal and ligand discrete supramolecular cages can be assembled. Metallosupramolecular cages can encapsulate guest molecules,[49] and the cage can act as a molecular reaction flask, to catalyse reactions and control the reactivity of molecules.[25d] Encapsulation of a guest molecule can also potentially change the property of the guest, recently Nitschke *et. al.* encapsulated white phosphorous in a M_4L_6 tetrahedron, rendering P_4 air stable.[50]

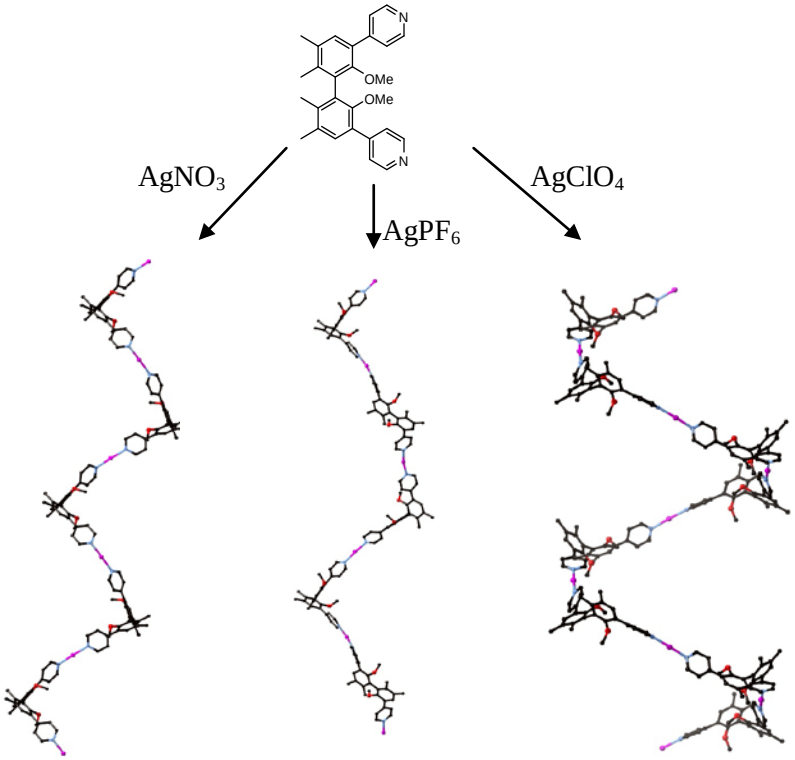

Figure 5.4. Anion directed self-assembly of helices with varying pitch depending on the anion used, 2_1 for nitrate, 3_1 for hexafluorophosphate and 4_1 for perchlorate.[47]

Host-guest supramolecular assemblies can also be formed by the enclathration of guest molecules between supramolecular assemblies rather than inside one discrete unit. One of the first examples of a clathrate compound was by Pedersen, investigating the enclathration of alkali metal ions by an extensive series of crown ethers.[51] Often the guest and host have the same symmetry,[52] but this is not always the case.[53] Enclathration of guest molecules can be selective, leading to applications in separation of organic compounds and sensing.[54] The guest is often held in position by hydrogen bonding or edge-to-face and face-to-face $\pi - \pi$ interactions.[52,54] It can be difficult to design or predict the formation of enclathration complexes as they are dependent on the packing and interactions present in the supramolecular assembly. Benzene is a common guest molecule in both encapsulation and enclathration species due to its ability to form $\pi - \pi$ interactions with the aromatic components of the ligand. Enclathration complexes are not limited to metallosupramolecular assemblies, suitable organic molecules can also enclathrate other organic guest molecules, usually in the solid state.[52,55]

The design of ligands in supramolecular chemistry allows control over the distances between two metal atoms, with aromatic or alkyne spacer groups commonly employed to increase the distance between two metal atoms.[56] Ligands can also be synthesised that bridge two metal atoms in close proximity by using

functional groups with two donor atoms positioned close together. The carboxylate functional group is able to bridge two metal atoms in a variety of different ways, as shown in figure 5.5a,[57] it is also possible for carboxylate ligands to coordinate to only one metal atom. Paddle wheel complexes where four carboxylate groups bridge two metal atoms, shown in figure 5.5b, have been well studied with a variety of different metal atoms[58,59,60] and copper(II) paddle wheel complexes have received particular attention due to the antiferromagnetic magnetic exchange that occurs between the copper metal centres.[57,61] Other functional groups besides carboxylates are able to bridge two metal centres in close proximity, for example 2-pyridone can act as a close analogue of carboxylate bridging, due to the three atom bridge present (O-C-O for carboxylate, N-C-O for 2-pyridone).[62] Bridging carboxylate ligands,[58] or other bridging co-ligands,[61] can be used to form supramolecular assemblies involving paddle wheel complexes, and this approach has been pioneered by Cotton.[60,63] Bridging two metals in close proximity allows for interesting metal-metal interactions to occur. Magnetic exchange and electronic coupling are often observed in complexes where the two metal atoms are in close proximity.[60,64]

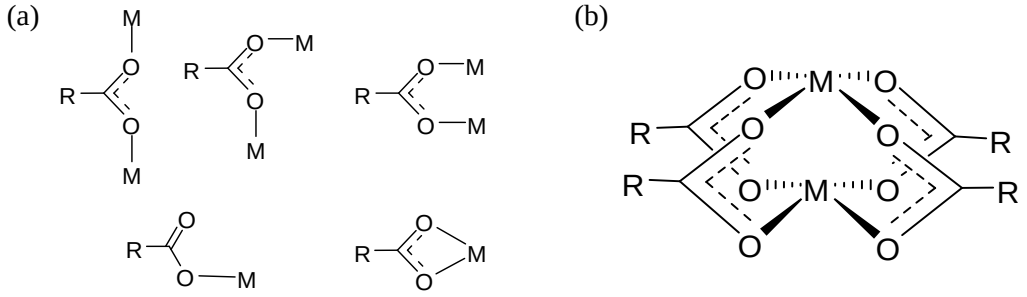

Figure 5.5. (a) Various coordination motifs for coordination of metal atoms to carboxylate functional groups,[57] (b) paddle wheel complex formed from four carboxylate ligands.

Single crystal X-ray diffraction is the most common method used to study metallosupramolecular assemblies in the solid state. Other techniques can also be employed, such as NMR and UV/vis spectroscopy, but the 3-dimensional determination of the overall supramolecular structure is unequivocally obtained using X-ray crystallography. X-ray crystallography requires the growth of single crystals suitable for diffraction, as well as crystals that are stable for the course of the data collection, this is easier said than done in many cases! There are many different techniques available for the growth of suitable crystals, such as vapour diffusion, layering and slow evaporation.[65] A vibration free environment is also preferred for crystal growth, although some crystals grown during the course of this study were obtained after significant earthquakes and lengthy periods of time spent out of the department. Caution needs to be applied when considering long intermolecular interactions in supramolecular assemblies as some apparent interactions are a result of crystal packing effects.[7]

5.2 Synthesis of Ligands

To investigate the influence of a N,N'-tethered backbone on 2,2'-biimidazole four different ligands were prepared. Three of these ligands N,N'-dimethylene-2,2'-biimidazole, **5.1**, N,N'-trimethylene-2,2'-biimidazole, **5.2**, and N,N'-(α,α'-o-xylylene)-2,2'-biimidazole, **5.3**, were synthesised following the method of Thummel *et al*.[66] Firstly, 2,2'-biimidazole was prepared from the condensation of glyoxal with ammonium acetate, and then the appropriate dihalogenated backbone was substituted onto the 2,2'-biimidazole under basic conditions, as shown in scheme 5.1.

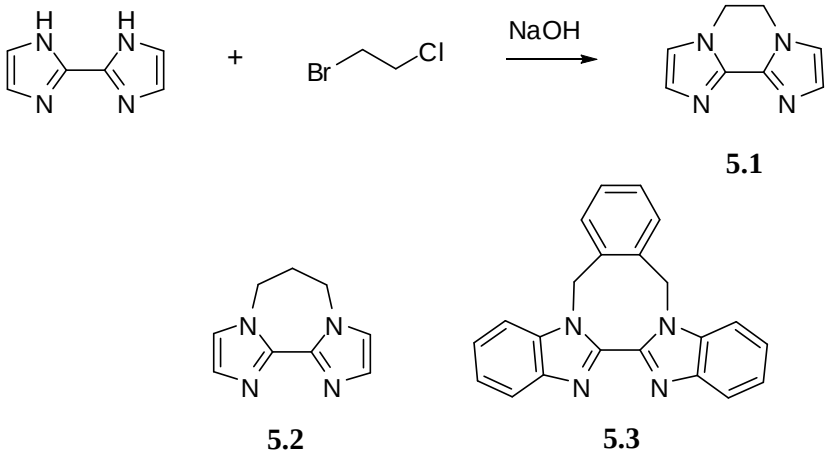

5.1 **5.2** **5.3**

Scheme 5.1. Synthesis of **5.1**, showing the general method for the synthesis of **5.2** and **5.3**.

Very little has reported on the coordination chemistry of **5.1**, **5.2** and **5.3** since their preparation first appeared in the literature in 1989. In fact, the only coordination compounds prepared from these three ligands appear in a paper by the same authors in 1990.[67] The preparation of Ru(**5.1**)$(bpy)_2(OH_2)^{2+}$, Ru(**5.2**)$_3^{2+}$, Ru(**5.2**)$(bpy)_2^{2+}$ and Ru(**5.3**)$(bpy)_2^{2+}$ are described in this paper. Interestingly, the ruthenium tris complexes of **5.1** and **5.3** could not be prepared, and the coordination of **5.1** in the Ru(**5.1**)$(bpy)_2(OH_2)^{2+}$ complex is described as monodentate, with the other coordination site filled by a water molecule, this is a result of the decrease in bite angle of **5.1** compared to 2,2'-bipyridine.

Coordination complexes of a similar biheterocycle to **5.1**, N,N'-dimethylene-2,2'-biimidazoline, **5.4**, (figure 5.6a) have been reported where **5.4** shows three different modes of coordination to various metal atoms.[68] In combination with $Mn(ClO_4)_2$,[68a] a tris chelating complex is formed with **5.4**, whilst in combination with $Cu(ClO_4)_2$[68a] and $Zn(NO_3)_2$[68b] a four coordinate complex is formed where one molecule of **5.4** chelates the metal atom whilst the two other molecules of **5.4** coordinate to the metal centre in a monodentate fashion. Molecules of **5.4** can also bridge two metal atoms in close proximity, when combined with $Cu(ClO_4)_2$[68a] or $Pd(PhCN)_2Br_2$[68b] four molecules of **5.4** bridge two metal centres, and

when $Cu(CH_3CN)_4BF_4$ was combined with **5.4** three molecules of **5.4** bridge the two copper centres.[68a] A monodentate complex with $HgCl_2$ has also been prepared.[68b] Silver complexes have also been prepared with **5.4**, bridging and monodentate coordination modes of **5.4** are observed.[68b]

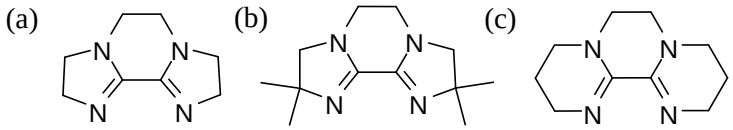

5.4 **5.5** **5.6**

Figure 5.6. (a) N,N'-dimethylene-2,2'-biimidazoline **5.4**, (b) **5.5**, and (c) **5.6**

A derivative of **5.4** with dimethyl substitution α to the imino nitrogen atoms, **5.5**, (figure 5.6b) has been prepared and a coordination complex with $Cd(ClO_4)_2$ reported.[69] Three molecules of **5.5** chelate the cadmium metal centre to form a tris coordination complex. A derivative of **5.4** where the five membered heterocycles have been increased in size to six membered heterocycles, **5.6**, (figure 5.6c) has been prepared. Coordination complexes with various Pd, Zn, Hg, Cu and Ag salts have been prepared and in all cases molecules of **5.6** chelate the metal centre owing to the increase in bite angle.[68b]

N,N'-o-benzyl-2,2'-biimidazole, **5.7**, was synthesised by a modified literature procedure,[70] shown below in scheme 5.2. Firstly 1,2-dibromobenzene was employed in a Cu_2O catalysed coupling with imidazole to form 1,2-diimidazoylbenzene, **5.8**, which was then employed in a $CuBr.SMe_2$ mediated intramolecular coupling, employing O_2 as the terminal oxidant, to generate **5.7** in 24% yield from **5.8**. Despite the recent synthesis of **5.7**, no coordination chemistry has been reported in the literature.

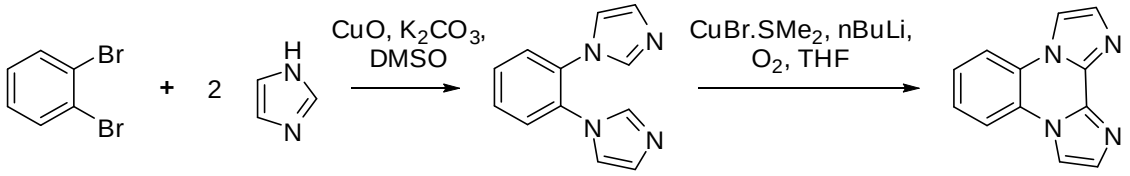

5.8 **5.7**

Scheme 5.2. Synthesis of **5.7**.

A crystal suitable for X-ray crystallography was grown from the slow evaporation of a dichloromethane solution of **5.7**. Compound **5.7** crystallised in the monoclinic space group $P2_1/n$, with one molecule of **5.7** in the asymmetric unit, shown in figure 5.7a. The C2···C13 bond distance is 1.433(2) Å, slightly longer than the bonds in the aromatic imidazole rings of this structure (average bond distance = 1.369(2) Å), and longer than the average C···C bond in benzene (ca. 1.39 Å). As expected the molecules display face-to-

face π – π stacking (centroid – centroid distance = 3.317(1) Å and 3.281(1) Å), and the stacks of **5.7** form weak hydrogen bonds with molecules in an adjacent stack though the external imidazole nitrogen atoms and imidazole hydrogen atoms (N···C range from 3.280(2) Å to 3.423(2) Å), as shown in figure 5.7b.

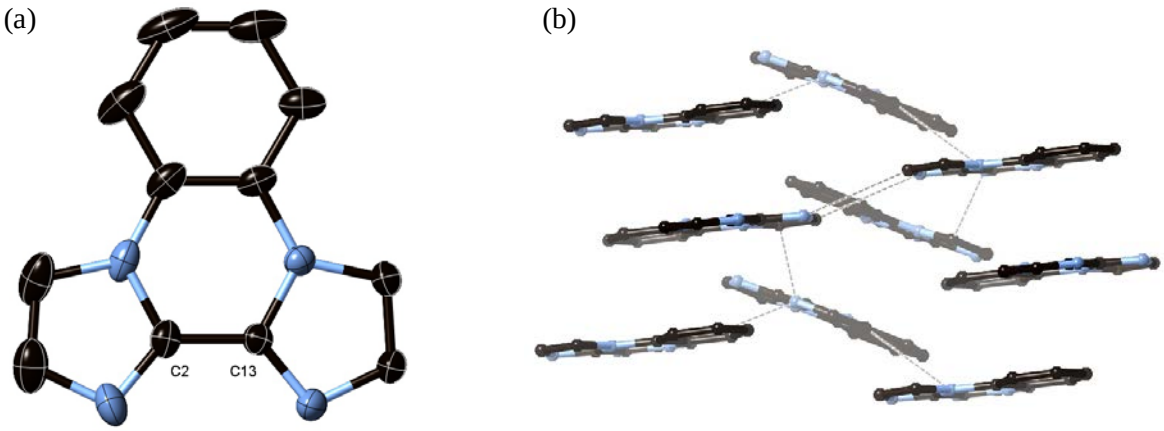

Figure 5.7. (a) Asymmetric unit of **5.7**, (b) π – π stacking and hydrogen bonding interactions between adjacent stacks of **5.7**, hydrogen atoms have been removed for clarity, donor acceptor hydrogen bond interactions indicated by dashed lines.

A crystal of **5.8** suitable for X-ray crystallography was also grown from the slow evaporation of a dichloromethane solution of **5.8**. The molecule crystallises in the monoclinic space group *C*2/*c*, with one molecule of **5.8** present in the asymmetric unit, shown in figure 5.8. As expected the imidazole rings are twisted out of plane to the benzene ring (41.4(1)˚ and 75.2(1)˚). Molecules of **5.8** display edge-to-face π – π interactions between the benzene rings of neighbouring molecules (edge carbon to centroid distance = 3.491(2) Å), and the imidazole rings of neighbouring molecules also show edge-to-face π – π interactions (edge carbon···centroid distance = 3.669(2) Å), and weak face-to-face π – π interactions (centroid to centroid distance = 3.735(2) Å).

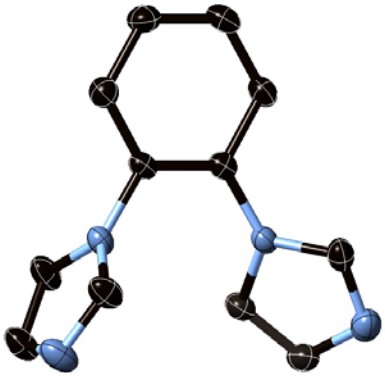

Figure 5.8. Asymmetric unit of **5.8**, hydrogen atoms have been removed for clarity.

5.3 Silver complexes with **5.1**

Supramolecular assemblies of d^{10} silver(I) salts with a range of nitrogen based heterocycles have been reported extensively in the literature.[71] Silver atoms can accommodate a wide range of coordination geometries and varying coordination numbers,[71d,72] giving rise to a diverse range of structures in combination with heterocyclic ligands. [71a,71d,e,71i] Due to the fluid nature of the interaction between the silver atom and the ligand, weaker interactions are allowed to dominate the formation of the overall structure.[73] Supramolecular assemblies of silver complexes have been reported where the structure is determined by weak hydrogen bonding,[73b,c] anion interactions[47,74] and π – π stacking interactions.[75]

By bridging the biimidazole scaffold with an ethyl backbone though two of the nitrogen atoms forming ligand **5.1**, the potentially strong hydrogen bonding interactions of these nitrogen atoms are blocked. The two nitrogen atoms that are available for bonding are discouraged from potential chelation of metal atoms by a narrow chelating angle imposed by the five membered rings of the biimidazole scaffold (~ 40˚, ca 60˚ for 2,2'-bipyridine).[66] This narrow chelating angle and the availability for bonding of only two nitrogen atoms of the biimidazole scaffold should encourage **5.1** to convergently bridge two metal atoms in close proximity.

*5.3.1 Synthesis of $[Ag_2$**5.1**$_2][NO_3]_2$, complex **5.9***

Complex **5.9** was formed from the reaction of **5.1** and silver nitrate in acetonitrile.[76] Crystals suitable for X-ray crystallography were formed from the reaction mixture after 48h in a 33% yield. Complex **5.9** crystallises in the monoclinic space group $P2_1/c$, and two silver atoms are indeed convergently bridged by two molecules of **5.1**, shown in figure 5.9. There are two crystallographically independent, discrete Ag_2L_2 units present in the asymmetric unit.

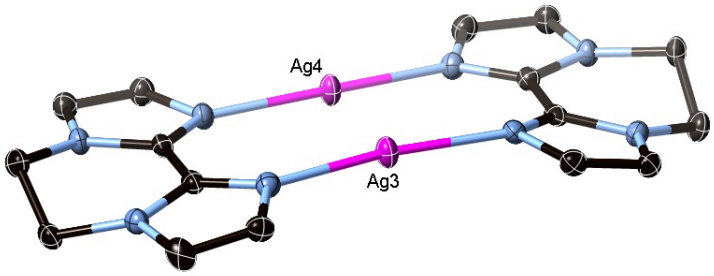

Figure 5.9. One of the discrete Ag_2L_2 units of complex **5.9**, nitrate anions and hydrogen atoms have been omitted for clarity.

The silver atoms in the Ag_2L_2 unit have a slightly bent linear geometry (N-Ag-N angles range from 164.9(1) to 172.3(1)˚), with Ag···N bond distances ranging from 2.109(3) to 2.166(3) Å. The silver atoms

in each unit are in close proximity to each other (Ag1···Ag2 = 2.892(1) Å and Ag3···Ag4 = 2.904(1) Å), only slightly longer than the silver – silver distance in metallic silver (2.884 Å)[77] and the two silver atoms in each unit can be considered to have weak silver – silver interactions.[78] Distances between silver atoms in neighbouring units are considerably longer (3.874(4) Å − 4.178(4) Å). Due to the constraint imposed on the ligand by the ethyl backbone the imidazole rings are distorted out of plane relative to each other (9.8(2)˚ − 12.4(2)˚), the N-C-C-N torsion angles of the backbone range from 45.5(3)˚ to 47.2(3)˚ again demonstrating the significant distortion of **5.1**.

Nitrate counter ions hold the Ag_2L_2 units in position through weak Ag···O bonds (2.742(3) Å – 3.291(4) Å). Each silver atom in the Ag_2L_2 unit is weakly bound to two nitrate anions and each nitrate anion is interacting with two silver atoms in two different units, thus forming a staircase arrangement, shown in figure 5.10. The imidazole rings of **5.1** display weak face-to-face π – π stacking with adjacent Ag_2L_2 units above and below with centroid to centroid distances ranging from 3.418(2) Å to 3.645(2) Å.

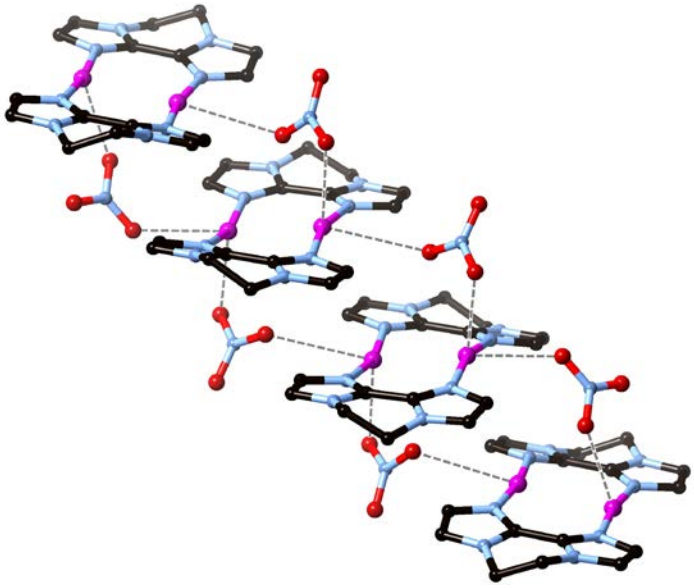

Figure 5.10 Staircase arrangement of Ag_2L_2 units in complex **5.9**, silver – nitrate interactions are indicated as dashed lines, hydrogen atoms have been omitted for clarity.

*5.3.2 Synthesis of $[Ag_3$**5.1**$_4][ClO_4]_3 \cdot CH_3CN$, complex **5.10***

Moving to a less coordinating counter ion, for example perchlorate, but maintaining the same ratio of silver salt to **5.1** gave a complex, **5.10**,[76] that crystallises in the monoclinic space group *Pc*. The colourless crystals were obtained in a 45% yield by vapour diffusion of diisopropyl ether into an acetonitrile solution of the reaction mixture. Using a less coordinating counter ion allows for different coordination of the silver atoms to **5.1**, and indeed a discrete Ag_3L_4 complex was formed, as shown in figure 5.11a. Each

ligand in complex **5.10** convergently bridges two silver atoms in a similar fashion to complex **5.9** (Ag···N bond distances range from 2.112(3) Å to 2.390(2) Å), but the central silver atom of the Ag_3L_4 unit coordinates to all four molecules of **5.1**. This produces a distorted tetrahedral geometry (N-Ag-N angles range from 91.8(1)˚ to 132.9(1)˚, τ_4 = 0.81) around the central silver atom, whilst the two remaining silver atoms have slightly bent linear geometries (N-Ag-N angles are 174.8(2)˚ and 174.7(2)˚). There is one Ag_3L_4 unit present in the asymmetric unit, along with three perchlorate anions (one of which is disordered over two positions), and one molecule of acetonitrile.

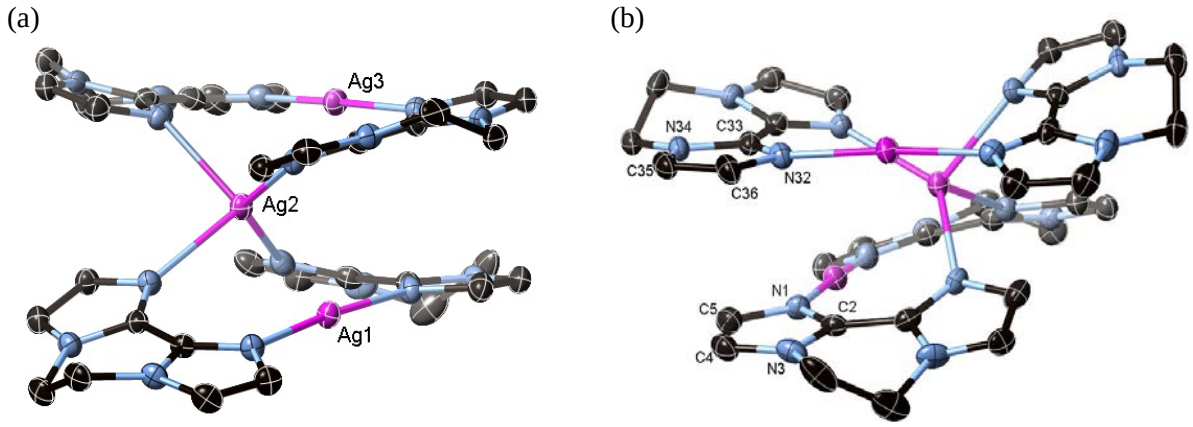

Figure 5.11.(a) The Ag_3L_4 unit formed in complex **5.10**, perchlorate counter ions, (b) π – π stacking interactions between ligands in the Ag_3L_4 unit of complex **5.10**, acetonitrile solvent molecules and hydrogen atoms have been removed for clarity.

The three silver atoms in complex **5.10** are again in close proximity to each other (Ag1···Ag2 = 3.048(1) Å and Ag2···Ag3 = 3.086(1) Å), with an Ag1···Ag2···Ag3 angle of 111.0(1)˚. The imidazole rings of **5.1** show significantly more twisting out of plane (16.6(2)˚ – 18.0(2)˚) and slightly larger torsion angles of the backbone (N-C-C-N range from 47.9(4)˚ to 51.1(4)˚) than in complex **5.9**. This twisting is required by the change in coordination around the silver atoms, allowing the central silver atom to coordinate all four molecules of **5.1**. Weak face-to-face π – π stacking interactions are present between the imidazole rings (N1 – C5 and N32 − C36) in the Ag_3L_4 unit, shown in figure 5.11b.

One disordered perchlorate molecule is weakly coordinated to Ag3 (Ag···O = 3.170(12) Å), with the oxygen atom having only 62% occupancy, whilst the acetonitrile solvent molecule is only weakly coordinated to Ag1 (Ag···N = 3.006(5) Å). The central silver atom, Ag2, is prevented from interactions with perchlorate anions or acetonitrile solvent molecules by its coordination to four molecules of **5.1**. Each Ag_3L_4 unit displays weak π – π stacking to adjacent Ag_3L_4 units (centroid to centroid distances

range from 3.391(3) Å to 3.573(2) Å) and the remaining perchlorate anions occupy weak hydrogen bonding pockets formed by **5.1**, shown in figure 5.12.

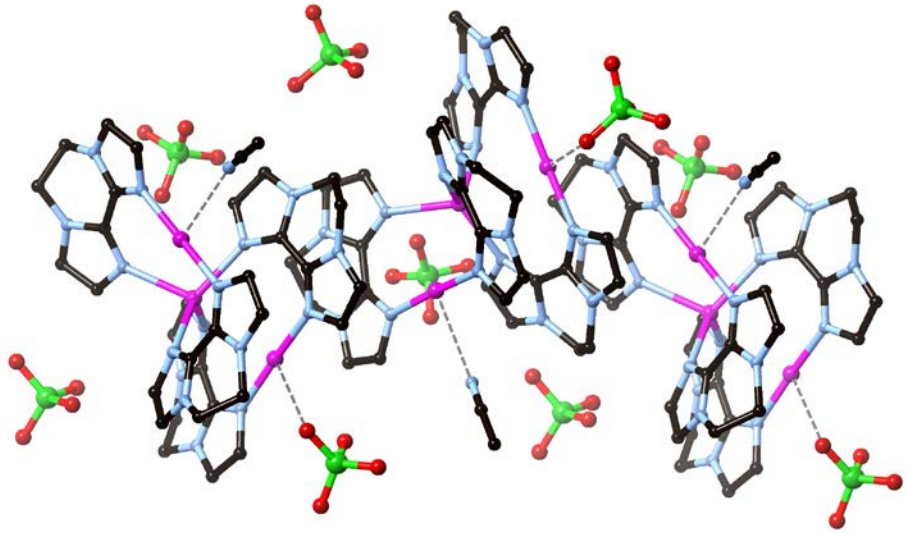

Figure 5.12. View of the π – π stacking between Ag_3L_4 subunits in complex **5.10**, the weakly coordinating perchlorate anions and acetonitrile molecules and the positioning of the remaining perchlorate anions are also shown, silver-acetonitrile and silver-perchlorate interactions are indicated as dashed lines, perchlorate anion disorder is not shown and hydrogen atoms have been removed for clarity.

*5.3.3 Synthesis of poly-[Ag_2**5.1**$_3$][PF_6]$_2$, complex **5.11***

An even weaker coordinating counter ion, in this case silver hexafluorophosphate, was also reacted with **5.1**, forming complex **5.11**.[76] In this case the presence of such a weakly coordinating counter ion allows formation of a polymer rather than discrete units, as observed for complexes **5.9** and **5.10** with nitrate and perchlorate counter ions respectively. Colourless crystals suitable for X-ray crystallography were obtained in 21% yield from the methanol solution of the reaction mixture after 48 hours. The complex crystallises in the orthorhombic space group *Pbcn*, with one and a half molecules of **5.1**, one silver atom and one hexafluorophosphate counter ion present in the asymmetric unit. Two ligands again convergently bridge two silver atoms to form the common Ag_2L_2 subunit seen in the previous complexes. These Ag_2L_2 subunits are linked together by a divergently bridging **5.1** forming a one dimensional polymer, a portion of which is shown below in figure 5.13.

Again the silver atoms are in close proximity to each other with the silver atoms of the Ag_2L_2 subunits significantly closer together (Ag···Ag = 3.043(1) Å) than the silver atoms linked by only one molecule of **5.1** (Ag···Ag = 3.568(1) Å). Each silver atom is now three coordinate with a distorted trigonal planar geometry (N-Ag-N angles range from 95.6(1)˚ to 149.9(1)˚), and the Ag···N distances are significantly

longer for the molecules of **5.1** that link the Ag_2L_2 subunits together ($Ag^{\cdots}N$ = 2.393(2) Å) than the molecules of **5.1** in the Ag_2L_2 subunits ($Ag^{\cdots}N$ = 2.161(2) Å and 2.191(2) Å). The twist in the imidazole rings of the molecules of **5.1** bridging the Ag_2L_2 units is smaller (19.6(2)˚), but the torsion angle of the ethyl bridging backbone greater (N-C-C-N = 51.6(3)˚) than the molecules of **5.1** in the Ag_2L_2 subunit (21.5(1)˚ and 50.8(2)˚, respectively). This twist is the largest degree of twisting observed in the three complexes **5.9** – **5.11**.

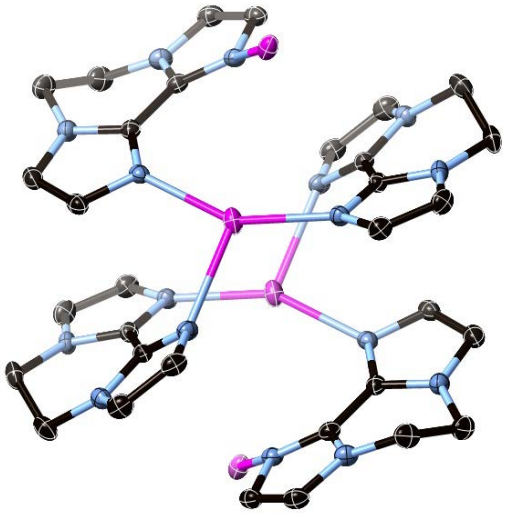

Figure 5.13. Part of the one-dimensional polymer formed in complex **5.11**. Both the divergent and convergent binding of **5.1** is shown. Hexafluorophosphate anions and hydrogen atoms have been removed for clarity.

The polymer grows along the *c*-axis of the unit cell, and the ligands weakly hydrogen bond to the hexafluorophosphate anion (shortest $C^{\cdots}F$ interaction = 3.367(3) Å), shown in figure 5.14. Each polymer chain is linked through weak hydrogen bonding interactions via the hexafluorophosphate anions.

Complexes **5.9**, **5.10**, and **5.11** clearly demonstrate the control that different anions have over the coordination of **5.1** to silver atoms,[76] the more weakly coordinating the counter ion the more distortion is tolerated in the molecules of **5.1**. In each complex a discrete Ag_2L_2 unit is present, with two molecules of **5.1** convergently bridging two silver atoms. As the anion coordinating strength decreases the silver atoms are allowed to interact with more molecules of **5.1**, eventually forming a polymer incorporating the Ag_2L_2 subunit. Strongly coordinating anions, like nitrate in complex **5.9**, interact more strongly with the silver atoms, while the least coordinating anion, hexafluorophosphate in complex **5.11** has only hydrogen bonds to **5.1**.

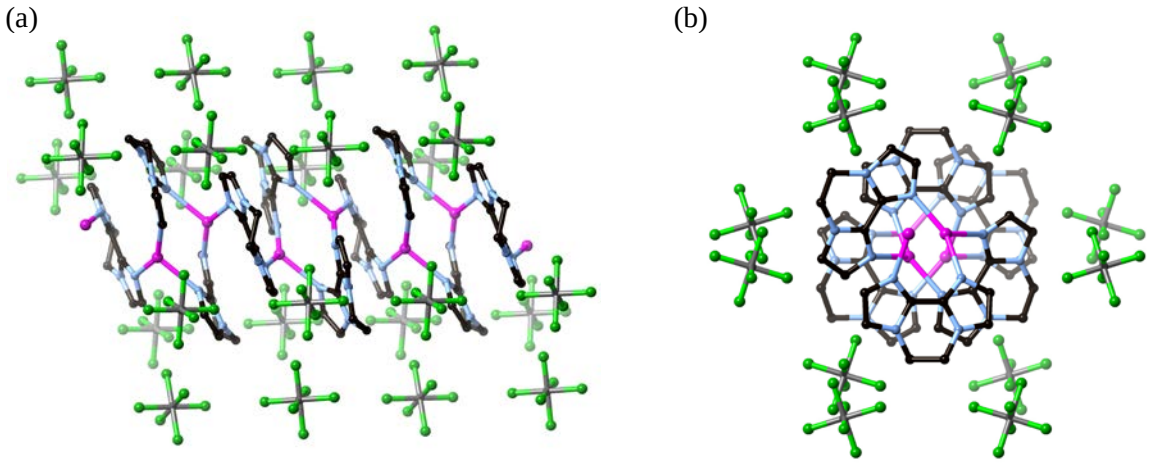

Figure 5.14. (a) An extended section of the polymer formed in complex **5.11**, (b) view of the polymer down the c-axis of the unit cell, hydrogen atoms have been removed for clarity.

5.4 Copper(I) complexes of **5.1**

The ability of **5.1** to convergently bridge two metal atoms, shown above using various silver(I) salts prompted an investigation into the coordination ability of **5.1** to other metal ions. Initally, copper(I) salts were investigated as copper(I) is a d^{10} metal ion similar to silver(I), and has also been used extensively in the formation of supramolecular assemblies. Copper(I) ions have a more defined coordinated geometry than silver(I) ions, copper(I) ions are usually have a tetrahedral geometry, as opposed to the promiscuous nature of the silver(I) ion which can have coordination numbers ranging from 2 – 9.[79]

*5.4.1 Synthesis of [Cu_2**5.1**$_3$][BF_4]$_2$·C_6H_6, complex **5.12***

Firstly, **5.1** was reacted with $Cu(CH_3CN)_4BF_4$ in hot acetonitrile, to form complex **5.12**, which was cooled and subjected to slow diffusion with benzene. Overnight large, colourless cube-shaped crystals suitable for X-ray crystallography were formed in 47% yield from the reaction mixture. Complex **5.12** crystallises in the chiral, cubic space group $P4_332$, forming a Cu_2L_3 dinuclear triple helicate. Again each molecule of **5.1** convergently bridges both copper atoms, as shown in figure 5.15. There is one sixth of complex **5.12**, one third of a BF_4 anion (disordered over two positions), and one third of a molecule of benzene present in the asymmetric unit. The copper atoms in the complex are separated by 2.714(1) Å, and the copper atoms have a slightly distorted trigonal planar geometry (N-Cu-N angle = 118.7(1)˚), with all Cu···N distances = 1.983(2) Å. The imidazole rings of **5.1** are twisted out of plane relative to each other by 12.4(2)˚, comparable to the twisting observed in complex **5.9**, with torsion angle of the ethyl bridging backbone comparable also (N-C-C-N = 51.4(5)˚).

The ethyl backbones of all three molecules of **5.1** that make up the Cu_2L_3 triple helicate twist in the same direction, this common directionality in the backbone twisting of **5.1** imparts chirality into complex **5.12**. Ligand **5.1** is achiral so there is no preference for the backbone to twist in one direction over the other, it is assumed that the sample of complex **5.12** obtained is racemic and that the crystals formed from the reaction are a 1:1 ratio of enantiomers. The N-Cu-Cu-N torsion angle of complex **5.12** is 7.8(1)˚, showing the small pitch of the dinuclear triple helicate.

A molecule of benzene is positioned in a pocket between each of the **5.1** molecules of the Cu_2L_3 helicate. Three Cu_2L_3 units self assemble to enclathrate each molecule of benzene, as shown in figure 5.16. Two tetrafluoroborate anions are positioned at apertures of this self assembled capsule above and below the benzene molecule, interacting with the ethyl backbone hydrogen atoms (C···F = 3.251(12) Å, 3.288(6) Å and 3.296(5) Å). The tetrafluoroborate anions are disordered over two positions, each with 50% occupancy, one fluorine atom points directly at the centre of the benzene ring half of the time, shown in figure 5.17a, and the other half of the time three fluorine atoms close the aperture at the top and bottom of the cage, shown in figure 5.17b. The tetrafluoroborate anions also interact with the imidazole hydrogen atoms (C···F = 3.127(12) Å and 3.491(11) Å) of **5.1** to close the apertures at the sides of the cage.

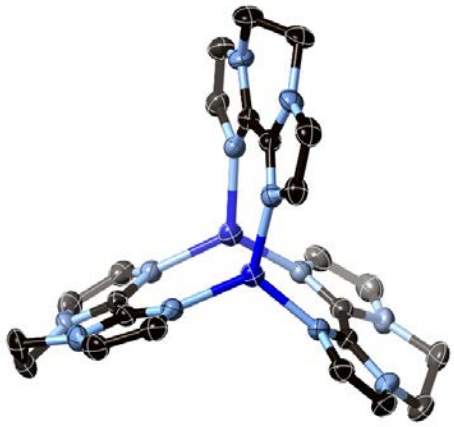

Figure 5.15. Cu_2L_3 helicate formed in complex **5.12**, tetrafluoroborate anions, benzene solvent molecules and hydrogens have been omitted for clarity.

The enclathrated benzene molecule displays edge-to-face π – π interactions with the twelve imidazole rings involved in the enclathration, edge to centroid distances range from 3.614(4) Å – 3.793(3) Å. There are no other strong interactions holding the molecule of benzene in place.

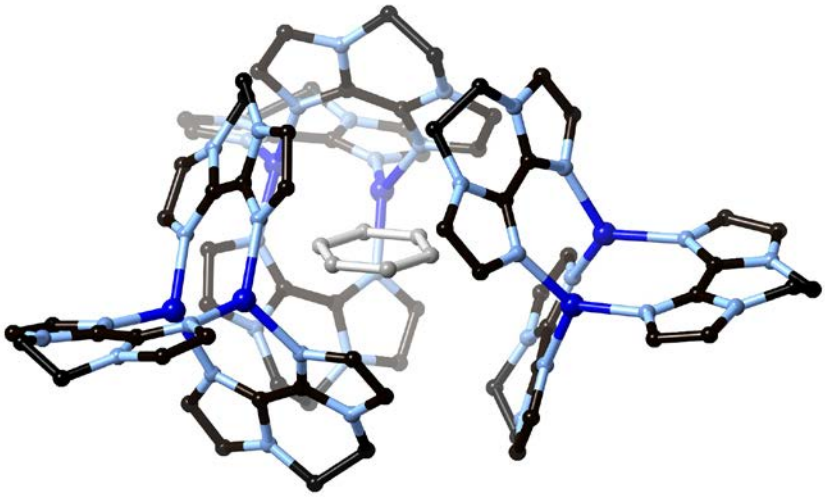

Figure 5.16. Enclathration of one molecule of benzene by three units of complex **5.12**, the benzene molecule is shown in grey, tetrafluoroborate anions and hydrogen atoms have been removed for clarity.

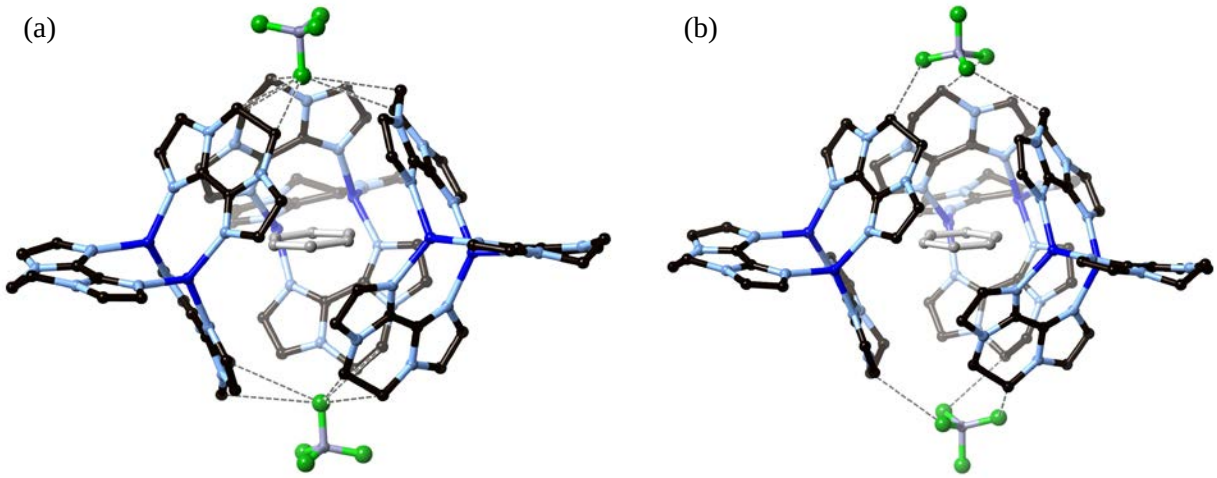

Figure 5.17. Positioning of the disordered tetrafluoroborate anions at the aperture of the enclathrating capsule formed by three complex **5.12** units, the benzene molecule is shown in grey, hydrogen bonds are indicated as dashed lines, and the hydrogen atoms not involved in hydrogen bonding have been removed for clarity.

*5.4.2 Synthesis of [Cu_2**5.1**$_3$][ClO_4]$_2$·C_6H_6, complex **5.13***

Using an anion with the same symmetry as tetrafluoroborate, namely perchlorate, another Cu_2L_3 helicate which enclathrates benzene, complex **5.13**, was prepared using $Cu(CH_3CN)_4ClO_4$ and **5.1**. Crystals suitable for X-ray crystallography were prepared in 56% yield in an analogous fashion to complex **5.12** above, with the slow diffusion of benzene into an acetonitrile solution of the reaction mixture to form colourless cube shaped crystals overnight. The complex crystallises in the chiral, cubic space group

$P4_132$, enantiomorphous to the $P4_332$ space group that complex **5.12** crystallises in. There is one sixth of complex **5.13**, one third of a ClO_4 anion (disordered over two positions), and one third of a molecule of benzene present in the asymmetric unit.

Complex **5.13** also forms a dinuclear triple helicate, with comparable Cu···Cu and Cu···N distances to **5.12** (2.726(1) Å and 1.982(3) Å respectively) with a trigonal planar geometry around the copper atoms (N-Cu-N angle = 118.7(4)˚) (see figure 5.15). The twisting of the imidazole rings of **5.1** is slightly larger than in **5.12** (13.0(2)˚) with a similar torsion angle (N-C-C-N = 51.6(6)˚). The N-Cu-Cu-N torsion angle = 8.2(2)˚, which is also slightly larger than complex **5.12**.

The perchlorate anions are again disordered over two positions, and held in place by the same weak interactions with the ethyl backbone hydrogen atoms (C···O = 3.316(7) Å, 3.335(5) Å and 3.343(9) Å) and imidazole hydrogen atoms (C···O = 3.283(7) Å and 3.383(18) Å) of **5.1**. In this case the two positions over which the perchlorate is disordered are not occupied equally, the position where one oxygen points towards the plane of the benzene ring is occupied 33% of the time (figure 5.17a), whilst the position where the anion forms three O···H hydrogen bonds to close the apertures at the top and bottom of the cage is occupied 66% of time (figure 5.17b).

*5.4.3 Synthesis of $[Cu_2$**5.1**$_3][NO_3]_2 \cdot C_6H_6$, complex **5.14***

An anion that also possesses a threefold axis, similar to tetrafluoroborate and perchlorate, namely nitrate, was also used to form complex **5.14** with ligand **5.1**. Using a more coordinating anion has not disrupted the formation of a chiral Cu_2L_3 triple helicate that enclathrates a molecule of benzene. Complex **5.14** was prepared by the reaction of **5.1** with $Cu(PPh_3)_2NO_3$ in hot acetonitrile. Crystals suitable for X-ray diffraction were prepared in a 41% yield in a similar fashion to complexes **5.12** and **5.13**, by slowly diffusing benzene into an acetonitrile solution of the reaction mixture. Complex **5.14** crystallises in the cubic, chiral space group $P4_332$ with one sixth of complex **5.14**, one third of a disordered nitrate anion and one third of a benzene molecule present in the asymmetric unit. Again the Cu···Cu and Cu···N distances are comparable to **5.12** and **5.13** (2.707(1) Å and 1.976(2) Å respectively), and the geometry around the copper atom is also trigonal planar (N-Cu-N angle = 118.7(2)˚), see figure 5.15. The twisting in the imidazole rings of **5.1** (12.3(1)˚) and the torsion angle of the ethyl backbone (N-C-C-N = 49.9(5)˚) are also similar to complexes **5.12** and **5.13**. The N-Cu-Cu-N torsion angle for complex **5.14** is 8.1(1)˚ similar to complexes **5.12** and **5.13**.

The nitrate anion is disordered over three positions, each occupied 33% of the time. Two oxygen atoms of the nitrate are always present, with the remaining oxygen atom disordered over three positions. The nitrate anion closes the apertures above and below the enclathration complex with one of the nitrate oxygen atoms that is fully occupied forming hydrogen bonds to the ethyl backbone hydrogen atoms of **5.1** (C···O = 3.278(4) Å, 3.398(5) Å and 3.543(7) Å), and imidazole hydrogen atoms of **5.1** (C···O = 3.326(7) Å and 3.403(5) Å) in a similar manner to **5.12** and **5.13**, shown in figure 5.18.

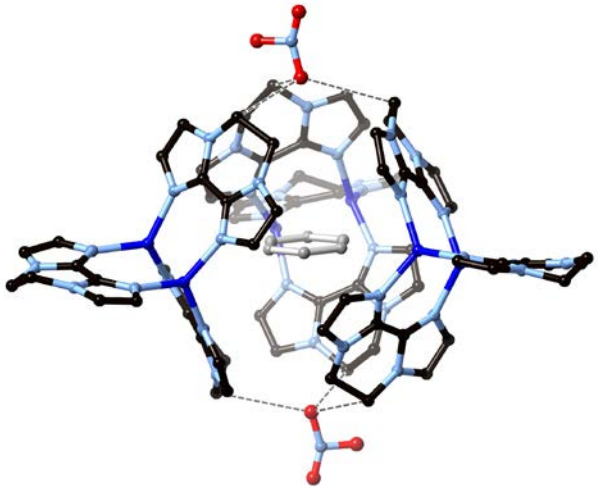

Figure 5.18. Nitrate anions forming hydrogen bonds to close the apertures of complex **5.14**, hydrogen bonds are indicated as dashed lines, nitrate anion disorder is not shown and hydrogen atoms not involved in hydrogen bonding have been removed and the benzene molecule is shown in grey for clarity.

All three enclathration complexes **5.12** – **5.14** were redissolved in acetonitrile and an NMR spectrum collected. All three complexes display downfield shifted peaks, relative to uncoordinated **5.1**, corresponding to the imidazole hydrogen atoms of coordinated **5.1**, indicative of the dinuclear triple helicate complex present in the solution phase. A peak in the NMR spectrum is also observed for the benzene molecule present in the crystal structure, with an integral corresponding to one benzene molecule for each complex, as expected, the NMR spectrum of complex **5.12** is shown in figure 5.19, the NMR spectrum of complexes **5.13** and **5.14** were very similar. The benzene peak is not shifted upfield compared to solvent benzene and hence it is unlikely that the benzene molecule is enclathrated in solution. An NMR titration was also undertaken, with 5 x 20 μL 0.0830 mol.L^{-1} acetonitrile aliquots of copper(I) tetrakis acteonitrile salt solution added to 1 mL of 0.0124 mol.L^{-1} acetonitrile solution of **5.1** to form the Cu_2L_3 unit, then another equivalent of copper(I) tetrakis acetonitrile salt solution is added to reach two equivalences of copper(I). The two imidazole peaks of uncoordinated **5.1** coalesce to one peak after the addition of one aliquot of tetrakis acteonitrile salt and only separate into two imidazole peaks of bound **5.1** once an excess of copper(I) tetrakis acetonitrile salt is added. Shown in figure 5.20 are the

NMR spectra for the titration performed to form complex **5.12**. An NMR spectrum was retaken of the titration sample after one hour but the peaks had not separated further. The coalescence of peaks, rather than disappearance peaks corresponding to uncoordinated **5.1** and appearance of peaks corresponding to coordinated **5.1** indicates that the formation of the dinuclear triple helicate is dynamic in solution. To try and observe the appearance and disappearance of peaks corresponding to uncoordinated and coordinated **5.1** rather than the coalescence of peaks and then separation, the titration was repeated with a drop of benzene added to the initial solution of **5.1**, as perhaps the benzene molecule templates formation of the Cu_2L_3 unit, but unfortunately the same coalescence of peaks was observed. NMR titrations were performed with **5.1** and the corresponding copper salts for complex **5.13** and **5.14**, they were similar to the titration shown in figure 5.20.

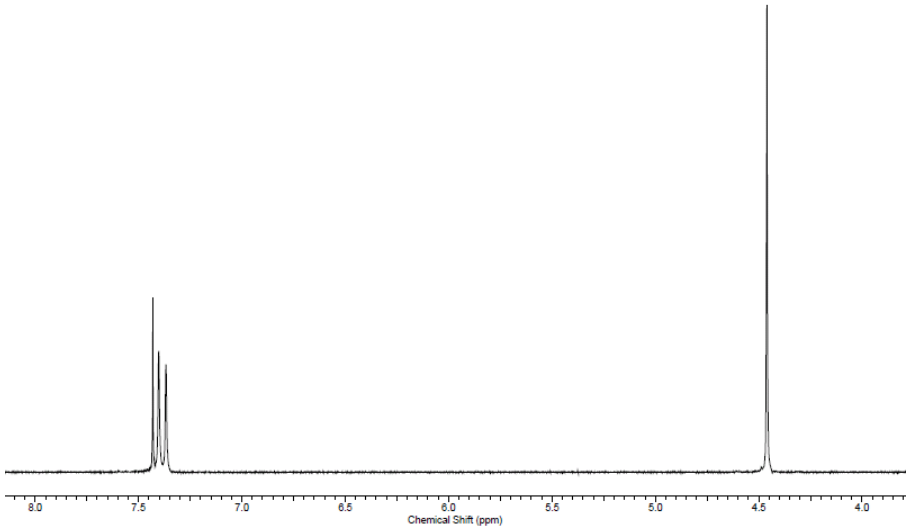

Figure 5.19. NMR spectrum of complex **5.12**.

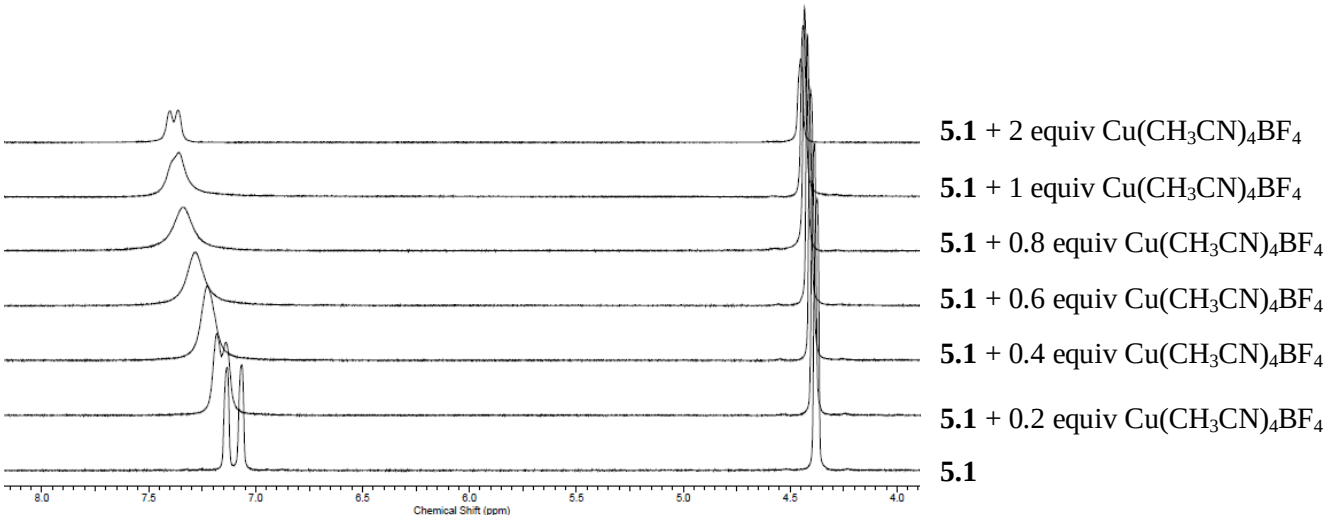

Figure 5.20 NMR titration to form complex **5.12**.

The stability of the enclathrated complexes **5.12** and **5.14** in the solid state was monitored by TGA. Both complexes retain the enclathrated benzene molecule up 300˚C before decomposition of the complex occurs. All three complexes appear to be stable in solution, with ESI-MS peaks corresponding to $Cu_2L_3^{2+}$, $Cu_2L_2^{2+}$ and CuL_2^{+} present, but no enclathrated benzene molecule was observed, as in the NMR spectrum.

*5.4.4 Synthesis of $[Cu_2$**5.1**$_3][PF_6]_2 \cdot 2C_6H_6$, complex **5.15***

Finally, using another anion with different geometry, in this case the octahedral anion hexafluorophosphate, formed complex **5.15**, in combination with **5.1**. Crystals suitable for X-ray crystallography were formed in a much lower yield (4%) in a similar fashion to complexes **5.12**, **5.13**, and **5.14** with the slow diffusion of benzene into an acetonitrile solution of the reaction mixture. Despite repeated attempts, in only one case could crystals of complex **5.15** be grown, allowing characterisation through X-ray crystallography only. Again a Cu_2L_3 dinuclear triple helicate is formed, with coordination of **5.1** similar to that shown in figure 5.15, but complex **5.15** crystallises in the monoclinic space group *P*2/*n*. Half of two crystallographically distinct Cu_2L_3 units are present in the unit cell, along with two hexafluorophosphate anions and half of four benzene molecules. The Cu···Cu distances (2.708(1) Å and 2.710(1) Å) and Cu···N distances (ranging from 1.936(3) Å to 2.026(4) Å) are similar to the three complexes described above and the copper atom also has a distorted trigonal planar geometry (N-Cu-N angles range from 103.5(1)˚ to 133.1(1)˚). The twist in the imidazole ring of **5.1** (ranging from 12.3(2)˚ to 13.6(3)˚) and the torsion angles of the ethyl backbone (N-C-C-N ranges from 48.8(5)˚ to 51.9(9)˚) are also similar to the three complexes described above. The N-Cu-Cu-N torsion angles range from 5.1(1)˚ to 12.8(2)˚.

The difference in using an octahedral anion can be clearly seen when the packing of **5.15** is examined, and a comparison made to the benzene enclathration complexes **5.12** – **5.14**. With a hexafluorophosphate anion the Cu_2L_3 tripe helicate unit common to all four complexes does not enclathrate a benzene molecule. Instead benzene molecules occupy only two of the available three sites between the ligands of the Cu_2L_3 unit, this interaction with only two benzene molecules rather than three forms a chain of Cu_2L_3 units, stabilized by weak face-to-face $\pi - \pi$ interactions with benzene molecules (centroid to centroid distances = 3.775(2) Å and 3.836(2) Å), as shown in figure 5.21. The third site, unoccupied by a molecule of benzene displays face-to-face $\pi - \pi$ stacking of imidazole rings between adjacent chains (centroid to centroid distance = 3.657(2) Å), as shown in figure 5.22.

The hexafluorophosphate anions form weak hydrogen bonds to both the hydrogen atoms of the ethyl backbone and the imidazole rings of **5.1**. One axial fluorine atom of the hexafluorophosphate anion sits in

hydrogen bonding pockets at each end of the Cu_2L_3 unit formed by the imidazole hydrogen atoms of all three molecules of **5.1** (C···F interactions range from 3.333(6) Å to 3.452(5) Å). Each hexafluorophosphate anion forms hydrogen bonds to five Cu_2L_3 units, disrupting the formation of the benzene enclathrulation complexes discussed above. The benzene molecules also have edge-to-face π interactions with benzene molecules in neighbouring chains, to form a channel of benzene molecules in the crystal structure.

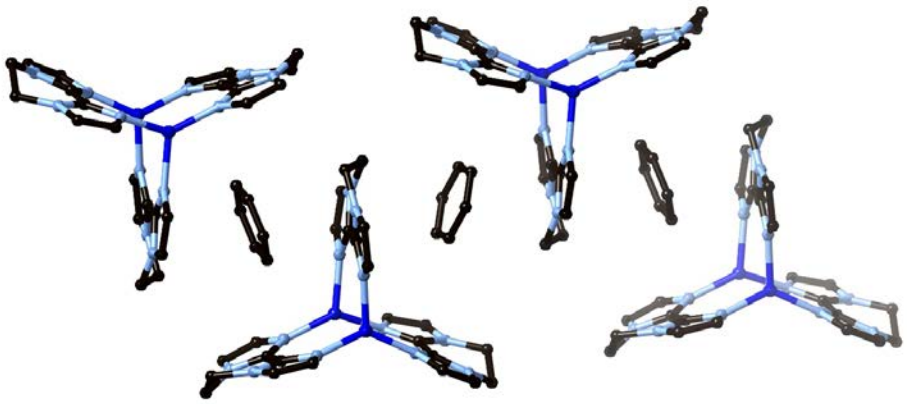

Figure 5.21. Benzene molecules in complex **5.15** interacting with Cu_2L_3 units to form a chain, hexafluorophosphate anions and hydrogen atoms have been removed for clarity.

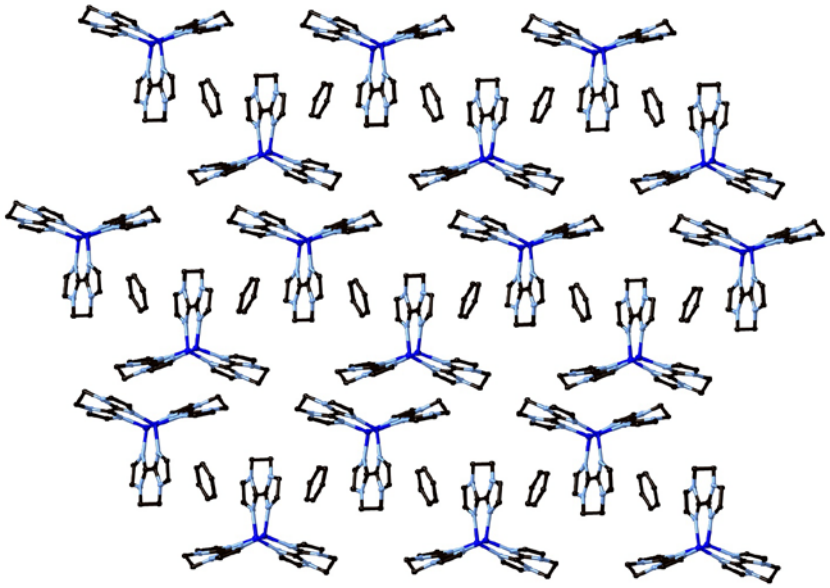

Figure 5.22. (a) π – π stacking between imidazole rings in adjacent chains, hexafluorophosphate anions and hydrogen atoms removed for clarity.

*5.4.5 Synthesis of [Cu_2**5.1**$_3$][ClO_4]$_2$·CH_3CN, complex **5.16***

All four complexes incorporate the diffusion solvent benzene in their crystal structures, so diffusion of solvents with the same (D_{3h}) symmetry seen in the asymmetric unit were used in an attempt form another enclathration complex analogous to complexes **5.12** to **5.14**. Initially hexafluorobenzene was used as a diffusion solvent as it is has the same symmetry as benzene, although hexafluorobenzene is considerably more electron deficient core than benzene. It is unclear if the symmetry of the anion, the electronic nature of the enclathrated molecule, the molecular volume, or a combination of all three, will enhance or disrupt the formation of the enclathrating complex.

The copper(I) salts of all three anions, tetrafluoroborate, perchlorate and nitrate, that form complexes to enclathrate benzene were set up for vapour diffusion under identical conditions, with hexafluorobenzene used as the diffusion solvent. Single crystals that were suitable for X-ray diffraction were formed from the reaction mixture containing $Cu(CH_3CN)_4ClO_4$ and **5.1** to form complex **5.16** in 41% yield. Complex **5.16** crystallised in the triclinic space group *P*-1, with one Cu_2L_3 unit, two perchlorate anions and one molecule of acetonitrile present in the asymmetric unit. Again the copper atoms have a distorted trigonal planar geometry (N-Cu-N angles range from 97.0(1)˚ to 139.7(1)˚), the Cu···Cu distances (2.684(1) Å) and Cu···N distances (ranging from 1.934(2) Å to 2.061(2) Å), along with the twisting of the imidazole rings of **5.1** (7.6(1)˚, 9.5(1)˚ and 14.6(1)˚) and the torsion angles of the ethyl backbone (N-C-C-N range from 46.0(2)˚ to 49.8(2)˚) are comparable to complexes **5.12** – **5.15** which also form a Cu_2L_3 unit, similar to that shown in figure 5.15. Two of the N-Cu-Cu-N torsion angles are the largest seen in all five Cu_2L_3 helicates formed (16.6(1)˚ and 21.0(1)˚) and the third is considerably smaller (2.4(1)˚).

Complex **5.16** does not enclathrate hexafluorobenzene as hoped; in fact hexafluorobenzene is not present at all in the X-ray crystal structure. The perchlorate anions in complex **5.16** occupy the same two hydrogen bonding pockets formed by the imidazole hydrogen atoms of **5.1** that are occupied by the hexafluorophosphate anions in complex **5.15**. The three oxygen atoms of the perchlorate anion are staggered between the three imidazole hydrogen atoms of the Cu_2L_3 unit with C···O distances ranging from 3.236(3) Å to 3.943(4) Å, as shown in figure 5.23. The axial oxygen atom of the perchlorate not involved in the hydrogen bonding pocket hydrogen bonds to hydrogen atoms of the ethyl backbone of **5.1** in an adjacent Cu_2L_3 unit (shortest C···O bond = 3.226(3) Å).

The acetonitrile solvent molecule present is positioned in between two **5.1** ligands of the Cu_2L_3 unit, these two ligands are also involved in weak face-to-face π – π stacking to another Cu_2L_3 unit through both imidazole rings of **5.1** (plane to centroid distances = 3.425(4) Å and 3.756(2) Å). This π – π stacking

interaction forms a chain of Cu_2L_3 units, as shown in figure 5.24. The third ligand not involved in the π – π stacking hydrogen bonds to the axial perchlorate oxygen atoms through the ethyl backbone hydrogens, linking the chains of Cu_2L_3 units together.

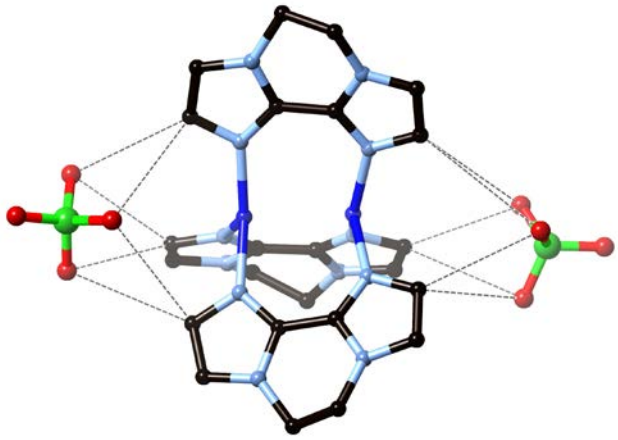

Figure 5.23. The two hydrogen bonding pockets occupied by perchlorate anions in complex **5.16**, hydrogen bonds are indicated as dashed lines, acetonitrile solvent molecules and hydrogen atoms have been removed for clarity.

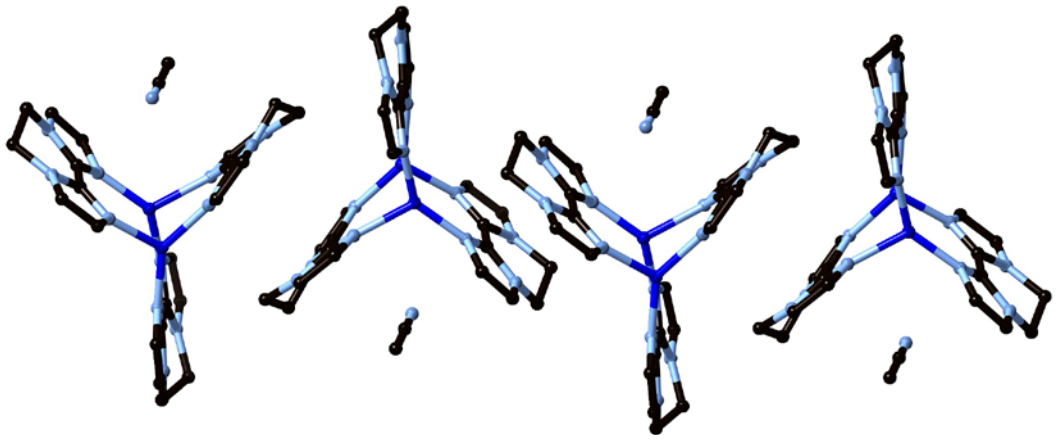

Figure 5.24. π – π stacking between the imidazole rings of **5.1** in complex **5.16** forming a chain of Cu_2L_3 units, perchlorate anions and hydrogen atoms have been removed for clarity.

The electron deficient core of the hexafluorobenzene molecule may not be able to form the edge-to-face π – π interactions required for the formation of an enclathration complex, or the hexafluorobenzene may be too large to be enclathrated by the Cu_2L_3 units. A much larger molecule, namely mesitylene, was also used for vapour diffusion under identical conditions to the formation of complexes **5.12** to **5.14**, but unfortunately no crystals suitable for single crystal X-ray diffraction were obtained. This indicates that the size and the electronic nature of the molecule to be enclathrated is important.

Fluorobenzene was also used as a diffusion solvent under identical conditions to the formation of complexes **5.12** to **5.14**. Crystals suitable for X-ray diffraction were obtained from the reaction mixture of **5.1** and $Cu(CH_3CN)_4BF_4$. The complex thus formed crystallised in the cubic, chiral space group $P4_132$, with one sixth of a Cu_2L_3 unit, one third of a BF_4 anion (disordered over two positions), and one third of a molecule of fluorobenzene present in the asymmetric unit (see figure 5.15). The fluorine atom of the fluorobenzene molecule is disordered over three positions of the benzene ring, as opposed to disordered over all six positions. Each fluorobenzene molecule is enclathrated by three Cu_2L_3 units (see figure 5.16). The formation of the enclathration species must be in some part dependent on the size and electronic nature of the molecule to be enclathrated, as when hexafluorobenzene was used to form complex **5.16**, no enclathration was observed (figure 5.24), but fluorobenzene does form the enclathration species.

Hexafluorophosphate is the only anion in this series not to form an enclathration complex when combined with copper(I) ions and **5.1** (figure 5.21). An experiment was undertaken to determine if the enclathration species would form preferentially when an anion with the correct symmetry was added to a solution of $Cu(CH_3CN)_4PF_6$ and **5.1**. A solution of **5.1** and $Cu(CH_3CN)_4PF_6$ in acetonitrile was heated and left to cool, after 5 minutes an acetonitrile solution containing one equivalence of $NaClO_4$ was added, and benzene was diffused into the mixed anion solution. Crystals suitable for X-ray crystallography were obtained after 48 hours, the structure so obtained is identical to complex **5.13**. Addition of an acetonitrile solution of tetrabutylammonium tetrafluoroborate to a solution of **5.1** and $Cu(CH_3CN)_4$, and the subsequent slow diffusion of benzene also gives crystals suitable for X-ray crystallography where the structure obtained is identical to that of complex **5.12**.

*5.4.6 Synthesis of poly-[Cu_2**5.1**]I_2, complex **5.17***

Finally, CuI was reacted with **5.1** to form complex **5.17**. Very small, colourless needles suitable for X-ray diffraction were formed instantly in a 35% yield when hot acetonitrile solutions of **5.1** and CuI were mixed together. Complex **5.17** crystallises in the monoclinic space group $P2_1/c$, there is one molecule of **5.1**, two copper atoms and two iodide anions present in the asymmetric unit.

Complex **5.17** forms a one dimensional polymer that grows along the c-axis of the unit cell, where again molecules of **5.1** convergently bridge two copper atoms (Cu···Cu = 2.640(1) Å), the shortest Cu···Cu distance observed for the copper complexes formed with **5.1**. The separation between these two copper atoms is verging on the separation seen between copper atoms in metallic copper (ca. 2.56 Å).[80] The Cu···N distances are comparable to the previous complexes (2.001(2) Å and 2.010(2) Å), as is the twist in the imidazole rings of **5.1** (8.1(1)˚). Each copper atom is also bound to three iodide ions (Cu···I = 2.637(1)

Å – 2.775(1) Å) to give the copper atom a distorted tetrahedral geometry (angles around the copper centre range from 105.5(1)˚ to 115.83(1)˚, τ_4(Cu1) = 0.92, τ_4(Cu2) = 0.95). Each iodide ion bridges three copper atoms, to form a copper – iodide wire framework, as shown in figure 5.25.

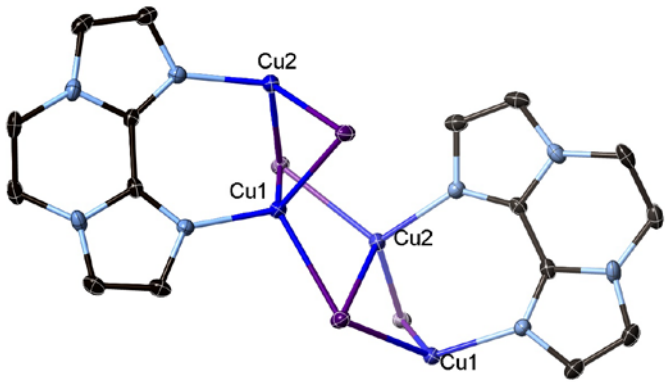

Figure 5.25. A section of the polymer chain formed in complex **5.17**, hydrogen atoms have been removed for clarity.

The copper atoms that are convergently bound to a molecule of **5.1** are grown up into a polymer by iodide atoms that bridge these subunits together. The separation between the copper atoms not bridged by **5.1** and only bridged by iodide atoms is considerably longer (Cu···Cu = 2.8129(5) Å) than the copper atoms that are bridged by molecules **5.1**. The copper-iodide wire framework is insulated by the molecules of **5.1** that alternate along each side of the wire. Both imidazole rings of **5.1** face-to-face π – π stack with the two imidazole rings of **5.1** in an adjacent polymer chain (centroid to centroid distance = 3.471(5) Å), separating the one dimensional chains of **5.17**, shown in figure 5.26.

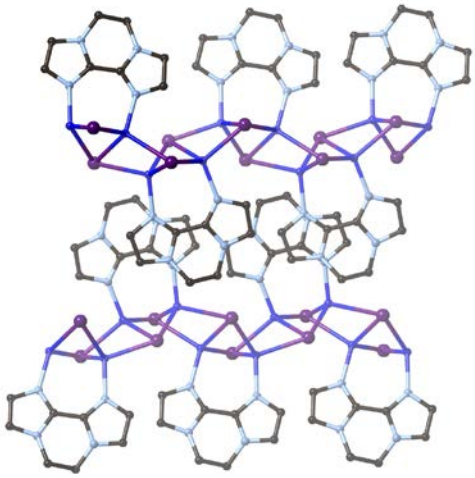

Figure 5.26. π – π stacking between adjacent polymer chains in complex **5.17**, hydrogen atoms have been removed for clarity.

Complexes **5.12** to **5.17** clearly show that the more defined coordination geometry around the copper(I) centre results in much less variation of the coordination chemistry of ligand **5.1**. Complexes **5.12** to **5.16** all display a dinuclear triple helicate motif, no matter the counter ion present, in stark contrast to the coordination of **5.1** to various silver(I) salts. The convergent bridging of **5.1** is maintained moving to the copper(I) salts and the distortion in **5.1** is similar to that seen in the silver(I) salts. Only when moving to a strongly coordinating iodide anion (complex **5.17**) does **5.1** fail to form a dinuclear triple helicate and a one dimensional copper iodide wire polymer is observed, although the convergent bridging of **5.1** is maintained.

5.5 Copper(II) complexes of **5.1**

With the successful formation of Cu_2L_3 triple helicates from the reactions of various copper(I) salts and **5.1**, the reaction of **5.1** and copper(II) salts was also investigated. In contrast to the d^{10} silver(I) and copper(I) salts, d^9 copper(II) centres prefer five coordinate geometries, varying between square planar and trigonal bipyramidal. The change in coordination environment around the metal centre should lead to different coordination of **5.1** around the copper centre and in turn this should promote the formation of different supramolecular assemblies not yet seen for **5.1**.

*5.5.1 Synthesis of $[Cu_2$**5.1**$_4][ClO_4]_2 \cdot 3CH_3CN \cdot 0.5C_6H_6$, complex **5.18***

Initially **5.1** was reacted with $Cu(ClO_4)_2$, to form complex **5.18**, crystals suitable for X-ray crystallography were obtained in 25% yield by the slow diffusion of benzene into the acetonitrile reaction mixture. Complex **5.18** crystallises in the monoclinic space group *P*2/*c* with half of two crystallographically distinct Cu_2L_4 units present in the asymmetric unit, along with four perchlorate anions (three of which are disordered), half a molecule of benzene and three acetonitrile molecules. Indeed, the change in copper oxidation state has lead to a change in the coordination geometry, with each copper atom now square pyramidal (N-Cu-N angles range from 89.0(1)˚ to 91.0(1)˚, and N-Cu-O angles range from 81.0(2)˚ to 105.4(1)˚). The change in coordination geometry has not affected the ability of **5.1** to bridge two copper atoms, but the dinuclear triple helicate formed for most of the copper(I) salts is not formed. Instead, the square planar geometry of complex **5.18**, with all four coordinating nitrogen atoms in the basal plane, allows the formation of a Cu_2L_4 dinuclear quadruple helicate with four molecules of **5.1** bridging two copper atoms. The square planar coordination geometry of the copper(II) atoms is completed by a coordinating perchlorate anion, as shown in figure 5.27. This dinuclear quadruple helicate motif is rarely observed in metallosupramolecular chemistry, presumably due to the steric demand of placing four ligands around only two metal centres, but it has been observed previously in copper(II)[68a] and palladium[68b] complexes for a very similar ligand, N,N'-dimethylene-2,2'-biimidazoline, **5.4**.

The copper atoms in the two crystallographically distinct Cu_2L_4 units are separated by 2.956(1) Å and 2.945(1) Å, almost 0.3 Å further apart than the copper(I) complexes described above. The Cu···N bonds in complex **5.18** range from 1.995(3) Å to 2.014(4) Å, similar to those found in previous complexes, and each helicate unit is capped by a disordered perchlorate anion, with Cu···O bonds ranging from 2.284(5) Å to 2.312(4) Å. The twist in the imidazole rings of **5.1** is significantly larger (twist angles range from 17.3(2)˚ – 22.7(2)˚) than those found in the complexes **5.12** to **5.16** formed with various copper(I) salts, most likely due to the steric hindrance caused by the addition of one extra molecule of **5.1** to bridge the two copper atoms. The torsion angles of the ethyl backbone are similar to those observed for the dinuclear triple helicate motifs (N-C-C-N range from 48.0(4)˚ to 50.9(7)˚).

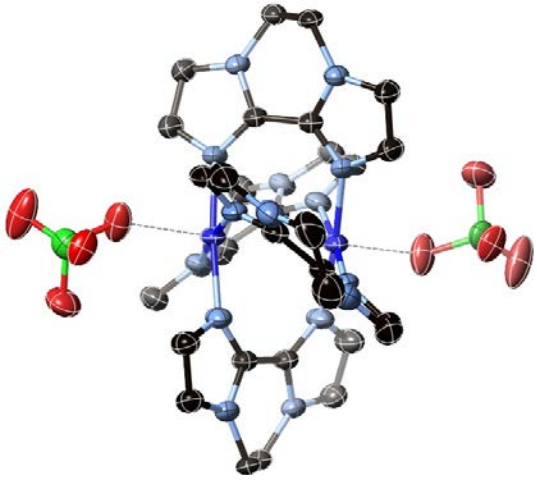

Figure 5.27. One of the crystallographically distinct dinuclear quadruple helicates formed in complex **5.18**, coordinating perchlorate anion disorder not shown, solvent molecules and hydrogen atoms have been removed for clarity.

Both the capping perchlorate anions and the imidazole hydrogen atoms of complex **5.18** show weak hydrogen bonding interactions (C···O range from = 3.065(6) Å to 3.886(10) Å) with imidazole hydrogen atoms and perchlorate anions of adjacent units, shown in figure 5.28. These interactions form a hydrogen bonding chain of Cu_2L_4 helicate units. Free perchlorate anions and benzene and acetonitrile molecules sit in the void space with minimal interactions to complex **5.18** units.

This Cu_2L_4 helicate unit possesses a similar motif to the well known $Cu(OAc)_2$ paddle wheel, where four acetate molecules bridge two copper atoms separated by only 2.65 Å.[81] Paddle wheel complexes between two copper(II) centres have been well documented in the literature,[60] with the two copper centres usually bridged by four carboxylate units,[57,61] other bridging ligands have also been used in the formation of

paddle wheel complexes.[62] The two copper centres are usually strongly antiferromagnetically coupled,[64] unfortunately no magnetic measurements on complex **5.18** were undertaken.

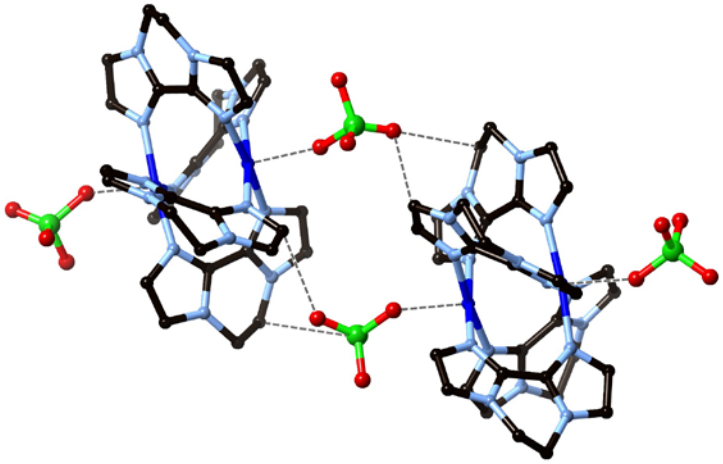

Figure 5.28. Weak hydrogen bonding interactions between adjacent units of complex **5.18**, silver – perchlorate interactions and hydrogen bonds are indicated as dashed lines, coordinating perchlorate anion disorder is not shown, noncoordinating perchlorate anions, solvent molecules and hydrogen atoms not involved in hydrogen bonding have been removed for clarity.

*5.5.2 Synthesis of [Cu_2**5.1**$_2(CH_3COO)_2$]·2CH_3CN, complex **5.19***

Ligand **5.1** was also reacted with copper acetate to form complex **5.19**. Blue, plate shaped crystals suitable for X-ray crystallography were formed over four weeks from the acetonitrile reaction mixture in a 61% yield. Complex **5.19** crystallises in the triclinic space group *P*-1, half of a $Cu_2L_2(OAc)_2$ unit is present in the asymmetric unit along with one molecule of acetonitrile. Two molecules of **5.1** convergently bridge two copper atoms, which are also bridged by two acetate molecules to form a $Cu_2L_2(OAc)_2$ unit. Two additional acetate molecules complete the square pyramidal geometry of the copper(II) ions (N-Cu-N = 175.6(1)˚, O-Cu-O = 82.1(1)˚, 96.8(1)˚ and 178.8(1)˚, N-Cu-O range from 88.8(1)˚ to 92.3(1)˚, τ_5 = 0.05), as shown in figure 5.29.

The two copper atoms are separated by a distance of 3.167(1) Å, significantly longer than the Cu···Cu observed in the copper acetate paddle wheel, and slightly longer than the separation in complex **5.18** above. The Cu···N distances (2.027(3) Å and 2.029(3) Å), and the Cu···O distances (bridging acetate Cu···O = 1.944(3) Å and 2.247(3) Å, capping acetate Cu···O = 1.937(3) Å) are similar to those seen in complexes discussed previously. The two imidazole rings of **5.1** twist out of plane by 10.6(2)˚, significantly smaller than the twisting in complex **5.18**, but comparable to the twisting observed in complexes **5.12** – **5.14**, as is the torsion angle of the ethyl backbone (N-C-C-N angle = 47.6(5)˚). The

decrease in twisting and torsion angles compared to **5.18** is most likely due to the decrease in the number of molecules of **5.1** around the two copper atoms, reducing the steric strain and therefore the distortion from planarity of the imidazole rings.

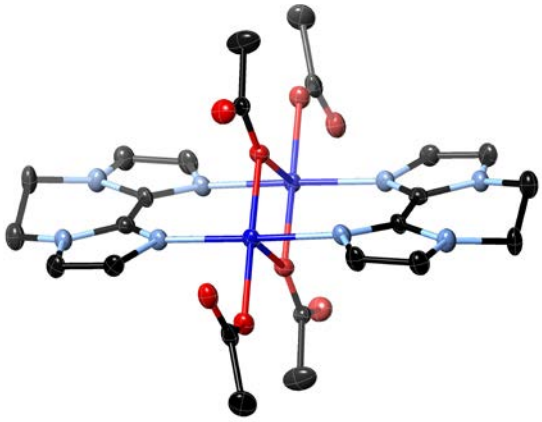

Figure 5.29. The $Cu_2L_2(OAc)_2$ unit formed in complex **5.19**, acetonitrile solvent molecules and hydrogen atoms have been removed for clarity.

Each $Cu_2L_2(OAc)_2$ unit displays face-to-face π – π stacking interactions between each of the imidazole rings of **5.1** with an imidazole ring of another $Cu_2L_2(OAc)_2$ unit positioned both above and below this unit (centroid to centroid distances = 3.636(3) Å and 3.684(3) Å). There is weak hydrogen bonding interactions between the bridging acetate molecules and the capping acetate molecules to the ethyl and imidazole backbone hydrogen atoms of **5.1** (C···O range from 3.383(5) Å to 3.828(5) Å, and C–H···O angles range from 154.9(2)˚ to 117.8(2)˚) in adjacent $Cu_2L_2(OAc)_2$ units. The π − π stacking interactions and hydrogen bonding is shown in figure 5.30.

The change in coordination geometry from copper(I) salts to copper(II) salts has not affected the ability of **5.1** to convergently bridge two copper atoms. To complete the coordination sphere of the copper(II) centres anions are also bound to the copper centre, in the case of complex **5.19** the acetate anions also bridge the copper centres.

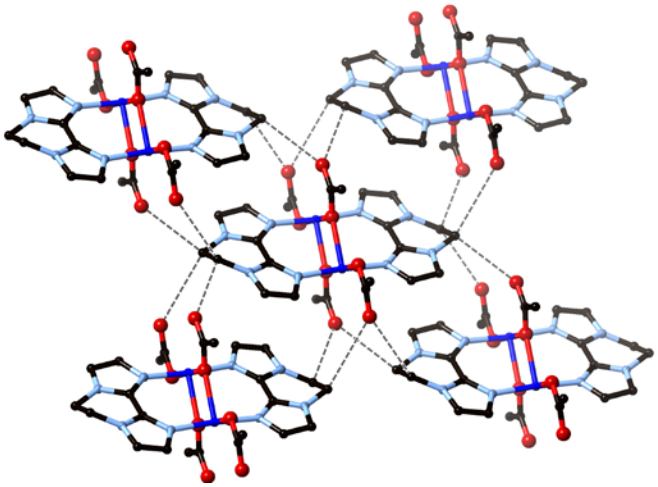

Figure 5.30. π stacking and hydrogen bonding between one $Cu_2L_2(OAc)_2$ unit of complex **5.19**, hydrogen bonds are indicated as dashed lines, acetonitrile solvent molecules and hydrogen atoms have been omitted for clarity.

5.6 Cadmium and cobalt complexes of **5.1**

*5.6.1 Synthesis of [Cd**5.1**$_2$(NO$_3$)$_2$OH$_2$], complex **5.20***

Finally **5.1** was reacted with metals that have a more rigid coordination environment around the metal centre. Initially, cadmium nitrate was reacted with **5.1** to form complex **5.20**. Crystals suitable for X-ray diffraction were grown from the slow diffusion of diisopropyl ether into an acetonitrile solution of the reaction mixture, producing colourless needles in 65% yield over the course of one week. The complex crystallises in the monoclinic space group $P2_1/n$ with two molecules of complex **5.20** present in the asymmetric unit.

For the first time in the course of this study ligand **5.1** is not bridging two metal centers, instead **5.1** is coordinated to the cadmium atom through only one nitrogen atom (Cd···N = 2.300(3) Å and 2.305(3) Å). Both nitrogen atoms bind to the cadmium centre in an axial position, whilst the other available nitrogen atoms of both molecules of **5.1** form strong hydrogen bonds to the same molecule of water (N···O = 2.682(4) Å and 2.723(4) Å, O–H···N = 141(3)˚ and 151(2)˚), which is also coordinated to the cadmium centre (Cd···O = 2.240(2) Å) in an equatorial position, as shown in figure 5.31. Two nitrate anions chelate the cadmium ion in an equatorial position to the cadmium atom through two of the oxygen atoms (Cd···O range = 2.398(3) Å to 2.488(3) Å) to complete the pentagonal bipyrimidal coordination sphere required by the cadmium atom (O-Cd-O angles range from 51.8(1)˚ to 92.1(1)˚, N-Cd-O range from 83.3(1)˚ to 96.8(1)˚, N-Cd-N = 174.7(1)˚).

The failure of **5.1** to bridge two metal atoms is presumably due to the more rigid coordination environment around the cadmium atom and the inability of **5.1** to distort to allow two cadmium atoms to come together in such close proximity. The twisting of the imidazole rings in **5.1** gives some insight into this distortion, with the imidazole rings twisted out of plane by 16.2(1)˚ and 15.2(1)˚ by coordination to the cadmium centre and hydrogen bonding to the coordinated water molecule. The largest degree of twisting of the imidazole rings in **5.1** was observed in the formation of the dinuclear quadruple helicate of complex **5.18**, here the twist angles ranged from 17.3(2)˚ to 22.7(2)˚. The torsion angles of the ethyl backbone of **5.1** are comparable to the other complexes (N-C-C-N = 47.8(4)˚ and 48.2(4)˚).

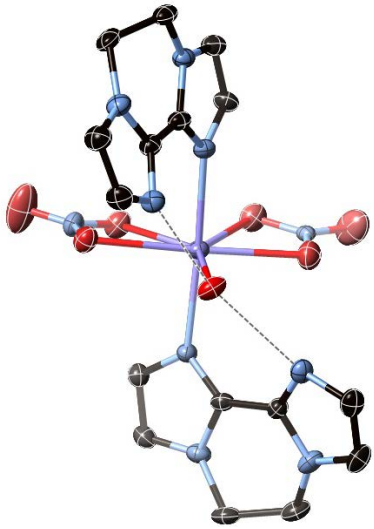

Figure 5.31. Asymmetric unit of complex **5.20**, hydrogen bonds are indicated as dashed lines, hydrogen atoms not involved in hydrogen bonding have been removed for clarity.

The remaining oxygen atom of the coordinated nitrate molecules weakly hydrogen bond to imidazole hydrogen atoms of **5.1** and hydrogen atoms of the ethyl backbone of **5.1** in two adjacent units. The imidazole rings of **5.1** face-to-face $\pi - \pi$ stack (3.659(4) Å to 3.925(2) Å) to imidazole rings in adjacent complexes as shown in figure 5.32.

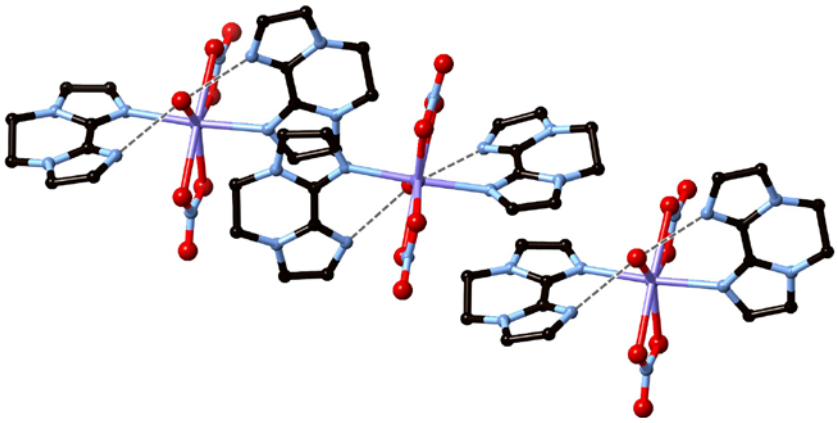

Figure 5.32. Face-to-face π – π stacking in complex **5.20**, hydrogen bonds shown as dashed lines, hydrogen atoms not involved in hydrogen bonding have been removed for clarity.

*5.6.2 Synthesis of [Co**5.1**$_2$(OH$_2$)$_4$][NO$_3$]$_2$, complex **5.21***

Cobalt nitrate was also used to form complex **5.21** with **5.1**. Crystals suitable for X-ray crystallography were obtained in 24% yield in a similar fashion to complex **5.20** with the slow diffusion of diisopropyl ether into an acetonitrile solution of the reaction mixture. Black plates of complex **5.21** crystallise in the monoclinic space group $P2_1/n$, with one half of complex **5.21** present in the asymmetric unit.

Again **5.1** does not bridge two cobalt atoms in complex **5.21** and instead two molecules of **5.1** coordinate to the one cobalt atom in a monodentate fashion in the axial position through one nitrogen atom (Co···N = 2.166(1) Å), whilst the other available nitrogen atom of **5.1** hydrogen bonds to a water molecule (N···O = 2.656(2) Å, O–H···N = 166.2(2)˚) which is coordinated in an equatorial position to the cobalt atom (Co···O = 2.112(1) Å), in a similar manner to **5.20** and shown in figure 5.34. Two other water molecules also coordinate to the cobalt atom to compete the octahedral coordination sphere around the cobalt atom (O-Co-O range from 89.8(1)˚ to 92.2(1)˚). Each nitrate anion hydrogen bonds (O···O = 2.734(1) Å and 2.797(1) Å, O–H···O = 171.0(2)˚ and 179.9(2)˚, respectively) to two coordinated, adjacent, water molecules, also shown in figure 5.33.

The nitrate anions are also involved in hydrogen bonding to coordinated water molecules (O···O = 2.726(2) Å) in adjacent complexes of **5.21** through the remaining oxygen atom of the nitrate anion. This forms an extensive hydrogen bonding network, where the nitrate anions link each complex to four adjacent complexes, shown in figure 5.34. The twisting of the imidazole rings of **5.1** and the torsion angle of the backbone are similar to complex **5.20** (12.4(1)˚ and 47.0(1)˚, respectively).

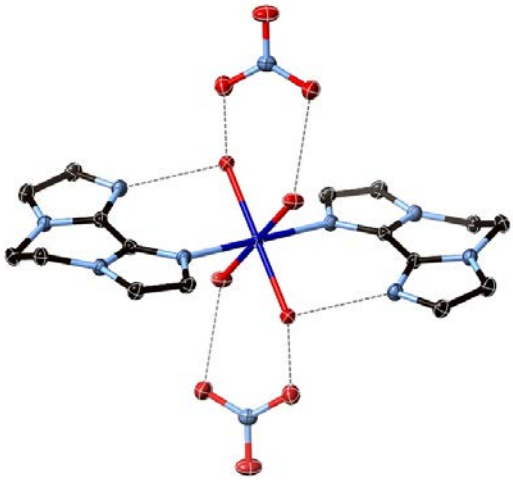

Figure 5.33. Coordination of **5.1** and water molecules to cobalt in complex **5.21**, with hydrogen bonded nitrate anions shown, hydrogen bonds are indicated as dashed lines, hydrogen atoms removed for clarity.

Moving to metal salts with more rigid coordination geometry and more coordination sites around the metal centre has prevented **5.1** from bridging two metal centres. Ligand **5.1** coordinates in a monodentate fashion in both complexes **5.20** and **5.21**, with the other nitrogen atom of **5.1** hydrogen bonding to a coordinated water molecule. Both complexes coordinate water molecules or anions to complete the coordination sphere of the metal.

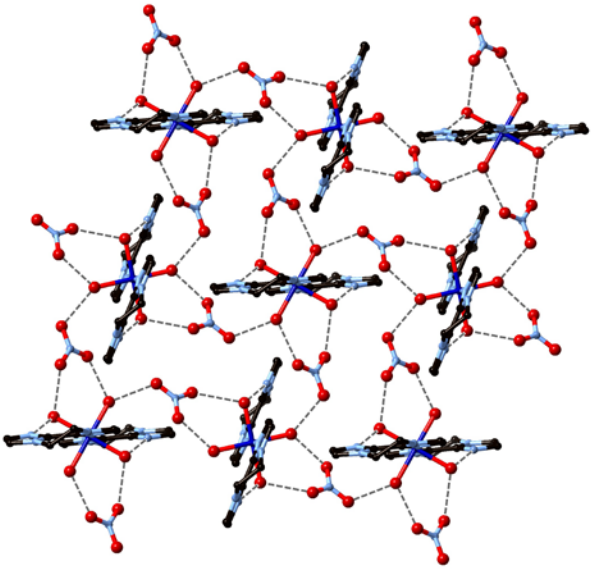

Figure 5.34. Nitrate anions and water molecules hydrogen bonding to link units of complex **5.21** together, hydrogen bonds are indicated as dashed lines, hydrogen atoms have been removed for clarity.

5.7 Copper(II) complexes of **5.2**

Ligand **5.2** differs to ligand **5.1** by the addition of one sp^3 carbon atom to the backbone of **5.1**. Although initially this may seem like a trivial change to make in the ligand, the complexes formed from **5.1** discussed above demonstrate that considerable strain is imparted on imidazole rings of **5.1** by the N,N'-ethyl bridged backbone. This strain manifests itself in the twisting of the imidazole rings of **5.1** way from coplanarity, and also prevents **5.1** from chelating metal atoms due to the narrow chelation angle. Moving from an ethyl bridging to a propyl bridging backbone linking the biimidazole moiety may decrease the inherent strain in the ligand, and hence decrease the twisting out of plane of the imidazole rings. To this end the coordination chemistry of **5.2** was investigated with a range of metal salts with various anions to probe the difference in coordination of **5.1** and **5.2**. Unfortunately, single crystals suitable for X-ray crystallography were only obtained from reaction mixtures where copper(II) salts were used, further investigation into the coordination of **5.2** to other metal centres (silver(I) and copper(I) salts) was not pursued further.

*5.7.1 Synthesis of [Cu**5.2**$SO_4(OH_2)_2$], complex **5.22***

Initially, a strongly coordinating anion, sulfate, was used to react with **5.2**. Combining an acetonitrile solution of **5.2** with an acetonitrile solution of $CuSO_4$ gave light green crystals suitable for X-ray diffraction over the course of two weeks in 32% yield. Complex **5.22** crystallises in the orthorhombic space group *Pnma* with half of complex **5.22** present in the asymmetric unit.

The propyl bridge of **5.2** has made a considerable difference in the coordination of **5.2** to the copper atom. As expected the propyl bridge has allowed **5.2** to chelate to the copper atom (Cu···N = 2.012(2) Å) and the imidazole rings of **5.2** are almost coplanar (2.9(1)˚), in stark contrast to the coordination of **5.1** to copper(II) salts. The sulfate anion is also coordinated to the copper atom (Cu···O = 2.175(2) Å) occupying an axial site, along with two water molecules (Cu···O = 1.955(1) Å) coordinated in a distorted equatorial position, giving the copper centre of complex **5.22** a distorted square pyramidal geometry where the copper centre is raised 0.248(1) Å from the basal plane (N-Cu-N = 82.4(1)˚, O-Cu-O = 89.5(1)˚ and 95.6(1)˚, N-Cu-O = 92.3(1)˚, 98.9(1)˚ and 165.2(1)˚), as shown in figure 5.35.

A chain of complex **5.22** units forms through two strong hydrogen bonds between two oxygen atoms of the sulfate anions and the two coordinated water molecules of **5.22** in an adjacent unit (O···O = 2.649(2) Å), shown in figure 5.36. Each hydrogen bonded chain is then linked to adjacent chains through strong hydrogen bonds, again between the sulfate anion oxygen atoms and the coordinated water molecules (O···O = 2.636(2) Å). Each unit of complex **5.22** is hydrogen bonded to three other units, these hydrogen

bonding interactions are also shown in figure 5.36. The hydrogen bonded network is further supported by face-to-face π – π interactions between the imidazole rings of **5.2** in adjacent units (centroid to centroid distance = 3.531(2) Å).

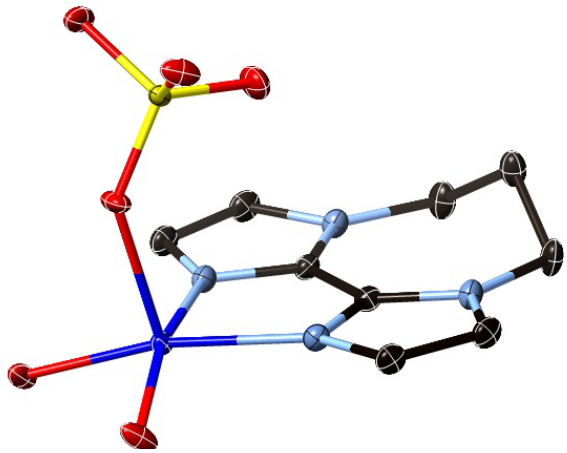

Figure 5.35. Ligand **5.2** chelating one copper atom in complex **5.22**, hydrogen atoms have been removed for clarity.

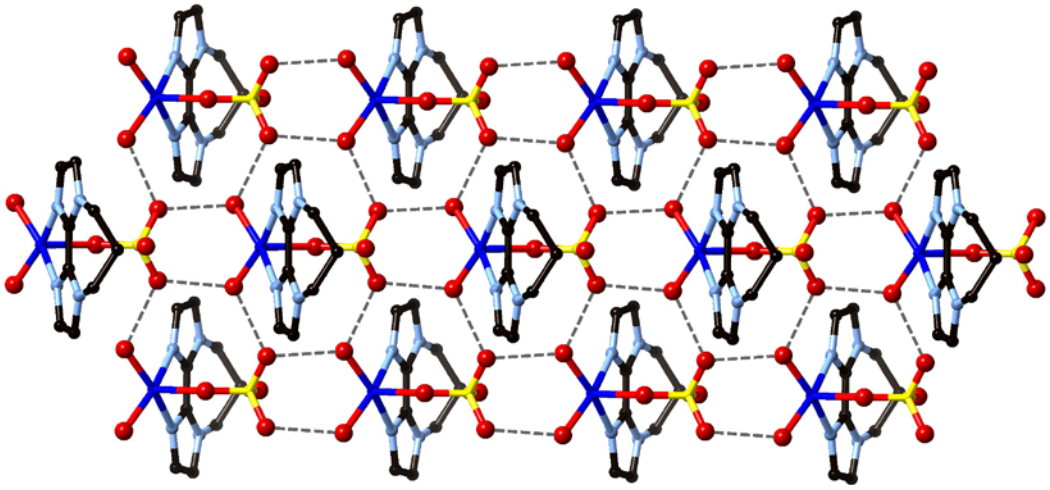

Figure 5.36. Hydrogen bonding interactions between adjacent units of complex **5.22**, hydrogen bonds are indicated as dashed lines and hydrogen atoms have been removed for clarity.

*5.7.2 Synthesis of [Cu**5.2**Cl_2], complex **5.23***

Ligand **5.2** was then reacted with another copper(II) salt also containing a strongly coordinating anion, in this case copper chloride, to form complex **5.23**. Dark green, rod like crystals suitable for X-ray crystallography were obtained from the acetonitrile reaction mixture after two weeks in 27% yield.

Complex **5.23** crystallises in the orthorhombic space group *Pbca* with one molecule of complex **5.23** present in the asymmetric unit.

Again **5.2** is able to chelate to the copper atom (Cu···N = 2.001(2) Å and 2.029(2) Å) and the two chloride ions also coordinate to the copper atom (Cu···Cl = 2.238(1) Å and 2.243(1) Å) giving the copper atom a distorted square planar geometry (angles around the copper centre range from 80.7(1)˚ to 98.1(1)˚, τ_4 = 0.19), as shown in figure 5.37. The central carbon atom of the propyl bridging backbone of **5.2** is disordered over two positions above and below the plane of the imidazole rings with one position is 60% occupied, the other 40%. The imidazole rings of **5.2** are again almost coplanar with a twist of only 2.4(1)˚.

Face-to-face and edge-to-face $\pi - \pi$ stacking interactions are present in complex **5.23** (ranging from 3.368(3) Å to 3.797(1)Å), and weak hydrogen bonds are also present from the chloride ions to the hydrogen atoms of the propyl bridged backbone of **5.2** in an adjacent molecule (C···Cl range from 3.557(5) Å to 3.906(3) Å).

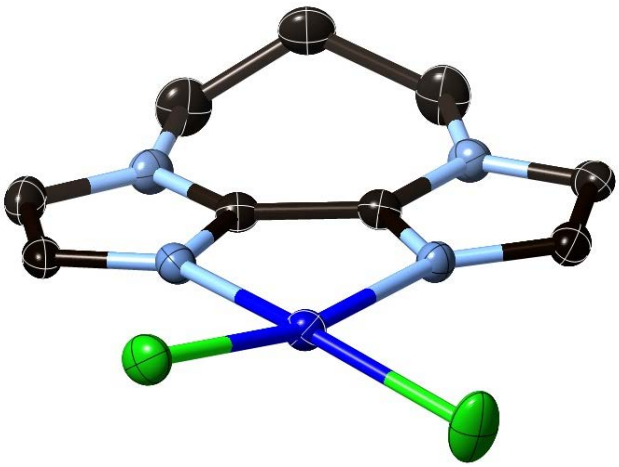

Figure 5.37. Asymmetric unit of complex **5.23**, disorder in the propyl backbone is not shown and hydrogen atoms have been removed for clarity.

*5.7.3 Synthesis of [Cu**5.2**$_2$(OH$_2$)$_2$][NO$_3$]$_2$, complex **5.24***

A copper(II) salt with a weakly coordinating anion, copper nitrate, was then used to form complex **5.24** when reacted with **5.2**. The use of a weaker anion should for the coordination of more than molecule of **5.2** to the copper centre. Dark green crystals suitable for X-ray diffraction were formed from the slow diffusion of diisopropyl ether into an acetonitrile solution of the reaction mixture in 10% yield. The complex crystallises in the monoclinic space group $P2_1/n$ with half a molecule of **5.24** present in the

asymmetric unit along with one nitrate anion. The weaker nitrate anion has allowed for two molecules of **5.2** to chelate to one copper atom, related by an inversion centre on the copper atom, with Cu···N distances = 2.032(1) Å and 2.046(2) Å, and again the twisting of the imidazole rings of **5.2** is minimal (0.9(1)˚). The coordination sphere of the octahedral copper atom (N-Cu-N = 82.0(1)˚ and 98.1(1)˚, N-Cu-O range from 89.7(1)˚ to 90.3(1)˚) is completed by two water molecules coordinated to the copper atom in axial positions (Cu···O = 2.376(1) Å), as shown in figure 5.38.

The nitrate counter ions hydrogen bond to two different water molecules in adjacent units of complex **5.24** (O···O = 2.843(2) Å and 2.887(2) Å), and each water molecule is in turn hydrogen bonding to two different nitrate anions. The third oxygen atom of the nitrate molecule is constrained in a hydrogen bonding pocket of a third unit of complex **5.24** (C···O = 3.254(2) Å and 3.565(2) Å), formed from the imidazole hydrogen atoms of **5.2**. These three hydrogen bonding interactions form a 3-dimensional network of complex **5.24** linked together by nitrate anions, as shown in figure 5.39.

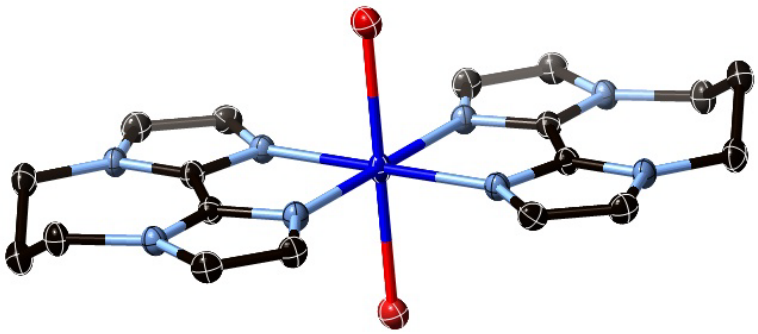

Figure 5.38. Two molecules of **5.2** chelating one copper molecule in complex **5.24**, nitrate anions and hydrogen atoms have been removed for clarity.

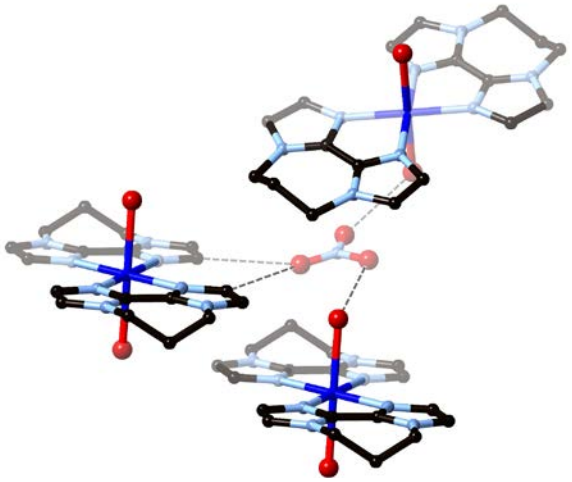

Figure 5.39. One nitrate anion hydrogen bonding to three different units of complex **5.24** through coordinated water molecules and imidazole hydrogen atoms, hydrogen bonds are indicated as dashed lines, hydrogen atoms have been removed for clarity.

*5.7.4 Synthesis of [Cu**5.2**$_2$(OH$_2$)$_2$]I$_2$, complex **5.25***

Ligand **5.2** was also reacted with CuI to form complex **5.25**. Dark green needles suitable for X-ray crystallography were obtained from the acetonitrile solution of the reaction mixture over the course of two weeks in 11% yield. The complex crystallises in the monoclinic space group $P2_1/n$ with half a molecule of **5.25** and one iodide anion present in the asymmetric unit. Like complex **5.24** above two molecules of **5.2** chelate one copper atom (Cu···N = 2.019(2) Å and 2.023(2) Å), and again the molecules of **5.2** are crystallographically related through an inversion centre on the copper atom. Two molecules of water are also coordinated to the copper atom (Cu···O = 2.364(3) Å) in axial positions to fufill the octahedral coordination geometry around the copper atom (N-Cu-N = 82.3(1)˚ and 97.7(1)˚ and N-Cu-O range from 87.3(1)˚ to 92.7(1)˚) . The bonding of **5.2** and the water molecules around the copper atom resembles that of complex **5.24**, refer to figure 5.38. Again the twisting of the imidazole rings in **5.2** is minimal (1.5(1)˚). During the course of the reaction copper(I) centre has been oxidised to a copper(II) centre.

The iodide ions form two moderate hydrogen bonds to water molecules from two neighbouring units of complex **5.25**, and each water molecule of the complex is in turn hydrogen bonded to two different iodide ions (O···I = 3.482(3) Å and 3.601(3) Å). This forms an extended two dimensional hydrogen bonding network, as shown in figure 5.40, where each unit of complex **5.25** interacts with four others through hydrogen bonding via an iodide ion. Loops involving four units of complex **5.25** and four iodide ions are formed, each iodide atom participates in two loops, while each complex unit participates in four loops

through both of the water molecules above and below the plane of **5.2**. Two chelating molecules of **5.2** from two neighbouring units point into each loop, filling the cavity. Sheets of the two dimensional network are interacting through weak hydrogen bonds formed by the imidazole hydrogen atoms and iodide ions of a neighbouring network (C···I = 4.019(3) Å and 4.469(3) Å).

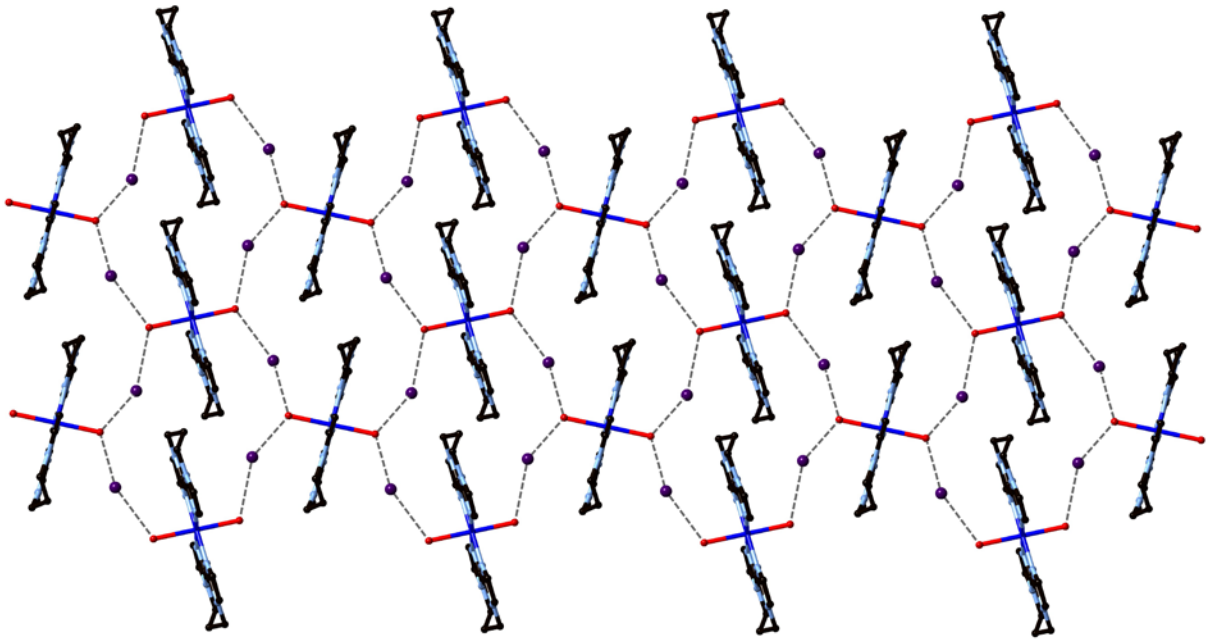

Figure 5.40. Extended 2-D hydrogen bonding network formed by the hydrogen bonding between water molecules of complex **5.25** and iodide ions, hydrogen bonds shown by dashed lines, hydrogen atoms not involved in hydrogen bonding have been omitted for clarity.

*5.7.5 Synthesis of [Cu**5.2**$_2$(OH$_2$)$_2$][ClO$_4$]$_2$, complex **5.26***

Finally **5.2** was reacted with copper(II) perchlorate, the weakest coordinating anion used for the formation of complexes with **5.2**, to form complex **5.26**. Light green crystals suitable for X-ray crystallography were obtained from the slow diffusion of diisopropyl ether into an acetonitrile solution of complex **5.26** in 12% yield. The complex crystallises in the monoclinic space group $P2_1/n$ with half a molecule of **5.26**, one perchlorate ion (disordered over two positions) present in the asymmetric unit. The middle carbon atom in the propyl backbone of ligand **5.2** is disordered over two positions, above and below the plane of the imidazole rings, as observed in complex **5.23**, one position is occupied 67% of the time, the other 33%.

Again two molecules of **5.2** chelate one copper atom (Cu···N = 2.024(4) Å and 2.028(4) Å), with two molecules of water coordinated to the copper atom in the axial position (Cu···O = 2.396(6) Å) to fulfill the coordination requirements of the copper atom. The twisting of the imidazole rings of **5.2** is again small (2.4(2)˚). The coordination of **5.2** and the water molecules around the copper atom resembles that

observed in complex **5.24**, refer to figure 5.38. The perchlorate anion is disordered over two positions with each position occupied 50% of the time.

One perchlorate anion hydrogen bonds to water molecules two neighbouring units of complex **5.26** (O···O = 2.500(20), 2.749(10) Å, 2.794(12) Å and 2.816(17) Å), as shown in figure 5.41, to form a two dimensional hydrogen bonding network, like that described for complex **5.25**.

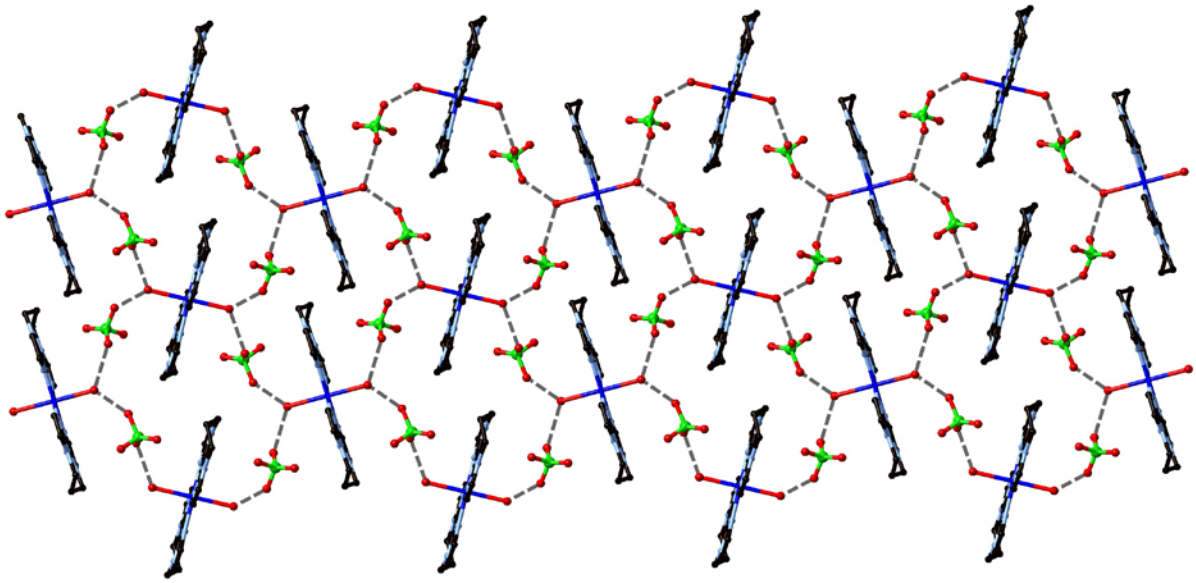

Figure 5.41. Extended 2-D hydrogen bonding network formed by the hydrogen bonding between water molecules of complex **5.26** and perchlorate anions, hydrogen bonds shown by dashed lines, perchlorate anion disorder and hydrogen atoms have been omitted for clarity.

Increasing the length of the N,N'-linking backbone has resulted in the chelation of copper(II) salts in all cases. When strongly coordinating anions are present only one molecule of **5.2** coordinates to the copper centre, the use of weaker anions allows the formation of a conserved coordination motif around the copper centre involving chelation of two molecules of **5.2** with two axial water molecules also coordinating.

5.8 Other complexes

Despite numerous attempts single crystals suitable for X-ray crystallography of complexes formed with various silver(I), copper(I) and copper(II) salts and **5.7** were not obtained. Attempts to crystallise the complex formed from $Ru(bpy)_2Cl_2$ and **5.7** with a variety of different methods was unsuccessful. Highly twinned crystals were grown, and these crystals were diffracted but gave poor data and a poor refinement. Despite the poor data enough information is given from the crystal structure solution to determine that **5.7**

coordinates in a monodentate fashion through one imidazole nitrogen atom, in accordance with Thummel *et al*'s preparation of a complex with $Ru(bpy)_2Cl_2$ and **5.7**[67] of which no crystal was isolated. The other coordination site of the ruthenium centre appears to be occupied by a molecule of acetonitrile.

5.9 Summary

The difference in backbone tether, metal ion and counterion used in the coordination chemistry of 2,2'-biimidazole ligands all play a significant role in the metallosupramolecular chemistry of these 2,2'-biimidazole ligands. In this chapter the coordination chemistry of N,N'-dimethylene-2,2'-biimidazole, **5.1**, and N,N'-trimethylene-2,2'-biimidazole, **5.2** were investigated with silver(I), copper(I) and copper(II), cadmium(II) and cobalt(II) metal ions and a range of counter ions. The lability of the silver(I) ion allowed for anion control of the metallosupramolecular structures formed with **5.1**, discrete structures were obtained with moderately coordinating anions and non coordinating anions allowed for a polymeric structure to be formed. In each case **5.1** bridges two silver(I) metal ions.

Dinuclear triple helicates were formed when **5.1** was coordinated to copper(I) ions no matter the anion present or its coordination strength. In three cases the dinuclear triple helicate enclathrates a benzene molecule, but when hexafluorophosphate is the anion no enclathration complex is formed. ^{1}H-NMR titrations show the dynamic nature of the helicate formation in solution, and anion competition studies show the enclathration complexes are formed preferentially over the hexafluorophosphate structure. Fluorobenzene is also enclathrated in the same manner by these dinuclear triple helicates, but hexafluorobenzene and mesitylene are not, demonstrating the dependence of the enclathration species on its size and electronic nature.

Ligand **5.1** also bridges copper(II) ions, but when complexed with cadmium(II) and cobalt(II) ions **5.1** is no longer bridging and instead coordinates in a monodentate fashion. The nitrogen atom of **5.1** not involved in metal coordination, participates in hydrogen bonding with a coordinated water molecule on the cadmium(II) or cobalt(II) metal ion.

The strain of the tethered backbone of **5.1** imparts a non-planar geometry onto the imidazole rings, pulling the nitrogen atoms apart and allowing the bridging if metal ions. In contrast the addition of only one more carbon atom, forming **5.2**, releases the strain on the imidazole ring and allowing for chelation. The reaction of **5.2** and copper(II) metal ions forms discrete coordination complexes in each case, with either one or two ligands bound to the copper(II) ion.

5.10 References

(1) Lehn, J.-M. *Angew. Chem. Int. Ed.* **1990**, *29*, 1304.

(2) Lindoy, L. F.; Atkinson, I. M. *Self-Assembly in Supramolecular Systems*; Royal Society of Chemistry: Cambridge, 2000.

(3) Fyfe, M. C. T.; Stoddart, J. F. *Acc. Chem. Res.* **1997**, *30*, 393.

(4) Lehn, J. M. *Supramolecular Chemistry*; VCH: Weinheim, 1995.

(5) Steed, J. W.; Atwood, J. L. *Supramolecular Chemistry*; John Wiley & Sons: West Sussex, 2000.

(6) Lehn, J.-M. *PNAS* **2002**, *99*, 4763.

(7) Steiner, T. *Angew. Chem. Int. Ed.* **2002**, *41*, 48.

(8) (a) Desiraju, G. R. *Acc. Chem. Res.* **1991**, *24*, 290, (b) Desiraju, G. R. *Acc. Chem. Res.* **1996**, *29*, 441.

(9) Aakeroy, C. B.; Seddon, K. R. *Chem. Soc. Rev.* **1993**, *22*, 397.

(10) Hunter, C. A. *Chem. Soc. Rev.* **1994**, *23*, 101.

(11) Janiak, C. *J. Chem. Soc. Dalton Trans.* **2000**, 3885.

(12) Fitchett, C. M., PhD. Thesis, University of Canterbury, 2002.

(13) Hunter, C. A.; Lawson, K. R.; Perkins, J.; Urch, C. J. *J. Chem. Soc. Perkin Trans. 2* **2001**, 651.

(14) Hunter, C. A.; Sanders, J. K. M. *J. Am. Chem. Soc* **1990**, *112*, 5525.

(15) Martinez, C. R.; Iverson, B. L. *Chem. Sci.* **2012**, *3*, 2191.

(16) (a) Grimme, S. *Angew. Chem. Int. Ed.* **2008**, *47*, 3430, (b) Bloom, J. W. G.; Wheeler, S. E. *Angew. Chem. Int. Ed.* **2011**, *50*, 7847.

(17) Gamez, P.; Mooibroek, T. J.; Teat, S. J.; Reedijk, J. *Acc. Chem. Res.* **2007**, *40*, 435.

(18) Constable, E. C. *Chemistry and Industry* **1994**, 56.

(19) Zampeze, J. A., PhD. Thesis, University of Canterbury, 2007.

(20) Piguet, C.; Bernardinelli, G.; Hopfgartner, G. *Chem. Rev.* **1997**, *97*, 2005.

(21) (a) Raymo, F. M.; Stoddart, J. F. *Chem. Rev.* **1999**, *99*, 1643, (b) Niu, Z.; Gibson, H. W. *Chem. Rev.* **2009**, *109*, 6024.

(22) (a) Wenz, G.; Han, B.-H.; Müller, A. *Chem. Rev.* **2006**, *106*, 782, (b) Harada, A.; Hashidzume, A.; Yamaguchi, H.; Takashima, Y. *Chem. Rev.* **2009**, *109*, 5974.

(23) Forgan, R. S.; Sauvage, J.-P.; Stoddart, J. F. *Chem. Rev.* **2011**, *111*, 5434.

(24) Seidel, S. R.; Stang, P. J. *Acc. Chem. Res.* **2002**, *35*, 972.

(25) (a) Dul, M.-C.; Pardo, E.; Lescouëzec, R.; Journaux, Y.; Ferrando-Soria, J.; Ruiz-García, R.; Cano, J.; Julve, M.; Lloret, F.; Cangussu, D.; Pereira, C. L. M.; Stumpf, H. O.; Pasán, J.; Ruiz-Pérez, C. *Coord. Chem. Rev.* **2010**, *254*, 2281, (b) Ruben, M.; Rojo, J.; Romero-Salguero, F. J.; Uppadine, L. H.; Lehn, J.-M. *Angew. Chem. Int. Ed.* **2004**, *43*, 3644, (c) Wurthner, F.; You, C.-

C.; Saha-Moller, C. R. *Chem. Soc. Rev.* **2004**, *33*, 133, (d) Fiedler, D.; Leung, D. H.; Bergman, R. G.; Raymond, K. N. *Acc. Chem. Res.* **2005**, *38*, 351.

(26) (a) Chakrabarty, R.; Mukherjee, P. S.; Stang, P. J. *Chem. Rev.* **2011**, *111*, 6810, (b) Swiegers, G. F.; Malefetse, T. J. *Chem. Rev.* **2000**, *100*, 3483.

(27) Leininger, S.; Olenyuk, B.; Stang, P. J. *Chem. Rev.* **2000**, *100*, 853.

(28) Yang, L.; Powell, D. R.; Houser, R. P. *Dalton Trans.* **2007**, 955.

(29) Addison, A. W.; Rao, T. N.; Reedijk, J.; van Rijn, J.; Verschoor, G. C. *J. Chem. Soc. Dalton Trans.* **1984**, 1349.

(30) Steel, P. J. *Acc. Chem. Res.* **2005**, *38*, 243.

(31) Gavrilova, A. L.; Bosnich, B. *Chem. Rev.* **2004**, *104*, 349.

(32) Steel, P. J. *Molecules* **2004**, *9*, 440

(33) Kaes, C.; Katz, A.; Hosseini, M. W. *Chem. Rev.* **2000**, *100*, 3553.

(34) (a) Xia, C.-K.; Lu, C.-Z.; Yuan, D.-Q.; Zhang, Q.-Z.; Wu, X.-Y.; Xiang, S.-C.; Zhang, J.-J.; Wu, D.-M. *Cryst. Eng. Comm.* **2006**, *8*, 281, (b) Jana, A. D.; Ghosh, A. K.; Ghoshal, D.; Mostafa, G.; Chaudhuri, N. R. *Cryst. Eng. Comm.* **2007**, *9*, 304, (c) Tadokoro, M.; Shiomi, T.; Isobe, K.; Nakasuji, K. *Inorg. Chem.* **2001**, *40*, 5476, (d) Hester, C. A.; Baughman, R. G.; Collier, H. L. *Polyhedron* **1997**, *16*, 2893, (e) Kirchner, C.; Krebs, B. *Inorg. Chem.* **1987**, *26*, 3569.

(35) Sang, R.-L.; Xu, L. *Eur. J. Inorg. Chem.* **2006**, *2006*, 1260.

(36) Atencio, R.; Chacon, M.; Gonzalez, T.; Briceno, A.; Agrifoglio, G.; Sierraalta, A. *Dalton Trans.* **2004**, 505.

(37) Gruia, L. M.; Rochon, F. D.; Beauchamp, A. L. *Acta. Cryst. E.* **2005**, *61*, m1604.

(38) Sang, R.-L.; Xu, L. *Inorg. Chim. Acta.* **2006**, *359*, 2337.

(39) Sang, R.; Xu, L. *Inorg. Chem.* **2005**, *44*, 3731.

(40) (a) Hay, B. P.; Gutowski, M.; Dixon, D. A.; Garza, J.; Vargas, R.; Moyer, B. A. *J. Am. Chem. Soc* **2004**, *126*, 7925, (b) Amendola, V.; Fabbrizzi, L.; Mosca, L. *Chem. Soc. Rev.* **2010**, *39*, 3889, (c) Fisher, M. G.; Gale, P. A.; Light, M. E.; Quesada, R. *Cryst. Eng. Comm.* **2008**, *10*, 1180, (d) Cui, X.; Delgado, R.; Carapuca, H. M.; Drew, M. G. B.; Felix, V. *Dalton Trans.* **2005**, 3297.

(41) (a) Rotger, C.; Soberats, B.; Quiñonero, D.; Frontera, A.; Ballester, P.; Benet-Buchholz, J.; Deyà, P. M.; Costa, A. *Eur. J. Org. Chem.* **2008**, *2008*, 1864, (b) Wu, B.; Huang, X.; Xia, Y.; Yang, X.-J.; Janiak, C. *Cryst. Eng. Comm.* **2007**, *9*, 676, (c) Zhu, X.; Lü, J.; Li, X.; Gao, S.; Li, G.; Xiao, F.; Cao, R. *Cryst. Growth. Des.* **2008**, *8*, 1897.

(42) (a) Mendy, J. S.; Pilate, M. L.; Horne, T.; Day, V. W.; Hossain, M. A. *Chem. Commun.* **2010**, *46*, 6084, (b) Miguel, P. J. S.; Roitzsch, M.; Yin, L.; Lax, P. M.; Holland, L.; Krizanovic, O.;

Lutterbeck, M.; Schurmann, M.; Fusch, E. C.; Lippert, B. *Dalton Trans.* **2009**, 10774, (c) Huang, B.; Santos, S. M.; Felix, V.; Beer, P. D. *Chem. Commun.* **2008**, 4610.

(43) (a) Jia, C.; Wu, B.; Li, S.; Yang, Z.; Zhao, Q.; Liang, J.; Li, Q.-S.; Yang, X.-J. *Chem. Commun.* **2010**, *46*, 5376, (b) Xia, Y.; Wu, B.; Liu, Y.; Yang, Z.; Huang, X.; He, L.; Yang, X.-J. *Cryst. Eng. Comm.* **2009**, *11*, 1849, (c) Ravikumar, I.; Lakshminarayanan, P. S.; Arunachalam, M.; Suresh, E.; Ghosh, P. *Dalton Trans.* **2009**, 4160.

(44) (a) Perera, T.; Marzilli, P. A.; Fronczek, F. R.; Marzilli, L. G. *Inorg. Chem.* **2010**, *49*, 5560, (b) Amendola, V.; Bergamaschi, G.; Boiocchi, M.; Fabbrizzi, L.; Milani, M. *Chem. Eur. J.* **2010**, *16*, 4368, (c) Smith, J. D.; Saykally, R. J.; Geissler, P. L. *J. Am. Chem. Soc* **2007**, *129*, 13847.

(45) Custelcean, R. *Chem. Soc. Rev.* **2010**, *39*, 3675.

(46) Gimeno, N.; Vilar, R. *Coord. Chem. Rev.* **2006**, *250*, 3161.

(47) Yuan, G.; Zhu, C.; Liu, Y.; Xuan, W.; Cui, Y. *J. Am. Chem. Soc* **2009**, *131*, 10452.

(48) (a) de Hoog, P.; Gamez, P.; Mutikainen, I.; Turpeinen, U.; Reedijk, J. *Angew. Chem. Int. Ed.* **2004**, *43*, 5815, (b) Berryman, O. B.; Johnson, D. W. *Chem. Commun.* **2009**, 3143, (c) Demeshko, S.; Dechert, S.; Meyer, F. *J. Am. Chem. Soc* **2004**, *126*, 4508.

(49) Kumazawa, K.; Yamanoi, Y.; Yoshizawa, M.; Kusukawa, T.; Fujita, M. *Angew. Chem. Int. Ed.* **2004**, *43*, 5936.

(50) Mal, P.; Breiner, B.; Rissanen, K.; Nitschke, J. R. *Science* **2009**, *324*, 1697.

(51) Pedersen, C. J. *J. Am. Chem. Soc* **1967**, *89*, 7017.

(52) Kumar, V. S. S.; Pigge, F. C.; Rath, N. P. *Cryst. Eng. Comm.* **2004**, *6*, 531.

(53) Copp, S. B.; Subramanian, S.; Zaworotko, M. J. *J. Chem. Soc. Chem. Commun.* **1993**, 1078.

(54) Bishop, R. *Chem. Soc. Rev.* **1996**, *25*, 311.

(55) Rahman, A. N. M. M.; Bishop, R.; Craig, D. C.; Marjo, C. E.; Scudder, M. L. *Cryst. Growth. Des.* **2002**, *2*, 421.

(56) Eddaoudi, M.; Kim, J.; Rosi, N.; Vodak, D.; Wachter, J.; O'Keeffe, M.; Yaghi, O. M. *Science* **2002**, *295*, 469.

(57) Youngme, S.; Cheansirisomboon, A.; Danvirutai, C.; Pakawatchai, C.; Chaichit, N.; Engkagul, C.; van Albada, G. A.; Costa, J. S.; Reedijk, J. *Polyhedron* **2008**, *27*, 1875.

(58) Koberl, M.; Cokoja, M.; Bechlars, B.; Herdtweck, E.; Kuhn, F. E. *Dalton Trans.* **2011**, *40*, 11490.

(59) Cotton, F. A.; Kim, Y. *J. Am. Chem. Soc* **1993**, *115*, 8511.

(60) Cotton, F. A.; Lin, C.; Murillo, C. A. *Acc. Chem. Res.* **2001**, *34*, 759.

(61) Barquín, M.; Cocera, N.; González Garmendia, M. J.; Larrínaga, L.; Pinilla, E.; Torres, M. R. *J. Coord. Chem.* **2010**, *63*, 2247.

(62) Kozlevčar, B.; Radišek, M.; Jagličić, Z.; Merzel, F.; Glažar, L.; Golobič, A.; Šegedin, P. *Polyhedron* **2007**, *26*, 5414.

(63) Cotton, F. A.; Lin, C.; Murillo, C. A. *PNAS* **2002**, *99*, 4810.

(64) Rao, V. M.; Sathyanarayana, D. N.; Manohar, H. *J. Chem. Soc. Dalton Trans.* **1983**, 2167.

(65) Spingler, B.; Schnidrig, S.; Todorova, T.; Wild, F. *Cryst. Eng. Comm.* **2012**, *14*, 751.

(66) Thummel, R. P.; Goulle, V.; Chen, B. *J. Org. Chem.* **1989**, *54*, 3057.

(67) Goulle, V.; Thummel, R. P. *Inorg. Chem.* **1990**, *29*, 1767.

(68) (a) Widlicka, D. W.; Wong, E. H.; Weisman, G. R.; Lam, K.-C.; Sommer, R. D.; Incarvito, C. D.; Rheingold, A. L. *Inorg. Chem. Commun.* **2000**, *3*, 648, (b) Li, J.; Widlicka, D. W.; Fichter, K.; Reed, D. P.; Weisman, G. R.; Wong, E. H.; DiPasquale, A.; Heroux, K. J.; Golen, J. A.; Rheingold, A. L. *Inorg. Chim. Acta.* **2010**, *364*, 185.

(69) Widlicka, D. W.; Wong, E. H.; Weisman, G. R.; Sommer, R. D.; Incarvito, C. D.; Rheingold, A. L. *Inorg. Chim. Acta.* **2002**, *341*, 45.

(70) Matsumoto, S.; Batmunkh, E.; Akazome, M.; Takata, Y.; Tamano, M. *Org. & Biomol. Chem.* **2011**, *9*, 5941.

(71) (a) Steel, P. J.; Fitchett, C. M. *Coord. Chem. Rev.* **2008**, *252*, 990, (b) Fitchett, C. M.; Steel, P. J. *Polyhedron* **2007**, *26*, 400, (c) Li, C.-P.; Wu, J.-M.; Du, M. *Inorg. Chem.* **2011**, *50*, 9284, (d) Liddle, B. J.; Hall, D.; Lindeman, S. V.; Smith, M. D.; Gardinier, J. R. *Inorg. Chem.* **2009**, *48*, 8404, (e) Chen, C.; Kang, B.; Su, C. *Aust. J. Chem.* **2006**, *59*, 3, (f) Stephenson, A.; Ward, M. D. *Chem. Commun.* **2012**, *48*, 3605, (g) Halder, P.; Zangrando, E.; Paine, T. K. *Dalton Trans.* **2009**, 5386, (h) Fitchett, C. M.; Steel, P. J. *Dalton Trans.* **2006**, 4886, (i) Slenters, T. V.; Sagué, J. L.; Brunetto, P. S.; Zuber, S.; Fleury, A.; Mirolo, L.; Robin, A. Y.; Meuwly, M.; Gordon, O.; Landmann, R.; Daniels, A. U.; Fromm, K. M. *Materials* **2010**, *3*, 3407.

(72) (a) Young, A. G.; Hanton, L. R. *Coord. Chem. Rev.* **2008**, *252*, 1346, (b) Zhang, T.; Song, H.; Dai, X.; Meng, X. *Dalton Trans.* **2009**, 7688.

(73) (a) Chakraborty, B.; Halder, P.; Paine, T. K. *Dalton Trans.* **2011**, *40*, 3647, (b) McMorran, D. A. *Inorg. Chem.* **2008**, *47*, 592, (c) Feazell, R. P.; Carson, C. E.; Klausmeyer, K. K. *Inorg. Chem.* **2006**, *45*, 935.

(74) (a) Carlucci, L.; Ciani, G.; Proserpio, D. M.; Visconti, M. *Cryst. Eng. Comm.* **2011**, *13*, 5891, (b) Wei, W.; Yu, H.; Jiang, F.; Liu, B.; Ma, J.; Hong, M. *Cryst. Eng. Comm.* **2012**, *14*, 1693.

(75) Blake, A. J.; Baum, G.; Champness, N. R.; Chung, S. S. M.; Cooke, P. A.; Fenske, D.; Khlobystov, A. N.; Lemenovskii, D. A.; Li, W.-S.; Schroder, M. *J. Chem. Soc. Dalton Trans.* **2000**, 4285.

(76) Gulbransen, J. L.; Fitchett, C. M. *Cryst. Eng. Comm.* **2012**, *14*, 5394.

(77) Bosch, E.; Barnes, C. L. *Inorg. Chem.* **2002**, *41*, 2543.

(78) (a) Pyykkö, P. *Chem. Rev.* **1997**, *97*, 597, (b) Schmidbaur, H.; Schier, A. *Chem. Soc. Rev.* **2008**, *37*, 1931, (c) Burgess, J. M., PhD. Thesis, University of Canterbury, 2009.

(79) (a) Dennehy, M.; Quinzani, O. V.; Mandolesi, S. D.; Burrow, R. A. *J. Mol. Struct.* **2011**, *998*, 119, (b) Ronson, T. K.; Adams, H.; Ward, M. D. *Eur. J. Inorg. Chem.* **2005**, *2005*, 4533, (c) J. Blake, A.; R. Champness, N.; N. Khlobystov, A.; A. Lemenovskii, D.; Li, W.-S.; Schroder, M. *Chem. Commun.* **1997**, 1339, (d) Suenaga, Y.; Gang Yan, S.; Ping Wu, L.; Ino, I.; Kuroda-Sowa, T.; Maekawa, M.; Munakata, M. *J. Chem. Soc. Dalton Trans.* **1998**, 1121.

(80) Simon, N. J.; Drexler, E. S.; Reed, R. P. "Properties of copper and copper alloys at cryogenic temperatures," Natl. Inst. Stand. Technol. (MSEL), 1992.

(81) van Niekerk, J. N.; Schoening, F. R. L. *Nature* **1953**, *171*, 36

Chapter Six:

Conclusions and future work

6.1 Conclusions

This thesis has described the preparation of a series of model compounds with heterocyclic five – membered rings substituted with multiple peripheral aryl rings and the ability of the peripheral aryl rings to undergo oxidative cyclodehydrogenation and photocyclisation to form carbon-carbon bonds, with a view towards the synthesis of curved heterocyclic aromatic systems. Synthetic strategies were used for the preparation of 2,3-diarylindole, 2,3,4,5-tetraarylpyrrole and pentaarylpyrrole compounds where the aryl group could be easily varied allowing for more activating and solubilising substituents to be attached to the peripheral aryl groups. Carbon-carbon bonds were formed between the peripheral aryl rings for each class of compound using either oxidative cyclodehydrogenation or photocyclisation and determination of the position of the carbon-carbon bond(s) in the resulting compounds was determined by ^{1}H-NMR spectroscopy and X-ray crystallography where appropriate.

6.1.1 Oxidative cyclodehydrogenation

Various conditions for oxidative cyclodehydrogenation were investigated during the course of this study. The use of $AlCl_3$/oxidant as the reagent for oxidative cyclodehydrogenation was trialled with both 2,3-diarylindole and 2,3,4,5-tetraarylpyrrole model compounds and pentaphenylpyrrole. In each case a low yield of cyclodehydrogenated product was obtained that could not be isolated from the reaction mixture. $FeCl_3$ was also used as a reagent for oxidative cyclodehydrogenation, added to the reaction both as a solid or dissolved in nitromethane. In most cases the formation of multiple products was observed, and in the cases where products could be isolated from the reaction mixture the formation of only one carbon-carbon bond between the peripheral aryl rings in the 2- and 3-position of the heterocyclic core was observed, resulting the formation of dibenzo[*a*,c]carbazoles from the corresponding 2,3-diarylindoles and N-benzyl-2,3-diaryl-dibenzo[*e,g*]indoles from the corresponding N-benzyl-2,3,4,5-tetraarylpyrroles. These reactions proceeded in low yields. In only one case did oxidative cyclodehydrogenation form more than one carbon-carbon bond, when N-ethyl-2,3,4,5-tetraphenylpyrrole was subjected to oxidative cyclodehydrogenation with 45 equivalents of $FeCl_3$ and 3,6,12,15-tetrachloro-9-ethyl-tetrabenzo[*a,c,g,i*]carbazole was isolated. Carbon-carbon bonds were formed between the phenyl rings in the 2- and 3-position of the pyrrole ring, as well as between the phenyl rings in the 4- and 5-position. Chlorination of all four phenyl rings also occurs and the X-ray crystal structure obtained demonstrates the significant distortion in the aromatic tetrabenzo[*a,c,g,i*]carbazole system, due to the steric strain between the two ortho hydrogen atoms of the peripheral aryl rings in the 3- and 4-position of the pyrrole core. The aryl rings in the 3- and 4-position of the pyrrole core are twisted at an angle of 38˚ to each other.

6.1.2 Photocyclisation

Photocyclisation reactions of the 2,3-diarylindole, 2,3,4,5-tetraarylpyrrole and pentaarylpyrrole compounds were also investigated during the course of this study. The photocyclisation reactions proceeded in high yields to form dibenzo[*a*,*c*]carbazoles from 2,3-diarylindoles, and N-ethyl-2,3-diaryl-dibenzo[*e*,*g*]indoles from N-ethyl-2,3,4,5-tetraarylpyrroles. The N-benzyl-2,3,4,5-tetraarylpyrrole compounds formed multiple products when subjected to photocyclisation and 3-benzyl-2,3-diaryl-dibenzo[*e*,*g*]indole compounds were isolated from the reaction mixture in low yields. The compounds have formed a carbon-carbon bond between the aryl rings in the 2- and 3-position of the pyrrole core but the benzyl group has also undergone a 1,3-shift to losing the aromaticity in the pyrrole ring and sp^3 hybridising the carbon atom in the 3-position of this ring. The carbon-carbon bond formation and 1,3-shift in one pot is unprecedented. Photocyclisation allowed for the preparation of reasonable quantities of N-ethyl-2,3-diaryl-dibenzo[*e*,*g*]indoles to investigate the possible step-wise carbon-carbon bond formation of the pyrrole systems, but subsequent oxidative cyclodehydrogenation was unsuccessful and photocyclisation returned only starting materials. ^{1}H-NMR spectroscopy and mass spectroscopy indicate the formation of one carbon-carbon bond when pentaphenylpyrrole was subjected to photocyclisation conditions, which has tentatively been assigned to the carbon-carbon bond formation between the phenyl rings in the 2- and 3-position of the pyrrole core.

6.3 Metallosupramolecular chemistry

The metallosupramolecular chemistry of two backbone linked 2,2'-biimidazole compounds were investigated with a variety of different metal ion and counter ions. The length of the backbone played a significant role in controlling the bridging or chelating ability of the 2,2'-biimidazole. Complexes of silver(I), copper(I) and copper(II) ions all formed where the ethyl bridged 2,2'-biimidazole ligand was bridging two metal centres. In contrast cadmium(II) and cobalt(II) ions formed monodenate complexes with the ethyl bridged 2,2'-biimidazole ligand and the free nitrogen atom formed hydrogen bonds to a coordinated water molecule. The propyl bridged 2,2'-biimidazole ligand formed exclusively chelating complexes with copper(II) ions, with either one or two ligands chelating the metal centre depending on the coordinating strength of the anion used.

<u>6.2 Future work</u>

6.2.1 2,3-diarylindole compounds

The variability of the 2,3-diarylindole model compounds investigated in this thesis was limited to alkyl substitution on the nitrogen atom and electron donating and solubilising substitution at the 4-position of the peripheral aryl ring. Further work towards investigating the oxidative cyclodehydrogenation and

photocyclisation of these compounds, and increasing the yield and stability of the compounds formed through oxidative cyclodehydrogenation, could incorporate the use of electron withdrawing groups on the nitrogen atom, such as benzoyl and acyl groups. Different substituents could also be incorporated around the phenyl ring on the indole core to probe the role the electronic nature of the indole ring plays in the carbon-carbon bond forming reaction.

6.2.2 2,3,4,5-tetraarylpyrrole compounds

The isolation of 3,6,12,15-tetrachloro-9-ethyl-tetrabenzo[*a*,*c*,*g*,*i*]carbazole from the oxidative cyclodehydrogenation reaction opens up the possibility of using transition metal catalysed reactions to appended different functionality to all four phenyl rings after cyclodehydrogenation reaction. The incorporation of 4-bromo substituents on the peripheral aryl groups would also allow these reactions to take place. Incorporation of a 4-bromo substituent on the peripheral aryl groups would also be interesting as the bromo substitution would remove electron density from the phenyl rings and is also ortho, para activating, possibly altering the oxidative cyclodehydrogenation reaction. The nature of the peripheral phenyl rings could also be modified to larger fused systems, like naphthalene, so that the resulting cyclodehydrogenated compounds would posses more fused rings and may be more rigid, allowing more structure to be seen in their UV/vis and emission spectra. Preliminary work has also been carried out to probe why the N-benzyl group of the 2,3,4,5-tetraarylpyrrole is able to undergo rearrangement during photocyclisation and the N-ethyl group and N-benzyl-2,3-diarylindoles does not. This can be further extended to understand the nature of the photocyclisation and difference in photocyclisation for the N-substituted-2,3,4,5-tetraarylpyrrole compounds. The photocyclisation of heteroaromatic compounds with peripheral aryl groups has not been extensively explored in the literature. The work presented in this thesis can be used as a platform to explore photocyclisation of heteroaromatic compounds, with a view towards the formation of compounds with multiply fused aromatic rings.

6.2.3 Pentaarylpyrrole compounds

Only a small quantity of pentaarylpyrrole compounds described in this thesis were made, and as a result this limited the investigation of the ability of these compounds to undergo oxidative cyclodehydrogenation and photocyclisation. Alternative reagents, like DDQ/H^+, also need to be investigated for their ability to form carbon-carbon bonds on this particular system. Further work is also needed to form a comprehensive family of pentaarylpyrrole compounds using the Suzuki coupling reaction of aryl boronic acids and 1,2,5-triaryl-3,4-dibromopyrroles. Not explored in this thesis was the synthesis of compounds with activating substituents, such as fluorine, in the ortho positions of the peripheral phenyl rings. These activating groups may provide a route to form a curved aromatic system

with a heterocyclic pyrrole ring at the core. Harsher conditions for the cyclodehydrogenation reaction were also not explored, for example flash vacuum pyrolysis, which may provide the extra energy required to form a curved corannulene-like compound.

Thin films of the cyclodehydrogenated and photocyclised compounds prepared here, along with their precursors, were not prepared during this study. The thin films of these compounds need to be prepared in order to measure their optical properties to assess the possibility of their use in organic devices.

6.2.4 Backbone linked 2,2'-biimidazole ligands

Only two ligands were used in this study of the coordination chemistry of backbone linked 2,2'-biimidazole ligands. The synthesis of a phenyl-linked backbone was also reported in this thesis, although no coordination complexes were isolated. The synthesis of 2,2'-biimidazole ligands with different backbones would extend the work completed here. A methylene bridged backbone 2,2'-biimidazole should pull the nitrogen atoms of the 2,2'-biimidazole even further apart, leading to new coordination motifs. Oxidation of the ethyl linked 2,2'-biimidazole to form an ethene linked 2,2'-biimidazole should decrease the torsion seen in the ethylene backbone and induce even more strain into the ligand, affecting the ability of the ligand to coordinate to metal ions.

Chapter Seven:

Experimental

General Information

Unless otherwise specified, all reagents and starting materials were reagent grade, purchased from standard suppliers and used as received. Water was purified by reverse osmosis *in-house*. Where anhydrous solvents were required, the HPLC-grade solvent was either distilled from standard drying agents or dried by passing over a sealed column of activated alumina. Melting points were recorded on an Electrothermal melting point apparatus and are uncorrected. Elemental analysis was carried out by Campbell Microanalytical Laboratory, University of Otago. Except where otherwise specified, all reactions were carried out in air.

Infrared Spectroscopy

All infrared spectra were recorded on a Perkin-Elmer Spectrum One FTIR instrument operating in diffuse reflectance mode with samples prepared as KBr mulls (KBr). The following abbreviations are used: s: strong, m: medium, w: weak, sh: shoulder, br: broad.

Mass spectroscopy

Mass spectra were recorded by Dr Marie Squire and Dr Meike Holzenkaempfer on either a DIONEX Ultimate 3000 or Bruker MaXis 4G spectrometer, both of which were operated in high resolution positive ion electrospray mode. Samples were dissolved and diluted to the required concentration in HPLC grade acetonitrile or methanol.

Nuclear Magnetic Resonance

All spectra were recorded on a Varian INOVA 500, Varian Unity 300, or an Agilent 400-MR instrument operating at 500, 300 and 400 MHz, respectively, for ^{1}H, and 125, 75 and 125 MHz, respectively, for ^{13}C. All samples were dissolved in commercially available deuterated solvents $CDCl_3$ and CD_3CN. Spectra were referenced to the residual solvent peaks and/or TMS. COSY, HSQC and HMBC experiments were employed where required, using standard Varian and Agilent pulse sequences.

UV/visible spectroscopy

UV/Visible spectra were recorded on a Varian CARY UV/Visible spectrometer in the range 225 – 800 nm for dichloromethane and 200 – 800 nm for acetonitrile. Samples were measured at room temperature in quartz curvettes of path length 1 cm and approximate capacity 3 mL.

Fluorometry

Emission spectra were recorded on a Horiba Fluorolog-3 spectrometer in the range 300 – 600 nm for dichloromethane. Samples were measured at room temperature in quartz curvettes of path length 1 cm and approximate capacity 3 mL.

X-Ray Crystallography

Refinement data is presented in Appendix 1. X-ray crystallographic data collection and refinement was carried out with either a Bruker APEXII instrument, using graphite-monochromated Mo Kα (λ = 0.71073 Å) radiation, or an Oxford-Agilent SuperNova instrument with focused microsource Cu Kα (λ = 1.5418 Å) radiation and ATLAS CCD area detector. All structures were solved using direct methods with SHELXS[1] and refined on F^2 using all data by full matrix least-squares procedures with SHELXL-97[2] within OLEX-2.[3] Non-hydrogen atoms were refined with anisotropic displacement parameters. Hydrogen atoms were included in calculated positions, or were manually assigned from residual electron density where appropriate, with isotropic displacement parameters 1.2 times the isotropic equivalent of their carrier atoms. The functions minimized were $\Sigma w(F2o-F2c)$, with $w=[\sigma 2(F2o)+aP2+bP]$-1, where $P=[\max(Fo)2+2F2c]/3$. Some of the refinements reported may change a little upon preparation for final publication. Graphical representations of crystallographic data were prepared using the CrystalMaker. Crystallographic data for all compounds is included in .cif format as electronic supplementary information.

Chapter Two

The following compounds were prepared according to literature methods, and all characterisation data were found to be consistent with that provided; 4,4'-dimethylbenzoin **2.3a**,[4] N*H*-2,3-bis(4-methoxyphenyl)indole **2.2**,[5] and N-ethyl-2,3-bis(4-methoxyphenyl)indole **2.6**,[5] 4'-chloro-2,2':6',2''terpyridine **2.28**[6] and [Ru(terpy)(Cl-terpy][PF_6]$_2$, **2.29**.[7]

Synthesis of 4,4'-di*tert*butylbenzoin, **2.4a**[8]

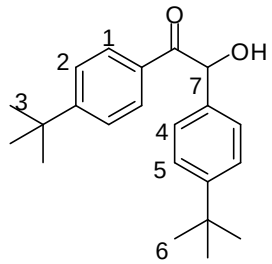

In a round bottom flask potassium cyanide (3.20 g, 49.1 mmol) was dissolved in 15 mL of water, and a solution of 4-*tert*butylbenzaldehyde (15.0 g, 15.5 mL, 92.5 mmol) in 25 mL of ethanol was added. The reaction mixture was refluxed for two hours, and a white solid precipitated. After cooling the solid was filtered, and recrystallised from ethanol. Yield: 12.8 g (85%). m.p. 157 – 158 ˚C; ^{1}H NMR (300MHz, $CDCl_3$): δ_H 7.87 (d, 2H, *J* = 8 Hz, H2), 7.40 (d, 2H, *J* = 8 Hz, H5), 7.34 (d, 2H, *J* = 8 Hz, H4), 7.27 (d, 2H, *J* = 8 Hz, H1), 5.90 (s, 1H, H7), 1.36 (s, 9H, CH_3, H6), 1.40 (s, 9H, CH_3, H3).

Synthesis of N*H*-2,3-diarylindoles, **2.1** – **2.4**

General procedure for the synthesis of N*H*-2,3-diarylindoles, **2.1** – **2.4**

Following a modified literature procedure,[5] in a round bottom flask was added aniline, the appropriately substituted anisoin and conc. hydrochloric acid and the mixture was heated to reflux for one hour at 110˚C. The temperature was then increased to 180˚C and water was distilled off for one hour. The solution was left to cool overnight and then portioned between 50mL diethyl ether and 50mL water. The layers were separated and the water layer was washed with 2x 50mL diethyl ether. The combined diethyl ether layers were washed with 3x 100mL 10% hydrochloric acid, 3x 100mL water, 3x 100mL 5% sodium hydroxide, 3x 100mL water and 2x 50mL brine. The organic layers were then dried with sodium sulfate and the solvent removed *in vacuo*. The solid was further dried under a high vacuum.

Synthesis of N*H*-2,3-diphenylindole, **2.1**[9]

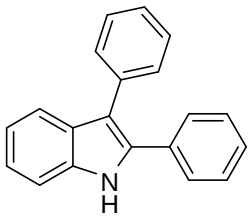

Benzoin (1.57 g, 7.4 mmol), aniline (3.48 g, 3.4 mL, 37.0 mmol), conc. hydrochloric acid (0.50 mL). Yield: 0.93 g (47%). m.p. = 120 – 123 ˚C; ^{1}H NMR (300MHz, $CDCl_3$): δ_H 8.21 (s, 1H, N*H*), 7.68 (d, 1H, *J* = 8 Hz), 7.46 – 7.15 (m, 13H).

Synthesis of N*H*-2,3-bis(4-methylphenyl)indole, **2.3**[10]

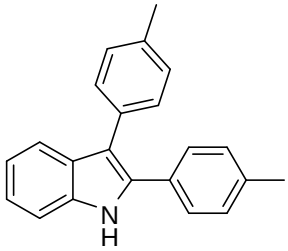

2.3a (1.30 g, 5.39 mmol), aniline (4.02 g, 3.95 mL, 43.2 mmol), conc. hydrochloric acid (0.370 mL). Yield: 0.840 g (52%). m.p. = 218 – 220 ˚C; ^{1}H NMR (500MHz, $CDCl_3$): δ_H 8.19 (s, 1H, N*H*), 7.68 (d, 1H, *J* = 8 Hz), 7.43 (d, 1H, *J* = 8 Hz), 7.36 – 7.33 (m, 4H), 7.26 – 7.20 (m, 3H), 7.17 – 7.14 (m, 3H), 2.41 (s, 3H, CH_3), 2.37 (s, 3H, CH_3).

Synthesis of N*H*-2,3-bis(4-*tert*butylphenyl)indole, **2.4**

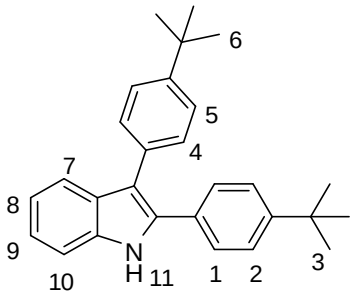

2.4a (1.56 g, 4.80 mmol), aniline (3.57 g, 3.50 mL, 38.4 mmol), conc. hydrochloric acid (0.30 mL). Yield: 0.92 g (50%). m. p. 123 – 125 ˚C; ^{1}H NMR (500MHz, $CDCl_3$): δ_H 8.18 (s, br, 1H, N*H*, H11), 7.69 (d, 1H, *J* = 8 Hz, H7), 7.42 – 7.34 (m, 9H, H1, H2, H4, H5, H10), 7.24 (t, 1H, *J* = 8 Hz, H9), 7.13 (t, 1H, *J* = 8 Hz, H8), 1.38 (s, 9H, H3), 1.34 (s, 9H, H6); ^{13}C NMR (125MHz, $CDCl_3$): δ_C 150.6 C2a, 148.9 C5a, 135.8 C1a, 133.8 C4a, 132.1, 1230.0, 129.7, 127.6, 125.6, 125.3, 122.4 C9, 120.2 C8, 119.9 C7, 114.6, 110.7 C10, 31.5 C3, 31.2 C6; MS(ESI): m/z: calc for $C_{28}H_{31}NNa$ ([**2.4** + Na]$^+$): 404.2354, found: 404.2351; IR (KBr) *v*/cm^{-1}: 3411 m, 2970 s, br, 2903 m, sh, 2867 m, sh, 1523 m, 1456 s, 1363 m, 1329 m, 1268 m, 1114 m, 1016 m, 969 m, 838 s, 739 s; UV-Vis λ_{max} (ε): 249 nm (31542), 310 nm (20477); Fluorometry λ_{max}: 417 nm.

Synthesis of N-ethyl-2,3-diarylindoles, **2.5** – **2.8**

General procedure for the synthesis of N-ethyl-2,3-diarylindoles, **2.5** – **2.8**

Following a modified literature procedure,[11] in a round bottom flask flushing with N_2, was added the appropriate N*H*-2,3-diarylindole and 10 mL dry dimethylformamide. The solution was cooled to 0˚C using an ice bath and sodium hydride was added. The solution was stirred at 0˚C for 10 minutes and then ethyl bromide was added and the solution was stirred at room temperature overnight. The solution was poured into 100 mL water and extracted with 3x 75 mL ethyl acetate. The combined organic layers were washed with 3x 200 mL water, dried with sodium sulfate and the solvent removed *in vacuo*. The solid obtained was recrystallised from ethyl acetate / hexanes.

Synthesis of N-ethyl-2,3-diphenylindole, **2.5**[12]

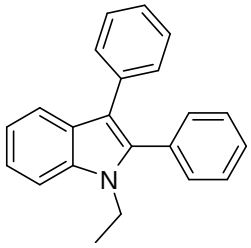

2.1 (1.08 g, 4 mmol), sodium hydride (0.30 g, 12 mmol), ethyl bromide (0.53 g, 0.36 mL, 4.8 mmol). Yield: 0.80 g (67%). m.p. = 127 – 128 ˚C; ^{1}H NMR (500MHz, $CDCl_3$): δ_H 7.81 (d, 1H, *J* = 8 Hz), 7.44 (d, 1 H, *J* = 8 Hz), 7.40 – 7.15 (m, 12H), 4.14 (q, 2H, *J* = 7 Hz, CH_2), 1.24 (t, 3H, *J* = 7 Hz, CH_3).

Synthesis of N-ethyl-2,3-bis(4-methoxyphenyl)indole, **2.6**[13]

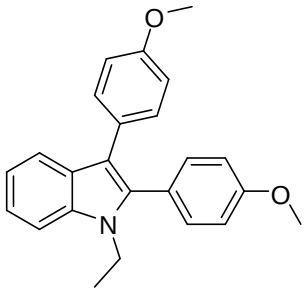

2.2 (1 g, 3 mmol), sodium hydride (0.22 g, 9.25 mmol), ethyl bromide (0.39 g, 0.28 mL, 3.63 mmol). Yield: 0.70 g (65%). m.p. = 101 – 105 ˚C; ^{1}H NMR (500MHz, $CDCl_3$): δ_H 7.76 (d, 1H, *J* = 8 Hz), 7.42 (d, 1H, *J* = 8 Hz), 7.27 – 7.21 (m, 5H), 7.16 (t, 1H, *J* = 8 Hz), 6.92 (d, 2H, *J* = 9 Hz), 6.82 (d, 2H, *J* = 9 Hz), 4.12 (q, 2H, *J* = 7 Hz, CH_2), 3.85 (s, 3H, OCH_3), 3.80 (s, 3H, OCH_3), 1.28 (t, 3H, *J* = 7 Hz, CH_3).

Synthesis of N-ethyl-2,3-bis(4-methylphenyl)indole, **2.7**

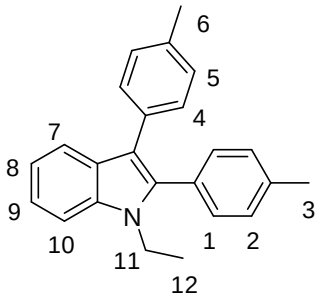

2.3 (1 g, 3.36 mmol), sodium hydride (0.24 g, 10.1 mmol), ethyl bromide (0.44 g, 0.30 mL, 4.03 mmol). Yield: 0.92 g (84%). m.p. 115 – 118 ˚C; ^{1}H NMR (500MHz, $CDCl_3$): δ_H 7.79 (d, 1H, *J* = 8 Hz, H7), 7.43 (d, 1H, *J* = 8 Hz, H10), 7.28 – 7.17 (m, 8H, H1, H2, H4, H8, H9), 7.08 (d, 2H, *J* = 8 Hz, H5), 4.12 (q, 2H, *J* = 7.5 Hz, CH_2, H11), 2.40 (s, CH_3, 3H, H3), 2.33 (s, CH_3, 3H, H6), 1.29 (t, 3H , *J* = 7.5 Hz, CH_3, H12); ^{13}C NMR (125MHz, $CDCl_3$): δ_C 137.8, 137.2, 136.0, 134.8, 132.3, 130.9, 129.6, 129.3, 129.1, 128.9 C5, 127.3, 121.8, 119.9, 119.7 C7, 115.0, 109.7 C10, 38.5 C11, 21.4 C3, 21.2 C6, 15.4 C12; ESMS: calc for $C_{24}H_{24}N$ ([**2.7** + H]$^+$) = 326.1909, found: 326.1903; IR (KBr) ν/cm^{-1}: 2979 m, 2917 m, 1520 m, 1460 s, 1349 s, 1332 m, 1237 m, 1096 m, 1019 m, 932 m, 836 m, 819 s, 801 s, 746 s; UV-Vis λ_{max} (ε): 240 nm (18386), 289 nm (10658); Fluorometry λ_{max}: 420 nm.

Synthesis of N-ethyl-2,3-bis(4-*tert*butylphenyl)indole, **2.8**

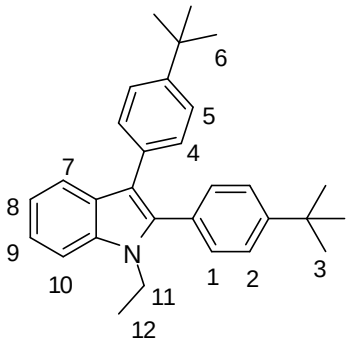

2.4 (1 g, 2.62 mmol), sodium hydride (0.18 g, 7.86 mmol), ethyl bromide (0.34 g, 0.25 mL, 3.17 mmol). Yield: 0.73 g (68%). m.p. 134 – 137 ˚C; ^{1}H NMR (500MHz, $CDCl_3$): δ_H 7.82 (d, 1H, *J* = 8 Hz, H7), 7.43 – 7.38 (m, 5H), 7.28 – 7.23 (m, 5H), 7.16 (t, 1H, *J* = 8 Hz, H8), 4.11 (q, 2H, *J* = 7 Hz, CH_2, H11), 1.36 (s, 9H, H3), 1.31 (s, 9H, H6), 1.28 (t, 3H, *J* = 7 Hz, CH_3, H12); ^{13}C NMR (125MHz, $CDCl_3$): δ_C 151.1, 148.0, 137.5, 136.2, 132.5, 130.9, 129.5, 127.7, 125.5, 125.2, 122.0, 120.2 C7, 120.0 C8, 115.1, 109.9, 38.8 C11, 31.7 C3, 31.2 C6, 15.7 C12; ESMS: calc for $C_{30}H_{35}NNa$ ([**2.8** + Na]$^+$) = 432.2662, found: 432.2661; IR (KBr) ν/cm^{-1}: 2956 s, 2902 s, sh, 2865 s, sh, 1464 s, 1362 s, 1335 s, 1268 s, 1236 s, 1111 m, 1018 m, 934 m, 839 s, 748 s, 740 s; UV-Vis λ_{max} (ε): 235 nm (30065), 288 nm (14707); Fluorometry λ_{max}: 421 nm.

Synthesis of N-benzyl-2,3-diarylindoles, **2.9** – **2.12**

General procedure for the synthesis of N-benzyl-2,3-diarylindoles, **2.9** – **2.12**

Following a modified literature procedure,[11] in a round bottom flask flushing with N_2, was added the appropriate N*H*-2,3-diarylindole and 10 mL dry dimethylformamide. The solution was cooled to 0˚C using an ice bath and sodium hydride was added. The solution was stirred at 0˚C for 10 minutes and then benzyl bromide was added and the solution stirred at room temperature overnight. The solution was poured into 100 mL water and extracted with 3x 75 mL ethyl acetate. The combined organic layers were washed with 3x 200 mL water, dried with sodium sulfate and the solvent removed *in vacuo*. The solid was recrystallised from ethyl acetate/hexanes.

Synthesis of N-benzyl-2,3-diphenylindole, **2.9**[14]

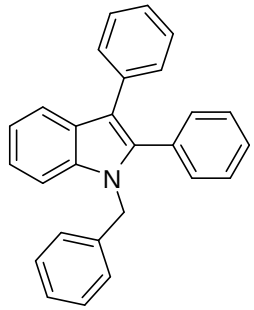

2.1 (0.8 g, 2.96 mmol), sodium hydride (0.2 g, 9.12 mmol), benzyl bromide (0.6 g, 0.41mL, 3.6 mmol). Yield: 0.72 g (68%). m.p. = 139 - 141 ˚C; ^{1}H NMR (500MHz, $CDCl_3$): δ_H 7.83 (d, 1H, *J* = 8 Hz), 7.34 – 7.18 (m, 17H), 7.02 (d, 1H, *J* = 8 Hz), 5.30 (s, 2H, CH_2).

Synthesis of N-benzyl-2,3-bis(4-methoxyphenyl)indole, **2.10**

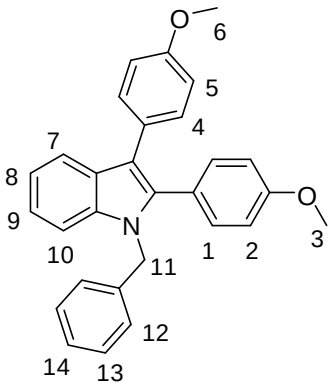

2.2 (1 g, 3 mmol), sodium hydride (0.22 g, 9.25 mmol), benzyl bromide (0.62 g, 0.44 mL, 3.63 mmol). Yield: 0.87 g (69%). m.p. 156 – 158 ˚C; ^{1}H NMR (400MHz, $CDCl_3$): δ_H 7.78 (d, 1H, *J* = 8 Hz, H7), 7.28 – 7.22 (m, 6H), 7.18 – 7.15 (m, 4H, H8, H10), 7.02 (d, 2H, *J* = 8 Hz), 6.85 – 6.81 (m, 4H, H9), 5.28 (s, CH_2, 2H, H11), 3.80 (s, OCH_3, 3H, H3), 3.79 (s, OCH_3, 3H, H6); ^{13}C NMR (125MHz, $CDCl_3$): δ_C 159.7, 157.8, 132.5, 131.2, 128.9, 128.0, 127.8, 127.4, 126.4 C10, 124.3, 122.4, 120.5, 119.8 C7, 115.1, 114.2, 114.0, 110.7, 55.5 C3, 55.4 C6, 47.8 C11; ESMS: calc for $C_{29}H_{25}NO_2Na$ ([**2.10** + Na]$^+$) = 442.1783, found 442.1794; IR (KBr) *ν*/cm^{-1}: 3042 w, 2936 w, 2835 w, 1610 m, 1517 s, 1495 s, 1463 s, 1287 s, 1245 s, 1175 s, 1030 s, 934 m, 835 s, 782 m, 747 s, 726 s; UV-Vis λ_{max} (ε): 247 nm (18433), 290 nm (10363); Fluorometry λ_{max}: 417 nm.

Synthesis of N-benzyl-2,3-bis(4-methylphenyl)indole, **2.11**

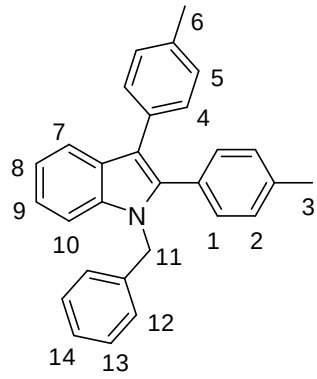

2.3 (1 g, 3.36 mmol), sodium hydride (0.24 g, 10.1 mmol), benzyl bromide (0.69 g, 0.48 mL, 4.03 mmol). Yield: 1.03 g (79%). m.p. 126 – 129 ˚C; ^{1}H NMR (400MHz, $CDCl_3$): δ_H 7.81 (d, 1H, *J* = 8 Hz, C7), 7.27 – 7.10 (m, 14H), 7.03 (d, 2H, *J* = 7 Hz), 5.29 (s, CH_2, 2H, H11), 2.35 (s, CH_3, 3H, H3), 2.34 (s, CH_3, 3H, H6); ^{13}C NMR (125MHz, $CDCl_3$): δ_C 138.3, 137.9, 136.9, 134.9, 132.2, 130.9, 129.7, 129.1, 128.9, 128.8, 128.6, 127.5, 127.1, 126.1, 122.1, 120.2, 119.7 C7, 115.3, 110.4, 47.5 C 11, 21.3 C3, 21.2 C6; ESMS: calc for $C_{29}H_{26}N$ ([**2.11** + H]$^+$) = 388.2065, found 388.2044; IR (KBr) *ν*/cm^{-1}: 3033 m, br, 2919 m, br, 1519 m, 1495 m, 1461 s, 1451 s, 1363 s, 1353 s, 829 s, 817 s, 744 s, 722 m, 699 m; UV-Vis λ_{max} (ε): 242 nm (20729), 291 nm (13050); Fluorometry λ_{max}: 415 nm.

Synthesis of N-benzyl-2,3-bis(4-*tert*butylphenyl)indole, **2.12**

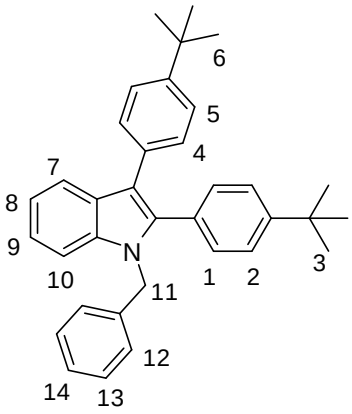

2.4 (1 g, 2.08 mmol), sodium hydride (0.2 g, 8 mmol), benzyl bromide (0.54 g, 0.37 mL, 3.15 mmol). Yield: 0.65 g (66%). m.p. 138 – 141 ˚C; ^{1}H NMR (400MHz, $CDCl_3$): δ_H 7.85 (d, 1H, *J* = 8 Hz, C7), 7.32-7.15 (m, 14H), 7.03 (d, 2H, *J* = 8 Hz), 5.29 (s, 2H, H11), 1.33 (s, 9H, CH_3, H3), 1.32 (s, 9H, CH_3, H6); ^{13}C NMR (125MHz, $CDCl_3$): δ_C 150.1, 148.0, 138.3, 137.8, 136.9, 132.2, 130.7, 129.4, 128.8, 128.6, 127.6, 127.0, 126.2, 125.2, 125.0, 122.0, 120.1, 119.9 C7, 115.2, 110.4, 47.6 C11, 31.4 C3, 31.3 C6; ESMS: calc for $C_{35}H_{37}NNa$ ([**2.12** + Na]$^+$) = 494.2818, found 494.2826; IR (KBr) ν/cm^{-1}: 2961 s, 2902 m, sh, 2868 m, sh, 1462 s, 1363 s, 839 s, 748 s, 739 s, 727 m; UV-Vis λ_{max} (ε): 233 nm (27928), 290 nm (14247); Fluorometry λ_{max}: 416 nm.

Synthesis of 1,2,3-triphenylindole, **2.13**

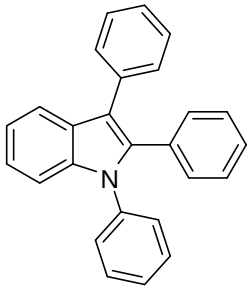

Following a modified literature procedure,[15] in an oven dry Schlenk tube cooled under vacuum and backfilled with argon was added **2.1** (0.270 g, 1mmol), iodobenzene (0.204 g, 0.11 ml, 1mmol) and potassium hydroxide (0.140 g, 2.5 mmol). 3 mL of dry dimethylsulfoxide was added and the reaction mixture was heated at 120 ˚C overnight under an argon atmosphere. The reaction mixture was cooled and 15 mL of sat. aqueous ammonium chloride solution was added. The solution was extracted with 2x 20 mL ethyl acetate, the organic layers combined and dried with $MgSO_4$. The solvent was removed *in vacuo* and purification with flash column chromatography gave **2.13**. Crystals suitable for X-ray crystallography were grown from the slow evaporation of a dichloromethane solution of **2.13** Yield: 0.090 g (26%). m.p. 185 – 187 ˚C; ^{1}H NMR (400MHz, $CDCl_3$): δ_H 7.83 (d, 1H, *J* = 7 Hz), 7.72 (d, 1H, *J* = 8.4 Hz), 7.39 – 7.32 (m, 8H), 7.24 – 7.22 (m, 3H), 7.18 – 7.09 (m, 4H).

Attempted syntheses of dibenzo[*a*,*c*]carbazoles using $FeCl_3$

General procedure for oxidative cyclodehydrogenation using $FeCl_3$ dissolved in nitromethane

In an oven dry schlenk tube cooled under vacuum and backfilled with argon was added iron (III) chloride and placed back under vacuum for 15 minutes. In an oven dry three-necked round bottom flask cooled whilst flushing with argon was added the appropriate indole (~ 0.150 g) and the solid was flushed with argon for five minutes. 150 mL dry dichloromethane was added and the solution was stirred with argon bubbling through for five minutes. The schlenk tube was refilled with argon and the iron (III) chloride was dissolved in nitromethane. The nitromethane solution was added dropwise to the dichloromethane solution and the solution was stirred with argon bubbling through for six hours, then the bubbling argon

was removed and the solution was stirred under argon overnight. The reaction was quenched with 100 mL methanol and then 100 mL water was added. The layers were separated and the organic layer was washed with 50mL of water, dried with $MgSO_4$ and the solvent removed *in vacuo*. Purification by flash column chromatography was attempted usually using SiO_2, 9:1 hexanes : ethyl acetate or SiO_2 4:1 hexanes:ethyl acetate.

General procedure for oxidative cyclodehydrogenation using $FeCl_3$ added to the reaction as a solid

In an oven dry schlenk tube cooled under vacuum and backfilled with argon was added iron (III) chloride and placed back under vacuum for 15 minutes. In an oven dry three-necked round bottom flask cooled whilst flushing with argon was added the appropriate indole (~ 0.150 g), and the solid was flushed with argon for five minutes. 150 mL dry dichloromethane was added and the solution was stirred with argon bubbling through for five minutes. The schlenk tube was refilled with argon and the solid iron (III) chloride was added in one go to the dichloromethane solution. The solution was stirred with argon bubbling through for six hours, then the bubbling argon was removed and the solution was stirred under argon overnight. The reaction was quenched with 100 mL methanol and then 100 mL water was added. The layers were separated and the organic layer was washed with 50 mL of water, dried with $MgSO_4$ and the solvent removed *in vacuo*. Purification by flash column chromatography was attempted usually using SiO_2, 9:1 hexanes:ethyl acetate or SiO_2, 4:1 hexanes:ethyl acetate

Synthesis of 9-benzyl-3,6-dimethoxy-9H-dibenzo[*a*,*c*]carbazole, **2.20**

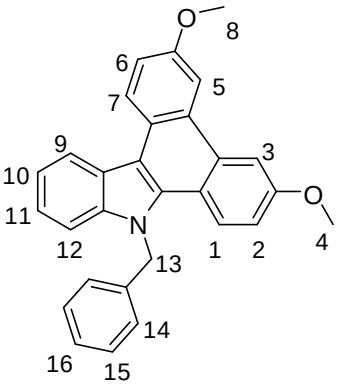

2.10 (0.150g, 0.358 mmol), $FeCl_3$ (0.87 g, 5.36 mmol), the dark red residue was purified by flash chromatography (SiO_2, 4:1 hexanes:ethyl acetate). Crystals suitable for X-ray crystallography were obtained by slow diffusion of diisopropyl ether into a benzene solution of **2.20**. Yield: 0.035 g (23%). m.p. 191 – 194 ˚C; ^{1}H NMR (400MHz, $CDCl_3$): δ_H 8.84 (d, br, 1H, H1), 8.59 (d, br, 1H, H9), 8.17 (d, 1H, *J* = 8.4 Hz, H7), 8.15 (s, 1H, H3), 8.10 (s, 1H, H5), 7.45 – 7.30 (m, 9H, H2, H10), 7.12 (d, 1H, *J* = 8.4 Hz, H6), 5.96 (s, 2H, CH_2, H13), 4.06 (s, 3H, OCH_3, H8), 4.00 (s, 3H, OCH_3, H4); ^{13}C NMR (125MHz, $CDCl_3$): δ_C 157.4, 137.6, 132.2, 129.1, 127.5, 126.0, 125.1 C1, 124.5 C7, 123.6, 121.4 C9, 120.6, 116.5 C6, 115.3, 109.7, 106.9 C3, 106.4 C5, 55.6 C8, 55.4 C4, 50.2 C13; ESMS: calc for $C_{29}H_{24}NO_2$ ([**2.20** + H]$^+$) = 418.1802, found 418.1786; calc for $C_{29}H_{23}NO_2$ ([**2.20**·]$^+$) = 417.1723, found, 417.1726; IR (KBr)*v*/cm^{-1}: 2953 w, 2927 w, 1616 m, 1529 m, 1469 s, 1238 s, 1207 s, 1038 s, 836 s, 803 s, 732 s, 702 m; UV-Vis λ_{max} (ε): 276 nm (49464), 309 nm (19528), 327 nm (16030), 378 nm (3900), 398 nm (4416); Fluorometry λ_{max}: 415 nm, 431 nm.

Attempted syntheses of dibenzo[*a*,*c*]carbazoles using $AlCl_3$/oxidant

Attempted synthesis of **2.16** using $AlCl_3/CuCl_2$

In an oven dry schlenk tube cooled under vacuum and backfilled with argon was added $AlCl_3$ (0.34 g, 2.52 mmol) and the tube was placed back under vacuum for 15 minutes. The tube was backfilled with argon and $CuCl_2$ (0.34 g, 2.52 mmol) and 1-ethyl-2,3-di(4-methoxyphenyl)indole, **2.6**, (0.100 g, 0.280 mmol) were added. 30 mL of degassed CS_2 was added to the solids and the reaction mixture was stirred under argon for four days, whilst monitoring with TLC. The CS_2 was then evaporated and the remaining solid was stirred for two hours with 50 mL 1 $mol.L^{-1}$ HCl solution. The solid was filtered and purification using flash column chromatography (Al_2O_3, 3:1 hexanes:ethyl acetate), did not isolate any products.

Attempted synthesis of **2.16** using $AlCl_3/Cu(OTf)_2$

The same general procedure was used as described above for the attempted synthesis of **2.16** using $AlCl_3/Cu(OTf)_2$.

2.6 (0.050 g, 0.140 mmol), $AlCl_3$ (0.17 g, 1.26 mmol), $Cu(OTf)_2$ (0.46 g, 1.26 mmol).

General procedure for the synthesis of dibenzo[*a*,*c*]carbazoles, using photocyclisation

In an oven dry quartz tube flushed with argon, 400 mL of dry toluene was added, and sparged with argon for 5 minutes. The appropriate indole was added, along with I_2 and propylene oxide. The solution was sparged with argon for 15 minutes and then irradiated with 300 nm light in a Rayonet photoreactor vernight with argon bubbling through the solution continuously. The solution was then washed with 200 mL $Na_2S_2O_3$ solution and 100 mL water, dried with $MgSO_4$ and the solvent removed *in vacuo*. The residue was purified by flash column chromatography.

Synthesis of 3,6-dimethyl-9H-dibenzo[*a*,*c*]carbazole, **2.25**

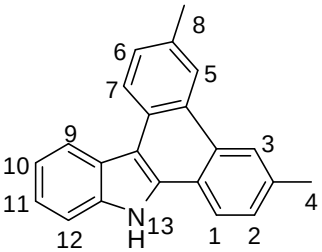

2.3 (0.150 g, 0.504 mmol), I_2 (0.140 g, 0.555 mmol), propylene oxide (2 mL), purification with flash column chromatography (SiO_2, 1:1 hexanes:dichloromethane). Yield: 0.086 g (58%). m.p. 202 – 205 ˚C; ^{1}H NMR (400MHz, $CDCl_3$): δ_H 8.83 (s, br, 1H, H13), 8.69 (d, 1H, *J* = 8 Hz, H7), 8.59 (s, 1H, H3), 8.56 (s, 1H, H5), 8.51 (d, 1H, *J* = 7.5 Hz, H9), 8.02 (d, 1H, *J* = 8 Hz, H1), 7.63 (d, 1H, *J* = 8 Hz, H6), 7.58 (d, 1H, *J* = 7.5 Hz, H12), 7.51 (d, 1H, *J* = 8 Hz, H2), 7.41 (t, 1H, *J* = 7.5 Hz, H11), 7.39 (t, 1H, *J* = 7.5 Hz, H10), 2.66 (s, 6H, H4, H8); ^{13}C NMR (125MHz, $CDCl_3$): δ_C 138.1 C12a, 135.8 C1aa, 133.5 C1a, 132.9 C8a, 130.0 C4a, 128.8 C12, 128.2 C2, 127.8 C7a, 126.9 C7aa, 124.9 C9a, 123.9 C3, 123.6 C7, 123.5 C11, 123.4 C5, 121.7 C9, 120.4 C1, 120.3 C10, 111.2

C6, 22.2 C4, 21.9 C8; ESMS: calc for $C_{27}H_{22}N$ ([**2.25**·]$^+$) = 295.1356, found 295.1354; IR (KBr)ν/cm^{-1}: 3420 s, 2915 m, 1539 s, 1469 s, 1359 m, 1291 s, 873 m, 800 s, 738 s, 540 s; UV-Vis λ_{max} (ε): 272 nm (72416), 299 nm (22763), 325 nm (21116), 357 nm (4836), 377 nm (4956); Fluorometry λ_{max}: 390 nm, 407 nm.

Synthesis of 3,6-di*tert*butyl-9H-dibenzo[*a*,*c*]carbazole, **2.26**

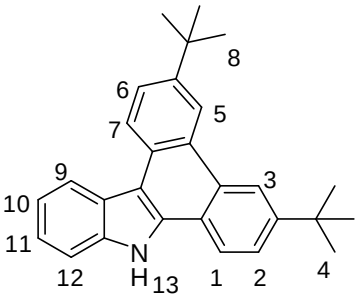

2.4 (0.150 g, 0.393 mmol), I_2 (0.110 g, 0.432 mmol), propylene oxide (2 mL), purification with flash column chromatography (SiO_2 3:2 hexanes:dichloromethane). Crystals suitable for X-ray crystallography were obtained by recrystallisation from ethyl acetate and hexanes. Yield: 0.060 g (40%). m.p. 192 – 194 ˚C; ^{1}H NMR (400MHz, $CDCl_3$): δ_H 8.87 – 8.81 (m, 3H, H3, H5, H13), 8.74 (d, 1H, *J* = 8Hz, H7), 8.53 (d, 1H, *J* = 8 Hz, H9), 8.06 (d, 1H, *J* = 8 Hz, H1), 7.84 (d, 1H, *J* = 8 Hz, H6), 7.76 (d, 1H, *J* = 8 Hz, H2), 7.64 (d, 1H, *J* = 8 Hz, H12), 7.44 – 7. 36 (m, 2 H, H10, H11), 1.56 (s, 9H, CH_3, H4), 1.55 (s, 9H CH_3, H8); ^{13}C NMR (125MHz, $CDCl_3$): δ_C 148.8, 145.6, 133.6, 129.9, 125.3 C6, 124.7 C2, 123.6 C7, 121.7 C9, 120.6 C1, 120.4 C10, 119.5 C3, 119.1 C5, 111.3 C12, 31.6 C4, 31.5 C8; ESMS: calc for $C_{28}H_{30}N$ ([**2.26** + H]$^+$) = 380.2373, found 380.2355, calc for $C_{28}H_{29}N$ ([**2.26**·]$^+$) = 379.2295, found 379.2301; IR (KBr)ν/cm^{-1}: 3435 s, sh, 3414 s, 2961 s, 2903 s, sh, 2867 s, sh, 1534 m, 1461 s, 1359 s, 1265 m, 1255 m, 880 m, 812 s, 738 s, 601 m; UV-Vis λ_{max} (ε): 272 nm (74773), 297 nm (22095), 321 nm (22128), 355 nm (5805), 373 nm (5599); Fluorometry λ_{max}: 384, 401.

Synthesis of 9-ethyl-9H-dibenzo[*a*,*c*]carbazole, **2.15**

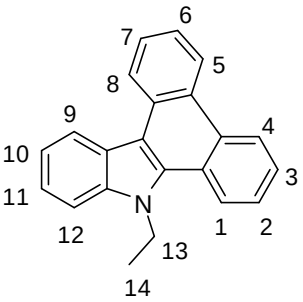

2.5 (0.150 g, 0.504 mmol), I_2 (0.140 g, 5.55 mmol), propylene oxide (1.5 mL), purification with flash column chromatography (SiO_2 3:2 hexanes:dichloromethane). Crystals suitable for X-ray crystallography were obtained by recrystallisation from ethyl acetate and hexanes. Yield: 0.095 g (64%). m.p. 114 – 118 ˚C; ^{1}H NMR (400MHz, $CDCl_3$): δ_H 8.90 (d, br, 2H, H4, H5), 8.79 (d, 1H, *J* = 8.6 Hz, H1), 8.65 (d, 1H, *J* = 8 Hz, H9), 8.56 (d, 1H, *J* = 7.4 Hz, H8), 7.77-7.69 (m, 3H, H3, H6, H7), 7.67 (d, 1H, *J* = 8 Hz, H12), 7.59 (t, 1H, *J* = 7.4 Hz, H2), 7.51 (t, 1H, *J* = 8 Hz, H11), 7.42 (t, 1H, *J* = 8 Hz, H10), 4.90 (q, 2H, CH_2, *J* = 7 Hz, H13), 1.74 (t, 3H, CH_3, *J* = 7 Hz, H14); ^{13}C NMR (125MHz, $CDCl_3$): δ_C 140.0 C12a, 133.6 C1aa, 130.9 C8a, 130.0 C1a, 127.3 C6, 126.8 C7, 126.4 C3, 125.5 C4a, 124.2 C5, 123.7 C4, 123.6 C11, 123.5 C1, 123.4 C2, 122.5 C8, 121.9 C9, 120.3 C10, 113.6 C5a, 109.4 C12, 40.9 C13, 15.3 C14; ESMS: calc for $C_{22}H_{18}N$ ([**2.15** + H]$^+$) = 296.1434, found 296.1428, calc for $C_{22}H_{17}N$ ([**2.15**·]$^+$) = 295.1356, found 295.1358; IR (KBr)ν/cm^{-1}:

2969 m, 1608 m, 1516 s, 1467 s, 1444 s, 1371 s, 1350 s, 1224 m, 1156 m, 1094 m, 935 m, 745 s, 733 s, 716 s; UV-Vis λ_{max} (ε): 275 nm (52363), 297 nm (15472), 326 nm (17219), 359 nm (4877), 378 nm (4659); Fluorometry λ_{max}: 389 nm, 407 nm.

Synthesis of 9-ethyl-3,6-dimethoxy-9H-dibenzo[*a*,*c*]carbazole, **2.16**

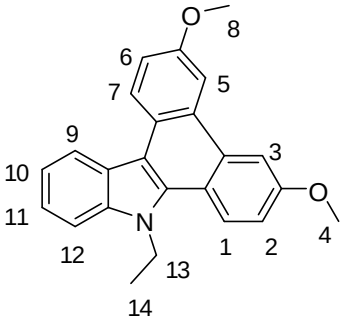

2.6 (0.150 g, 0.420 mmol), I_2 (0.120 g, 0.462 mmol), propylene oxide (1.5 mL), purification with flash column chromatography (SiO_2, dichloromethane). Yield: 0.090 g (60%). m.p. 96 – 99 ˚C; ^{1}H NMR (400MHz, $CDCl_3$): δ_H 8.76 (d, 1H, *J* = 9 Hz, H1), 8.54 (d, 1H, *J* = 8 Hz, H7), 8.37 (d, 1H, *J* = 9 Hz, H9), 8.11 (s, 1H, H5), 8.04 (s, 1H, H3), 7.57 (d, 1H, *J* = 8 Hz, H2), 7.48 (t, 1H, *J* = 7.5 Hz, H11), 7.40 (d, 1H, *J* = 8 Hz, H6), 7.29 (t, 1H, *J* = 7.5 Hz, H10), 7.21 (d, 1H, *J* = 7.5 Hz, H12), 4.72 (q, 2H, CH_2, *J* = 7 Hz, H13), 4.03 (s, 6H, OCH_3, H4, H8), 1.66 (t, 3H, CH_3, *J* = 7 Hz, H14); ^{13}C NMR (125MHz, $CDCl_3$): δ_C 157.2 C2a, 155.9 C6a, 139.87 C12a, 132.8, 132.2 C1aa, 127.7 C3a, 124.9 C1, 124.1 C9, 123.5 C5a, 123.3 C11, 121.4 C7, 120.1 C6, 118.4, 116.3 C10, 115.5 C12, 112.1 C1a, 109.2 C2, 106.8 C3, 106.3C5, 55.6 C4, 55.5 C8, 40.9 C13, 15.2 C14; ESMS: calc for $C_{24}H_{22}NO_2$ ([**2.16** + H]$^+$) = 356.1645, found 356.1630, calc for $C_{24}H_{21}NO_2$ ([**2.16**·]$^+$) = 355.1567, found 355.167; IR (KBr)*ν*/cm^{-1}: 2983 m, 2929 m, 1616 m, 1574 m, 1528 m, 1465 s, 1377 m, 1236 s, 1038 m, 833 m, 800 m, 789 m, 737 m; UV-Vis λ_{max} (ε): 277 nm(59286), 310 nm (23439), 329 nm (18347), 380 nm (4693), 400 nm (5080); Fluorometry λ_{max}: 420 nm, 435 nm.

Synthesis of 9-ethyl-3,6-dimethyl-9H-dibenzo[*a*,*c*]carbazole, **2.17**

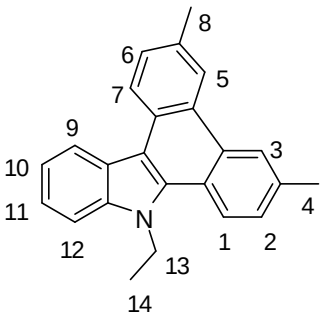

2.7 (0.150 g, 0.461 mmol), I_2 (0.130 g, 0.507 mmol), propylene oxide (1.5 mL), purification with flash column chromatography (SiO_2, 3:2 hexanes:dichloromethane). Crystals suitable for X-ray crystallography were obtained by recrystallisation from ethyl acetate and hexanes. Yield: 0.130 g (85%). m.p. 137 – 141 ˚C; ^{1}H NMR (400MHz, $CDCl_3$): δ_H 8.77 (d, 1H, *J* = 8.4 Hz, H1), 8.67 (s, 1H, H3), 8.60 (d, 1H, *J* = 8 Hz, H9), 8.57 (s, 1H, H5), 8.45 (d, 1H, *J* = 8.4 Hz, H7), 7.63 (d, 1H, *J* = 8.4 Hz, H2), 7.57 (d, 1H, *J* = 8.4 Hz, H6), 7.53 (d, 1H, *J* = 8 Hz, H12), 7.49 (t, 1H, *J* = 8 Hz, H11), 7.39 (t, 1H, *J* = 8 Hz, H10), 4.87 (q, 2H, CH_2, H13), 2.67 (s, 3H, CH_3, H4), 2.66 (s, 3H, CH_3, H8), 1.72 (t, 3H, CH_3, H14); ^{13}C NMR (125MHz, $CDCl_3$): δ_C 140.0 C12a, 135.0 C6a, 133.4 C1aa, 132.7 C2a, 130.9 C7a, 128.7 C2, 127.9 C1a, 127.8 C6, 126.8 C7aa, 124.1 C3, 123.7 C3a, 123.4 C1, 123.3 C11, 123.2 C9, 122.4 C7, 121.8 C5, 121.5 C5a, 120.1 C10, 113.0 C9a, 109.3 C12, 40.8 C13, 21.9 C4, 21.8 C8, 15.3 C14; ESMS: calc for $C_{24}H_{22}N$

([**2.17** + H]$^+$) = 324.1747, found 324.1733, calc for $C_{24}H_{21}H$ ([**2.17**·]$^+$) = 323.1669, found 323.1668; IR (KBr)ν/cm^{-1}: 2975 w, 2919 w, 1528 s, 1466 s, 1371 m, 1348 m, 1333 m, 1297 m, 1226 m, 802 s, 739 s; UV-Vis λ_{max} (ε): 277 nm (61425), 302 nm (19026), 327 nm (19612), 365 nm (5226), 384 nm (5212); Fluorometry λ_{max}: 397 nm, 414 nm.

Synthesis of 9-ethyl-3,6-di*tert*butyl-9H-dibenzo[*a*,*c*]carbazole, **2.18**

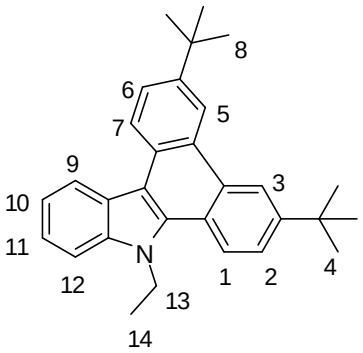

2.8 (0.150 g, 0.366 mmol), I_2 (0.100 g, 0.403 mmol), propylene oxide (1.5 mL), purification with flash column chromatography (SiO_2, 3:2 hexanes:dichloromethane). Yield: 0.133 g (89%). m.p. 135 – 138 ˚C; ^{1}H NMR (400MHz, $CDCl_3$): δ_H 8.92 (s, 1H, H3), 8.83 (d, 1H, *J* = 8.8 Hz, H1), 8.81 (s, 1H, H5), 8.62 (d, 1H, *J* = 7.6 Hz, H9), 8.51 (d, 1H, *J* = 8.8 Hz, H7), 7.84 (d, 1H, *J* = 8.4 Hz, H2), 7.79 (d, 1H, *J* = 8.4 Hz, H6), 7.63 (d, 1H, *J* = 7.6 Hz, H12), 7.50 (t, 1H, *J* = 7.6 Hz, H11), 7.41 (t, 1H, *J* = 7.6 Hz, H10), 4.87 (q, 2H, CH_2, *J* = 7 Hz, H13), 1.73 (t, 1H, CH_3, *J* = 7 Hz, H14), 1.56 (s, 18H, CH_3, H4, H8); ^{13}C NMR (125MHz, $CDCl_3$): δ_C 148.0 C6a, 145.8 C2a, 139.9 C12a, 133.5 C1aa, 130.8 C7aa, 127.9 C5a, 126.6 C3a, 125.3 C2, 124.4 C6, 123.7 C9a, 123.4 C1, 123.3 C11, 122.4 C7, 121.8 C9, 121.5 C7a, 120.1 C10, 119.8 C3, 118.9 C5, 113.0 C1a, 109.3 C12, 40.9 C13, 31.5 C4, 31.4 C8, 15.3 C14; ESMS: calc for $C_{30}H_{34}N$ ([**2.18** + H]$^+$) = 408.2686, found 408.2684; IR (KBr)ν/cm^{-1}: 2956 s, 2902 m, sh, 2866 m, sh, 1525 m, 1463 s, 1372 m, 1361 m, 1344 m, 1333 m, 1260 m, 879 m, 814 m, 733 s, 602 m; UV-Vis λ_{max} (ε): 277 nm (63644), 299 nm (18444), 327 nm (19505), 362 nm (5523), 381 nm (5688); Fluorometry λ_{max}: 392nm, 410 nm.

Synthesis of 9-benzyl-9H-dibenzo[*a*,*c*]carbazole, **2.19**

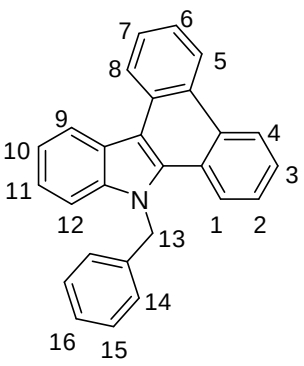

2.9 (0.150 g, 0.417 mmol), I_2 (0.120 g, 0.459 mmol), propylene oxide (1.5 mL), purification with flash column chromatography (SiO_2, 3:2 hexanes:dichloromethane). Yield: 0.125 g (84%). m.p. 141 – 143 ˚C; ^{1}H NMR (400MHz, $CDCl_3$): δ_H 8.94 (d, 1H, *J* = 7.6 Hz, H4), 8.86 (d, 1H, *J* = 8.4 Hz, H5), 8.80 (d, 1H, *J* = 7.6 Hz, H1), 8.70 (s, 1H, *J* = 8.4 Hz, H9), 8.27 (d, 1H, *J* = 8.4 Hz, H8), 7.791 (t, 1H, *J* = 7.6 Hz, H3), 7.63 – 7.61 (m, 2H, H2, H7), 7.51 – 7.44 (m, 4H, H6, H10), 7.38 – 7.32 (m, 5H), 6.03 (s, 2H, CH_2, H13); ^{13}C NMR (125MHz, $CDCl_3$): δ_C 141.2 C12a, 137.4 C1aa, 134.7 C8aa, 130.9, 129.9, 129.1, 127.5, 127.4 C3, 127.0, 126.5, 126.0, 125.7, 124.1, 124.0, 123.8 C5, 123.7 C4, 123.5 C1, 123.2, 122.9 C7, 121.9 C9, 120.9, 110.0, 50.2 C13; ESMS: calc for $C_{27}H_{20}N$ ([**2.19** + H]$^+$) = 358.1590, found 358.1594; IR (KBr)ν/cm^{-1}: 3041 w, 1514 m, 1470 s, 1359 m, 1334 m, 1210 w, 1155 w, 746 s, 729

m, 719 m; UV-Vis λ_{max} (ε): 274 nm (56103), 295 nm (16745), 324 nm (19190), 357 nm (5568), 375 nm (5247); Fluorometry λ_{max}: 385 nm, 402 nm.

Synthesis of 9-benzyl-3,6-dimethyl-9H-dibenzo[*a*,*c*]carbazole, **2.21**

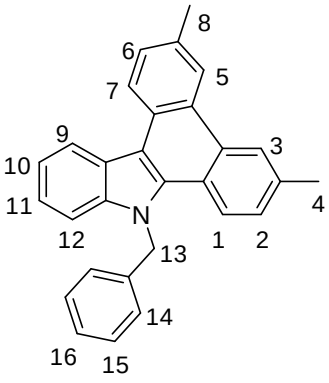

2.11 (0.150 g, 0.387 mmol), I_2 (0.110 g, 0.426 mmol), propylene oxide (1.5 mL), purification with flash column chromatography (SiO_2, 3:2 hexanes:dichloromethane). Crystals suitable for X-ray crystallography were obtained by recrystallisation from ethyl acetate and hexanes. Yield: 0.084 g (56%). m.p. 216 – 218 ˚C; ^{1}H NMR (400MHz, $CDCl_3$): δ_H 8.81 (d, 1H, *J* = 8.4 Hz, H1), 8.63 (m, 2H, H3, H7), 8.57 (s, 1H, H5), 8.16 (d, 1H, *J* = 7.6 Hz, H9), 7.60 (d, 1H, *J* = 8.4 Hz, H2), 7.47 – 7.29 (m, 10 H), 6.00 (s, 2H, CH_2, H13), 2.67 (s, 3H, CH_3, H4), 2.60 (s, 3H, CH_3, H8); ^{13}C NMR (125MHz, $CDCl_3$): δ_C 141.7, 137.6, 135.2, 134.8, 133.0, 131.2, 129.1, 128.9 C2, 127.9, 127.8, 127.5, 127.1, 126.0, 124.0, 123.8 C1, 123.5 C3, 123.4 C5, 122.8 C2, 121.8 C7, 121.1, 120.6, 109.8, 50.1 C13, 22.0 C4, 21.9 C8; ESMS: calc for $C_{29}H_{24}N$ ([**2.21** + H]$^+$) = 386.1904, found 386.1873, calc for $C_{29}H_{23}N$ ([**2.21**·]$^+$) = 385.1825, found 385.1828; IR (KBr)*ν*/cm^{-1}: 2917 w, br, 1528 m, 1467 m, 1454 m, 1357 m, 1332 m, 803 s, 735 s, 696 w; UV-Vis λ_{max} (ε): 276 nm (65698), 300 nm (19672), 326 nm (21264), 363 nm (5463), 382 nm (5570); Fluorometry λ_{max}: 394 nm, 411 nm.

Synthesis of 9-benzyl-3,6-di*tert*butyl-9H-dibenzo[*a*,*c*]carbazole, **2.22**

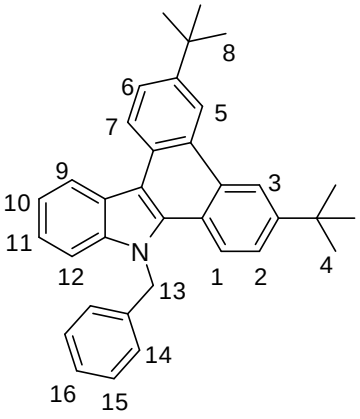

2.12 (0.150 g, 0.318 mmol), I_2 (0.090 g, 0.350 mmol), propylene oxide (1.5 mL), purification with flash column chromatography (SiO_2, 7:3 hexanes:dichloromethane). Yield: 0.120 g (78%). m.p. 179 – 182 ˚C; ^{1}H NMR (400MHz, $CDCl_3$): δ_H 8.87 (s, 1H, H3), 8.85 (d, 1H, *J* = 7.6 Hz, H1), 8.80 (s, 1H, H5), 8.66 (d, 1H, *J* = 8.8 Hz, H9), 8.21 (d, 1H, *J* = 8.8 Hz, H7), 7.85 (d, 1H, *J* = 8.8 Hz, H2), 7.54 (d, 1H, *J* = 8.8 Hz, H6), 7.49-7.31 (m, 8H), 6.01 (s, 2H, CH_2, H13), 1.56 (s, 9H, CH_3, H4), 1.49 (s, 9H, CH_3, H8); ^{13}C NMR (125MHz, $CDCl_3$): δ_C 148.1 C2a, 146.1 C6a, 141.2 C12a, 137.7 C1aa, 134.5 C7aa, 130.9, 129.1, 127.8, 127.5, 126.7, 126.0 C1a, 125.4, 124.5 C2, 124.0, 123.8 C6, 123.5 C1, 122.7 C7, 121.8 C9, 121.1, 120.6, 119.7 C3, 119.0 C5, 113.3, 109.8 C12, 50.1 C13, 31.6 C4, 31.4 C8; ESMS: calc for $C_{35}H_{36}N$ ([**2.22** + H]$^+$) = 470.2842, found 470.2830, calc for $C_{35}H_{35}N$ ([**2.22**·]$^+$) = 469.2763, found 469.2769; IR (KBr)*ν*/cm^{-1}: 2962 s, 2903 m, sh, 2868 m, sh, 1568 m, 1525 m, 1468 s, 1454 s, 1358 s, 1258 m, 948 m, 810 s, 733 s, 600 m; UV-Vis λ_{max}

(ε): 276 nm (66433), 297 nm (19674), 325 nm (20986), 360 nm (6390), 379 nm (6227); Fluorometry λ_{max}: 389 nm, 407 nm.

Attempted synthesis of 1-(2,2':6',2''terpyridine)-2,3-di(4-methoxyphenyl)indole

Method A: Following the general procedure outlined above for the the synthesis of N-ethyl-2,3,diarylindoles **2.5** – **2.8**, **2.2** (0.100 g, 0.304 mmol), sodium hydride (0.050 g, 0.912mmol), **2.28** (0.098 g, 0.364 mmol) were used. After quenching the reaction ^{1}H-NMR spectroscopy and ESMS indicate only starting materials present.

Method B: Following a modified literature procedure,[16] **2.2** (0.110 g, 0.336 mmol), and KO^{t}Bu (0.045 g, 0.404 mmol) were placed in a round bottom flask flushing with nitrogen and then 20 mL of dry dimethylformamide was added. The reaction mixture was stirred for thirty minutes under a nitrogen atomosphere and then **2.28** (0.110 g, 0.404 mmol) was added. The reaction mixture was stirred at 100 ˚C for five hours under a nitrogen atomosphere and then poured into 100 mL water. The reaction mixture was extracted with 3x 50 mL ethyl acetate, and the combined organic layer were washed with 2x 100 mL water. The organic layer was dried with $MgSO_4$ and the solvent removed *in vacuo*. ^{1}H-NMR spectroscopy and ESMS indicate only starting materials present.

Method C: Following the general procedure outlined above for the the synthesis of N-ethyl-2,3,diarylindoles **2.5** – **2.8**, **2.2** (0.035 g, 0.101 mmol), sodium hydride (0.010 g, 0.302 mmol), **2.29** (0.075 g, 0.084 mmol) were used. After quenching the reaction ^{1}H-NMR spectroscopy and ESMS indicate only starting materials present.

Synthesis of 1-(2,2':6',2''terpyridine)indole

Following the general procedure outlined above for the the synthesis of N-ethyl-2,3,diarylindoles **2.5** – **2.8**, indole (0.016 g, 0.135 mmol), sodium hydride (0.01 g, 0.410 mmol), and **2.29** (0.100 g, 0.112 mmol) were used. Purification with flash column chromatography (SiO_2, 14:3:2 acetonitrile:sat. KNO_3:H_2O) afforded 1-(2,2':6',2''terpyridine)indole by ESMS. ESMS: calc for $C_{38}H_{27}N_7Ru^{2+}$ = 341.5685, found 341.5688, calc for $C_{38}H_{27}N_7RuPF_6^+$ = 828.1018, found 828.1032.

Chapter Three

The following compounds were prepared according to literature methods, and all characterisation data were found to be consistent with that provided; N*H*-2,3,4,5-tetraphenylpyrrole, **3.1**[17], deoxyanisoin,[18] N-ethyl-2,3,4,5-tetraphenylpyrrole, **3.5**,[11] 9,10-phenanthrenediylbis(phenyl)methanone **3.43**[19] and 1,3-diphenylcyclopenta[*l*]phenanthrene-2-one **3.44**.[19]

Synthesis of N*H*-2,3,4,5-tetraarylpyrroles, **3.3**, **3.4**

General procedure for the synthesis of N*H*-2,3,4,5-tetraarylpyrroles, **3.3**, **3.4**

Following a modified literature procedure,[17] the appropriate benzoin was dissolved in glacial actic acid, zinc dust and ammonium acetate were then added and the mixture was refluxed for two hours. Boiling water was added and upon cooling a white precipitate formed. The precipitate was collected by filtration, dissolved in dichloromethane, washed with water and dried with $MgSO_4$. The solvent was removed *in vacuo* and the solid was recrystallised from dichloromethane and hexanes.

Synthesis of N*H*-2,3,4,5-tetra(4-methylphenyl)pyrrole **3.3**

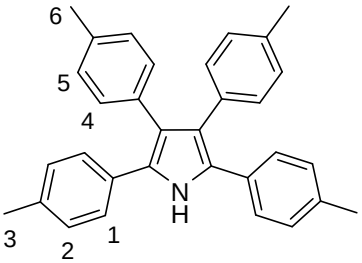

2.3a (2.40 g, 10 mmol), zinc (0.65 g, 10 mmol), ammonium acetate (6.0 g, 78 mmol). Yield: 1.10 g (52%). m.p. 237 – 239 ˚C; ^{1}H NMR (500MHz, $CDCl_3$): δ_H 8.31 (s, br, 1H, N*H*), 7.16 (d, 4H, *J* = 8.5 Hz), 7.07 (d, 4H, *J* = 8.5 Hz), 6.67 (s, 8H), 2.33 (s, 3H, CH_3), 2.30 (s, 3H, CH_3); ESMS: calc for $C_{32}H_{30}N$ ([**3.3** + H]$^+$) = 428.2373, found 428.2374, calc for $C_{32}H_{29}N$ ([**3.3**·]$^+$) = 427.2295, found 427.2297; IR (KBr)*ν*/cm^{-1}: 3418 m, 3018 m, 2918 m, 1520 s 1500 s, 1293 m, 1262 m, 112 m, 836 m, 817 s, 736 m, 505 m; UV-Vis λ_{max} (ε): 238 nm (14879), 262 nm (15138), 309 nm(16400); Fluorometry λ_{max}: 394 nm.

Synthesis of N*H*-2,3,4,5-tetra(4-*tert*butylphenyl)pyrrole **3.4**

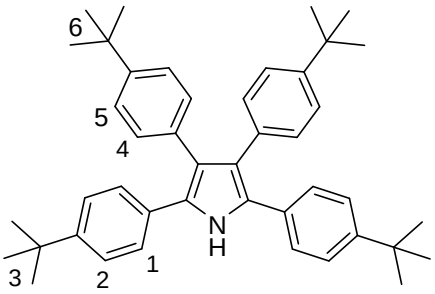

2.4a (1.90 g, 5.89 mmol), zinc (0.40 g, 5.89 mmol), ammonium acetate (3.50 g, 45.9 mmol). Yield: 0.75 g (43%). m.p. 241 – 245 ˚C; ^{1}H NMR (500MHz, $CDCl_3$): δ_H 8.28 (s, br, 1H, N*H*) 7.26 (d, 4H, *J* = 8 Hz, H1), 7.21 (d, 4H, *J* = 8 Hz, H2), 7.15 (d, 4H, *J* = 8 Hz, H4), 7.01 (d, 4H, *J* = 8 Hz, H5), 1.30 (s, 9H, CH_3, H3), 1.29 (s, 9H, CH_3, H6); ^{13}C NMR (125MHz, $CDCl_3$): δ_C 149.2 C2a, 148.3

C5a, 132.6, 130.5 C5, 130.2, 128.3, 128.0, 126.5 C2, 125.4 C1, 125.3, 124.5 C4, 31.4 C3, 31.3 C6; ESMS calc for $C_{44}H_{54}N$ ([**3.4** + H]$^+$) = 596.4256, found 596.4284, calc for $C_{44}H_{53}N$ ([**3.4**$^{\cdot}$]$^+$) = 595.4177, found 595.4237; IR (KBr)ν/cm^{-1}: 3425 m, 2956 s, 2903 m, sh, 2868 m, sh, 1521 m, sh, 1497 m, 1462 m, 1362 m, 1268 m, 836 s, 566 m, 537 m; UV-Vis λ_{max} (ε): 236 nm (18524), 265 nm (17423), 316 nm (20350); Fluorometry λ_{max}: 392 nm.

Attempted synthesis of N*H*-2,3,4,5-tetra(4-methoxyphenyl)pyrrole, **3.2**

Synthesis of 1,2,3,4-tetra(4-methoxyphenyl)-1,4-butadione[20]

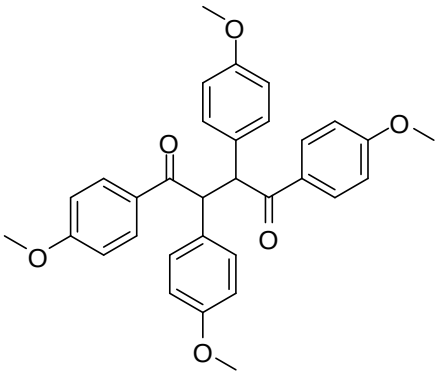

Following a modified literature procedure,[11] KO^{t}Bu (0.310 g, 2.8 mmol) was added to an oven dry Schlenk flask, cooled under vacum and backfiled with argon, dissolved in 10 mL dry tetrahydrofuran and then cooled to – 75 ˚C using an acetone/dry ice bath. Deoxyanisoin (1.0 g, 3.9 mmol) was added to an oven dry Sclenk tube cooled under vacuum and backfilled with argon, dissolved in 10 mL dry tetrahydrofuran and added to the reaction mixture dropwise. I_2 (0.71 g, 2.8 mmol) was dissolved in 20 mL dry tetrahydrofuran and added to the reaction mixture dropwise. The reaction mixture was stirred for two hours at 0 ˚C using an ice bath. 50 mL sat. aqeous $Na_2S_2O_5$ was added to quench the reaction, and the aqueous layer was extracted with 3x 20 mL ethyl acetate. The combined organic residue was washed with 1x 50 mL brine, dried with $MgSO_4$ and the solvent was removed *in vacuo*. Recrystallise from hexanes to give 1,2,3,4-tetra(4-methoxyphenyl)-1,4-butadione. Yield: 0.68 g (68%). m.p. 210 – 212 ˚C; ^{1}H NMR (500MHz, $CDCl_3$): δ_H 7.97 (d, 4H, *J* = 9 Hz), 6.94 (d, 4H, *J* = 9 Hz), 6.83 (d, 4H, *J* = 9 Hz), 6.66 (d, 4H, *J* = 9 Hz), 5.27 (s, 2H), 3.79 (s, 6H, OCH_3), 3.69 (s, 6H, OCH_3).

Attempted synthesis of N*H* -2,3,4,5-tetra(4-methoxyphenyl)pyrrole, **3.2**

Following a modified literature procedure,[11] 1,2,3,4-tetra(4-methoxyphenyl)-1,4-butadione (0.5 g, 9.8 mmol) and ammonium acetate (0.75 g, 9.8 mmol) were added to a round bottom flask and dissolved in 20 mL glacial acetic acid. The reaction mixture was heated to 130 ˚C and stirred overnight. The reaction mixture was poured into 100 mL water, and the precipitate formed was filtered and dissolved in 50 mL ethyl acetate. The ethyl acetate was washed with 2x 20 mL of sat. aqueous Na_2CO_3 and 2x 20 mL water and dried with $MgSO_4$. The solvent was removed *in vacuo*. The ^{1}H-NMR spectrum of the resulting residue matched that of the starting material.

Synthesis of N-ethyl-2,3,4,5-tetraarylpyrroles, **3.6**, **3.7**

General procedure for the synthesis of N-ethyl-2,3,4,5-tetraarylpyrroles, **3.6**, **3.7**

Following a modified literature procedure,[11] in a round bottom flask flushing with N_2, was added the appropriate N*H*-2,3,4,5-tetraarylpyrrole and 25 mL dry dimethylformamide. The solution was cooled to 0˚C using an ice bath and sodium hydride was added. The solution was stirred at 0˚C for 10 minutes and then ethyl bromide was added and the solution stirred at room temperature overnight. The solution was poured into 100 mL water and extracted with 3x 75 mL ethyl acetate. The combined organic layers were washed with 3x 200 mL water, dried with sodium sulfate and the solvent removed *in vacuo*. The solid obtained was recrystallised from ethyl acetate / hexanes.

Synthesis of N-ethyl-2,3,4,5-tetra(4-methylphenyl)pyrrole, **3.6**

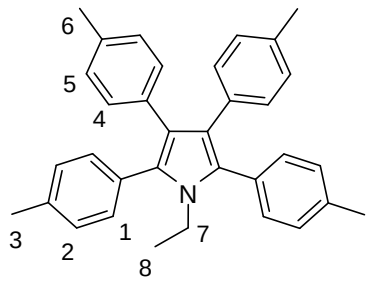

3.3 (0.300 g, 0.702 mmol), sodium hydride (0.050 g, 2.1 mmol), ethyl bromide (0.095 g, 0.06 mL, 0.845 mmol). Yield: 0.220 g (69%). m.p. 161 – 165 ˚C; ^{1}H NMR (500MHz, $CDCl_3$): δ_H 7.21 (d, 4H, *J* = 8 Hz, H1), 7.12 (d, 4H, *J* = 8 Hz, H2), 6.82 (s, 8H, H4, H5), 3.84 (q, 2H, CH_2, *J* = 7 Hz, H7), 2.36 (s, 3H, CH_3, H3), 2.21 (s, 3H, CH_3, H6), 0.95 (t, 3H, CH_3, *J* = 7 Hz, H8); ^{13}C NMR (125MHz, $CDCl_3$): δ_C 136.8, 134.0, 132.8, 131.3, 130.6, 130.4, 128.8, 128.1, 121.7, 39.3 C7, 21.3 C3, 21.1 C6, 16.7 C8; ESMS calc for $C_{34}H_{34}N$ ([**3.6** + H]$^+$) = 456.2686, found 456.2693; IR (KBr)*ν*/cm^{-1}: 2973 m, br, 1522 s, 1498 s, 1338 m, 1114 m, 1021 s, 834 m, sh, 817 s, 741 m, 524 s; UV-Vis λ_{max} (ε): 256 nm (22312), 289 nm (14988); Fluorometry λ_{max}: 392 nm.

Synthesis of N-ethyl-2,3,4,5-tetra(4-*tert*butylphenyl)pyrrole, **3.7**

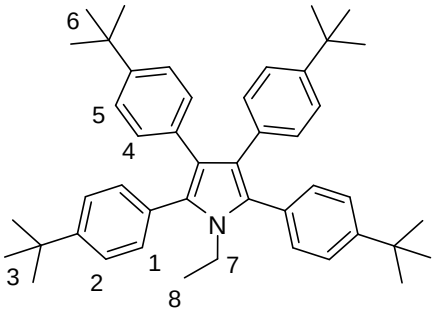

3.4 (0.340 g, 0.571 mmol), sodium hydride (0.04 g, 1.71 mmol), ethyl bromide (0.075 g, 0.05 mL, 0.685 mmol). Yield: 0.140 g (39%). m.p. 171 – 174 ˚C; ^{1}H NMR (500MHz, $CDCl_3$): δ_H 7.31 (d, 4H, *J* = 8 Hz, H1), 7.25 (d, 4H, *J* = 8 Hz, H2), 6.99 (d, 4H, *J* = 8 Hz, H4), 6.84 (d, 4H, *J* = 8 Hz, H5), 3.85 (q, 2H, CH_2, *J* = 7 Hz, H7), 1.32 (s, 9H, H3, H3', H3''), 1.22 (s, 9H, H6, H6', H6''), 0.94 (t, 3H, CH_3, *J* = 7 Hz, H8); ^{13}C NMR (125MHz, $CDCl_3$): δ_C 171.2 C2a, C5a, 149.8 C1a, 147.1 C4a, 132.8, 131.1 C2, 130.7 C5, 130.5, 130.4, 124.8 C1, 124.0 C4, 121.9, 39.6 C7, 31.5 C3, 31.3 C6, 16.7 C8; ESMS calc for $C_{46}H_{57}NNa$ ([**3.7** + Na]$^+$) = 646.4389, found 646.4381; IR (KBr)*ν*/cm^{-1}: 2961 s, br, 1739 w, 1462 m, 1362 m, 1269 m, 836 s, 569 m; UV-Vis λ_{max} (ε): 255 nm (24323), 287 nm (17437); Fluorometry λ_{max}: 393 nm.

Synthesis of N-benzyl-2,3,4,5-tetraarylpyrroles, **3.8 – 3.10**

General procedure for the synthesis of N-ethyl-2,3,4,5-tetraarylpyrroles, **3.8 – 3.10**

Following a modified literature procedure,[11] in a round bottom flask flushing with N_2, was added the appropriate N*H*-2,3,4,5-tetraarylpyrrole and 25 mL dry dimethylformamide. The solution was cooled to 0˚C using an ice bath and sodium hydride was added. The solution was stirred at 0˚C for 10 minutes and then benzyl bromide was added and the solution stirred at room temperature overnight. The solution was poured into 100 mL water and extracted with 3x 75 mL ethyl acetate. The combined organic layers were washed with 3x 200 mL water, dried with sodium sulfate and the solvent removed *in vacuo*. The solid obtained was recrystallised from ethyl acetate / hexanes.

Synthesis of N-benzyl-2,3,4,5-tetraphenylpyrrole, **3.8**

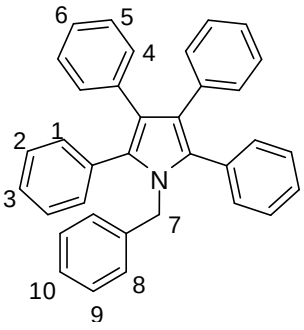

3.1 (1.60 g, 4.17 mmol), sodium hydride (0.30 g, 12.51 mmol), benzyl bromide (0.86 g, 0.60 mL, 5.01 mmol). Yield: 1.30 g (68%). m.p. 186 – 188 ˚C; ^{1}H NMR (500MHz, $CDCl_3$): δ_H 7.20 – 7.13 (m, 15H), 7.04 (d, 4H, *J* = 7 Hz), 6.98 (d, 4H, *J* = 7 Hz), 6.76 (d, 2H, *J* = 7 Hz), 5.08 (s, 2H, CH_2, H7); ^{13}C NMR (125MHz, $CDCl_3$): δ_C 139.2, 135.6, 132.8, 131.9, 131.5, 130.9, 128.2, 128.0, 127.9, 127.4, 127.3, 126.7, 126.0, 125.1, 122.6, 48.2 C7; ESMS calc for $C_{35}H_{28}N$ ([**3.8** + H]$^+$) = 462.2216, found 462.2225; IR (KBr)*ν*/cm^{-1}: 3063 w, 3030 w, 1601 m, 1501 m, 1337 m, 1073 w, 1028 w, 757 m, 739 m, 703 s; UV-Vis λ_{max} (ε): 251 nm (27416), 291 nm (16018); Fluorometry λ_{max}: 392 nm.

Synthesis of N-benzyl-2,3,4,5-tetra(4-methylphenyl)pyrrole, **3.9**

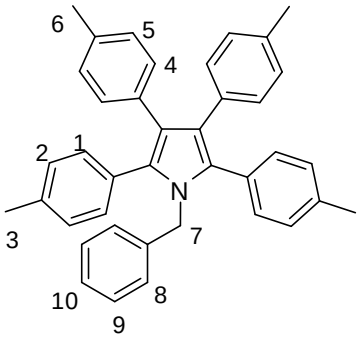

3.3 (1.40 g, 3.28 mmol), sodium hydride (0.25 g, 9.82 mmol), benzyl bromide (0.68 g, 0.45 mL, 3.94 mmol). Yield: 1.30 g (75%). m.p. 213 – 217 ˚C; ^{1}H NMR (500MHz, $CDCl_3$): δ_H 7.14 (d, 2H, *J* = 7.5 Hz, H8), 7.04 (d, 4H, *J* = 7.5 Hz, H1), 6.98 (d, 4H, *J* = 7.5 Hz, H2), 6.85 (s, 9 H), 6.74 (d, 2H, *J* = 7 Hz), 5.02 (s, 2H, CH_2, H7), 2.27 (s, 3H, CH_3, H3), 2.22 (s, 3H, CH_3, H6); ^{13}C NMR (125MHz, $CDCl_3$): δ_C 139.5, 136.8, 134.1, 132.8, 131.6, 131.4, 130.6, 130.0, 128.7, 128.1, 128.0, 126.5, 126.0, 122.2, 48.0 C7, 21.2 C3, 21.1 C6; ESMS calc for $C_{39}H_{36}N$ ([**3.9** + H]$^+$) = 518.2842, found 518.2852; IR (KBr)*ν*/cm^{-1}: 3027 w, sh, 2917 w, 1520 s, 1494 s, 1454 s, 1351 s, 1113 m, 836 s, 824 s, 734 m, 525 m; UV-Vis λ_{max} (ε): 253 nm (25573), 284 nm (16291); Fluorometry λ_{max}: 396 nm.

Synthesis of N-benzyl-2,3,4,5-tetra(4-*tert*butylphenyl)pyrrole, **3.10**

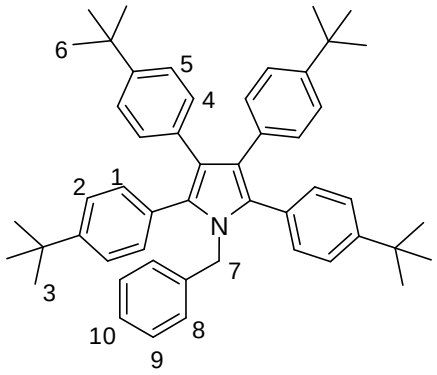

3.4 (0.80 g, 1.34 mmol), sodium hydride (0.10 g, 4.02 mmol), benzyl bromide (0.27 g, 0.2 mL, 1.61 mmol). Yield: 0.40 g (43%). m.p. 277 – 282 ˚C; ^{1}H NMR (500MHz, $CDCl_3$): δ_H 7.18 (d, 4H, *J* = 8.5 Hz, H8), 7.11 – 7.09 (m, 7H), 7.02 (d, 4H, *J* = 8.5 Hz, H4), 6.90 (d, 4H, *J* = 8.5 Hz, H5), 6.69 – 6.67 (m, 2H), 5.00 (s, 2H, CH_2, H7), 1.27 (s, 9H, CH_3, H3), 1.23 (s, 9H, CH_3, H6); ^{13}C NMR (125MHz, $CDCl_3$): δ_C 149.8, 127.3, 139.6, 132.8, 131.7, 131.2, 130.4, 130.1, 127.9, 126.4, 126.2, 124. 7, 124.0, 122.3, 48.3 C7, 31.4 C3, 31.3 C6; ESMS calc for $C_{51}H_{60}N$ ([**3.10** + H]$^+$) = 686.4720, found 686.4743; IR (KBr)*ν*/cm^{-1}: 2965 s, 2902 w, sh, 2867 w, sh, 1495 w, 1362 m, 1268 w, 1130 w, 1019 w, 837 m, 820 w, 564 w; UV-Vis λ_{max} (ε): 253 nm (26405), 289 nm (17660); Fluorometry λ_{max}: 399 nm.

General procedure for oxidative cyclodehydrogenation using $FeCl_3$ dissolved in nitromethane

In an oven dry schlenk tube cooled under vacuum and backfilled with argon was added iron (III) chloride and placed back under vacuum for 15 minutes. In an oven dry three-necked round bottom flask cooled whilst flushing with argon was added the appropriate N-substituted-2,3,4,5-tetraarylpyrrole (~ 0.150 g), and the solid was flushed with argon for five minutes. 150 mL dry dichloromethane was added and the solution was stirred with argon bubbling through for five minutes. The schlenk tube was refilled with argon and the iron (III) chloride was dissolved in nitromethane. The nitromethane solution was added dropwise to the dichloromethane solution and the solution was stirred with argon bubbling through for six hours, then the bubbling argon was removed and the solution was stirred under argon overnight. The reaction was quenched with 100 mL methanol and then 100 mL water was added. The layers were separated and the organic layer was washed with 50mL of water, dried with $MgSO_4$ and the solvent removed *in vacuo*. Purification by flash column chromatography was attempted usually using SiO_2, 9:1 hexanes : ethyl acetate or SiO_2 4:1 hexanes:ethyl acetate.

General procedure for oxidative cyclodehydrogenation using $FeCl_3$ added to the reaction as a solid

In an oven dry schlenk tube cooled under vacuum and backfilled with argon was added iron (III) chloride and placed back under vacuum for 15 minutes. In an oven dry three-necked round bottom flask cooled whilst flushing with argon was added the appropriate N-substituted-2,3,4,5-tetraarylpyrrole (~ 0.150 g), and the solid was flushed with argon for five minutes. 150 mL dry dichloromethane was added and the solution was stirred with argon bubbling through for five minutes. The schlenk tube was refilled with argon and the solid iron (III) chloride was added in one go to the dichloromethane solution. The solution

was stirred with argon bubbling through for six hours, then the bubbling argon was removed and the solution was stirred under argon overnight. The reaction was quenched with 100 mL methanol and then 100 mL water was added. The layers were separated and the organic layer was washed with 50 mL of water, dried with $MgSO_4$ and the solvent removed *in vacuo*. Purification by flash column chromatography was attempted usually using SiO_2, 9:1 hexanes:ethyl acetate or SiO_2, 4:1 hexanes:ethyl acetate.

Synthesis of 3,6,12,15-tetrachloro-9-ethyl-tetrabenzo[*a*,*c*,*g*,*i*]carbazole, **3.14**

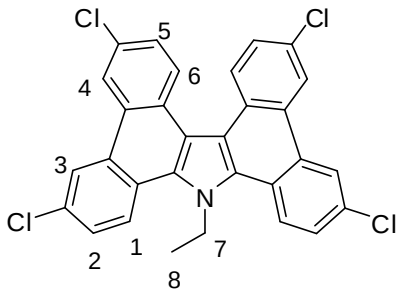

3.5 (0.180 g, 0.458 mmol), $FeCl_3$ (3.37 g, 20.61 mmol), upon attempting to dissolve in dichloromethane to purify by column chromatogaphy a solid formed. This solid was collected, and washed with a small amount of dichloromethane to give **3.14**. Yield: 0.019 g (8%). m.p. ˚C 306 – 307 ; ^{1}H NMR (500MHz, $CDCl_3$): δ_H 8.70 (d, 1H, *J* = 9 Hz, H1), 8.69 (s, 2H, H3), 8.58 (s, 2H, H4), 8.44 (d, 2H, *J* = 9 Hz, H6), 7.70 (d, 2H, *J* = 9 Hz, H5), 7.55 (d, 2H, *J* = 9 Hz, H2), 5.12 (q, 2H, CH_2, *J* = 7 Hz, H7), 1.70 (t, 3H, CH_3, *J* = 7 Hz, H8); ^{13}C NMR (125MHz, $CDCl_3$): δ_C 135.3, 132.0, 131.4,131.0, 128.6, 127.9, 127.1, 127.0, 126.9, 124.4, 123.9, 123.8, 117.3, 45.2 C7, 16.1 C8; IR (KBr)*v*/cm^{-1}: 2975 w, 2925 w, 1566 s, 1518 m, 1433 s, 1350 m, 1131 m, 1100 m, 1027 m, 953 m, 875 s, 802 s, 697 w, 541 w.

Synthesis of N-benzyl-2,3-diphenyl-dibenzo[*e*,*g*]indoles **3.15** – **3.17**

Synthesis of N-benzyl-2,3-diphenyl-dibenzo[*e*,*g*]indole, **3.15**

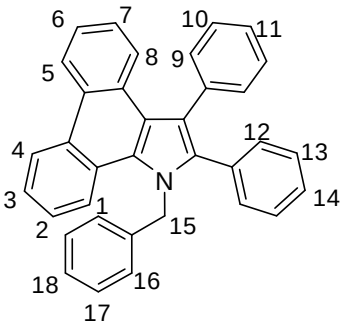

3.8 (0.150 g, 0.325 mmol), iron (III) chloride (0.81 g, 4.87 mmol), purification with flash column chromatography (SiO_2, 9:1 hexanes:ethyl acetate). Crystals suitable for X-ray crystallography were obtained by diffusion of methanol into a benzene solution of **3.15**. Yield: 0.045 g (30%). m.p. 243 – 244 ˚C; ^{1}H NMR (400MHz, $CDCl_3$): δ_H 8.77 (d, 1H, *J* = 8.4 Hz, H4), 8.68 (d, 1H, *J* = 8.8 Hz, H5), 8.15 (d, 1H, *J* = 8.4 Hz, H1), 7.84 (d, 1H, *J* = 8.8 Hz, H8), 7.48 – 7.27 (m, 17H, H3, H2, H6, H7), 7.13 (d, 2H, *J* = 8 Hz, H9), 5.73 (s, 2H, CH_2, H15); ^{13}C NMR (125MHz, $CDCl_3$): δ_C 138.8, 138.6, 137.3, 131.7, 131.6, 131.4, 129.3, 128.9, 128.8, 128.2, 127.9, 127.8, 127.6, 127.2, 126.6, 126.3, 126.2, 125.8, 124.2 C8, 124.0, 123.9, 123.8 C4, 123.2 C5, 121.8 C1, 119.7, 119.6, 51.1 C15; ESMS calc for $C_{35}H_{26}N$ ([**3.15** + H]$^+$) = 460.2060, found 460.2056; IR (KBr)*v*/cm^{-1}: 3056 w, br, 1608 m, 1512 m, 1441 m, 1357 m, 1031 m, 761 s, 728 s, 701 s; UV-Vis λ_{max} (ε): 267 nm (62766), 294 nm (28055), 318 nm (17661), 365 nm (3071); Fluorometry λ_{max}: 394 nm.

Synthesis of N-benzyl-2,3-di(4-methylphenyl)-6,9-dimethyl-dibenzo[*e*,*g*]indole, **3.16**

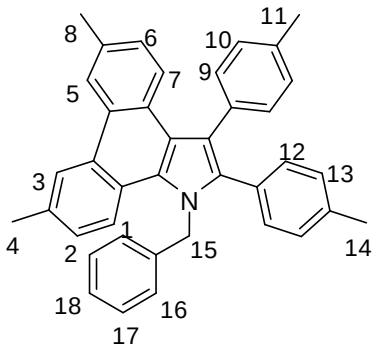

3.9 (0.150 g, 0.290 mmol), iron (III) chloride (0.71 g, 4.35 mmol), purification with flash column chromatography (SiO_2, 9:1 hexanes:ethyl acetate). Crystals suitable for X-ray crystallography were obtained by diffusion of methanol into a benzene solution of **3.16**. Yield: 0.057 g (38%). m.p. 256 – 257 ˚C; ^{1}H NMR (400MHz, $CDCl_3$): δ_H 8.53 (s, 1H, H3), 8.45 (s, 1H, H5), 7.99 (d, 1H, *J* = 7.2 Hz, H1), 7.71 (d, 1H, *J* = 7.2 Hz, H7), 7.30 – 7.25 (m, 4H), 7.23 (d, 1H, *J* = 7.2 Hz, H2), 7.17 (d, 1H, *J* = 7.2 Hz, H6), 7.14 – 7.10 (m, 5H), 7.05 (d, 2H, *J* = 6.4 Hz, H9), 6.96 (d, 2H, *J* = 6.4 Hz, H10), 5.67 (s, 2H, CH_2, H15), 2.53 (s, 6H, CH_3, H4, H8), 2.39 (s, 3H, CH_3, H14), 2.27 (s, 3H, CH_3, H11); ^{13}C NMR (125MHz, $CDCl_3$): δ_C 138.9, 138.2, 137.3, 135.8, 134.4, 133.1, 132.9, 131.4, 131.2 C9, 129.2, 129.0, 128.9 C2, 128.6 C10, 127.8, 127.6 C2, 127.5, 127.0, 126.9, 125.8, 124.1 C7, 123.8 C3, 123.0 C5, 121.7 C1, 119.0, 51.3 C15, 21.8 C4, 21.7 C8, 21.3 C14, 21.2 C11; ESMS calc for $C_{39}H_{34}N$ ([**3.16** + H]$^+$) = 516.2686, found 516.2684; IR (KBr)*ν*/cm^{-1}: 2914 w, br, 1525 s, 1496 m, 1453 s, 1355 s, 1033 w, 1024 w, 955 w, 821 s, 806 m, 749 s, 732 s, 547 m; UV-Vis λ_{max} (ε): 269 nm (64982), 299 nm (30645), 322 nm (17828), 373 nm (3551); Fluorometry λ_{max}: 393nm, 403 nm.

Synthesis of N-benzyl-2,3-di(4-*tert*butylphenyl)-6,9-di*tert*butyl-dibenzo[*e*,*g*]indole, **3.17**

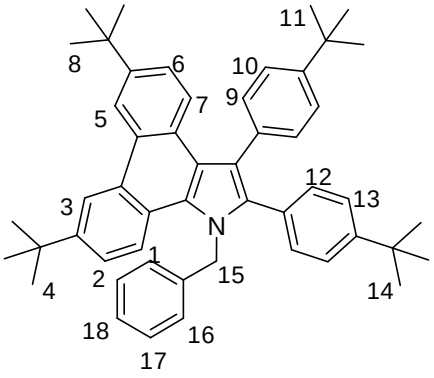

3.10 (0.150 g, 0.219 mmol), iron (III) chloride(0.53 g, 3.28 mmol), purification with flash column chromatography (SiO_2, 9:1 hexanes:ethyl acetate). Crystals suitable for X-ray crystallography were obtained by diffusion of methanol into a benzene solution of **3.17**. Yield: 0.038 g (25%). m.p. 294 – 295 ˚C; ^{1}H NMR (400MHz, $CDCl_3$): δ_H 8.75 (s, 1H, H3), 8.66 (s, 1H, H5), 8.04 (d, 1H, *J* = 7.2 Hz, H1), 7.79 (d, 1H, 6.8 Hz, H7), 7.40 (d, 1H, *J* = 7.2 Hz, H2), 7.35 – 7.24 (m, 8H), 7.13 (s, br, 4H, H9), 7.05 (d, 2H, *J* = 6.4 Hz, H10), 5.71 (s, 2H, CH_2, H15), 1.45 (s, 18H, CH_3, H4, H8), 1.36 (s, 9H, CH_3, H14), 1.24 (s, 9H, CH_3, H11); ^{13}C NMR (125MHz, $CDCl_3$): δ_C 150.24, 149.0, 145.9, 139.2, 138.3, 134.4, 131.2, 130.9 C10, 129.1, 128.9, 128.8, 127.9, 127.4, 127.0, 125.9, 124.8, 124.6, 124.1 C2, 123.9 C7, 121.6 C1, 119.5 C3, 119.4, 118.8 C5, 51.0 C15, 31.5 C4, 31.4 C8, 31.3 C14, 31.2 C11; ESMS calc for $C_{51}H_{58}N$ ([**3.17** + H]$^+$) = 684.4564, found 684.4580; IR (KBr)*ν*/cm^{-1}: 2961 s, 2903 w, sh, 2867 w, sh, 1456 w, 1361 m, 1265 w, 1025 w, 839 w, 599 w; UV-Vis λ_{max} (ε): 269 nm (62144), 296 nm (29750), 323 nm (17470), 369 nm (3472); Fluorometry λ_{max}: 389 nm, 399 nm.

General procedure for the photocyclisation reactions

In an oven dry quartz tube flushed with argon, 400 mL of dry toluene was added, and sparged with argon for 5 minutes. The appropriate N-substituted-2,3,4,5-tetraarylpyrrole was added, along with I_2 and propylene oxide. The solution was sparged with argon for 15 minutes and then irradiated with 300 nm light in a Rayonet photoreactor vernight with argon bubbling through the solution continuously. The solution was then washed with 200 mL $Na_2S_2O_3$ solution and 100 mLwater, dried with $MgSO_4$ and the solvent removed *in vacuo*. The residue was purified by flash column chromatography.

Synthesis of N-ethyl-2,3-diphenyl-dibenzo[*e*,*g*]indoles, **3.27** – **3.29**

Synthesis of N-ethyl-2,3-diphenyl-dibenzo[*e*,*g*]indole, **3.27**

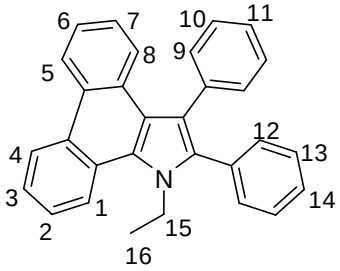

3.5 (0.150 g, 0.375 mmol), I_2 (0.310 g, 1.24 mmol), propylene oxide (2 mL), purification with flash column chromatography (SiO_2, 3:2 hexanes:dichloromethane). Yield: 0.110 g (73%). m.p. 174 – 175 ˚C; ^{1}H NMR (400MHz, $CDCl_3$): δ_H 8.82 (d, 1H, *J* = 8.8 Hz, H4), 8.68 (d, 1H, *J* = 8.8 Hz, H5), 8.45 (d, 1H, *J* = 8.8 Hz, H1), 7.78 (d, 1H, *J* = 8.4 Hz, H8), 7.66 (t, 1H, *J* = 7.2 Hz, H2), 7.58 (t, 1H, *J* = 7.2 Hz, H3), 7.43 (t, 1H, *J* = 7.2 Hz, H7), 7.36 – 7.22 (m, 11H, H6, H9, H10, H11, H12, H13, H14), 4.55 (q, 2H, CH_2, *J* = 7.2 Hz, H15), 1.47 (t, 3H, CH_3, *J* = 7.2 Hz, H16); ^{13}C NMR (125MHz, $CDCl_3$): δ_C 137.4 C1aa, 132.4, 131.6, 131.5, 129.3, 128.1, 128.0, 127.8, 126.5 C2, 126.4, 126.1 C12aa, 124.3, 124.2 C4, 124.1 C8, 123.9 C3, 123.8 C7, 123.2 C5, 121.4 C1, 41.9 C15, 16.2 C16; ESMS calc for $C_{30}H_{24}N$ ([**3.27** + H]$^+$) = 398.1903, found 398.1905; IR (KBr)ν/cm^{-1}: 3056 w, 2991 w, 1608 m, 1516 m, 1442 m, 1354 m, 1171 w, 1069 w, 1028 m, 750 s, 725 s, 705 s; UV-Vis λ_{max} (ε): 267 nm (65681), 296 nm (28569), 319 nm (16423), 365 nm (2655); Fluorometry λ_{max}: 394 nm.

Synthesis of N-ethyl-2,3-di(4-methylphenyl)-6,9-dimethyl-dibenzo[*e*,*g*]indole, **3.28**

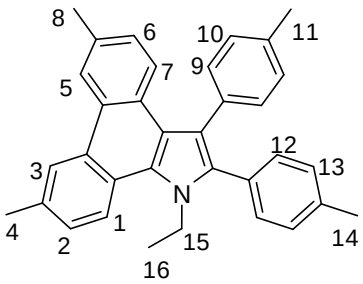

3.6 (0.150 g, 0.329 mmol), I_2 (0.270 g, 1.09 mmol), propylene oxide (1.5 mL), purification with flash column chromatography (SiO_2, 3:2 hexanes:dichloromethane). Crystals suitable for X-ray crystallography were obtained by diffusion of methanol into a benzene solution of **3.28**. Yield: 0.110 g (71%). m.p. 168 – 170 ˚C; ^{1}H NMR (400MHz, $CDCl_3$): δ_H 8.59 (s, 1H, H3), 8.45 (s, 1H, H5), 8.30 (d, 1H, *J* = 8.4 Hz, H1), 7.66 (d, 1H, *J* = 8 Hz, H7), 7.45 (d, 1H, *J* = 9.2 Hz, H2), 7.23 – 7.19 (m, 4H), 7.13 – 7.07 (m, 5H), 4.49 (q, 2H, CH_2, *J* = 7.2 Hz, H15), 2.63 (s, 3H, CH_3, H4), 2.52 (s, 3H, CH_3 H8), 2.35 (s, 6H, CH_3, H11, H14), 1.43 (t, 3H, CH_3, *J* = 7.2 Hz, H16); ^{13}C NMR (125MHz, $CDCl_3$): δ_C 137.5, 137.3 C13a, 135.6 C10a, 134.4, 133.0

C2a, 132.7 C6a, 131.5, 131.3, 129.6, 129.1, 128.8 C2, 128.7, 127.8, 127.5, 127.4, 126.9, 126.8, 124.1 C3, 123.9 C7, 123.0 C5, 122.2, 121.3 C1, 119.2, 118.8, 41.7 C15, 21.8 C11, 21.7 C14, 21.3 C8, C4, 16.2 C16; ESMS calc for $C_{34}H_{32}N$ ([**3.28** + H]$^+$) = 454.2535, found 454.2521; IR (KBr)ν/cm^{-1}: 2916 s, br, 1908 w, 1527 s, 1453 s, 1373 m, 1351 m, 1024 m, 821 s, 804 s, 745 m, 548 m; UV-Vis λ_{max} (ε): 268 nm (61052), 301 nm (27660), 323 nm (14852), 374 nm (3140); Fluorometry λ_{max}: 394 nm, 405 nm.

Synthesis of N-ethyl-2,3-di(4-*tert*butylphenyl)-6,9-di*tert*butyl-dibenzo[*e*,*g*]indole, **3.29**

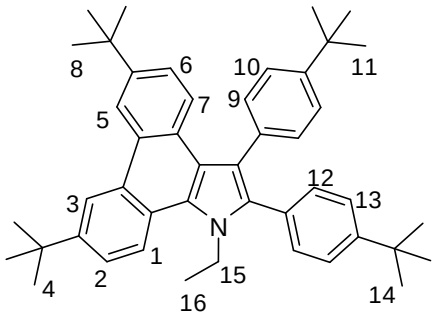

3.6 (0.06 g,0.0962 mmol), I_2 (0.081 g, 0.317 mmol), propylene oxide (1 mL), purification with flash column chromatography (SiO_2, 3:2 hexanes:dichloromethane). Yield: 0.040 g (69%). m.p. 230 – 232 ˚C; ^{1}H NMR (400MHz, $CDCl_3$): δ_H 8.82 (s, 1H, H3), 8.68 (s, 1H, H5), 8.37 (d, 1H, *J* = 8.4 Hz, H1), 7.74 (d, 1H, *J* = 8.4 Hz, H7), 7.71 (d, 1H, *J* = 8.4 Hz, H2), 7.34 – 7.21 (m, 9H), 4.52 (q, CH_2, *J* = 7 Hz, H15), 1.57 (s, 9H, CH_3, %4), 1.52 (s, 9H, CH_3, H8), 1.44 (s, 18H, CH_3, H11, H14), 1.34 (t, 3H, CH_3, *J* = 7 Hz, H16) ; ^{13}C NMR (125MHz, $CDCl_3$): δ_C 150.3 C2, 148.9 C6, 145.9 C13, 145.7 C10, 137.7, 134.5, 131.3, 131.1, 129.6, 129.1, 127.3, 127.1, 126.9, 124.7, 124.6, 124.2, 124.1, 123.8, 122.3 C7, 121.1 C1, 119.8 C3, 119.4 C5, 119.0, 118.7, 41.7 C15, 31.5 C4, 31.4, C8, 31.3 C11, C14, 16.3 C16; ESMS calc for $C_{46}H_{56}N$ ([**3.29** + H]$^+$)= 622.4407, found 622.4421; IR (KBr)ν/cm^{-1}: 2961 s, 2903 m, sh, 2868 m, sh, 1461 m, 1362 s, 1266 m, 1022 w, 850 w, 600 w; UV-Vis λ_{max} (ε): 269 nm (64653), 298 nm (30069), 324 nm (16262), 371 nm (3291); Fluorometry λ_{max}: 390 nm, 400 nm.

Synthesis of 3-benzyl-2,3-diaryl-bibenzo[*e*,*g*]indoles **3.36** – **3.38**

Synthesis of 3-benzyl-2,3-diphenyl-dibenzo[*e*,*g*]indole, **3.36**

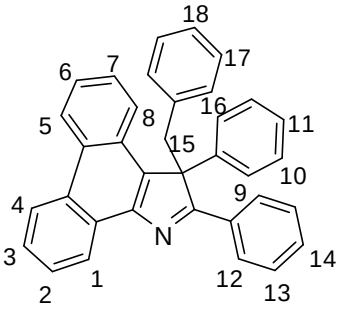

3.8 (0.150 g, 0.325 mmol), I_2 (0.270 g, 1.07 mmol), propylene oxide (1.5 mL), purification with flash column chromatography (SiO_2, 3:2 hexanes:dichloromethane). Yield: 0.005 g (4%). m.p. 218 – 220 ˚C; ^{1}H NMR (500MHz, $CDCl_3$): δ_H 8.78 (d, 1H, *J* = 8 Hz, H4), 8.72 (m 2H, H5), 7.93 (d, 2H, 7 Hz), 7.89 (d, 1H, 7.6 Hz, H1), 7.68 (m, 2H, H6), 7.60 (t, 1H, *J* = 6.8 Hz, H3), 7.52 (t, 1H, *J* = 7.6 Hz, H2), 7.45 – 7.27 (m, 10H), 6.81 (t, 1H, *J* = 7.6 Hz, H18), 6.63 (t, 2H, *J* = 7.6 Hz, H17), 6.11 (d, 2H, *J* = 7.6 Hz, H16), 4.32 (d, 1H, *J* = 12.4 Hz, H15), 4.05 (d, 1H, *J* = 12.4 Hz, H15); ^{13}C NMR (125MHz, $CDCl_3$): δ_C 145.9, 131.8, 131.5,129.5, 128.9, 128.7, 128.6 C16, 127.1, 127.0 C2, 126.9 C17, 126.8 C18, 126.6, 125.6 C3, 124.9 C4, 124.0, 123.4 C1, 122.7 C5, 40.7 C15; ESMS calc for $C_{35}H_{26}N$ ([**3.36** + H]$^+$) =

460.2060, found 460.2070; IR (KBr)ν/cm^{-1}: 3060 w, 3028 w, 1524 m, 1493 m, 1443 m, 1315 w, 1027 w, 753 s, 725 m, 702 s, 526 m; UV-Vis λ_{max} (ε): 258 nm (40432), 291 nm (23671), 301 nm (17474), 364 nm (13590); Fluorometry λ_{max}: 453 nm.

Synthesis of 3-benzyl-2,3-di(4-methylphenyl)-6,9-dimethyl-dibenzo[*e*,*g*]indole, **3.37**

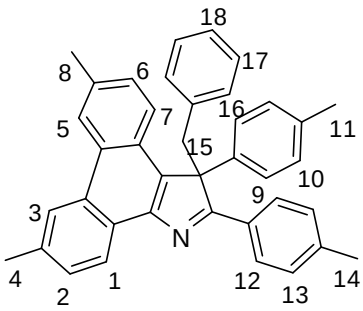

3.9 (0.150 g, 0.290 mmol), I_2 (0.150 g, 0.608 mmol), propylene oxide (1.5 mL), purification with flash column chromatography (SiO_2, 3:2 hexanes:dichloromethane). Crystals suitable for X-ray crystallography were obtained by diffusion of methanol into a benzene solution of **3.37**. Yield: 0.007 g (5%). m.p. 274 – 276 ˚C; ^{1}H NMR (400MHz, $CDCl_3$): δ_H 8.54 (s, 1H, H3), 8.49 (s, 1H, H5), 7.85 (d, 2H, *J* = 7.6 Hz, H12), 7.78 (d, 1H, *J* = 8.4 Hz, H1), 7.49 (d, 1H, *J* = 7.6 Hz, H7), 7.33 (d, 1H, *J* = 7.6 Hz, H2);7.27 (m, 2H, H9), 7.20 (d, 2H, *J* = 7.6 Hz, H13), 7.12 (m, 3H, H6, H10), 6.80 (t, 1H, *J* = 7.2 Hz, H18), 6.63 (t, 2H, *J* = 7.2 Hz, H17), 6.13 (d, 2H, *J* = 7.2 Hz, H16), 4.27 (d, 1H, *J* = 12.8 Hz, H15), 4.00 (d, 1H, *J* = 128 Hz, H15), 2.64 (s, 3H, CH_3), 2.60 (s, 3H, CH_3), 2.40 (s, 3H, CH_3), 2.30 (s, 3H, CH_3); ^{13}C NMR (125MHz, $CDCl_3$): δ_C 148.6 C4a, 140.5 C14a, 136.7, 136.6, 136.0, 135.9, 134.9, 134.6, 131.3, 131.0, 130.0, 129.6 C11, 129.3, 129.0 C16, 128.5 C2, 128.3 C12, 128.2 C7, 126.9 C17, 126.3 C18, 126.0, 124.9, 124.6, 123.7, 123.1 C1, 122.5 C5, 68.1 C16a, 40.7 C15, 22.3 C4, 22.1 C8, 21.6 C14, 21.1 C11; ESMS calc for $C_{39}H_{34}N$ ([**3.37** + H]$^+$) = 516.2686, found 516.2694; IR (KBr)ν/cm^{-1}: 3032 w, 2918 m, br, 1608 w, 1509 s, 1311 w, 1183 m, 1021 w, 819 s, 809 m, sh, 763 w, 739 w, 701 s, 524 s; UV-Vis λ_{max} (ε): 262 nm (30986), 281 nm (24451), 294 nm (19158), 306 nm (13655), 375 nm (9741); Fluorometry λ_{max}: 463 nm.

Synthesis of 3-benzyl-2,3-di(4-*tert*butylphenyl)-6,9-di*tert*butyl-dibenzo[*e*,*g*]indole, **3.38**

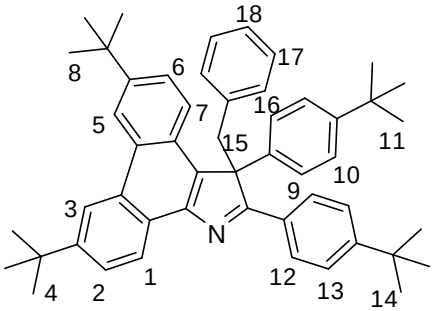

3.10 (0.150 g, 0.219 mmol), I_2 (0.190 g, 0.722 mmol), propylene oxide (1.5 mL), purification with flash column chromatography (SiO_2, 7:3 hexanes:dichloromethane). Yield: 0.006 g (4%). m.p. 251 – 252 ˚C; ^{1}H NMR (400MHz, CD_2Cl_2): δ_H 8.79 (s, 1H, H3), 8.74 (s, 1H, H5), 8.61 (d, 1H, *J* = 8.8 Hz, H7), 7.89 (d, 3H, *J* = 8.4 Hz, H1, H12), 7.78 (d, 1H, *J* = 8.8 Hz, H6), 7.64 (d, 1H, *J* = 7.6 Hz, H2), 7.44 (d, 2H, *J* = 8.8 Hz, H13), 7.36 (d, 2H, *J* = 8 Hz, H9), 7.31 (m, br, 2H, H10), 6.83 (t, 1H, *J* = 7.6 Hz, H18), 6.60 (t, 2H, *J* = 7.6 Hz, H17), 6.19 (d, 2H, *J* = 7.6 Hz, H16), 4.35 (d, 1H, *J* = 12.4 Hz, H15), 4.08 (d, 1H, *J* = 12.4 Hz, H15), 1.47 (s, 9H, CH_3, H4), 1.45 (s, 9H, CH_3, H8), 1.31 (s, 9H, CH_3, H14), 1.23 (s, 9H, CH_3, H11); ^{13}C NMR (125MHz, CD_2Cl_2): δ_C 135.8,

135.5, 129.0, 128.1, 126.9, 126.2, 125.8, 125.5, 125.2, 125.0, 124.1, 123.0, 119.6, 1183, 40.5 C15, 31.2 C4, 31.1 C8, 30.9 C14, 30.8, C11; ESMS calc for $C_{51}H_{58}N$ ([**3.38** + H]$^+$) = 684.4564, found 684.4583; IR (KBr)*v*/cm^{-1}: 2961 s, 2905 m, sh, 2868 m, sh, 1606 w, 1507 m, 1363 m, 1264 m, 111 w, 1017 w, 838 m, 700 m; UV-Vis λ_{max} (ε): 262 nm (43251), 279 nm (34494), 295 nm (28320), 307 nm (19733), 375 nm (15564); Fluorometry λ_{max}: 461 nm.

Synthesis of N-substituted-2,3-di(4-methylphenyl)-6,9-dimethyl-dibenzo[*e,g*]indoles, **3.16**, **3.28** using DDQ/CH_3SO_3H

Following a modified literature procedure,[21] in an oven dried Schlenk tube, cooled under vacuum, and backfilled with argon, was added the appropriate N-substituted-2,3,4,5-tetra(4-methylphenyl)pyrrole (1 equiv). 20 mL of dry dichloromethane and 2 mL of CH_3SO_3H was added and the solution was cooled to 0 ˚C using an ice bath. DDQ was added (3 equiv) and the reaction was stirred at room temperature overnight, and then quenched with 20 mL sat. aqueous $NaHCO_3$. The organic layer was washed with 50 mLwater, then 50 mL brine. The organic layer was dried with $MgSO_4$ and the solvent was removed *in vacuo* and the residue was purified with flash column chromatography (SiO_2, 3:2 hexanes:dichloromethane).

Compounds **3.6** and **3.9** formed **3.28** and **3.16** respectively, ^{1}H NMR spectroscopy and ESMS matched that of compounds **3.28** and **3.16** described above.

Attempted synthesis of N-substituted-2,3-di(4-methylphenyl)-6,9-dimethyl-dibenzo[e,g]indoles, **3.16**, **3.28** using $CF_3COO)_2I^{III}C_6H_5$ (PIFA)/BF_3.OEt_2

Following a modified literature procedure,[22] in an oven dried Schlenk tube, cooled under vacuum, and backfilled with argon, was added **3.5** (0.200 g, 0.5 mmol). 10 mL of dry dichloromethane was added and the solution was cooled to – 40 ˚C using an acetonitrile/dry ice bath. PIFA (0.240 g, 0.55 mmol) and BF_3.OEt_2 (0.085 g, 0.08 mL, 0.60 mmol) were added to an oven dry Schlenk tube cooled under vacuum and backfilled with argon, and 10 mL of dry dichloromethane was added. This solution was cooled to – 40 ˚C and added dropwise to the reaction mixture. After three hours stirring at – 40 ˚C the reaction mixture was quenched with 20 mL sat. aqueous $NaHCO_3$. The organic layer was washed with 50 mL water and the mixture was dried with $MgSO_4$. The solvent was removed *in vacuo*. The ^{1}H-NMR spectrum of the crude residue matched that of the starting material.

Synthesis of 1,3-diphenyl-dibenzo[*e*,*g*]isoindole, **3.42**

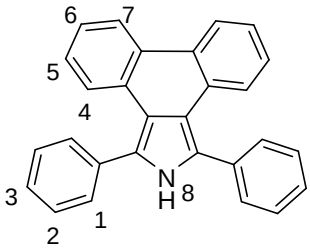

9,10-phenanthrenediylbis(phenyl)methanone, **3.43**, (0.20 g, 0.520 mmol) was added to a round bottom flask and dissolved in 20 mL glacial acetic acid. Zinc (0.07 g, 1.036 mmol) and ammonium acetate (0.16 g, 2.07 mmol) were added and the reaction mixture was refluxed overnight. The reaction mixture was added to 100 mL water and extracted with 2x 50 mL ethyl acetate. The combine organic layer was washed with 2x 100 mL sat. aqueous $NaHCO_3$, 100 mL water and 50 mL brine. The organic layer was then dried with $MgSO_4$ and the solvent removed *in vacuo*. Purification using flash column chromatography (SiO_2, 9:1 hexanes:ethyl acetate) gave 1,3-diphenyl-dibenzo[*e*,*g*]isoindole. Crystals suitable for X-ray crystallography were obtained by the slow evaporation of a dichloromethane solution of **3.42**. Yield: 0.035 g (20%). ^{1}H NMR (400MHz, $CDCl_3$): δ_H 8.37 (d, 2H, J = 8.4 Hz), 8.17 (d, 2H, J = 8 Hz), 7.82 (d, 4H, J = 7.2 Hz), 7.55 – 7.42 (m, 10H); ^{13}C NMR (125MHz, $CDCl_3$): δ_C 133.8, 130.1, 129.3, 128.8, 128.7, 128.5, 128.0, 127.1, 126.9, 124.1, 123.8, 123.0.

Attempted synthesis of 2-ethyl-1,3-diphenyl-dibenzo[*e*,*g*]indole, **3.41**

Following the general procedure outlined above for the the synthesis of N-ethyl-2,3,4,5-tetraarylpyrroles **3.6** and **3.7**, **3.42** (0.085 g, 0.23 mmol), sodium hydride (0.020 g, 0.69 mmol) and ethyl bromide (0.030 g, 0.02 mL, 0.28 mmol) were used. After removal of the solvent *in vacuo*, multiple products were present according to TLC. Purification using flash column chromatography was attempted (SiO_2, 3:2 hexanes:dichloromethane) but no products with data matching that expected for **3.41** was obtained.

Chapter Four

The following compounds were prepared according to literature methods, and all characterisation data were found to be consistent with that provided; pentaphenylpyrrole, **4.1**,[23] 1,2,3,4-tetraphenyl-1.4-butadione, **4.3**,[11] deoxybenzoin, **4.6**,[24] deoxyanisoin, **4.7**,[18] deoxy-4,4'-*tert*butylanisoin, **4.8**,[8] *tert*butylaniline, **4.11**,[25] 1,2,5-triphenyl-3,4-dibromopyrrole, **4.23**,[23] phenylboronic acid, **4.24**,[26] 1,4-diphenylbutane, **4.25**,[27],[28] 4-methoxyphenylboronic acid, **4.30**[29] and 4'-(4-aminophenyl)-2,2':6,2''terpyridine, **4.34**.[30]

Synthesis of 1,2,3,4-tetra(4-*tert*butylphenyl)-1,4-butadione, **4.5**

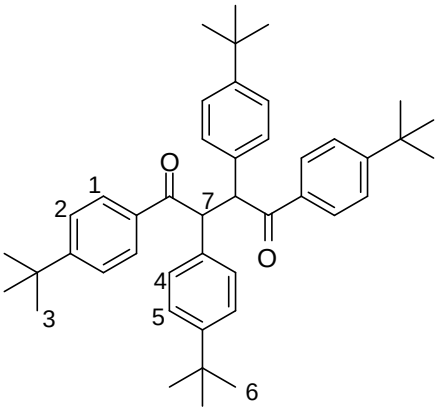

Following a modified literature procedure,[11] KO^{t}Bu (0.065 g, 0.58 mmol) was added to an oven dry Schlenk flask, cooled under vacum and backfiled with argon, dissolved in 10 mL dry tetrahydrofuran and then cooled to – 75 ˚C using an acetone/dry ice bath. Deoxy-4,4'-*tert*butylanisoin, **4.8**, (0.25 g, 0.81 mmol) was added to an oven dry Sclenk tube cooled under vacuum and backfilled with argon, dissolved in 10 mL dry tetrahydrofuran and added to the reaction mixture dropwise. I_2 (0.150 g, 0.58 mmol) was dissolved in 20 mL dry tetrahydrofuran and added to the reaction mixture dropwise. The reaction mixture was stirred for two hours at 0 ˚C using an ice bath. 50 mL sat. aqeous $Na_2S_2O_5$ was added to quench the reaction, and the aqueous layer was extracted with 2x 20 mL ethyl acetate. The combined organic residue was washed with 2x 20 mL brine, dried with $MgSO_4$ and the solvent was removed *in vacuo*. Recrystallised from hexanes/ethylacetate to give 1,2,3,4-tetra(4-*tert*butylphenyl)-1,4-butadione. Yield: 0.15 g (60%). m.p. 140 – 142 ˚C; ^{1}H NMR (500MHz, $CDCl_3$): δ_H 7.82 (d, 4H, *J* = 8.5 Hz, H5), 7.35 (d, 4H, *J* = 8.5 Hz, H4), 7.27 (d, 4H, *J* = 8.5 Hz, H2), 7.20 (d, 4H, *J* = 8.5 Hz, H1), 5.84 (s, 2H, H7), 1.22 (s, 18H, H6), 1.20 (s, 18H, H3); ^{13}C NMR (125MHz, $CDCl_3$): δ_C 198.4 C7a, 157.8 C2a, 151.4 C5a, 136.3 C1a, 130.9 C4a, 129.2 C5, 127.4 C1, 126.1 C2, 125.7 C4, 75.6 C7, 31.3 C6, 31.0 C3; ESMS calc for $C_{44}H_{52}O_2$ ([**4.5** + H]$^+$) = 615.4202, found 615.4191; IR (KBr)ν/cm^{-1}: 3402 s, 3425 s, 2959 s, 1673 s, 1604 m, 1463 m, 1410 m, 1267 m, 1220 m, 1185 m, 1089 m, 980 m, 872 m, 826 m, 818 m, 654 m, 580 m.

General procedure for the synthesis of 2,3,4,5-tetraarylfurans, **4.14 – 4.16**

In a round bottom flask was added the appropriate 1,2,3,4-tetraaryl-1,4-butadione, aniline and 20 mL glacial acetic acid. The reaction mixture was heated to refux and refluxed for two hours. A white precipate formed, which was filtered to give the corresponding 2,3,4,5-tetraarylfuran.

Synthesis of 2,3,4,5-tetraphenylfuran, **4.14**[31]

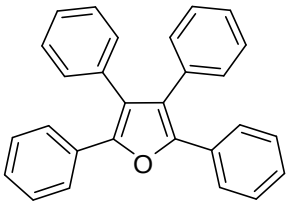

4.3 (0.150 g, 0.380 mmol), aniline (0.110 g, 0.11 mL, 1.15 mmol). Yield: 0.120 g (84%). m.p. 190 – 193 ˚C; ^{1}H NMR (500MHz, $CDCl_3$): δ_H 7.51 (d, 4H, *J* = 7.5 Hz), 7.26 – 7.22 (m, 12H), 7.17 – 7.14 (m, 4H).

Synthesis of 2,3,4,5-tetra(4-methoxyphenyl)furan, **4.15**[32]

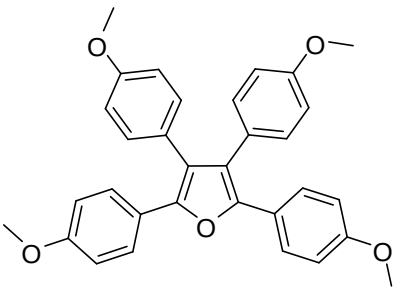

4.4 (0.120 g, 0.240 mmol), aniline (0.070 g, 0.07 mL, 0.720 mmol). Yield: 0.095 g (80%). m.p. 201 – 204 ˚C; ^{1}H NMR (500MHz, $CDCl_3$): δ_H 7.44 (d, 4H, *J* = 9 Hz), 7.06 (d, 4H, *J* = 9Hz), 6.81 (d, 4H, *J* = 9 Hz), 6.79 (d, 4H, *J* = 9 Hz), 3.80 (s, 6H, CH_3), 3.79 (s, 6H, CH_3).

Synthesis of 2,3,4,5-tetra(4-*tert*butylphenyl)furan, **4.16**[31]

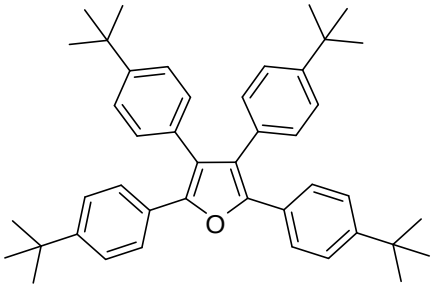

4.5 (0.100 g, 0.162 mmol), aniline (0.45 g, 0.45 mL, 0.488 mmol). Yield: 0.080 g (82%). m.p. 198 – 200 ˚C; ^{1}H NMR (500MHz, $CDCl_3$): δ_H 7.42 (d, 4H, *J* = 8.5 Hz), 7.16 (d, 4H, *J* = 8.5 Hz), 7.12 (d, 4H, *J* = 8.5 Hz), 6.99 (d, 4H, *J* = 8.5 Hz), 1.25 (s, 18H, CH_3), 1.23 (s, 18H, CH_3).

General procedure for the synthesis of N-substituted-N-benzoyl-phenylglycines, **4.18** and **4.21**

In a round bottom flask was added phenyl acetic acid (10.0 g, 73.4 mmol), 80 mL ethanol and 5 mL conc. H_2SO_4 and the reaction mixture was refluxed overnight. The reaction mixture was cooled and the solvent removed *in vacuo*. Purification using flash column chromatography (Al_2O_3, 1:1 hexanes:ethyl acetate) gave 10.50 g (95%) phenyl acetic acid ethyl ester.

Following literature procedure,[33] in a round bottom flask was added sodium bromate (11.9 g, 78.9 mmol) dissolved in 40 mL water. Over the course of 15 minutes phenyl acetic acid ethyl ester (4.0 g, 26.3 mmol) dissolved in 50 mL of ethyl acetate was added, followed by sodium metabisulfite (7.6 g, 39.5 mmol)

dissolved in 100 mL water. The reaction mixture was stirred at room temperature for five hours. The reaction mixture was extracted with 3x 100 mL diethyl ether, and the combined organic layers were washed with 100 mL sat. aqueous sodium thiosulfate, dried with $MgSO_4$ and the solvent removed *in vacuo*. Purification using flash column chromatography (SiO_2, 9:1 hexanes:ethyl acetate) gave 4.5 g (70%) of α-bromophenyl acetic acid ethyl ester.

In a round bottom flask, α-bromophenyl acetic acid ethyl ester (0.60 g, 2.5 mmol), the appropriate amine (1 equiv) and triethylamine (1 equiv) were added, followed by 20 mL dry toluene. The reaction mixture was refluxed for overnight, and then cooled. The solution was washed with 50 mL water, dried with $MgSO_4$ and the solvent removed *in vacuo*. The resulting residue was recrystallised from pentane to give the corresponding α-amino phenyl acetic acid ethyl ester (methyl amino 0.38 g (78%) and phenyl amino 0.30 g (47%)).

In a round bottom flask, the appropriate α-amino phenyl acetic acid ethyl ester (0.40 mmol), benzoyl chloride (0.60 g, 0.05 mL, 0.40 mmol) and triethylamine (0.40 g, 0.55 mL, 0.40 mmol) were added, followed by 20 mL dry toluene. The reaction mixture was refluxed overnight, and then cooled. The resulting precipitate was filtered to give the appropriate α-benzoylamino phenyl acetic acid ethyl ester (methylamino 0.084 g (71%) and phenylamino 0.075 g (52%)).

In a round bottom flask the appropriate α-benzoylamino phenyl acetic acid ethyl ester (2 mmol), NaOH (0.090 g, 2.2 mmol), 2 mL water and 5 mL ethanol were added and refluxed for 45 minutes. The resulting solution was diluted with 10 mL water, acidified with 10% HCL and extracted into 20 mL dichloromethane. The dichloromethane solution was dried with $MgSO_4$, and the solvent removed *in vacuo*. The resulting residue was recrystallised from chloroform to give **4.18** (0.65 g (95%) or **4.21** (0.50 g (92%).

General procedure for the synthesis of münchnones, **4.17** and **4.20**

In an on oven dry Schlenk tube cooled under vacuum and backfilled with argon was added the appropriate N-substituted-N-benzoyl-phenylglycine (0.33 mmol) and 2 mL freshly distilled acetic anhydride. The reaction mixture was heated at 50 ˚C for 30 minutes and cooled. The reaction mixture was stirred in 10 mL diethyl ether and the resulting solid was filtered, to give the corresponding münchnone. In each case **4.17** and **4.20** quickly changed from a solid to an oily residue, and as a result were too unstable to characterised.

General procedure for the synthesis of N-substituted-2,3,4,5-tetraphenylpyrroles, **4.1** and **4.19**

In an on oven dry Schlenk tube cooled under vacuum and backfilled with argon was added the appropriate N-substituted-N-benzoyl-phenylglycine, 5 mL freshly distilled acetic acid and diphenyl

acetylene (0.60 g, 3.41 mmol). The recation mixture was heated at 130 ˚C for seven hours. The solution was cooled and the solvent removed *in vacuo*. The remaining reside was washed with methanol to give the corresponding pyrrole.

Synthesis of N-methyl-2,3,4,5-tetraphenylpyrrole, **4.19**[34]

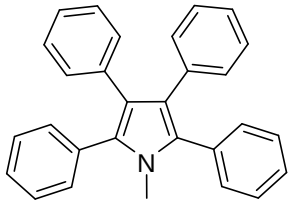

4.21 (0.31 g, 1.22 mmol). Yield: 0.100 g (21%). m.p. 205 – 207 ˚C; ^{1}H NMR (500MHz, $CDCl_3$): δ_H 7.34 – 7.25 (m, 10H), 7.09 – 7.01 (m, 6H), 6.94 – 6.89 (m, 4H), 3.45 (s, 3H, CH_3).

Synthesis of pentaphenylpyrrole **4.1**[23]

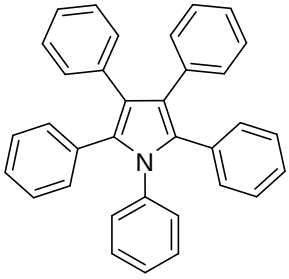

4.18 (0.232 g, 0.70 mmol). Crystals suitable for X-ray crystallography were obtained by the slow evaporation of a dichloromethane solution of **4.1**. Yield: 0.045 g (15%). m.p. 275 – 279 ˚C; ^{1}H NMR (500MHz, $CDCl_3$): δ_H 7.14 – 7.11 (m, 4H), 7.09 – 7.05 (m, 11H), 6.94 – 6.89 (m, 10H); ESMS calc for $C_{34}H_{26}N$ ([**4.1** + H]$^+$) = 448.2060, found 448.2068.

General procedure for the synthesis of 1,2,5-triarylpyrroles, **4.22**, **4.26** and **4.27**

1,4-diphenyl-1,4-butanedione, **4.25**, and the appropriate aniline (1.2 equiv) were added to a round bottom flask and then 10 mL of glacial acetic acid was added. The mixture was refluxed for two hours, and then cooled to room temperature. The resulting white solid was filtered and washed with acetone.

Synthesis of 1,2,5-triphenylpyrrole, **4.22**[35]

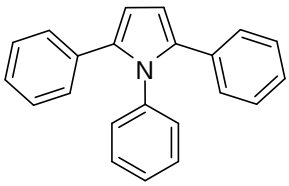

4.25 (0.50 g, 2.0 mmol), aniline (0.23 g, 0.23 mL, 2.5 mmol). Yield: 0.36 g (61%). m.p. 228 – 231 ˚C; ^{1}H NMR (500MHz, $CDCl_3$): δ_H 7.25 – 7.22 (m, 4H), 7.19 – 7.14 (m, 5H), 7.09 – 7.03 (m, 6H), 6.48 (s, 2H).

Synthesis of 1-(4-methoxyphenyl)-2,5-diphenylpyrrole, **4.26**[35]

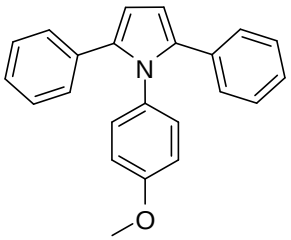

4.25 (0.50 g, 2.1 mmol), 4-anisidine (0.33 g, 2.6 mmol). Yield: 0.40 g (60%). m.p. 225 – 229 ˚C; ^{1}H NMR (500MHz, $CDCl_3$): δ_H 7.20 – 7.14 (m, 6H), 7.08 (d, 4H, *J* = 7 Hz), 6.96 (d, 2H, *J* = 8.5 Hz), 6.76 (d, 2H, *J* = 8.5 Hz), 6.47 (s, 2H), 3.78 (s, 3H, CH_3).

Synthesis of 1-(4-*tert*butylphenyl)-2,5-diphenylpyrrole, **4.27**

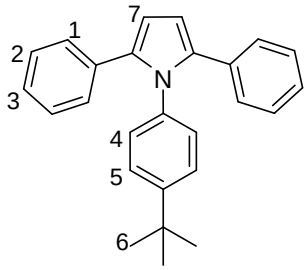

4.25 (0.30 g, 1.25 mmol), 4-*tert*butylaniline (0.23 g, 1.56 mmol). Yield: 0.27 g (62%). m.p. 241 – 242 ˚C; ^{1}H NMR (500MHz, $CDCl_3$): δ_H 7.23 (d, 2H, *J* = 8 Hz, H5), 7.16 – 7.14 (m, 6H, H1, H3), 7.07 – 7.04 (m, 4H, H2), 6.95 (d, 2H, *J* = 8 Hz, H4), 6.48 (s, 2H, H7), 1.29 (s, 9H, CH_3, H6); ^{13}C NMR (125MHz, $CDCl_3$): δ_C 133.3 C7a, 128.6 C2, 128.3 C4, 127.8 C3, 126.1 C1, 125.6 C5, 109.7 C7, 31.3 C6; ESMS calc for $C_{26}H_{25}NNa$ ([**4.27** + Na]$^+$) = 374.1879, found 374.1878; IR (KBr)*v*/cm^{-1}: 3050 w, 2965 m, 2904, w, sh, 1869, w, sh, 1599 m, 1516 s, 1485 s, 1396 m, 838 m, 759 s, 747 m, sh, 698 s, 604 w.

General procedure for the synthesis of 1,2,5-triaryl-3,4-dibromopyrroles, **4.28** and **4.29**

Following a modified literature procedure,[23] in a round bottom flask flushing with argon was added the appropriate 1,2,5-triarylpyrrole. After flushing with argon for a further 5 minutes 40mL of dry dimethylformamide was added and the solution cooled to 0˚C in an ice bath. In another round bottom flask flushing with argon was added N-bromosuccinamide and 10mL of dry dimethylformamide. This solution was added dropwise to the solution of the 1,2,5-triarylpyrrole at 0˚C. The solution was stirred overnight at room temperature. 300 mL of water was added to the solution and the white precipitate formed was filtered and washed with water and ethanol. The 1,2,5-triaryl-3,4-dibromopyrrole formed was then recrystallised from ethyl acetate.

Synthesis of 1-(4-methoxyphenyl)-2,5-diphenyl-3,4-dibromopyrrole, **4.28**

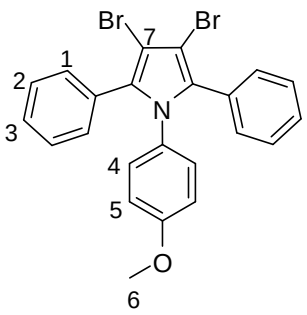

4.26 (1.50 g, 4.60 mmol), N-bromosuccinamide (1.8 g, 10.1 mmol). Yield: 1.60 g (71%). m.p. 182 – 184 ˚C; ^{1}H NMR (500MHz, $CDCl_3$): δ_H 7.26 – 7.22 (m, 6H, H1, H3), 7.19 – 7.17 (m, 4H, H2), 6.77 (d, 2H, *J* = 7 Hz, H4), 6.61 (d, 2H, *J* = 7 Hz, H5), 3.70 (s, 3H, OCH_3, H6); ^{13}C NMR (125MHz, $CDCl_3$): δ_C 158.5 C5a, C4a, 132.5 C7, 130.7 H2, 129.6 C4, 127.8 C3, 127.6 C1, 113.7 C5, 55.3 C6; ESMS calc for $C_{23}H_{18}NOBr_2$ ([**4.28** + H]$^+$) = 481.9750, found 481.9750; IR (KBr)*v*/cm^{-1}: 3057 w, 2968 w, 2840 w, 1597, w, 1514 s, 1478 m, 1459 m, 1441m, 1297 m, 1251 s, 1031 m, 834 m, 779 m, 765 m, 746 m, 700 m; UV-Vis λ_{max} (ε): 236 nm (14833), 284 nm (15251).

Synthesis of 1-(4-*tert*butylphenyl)-2,5-diphenyl-3,4-dibromopyrrole, **4.29**

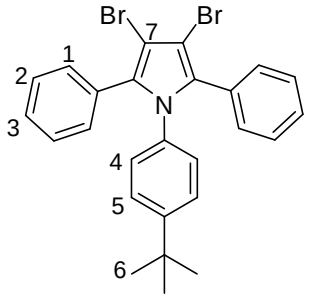

4.27 (0.72 g, 2.1 mmol), N-bromosuccinamide (0.80 g, 4.5 mmol). Yield: 0.85 g (79%). m.p. 166 – 168 ˚C; ^{1}H NMR (500MHz, $CDCl_3$): δ_H 7.26 – 7.21 (m, 6H, H1, H3), 7.17 – 7.15 (m, 4H, H2), 7.10 (d, 2H, *J* = 9 Hz, H5), 6.75 (d, 2H, *J* = 9 Hz, H4), 1.21 (s, 9H, CH_3, H6); ^{13}C NMR (125MHz, $CDCl_3$): δ_C 150.6 C5a, 135.3 C1a, 132.3 C7, 130.7 C2, 128.0 C4, 127.7 C3, 127.6 C1, 125.4 C5, 31.2 C6; ESMS calc for $C_{26}H_{23}NBr_2Na$ ([**4.29** + Na]$^+$) = 530.0089, found 532.0067; IR (KBr)*v*/cm^{-1}: 3052, w, 2967 s, 2905 w, sh, 2872 w, sh, 1600 w, 1516 m, 1484 m, 1331 s, 1030 w, 843 m, 775 m, 752 m, 701 s.

General procedure for the synthesis of pentaarylpyrroles, **4.12**, **4.13**, **4.31**, **4.32**

In a round bottom Schlenk flask, the appropriate 1,2,5-triaryl-3,4-dibromopyrrole, the appropriate aryl boronic acid and tetrakis(triphenylphosphine)palladium(0) were added and the flask vacuum/argon exchanged three times. 50 mL of degassed toluene and 2 mL degassed 2 mol.L^{-1} potassium carbonate solution were added and the reaction mixture was stirred overnight at 110 ˚C. The reaction mixture was cooled and the solvent was removed *in vacuo*. The resulting residue was purified by flash column chromatography (SiO_2, dichloromethane) and then recrystallised from ethyl acetate.

Synthesis of 1-(4-methoxyphenyl)-2,3,4,5-tetraphenylpyrrole, **4.12**[10]

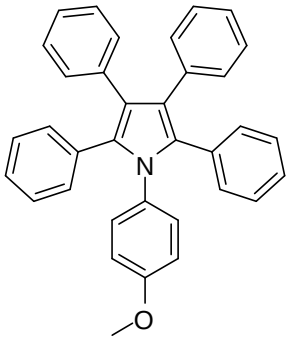

4.28 (0.46 g, 0.95 mmol), phenyl boronic acid, **4.24**, (0.35 g, 2.9 mmol), tetrakis(triphenylphosphine)palladium(0) (0.05 g). Yield: 0.15 g (33%). m.p. 265 – 268 ˚C; ^{1}H NMR (500MHz, $CDCl_3$): δ_H 7.08 – 7.05 (m, 12H),6.95 – 6.90 (m, 8H), 6.85 (d, 2H, *J* = 8.5 Hz), 6.65 (d, 2H, *J* = 8.5 Hz), 3.74 (s, 3H, OCH_3, H9); ESMS calc for $C_{35}H_{28}NO$ ([**4.12** + H]$^+$) = 478.2165, found 478.2163; UV-Vis λ_{max} (ε): 258 nm (28545), 296 nm (17402).

Synthesis of 1-(4-*tert*butylphenyl)-2,3,4,5-tetraphenylpyrrole, **4.13**

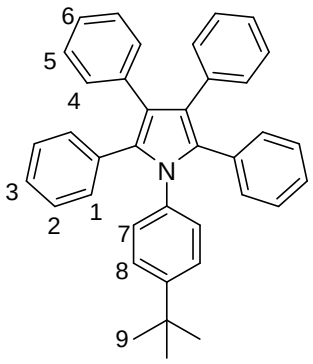

4.29 (0.50 g, 0.98 mmol), phenyl boronic acid, **4.24**, (0.36 g, 2.9mmol), tetrakis(triphenylphosphine)palladium(0) (0.05 g). Yield: 0.13 g (26%). m.p 282 – 283 ˚C; ^{1}H NMR (500MHz, $CDCl_3$): δ_H 7.12 (d, 2H, *J* = 7 Hz, H8), 7.08 – 7.02 (m, 12H), 6.94 (m, 4H), 6.89 (d, 4H, *J* = 7.5 Hz), 6.83 (d, 2H, *J* = 7 Hz, H7), 1.24 (s, 9H, CH_3, H9); ^{13}C NMR (125MHz, $CDCl_3$): δ_C 149.9 C8a, 135.8, 135.4, 132.3, 131.6, 131.4, 131.1, 128.5 C7, 127.5, 127.4, 126.3, 125.3, 125.1 C8, 122.7, 31.2 C9; ESMS calc for $C_{38}H_{33}NNa$ ([**4.13** + Na]$^+$) = 526.2505, found 526.2516; IR (KBr)*ν*/cm^{-1}: 3047 m, 2959 s, 2904 w, sh, 2868 w, sh, 1601 m, 1508 s, 1484 m, 1467 m, 1443 m, 1370 s, 1266 w, 1148 w, 1113 w, 1073 w, 1024 m, 914 m, 846 m, 800 m, 786 m, 749 m, 734 m, 701 s; UV-Vis λ_{max} (ε): 259 nm (28678), 294 nm (16777).

Synthesis of 1,2,5-triphenyl-3,4-(4-methoxyphenyl)pyrrole, **4.31**

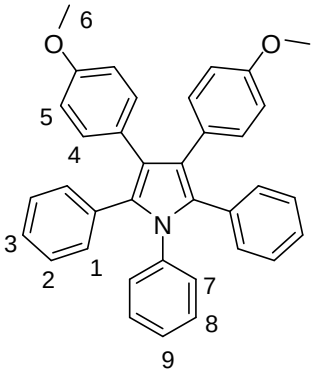

4.23 (0.86 g, 0.95 mmol), 4-methoxy phenyl boronic acid, **4.30**, (0.44 g, 2.9 mmol), tetrakis(triphenylphosphine)palladium(0) (0.25 g). Yield: 0.13 g (26%). m.p 274 – 275 ˚C; ^{1}H NMR (500MHz, $CDCl_3$): δ_H 7.13 – 7.06 (m, 8H), 6.93 – 6.87 (m, 7H), 6.86 (d, 4H, *J* = 8 Hz, H4), 6.65 (d, 4H, *J* = 8 Hz, H5), 3.75 (s, 6H, OCH_3, H6) ; ^{13}C NMR (125MHz, $CDCl_3$): δ_C 157.3 C5a, 132.4, 132.0 C4, 131.4, 131.3, 129.2, 128.2, 127.7, 127.5, 126.7, 126.3, 122.3, 113.1 C5, 55.0 C6; ESMS calc for $C_{36}H_{30}NO_2$ ([**4.31** + H]$^+$) = 508.2271, found 508.2274; IR (KBr)*ν*/cm^{-1}: 3040 w, 2950 w, 2930 w, 2832 w, 1537 m, 1509 s, 1496 m, sh, 1486 m, sh, 1369 m, 1292 m, 1245 s, 1181 m, 1107 w, 1033 m, 838 m, 795 w, 770 m, 699 s; UV-Vis λ_{max} (ε): 255 nm (32112), 297 nm (21821).

Synthesis of 1,3,4-(4-methoxyphenyl)-2,5-diphenylpyrrole, **4.32**

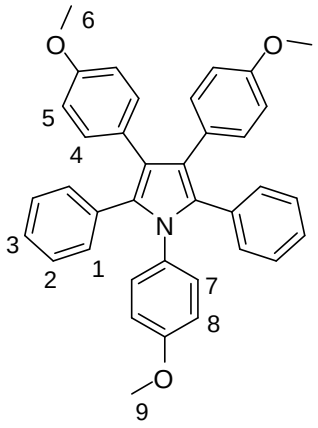

4.28 (0.92 g, 1.9 mmol), 4-methoxy phenyl boronic acid, **4.30**, (0.87 g, 5.7 mmol), tetrakis(triphenylphosphine)palladium(0) (0.20 g). Yield: 0.25 g (25%). m.p 223 – 226 ˚C; ^{1}H NMR (500MHz, $CDCl_3$): δ_H 7.08 – 7.06 (m, 6H), 6.92 – 6.90 (m, 4H), 6.87 – 6.83 (m, 6H), 6.66 – 6.63 (m, 6H), 3.75 (s, 6H, OCH_3, H6), 3.73 (s, 3H, OCH_3, H9); ^{13}C NMR (125MHz, $CDCl_3$): δ_C 158.0, 15.7.3, 132.5, 132.0, 131.4, 130.0, 127.8, 127.5, 126.2, 122.1, 113.4, 113.0, 55.3 C9, 55.0 C6; ESMS calc for $C_{37}H_{32}NO_3$ ([**4.32** + H]$^+$) = 538.2377, found 538.2385; IR (KBr)ν/cm^{-1}: 3039 w, 3005 w, 2954 w, 2931 w, 2833 m, 1600 w, 1577 w, 1536 m, sh, 1514 s, 1486 m, 1466 m, 1440 m, 1301 m, 1287 m, 1245 s, 1181 m, 1108 w, 1034 s, 834 s, 767 m, 699 m; UV-Vis λ_{max} (ε): 256 nm (32053), 296 nm (21900).

Attempts at oxidative cyclodehydrogenation of **4.1**

Method A: In an oven dry schlenk tube cooled under vacuum and backfilled with argon was added iron (III) chloride (0.71 g, 4.4 mmol) and placed back under vacuum for 15 minutes. In an oven dry three-necked round bottom flask cooled whilst flushing with argon was added pentaphenylpyrrole, **4.1**, (0.05 g, 0.11 mmol), and the solid was flushed with argon for five minutes. 50 mL dry dichloromethane was added and the solution was stirred with argon bubbling through for five minutes. The schlenk tube was refilled with argon and the iron (III) chloride was added to the dichloromethane solution in one go. The solution was stirred with argon bubbling through for six hours, then the bubbling argon was removed and the solution was stirred under argon overnight. The reaction was quenched with 50 mL methanol and then 50 mL water was added. The layers were separated and the organic layer was washed with 50mL of water, dried with $MgSO_4$ and the solvent removed *in vacuo*. Purification by flash column chromatography was attempted usually using SiO_2, 4:1 hexanes : ethyl acetate, did not isolate any products.

Method B: In an oven dry schlenk tube cooled under vacuum and backfilled with argon was added $AlCl_3$ (0.44 g, 2.60 mmol) and the tube was placed back under vacuum for 15 minutes. The tube was backfilled with argon and $CuCl_2$ (0.55 g, 2.60 mmol) and pentaphenylpyrrole, **4.1**, (0.040 g, 0.090 mmol) was added. 30 mL of degassed CS_2 was added to the solids and the reaction mixture was stirred under argon for six days, whilst monitoring with TLC. The CS_2 was evaporated and the remaining solid was stirred for two hours with 10 mL 10% NH_3 solution and 10 mL dichloromethane. The aqueous layer was extracted with 10 mL dichloromethane and the combined organic layers were washed with 10 mL 10% NH_3

solution and then 10 mL water. Purification using flash column chromatography (SiO_2, 9:1 hexanes:ethyl acetate), did not isolate any products.

Photocyclisation of **4.1**

In an oven dry quartz tube flushed with argon, 200 mL of dry toluene was added, and sparged with argon for 5 minutes. Pentaphenylpyrrole, **4.1**, (0.05 g, 0.110 mmol) was added, along with I_2 (0.150 g, 0.57 mmol) and propylene oxide 5mL. The solution was sparged with argon for 15 minutes and then irradiated with 300 nm light in a Rayonet photoreactor overnight with argon bubbling through the solution continuously. The solution was then washed with 200 mL $Na_2S_2O_3$ solution and 100 mL water, dried with $MgSO_4$ and the solvent removed *in vacuo*. Yield: 0.04 g (81%). m.p. 309 – 311 ˚C; ^{1}H NMR (500MHz, $CDCl_3$): δ_H 8.72 (d, 1H, *J* = 8.4 Hz), 8.68 (d, 1H, *J* = 9.2 Hz), 7.84 (d, 1H, *J* = 7.6 Hz), 7.43 – 7.28 (m, 12H), 7.19 – 7.17 (m, 2H), 7.05 – 6.99 (m, 6H); ESMS calc for $C_{34}H_{24}N$ = 446.1903, found 446.1899; IR (KBr)*v*/cm^{-1}: 3054 w, 1495 s, 1476 w, 1449 s, 1398 m, 1071 w, 755 s, 726 m, 701 s;

Attempted synthesis of 1-(4'(4-aminophenyl)2.2':6,2''-terpyridine)-2,5-diphenylpyrrole, **4.33**

1,4-diphenyl-1,4-butanedione, **4.25**, (0.150 g, 0.62 mmol) and **4.34** (0.250 g, 0.77 mmol) were added to a round bottom flask and then 25 mL of glacial acetic acid was added. The mixture was refluxed for two hours, and then cooled to room temperature. 50 mL of water was added and the solution was extracted with 50 mL dichloromethane. The organic layer was washed with 3x 100 mL water, dried with $MgSO_4$ and the solvent removed *in vacuo*. ESMS indicates the formation of 4'-(4-acetylphenyl)-2,2':6,2''terpyridine. ESMS calc for $23_4H_{19}N_4O$ = 367.1553, found 367.1552.

Chapter 5

Synthesis of ligands **5.1**, **5.2**, **5.3** and **5.7**

The following compounds were prepared according to literature methods, and all characterisation data were found to be consistent with that provided; 2,2-biimidazole, N,N'-dimethylene-2,2'-biimidazole **5.1**,[36] N,N'-trimethylene-2,2'-biimidazole **5.2**,[36] and N,N'-(α,α'-o-xylylene)-2,2'-biimidazole **5.3**,[36] 1,2-diimidazoylbenzene, **5.8**.[37]

Synthesis of N,N'-o-benzyl-2,2'-biimidazole **5.7**[37]

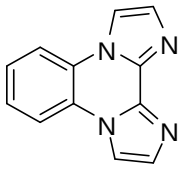

Under standard Schlenk conditions, **5.8** (0.321 g, 1.53 mmol) was added to a Schlenk tube and placed under vacuum for 10 minutes. 30 mL of anhydrous tetrahydrofuran was added into the Schlenk tube, and the solution was cooled to -78 ˚C using an acetone/ dry ice bath. Over the course of 5 minutes ^{n}BuLi (2.1 mL, 3.36 mmol, 1.6 M) was added dropwise with stirring, and the solution was left to stir for 90 minutes at 0 ˚C in an ice bath. After this time CuBr.SMe_2 (0.63 g, 3.06 mmol) was added in one go and the solution was left to stir under Ar for 30 minutes and a brown/red solution with a black precipitate formed. The solution was left to stir under an atmospher of O_2 overnight. The reaction mixture was added to 50 mL dichloromethane and 50 mL 10% NH_3 solution and stirred vigourosly overnight. The organic and aqueous layers were seperated, and the aqueous layer was washed with 50 mL of dichloromethane. The organic layers were then combined and washed with 50 mL 10% NH_3 solution, 50 mL water and 50 mL brine. The organic layer was then dried with Na_2SO_4 and the solvent removed *in vacuo*. The resultant brown solid was washed with tetrahydrofuran to give a white powder, **5.7**. Yield: 0.075 g (24%, 0.036 mmol). M.p. 258 – 260 ˚C; ^{1}H NMR (500MHz, $CDCl_3$): δ_H 7.88 (s, br, 2H), 7.87 (dd, 2H, J = 4 Hz and 6.4 Hz), 7.63 (s, br, 2H), 7.54 (dd, 2H, J = 4 Hz and 6.4 Hz).

Synthesis of silver complexes with **5.1**

Synthesis of $[Ag_2$**5.1**$_2][NO_3]_2$, **5.9**

5.1 (10 mg, 0.06 mmol) and $AgNO_3$ (6 mg, 0.03 mmol) were each dissolved in 5ml of acetonitrile and heated. The solutions were mixed and left to cool. Colourless needles of **1** suitable for X-ray crystallographic analysis were obtained after 48 h. Yield: 3.3 mg (33%). m.p. > 300 °C; Elemental anal. calcd (found) for $C_{16}H_{16}N_{10}O_6Ag_2$ (657.94): C, 29.11 (28.55); H, 2.44 (2.28); N, 21.22 (20.58) %; IR (KBr) ν/cm^{-1}: 3119 m, 3003 w, 2398 w, br, 1598 w, 1508 m, 1472 w, 1435 m, 1362 s, br, 1286 s, 1216 m, 1140 m, 1124 w, 1099 w, 1057 w, 965 w, 828 w, 788 m, 763 m, 722 m, 674 m.

Synthesis of $[Ag_3\mathbf{5.1}_4][ClO_4]_3 \cdot CH_3CN$, **5.10**

5.1 (10 mg, 0.06 mmol) and $AgClO_4$ (7 mg, 0.03 mmol) were each dissolved in 5ml of acetonitrile and heated. The solutions were mixed and left to cool. After 24 h 1 ml of this solution was used for vapour diffusion with diisopropyl ether. Colourless needles of **2** suitable for X-ray crystallographic analysis were obtained after 24 h. Yield: 5.7 mg (45%). Elemental anal. calcd (found) for $C_{32}H_{32}N_{16}O_{12}Cl_3Ag_3$ (1257.9): C, 31.32 (27.79); H, 2.71 (2.21); N, 18.26 (15.94) %; IR (KBr) ν/cm^{-1}: 3136 m, br, 1555 m, 1520 m, 1436 m, 1351 m, 1287 m, 1091 s, br, 967 m, 776 m, 674 m, 623 s.

Synthesis of poly-$[Ag_2\mathbf{5.1}_3][PF_6]_2$, **5.11**

5.1 (10 mg, 0.06 mmol) and $AgPF_6$ (8 mg, 0.03 mmol) were each dissolved in 5ml of methanol and heated. The solutions were mixed and left to cool. Colourless needles of **3** suitable for X-ray crystallograhic analysis were obtained after 48 h. Yield: 3.1 mg (21%). m.p. 289-292 ˚C; Elemental anal. calcd (found) for $C_{24}H_{24}N_{12}F_{12}P_2Ag_2$ (1293.7): C, 29.23 (28.15); H, 2.45 (2.40); N, 17.04 (15.94) %; IR (KBr) ν/cm^{-1}: 31078w, br, 1500 m, 1468 w, 1436 w, 1347 w, 1284 m, 1123 m, 1059 w, 841 s, br, 764 m, 720 w, 670 w, 559 s.

Synthesis of copper(I) complexes with **5.1**

General procedure for the preparation of complexes **5.12**, **5.13**, **5.14** and **5.15**.

5.1 and the appropriate Cu(I) salt were each dissolved in 5mL of acetonitrile and heated. The solutions were combined and left to cool. Benzene was slowly diffused into the combined solution and after 24h colourless cubes suitable for X-ray diffraction were obtained in each case.

Synthesis of $[Cu_2\mathbf{5.1}_3][BF_4]_2 \cdot C_6H_6$, **5.12**

5.1 (10 mg, 0.062 mmol) and $Cu(CH_3CN)_4BF_4$ (9.8 mg, 0.031 mmol). Yield: 6.2 mg (47%). m.p. 240 ˚C (decomp); ^{1}H NMR (500MHz, CD_3CN): δ_H = 7.37 (s, 1H, benzene), 7.34 (s, 1H), 7.31 (s, 1H), 4.40 (s, 2H); MS(ESI): m/z: calc for $[Cu_2\mathbf{5.1}_3]^{2+}$: 303.0414, found 303.0450; calc for $[Cu_2\mathbf{5.1}_2]^{2+}$: 223.0039, found: 223.0069; calc for $[Cu\mathbf{5.1}_2]^{+}$: 383.0788, found 383.0838; Elemental anal calcd (found) for $C_{30}H_{30}B_2N_{12}F_8Cu_2$ (858.14): C, 41.93 (41.93); H, 3.52 (3.53); N 19.56 (19.46) %; IR (KBr) ν/cm^{-1}: 3151 m, 3040 w, 2941 w, 1508 s, 1467 m, 1438 s, 1395 w, 1343 s, 1282 s, 1255 w, 1207 w, 1122 s 1062 s, br, 978 w, 961 w, 881 w, 784 s, 721 w, 693 m, 675 m; UV-Vis λ_{max} (ε): 204 nm (70051), 279 nm (44831), 288 nm (45908).

Synthesis of $[Cu_2\mathbf{5.1}_3][ClO_4]_2 \cdot C_6H_6$, **5.13**

5.1 (10 mg, 0.062 mmol) and $Cu(CH_3CN)_4ClO_4$ (10.2 mg, 0.031 mmol). Yield: 7.6 mg (56%). ^{1}H NMR (500 MHz, CD_3CN): δ_H = 7.37 (s, 1H, benzene), 7.34 (s, 1H), 7.31 (s, 1H), 4.40 (s, 2H). MS(ESI): m/z: calc for $[Cu_2\mathbf{5.1}_3]^{2+}$: 303.0414 found 303.0417; calc for $[Cu_2\mathbf{5.1}_2]^{2+}$: 223.0039, found: 223.0049; calc for $[Cu\mathbf{5.1}_2]^{+}$: 383.0788, found 383.0796; Elemental anal calc (found) for $C_{30}H_{30}N_{12}O_8Cl_2Cu_2$ (882.03): C, 40.73 (40.96); H, 3.42 (3.47); N, 19.00 (18.95) %; IR (KBr) ν/cm^{-1}: 3145 m, 3033 m, 2938 m, 2011 w, br, 1836 w, 1741 w, br, 1643 w, br, 1508 s, 1465 m, 1436 s, 1343 s, 1281 s, 1253 m, 1204 m, 1092 s, br, 961 m, 878 m, 781 s, 720 m, 692 s, 675 s, 623 s; UV-Vis λ_{max} (ε): 201 nm (79501), 279 nm (45341), 288 nm (46419).

Synthesis of $[Cu_2\mathbf{5.1}_3][NO_3]_2 \cdot C_6H_6$, **5.14**

5.1 (5 mg, 0.031mmol) and $Cu(PPh_3)_2NO_3$ (10.1 mg, 0.015 mmol). Yield: 2.5 mg (41%). m.p. 260-263 ˚C; MS(ESI): m/z: calc for $[Cu_2\mathbf{5.1}_3]^{2+}$: 303.0414, found 303.0413; calc for $[Cu_2\mathbf{5.1}_2]^{2+}$: 223.0039, found: 223.0039; calc for $[Cu\mathbf{5.1}_2]^{+}$: 383.0788, found 383.0793. Elemental anal calc (found) for $C_{30}H_{30}N_{14}O_6Cu_2$ (808.11): C, 44.50 (44.79); H, 3.73 (3.80); N, 24.22 (24.20)%; IR (KBr) ν/cm^{-1}: 3110 m, 3015 m, 2937 m, 2379 w, 1746 w, br, 1664 w, br, 1507 s, 1466 s, 1438 s, 1357 s, br, 1280 s, 1122 m, 830 m, 786 s, br, 722 m, 694 s, 675 s.

Synthesis of $[Cu_2\mathbf{5.1}_3][PF_6]_2 \cdot 2C_6H_6$, complex **5.15**

5.1 (10 mg, 0.062 mmol) and $Cu(CH_3CN)_4PF_6$ (11.5 mg, 0.031 mmol). Yield: 0.002 g (4%).

Synthesis of $[Cu_2\mathbf{5.1}_3][ClO_4]_2 \cdot CH_3CN$, **5.16**

5.1 (10 mg, 0.062 mmol) and $Cu(CH_3CN)_4ClO_4$ (10.2 mg, 0.031 mmol) were each dissolved in 5mL of acetontrile and heated. The solutions were combined and left to cool. Hexafluorobenzene was slowly diffused into the solution and after 24h colourless plates suitable for X-ray diffraction were obtained.
Yield: 7.2 mg (41%). Elemental anal calc (found) for $C_{26}H_{27}N_{13}O_8Cl_2Cu_2$ (845.01); C, 36.85 (36.86); H, 3.21 (3.13); N, 21.48 (21.24) %; IR (KBr) ν/cm^{-1}: 3140 m, br, 3081 w, 2989 w, 2245 w, 2013 w, br, 1715 w, 1609 w, 1515 s, 1466 m, 1443 s, 1398 w, 1346 s, 1288 s, 1250 w, 1106 s, br, 961 m, 937 w, 910 w, 865 w, 750 s, br, 724 m, 673 m, 623 s.

Synthesis of fluorobenzene enclathration complex with $Cu(CH_3CN)_4BF_4$

5.1 (10 mg, 0.062 mmol) and $Cu(CH_3CN)_4BF_4$ (9.8 mg, 0.031 mmol) were each dissolved in 5mL of acetontrile and heated. The solutions were combined and left to cool. Fluorobenzene was slowly diffused

into the solution and after 24h colourless plates suitable for X-ray diffraction were obtained. Yield: 7.1 mg (40%).

Anion competition experiment between PF_6^- and ClO_4^-

5.1 (10 mg, 0.062 mmol) and $Cu(CH_3CN)_4PF_6$ (11.5 mg, 0.031 mmol) were each dissolved in 5mL of acetontrile and heated. The solutions were combined and left to cool. After cooling an acetonitrile solution (2mL) of $NaClO_4$ (4mg, 0.031 mmol) was added, and then benzene was slowly diffused into the combined solutions. After 24h colourless plates suitable for X-ray diffraction were obtained.

Synthesis of poly-[Cu_2**5.1**]I_2, **5.17**

5.1 (10 mg, 0.0622 mmol) and CuI (5.9 mg, 0.0311 mmol) were each dissolved in 5mL of acetonitrile and heated. The solutions were combined and small colourless needles suitable for X-ray diffraction formed instantly. Yield: 5.8 mg (35%). m.p. > 300 ˚C. Elemental anal calc (found) for $C_8H_8N_4CuI_2$; C, 20.12 (19.34); H, 1.69 (1.48); N, 11.73 (10.98) %; IR (KBr) ν/cm^{-1}: 3118 m, 2987 w, 2943 w, 2245 w, 1604 w, 1523 m, sh, 1510 s, 1465 m, 1433 s, 1400 w, 1341 s, 1281 s, 1213 w, 1170 m, 1125 s, 1055 m, 967 m, 944 w, 917 w, 882 w, 851 m, 772 s, 742 s, 720 m, 673 m, 615 w, 484 m, 451 m.

Synthesis of copper(II) complexes with **5.1**

Synthesis of [Cu_2**5.1**$_4$][ClO_4]$_2$·3CH_3CN·0.5C_6H_6, **5.18**

5.1 (10 mg, 0.062 mmol) and $Cu(ClO_4)_2$ (11.5 mg, 0.031 mmol) were each dissolved in 5 mL acetonitrile and heated. The solutions were combined and left to cool. Benzene was slowly diffused into the solution and after 24h brown rods suitable for X-ray diffraction were obtained. Yield: 9.0 mg (25%). MS(ESI): m/z: calc for $[Cu_2\mathbf{5.1}_2]^{2+}$: 223.0039, found 223.0037. Elemental anal calc (found) for $C_{32}H_{32}N_{16}O_{16}Cl_4Cu_2$ (1165.42): C, 32.97 (32.78); H, 2.77 (2.74); N, 19.23 (18.79) %; IR (KBr) ν/cm^{-1}: 3147 w, 1736 w, 1622 w, 1515 m, 1441 m, 1356 m, 1286 m, 1110 s, br, 1080 s, br, 972 m, 921 w, 763 m, 725 m, 669 m, 625 s.

Synthesis of [Cu_2**5.1**$_2$(CH_3COO)$_2$]·CH_3CN, **5.19**

5.1 (5 mg, 0.0311 mmol) and $Cu(CH_3COO)_2$ (12.0 mg, 0.0622 mmol) were each dissolved in 5 mL acetonitrile and heated. The solutions were combined and left to cool, after 4 weeks blue plates suitable for X-ray diffraction were obtained. Yield: 13 mg (61%). m.p. 175-179 ˚C. MS(ESI): m/z: calc for $[Cu_2\mathbf{5.1}_2CH_3COO]^{1+}$: 282.0176, found 282.0174, calc for $[Cu_2\mathbf{5.1}_2]^{2+}$: 223.0039, found 223.0039. Elemental anal calc (found) for $C_{24}H_{31}N_9O_8Cu_2$ (700.56): C, 41.14 (40.87); H, 4.46 (4.73); N, 17.99 (17.61) %; IR (KBr) ν/cm^{-1}: 3141 w, 3004 w, 2922 w, 1587 s, br, 1510 m, 1426 s, 1415 s, 1393 m, 1346 s, 1291 m, 1135 m, 1060 w, 1026 w, 965 m, 925 w, 764 m, 725 m, 676 s, 619 m.

Synthesis of cadmium and cobalt complexes with **5.1**

Synthesis of [Cd**5.1**$_2$(NO_3)$_2$$OH_2$], **5.20**

51 (10 mg, 0.0622 mmol) and $Cd(NO_3)_2$ (9.6 mg 0.031 mmol) were each dissolved in 5mL of acetonitrile and heated. The solutions were combined and left to cool. Diisopropyl ether was slowly diffused in and small colourless needles suitable for X-ray diffraction were formed after one week. Yield: 12 mg (65%). m.p. 227-229 ˚C. Elemental anal calc (found) for $C_{16}H_{18}N_{10}O_7Cd$ (574.79); C, 33.43 (33.63); H, 3.16 (3.10); N, 24.37 (24.10) %; IR (KBr) ν/cm^{-1}: 3130 m, 3112 m, 2940 m, br, 2297 w, 1759 w, 1731 w, 1591 m, 1512m, 1469 s, 1443 s, 1430 s, 1372 m, 1340 s, 1303 s, 1280 s, 1210 m, 1174 w, 1127 s, 1095 m, 1082 m, 1058 m, 1028 s, 981 w, 956 s, 931 m, 914 m, 864 m, 821 m, 768 s, 753 s, 718 s, 675 s, 616 m, 590 m, 472 m.

Synthesis of [Co**5.1**$_2$(OH_2)$_4$][NO_3]$_2$, **5.21**

5.1 (10 mg, 0.0622 mmol) and $Co(NO_3)_2$ (9.1 mg, 0.031 mmol) were each dissolved in 5mL of acetonitrile and heated. The solutions were combined and left to cool. Diisopropyl ether was slowly diffused in and small back plates suitable for X-ray diffraction were formed after one week. Yield: 8.7 mg (24%). m.p. 159-162 ˚C. Elemental anal calc (found) for $C_{16}H_{24}N_{10}O_{10}Co$ (575.10); C, 33.40 (33.23); H, 4.20 (3.81); N, 24.34 (24.13) %; IR (KBr) ν/cm^{-1}: 3483 m, 3168 m, 3131 m, 3017 w, 2750 w, 2254 w, 1968 w, 1729 w, 1611 m, 1494 s, 1443 m, 1384 s, 1357 m, sh, 1273 s, 1134 m, 1060 w, 993 s, 955 w, sh, 860 m, 796 m, 756 m, 679 m,556 m.

Synthesis of copper(II) complexes with **5.2**

Synthesis of [Cu**5.2**SO_4(OH_2)$_2$], **5.22**

5.2 (10 mg, 0.0574 mmol) and $CuSO_4$ (7.2 mg, 0.0287 mmol) were each dissolved in 5mL of acetonitrile and heated. The solutions were combined and left to cool. After two weeks light green cubes suitable for X-ray crystallography were obtained. Yield: 6.8 mg (32%). m.p. 179 ˚C (decomp). Elemental anal calc (found) for $C_9H_{14}N_4O_6SCu$ (368.99); C, 29.23 (29.30); H, 3.82 (3.69); N, 15.15 (15.08) %; IR (KBr) ν/cm^{-1}: 2965 m, br, 2457 w, 2353 w, 1744 w, 1669 w, 1647 w, 1563 w, 1505 w, 1482 m, 1454 w, 1427 w, 1387 w, 1345 m, 1308 w, 1265 w, 1215 w, 1172 s, 1093 s, 1034 s, sh, 1015 s, 973 s, 950 m, 907 w, 899 w, 880 w, 792 s, 731 m, 682 m, 632 m, 620 m.

Synthesis of [Cu**5.2**Cl_2], **5.23**

5.2 (10 mg, 0.0574 mmol) and $CuCl_2$ (4.9 mg, 0.0287 mmol) were dissolved in 5mL of acetonitrile and heated. The solutions were combined and left to cool, after two weeks dark green needles suitable for X-ray crystallography were obtained. Yield: 4.8 mg (27%). m.p. 192 ˚C (decomp). Elemental anal calc

(found) for $C_9H_{10}N_4Cl_2Cu$ (306.96); C, 35.02 (35.12); H, 3.27 (3.06); N, 18.15 (18.03) %; IR (KBr) ν/cm^{-1}: 3106 m, 2934 m, 1724 w, 1649 m, 1556 m, 1499 m, 1474 s, 1434 m, 1380 m, 1345 m, 1308 w, 1256 m, 1212 m, 1151 s, 1094 w, 1069 w, 1032 m, 964 m, 946 m, 866 m, 766 m, sh, 750 s, 681 s, 643 m, 619 m.

Synthesis of [Cu**5.2**$_2$(OH$_2$)$_2$][NO$_3$]$_2$, **5.24**

5.2 (10 mg, 0.0574 mmol) and $Cu(NO_3)_2$ (6.9 mg, 0.0287 mmol) were each dissolved in 5mL of acetonitrile and heated. The solutions were combined and left to cool. Yield: 3.4 mg (10%). m.p. > 300 ˚C. Calc for $C_{18}H_{24}N_{10}O_8Cu$ (571.11); C, 37.80 (37.76); H, 4.23 (4.52), N, 24.49 (24.53) %; IR (KBr) ν/cm^{-1}: 3476 m, br, 3158 w, 3131 m, 2942 w, 2405 w, 1751 w, 1628 m, br, 1549 m, 1509 m, 1474 s, 1449 s, 1385 s, br, 1342 s, br, 1261 w, 1239 w, 1212 w, 1162 m, 1148 s, 1099 w, 1076 w, 1034 w, 964 m, 950 w, 827 w, 787 m, br, 688 m.

Synthesis of [Cu**5.2**$_2$(OH$_2$)$_2$]I$_2$, **5.25**

5.2 (10 mg, 0.0574 mmol) and CuI (5.5 mg, 0.0287 mmol) were dissolved in 5mL of acetonitrile and heated. The solutions were combined and left to cool, after two weeks dark green needles suitable for X-ray crystallography were obtained. Yield: 3.7 mg (11%). m.p. > 300 ˚C. Elemental anal calc (found) for $C_{18}H_{24}N_8O_2CuI$ (574.04); C, 30.81 (30.90); H, 3.45 (3.24); N, 15.97 (15.86) %; IR (KBr) ν/cm^{-1}: 3479 s, br, 3111 m, 2931 m, 2011 w, br, 1703 w, br, 1642 m, 1533 m, 1507 s, 1471 s, 1445 m, 1425 m, 1387 m, 1340 s, 1264 m, 1212 w, 1161 m, 1146 s, 1098 w, 1073 m, 1034 w, 964 s, 950 m, 878 w, 862 w, 776 s, 685 s, 641 w, 619 m.

Synthesis of [Cu**5.2**$_2$(OH$_2$)$_2$][ClO$_4$]$_2$, **5.26**

5.2 (10 mg, 0.0574 mmol) and $Cu(ClO_4)_2$ (10.6 mmol, 0.0287 mmol) were dissolved in 5mL of acetonitrile and heated. The solutions were combined and left to cool. Diisopropyl ether was diffused in and light green needles suitable for X-ray crystallography were obtained. Yield: 5.6 mg (12%). Elemental anal calc (found) for $C_{18}H_{24}N_8O_{10}Cl_2Cu$ (645.03); C, 33.42 (33.74); H, 3.74 (3.47); N, 17.32 (17.63) %; IR (KBr) ν/cm^{-1}: 3575 w, 3140 w, sh, 3132 m, 2944 w, 2327 w, 2030 w, br, 1722 w, br, 1643 w, 1610 w, br, 1556 m, 1510 m, 1476 s, 1450 m, 1426 w, 1388 m, 1344 m, 1262 w, 1213 w, 1150 s, sh, 1103 s, br, 965 m, 948 m, 882 w, 770 s, 688 m, 623 s, 525 w, 462 m.

7.5 References

(1) Sheldrick, G. M. *Acta Crystallogr., Sect. A* **2008**, *64*, 112

(2) Sheldrick, G. M. *Programs for X-ray Crystal Structure Refinement*; University of Gottingen, 1997.

(3) Dolomanov, O. V.; Bourhis, L. J.; Gildea, R. J.; Howard, J. A. K.; Puschmann, H. *J. Appl. Crystallogr.* **2009**, *42*, 339

(4) Butler, R. N.; Hanniffy, J. M.; Stephens, J. C.; Burke, L. A. *The Journal of Organic Chemistry* **2008**, *73*, 1354.

(5) Szmuszkovicz, J.; Glenn, E. M.; Heinzelman, R. V.; Hester, J. B.; Youngdale, G. A. *Journal of Medicinal Chemistry* **1966**, *9*, 527.

(6) Constable, E. C.; Ward, M. D. *Journal of the Chemical Society, Dalton Transactions* **1990**, 1405.

(7) Constable, E. C.; Harverson, P.; Housecroft, C. E.; Nordlander, E.; Olsson, J. *Polyhedron* **2006**, *25*, 437.

(8) Han, G. Y.; Han, P. F.; Perkins, J.; McBay, H. C. *J. Org. Chem.* **1981**, *46*, 4695.

(9) Shen, M.; Li, G.; Lu, B. Z.; Hossain, A.; Roschangar, F.; Farina, V.; Senanayake, C. H. *Organic Letters* **2004**, *6*, 4129.

(10) Chen, X.; Li, X.; Wang, N.; Jin, J.; Lu, P.; Wang, Y. *European Journal of Organic Chemistry* **2012**, *2012*, 4380.

(11) Kuo, W.-J.; Chen, Y.-H.; Jeng, R.-J.; Chan, L.-H.; Lin, W.-P.; Yang, Z.-M. *Tetrahedron* **2007**, *63*, 7086.

(12) Biswas, K. M.; Dhara, R. N.; Mallik, H.; Halder, S.; Sinha, C.; Saha, A.; Ganguly; De, P.; Brahmachari, A. S. *Monatsh. Chem.* **1996**, *127*, 111.

(13) Koulocheri, Sophia D.; Haroutounian, Serkos A. *European Journal of Organic Chemistry* **2001**, *2001*, 1723.

(14) Baccolini, G.; Dalpozzo, R.; Todesco, P. E. *J. Chem. Soc., Perkin Trans. 1* **1988**, 971.

(15) Cano, R.; Ramón, D. J.; Yus, M. *The Journal of Organic Chemistry* **2011**, *76*, 654.

(16) Accorsi, G.; Armaroli, N.; Cardinali, F.; Wang, D.; Zheng, Y. *Journal of Alloys and Compounds* **2009**, *485*, 119.

(17) MacLean, P. D.; Chapman, E. E.; Dobrowolski, S. L.; Thompson, A.; Barclay, L. R. C. *The Journal of Organic Chemistry* **2008**, *73*, 6623.

(18) Carter, P. H.; Cymerman, C. J.; Lack, R. E.; Moyle, M. *Organic Synthesis* **1960**, *40*, 16.

(19) Dennis, G. D.; Edwards-Davis, D.; Field, L. D.; Masters, A. F.; Maschmeyer, T.; Ward, A. J.; Buys, I. E.; Turner, P. *Australian Journal of Chemistry* **2006**, *59*, 135.

(20) Cymerman-Craig, J.; Moyle, M.; Rowe-Smith, P.; Wailes, P. C. *Australian Journal of Chemistry* **1956**, *9*, 391.

(21) Zhai, L.; Shukla, R.; Rathore, R. *Organic Letters* **2009**, *11*, 3474.

(22) Churruca, F.; SanMartin, R.; Carril, M.; Urtiaga, M. K.; Solans, X.; Tellitu, I.; Domínguez, E. *The Journal of Organic Chemistry* **2005**, *70*, 3178.

(23) Feng, X.; Tong, B.; Shen, J.; Shi, J.; Han, T.; Chen, L.; Zhi, J.; Lu, P.; Ma, Y.; Dong, Y. *The Journal of Physical Chemistry B* **2010**, *114*, 16731.

(24) Ballard, D. A.; Dehn, W. M. *Journal of the American Chemical Society* **1932**, *54*, 3969.

(25) Craig, D. *Journal of the American Chemical Society* **1935**, *57*, 195.

(26) Liu, S.-J.; Zhao, Q.; Fan, Q.-L.; Huang, W. *European Journal of Inorganic Chemistry* **2008**, *2008*, 2177

(27) Bailey, P. S.; Lutz, R. E. *Journal of the American Chemical Society* **1948**, *70*, 2412.

(28) (a) Lutz, R. E. *Org. Synth.* **1940**, *20*, 29, (b) Conant, J. B.; Lutz, R. E. *Journal of the American Chemical Society* **1923**, *45*, 1303

(29) Percec, V.; Bera, T. K.; De, B. B.; Sanai, Y.; Smith, J.; Holerca, M. N.; Barboiu, B.; Grubbs, R. B.; Fréchet, J. M. J. *The Journal of Organic Chemistry* **2001**, *66*, 2104.

(30) Koohmareh, G. A.; Sharifi, M. *J. Appl. Polym. Sci.* **2010**, *116*, 179.

(31) Hussain, M.; Khera, R. A.; Hung, N. T.; Langer, P. *Organic & Biomolecular Chemistry* **2011**, *9*, 370.

(32) Nakano, M.; Tsurugi, H.; Satoh, T.; Miura, M. *Organic Letters* **2008**, *10*, 1851.

(33) Kikuchi, D.; Sakaguchi, S.; Ishii, Y. *The Journal of Organic Chemistry* **1998**, *63*, 6023.

(34) Ban, I.; Sudo, T.; Taniguchi, T.; Itami, K. *Organic Letters* **2008**, *10*, 3607.

(35) Zheng, Q.; Hua, R. *Tetrahedron Letters* **2010**, *51*, 4512.

(36) Thummel, R. P.; Goulle, V.; Chen, B. *The Journal of Organic Chemistry* **1989**, *54*, 3057.

(37) Matsumoto, S.; Batmunkh, E.; Akazome, M.; Takata, Y.; Tamano, M. *Organic & Biomolecular Chemistry* **2011**, *9*, 5941.

Appendix 1:

Crystal data and structural refinement details

Table A1. Crystal data and structure refinement for **2.3**, **2.5**, **2.8**, **2.11** and **2.12**.

Compound	**2.3**	**2.5**	**2.8**	**2.11**	**2.12**
Emperical formula	$C_{66}H_{57}N_3$	$C_{22}H_{19}N$	$C_{30}H_{35}N$	$C_{32}H_{32}N$	$C_{35}H_{37}N$
Formula weight	892.15	297.38	409.59	430.59	471.66
Radiation source	CuKα	MoKα	CuKα	CuKα	CuKα
Temperature (K)	120.01(10)	115.15(10)	120.01(10)	120.01(10)	120.01(10)
Crystal system	monoclinic	monoclinic	monoclinic	monoclinic	monoclinic
Space group	$P2_1/c$	$P2_1/c$	$P2_1/c$	$P2_1/n$	$P2_1/c$
Unit cell dimensions: a (Å)	19.0427(4)	10.6885(3)	19.4295(7)	14.3654(4)	11.6427(5)
b (Å)	13.1257(3)	8.48170(3)	10.5714(3)	9.5078(2)	10.0763(4)
c (Å)	20.3761(4)	18.2331(6)	12.1842(4)	18.6740(6)	23.5686(8)
α (˚)	90.00	90.00	90.00	90.0	90.00
β (˚)	104.024(2)	91.469(2)	99.070(4)	105.746(3)	98.765(3)
γ (˚)	90.00	90.00	90.00	90.0	90.00
Volume ($Å^3$)	4941.18(19)	1652.41(9) $Å^3$	2471.31(15)	2454.82(11)	2732.68(18)
Z	4	4	4	4	4
Density (calculated) (Mg/m^3)	1.199	1.195	1.101	1.165	1.146
Absorption coefficient (mm^{-1})	0.525	0.069	0.468	0.500	0.489
F(000)	1896.0	632.0	888.0	924.0	1016.0
Crystal dimensions	0.31 x 0.12 x 0.09	0.35 × 0.25 × 0.03	0.27 x 0.18 x 0.06	0.21 x 0.19 x 0.08	0.29 x 0.24 x 0.11
Theta range for data collection (˚)	8.08 to 148.18	3.82 to 60.24	9.22 to 146.64	6.92 to 147.36	7.6 to 139.98
Reflections collected	19949	42210	8345	8964	9882
Independent reflections [R(int)]	9711 [0.0257]	4851 [0.0583]	4791 [0.0201]	4820 [0.0263]	5153 [0.0397]
Observed reflections [I>2σ(I)]	8278	3756	3895	3817	3726
Data / restraints / parameters	9711/0/628	4851/0/209	4791/0/317	4820/0/301	5153/0/331
Goodness-of-fit on F^2	1.030	1.074	1.047	1.056	1.017
R_1 [I>2σ(I)]	0.0443	0.0571	0.0495	0.0754	0.0481
wR_2 (all data)	0.1197	0.1799	0.1411	0.2554	0.1266
Flack parameter					

Table A2. Crystal data and structure refinement for **2.13**, **2.15**, **2.17**, **2.20** and **2.21**.

Compound	**2.13**	**2.15**	**2.17**	**2.20**	**2.21**
Emperical formula	$C_{26}H_{19}N$	$C_{22}H_{17}N$	$C_{24}H_{21}N$	$C_{29}H_{23}NO_2$	$C_{29}H_{23}N$
Formula weight	345.42	295.37	323.42	417.48	385.48
Radiation source	MoKα	CuKα	CuKα	CuKα	CuKα
Temperature (K)	113.15(10)	120.01(10)	120.01(10)	120.01(10)	120.01(10)
Crystal system	monoclinic	monoclinic	orthorhombic	triclinic	triclinic
Space group	$P2_1/n$	$P2_1/c$	*Pbca*	*P*-1	*P*-1
Unit cell dimensions: a (Å)	11.1554(5)	9.6538(3)	18.8849(4)	10.1458(4)	5.5885(3)
b (Å)	8.4340(4)	10.3800(2)	8.9852(2)	10.8567(5)	10.2475(5)
c (Å)	19.6631(10)	15.3298(4)	20.2021(4)	11.2936(5)	17.7072(8)
α (˚)	90.00	90.00	90.00	84.384(4)	87.263(4)
β (˚)	96.071(3)	102.907(3)	90.00	64.476(4)	88.399(4)
γ (˚)	90.00	90.00	90.00	66.539(4)	81.698(4)
Volume ($Å^3$)	1839.62(15)	1497.34(6)	3427.96(13)	1025.70(8)	1002.06(9)
Z	4	4	8	2	2
Density (calculated) (Mg/m^3)	1.247	1.310	1.253	1.352	1.278
Absorption coefficient (mm^{-1})	0.072	0.578	0.547	0.664	0.558
F(000)	728.0	624.0	1376.0	440.0	408.0
Crystal dimensions	0.18 x 0.09 x 0.07	0.28 x 0.17 x 0.10	0.29 x 0.15 x 0.05	0.16 x 0.10 x 0.06	0.31 x 0.27 x 0.11
Theta range for data collection (˚)	5.26 to 50.04	9.4 to 147.86	8.76 to 147.36	8.72 to 137	8.72 to 147.7
Reflections collected	31728	14893	8498	13116	8149
Independent reflections [R(int)]	3243 [0.0620]	2989 [0.0320]	3378 [0.0212]	3758 [0.0161]	3895 [0.0310]
Observed reflections [I>2σ(I)]	3058	2666	2831	3360	3316
Data / restraints / parameters	3243/0/245	2989/0/209	3378/0/229	3758/0/291	3895/0/273
Goodness-of-fit on F^2	1.345	1.064	1.026	1.053	1.185
R_1 [I>2σ(I)]	0.0973	0.0404	0.0403	0.0347	0.0491
wR_2 (all data)	0.2000	0.1100	0.1093	0.0976	0.1612
Flack parameter					

Table A3. Crystal data and structure refinement for **2.26**, **3.14**, **3.15**, **3.16** and **3.17**.

Compound	**2.26**	**3.14**	**3.15**	**3.16**	**3.17**
Emperical formula	$C_{28}H_{29}N$	$C_{30}H_{17}Cl_4N$	$C_{35}H_{25}N$	$C_{45}H_{39}N$	$C_{54}H_{57}N$
Formula weight	379.52	533.25	459.56	593.77	720.01
Radiation source	CuKα	MoKα	CuKα	CuKα	CuKα
Temperature (K)	120.01(10)	113.15(10)	120.01(10)	120.01(10)	130.15(10)
Crystal system	monoclinic	triclinic	monoclinic	monoclinic	orthorhombic
Space group	$P2_1/c$	P-1	$P2_1/c$	$P2_1/c$	$Pbcn$
Unit cell dimensions: a (Å)	14.2220(5)	9.9632(3)	10.1062(2)	5.95712(11)	37.2161(19)
b (Å)	11.7212(4)	11.2079(3)	13.1190(3)	24.7533(5)	10.0990(3)
c (Å)	12.9459(5)	11.9471(4)	18.1079(4)	22.2920(4)	23.5559(8)
α (˚)	90.00	64.541(2)	90.00	90.00	90.00
β (˚)	101.179(3)	74.712(2)	97.158(2)	94.0305(17)	90.00
γ (˚)	90.00	75.154(2)	90.00	90.00	90.00
Volume ($Å^3$)	2117.13(12)	1146.18(6)	2382.09(9)	3279.02(11)	8853.3(6)
Z	4	2	4	4	8
Density (calculated) (Mg/m^3)	1.191	1.545	1.281	1.203	1.080
Absorption coefficient (mm^{-1})	0.512	0.539	0.560	0.518	0.458
F(000)	816.0	544.0	968.0	1264.0	3104.0
Crystal dimensions	0.27 x 0.13 x 0.09	0.50 × 0.29 × 0.04	0.34 x 0.25 x 0.12	0.25 x 0.21 x 0.06	0.31 x 0.13 x 0.10
Theta range for data collection (˚)	11.34 to 130.16	3.84 to 68.08	8.34 to 147.94	5.34 to 147.64	7.5 to 134
Reflections collected	6931	24533	9069	18660	21923
Independent reflections [R(int)]	3614 [0.0173]	6734 [0.0607]	4678 [0.0219]	6468 [0.0193]	7884 [0.0463]
Observed reflections [I>2σ(I)]	3189	3429	3749	5731	5585
Data / restraints / parameters	3614/0/268	6734/0/317	4678/0/325	6468/0/419	7884/3/498
Goodness-of-fit on F^2	1.044	0.924	1.038	1.042	1.057
R_1 [I>2σ(I)]	0.0384	0.0459	0.0418	0.0599	0.0717
wR_2 (all data)	0.1075	0.1324	0.1132	0.1537	0.2160
Flack parameter					

Table A4. Crystal data and structure refinement for **3.28**, **3.37**, **3.42**, **4.1** and **4.14**.

Compound	**3.28**	**3.37**	**3.42**	**4.1**	**4.14**
Emperical formula	$C_{40}H_{37}N$	$C_{39}H_{33}N$	$C_{28}H_{19}N$	$C_{34}H_{25}N$	$C_{28}H_{20}O$
Formula weight	531.71	515.66	369.44	447.55	372.44
Radiation source	CuKα	CuKα	CuKα	MoKα	MoKα
Temperature (K)	120.01(10)	120.01(10)	120.01(10)	110.15(10)	121.15(10)
Crystal system	triclinic	triclinic	orthorhombic	monoclinic	monoclinic
Space group	*P*-1	*P*-1	*Pbca*	$P2_1/n$	$C2/c$
Unit cell dimensions: a (Å)	9.8521(3)	10.2655(5)	14.5573(3)	10.7089(4)	25.5834(12)
b (Å)	10.1991(4)	11.6330(5)	10.4805(2)	9.7575(4)	8.0040(4)
c (Å)	16.8567(6)	12.7175(6)	24.5848(6)	23.6999(9)	21.5645(10)
α (˚)	99.880(3)	109.469(4)	90.00	90.00	90.00
β (˚)	95.857(3)	101.265(4)	90.00	95.351(2)	117.152(3)
γ (˚)	116.117(3)	91.218(4)	90.00	90.00	90.00
Volume ($Å^3$)	1467.81(9)	1398.13(11)	3750.83(14)	2465.66(17)	3929.1(3)
Z	2	2	8	4	8
Density (calculated) (Mg/m^3)	1.203	1.225	1.308	1.206	1.259
Absorption coefficient (mm^{-1})	0.517	0.529	0.576	0.069	0.075
F(000)	568.0	548.0	1552.0	944.0	1568.0
Crystal dimensions	0.26 x 0.19 x 0.12	0.17 x 0.09 x 0.05	0.21 x 0.14 x 0.06	0.50 × 0.19 × 0.09	0.31 × 0.31 × 0.1
Theta range for data collection (˚)	5.44 to 147.68	7.54 to 147.92	7.2 to 147.8	3.46 to 50	3.58 to 51
Reflections collected	15596	10379	12515	45093	34864
Independent reflections [R(int)]	5812 [0.0197]	5488 [0.0215]	3714 [0.0355]	4341 [0.0762]	3660 [0.0787]
Observed reflections [I>2σ(I)]	5247	4674	3292	3038	2507
Data / restraints / parameters	5812/36/364	5488/0/365	3714/0/262	4341/0/316	3660/0/262
Goodness-of-fit on F^2	1.058	1.038	1.038	1.163	1.130
R_1 [I>2σ(I)]	0.0551	0.0444	0.0577	0.0500	0.0509
wR_2 (all data)	0.1416	0.1232	0.1699	0.1756	0.1671
Flack parameter					

Table A5. Crystal data and structure refinement for **4.15**, **4.32**, **5.7**, **5.8** and **5.9**.

Compound	**4.15**	**4.32**	**5.7**	**5.8**	**5.9**
Emperical formula	$C_{64}H_{56}O_{10}$	$C_{37}H_{31}NO_3$	$C_{12}H_8N_4$	$C_{12}H_{11}N_4$	$C_{16}H_{16}Ag_2N_{10}O_6$
Formula weight	985.09	537.63	208.22	211.25	660.13
Radiation source	MoKα	CuKα	MoKα	MoKα	MoKα
Temperature (K)	111.15(10)	120.01(10)	114.15(10)	113.15(10)	114.15(10)
Crystal system	triclinic	triclinic	monoclinic	monoclinic	monoclinic
Space group	*P*-1	*P*-1	$P2_1/n$	$C2/c$	$P2_1/c$
Unit cell dimensions: a (Å)	9.8656(14)	9.8317(6)	6.8793(2)	26.3747(11)	13.4409(8)
b (Å)	11.0149(18)	11.3469(6)	10.4066(4)	5.4938(2)	15.3904(8)
c (Å)	24.145(4)	13.6689(8)	13.3454(5)	19.1398(14)	19.3895(10)
α (˚)	87.821(10)	70.917(5)	90.00	90.00	90.00
β (˚)	81.527(11)	89.640(5)	95.882(2)	132.888(2)	91.252(3)
γ (˚)	78.580(11)	82.046(5)	90.00	90.00	90.00
Volume ($Å^3$)	2543.7(7)	1426.00(15)	950.37(6)	2031.96(19)	4010.0(4)
Z	2	2	4	8	8
Density (calculated) (Mg/m^3)	1.286	1.252	1.455	1.381	2.187
Absorption coefficient (mm^{-1})	0.086	0.622	0.093	0.088	2.016
F(000)	1040.0	568.0	432.0	888.0	2592
Crystal dimensions	0.32 × 0.14 × 0.07	0.23 x 0.17 x 0.08	0.54 × 0.13 × 0.12	0.58 × 0.19 × 0.05	0.16 × 0.11 × 0.02
Theta range for data collection (˚)	1.7 to 50.22	6.84 to 147.56	4.98 to 66.38	4.22 to 55	3.04 to 60
Reflections collected	49003	9643	27497	17915	98654
Independent reflections [R(int)]	9001 [0.0973]	5559 [0.0182]	3524 [0.0391]	2335 [0.0424]	11680 [0.0790]
Observed reflections [I>2σ(I)]	4877	4616	2338	1824	8356
Data / restraints / parameters	9001/0/695	5559/0/373	3524/0/145	2335/0/145	11680/0/613
Goodness-of-fit on F^2	1.016	1.043	1.024	1.129	1.045
R_1 [I>2σ(I)]	0.0550	0.0418	0.0487	0.0400	0.0357
wR_2 (all data)	0.1920	0.1195	0.1491	0.1523	0.0774
Flack parameter					

Table A6. Crystal data and structure refinement for **5.10**, **5.11**, **5.12**, **5.13** and **5.14**.

Compound	**5.10**	**5.11**	**5.12**	**5.13**	**5.14**
Emperical formula	$C_{34}H_{35}Ag_3Cl_3N_{17}O_{12}$	$C_{12}H_{12}AgF_6N_6P$	$C_{30}H_{30}B_2Cu_2F_8N_{12}$	$C_{30}H_{30}Cl_2Cu_2N_{12}O_8$	$C_{30}H_{30}Cu_2N_{14}O_6$
Formula weight	1303.75	493.12	859.36	884.64	809.76
Radiation source	MoKα	MoKα	MoKα	MoKα	MoKα
Temperature (K)	114.15(10)	114.15(10)	117.15(10)	116.15(10)	114.15(10)
Crystal system	monoclinic	orthorhombic	cubic	cubic	cubic
Space group	*Pc*	*Pbcn*	$P4_332$	$P4_132$	$P4_332$
Unit cell dimensions: a (Å)	11.8432(4),	21.9927(5)	15.0798(6)	15.1915(10)	14.9000(5)
b (Å)	12.4409(4),	12.7858(3)	15.0798(6)	15.1915(10)	14.9000(5)
c (Å)	15.8426(4)	11.2203(3)	15.0798(6)	15.1915(10)	14.9000(5)
α (˚)	90.00	90.00	90.00	90.00	90.00
β (˚)	109.1470(10)	90.00	90.00	90.00	90.00
γ (˚)	90.00	90.00	90.00	90.00	90.00
Volume ($Å^3$)	2205.12(12)	3155.08(13)	3429.2(2)	3505.9(4)	3307.95(19)
Z	2	8	4	4	4
Density (calculated) (Mg/m^3)	1.964	2.076	1.665	1.676	1.626
Absorption coefficient (mm^{-1})	1.583	1.456	1.328	1.435	1.353
F(000)	1292	1936	1736.0	1800.0	1656.0
Crystal dimensions	0.51 × 0.13 × 0.06	0.47 × 0.12 × 0.08	0.41 × 0.36 × 0.23	0.39 × 0.26 × 0.17	0.51 × 0.49 × 0.48
Theta range for data collection (˚)	3.28 to 62	3.68 to 60	6.04 to 61.02	6 to 58.84	4.74 to 56.04
Reflections collected	60862	80245	10847	12809	21241
Independent reflections [R(int)]	13766 [0.0339]	4581 [0.0443]	1760 [0.0501]	1634 [0.0546]	1344 [0.0566]
Observed reflections [I>2σ(I)]	12881	3806	1510	1443	1220
Data / restraints / parameters	13766/8/633	4581/0/235	1760/0/96	1634/0/95	1344/1/92
Goodness-of-fit on F^2	1.163	1.228	1.056	1.072	1.056
R_1 [I>2σ(I)]	0.0247	0.0236	0.0386	0.0398	0.0281
wR_2 (all data)	0.0783	0.0883	0.0767	0.0814	0.0774
Flack parameter			0.00(2)	0.03(2)	-0.02(2)

Table A7. Crystal data and structure refinement for **5.15**, **5.16**, fluorobenzene encapsulation, **5.17** and **5.18**.

Compound	**5.15**	**5.16**	fluorobenzene encapsulation	**5.17**	**5.18**
Emperical formula	$C_{36}H_{36}Cu_2F_{12}N_{12}P_2$	$C_{26}H_{27}Cl_2Cu_2N_{13}O_8$	$C_{30}H_{29}B_2Cu_2F_9N_{12}$	$C_8H_8Cu_2I_2N_4$	$C_{80}H_{85}Cl_8Cu_4N_{37}O_{32}$
Formula weight	1053.79	847.59	877.35	541.06	2614.61
Radiation source	CuKα	CuKα	CuKα	MoKα	MoKα
Temperature (K)	120.01(10)	120.01(10)	120.01(10)	114.15(10)	114.15(10)
Crystal system	monoclinic	triclinic	cubic	monoclinic	monoclinic
Space group	*P*2/*n*	*P*-1	$P4_132$	$P2_1/c$	*P*2/*c*
Unit cell dimensions: a (Å)	12.1604(2)	11.2261(5)	15.0849(2)	9.7533(3)	17.8116(5)
b (Å)	26.8329(5)	11.5771(5)	15.0849(2)	16.7961(4)	18.5505(6)
c (Å)	13.3566(2)	14.3370(7)	15.0849(2)	7.9741(2)	16.6880(5)
α (˚)	90.00	111.278(4)	90.00	90.00	90.00
β (˚)	105.0689(19)	95.599(4)	90.00	111.4780(10)	107.597(2)
γ (˚)	90.00	110.426(4)	90.00	90.00	90.00
Volume ($Å^3$)	4208.38(14)	1572.57(15)	3432.63(8)	1215.58(6)	5255.9(3)
Z	4	2	4	4	2
Density (calculated) (Mg/m^3)	1.663	1.790	1.698	2.956	1.652
Absorption coefficient (mm^{-1})	2.853	3.873	2.365	8.554	1.099
F(000)	2128.0	860.0	1768.0	992.0	2664.0
Crystal dimensions	0.37 × 0.16 × 0.05	0.41 × 0.38 × 0.26	0.34 × 0.16 × 0.09	0.08 × 0.07 × 0.04	0.42 × 0.14 × 0.08
Theta range for data collection (˚)	6.58 to 139.96	6.84 to 139.98	13.12 to 132.98	6 to 60	2.2 to 55.52
Reflections collected	24073	17185	3343	32195	120806
Independent reflections [R(int)]	7942 [0.0230]	5927 [0.0182]	1019 [0.0265]	3543 [0.0447]	12331 [0.0696]
Observed reflections [I>2σ(I)]	5334	5718	989	3110	8304
Data / restraints / parameters	7942/4/579	5927/0/461	1019/1/100	3542/0/145	12331/0/796
Goodness-of-fit on F^2	1.176	1.054	1.060	1.041	1.035
R_1 [I>2σ(I)]	0.0532	0.0295	0.0547	0.0207	0.0466
wR_2 (all data)	0.1259	0.0762	0.1576	0.0437	0.1559
Flack parameter			0.07(9)		

Table A8. Crystal data and structure refinement for **5.19**, **5.20**, **5.21**, **5.22** and **5.23**.

Compound	**5.19**	**5.20**	**5.21**	**5.22**	**5.23**
Emperical formula	$C_{14}H_{17}CuN_5O_4$	$C_{16}H_{18}CdN_{10}O_7$	$C_{16}H_{24}CoN_{10}O_{10}$	$C_9H_{14}CuN_4O_6S$	$C_9H_{10}N_4Cl_2Cu$
Formula weight	382.87	574.80	575.38	369.84	308.65
Radiation source	MoKα	MoKα	MoKα	MoKα	MoKα
Temperature (K)	114.15(10)	116.15(10)	114.15(10)	117.15(10)	114.15(10)
Crystal system	triclinic	monoclinic	monoclinic	orthorhombic	orthorhombic
Space group	*P*-1	$P2_1/n$	$P2_1/n$	*Pnma*	*Pbca*
Unit cell dimensions: a (Å)	9.3775(6)	9.8819(3)	10.4573(4)	17.5961(5)	9.0794(2)
b (Å)	9.6247(6)	14.4993(4)	10.4800(3)	9.8074(3)	12.5910(4)
c (Å)	10.3197(6)	15.2185(4)	10.5684(4)	7.3662(2)	19.4921(5)
α (˚)	75.145(4)	90.00	90.00	90.00	90.00
β (˚)	63.674(3)	108.6290(10)	101.689(2)	90.00	90.00
γ (˚)	79.154(4)	90.00	90.00	90.00	90.00
Volume ($Å^3$)	803.92(9)	2066.27(10)	1134.20(7)	1271.20(6)	2228.31(10)
Z	2	4	2	4	8
Density (calculated) (Mg/m^3)	1.582	1.848	1.685	1.932	1.840
Absorption coefficient (mm^{-1})	1.388	1.123	0.834	1.919	2.414
F(000)	394.0	1152.0	594.0	756.0	1240.0
Crystal dimensions	0.17 × 0.11 × 0.07	0.32 × 0.25 × 0.02	0.47 × 0.4 × 0.16	0.51 × 0.45 × 0.45	0.26 × 0.18 × 0.04
Theta range for data collection (˚)	4.4 to 52.9	3.98 to 55	5.54 to 56.56	6 to 52.74	4.18 to 62.74
Reflections collected	15384	45623	24846	24939	60423
Independent reflections [R(int)]	3271 [0.0613]	4739 [0.0584]	2804 [0.0378]	1377 [0.0382]	3673 [0.0558]
Observed reflections [I>2σ(I)]	2478	4175	2500	1332	2886
Data / restraints / parameters	3271/0/220	4739/4/313	2804/8/181	1377/0/109	3673/0/155
Goodness-of-fit on F^2	1.132	1.169	1.047	1.185	0.911
R_1 [I>2σ(I)]	0.0459	0.0341	0.0261	0.0255	0.0280
wR_2 (all data)	0.1489	0.1017	0.0690	0.0721	0.1204
Flack parameter					

Table A9. Crystal data and structure refinement for **5.24**, **5.25** and **5.26**.

Compound	**5.24**	**5.25**	**5.26**
Emperical formula	$C_{18}H_{24}CuN_{10}O_8$	$C_{18}H_{24}CuI_2N_8O_2$	$C_{18}H_{24}Cl_2CuN_8O_{10}$
Formula weight	572.01	701.79	646.89
Radiation source	MoKα	MoKα	MoKα
Temperature (K)	113.15(10)	113.15(10)	114.15(10)
Crystal system	monoclinic	monoclinic	monoclinic
Space group	$P2_1/n$	$P2_1/n$	$P2_1/n$
Unit cell dimensions: a (Å)	7.2965(4)	7.1026(2)	7.4380(3)
b (Å)	11.8046(7)	11.4709(3)	11.6175(4)
c (Å)	13.1310(8)	13.7992(4)	14.1375(5)
α (˚)	90.00	90.00	90.00
β (˚)	101.091(4)	96.3370(10)	92.112(2)
γ (˚)	90.00	90.00	90.00
Volume ($Å^3$)	1109.88(11)	1117.40(5)	1220.81(8)
Z	2	2	2
Density (calculated) (Mg/m^3)	1.712	2.086	1.760
Absorption coefficient (mm^{-1})	1.056	3.774	1.186
F(000)	590.0	678.0	662.0
Crystal dimensions	0.45 × 0.22 × 0.08	0.49 × 0.16 × 0.16	0.57 × 0.36 × 0.18
Theta range for data collection (˚)	4.68 to 56.68	5.94 to 57.36	4.54 to 58.46
Reflections collected	24688	26405	28285
Independent reflections [R(int)]	2769 [0.0507]	2877 [0.0366]	3308 [0.0475]
Observed reflections [I>2σ(I)]	2345	2637	2544
Data / restraints / parameters	2769/4/175	2877/4/148	3308/0/224
Goodness-of-fit on F^2	1.131	1.119	1.137
R_1 [I>2σ(I)]	0.0310	0.0228	0.0770
wR_2 (all data)	0.0955	0.0641	0.2039
Flack parameter			